ISSN 1881-9109
National Museum of Nature and Science Monographs No. 45

OLENEKIAN (EARLY TRIASSIC) STRATIGRAPHY AND FOSSIL ASSEMBLAGES IN NORTHEASTERN VIETNAM

Edited by
Yasunari Shigeta
Toshifumi Komatsu
Takumi Maekawa
Huyen Dang Tran

National Museum of Nature and Science
Tokyo, March 2014

National Museum of Nature and Science Monographs

No. 45

Olenekian (Early Triassic) stratigraphy and fossil assemblages in northeastern Vietnam

Edited by

Yasunari Shigeta

Toshifumi Komatsu

Takumi Maekawa

Huyen Dang Tran

National Museum of Nature and Science

Tokyo, March 2014

National Museum of Nature and Science
Ueno Park, Tokyo 110–8718
Japan

Published on March 31, 2014
Printed by Kokusai Bunkensha Co. Ltd., Tokyo
ISSN: 1881-9109
ISBN: 978-4-87803-038-3

Contents

Contributors

Huyen Dang Tran Department of Paleontology and Stratigraphy, Vietnam Institute of Geosciences and Mineral Resources (VIGMR), Hanoi, Vietnam (E-mail: rigmr@fpt.vn)

Tien Dinh Cong Department of Paleontology and Stratigraphy, Vietnam Institute of Geosciences and Mineral Resources (VIGMR), Hanoi, Vietnam (E-mail: dc_tien4985@yahoo.com)

Hisayoshi Igo Institute of Natural History, 3–14–24 Takada, Toshima-ku, Tokyo 171–0033, Japan (E-mail: igohisa@mac.com)

Andrzej Kaim American Museum of Natural History, Central Park West at 79th Street, New York, NY 10024–5192, U.S.A. and Instytut Paleobiologii PAN, ul. Twarda 51/55 00–818 Warszawa, Poland (E-mail: kaim@twarda.pan.pl)

Toshifumi Komatsu Graduate School of Science and Technology, Kumamoto University, 2–39–1 Kurokami, Chuo-ku, Kumamoto 860–8555, Japan (E-mail: komatsu@sci.kumamoto-u.ac.jp)

Huu Nguyen Dinh Department of Paleontology and Stratigraphy, Vietnam Institute of Geosciences and Mineral Resources (VIGMR), Hanoi, Vietnam (E-mail: rigmr@fpt.vn)

Phong Nguyen Duc Department of Paleontology and Stratigraphy, Vietnam Institute of Geosciences and Mineral Resources (VIGMR), Hanoi, Vietnam (E-mail: phongcs@gmail.com)

Alexander Nützel Bayerische Staatssammlung für Paläontologie und Geologie, Richard Wagner Str. 10, 80333 München, Germany (E-mail: a.nuetzel@lrz.uni-muenchen.de)

Takumi Maekawa Graduate School of Science and Technology, Kumamoto University, 2–39–1 Kurokami, Chuo-ku, Kumamoto 860–8555, Japan (E-mail: 127d9009@st.kumamoto-u.ac.jp)

Yuka Miyake Graduate School of Science and Technology, Kumamoto University, 2–39–1 Kurokami, Chuo-ku, Kumamoto 860–8555, Japan (E-mail: y.m.ctty@gmail.com)

Yasunari Shigeta Department of Geology and Paleontology, National Museum of Nature and Science, 4–1–1 Amakubo, Tsukuba, Ibaraki 305–0005, Japan (E-mail: shigeta@kahaku.go.jp)

Osamu Takahashi Department of Astronomy and Earth Sciences, Tokyo Gakugei University, 4–1–1 Nukuikitamachi, Koganei, Tokyo 184–8501, Japan (E-mail: takahasi@u-gakugei.ac.jp)

Gengo Tanaka BioGeos, Japan Agency for Marine-Earth Science and Technology, 2–15 Natsushima, Yokosuka, Kanagawa 237–0061, Japan (E-mail: gengostra@yahoo.co.jp)

Yukiyasu Tsutsumi Department of Geology and Paleontology, National Museum of Nature and Science, 4–1–1 Amakubo, Tsukuba, Ibaraki 305–0005, Japan (E-mail: ytsutsu@kahaku.go.jp)

Abstract

Reported herein are extensive data resulting from a through investigation of the stratigraphy and paleontology of the Olenekian Bac Thuy Formation (Lower Triassic) in Lang Son City and the surrounding Chi Lang District of northeastern Vietnam. The Bac Thuy Formation conformably overlies the siliciclastic sandstone and mudstone of the Induan to Olenekian Lang Son Formation (Lower Triassic) and is unconformably overlain by rhyolitic rocks of the Middle Triassic Khon Lang Formation. Commonly divided into three parts, the Bac Thuy Formation consists of a lower part comprised mainly of limestone and mudstone, a middle part characterized by organic-rich dark gray limestone and an upper part composed of thick mudstone, sandstone and limestone. Its depositional environment consists of tidal flat, wave-influenced carbonate platform, and slope and marginal basin plain deposits. The intervals of organic-rich dark gray limestone and mudstone intercalated in the succession of slope to marginal basin plane facies are characterized by monospecific fossil and ichno-fossil assemblages, which suggest anoxic to dysoxic conditions.

The Bac Thuy Formation is very fossiliferous. Various types of fossils, e.g. cephalopods, gastropods, bivalves and conodonts, are abundant throughout the sequence, whereas ostracods and radiolarians are present only in the middle part. Five distinct ammonoid faunas, the *Flemingites rursiradiatus* beds, *Urdyceras tulongensis* beds, *Owenites koeneni* beds, *Xenoceltites variocostatus* beds, *Tirolites* cf. *cassianus* beds and *Tirolites* sp. nov. beds, as well as three conodont zones, *Novispathodus* ex gr. *waageni* Zone, *Novispathodus pingdingshanensis* Zone and *Triassospathodus symmetricus* Zone are recognized in ascending order. Based on these ammonoid and conodont occurrences, the formation ranges in age from Middle Smithian (middle Early Olenekian) to Early Spathian (early Late Olenekian), and the Smithian/Spathian boundary occurs in the organic-rich dark gray mudstone in the middle part of the formation. Radiometric ages of zircons reveal that the age of the rhyolite in the basal part of the overlying Khon Lang Formation is 237.7±1.9 Ma, which infers a latest Ladinian to earliest Carnian age.

Ammonoid faunas exhibit a very strong relationship with other Tethyan faunas, but show a relatively weak relationship with faunas on opposite sides of the Panthalassa. In contrast, Lower Spathian bivalve occurrences demonstrate probable faunal exchanges between the Tethys and Panthalassa. The gastropod fauna is characterized only by larvae or early juveniles of taxa displaying a mostly planktotrophic type of development, which indicates an unfavourable benthic environment for gastropods. The radiolarian fauna dominated by entactinarians from the Upper Smithian includes a mixture of Paleozoic and Triassic types.

The ammonoid mode of occurrence suggests that while the supratidal to intertidal environment was uninhabitable, the majority of ammonoids probably lived in the subtidal flat to storm-wave-influenced shallow marine environment typical of a carbonate platform. After death their shells were transported from their biotope to the slope to marginal basin plane by gravity flow. Almost all bivalve species were also transported more or less from their original habitats to offshore environments. However, epifaunal *Crittendenia* and *Bositra* probably inhabited the hemipelagic deposits of the slope and marginal basin plane environments, judging from their mode of fossil occurrence and shell preservation.

The limestone in the lower part of the Bac Thuy Formation contains many larval and/or juvenile shells of gastropods, whose external ornamentation is exceptionally well preserved. Acid treatment of this same limestone also produced many small ammonoid specimens free of obscuring matrix, thus permitting observation of the unique three-dimensional geometry of their internal features.

One hundred nineteen taxa (cephalopods: 42, gastropods: 8, bivalves: 5, conodonts: 46, ostracods: 6, radiorarians: 12) including seven new species (ammonoid: *Gaudemandites langsonensis*; radiolarians: *Multisphaera triassorobusta*, *Retentactinia*? *kycungensis*, *R*.? *parvisphaera*, *Plenoentactinia*? *terespongia*, *Paroertlispongus spinorientalis*, ostracoda: *Paracypris vietnamensis*) are described.

Key words: Ammonoids, Bac Thuy Formation, biostratigraphy, conodonts, Lower Triassic, northeastern Vietnam, Olenekian, Smithian, Spathian, stratigraphy

ベトナム北東部のオレネキアン階（下部三畳系）層序と化石群（重田康成・小松俊文・前川匠・Huyen Dang Tran 編）

ベトナム北東部のランソン市とチーラン地域周辺に分布するオレネキアン階（下部三畳系）バクトゥイ層について，層序学的研究と古生物学的研究を通して得られた様々な結果を報告する．バクトゥイ層は，インドゥアン階～オレネキアン階の珪砕屑性岩類（砂岩や泥岩）より成るランソン層に整合で重なり，中部三畳系コンラン層の流紋岩類に不整合で覆われる．バクトゥイ層は，主に石灰岩や泥岩によって形成される下部，有機物に富む暗灰色の石灰岩や泥岩で特徴づけられる中部，厚い泥岩，砂岩，石灰岩より成る上部に分けられ，干潟，波浪が卓越する炭酸塩プラットフォームの浅海相，陸棚斜面，海盆縁辺の堆積環境から成る．陸棚斜面相から海盆縁辺相に見られる有機物に富む暗灰色の石灰岩や泥岩は，単調な化石群や生痕化石群で特徴づけられ，無酸素から貧酸素の環境を示す．

バクトゥイ層からは，様々な化石が産出する．頭足類，巻貝類，二枚貝類，コノドント類は，全層準を通して豊富に産出するが，貝形虫類や放散虫類は中部のみから産出する．アンモノイド化石層は，下位から *Flemingites rursiradiatus* 層，*Urdyceras tulongensis* 層，*Owenites koeneni* 層，*Xenoceltites variocostatus* 層，*Tirolites* cf. *cassianus* 層，*Tirolites* sp. nov. 層の 5 層が認められた．またコノドント化石帯は，下位から *Novispathodus* ex gr. *waageni* 帯，*Novispathodus pingdingshanensis* 帯，*Triassospathodus symmetricus* 帯の 3 帯が認められた．これらの化石に基づくと，バクトゥイ層の年代は，スミシアン中期（オレネキアン前期の中頃）～スパシアン前期（オレネキアン後期の前半）で，スミシアン／スパシアン境界はバクトゥイ層中部の有機物に富む暗灰色泥岩中に位置する．コンラン層最下部の流紋岩中のジルコンの放射年代は，237.7 ± 1.9 Ma であり，ラディニアン末期あるいはカーニアン最初期を示す．

バクトゥイ層のアンモノイド化石群は，他のテチス域の化石群と強い関連性を示すが，パンサラッサ海両岸の化石群とは比較的関係性が弱い．一方，スパシアン階下部の二枚貝化石は，テチス域とパンサラッサ域の間での動物群の交流を示す．巻貝化石は，プランクトン栄養型の浮遊幼生あるいは稚貝のみが産出するが，これは海底が巻貝類には好ましくない環境であったことを意味する。スミシアン階上部の放散虫化石群は，Entactinaria 目が優占し，古生代型と三畳紀型の種群が混在する．

アンモノイド化石の産状から，潮上帯～潮間帯は，生息に不適な環境であり，アンモノイドの大部分は潮下帯～暴風時に波浪の影響を受ける浅海の炭酸塩プラットフォームに生息していたと考えられる．バクトゥイ層のアンモノイドの多くは，死後，その殻が重力流により生息域から陸棚斜面や海盆縁辺に運搬されたものである．二枚貝類の多くも生息域から沖合環境へ殻が運搬されたと考えられるが，産状や殻の保存状態から判断して，表在性の *Crittendenia* や *Bositra* は陸棚斜面や海盆縁辺で生息していたと思われる．

バクトゥイ層下部の石灰岩には，表面装飾が例外的に保存良好な巻貝類の幼生や稚貝の殻が多数含まれている．また，酸処理により殻内部の充填物が除去され内部形態の三次元構造が観察可能となった多数の微小なアンモノイド化石を得ることができる．

本論文では，7 新種（アンモノイド類：*Gaudemandites langsonensis*，放散虫類：*Multisphaera triassorobusta*，*Retentactinia*? *kycungensis*，*R*.? *parvisphaera*，*Plenoentactinia*? *terespongia*，*Paroertlispongus spinorientalis*，貝形虫類：*Paracypris vietnamensis*）を含む 119 分類群（アンモノイド類：42，巻貝類：8，二枚貝類：5，コノドント類：46，貝形類：6，放散虫類：12）を記載した．

Huyen Dang Tran・Tien Dinh Cong・猪郷久義・Andrzej Kaim・
小松俊文・Huu Nguyen Dinh・Phong Nguyen Duc・Alexander Nützel・
前川匠・三宅優佳・重田康成・高橋修・田中源吾・堤之恭

Introduction

(by Y. Shigeta, T. Komatsu, H. T. Dang, T. Maekawa, O. Takahashi, G. Tanaka and Y. Tsutsumi)

Lower Triassic marine deposits, widely distributed in northeastern Vietnam, have attracted the attention of many scientists beginning with the early work of pioneering French geologists and paleontologists. During the early twentieth century, Jean-Baptiste-Henri Counillon (1860–1923) and Henri Mansuy (1857–1937) collected various types of Lower Triassic molluscan fossils in Lang Son Province, and Mansuy (1908) is credited with being the first worker to describe ammonoids from the area. Furthermore, the 1908 work of Mansuy represents the first description of Triassic ammonoids from the country of Vietnam. Then in 1940, Professor Josué Heilmann Hoffet (1901–1945), while working at the University of Indochina, (established in 1906, now the Vietnam National University, Hanoi), collected ammonoids from limestone beds, approximately 24 km southeast of Lang Son City.

During the late twentieth century, Vietnamese paleontologists began investigating the Lower Triassic outcrops in Lang Son Province and eventually described the ammonoids, bivalves and conodonts they collected. In 1977, Nguyen Dinh Huu described several important age diagnostic Olenekian ammonoids from the Na Trang area, near Lang Son City. Then, in 1980 Vu Khuc erected the Bac Thuy Formation for the numerous carbonate beds in Lang Son Province and later he also described several Olenekian ammonoids from the Bac Thuy and Na Trang areas (Vu Khuc, 1984, 1991). During the period from 1988 to 2005, Dr. Dang Tran Huyen and Nguyen Dinh Huu conducted an extensive study of the paleontology and stratigraphy of the formation (Dang and Nguyen K. Q., 2000; Dang and Nguyen, D. H., 2005; Dang, 2006). Dr. Bui Duc Thang studied conodonts from the formation and reported typical Smithian (= Early Olenekian) conodont assemblages (Bui, 1989). Taken together, these studies reveal that the Lower Triassic of northeastern Vietnam yields numerous well-preserved fossils from various horizons within a relatively complete biostratigraphic sequence.

Similar fossiliferous Lower Triassic deposits also crop out in South China, and these outcrops have been extensively studied by various authors beginning with the pioneer works of Chao (1950, 1959) who first documented the occurrence of rich Early Triassic ammonoid faunas in northwestern Guangxi. More recently, Lehrmann *et al*. (2001, 2003, 2007a, b) and Galfetti *et al.* (2008) conducted detailed studies of the lithofacies and depositional environments of the Lower Triassic in this area. Brayard and Bucher (2008) and Brühwiler *et al*. (2008) recognized several Griesbachian to Smithian-aged ammonoid faunas in northwestern Guangxi and constructed a new, very high resolution biostratigraphical zonation, portions of which can be correlated with various Tethyan localities as well as certain faunal horizons in the eastern Panthalassic basins. Kaim *et al.* (2010) discovered and described a well-preserved Greisbachian gastropod fauna, and Goudemand *et al.* (2012) described early Triassic conodont clusters from the area. Chen *et al.* (2013) reported on the size variation of conodonts in sediments representing the Smithian/Spathian boundary. These studies have contributed significantly to achieving an improved understanding of the environment and dynamics of the biotic recovery after the end-Permian mass extinction.

In order to better understand the regional correlation and reconstruction of Early Triassic depositional environments, tectonics, biofacies and marine ecosystems in northeastern Vietnam, Japanese and Vietnamese workers in 2005 organized a joint working group under the leadership of Dr. Toshifumi Komatsu. During the period from 2006 to 2012, various members of the group conducted several scientific expeditions to Lang Son Province (Fig.

Fig. 1. Photographs of the Geologic Museum in Hanoi and major members of the Japanese-Vietnamese Joint Resaearch Group. 1, Geologic Museum (Bao Tang Dia Chat) in Hanoi, Vietnam. Numerous specimens of Lower Triassic megafossils collected by Vu Khuc and Huu Nguyen Dinh from the Bac Thuy Formation are reposited here. 2, Dr. Huyen Dang Tran, Tien Dinh Cong and Dr. Toshifumi Komatsu. 3, Phuong Nguyen Duc (driver), Huu Nguyen Dinh, Takumi Maekawa, Dr. Yasunari Shigeta and Dr. Huyen Dang Tran at the Bac Thuy Railway Station. 4, Phong Nguyen Duc.

1), where they investigated all geological and paleontological aspects of the extensive outcrops including lithostratigraphy, biostratigraphy, isotope stratigraphy, sedimentology, paleobiology, and systematic paleontology.

These studies have resulted in several reports, some of which are preliminary in nature. They include descriptions of several Olenekian bivalves (e.g., *Crittendenia*) by Komatsu *et al*. (2013), and Komatsu *et al.* (2014) have reported that the depositional environment of the Bac Thuy Formation consists mainly of intertidal, wave and storm dominated shallow marine, slope, and marginal basin plain deposits. Komatsu *et al*. (2011) and Maekawa *et al*. (2012) have presented preliminary reports in regular meeting of the Palaeontological Society of Japan regarding the Smithian to Spathian conodont, bivalve, and ammonoid assemblages. In order to document the enormous amount of resultant data concerning the Lower Triassic in northeastern Vietnam, a decision was made to publish a monograph with financial support from the National Museum of Nature and Science with Dr. Yasunari Shigeta as chief editor. This volume includes a systematic paleontology section for the cephalopods, bivalves, gastropods, conodonts, ostracods and radiolarians collected from the Bac Thuy Formation, as well as a description of the formation's sedimentary environments and that of the upper part of the underlying Lang Son Formation. Also included is a section dealing with the zircon geochronology of the overlying Khon Lang Formation.

Research methods

Fossil-bearing rock samples were collected following a careful bed-by-bed approach with special attention devoted to taphonomic considerations. Megafossils were recovered from host rocks in the laboratory by use of air tool and/or air abrasion equipment. Silicon casts were made of specimens consisting only of outer molds. Over 100 limestone samples have been examined in an effort to investigate microfossils. Conodonts and micro gastropods were removed by applying 5–8% acetic acid to approximately 0.5 to 2 kg sample, then sieving residues (0.177 mm and 1 mm screens) and washing in water. Radiolarians were extracted by applying 5% hydrochloric acid to 0.5 kg samples for 24 hours, then sieving residues (0.300 mm and 0.075 mm screens) and washing in water. Ostracods were removed by applying 5% acetic acid for two weeks, then washing in water.

During field work, facies analyses of the beds were performed based on lithology, sedimentary structures, grain size, paleocurrent data, and fossil content in order to reconstruct depositional environments. In the laboratory, we observed the detailed sedimentary structures and fabrics of block samples and also prepared thin sections for petrographic analysis and observation of microfossils. Sedimentological terminology follows that of Tucker and Wright (1990), Tucker (1991), Reading and Collinson (1996), Mulder and Alexander (2001), and Mulder (2011).

Radiometric ages of rhyolite samples were obtained by zircon U-Pb dating using a Laser Ablation Inductively Coupled Plasma Mass Spectrometry (LA-ICP-MS) unit installed at the National Museum of Nature and Science, Tsukuba. Procedures for sample preparation and their subsequent analyses for zircon are the same as those described by Tsutsumi *et al.* (2012). The quadrupole ICP-MS is an Agilent 7700x, and the laser ablation system is an ESI NWR213. A spot size of 25 μm and laser power 4–5 J/cm^2 were adopted. He gas was used as the carrier gas instead of Ar gas to enhance a higher transport efficiency of ablated materials (e.g. Eggins *et al*., 1998). Common Pb corrections for the concordia diagrams as well as for each age were made using ^{208}Pb and ^{207}Pb, respectively (Williams, 1998), on the basis of the model for common Pb compositions proposed by Stacey and Kramers (1975). The pooled ages presented in this

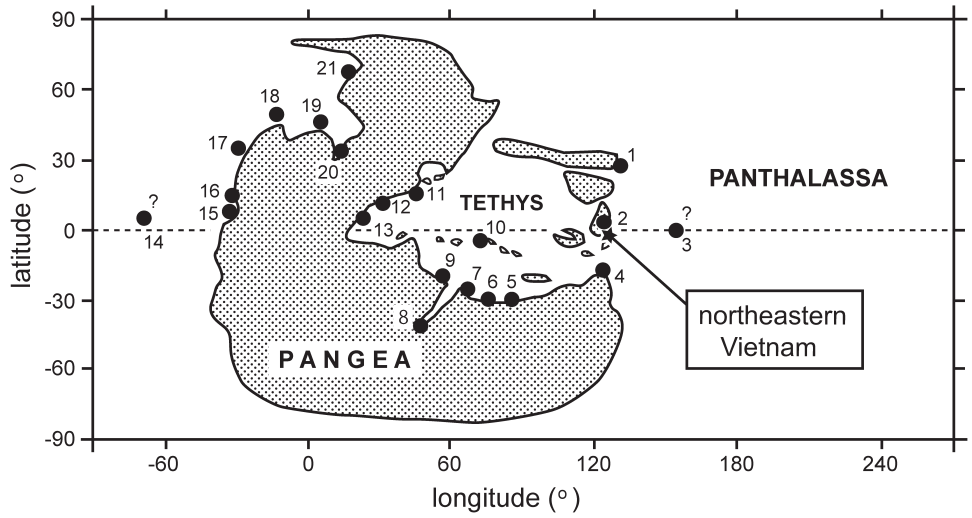

Fig. 2. Paleogeographical map of the Early Triassic showing the position of northeastern Vietnam and other areas. Paleomaps modified after Péron *et al*., 2005, Brayard *et al*., 2006 and Brayard *et al*., 2009. 1: South Primorye, 2: South China, 3: Kamura, Taho and Iwai limestones (Japan), 4: Timor, 5: South Tibet, 6: Spiti, 7: Salt Range, 8: Madagascar, 9: Oman, 10: Afghanistan, 11: Caucasus, 12: Chios, 13: Albania, 14: Chulitna (Alaska), 15: Nevada, 16: Idaho/Utah, 17: British Columbia, 18: Ellesmere Island, 19: Spitsbergen, 20: Greenland, 21: Olenek River area.

study were calculated using the Isoplot/Ex software (Ludwig, 2003).

Repository of specimens

All fossils and rock samples collected during our field work were transported from Vietnam to Japan with permission from the Vietnamese Government and other concerned authorities. All cephalopod, gastropod, ostracod and conodont specimens are reposited at the National Museum of Nature and Science, Tsukuba. Bivalves are stored in the Faculty of Science, Kumamoto University, Kumamoto, and radiolarian specimens are stored at Tokyo Gakugei University, Koganei.

Paleogeographical and geological setting

(by T. Komatsu, Y. Shigeta and H. T. Dang)

Tectonic activity of South China and Indochina blocks that probably began in the late Paleozoic continued throughout the Early to Middle Triassic (Metcalfe, 1998, 2009; Lepvrier *et al*., 2004; Nakano *et al*., 2008, 2010). According to Metcalfe (2009), the South China block originally rifted and separated from the northern margin of Gondwanaland in the Devonian and drifted northward in the Triassic. The Indochina craton was deeply subducted beneath the South China craton in the Early Triassic (Nakano *et al*., 2010).

In the Early Triassic, the Nanpanjiang and An Chau basins were widely exposed on the South China block (Enos *et al*., 2006; Lehrmann *et al*., 2007a, b; Galfetti *et al*., 2008; Komatsu *et al*., 2014). The Nanpanjiang basin is a vast, shallow to deep marine embayment in the southern part of the South China block. During the late Permian to Early Triassic, it was located in the eastern Tethys seaway near the equator (Metcalfe, 1998, 2009). The An Chau basin in Vietnam, which is located in the southern part of the South China block (Fig. 2), was continuous with the southeastern Nanpanjiang basin during the Triassic.

In the southwestern part of Guangxi Province, south China, the Nanpanjiang basin sur-

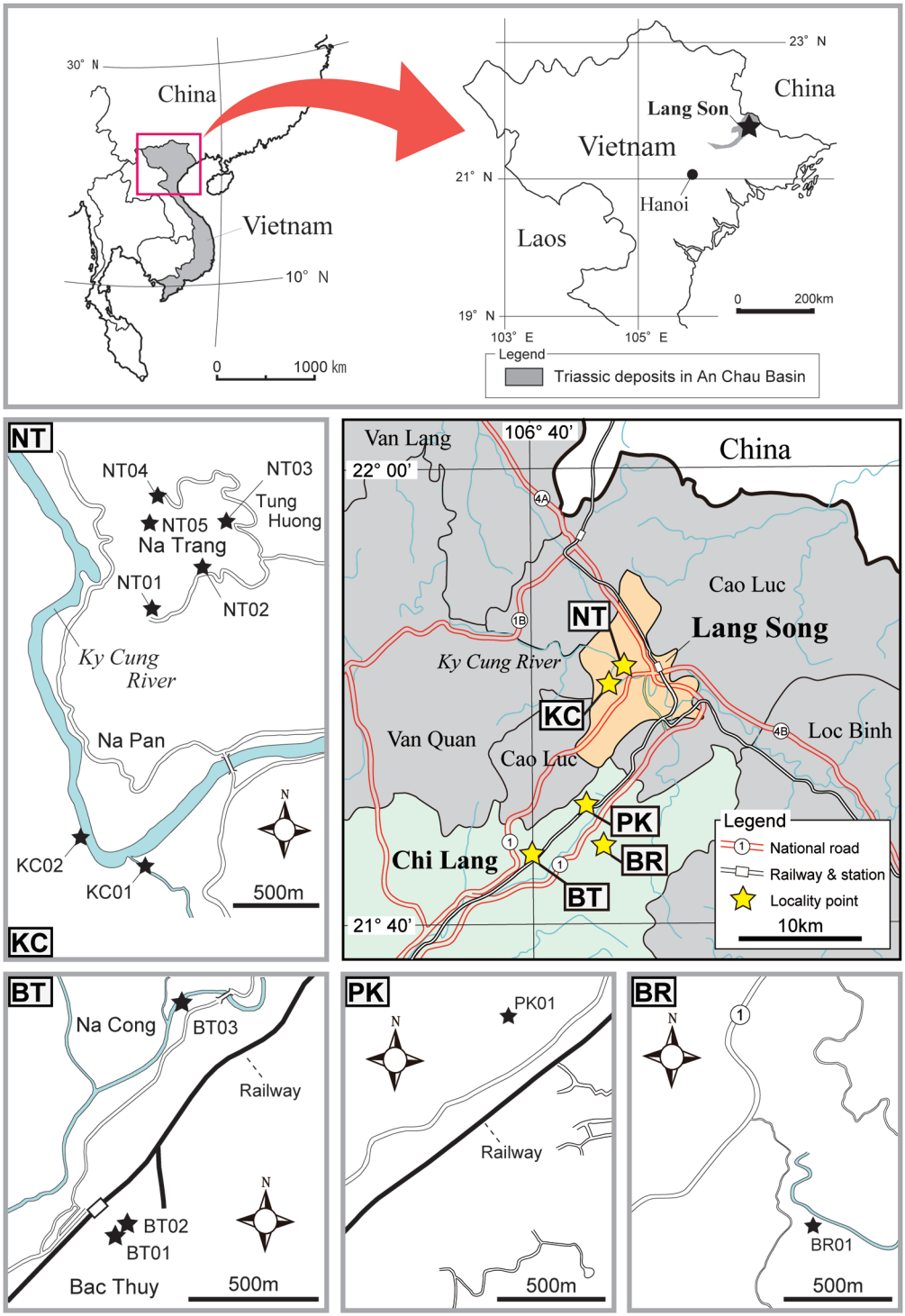

Fig. 3. Map showing the study area and An Chau basin in Lang Son Province, northeastern Vietnam. Studied sections (BT, KC, NT, PK and BR) are located in the central part of Lang Son Province.

rounds several large, isolated platforms, including the Chongzuo-Pingguo and Debao platforms (Lehrmann *et al*., 2007a, b). In the Chongzuo area of southwestern Guangxi Province, the Early Triassic Nanpanjiang basin is filled with mudstone and debris flow deposits of the Induan to Olenekian Luolou Formation and with isolated shallow marine platform deposits of the Induan Majiaoling and Induan to Olenekian Beisi formations (Lehrmann *et al*., 2007a, b). In Vietnam, the Early Triassic An Chau basin is filled mainly with marine deposits of the Lower Triassic Lang Son and Bac Thuy formations and the Middle Triassic volcanic rocks of the Khon Lang Formation. Komatsu *et al.* (2014) reported the Olenekian Bac Thuy Formation is lithologically equivalent to the Luolou Formation in the Nanpanjiang basin.

According to Lehrmann *et al*. (2007b), who examined long-term subsidence patterns during the Proterozoic to Triassic, the Yangtze platform and other, isolated platforms—including the Chongzuo-Pingguo platform and the Great Bank of Guizhou—were characterized by high subsidence and sedimentation rates during the Olenekian to Anisian in the Chongzuo area; peak subsidence rates occurred earlier in the southern basin (i.e., in the Pingguo and Chongzuo areas) than in the northern basin. During the Olenekian to Anisian, in the Nanpanjiang basin the huge accommodation space was filled with carbonate and siliciclastic gravity flow deposits. However, the timing and source area of the siliciclastic gravity flows in the southern Nanpanjiang basin are poorly understood, although Enos *et al.* (2006) suggested that the Middle Triassic turbidites originated from the east in association with the Jiangnan uplift in the northern basin.

In contrast, Lower Triassic siliciclastic sediments are common in the shallow to deep marine facies in the An Chau basin (Komatsu and Dang, 2007; Komatsu *et al.*, 2010, 2014). According to Komatsu *et al*. (2014), thick siliciclastic slump deposits accumulated in a slope environment are intercalated within the upper part of the Induan to early Olenekian Lang Son Formation. Many turbidite beds consisting of siliciclastics are embedded in the Olenekian Bac Thuy Formation. Climbing-ripple and current-ripple laminations in high- and low-density marginal basin turbidites indicate eastward, northeastward, and southeastward paleocurrent directions in the Bac Thuy Formation (Komatsu *et al*., 2014). These observations suggest that the Lower Triassic siliciclastic sediments in the southern Nanpanjiang basin originated mainly from the shelf in the An Chau basin or from a landmass in northern Vietnam. Moreover, it seems that the landmass was distributed in the western margin of the An Chau basin.

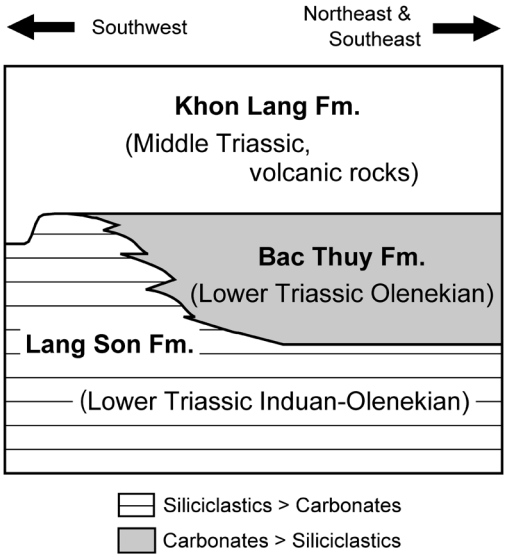

Fig. 4. Stratigraphic subdivisions of the Lower Triassic System in An Chau basin, northeastern Vietnam. The Olenekian Bac Thuy Formation consists of carbonates and siliciclastics.

Stratigraphy of the Bac Thuy Formation

(by T. Komatsu, T. Maekawa and Y. Shigeta)

The Bac Thuy Formation was established by Vu Khuc (1980), and its stratotype is locat-

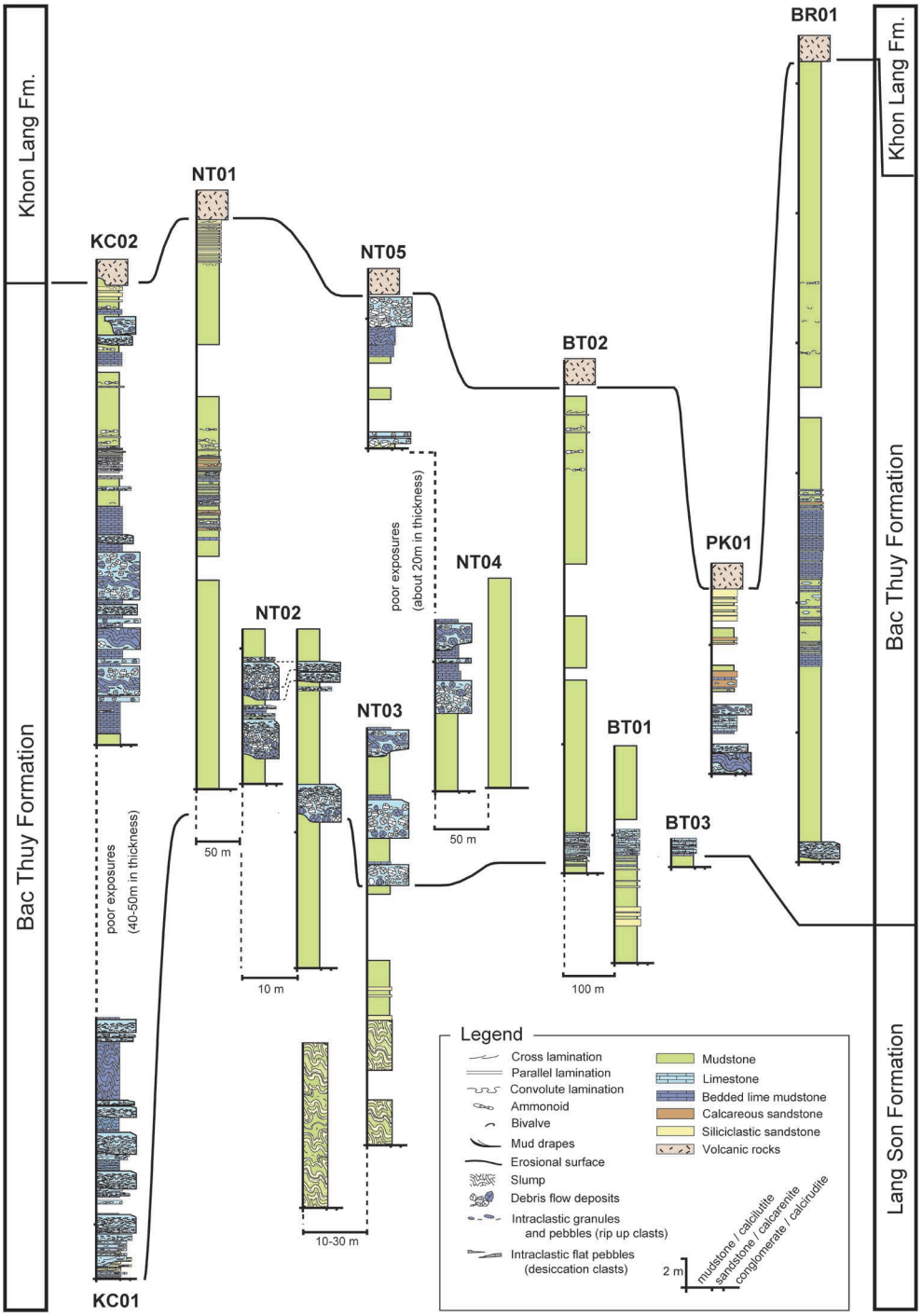

Fig. 5. Columnar sections of the Lang Son (upper part) and Bac Thuy formations in the central part of Lang Son Province.

ed near the Bac Thuy railway station in the Bac Thuy area (BT), Chi Lang District, Lang Son Province. It is also well exposed in the Pac Khanh (PK), Ban Ru (BR), Na Trang (NT) and Ky Cung River (KC) areas, in the central part of Lang Son Province (Fig. 3). The formation conformably overlies the Lower Triassic (Induan to Olenekian) Lang Son Formation, which consists mainly of siliciclastic sandstone and mudstone in the Na Trang, Bac Thuy and Ban Ru areas, and it is unconformably overlain by the Middle Triassic Khon Lang Formation, which consists predominately of rhyolitic rocks in these areas (Fig. 4). The Bac Thuy Formation is generally divided into three parts, namely a lower part consisting mainly of limestone and mudstone, a middle part characterized by organic-rich dark gray limestone and an upper part composed of thick mudstone, sandstone and limestone (Fig. 5).

Bac Thuy area

Exposures: Two sections, BT01 and BT02, near the Bac Thuy railway station (stratotype) and one section (BT03) at Na Cong, in Chi Lang District (Figs. 3, 5–11).

Thickness: 45 m at BT02 (Figs. 5, 8).

Lithology: The lowermost part of the Bac Thuy Formation (3 m thick) consists of a basal alternation of thin-bedded limestone and greenish gray mudstone that is overlain by 2 m thick interval of fossiliferous bedded limestone (Figs. 6, 9–11). This limestone bed interval, which contains abundant ammonoid shells and a thin slump bed, is also characterized by sutured stylolite (BT01–03). Although the middle part of the formation is not well exposed, the upper part is represented by a thick massive and dominant greenish-gray mudstone containing shelly sandstone layers.

Megafossils: The thin limestone beds of the basal limestone/greenish gray mudstone alternation and the lower part of the overlying fossiliferous limestone beds yield *Flemingites rursiradiatus* Chao, 1959, *Pseudaspidites muthianus* (Krafft and Diener, 1909), *Submeekoceras hsüyüchieni* (Chao, 1959) and *Jinyaceras* cf. *bellum* Brayard and Bucher, 2008. The middle part of the fossiliferous limestone beds intercalated with the thin slump bed contains *Urdyceras tulongensis* Brühwiler *et al*. 2010, *Ussuria kwangsiana* Chao, 1959, *Galfettites simplicitatis* Brayard and Bucher 2008, *Pseudaspidites muthianus*, *Submeekoceras hsüyüchieni*, *Jinyaceras* cf. *bellum*, *Paranannites sinensis* (Chao, 1959) and *Aspenites acutus* Hyatt and Smith, 1905. *Owenites koeneni* Hyatt and Smith, 1905 is the characteristic ammonoid in the upper part of the 2 m thick fossiliferous limestone beds, but *Preflorianites radians* Chao, 1959, *Dieneroceras*? *goudemandi* (Brayard and Bucher, 2008), *Leyeceras rothi* Brayard and Bucher, 2008, *Parussuria compressa* (Hyatt and Smith, 1905), *Nammalites* sp. indet. and *Pseudosageceras multilobatum* Noetling, 1905a also occur in this interval. Megafossils are not found in the middle part of the formation. *Xenoceltites*? sp. indet., *Tirolites* sp. nov., *Columbites* sp. indet., *Yvesgalleticeras*? sp. indet. and *Eodanubites*? sp. indet. occur in the greenish-gray mudstone of the upper part. The bivalves, *Crittendenia australasiatica* (Krumbeck, 1924), "*Pseudomonotis*" *himaica* (Bittner, 1899) and *Bositra* sp. indet. are also commonly found in the upper part of the formation.

Microfossils: Microfossils are abundant in the 2 m thick fossiliferous limestone bed interval in the lower part of the formation, but the basal thin limestone/mudstone alternation yields only poorly preserved microfossils. Conodonts, including *Novispathodus* ex gr. *waageni* (Sweet, 1970b), *Conservatella conservativa* (Müller, 1956), *Discretella discreta* (Müller, 1956), and *D*. *robustus* (Wang and Wang, 1976) are commonly found throughout the fossiliferous limestone interval. In particular, the lower part of this interval is especially rich, yielding various species of conodonts such as *Eurygnathodus costatus* Staesche,

Fig. 6. Basal part of the Bac Thuy Formation in BT01, which conformably overlies the Lang Son Formation.

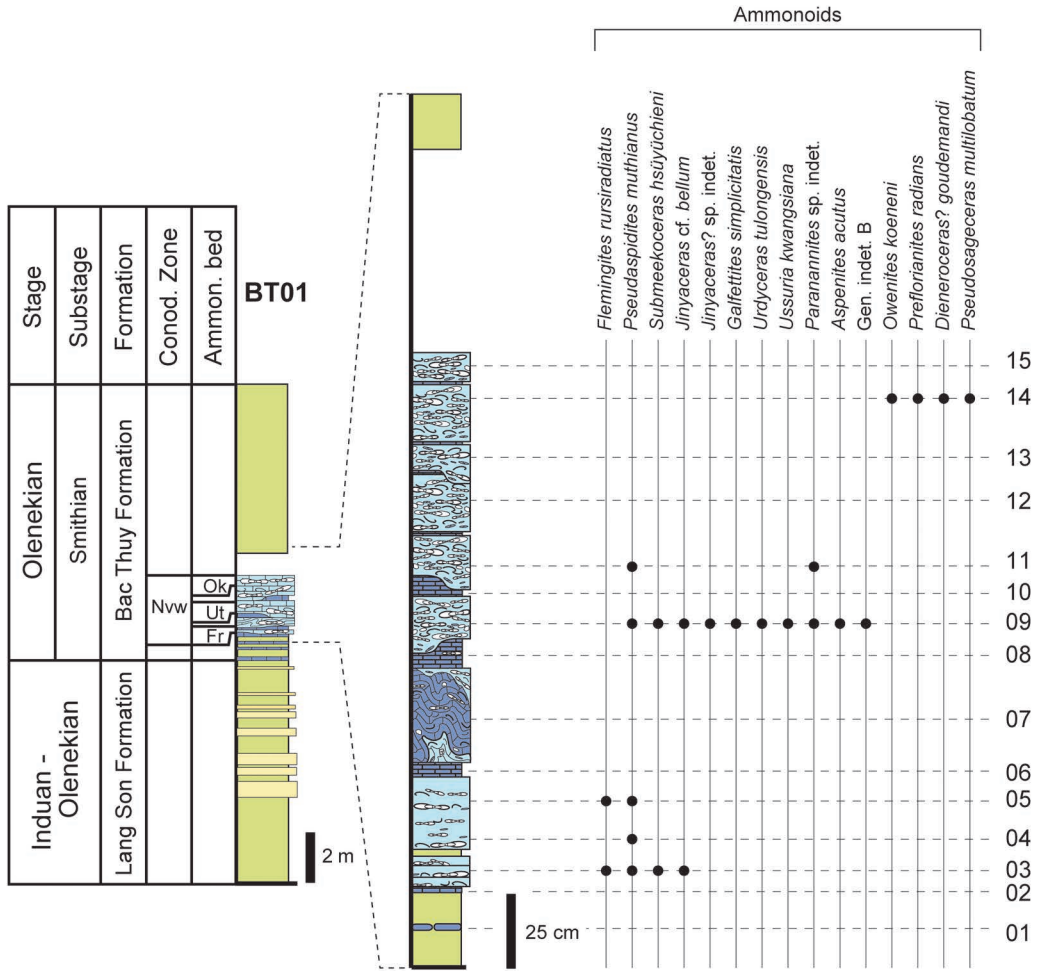

Fig. 7. Distribution of ammonoid, gastropod, and conodont taxa in BT01. Legend is shown in Fig. 5. Nvw: *Novispathodus* ex gr. *waageni* Zone, Fr: *Flemingites rursiradiatus* beds, Ut: *Urdyceras tulongensis* beds, Ok: *Owenites koeneni* beds.

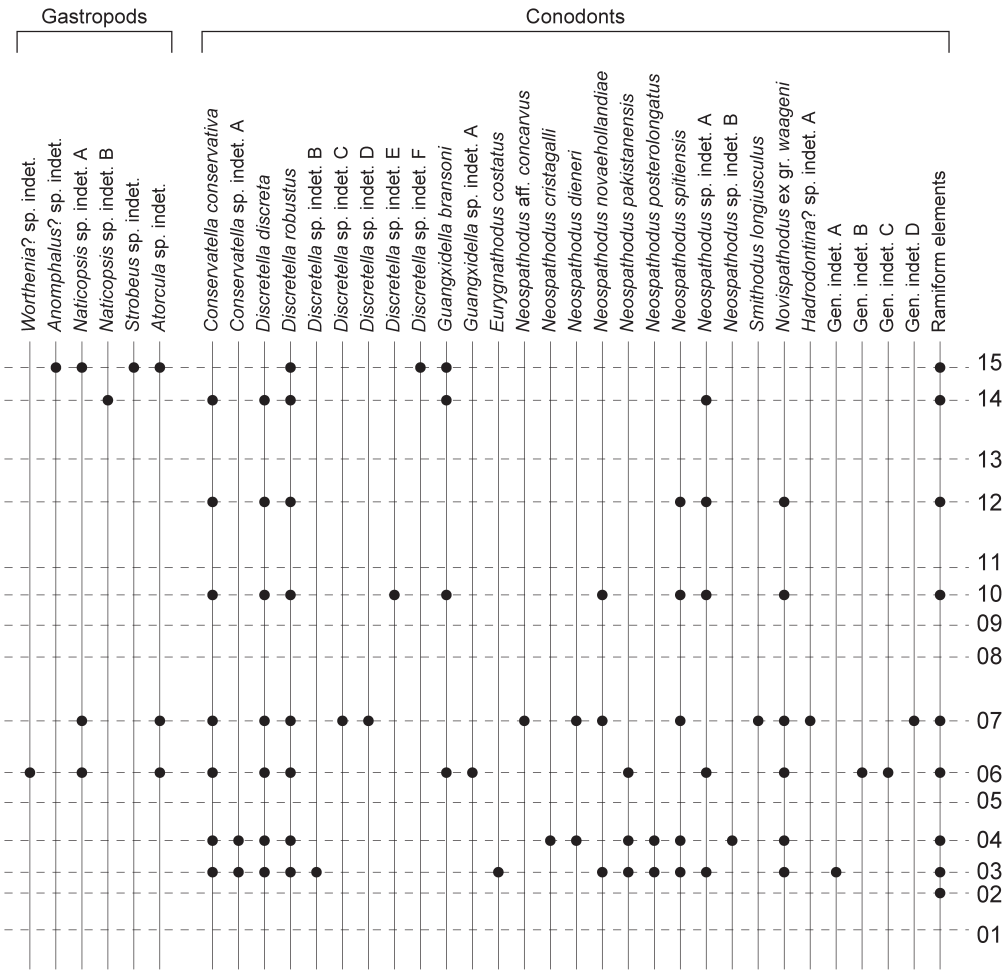
Gastropods
Conodonts
Worthenia? sp. indet.
Anomphalus? sp. indet.
Naticopsis sp. indet. A
Naticopsis sp. indet. B
Strobeus sp. indet.
Atorcula sp. indet.
Conservatella conservativa
Conservatella sp. indet. A
Discretella discreta
Discretella robustus
Discretella sp. indet. B
Discretella sp. indet. C
Discretella sp. indet. D
Discretella sp. indet. E
Discretella sp. indet. F
Guangxidella bransoni
Guangxidella sp. indet. A
Eurygnathodus costatus
Neospathodus aff. concarvus
Neospathodus cristagalli
Neospathodus dieneri
Neospathodus novaehollandiae
Neospathodus pakistanensis
Neospathodus posterolongatus
Neospathodus spitiensis
Neospathodus sp. indet. A
Neospathodus sp. indet. B
Smithodus longiusculus
Novispathodus ex gr. waageni
Hadrodontina? sp. indet. A
Gen. indet. A
Gen. indet. B
Gen. indet. C
Gen. indet. D
Ramiform elements
15
14
13
12
11
10
09
08
07
06
05
04
03
02
01

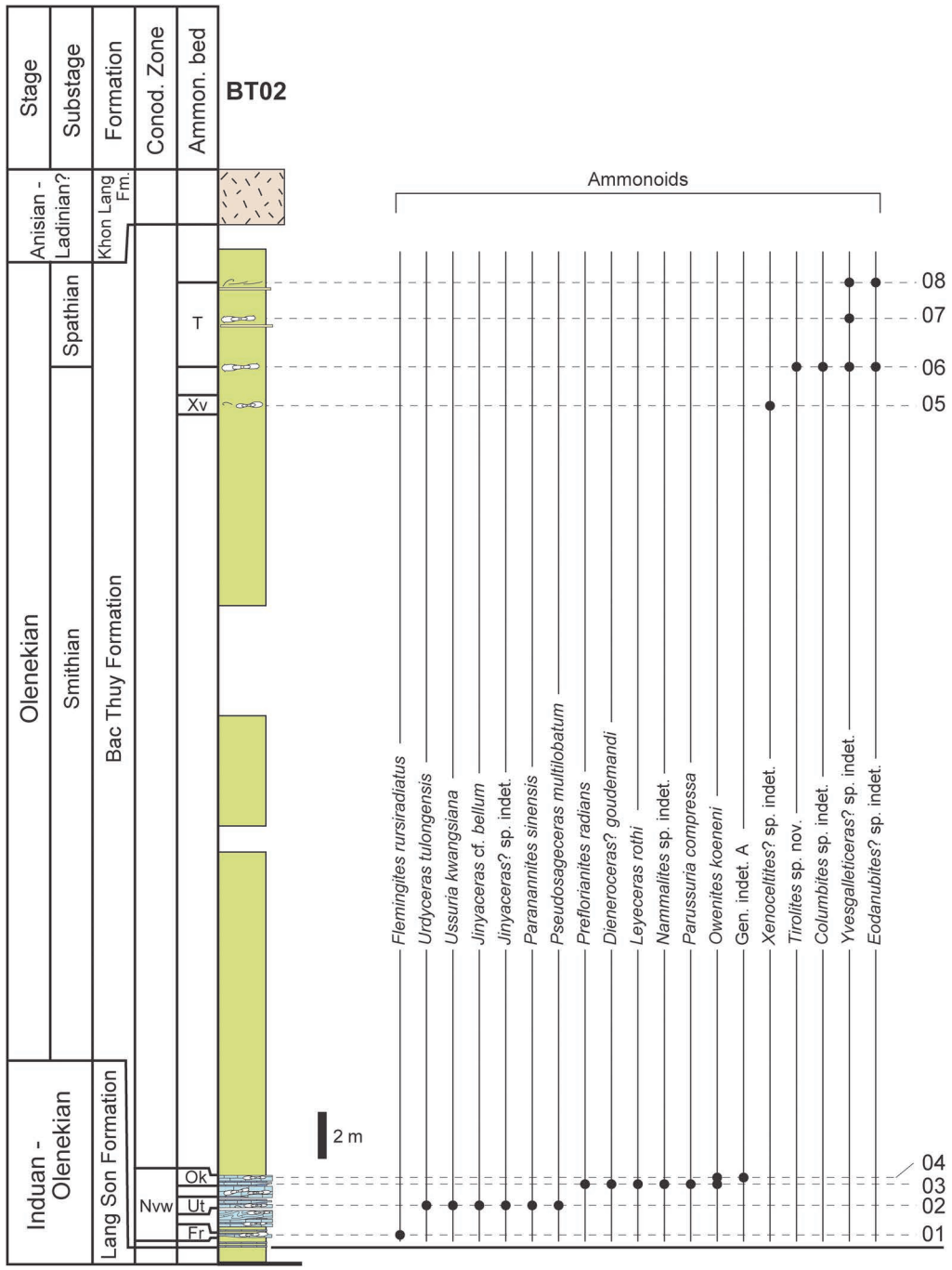

Fig. 8. Distribution of ammonoid, gastropod, bivalve, and conodont taxa in BT02. Legend is shown in Fig. 5. Nvw: *Novispathodus* ex gr. *waageni* Zone, Fr: *Flemingites rursiradiatus* beds, Ut: *Urdyceras tulongensis* beds, Ok: *Owenites koeneni* beds, Xv: *Xenoceltites variocostatus* beds, T: *Tirolites* sp. nov. beds.

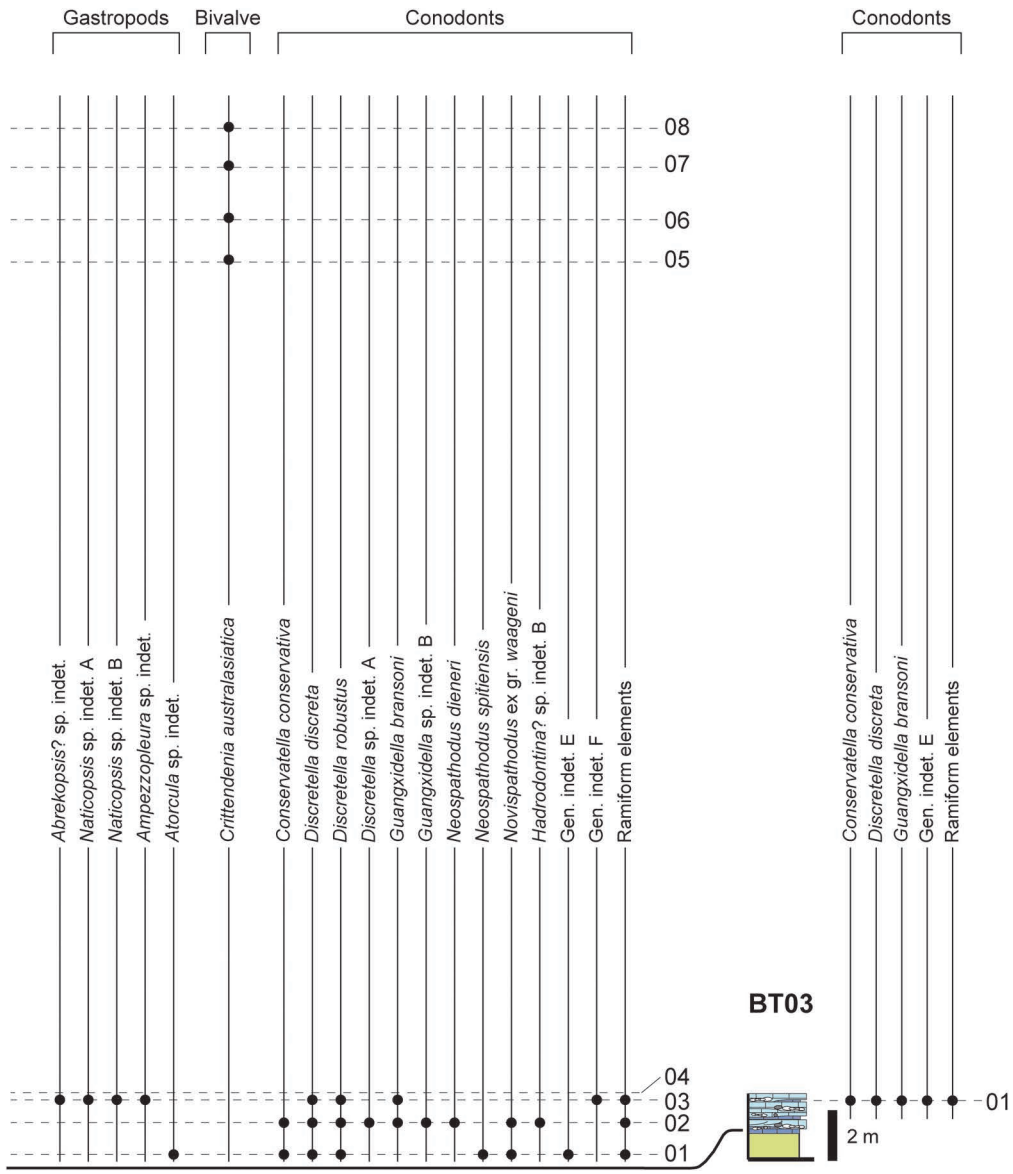
Gastropods
Bivalve
Conodonts
Conodonts
Abrekopsis? sp. indet.
Naticopsis sp. indet. A
Naticopsis sp. indet. B
Ampezzopleura sp. indet.
Atorcula sp. indet.
Crittendenia australasiatica
Conservatella conservativa
Discretella discreta
Discretella robustus
Discretella sp. indet. A
Guangxidella bransoni
Guangxidella sp. indet. B
Neospathodus dieneri
Neospathodus spitiensis
Novispathodus ex gr. waageni
Hadrodontina? sp. indet. B
Gen. indet. E
Gen. indet. F
Ramiform elements
08
07
06
05
04
03
02
01
BT03
2 m
Conservatella conservativa
Discretella discreta
Guangxidella bransoni
Gen. indet. E
Ramiform elements
01

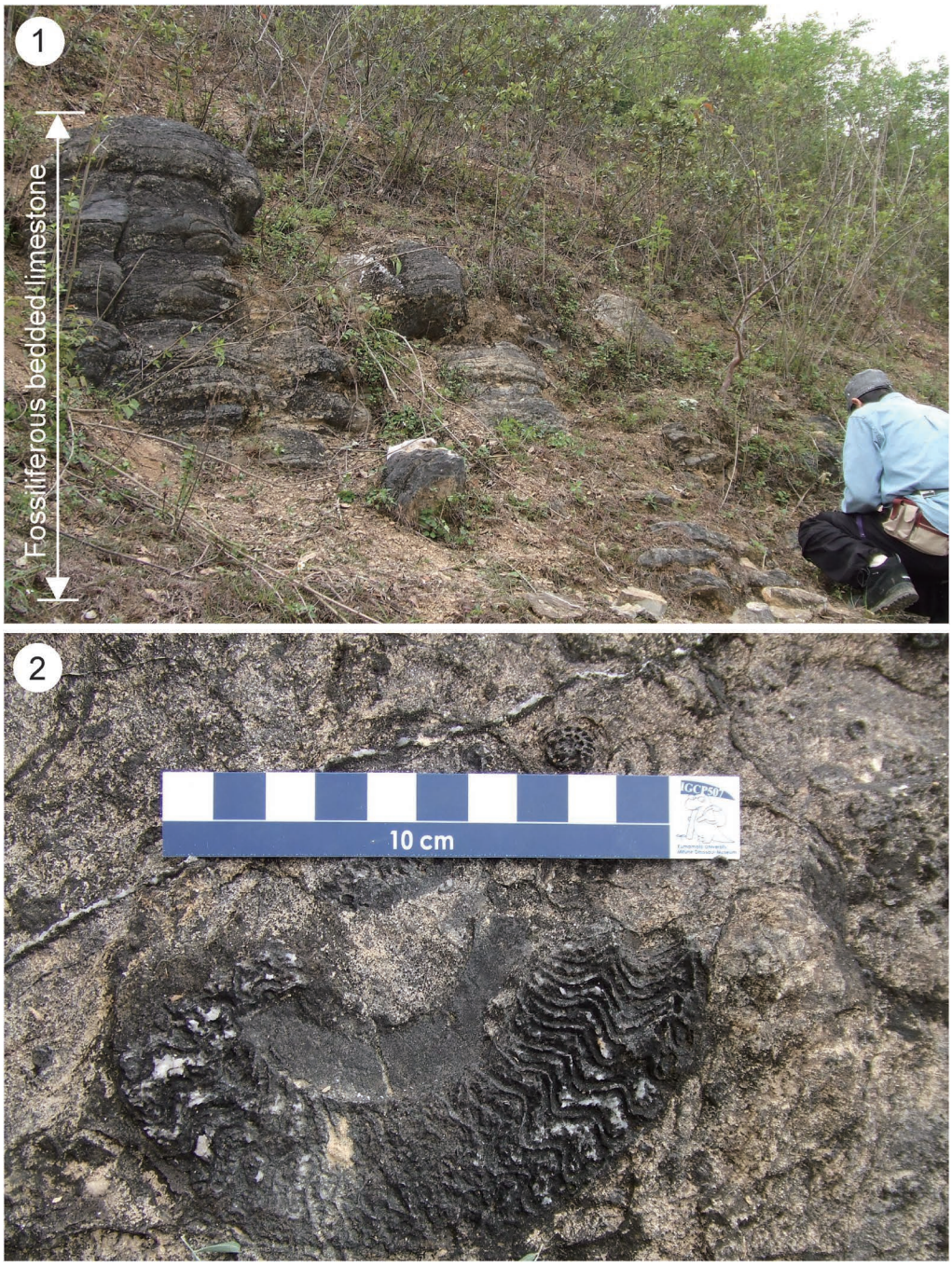

Fig. 9. Alternating thin-bedded limestone and mudstone and 2 m thick fossiliferous bedded limestone interval in the basal part of the BacThuy Formation in BT01. 1, 2 m thick bedded limestone interval containing abundant ammonoids, gastropods and conodonts. 2, Bedding plane in the 2 m thick fossiliferous bedded limestone interval at BT01-09. Many ammonoid sections are visible.

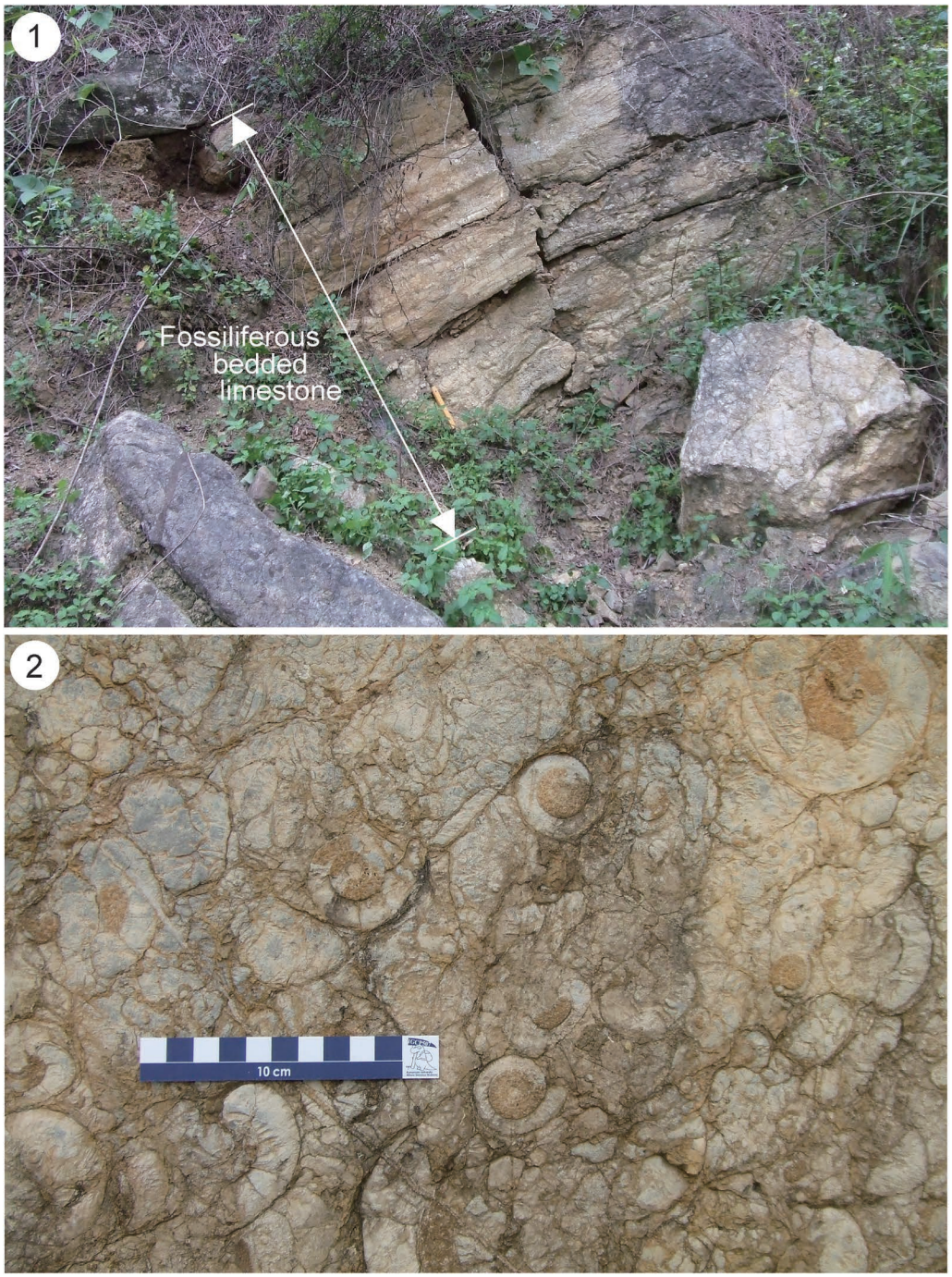

Fig. 10. 1, 2 m thick fossiliferous bedded limestone interval containing abundant ammonoids in the basal part of the Bac Thuy Formation in BT03. Scale is 20 cm. 2, Bedding plane in the ammonoid supported shell-concentration in the 2 m thick fossiliferous bedded limestone interval.

Fig. 11. Bedding plane in the ammonoid supported shell-concentration in the 2 m thick fossiliferous bedded limestone interval in the basal part of the Bac Thuy Formation in BT03. *Owenites koeneni* and *Preflorianites radians* occur abundantly in the ammonoid supported shell-concentration.

1964, *Neospathodus* aff. *concavus* Zhao and Orchard, 2007, *Ns*. *cristagalli* (Huckriede, 1958), *Ns*. *dieneri* Sweet, 1970a, *Ns. novaehollandiae* McTavish, 1973, *Ns*. *pakistanensis* Sweet, 1970b, *Ns*. *posterolongatus* Zhao and Orchard, 2007 and *Ns*. *spitiensis* Goel, 1977.

The middle part of the limestone bed interval is intercalated with a slump bed containing the conodonts, *Ns*. *dieneri*, *Ns. novaehollandiae*, *Ns*. *spitiensis*, *Guangxidella bransoni* (Müller, 1956), *Smithodus longiusculus* (Buryi, 1979), and two species of *Hadrodontina*?, as well as the gastropods *Worhtenia*? sp. indet., *Atorcula* sp. indet. and *Naticopsis* sp. indet. A.

The upper part of the limestone bed interval yields the conodont *Guangxidella bransoni*, and the gastropods *Anomphalus*? sp. indet., *Abrekopsis* sp. indet., *Strobeus* sp. indet., *Ampezzopleura* sp. indet. *Atorcula* sp. indet. and *Naticopsis* sp. indet. A and B. Microfossils are not found in the middle and upper parts of the formation.

Ky Cung River

Exposures: Two sections, KC01, 02 along the Ky Cung River near Na Pan, in Lang Son City (Figs. 3, 5, 12–16)

Thickness: Greater than 100 m (Figs. 5, 12, 15).

Lithology: The lower part of the formation (95 m thick), which is poorly exposed in this area, consists of limestone breccias, bedded limestone, carbonate slump beds and greenish gray mudstone (Figs. 13, 14, 16). Embedded in the basal part at KC01 are 4 m thick typical shallow marine carbonates consisting of oolites, lenticular to wavy beddings, tidal bundles containing mud drapes and cross-stratified limestone. Thin bivalve shells and small ammonoids commonly occur in the oolitic limestone and cross-stratified limestone, and desiccation cracks are typically found in the lenticular to wavy bedding (Komatsu *et al.*, 2014). The middle part of the formation (3 m thick) is characterized by organic-rich dark gray thin-bedded limestone yielding abundant radiolarians and bivalves, and mudstone containing dark gray calcareous nodules. The upper part of the formation (12 m thick) consists of thick mudstone intercalated with limestone breccias, thin bedded limestone, thin turbidite beds and sandstone/mudstone alternations. Ammonoid and bivalve shell lag deposits, and cross- and parallel-laminations characterize the thin turbidite beds.

Megafossils: Ammonoids are common in the limestone breccias and bedded limestone in the lower part of the formation. *Owenites koeneni* and *Dieneroceras*? *goudemandi* are dominant, but other taxa are also found in two different horizons as follows: *Juvenites sinuosus* (Kiparisova, 1947), *Paranannites sinensis*, *Preflorianites radians*, *Leyeceras rothi*, *Anaflemingites hochulii* Brayard and Bucher, 2008, *Parussuria compressa* and *Aspenites acutus* in the lower portion, and *Guodunites monneti* Brayard and Bucher, 2008 in the upper portion. The organic-rich dark gray carbonate beds in the middle part of the formation contain the following megafossils: ammonoid–*Xenoceltites variocostatus* Brayard and Bucher, 2008 and bivalves–abundant *Crittendenia australasiatica*, rare *Crittendenia langsonensis* Komatsu and Dang, 2013 and *Bositra limbata* (Guo, 1985).

The upper part of the formation yields the bivalves–*Crittendenia australasiatica*, *Leptochondria bittneri* (Kiparisova, 1938), "*Pseudomonotis*" *himaica*, *Bositra limbata* and *Bositra* sp. indet. and ammonoids, whose shells form thin lenticular shell concentrations (Figs. 17–19). Ammonoid composition changes toward the upward sequence within the upper part of the formation. *Tirolites* cf. *cassianus* (Quenstedt, 1849) is common in the greenish-gray mudstone of the lower portion, while *Tirolites* sp. nov., *Columbites* sp. indet., *Yvesgalleticeras*? sp. indet. are abundant in the middle portion. Also occurring in the middle portion are *Procarnites*? sp. indet., *Eodanubites*?

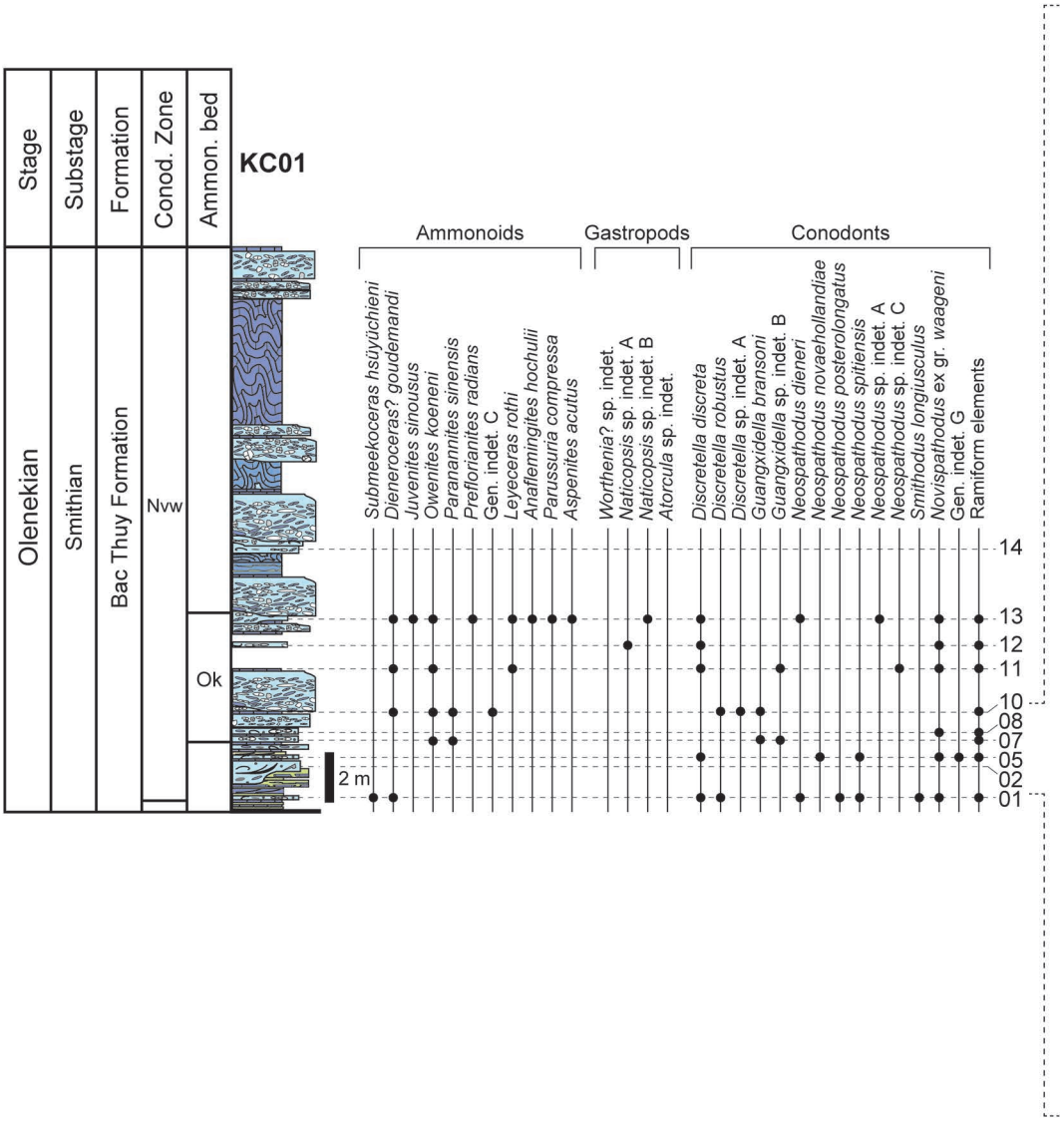

Fig. 12. Distribution of ammonoid, gastropod, and conodont taxa in KC01. Legend is shown in Fig. 5. Nvw: *Novispathodus* ex gr. *waageni* Zone, Ok: *Owenites koeneni* beds.

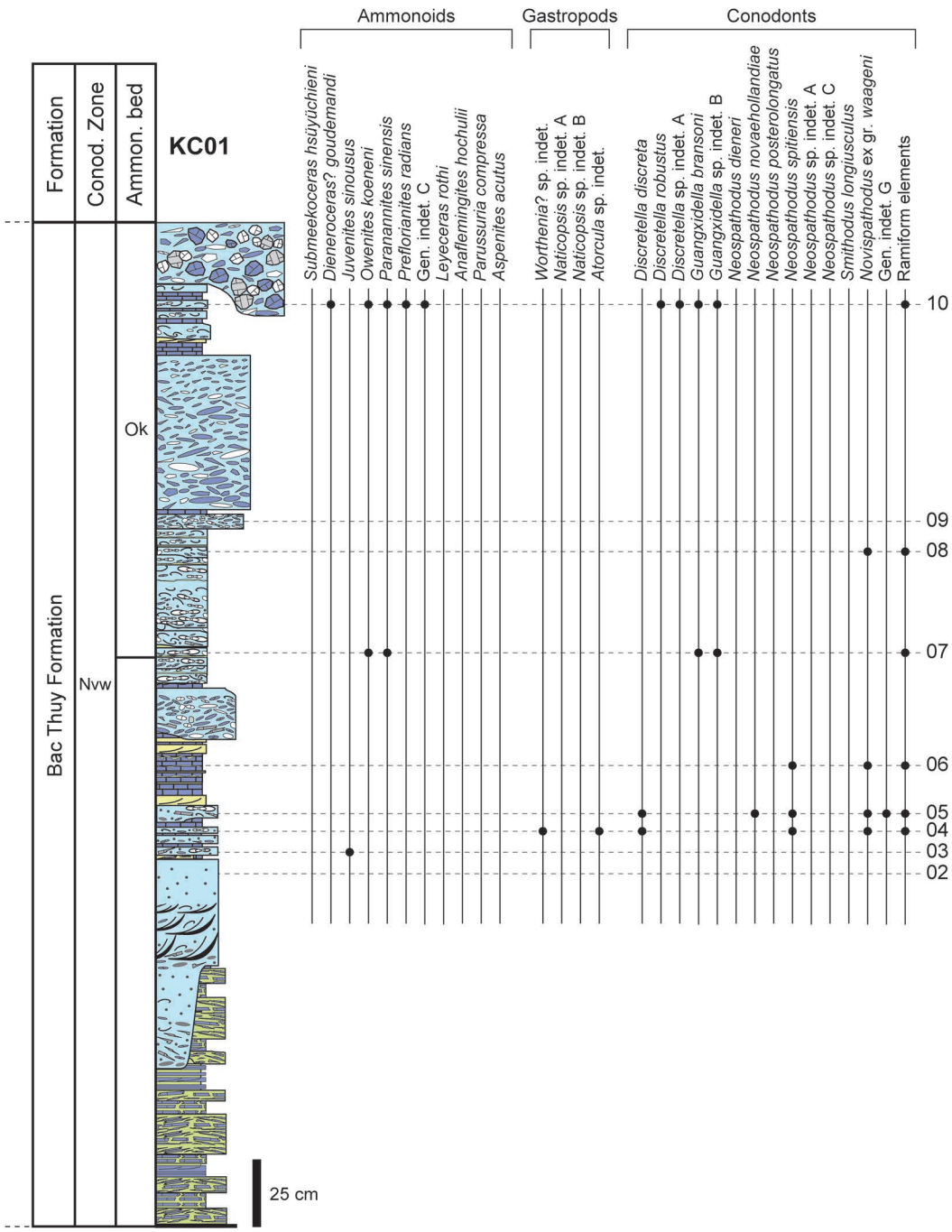
Formation
Conod. Zone
Ammon. bed
KC01
Bac Thuy Formation
Nvw
Ok
25 cm
Ammonoids
Gastropods
Conodonts
Submeekoceras hsüyüchieni
Dieneroceras? goudemandi
Juvenites sinousus
Owenites koeneni
Paranannites sinensis
Prefloranites radians
Gen. indet. C
Leyeceras rothi
Anaflemingites hochulii
Parussuria compressa
Aspenites acutus
Worthenia? sp. indet.
Naticopsis sp. indet. A
Naticopsis sp. indet. B
Atorcula sp. indet.
Discretella discreta
Discretella robustus
Discretella sp. indet. A
Guangxidella bransoni
Guangxidella sp. indet. B
Neospathodus dieneri
Neospathodus novaehollandiae
Neospathodus posterolongatus
Neospathodus spitiensis
Neospathodus sp. indet. A
Neospathodus sp. indet. C
Smithodus longiusculus
Novispathodus ex gr. waageni
Gen. indet. G
Ramiform elements
10
09
08
07
06
05
04
03
02

Fig. 13. Exposures of the lower part of the Bac Thuy Formation along a tributary of the Ky Cung River in KC01. 1, Limestone breccia, slump bed and bedded limestone. 2, Secondarily deformed bedded limestone (slump bedding).

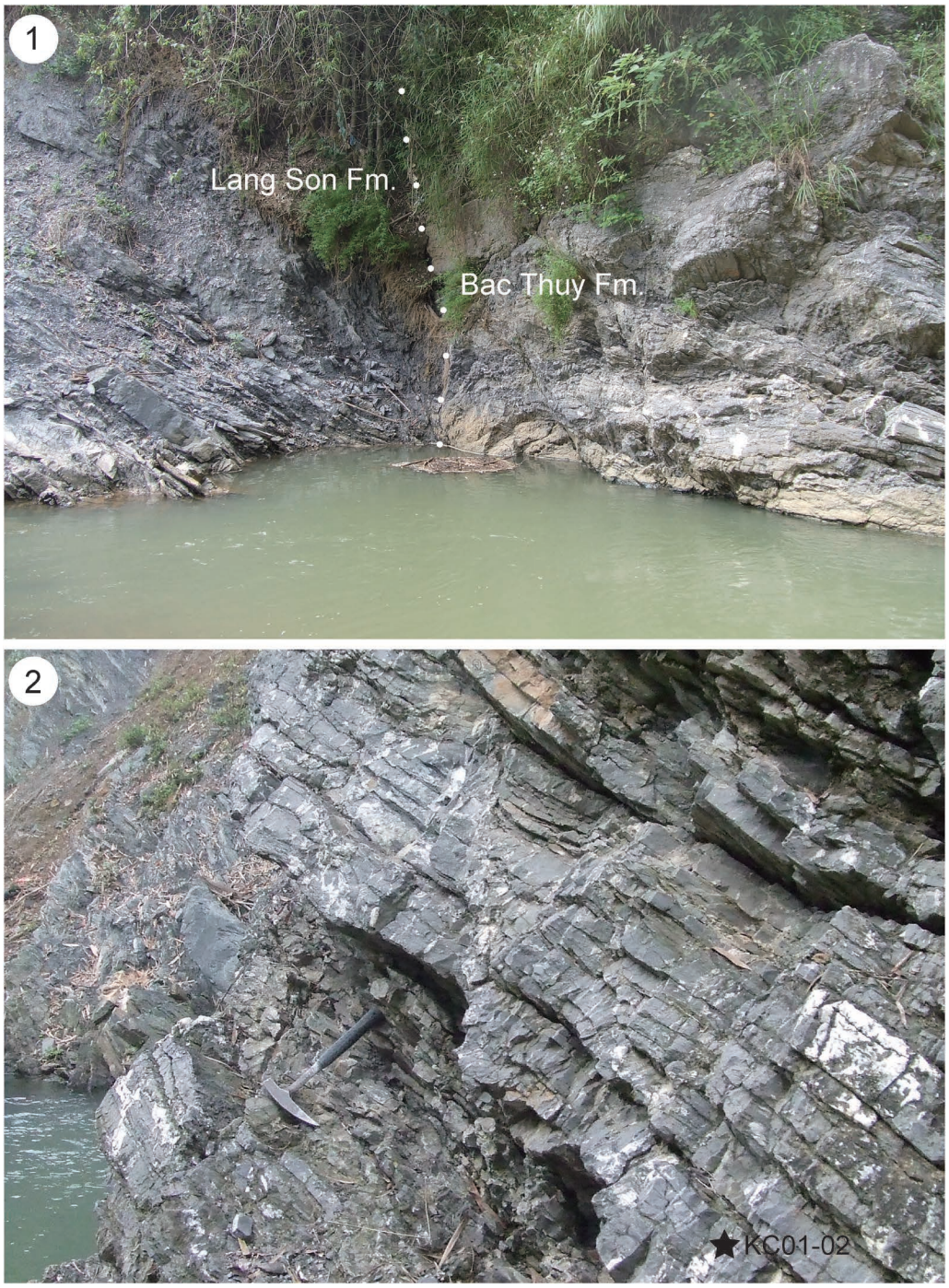

Fig. 14. Exposures of the lower part of the Bac Thuy Formation along a tributary of the Ky Cung River in KC01. 1, Outcrop showing the fault contact between shallow marine limestone of the Bac Thuy Formation and underlying Lang Son Formation in KC01. 2, Shallow marine carbonate lithofacies.

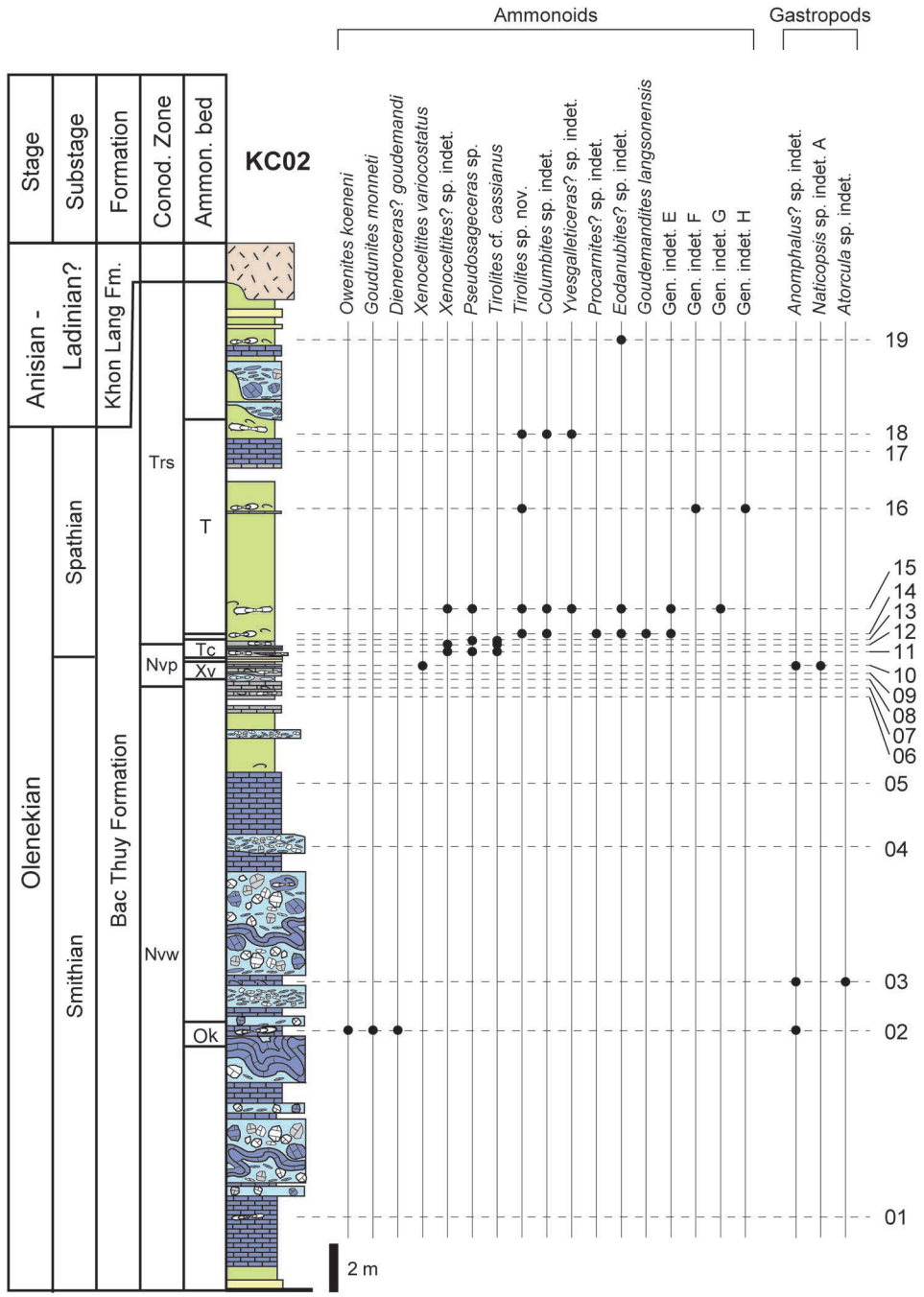

Fig. 15. Distribution of ammonoid, gastropod, bivalve, conodont, and radiolarian taxa in KC02. Legend is shown in Fig. 5. Nvw: *Novispathodus* ex gr. *waageni* Zone, Nvp: *Novispathodus pingdingshanensis* Zone, Trs: *Triassospathodus symmetricus* Zone, Ok: *Owenites koeneni* beds, Xv: *Xenoceltites variocostatus* beds, Tc: *Tirolites* cf. *cassianus* beds, T: *Tirolites* sp. nov. beds.

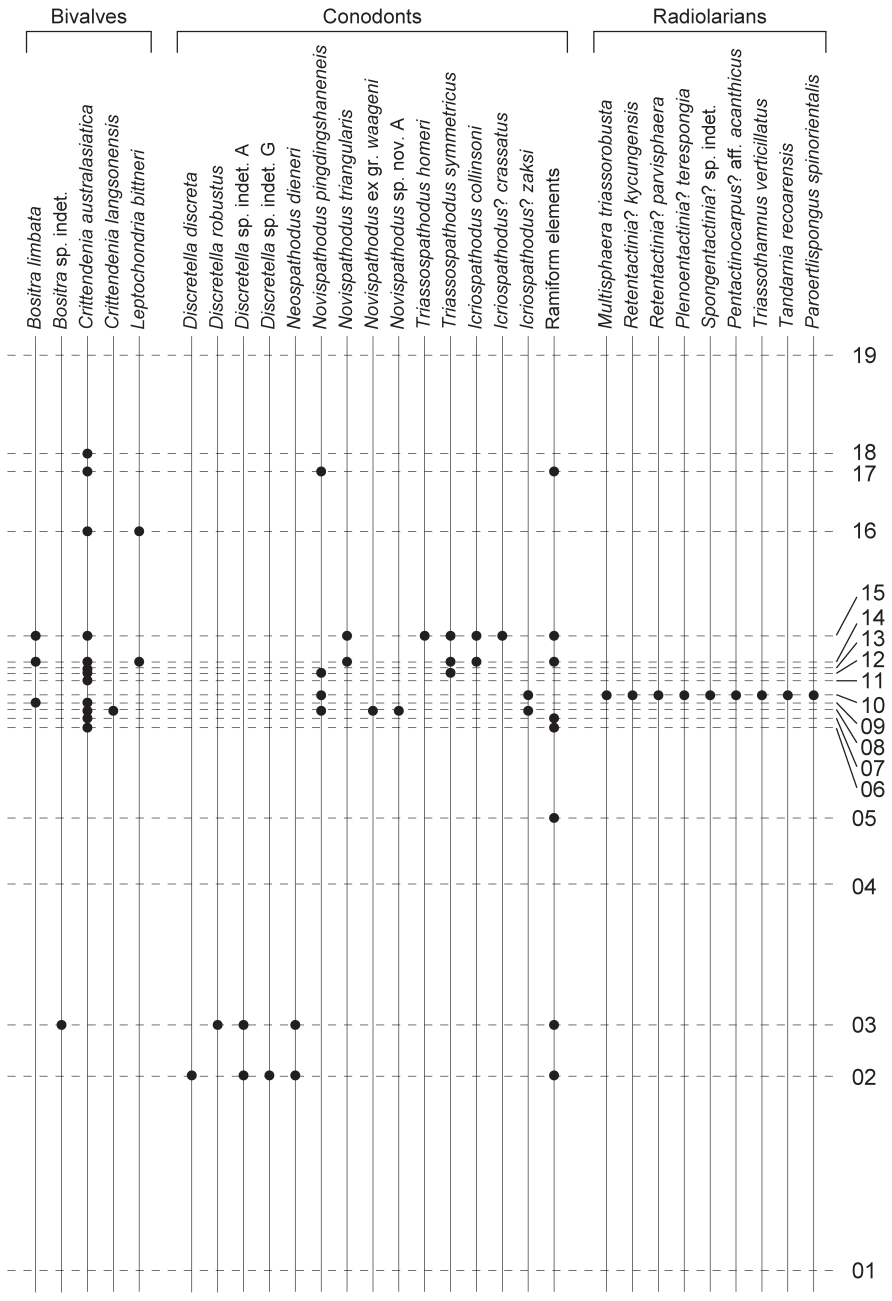
Bivalves
Conodonts
Radiolarians
Bositra limbata
Bositra sp. indet.
Crittendenia australasiatica
Crittendenia langsonensis
Leptochondria bittneri
Discretella discreta
Discretella robustus
Discretella sp. indet. A
Discretella sp. indet. G
Neospathodus dieneri
Novispathodus pingdingshaneneis
Novispathodus triangularis
Novispathodus ex gr. waageni
Novispathodus sp. nov. A
Triassospathodus homeri
Triassospathodus symmetricus
Icriospathodus collinsoni
Icriospathodus? crassatus
Icriospathodus? zaksi
Ramiform elements
Multisphaera triassorobusta
Retentactinia? kycungensis
Retentactinia? parvisphaera
Plenoentactinia? terespongia
Spongentactinia? sp. indet.
Pentactinocarpus? aff. acanthicus
Triassothamnus verticillatus
Tandarnia recoarensis
Paroertlispongus spinorientalis
19
18
17
16
15
14
13
12
11
10
09
08
07
06
05
04
03
02
01

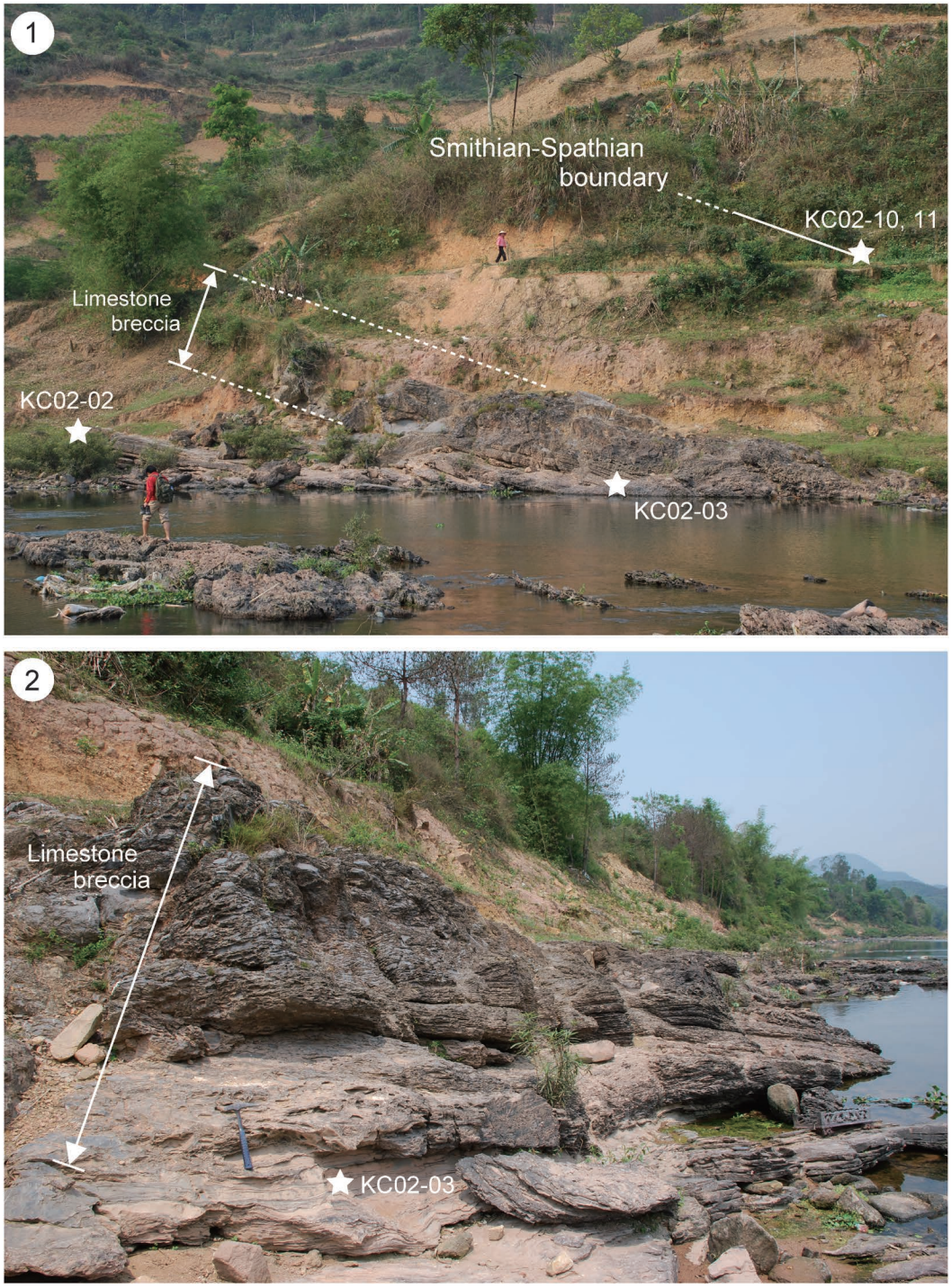

Fig. 16. Exposures of the lower and middle parts of the Bac Thuy Formation in KC02. 1, Limestone breccia, thin-bedded limestone and thick mudstone cropping out along the Ky Cung River. The Smithian/Spathian boundary is intercalated in alternating organic-rich dark gray bedded limestone and mudstone at KC02-10 and KC02-11. 2, Thick limestone breccia containing intraclasts composed mainly of oolitic and bioclastic shallow marine limestone and thin-bedded hemipelagic limestone.

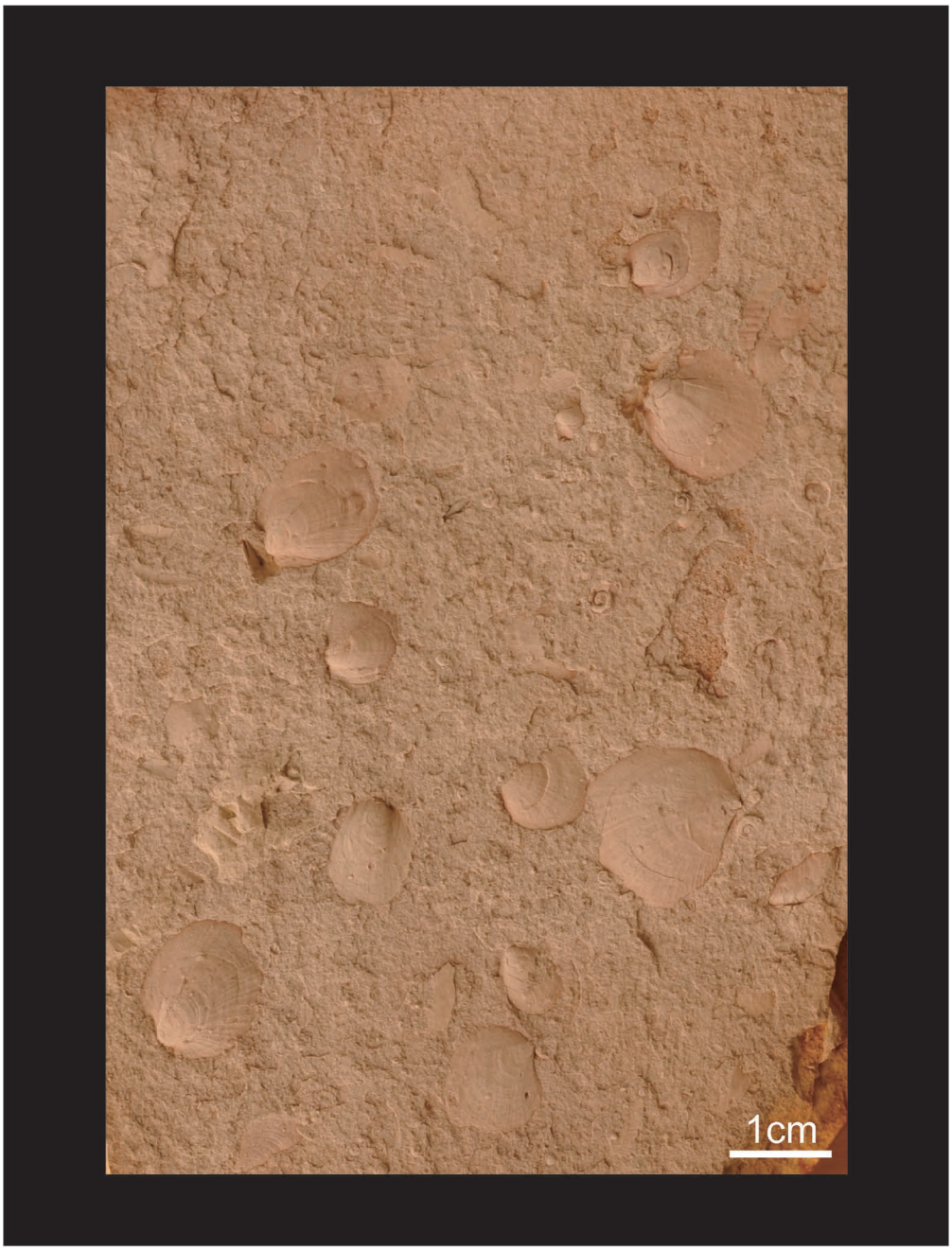

Fig. 17. Shell concentration (KMSP-5138) consisting of "*Pseudomonotis*" *himaica* and *Crittendenia australasiatica* in the Td division of a thin turbidite layer in thick hemipelagic mudstone at KC02-15. Disarticulated shells are scattered on the basal erosive surface of the low-density turbidite layer.

Fig. 18. Early Spathian ammonoids in a low-density turbidite layer from KC02-14.

Fig. 19. Early Spathian ammonoids in a low-density turbidite layer from KC02-14.

sp. indet. and *Goudemandites langsonensis* Shigeta and Nguyen sp. nov. Only rare specimens of *Eodanubites*? sp. indet. occur in the greenish-gray mudstone in the upper portion.

Microfossils: The bedded limestone in the lower part of the formation contains abundant microfossils as follows: conodonts–*Novispathodus* ex gr. *waageni*, *Ns*. *dieneri*, *Ns. novaehollandiae*, *Ns*. *posterolongatus*, *Ns*. *spitiensis*, *Discretella discreta*, *D*. *robustus*, *Guangxidella bransoni,* and *Smithodus longiusculus*, gastropods–*Worhtenia*? sp. indet., *Anomphalus*? sp. indet., *Atorcula* sp. indet. and *Naticopsis* sp. indet. A and B.

In the middle part of the formation, the dark gray thin-bedded limestone and calcareous nodules contain the following fossils: conodonts–*Novispathodus* ex gr. *waageni*, *Nv*. *pingdingshanensis* (Zhao and Orchard, 2007), *Nv*. sp. nov. A Goudemand and Orchard, 2012, and *Icriospathodus*? *zaksi* (Buryi, 1979), abundant radiolarians–*Multisphaera triassorobusta* Takahashi, sp. nov., *Retentactinia*? *kycungensis* Takahashi, sp. nov., *R*. *parvisphaera* Takahashi, sp. nov., *Plenoentactinia*? *terespongia* Takahashi, sp. nov., *Spongentactinia*? sp. indet., *Pentactinocarpus*? aff. *acanthicus* Dumitrica, 1978, *Triassothamnus verticillatus* (Dumitrica, 1978), *Tandarnia recoarensis* Dumitrica, 1982 and *Paroertlispongus spinorientalis* Takahashi, sp. nov., gastropod–*Anomphalus*? sp. indet.

In the upper part of the formation, the thin bedded limestone and thin layered shell concentrations contain conodonts as follows: abundant *Novispathodus triangularis* (Bender, 1970), *Triassospathodus homeri* (Bender, 1970), *T*. *symmetricus* (Orchard, 1995), *Icriospathodus collinsoni* (Solien, 1979), and rare *I*.? *crassatus* (Orchard, 1995) and *Nv*. *pingdingshanensis*.

Na Trang area

Exposures: Five sections, NT01–05 around Na Trang Village, in Lang Son City (Figs. 3, 5, 20–22)

Thickness: 50 m (Figs. 5, 21).

Lithology: The lower part of the formation (20–26 m thick, NT01–04) consists of thick greenish gray mudstone, limestone breccias and thin bedded limestone. The 0.2–4 m thick limestone breccias, characterized by structureless clast- or matrix supported textures, exhibit typical channel-like bodies. The middle part (6 m thick) is dominated by organic-rich dark gray thin-bedded limestone, mudstone and sandstone. Organic-rich dark gray calcareous nodules are abundant in the dark gray mudstone. These dark gray carbonates yield abundant radiolarians, and commonly contain monospecific ammonoids and bivalves. The sandstone is characterized by normal and inverse-grading, cross- and convolute-laminations. The upper part of the formation (18 m thick) is composed of thick greenish gray mudstone overlain by 3 m thick alternations of sandstone and mudstone (Fig. 22). The thick mudstone portion is commonly intercalated with thin shelly sandstone layers. The sandstone/mudstone alternations contain climbing ripples, parallel- and convolute-laminations. At NT05 the upper part is intercalated with limestone breccias and thin bedded limestone.

Megafossils: Fossils have not been found in the lower part of the formation, but the following megafossils have been collected from the organic-rich dark gray carbonates in the middle part: ammonoid–*Xenoceltites variocostatus*, nautiloid–*Trematoceras* sp. indet., and bivalves–abundant *Crittendenia australasiatica*, rare *Crittendenia langsonensis*, and a fragment of *Leptochondria bittneri*. The greenish-gray mudstone in the upper part contains the following ammonoids: *Tirolites* sp. nov., *Columbites* sp. indet. and *Eodanubites*? sp. indet., noutiloid–*Trematoceras* sp. indet., and the bivalves–*Crittendenia australasiatica*, *Leptochondria bittneri*, "*Pseudomonotis*" *himaica* and *Bositra* sp. indet.

Microfossils: In the middle part of the formation, the organic-rich dark gray thin-bedded

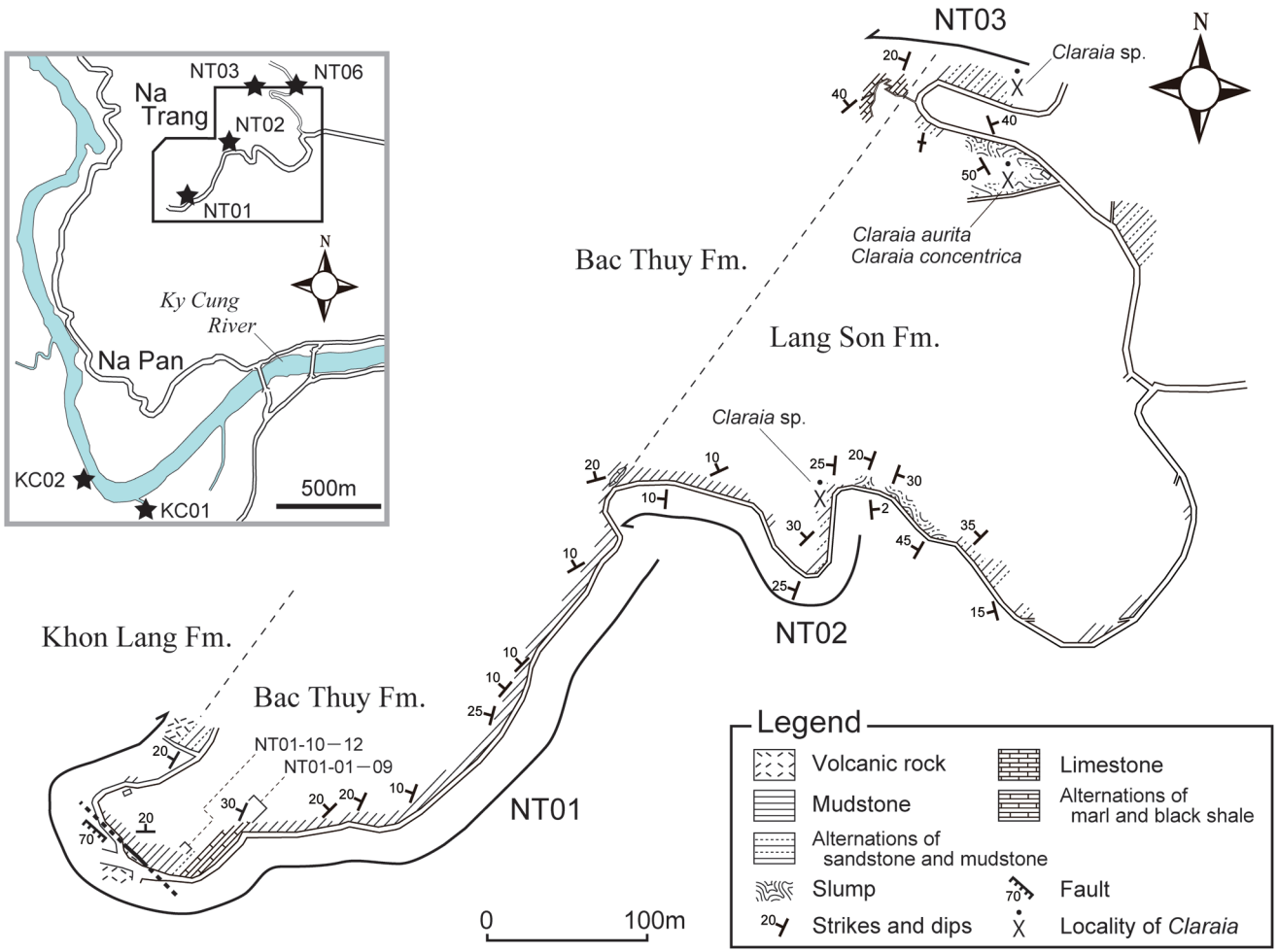

Fig. 20. Route map in the Na Trang area (NT01, 02, 03). The upper part of the Lang Son, Bac Thuy and Khon Lang formations are widely distributed in the area. The alternating organic-rich dark gray bedded limestone and mudstone contains abundant bivalves, ammonoids and radiolarians (NT01-01–09). The Spathian ammonoids, *Tirolites* and *Columbites*, are commonly found in thin turbidite layers (NT01-10, NT01-11).

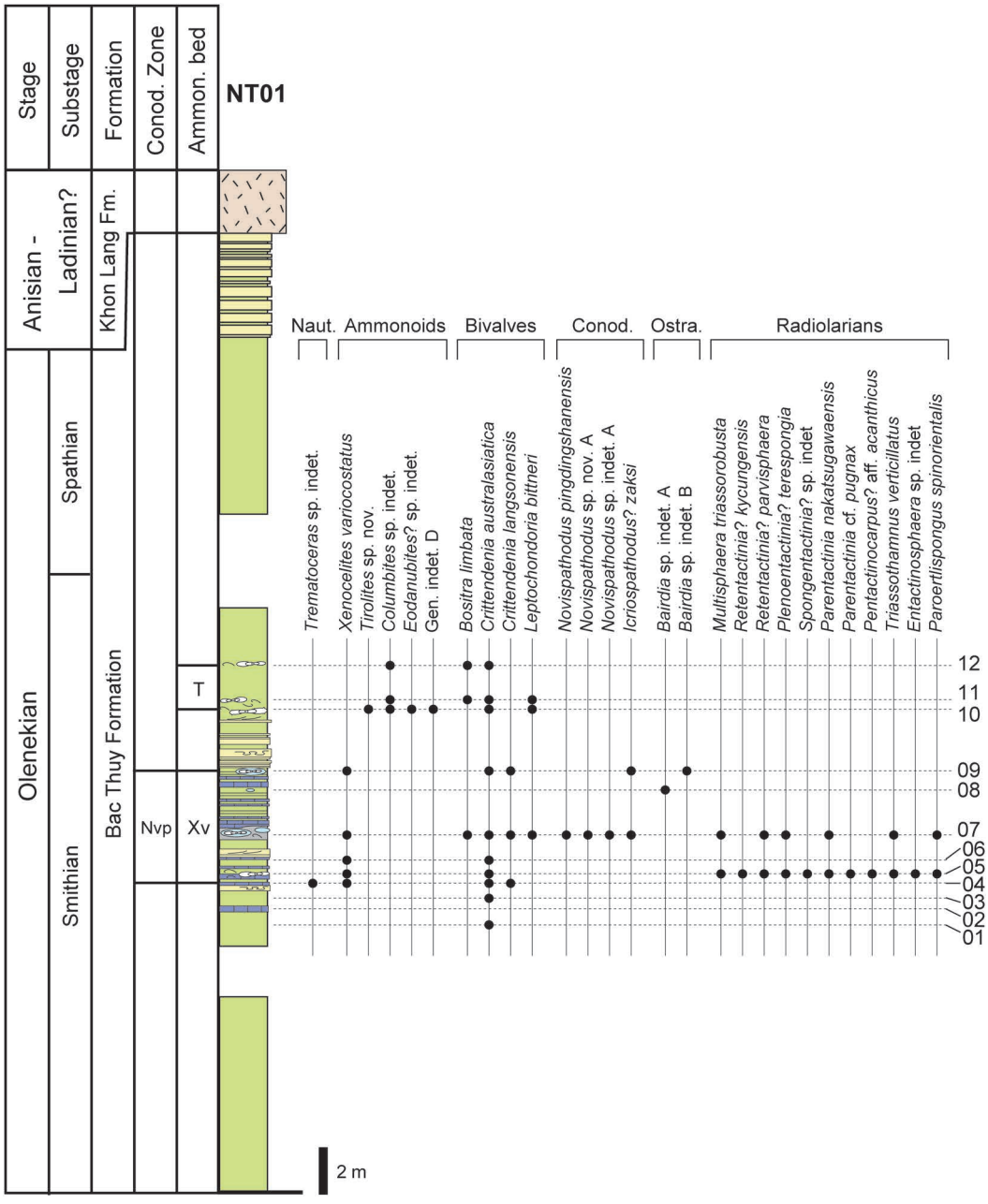

Fig. 21. Distribution of nautiloid, ammonoid, gastropod, bivalve, conodont, ostracoda and radiolarian taxa in NT01. Legend is shown in Fig. 5. Nvp: *Novispathodus pingdingshanensis* Zone, Xv: *Xenoceltites variocostatus* beds, T: *Tirolites* sp. nov. beds.

Fig. 22. Exposures of the upper part of the Bac Thuy Formation in NT01. 1, Hemipelagic mudstone intercalated with turbidite layers that contain abundant ammonoids and bivalves. 2. Outcrop showing unconformity between the Bac Thuy Formation consisting mainly of concentrated density flow to turbidity flow deposits and overlaying volcanic rocks of the Khon Lang Formation in NT01.

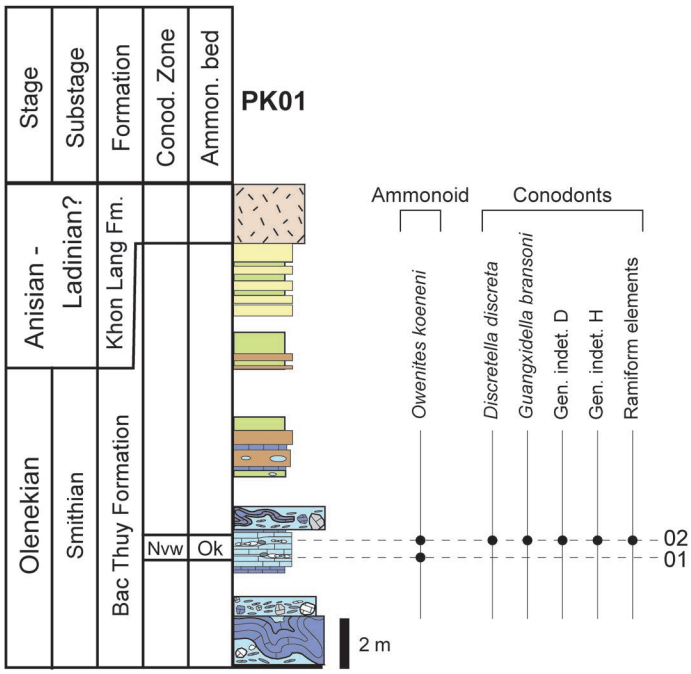

Fig. 23. Distribution of ammonoid and conodont taxa in PK01. Legend is shown in Fig. 5. Nvw: *Novispathodus* ex gr. *waageni* Zone, Ok: *Owenites koeneni* beds.

limestone contains rare conodonts–*Novispathodus pingdingshanensis*, *Novispathodus* sp. nov. A, and *Icriospathodus*? *zaksi*, abundant radiolarians–*Retentactinia*? *kycungensis* Takahashi, sp. nov., *Parentactinia nakatsugawaensis* Sashida, 1983, *P*. cf. *pugnax* Bumitrica, 1978, and *Paroertlispongus spinorientalis* Takahashi, sp. nov., and ostracods–two species of *Bairdia*.

Pac Khanh area

Exposures: One section, PK01, in Chi Lang District (Figs. 3, 5, 23, 24)

Thickness: Greater than 14 m (Figs. 5, 23).

Lithology: The lower part of the formation, which is poorly exposed in this area, consists mainly of limestone breccia, bedded limestone with abundant ammonoid shells, and greenish gray mudstone (Figs. 24). Ammonoid composition and mode of occurrence in the bedded limestone are quite similar to those of the ammonoids in the lower part of the Bac Thuy section stratotype. The middle part of the formation (2 m thick) is characterized by sandstone and dark gray mudstone containing organic-rich calcareous nodules. The upper part of the formation in the Pac Khanh section is distinguished by alternating sandstone and mudstone whose lithology resembles that of the uppermost Na Trang (NT01) and Ky Cung River (KC02) sections.

Megafossils: Because of the difficulty encountered in collecting macrofossils from the unusually hard limestone breccias and bedded limestone, only the ammonoid *Owenites koeneni* is recognized in the lower part of the formation. Megafossils have not been found in the middle and upper parts of the formation.

Microfossils: The conodonts, *Discretella discreta* and *Guangxidella bransoni* occur commonly in the bedded limestone in the lower part of the formation.

Fig. 24. Fossiliferous bedded limestone containing abundant ammonoids in the Bac Thuy Formation in PK01.

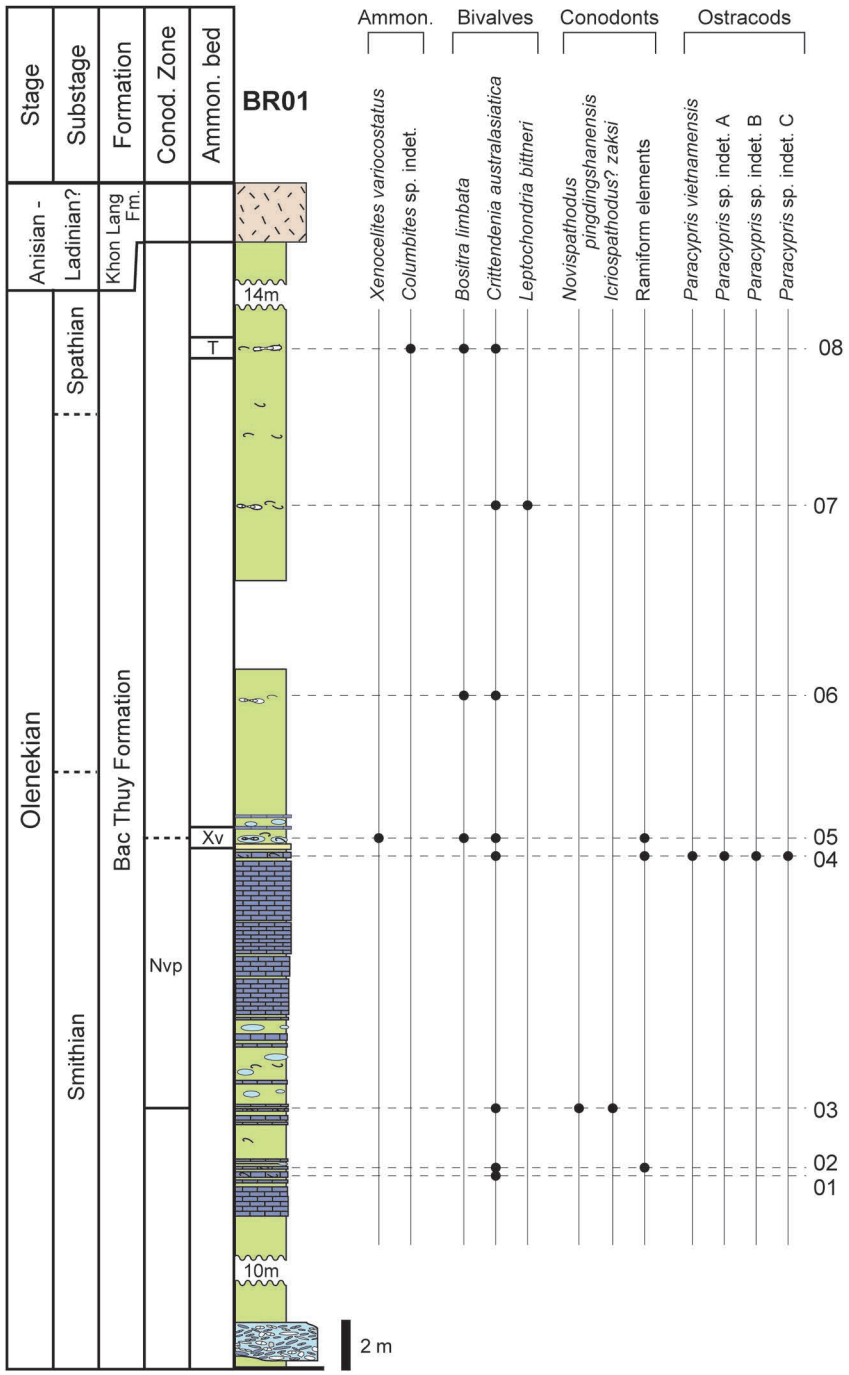

Fig. 25. Distribution of ammonoid, bivalve, conodont, and ostracoda taxa in BR01. Legend is shown in Fig. 5. Nvp: *Novispathodus pingdingshanensis* Zone, Xv: *Xenoceltites variocostatus* beds, T: *Tirolites* sp. nov. beds.

Ban Ru area

Exposures: One section, BR01, in Chi Lang District (Figs. 3, 5, 25)

Thickness: Greater than 185 m by Dang (2006). However, the lower part of the section was not closely examined (Figs. 5, 25).

Lithology: The lower part of the formation is composed mainly of mudstone, limestone breccias and bedded limestone, while the middle part of the formation (13 m thick) consists predominately of dark gray organic-rich thin-bedded limestone and mudstone containing dark gray calcareous nodules that commonly yield ostracods and bivalves. Lithologically, the middle part of the Ban Ru section closely resembles the middle parts of the Na Trang (NT01) and Ky Cung (KC02) sections. The upper part of the section (30 m thick), dominated by thick greenish gray mudstone, is lithologically similar to the upper parts of the Bac Thuy (BT02) and Na Trang (NT01) sections. Taken together, the thickness of the middle and upper parts of the Ban Ru (BR01) section exceeds 40 m, which is much thicker than the same intervals in the other section.

Megafossils: Megafossils have not been found in the lower part of the formation, but the ammonoid *Xenoceltites variocostatus* and bivalve *Crittendenia australasiatica* are quite common in the middle part. The upper part of the formation yields rare specimens of the ammonoid *Columbites* sp. indet., and bivalves *Crittendenia australasiatica*, *Bositra limbata* and "*Pseudomonotis*" *himaica*.

Microfossils: The organic-rich dark gray thim-bedded limestone in the middle part of the formation yields rare conodonts including *Novispathodus pingdingshanensis*, *Icriospathodus*? *zaksi*, as well as fragments of conodont elements. Also found are abundant ostracods, *Paracypris vietnamensis* Tanaka and Komatsu sp. nov. and *Paracypris* sp. A. Microfossils have not been found in the lower and upper parts of the formation.

Depositional environments of the Bac Thuy Formation

(by T. Komatsu, T. Maekawa, Y. Shigeta, H. T. Dang and P. D. Nguyen)

Depositional environments of the Triassic systems in the An Chau basin have been documented by Komatsu and Dang (2007), Komatsu *et al*. (2010) and Komatsu *et al*. (2014). The Olenekian stage in this basin, consisting of the upper part of the Lang Son and Bac Thuy formations, is composed of mixed carbonate and siliciclastic shallow marine to marginal basin deposits (Fig. 26). Dominated by siliciclastic facies, the upper part of Lang Son Formation is composed mainly of storm and wave-influenced shallow marine deposits, characterized by wave ripples and hummocky cross-stratification as well as slope deposits (Komatsu and Dang, 2007; Komatsu *et al.*, 2014). According to Komatsu *et al*. (2014), the Bac Thuy Formation consists of a tidal flat, wave-influenced carbonate platform, and slope and marginal basin plain deposits (Fig. 26). The lower part of Bac Thuy Formation is locally intercalated with tidal deposits and wave-influenced shallow marine carbonates at KC01 (Figs. 27–31). The tidal flat deposits are composed mainly of lenticular and wavy bedding with thin flat-bedded carbonates containing desiccation cracks (Fig. 27). Current ripples in the lenticular and wavy bedding exhibit bi-directional paleocurrents. These tidal deposits are intercalated with cross-stratified limestone characterized by tidal bundle carbonates containing mud drapes. The tidal bundles may have accumulated in response to migration of sand bars formed by tidal currents in intertidal to subtidal zones (Dalrymple, 1992, 2010). Desiccation cracks containing tepee structures are generally formed on the supratidal and upper intertidal zones in arid to semiarid environments (Wright 1990; Wright and Burchette, 1996; Pratt, 2010). The subtidal carbonates yield poorly preserved bivalves, ammonoids and conodonts (Figs. 28, 30, 31).

The shallow marine carbonates contain wave-ripples, low-angle cross-stratification (hummocky cross-stratification?, Fig. 29), ooids and abundant typical marine mollusks and microfossils (Figs. 29–31). The Smithian conodont, *Novispathodus waageni* (=*Neospathodus waageni*), is common in the shallow marine carbonates (Fig. 12). Marine molluscan fossil assemblages are characterized by abundant small bivalves and Smithian ammonoids such as *Owenites koeneni*. These thin bivalve shells typically show an edgewise arrangement (i.e., flat shells arranged perpendicular to the bedding, Kidwell *et al*., 1986) generated by strong wave currents (Fig. 31). Cyclic tidal deposits and wave-influenced shallow marine carbonates consist of typical retrogradational parasequence sets suggesting transgressive sequences (Komatsu *et al*., 2014). These tidal and wave influenced deposits were probably accumulated in a typical shallow marine environment on an isolated carbonate platform.

Slope and marginal basin-plain deposits, dominant in the upper part of Bac Thuy Formation, are widely distributed in Lang Son Province (BT02, KC02, NT01–05, PK01, BR01, in Figs. 32–35). These slope deposits are characterized by limestone breccias, high-density turbidites, slump beds and hemi-pelagic mudstone and limestone (Komatsu *et al*., 2014). Abundant concentrations of ammonoid shells, associated with limestone breccias or slump beds, are embedded in slope deposits (BT01–03, PK01).

Marginal basin-plain deposits consist of typical turbidite beds, minor limestone breccias and thick hemipelagic mudstone containing marl layers. These marl layers yield the Spathian ammonoids *Tirolites* and *Columbites*, the bivalve *Leptochondria bittneri* and conodonts *Triassospathodus* and *Icriospathodus*. The classical turbidite sets may represent frontal splay environments in the marginal basin plain. Clastics apparently were supplied from the west, hence the paleocurrent directions of the siliciclastic gravity flow deposits were approximately eastward (Komatsu *et al.*, 2014). These Olenekian carbonate and siliciclastic facies in the Bac Thuy Formation exhibit a typical transgressive succession.

The Smithian/Spathian boundary and latest Smithian anoxic to dysoxic facies, characterized by organic-rich dark gray bedded limestone and mudstone, are embedded in a succession ranging from slope to marginal basin-plain facies composed mainly of gravity flow and hemipelagic deposits (Komatsu *et al.*, 2014). The uppermost part of the organic-rich mudstone bed is intercalated with the Smithian/Spathian boundary as indicated by the first appearance of *Tilorites* cf. *cassianus* (KC02, NT01). The anoxic to dysoxic facies, composed of dark gray radiolarian and mollusk-shell bioclastic wackestone and dark gray mudstone, is characterized by rare bioturbation, small pyrite crystal aggregates and rich organic matter. The pyrite aggregates were possibly generated under anoxic sediments and/or under stagnant water conditions. The organic-rich dark gray mudstones contain weakly parallel and cross-laminations, and are intercalated with so-called high density turbidite beds characterized by massive, normal and inverse graded coarse grained calcareous sandstones (Fig. 34). Very small grazing traces (pascichnia), such as *Spirophycus* isp. and *Phycosiphon* isp. are commonly found in some layers (Fig. 29). These ichnofossil assemblages, dominated by pascichnia and characterized by low diversity and moderately high density, indicate opportunistic producers (Bromley, 1996). Ekdale and Mason (1988) proposed that pascichnia-dominated trace fossil assemblages were formed under less oxygenated conditions than domichnia-dominated assemblages, suggesting anoxic to dysoxic conditions.

The organic-rich carbonates and mudstone yield abundant low-diversity molluscan fossils and microfossils. Microfossil assemblages are mainly composed of spheroidal radiolarians

	Sedimentary environments		Lithology	Characteristic sedimentary structures, clasts, and fossils
Shallow carbonate platform	Tidal deposits	Intertidal -supratidal flat	Lenticular, wavy, and thin flat-bedded carbonates (wackestone, lime mudstone, and dolomite) and mudstone	・Current ripples and cross-lamination indicating bidirectional paleocurrents.
			Intraclastic rudstone and floatstone containing dolomite clasts (secondarily deformed or reworked deposits)	・Tepee structures and desiccation cracks. ・Imbrications and flat pebbles and cobbles containing upside-down geopetal structures.
		Subtidal -intertidal flat	Intraclastic, oolitic, and bioclastic limestone (rudstone and floatstone)	・Cross-stratification, with mud drapes and reactivation surfaces. ・Poorly preserved bivalve shells.
	Subtidal flat to wave-influenced shallow marine deposits		Alternating limestone (bioclastic, oolitic, and intraclastic floatstone and wackestone) and marl (wackestone and lime mudstone)	(Limestone) ・Normal grading and structureless. ・Abundant well-preserved marine mollusks. (Marl) ・Weak lamination.
	Transgressive lag deposits		Intraclastic limestone (rudstone)	・Normal grading and structureless. ・Poorly preserved molluscan shells.
Slope to marginal basin plain	Debris flow deposits		Limestone breccia (intraclastic floatstone and rudstone)	・Matrix- or clast-supported. ・Structurless (chaotic). ・Large intraclastic limestone clasts and slump beds.
	Concentrated density flow to turbidity flow deposits Hemipelagic siliciclastic deposits		Alternating siliciclastic sandstone and mudstone	(Sandstone) ・Normal grading, weakly parallel lamination, and climbing ripples, or structureless. (Mudstone) ・Weak parallel lamination and weak bioturbation, or structureless.
	Concentrated density flow deposits Hemipelagic calcareous deposits		Alternating limestone (bioclastic and intraclastic floatstone and rudstone) and marl (wackestone and lime mudstone)	(Limestone) ・Normally graded shell concentrations, structureless, with ammonoid imbrication. ・Abundant molluscan fossils, microfossils, and intraclastic marl clasts (rip-up clasts). (Marl) ・Weak bioturbation and structureless. ・Common molluscan fossils and microfossils.
	Turbidity flow deposits Hemipelagic siliciclastic deposits		Organic-rich dark gray limestone (wackestone) and mudstone containing marl layers	(Limestone) ・Parallel lamination and cross-lamination, or structureless. ・Common molluscan fossils, and microfossils. (Mudstone) ・Weak parallel lamination, or structureless. ・Common microfossils and calcareous nodules.
	Hemipelagic calcareous deposits		Bedded marl (wackestone and lime mudstone) containing mudstone layers	・Weak parallel lamination and weak bioturbation, or structureless. ・Common microfossils and rare bivalves.
	Hemipelagic siliciclastic deposits Turbidity flow deposits		Thick mudstone intercalated by sandstone and wackestone layers	(Mudstone) ・Weak parallel lamination and weak bioturbation, or structureless. (Sandstone) ・Cross-lamination and current ripple lamination.
	Slump deposits originating from hemipelagic calcareous deposits		Secondarily deformed marl beds	・Folded and deformed beds.
	Slump deposits originating from shelf deposits in the Lang Son Fm.		Secondarily deformed alternating siliciclastic sandstone and mudstone	

Fig. 26. Sedimentary facies and depositional environments. Modified from Komatsu *et al.* (2014).

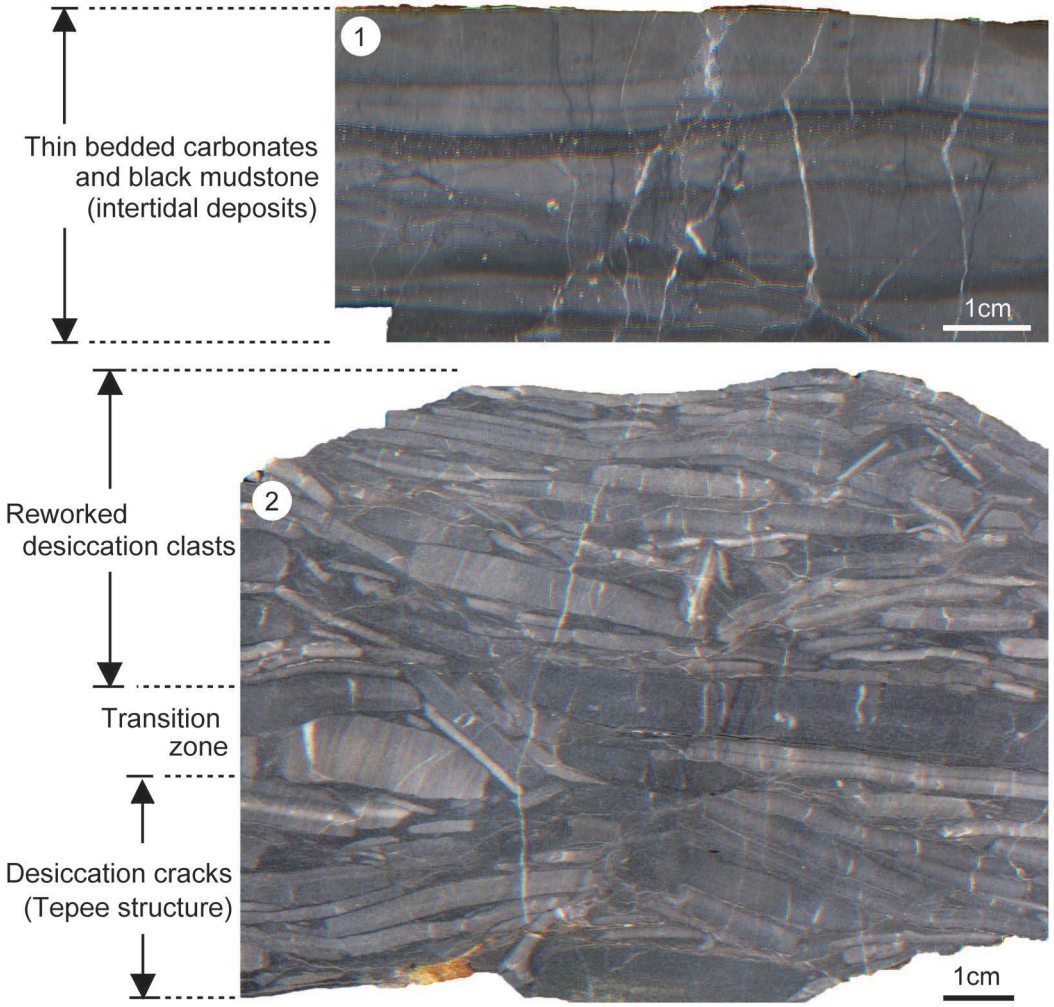

Fig. 27. Vertical cross sections of slabs from KC01. These deposits are interpreted to have accumulated in a tidal flat environment (Komatsu *et al*., 2014). 1, Alternating thin flat-bedded limestone and mudstone. 2, Intraclastic limestone containing tepee structures and desiccation cracks. Upper part of the slab is characterized by reworked desiccation clasts.

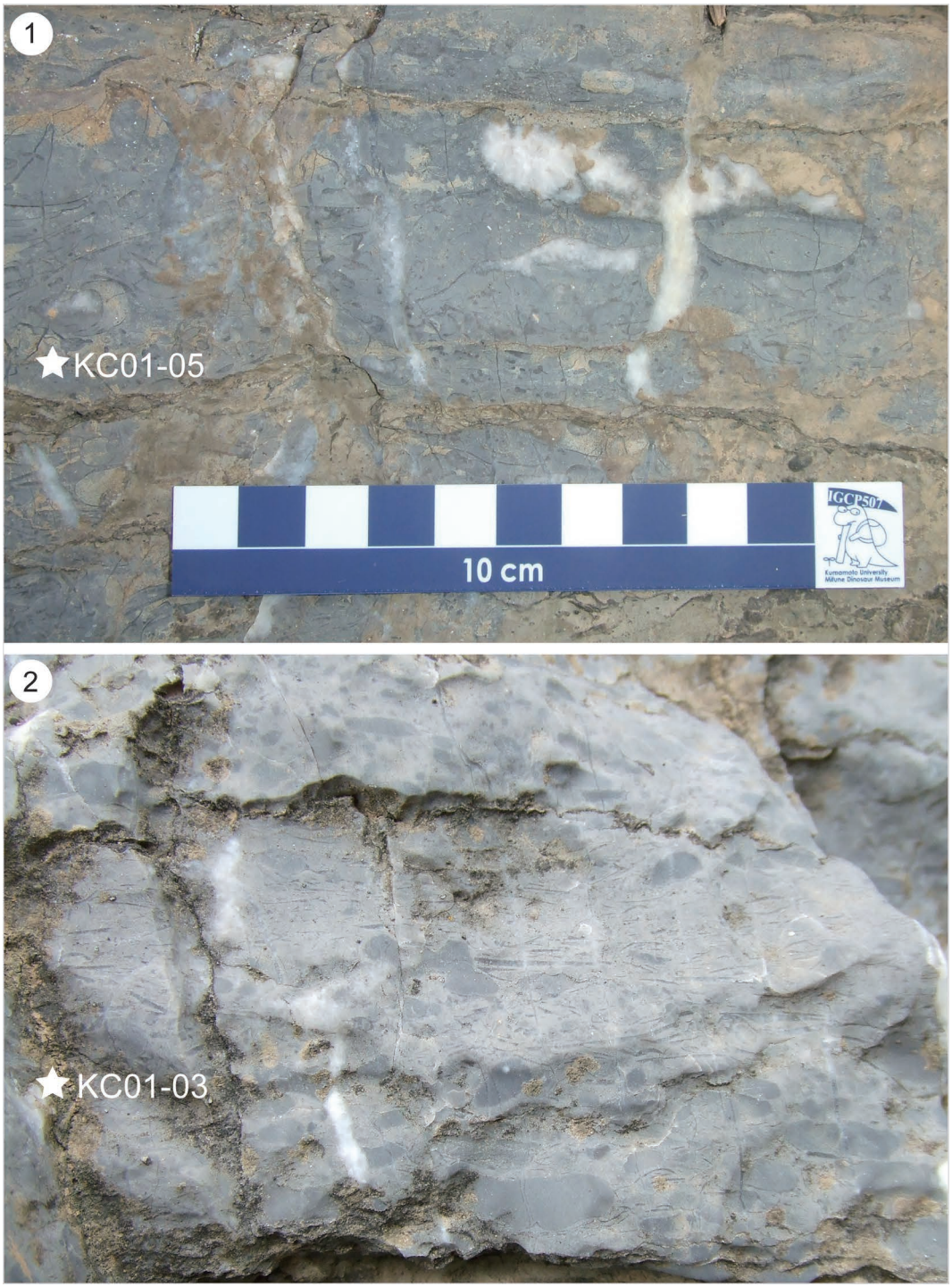

Fig. 28. Shallow marine carbonate lithofacies in KC01. 1, Bioclastic, oolitic and intraclastic limestone containing abundant thin-shelled bivalves and ammonoids at KC01-05. 2, Bioclastic, oolitic and intraclastic limestone at KC01-03.

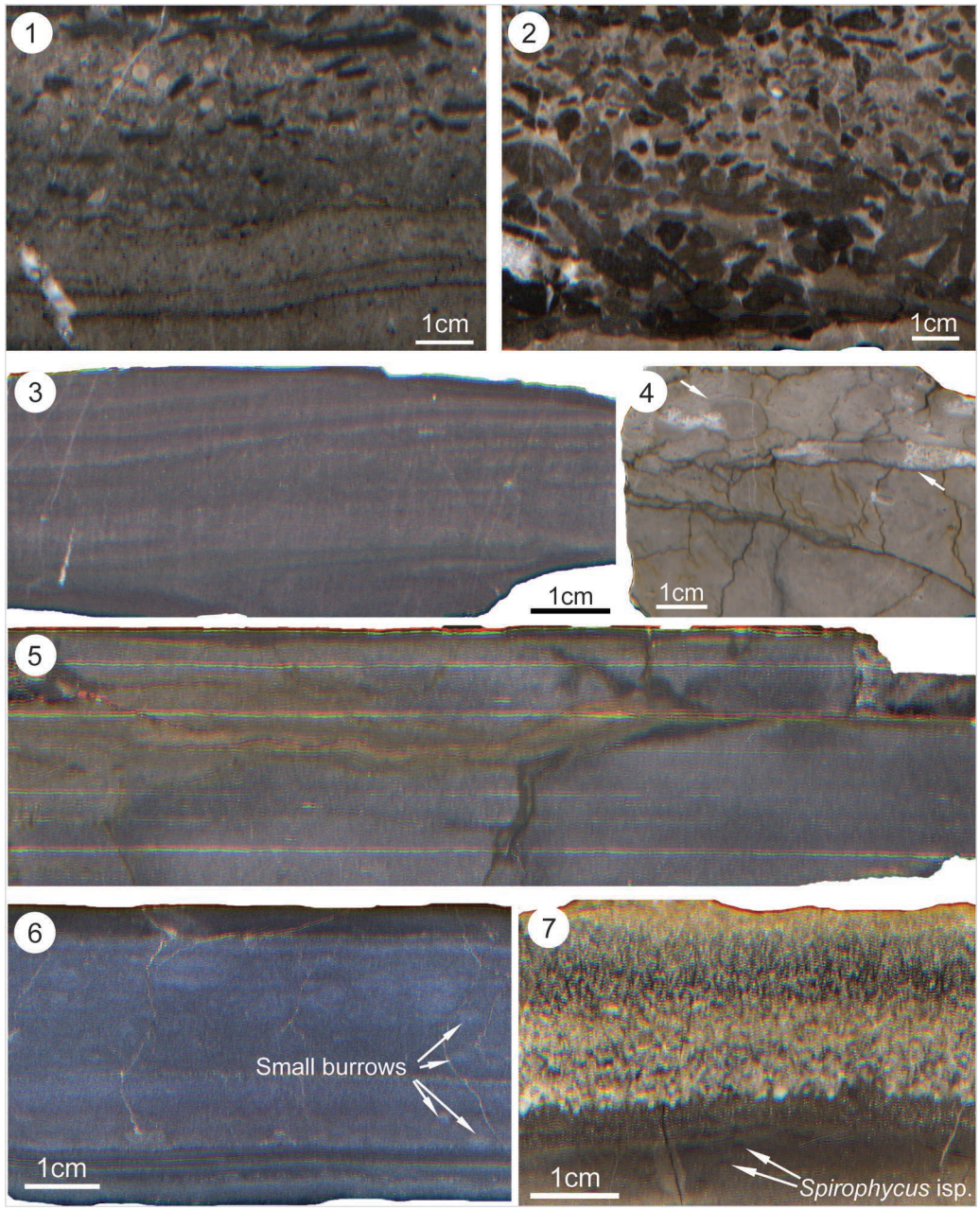

Fig. 29. 1–3, Vertical cross sections of shallow marine limestone slabs from KC01. 1, Intraclastic, oolitic, and bioclastic limestone from KC01-03. 2, Intraclastic limestone showing normal grading from KC01-09. 3, Low-angle cross-stratified limestone (hummocky cross-stratified limestone?) from KC01-05. 4, Vertical cross section of hemipelagic limestone slab from PK01. Bioclastic limestone contains ammonoid (arrows) and bivalve shells. The ammonoid shells show geopetal structures. 5, Laminated organic-rich dark gray mudstone from NT01. 6, Laminated organic-rich dark gray limestone containing small burrows in KC02 overlying well-laminated organic-rich black lime mudstone. 7, Calcareous sandstone showing normal grading and weakly bioturbated organic-rich, black lime mudstone containing tiny ichnofossils, *Spirophycus* isp. in NT01.

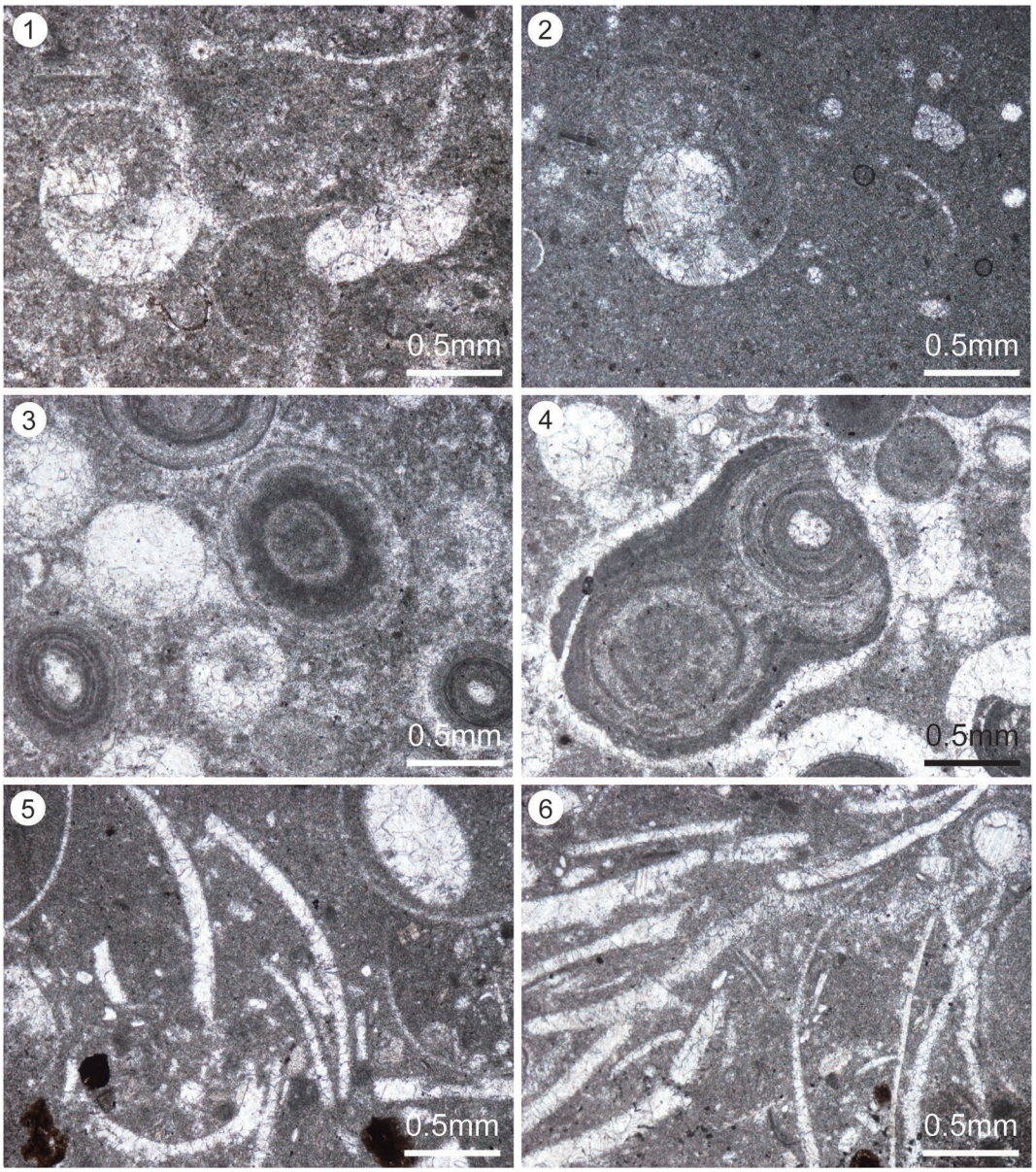

Fig. 30. Photomicrographs of vertical thin sections. 1–2, Bioclastic limestone containing juvenile ammonoids from KC01-03. 3–4, Oolitic limestone from KC01-08. 5–6, Bioclastic limestone containing fragmental and disarticulated thin-shelled bivalves from KC01-08. Thin-shelled bivalves are arranged edgewise and perpendicular to the bedding, which indicates formation by strong wave currents.

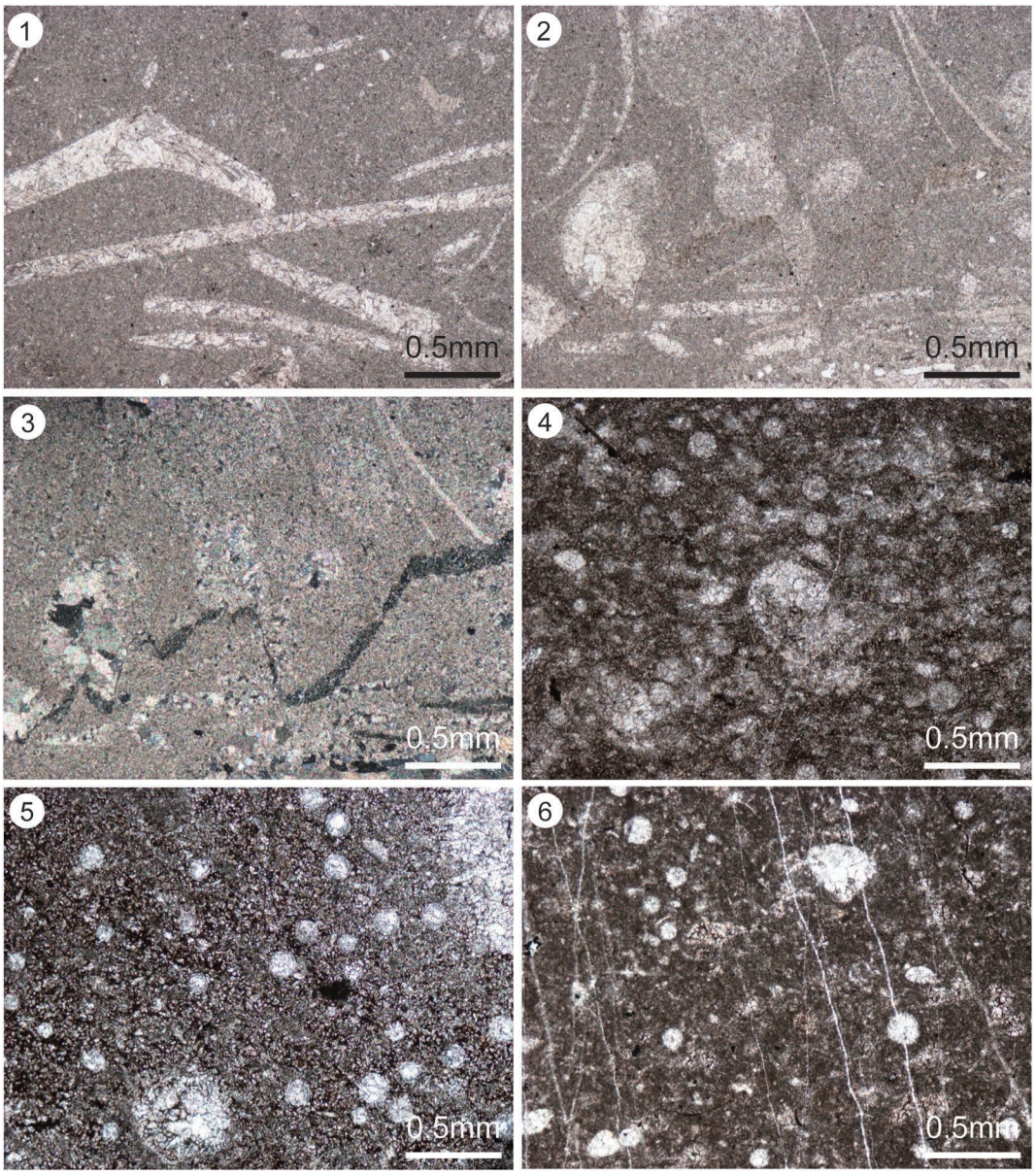

Fig. 31. Photomicrographs of vertical thin sections. 1–2, Bioclastic limestone containing thin-shelled bivalves and juvenile ammonoids from BT01-14. 3, Sutured stylolites commonly found in hemipelagic limestone from KC01-14. 4, Organic-rich dark gray calcareous nodule containing abundant spheroidal radiolarians from NT01-07. 5, Organic-rich dark gray limestone containing abundant spheroidal radiolarians from KC02-10. 6, Organic-rich dark gray calcareous nodule containing abundant spheroidal radiolarians and ostracods from BR01-05.

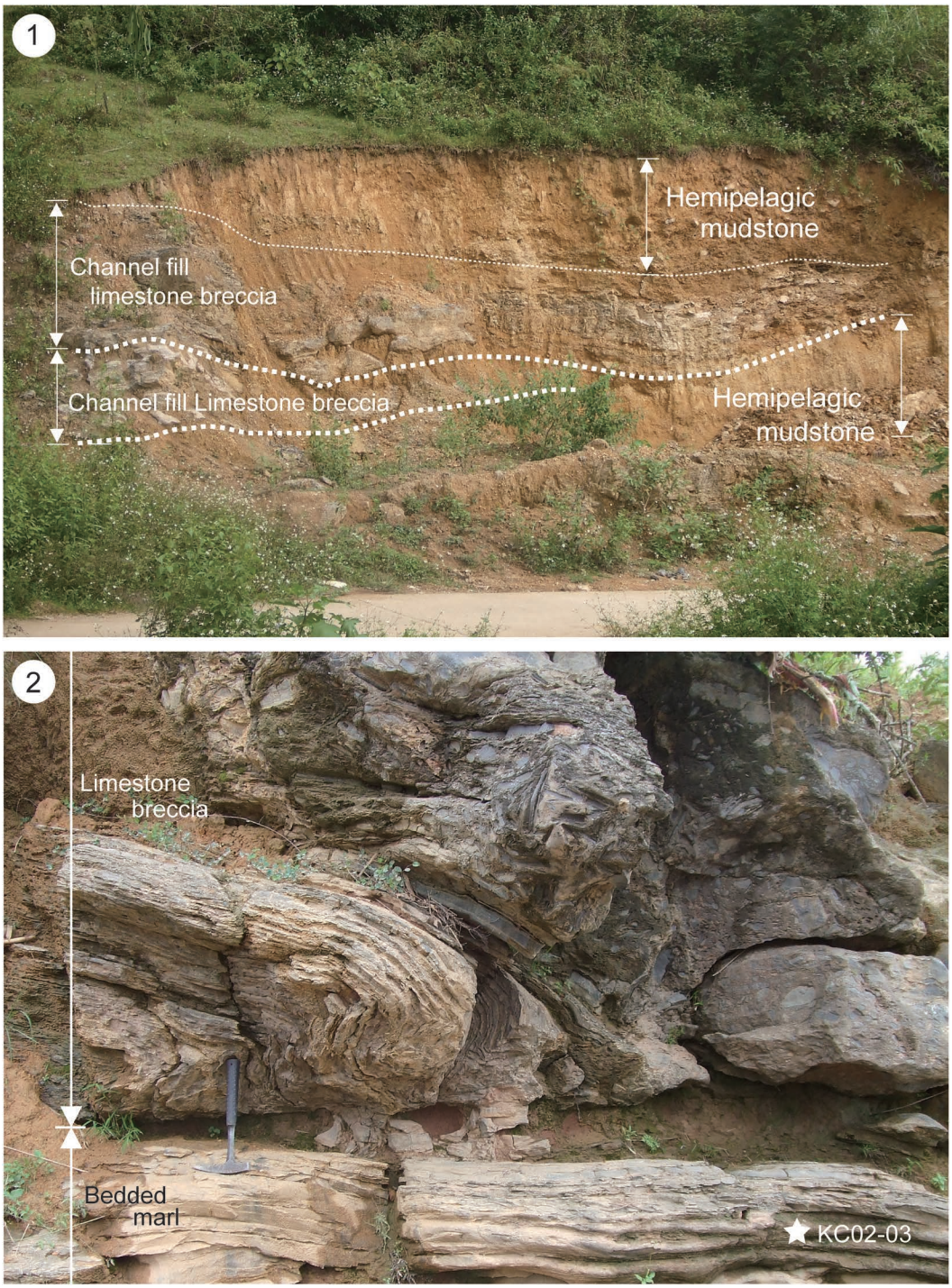

Fig. 32. Lithofacies of slope deposits. 1, Exposures of isolated channel-filling limestone breccias in hemipelagic mudstone in NT02. 2, Limestone breccia containing slump beds and overlying thin-bedded marl at KC02-03.

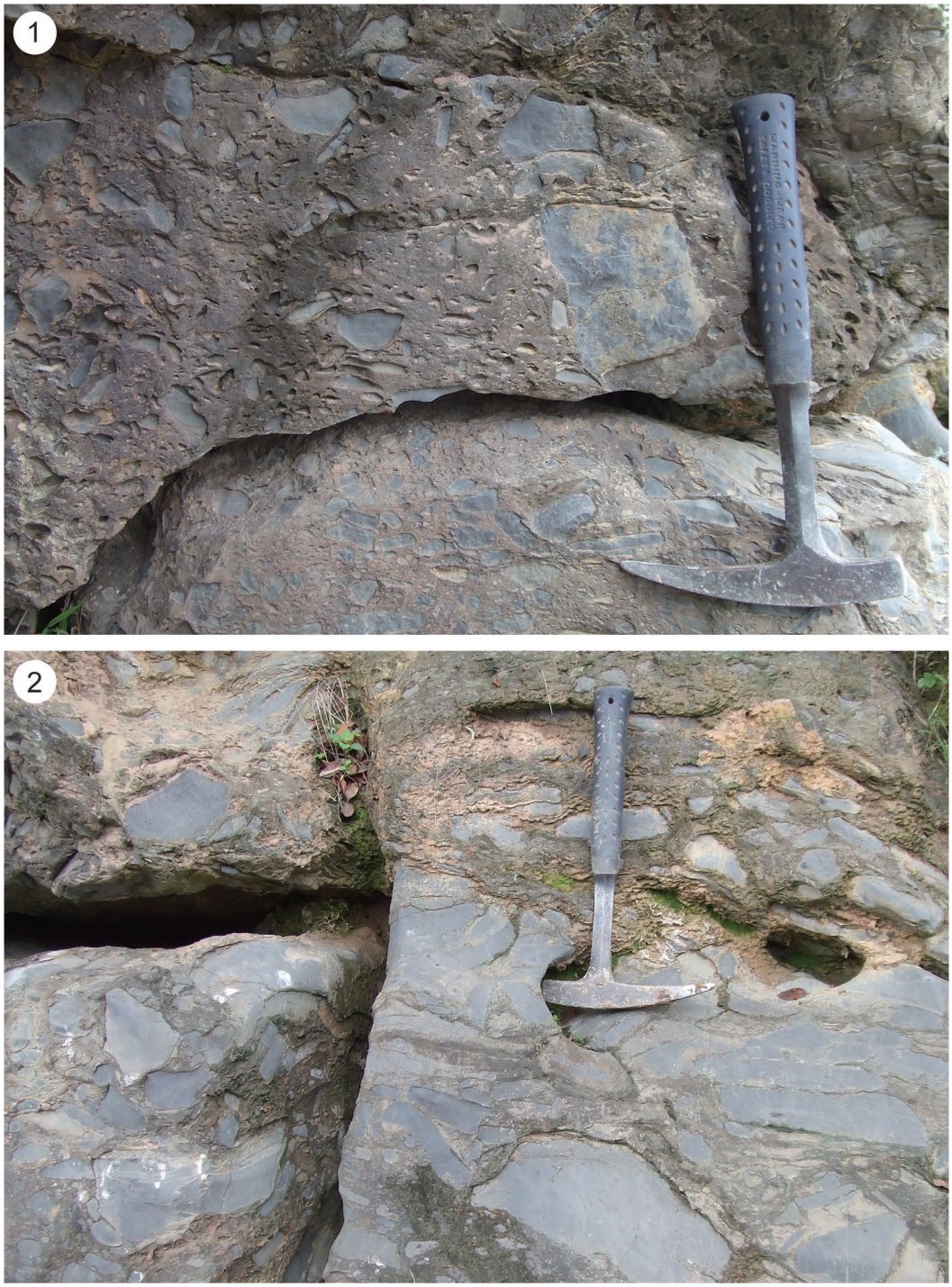

Fig. 33. Lithofacies of slope deposits in KC02. 1, Limestone breccia characterized by matrix- and clast-supports. 2, Clast-supported limestone breccia containing pebble and cobble intraclasts.

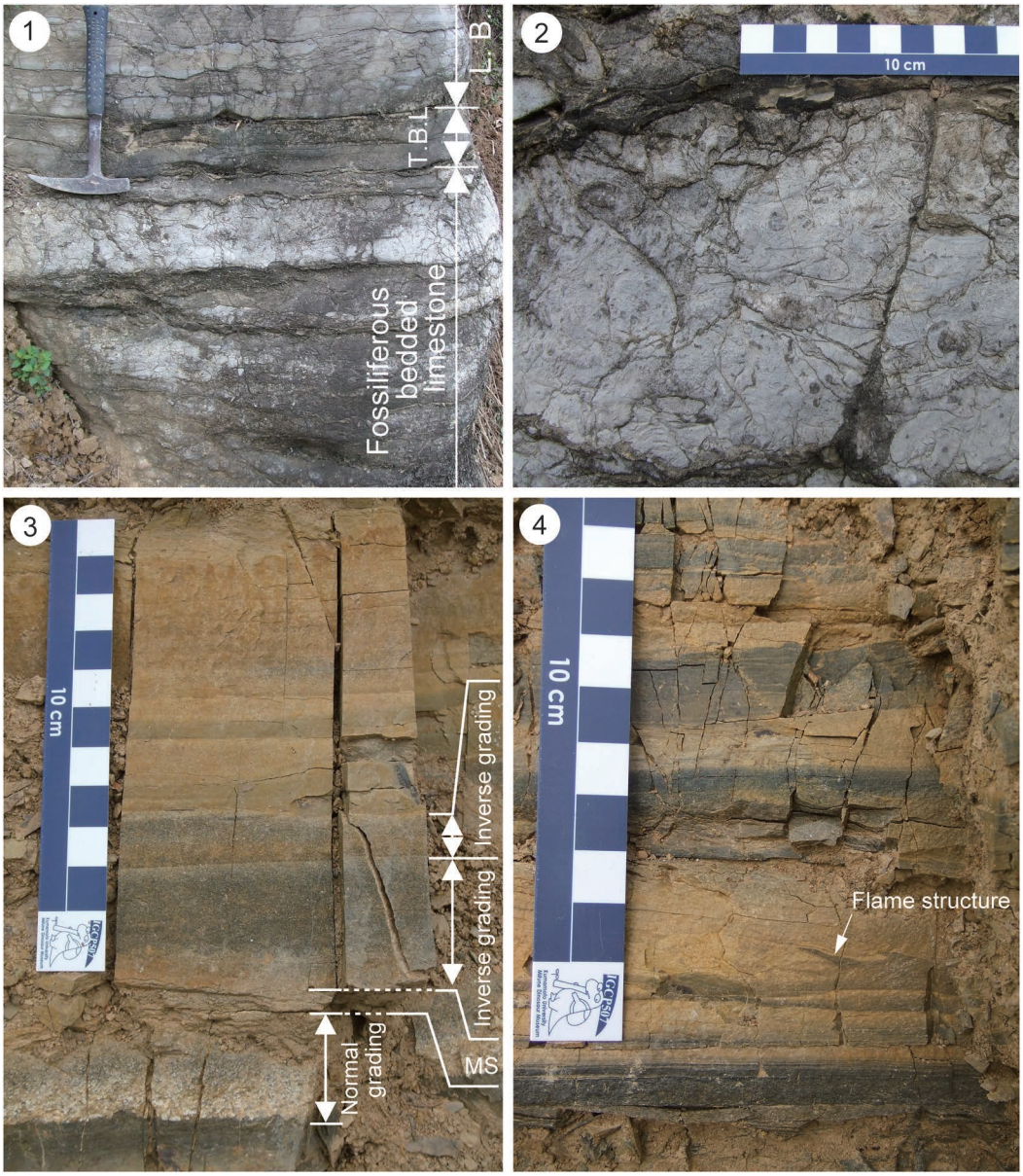

Fig. 34. 1–2, Fossiliferous bedded limestone in PK01. 1, Fossiliferous bedded limestone overlain by thin-bedded limestone (T. B. L) and limestone breccia (L. B.). 2, Fossiliferous bedded limestone containing abundant ammonoids (e.g. *Owenites koeneni*) at PK01-02. 3–4, Exposures of gravity flow deposits in NT01. 3, Gravelly and very coarse calcareous sandstone displaying normal and inverse grading. 4, Convolute- and parallel laminated calcareous sandstone and mudstone. The basal part of the calcareous sandstone occasionally contains flame structures.

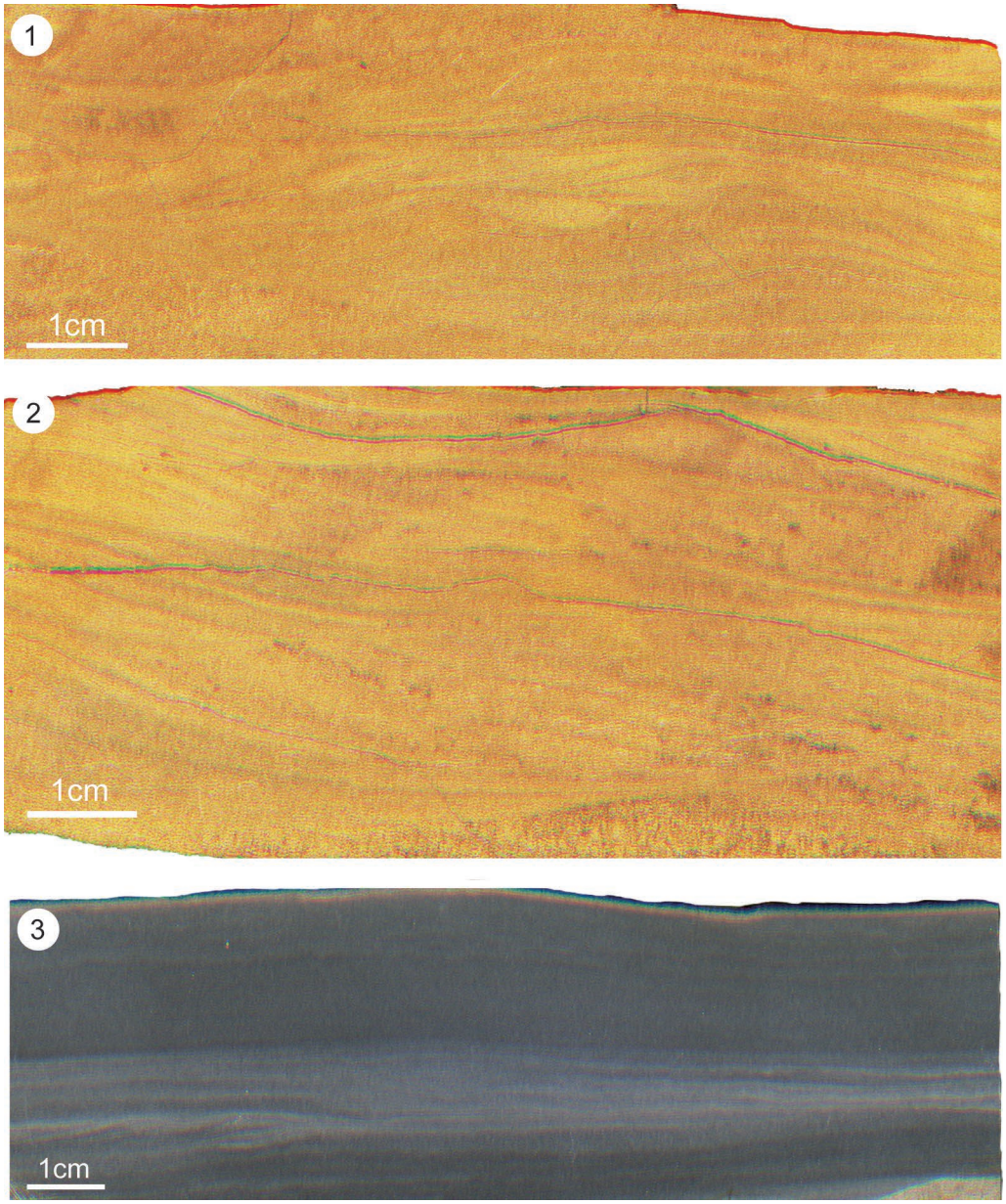

Fig. 35. Vertical cross sections of sandstone in the upper part of the Bac Thuy Formation. 1–2, Very fine siliciclastic sandstone contains climbing-ripple lamination from NT01. 3, Thin calcareous turbidite characterized by Tc and Td divisions is embedded in thick hemipelagic mudstone at KC02-15.

and poorly ornamented ostracods (Fig. 31). Komatsu *et al*. (2011, 2013) reported a monospecific ammonoid assemblage composed of *Xenoceltites variocostatus* and a thin-shelled epifaunal bivalve assemblage consisting mainly of *Crittendenia australasiatica* from this facies. In the Ban Ru area, a low diversity ostracod assemblage from the organic-rich dark gray bedded limestone is composed of several species of *Paracypris* of which *Paracypris vietnamensis* and *Paracypris* sp. A are abundant. A similar low diversity assemblage exists in the same lithologic unit in the Na Trang area, in which only two species of *Bairdia* are common.

Biostratigraphy

Ammonoid succession (by Y. Shigeta)

Based on carefully controlled bed-by-bed sampling, a total of five distinct Olenekian (Smithian and Spathian) ammonoid faunas are recognized in the studied area (Fig. 36). These faunas, ranging in age from the earliest Middle Smithian through the Early Spathian, represent a more or less continuous succession that can be correlated with other Tethyan sequences such as the Salt Range (Pakistan), Spiti (India), Tulong (South Tibet), Oman and South China as well as the eastern Panthalassa. Formal zones are not introduced for these assemblages because fossil occurrences are not stratigraphically continuous and our knowledge of Early Triassic ammonoid faunas in northeastern Vietnam is only in a preliminary stage. Hence, the term "beds" is used to describe each of the local faunal sequences.

Flemingites rursiradiatus *beds*: These beds, of earliest Middle Smithian age (Brayard *et al*., 2013), are well-documented from the lower part of the fossiliferous limestone beds in the basal portion of the Bac Thuy Formation in exposures at Bac Thuy (sections BT01, 02). *Flemingites rursiradiatus* as well as *Pseudaspidites muthianus, Submeekoceras hsüyüchieni* and *Jinyaceras* cf. *bellum* all co-occur in these beds. This fauna correlates with that from the *Flemingites rursiradiatus* beds in Guangxi, South China (Brayard and Bucher, 2008) and Oman (Brühwiler *et al*., 2012a), as well as the *Flemingites* beds in Spiti (Brühwiler *et al*., 2012c), *Flemingites flemingianus* beds of the Salt Range (Brühwiler *et al*., 2012b) and *Flemingites* sp. beds of Utah, USA (Brayard *et al.,* 2013).

Urdyceras tulongensis *beds*: This subdivision, which occurs in the middle part of the basal portion of the Bac Thuy Formation in exposures at Bac Thuy (sections BT01, 02), is characterized by the association of *Urdyceras tulongensis*, *Ussuria kwangsiana*, *Galfetites simplicitatis*, *Pseudaspidites muthianus*, *Submeekoceras hsüyüchieni*, *Jinyaceras* cf. *bellum*, *Paranannites sinensis* and *Aspenites acutus*.

Recently, Brühwiler *et al.* (2010) documented the occurrence of *Urdyceras tulongensis* in the *Brayardites compressus* beds (lower Middle Smithian) at Tulong, South Tibet, and since an equivalent fauna is not known from South China, Brühwiler *et al*. (2010, 2012c) pointed out that the *Brayardites compressus* beds can probably be correlated with an interval between the *Flemingites rursiradiatus* beds and the *Owenites koeneni* beds of South China. Although *Brayardites compressus* Brühwiler *et al*., 2010 has not yet been found in northeastern Vietnam, the occurrence of *U. tulongensis* supports the suggestion of Brühwiler *et al*. (2010, 2012c). Therefore, this subdivision is considered to be of early Middle Smithian age.

Owenites koeneni *beds*: This subdivision occurs in the upper part of the basal portion of the Bac Thuy Formation in the Bac Thuy sections (BT01, 02) and the Pac Khanh section (PK01) as well as in limestone breccia and bedded limestone in the lower portion of the Bac Thuy Formation exposed along the Ky Cung River (sections KC01, 02). These beds are mainly characterized by *Owenites koeneni* and *Dieneroceras*? *goudemandi*, but other taxa

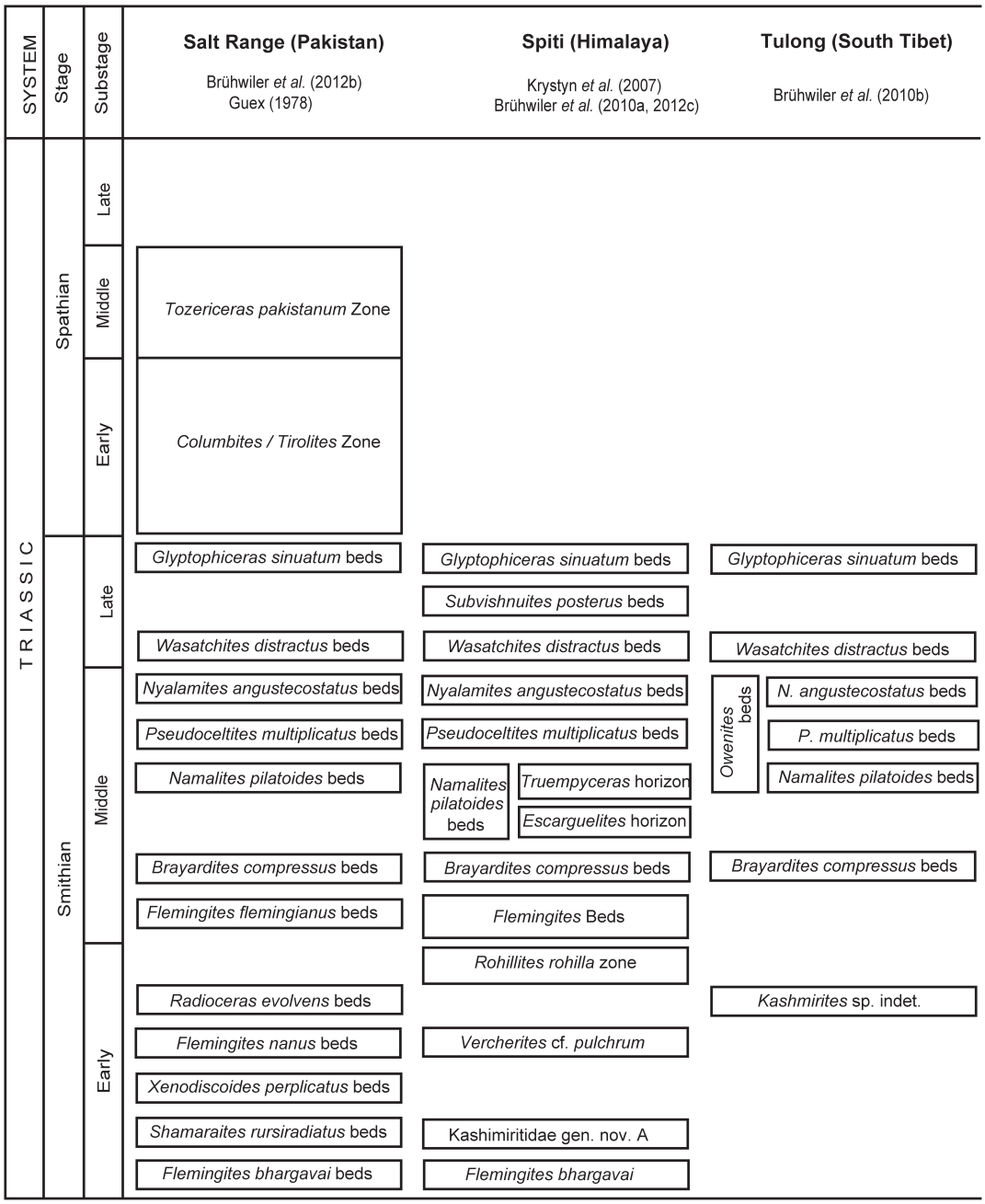

Fig. 36. Ammonoid and conodont biostratigraphic subdivision of the Lower Triassic of northeastern Vietnum and correlation with other regions. *N. p.*: *Novispathodus pingdingshanenesis*, *T. s.*: *Triassospathodus symmetricus*.

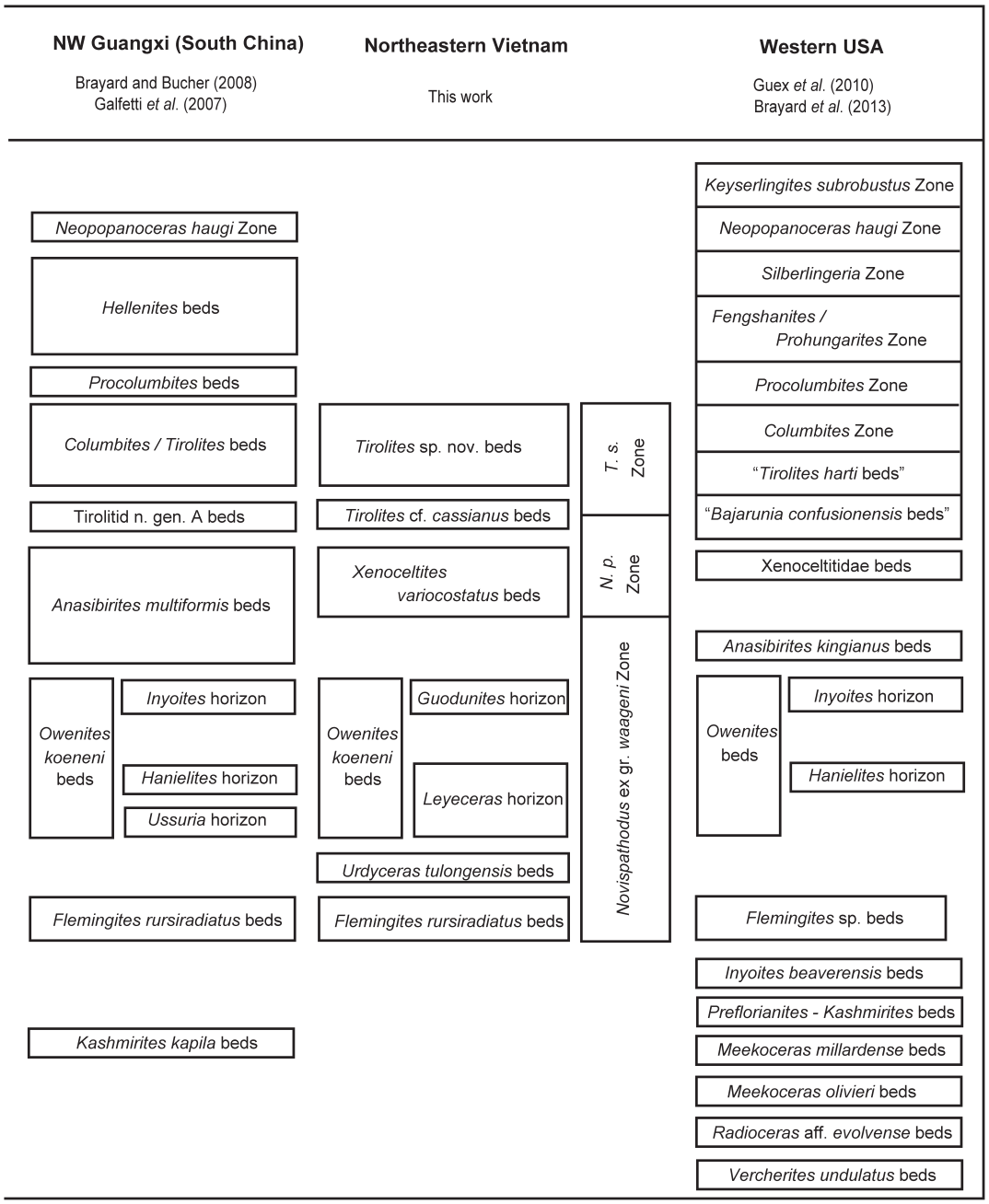
NW Guangxi (South China)
Brayard and Bucher (2008)
Galfetti et al. (2007)
Northeastern Vietnam
This work
Western USA
Guex et al. (2010)
Brayard et al. (2013)
Neopopanoceras haugi Zone
Hellenites beds
Procolumbites beds
Columbites / Tirolites beds
Tirolitid n. gen. A beds
Anasibirites multiformis beds
Owenites koeneni beds
Inyoites horizon
Hanielites horizon
Ussuria horizon
Flemingites rursiradiatus beds
Kashmirites kapila beds
Tirolites sp. nov. beds
Tirolites cf. cassianus beds
Xenoceltites variocostatus beds
Owenites koeneni beds
Guodunites horizon
Leyeceras horizon
Urdyceras tulongensis beds
Flemingites rursiradiatus beds
T. s. Zone
N. p. Zone
Novispathodus ex gr. waageni Zone
Keyserlingites subrobustus Zone
Neopopanoceras haugi Zone
Silberlingeria Zone
Fengshanites / Prohungarites Zone
Procolumbites Zone
Columbites Zone
"Tirolites harti beds"
"Bajarunia confusionensis beds"
Xenoceltitidae beds
Anasibirites kingianus beds
Owenites beds
Inyoites horizon
Hanielites horizon
Flemingites sp. beds
Inyoites beaverensis beds
Preflorianites - Kashmirites beds
Meekoceras millardense beds
Meekoceras olivieri beds
Radioceras aff. evolvense beds
Vercherites undulatus beds

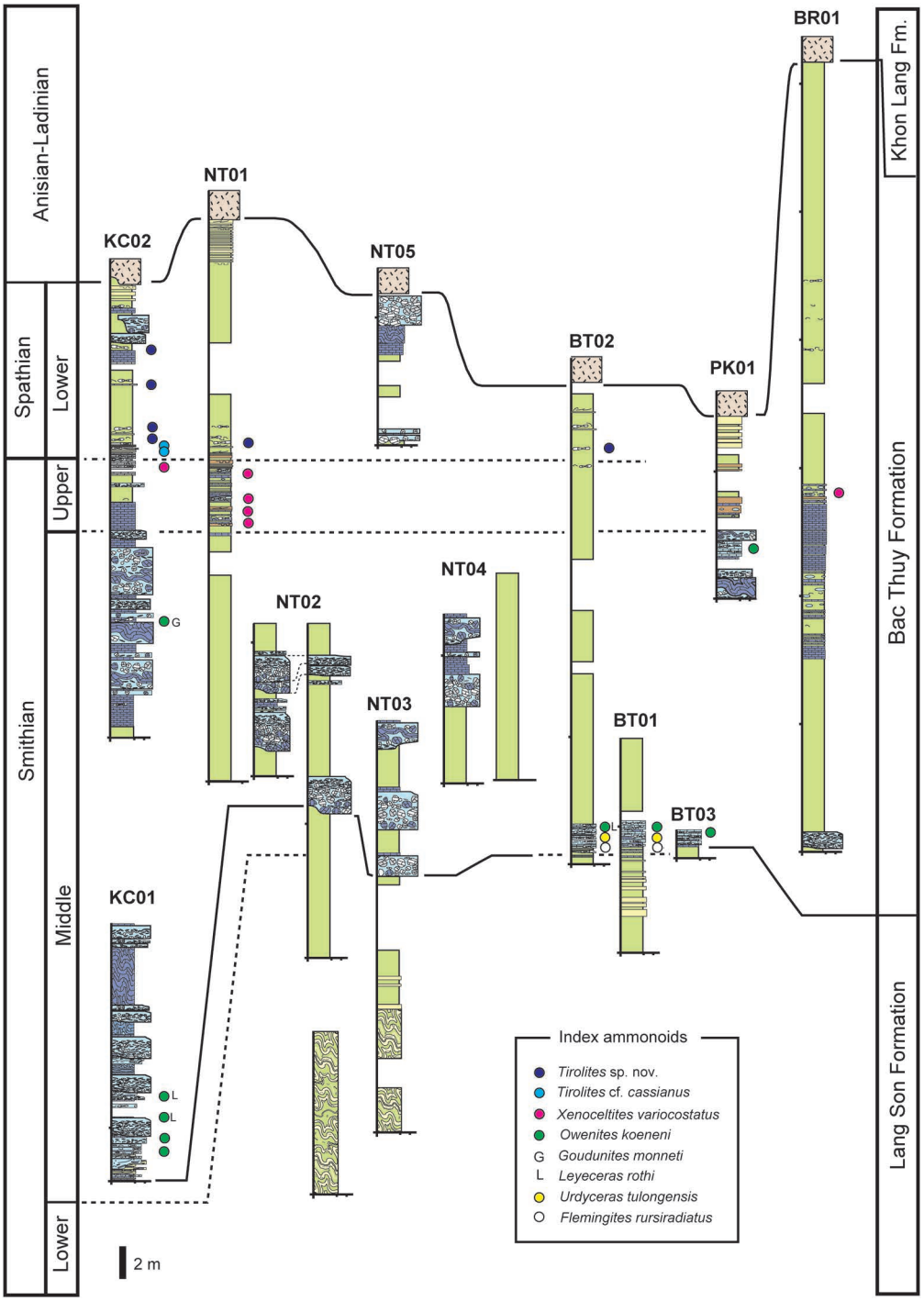

Fig. 37. Distribution of index ammonoid taxa in the Bac Thuy Formation.

are also found at two different horizons as follows: *Preflorianites radians*, *Leyeceras rothi*, *Anaflemingites hochulii*, *Juvenites sinuosus* and *Parussuria compressa* in the lower part (*Leyeceras* horizon), and *Guodunites monneti* in the upper part (*Guodunites* horizon).

In Guangxi, South China, Brayard and Bucher (2008) subdivided the Middle Smithian *Owenites koeneni* beds into three horizons in ascending order as follows: *Ussuria*, *Hanielites* and *Inyoites* horizons. The *Leyeceras* horizon, of middle Middle Smithian age, probably can be correlated with the *Ussuria* and *Hanielites* horizons as well as the *Nammalites pilatoides* beds in the Salt Range (Brühwiler *et al*., 2012b), Spiti (Brühwiler *et al*., 2012c) and Tulong (Brühwiler *et al*., 2010). The *Guodunites* horizon, of late Middle Smithian age, correlates with the *Inyoites* horizon of South China and Utah, USA (Brayard *et al*., 2013), the *Meekoceras gracilitatis* Zone in Nevada, USA (Jenks *et al*., 2010) and the *Nyalamites angustecostatus* beds in the Salt Range (Brühwiler *et al*., 2012b), Spiti (Brühwiler *et al*., 2012c) and South Tibet (Brühwiler *et al*., 2010).

Xenoceltites variocostatus *beds*: These beds, which are well-documented from the middle portion of the Bac Thuy Formation (sections NT01, KC02, BT02, BR01), are characterized by the unique occurrence of *Xenoceltites variocostatus*. This subdivision is middle to late Late Smithian in age, because *X. variocostatus* occurs in the upper part of the *Anasibilites multiformis* beds in Guangxi, South China (Brayard and Bucher, 2008), the *Glyptophiceras sinuatus* beds of South Tibet (Brühwiler *et al*., 2010) and the Salt Range (Brühwiler *et al*., 2012b) and the *Subvishnuites posterus* beds in Spiti (Brühwiler *et al*., 2012c).

Tirolites *cf.* cassianus *beds*: Of earliest Early Spathian age, these beds are well-documented in the upper portion of the Bac Thuy Formation exposed along the Ky Cung River (section KC02). Also found with *Tirolites* cf. *cassianus* are *Pseudosageceras* sp. and *Xenoceltites*? sp. *Tirolites cassianus* has long been recognized as one of the more important age-diagnostic species of the earliest Early Spathian in the Tethys (Krystyn, 1974; Posenato, 1992).

Tirolites *sp. nov. beds*: This subdivision, of Early Spathian age, occurs in the upper portion of the Bac Thuy Formation (sections NT01, KC02, BT02, BR01). Its fauna is characterized by the association of *Tirolites* sp. nov., *Columbites* sp., *Xenoceltites*? sp., *Yvesgalleticeras*? sp., *Procarnites*? sp., *Eodanubites*? sp. and *Goudemandites langsonensis* sp. nov. *Tirolites* and *Columbites* are typical age-diagnostic taxa of the Early Spathian (Kummel, 1969; Guex *et al*., 2010).

Conodont succession (by T. Maekawa and T. Komatsu)

The Lower Triassic section in the northeastern Vietnam can be divided into three conodont zones in ascending order as follows: *Novispathodus* ex gr. *waageni* Zone, *Novispathodus pingdingshanensis* Zone, and *Triassospathodus symmetricus* Zone (Fig. 36).

Novispathodus *ex gr.* waageni *Zone*: This zone begins with the first occurrence of *Novispathodus* ex gr. *waageni* and ends with the first occurrence of *Nv. pingdingshanensis*. The following taxa are associated: *Conservatella conservativa*, *C.* sp. indet. A, *Discretella discreta*, *D. robustus*, *D.* sp. indet. A through G, *Guangxidella bransoni*, *G.* sp. indet. A, *G.* sp. indet. B, *Eurygnathodus costatus*, *Neospathodus* aff. *concavus*, *Ns. cristagalli*, *Ns. dieneri*, *Ns. novaehollandiae*, *Ns. pakistanensis*, *Ns. posterolongatus*, *Ns. spitiensis*, *Ns.* sp. indet. A, *Ns.* sp. indet. B, *Ns.* sp. indet. C, *Smithodus longiusculus*, *Novispathodus pingdingshanensis*, *Hadrodontina*? sp. indet. A, and *H.*? sp. indet. B. The Zone encompasses the *Flemingites rursiradiatus*, *Urdyceras tulongensis*, *Owenites koeneni*, and part of the *Xenoceltites variocostatus* ammonoid beds in the Bac Thuy Formation. Conodonts are abundant in the in-

terval between the *Flemingites rursiradiatus* beds and *Owenites koeneni* beds, but are scarce in the *Xenoceltites variocostatus* beds.

Novispathodus waageni is a well-known species whose range covers the entire Smithian (Sweet *et al*., 1971; Orchard, 2007a). Sweet (1970b) first reported the species from the Mianwali Formation, West Pakistan and designated it as the guide species of Zone 7, which corresponds to the Smithian part of the formation. Subsequently, *Nv. waageni* has been reported from throughout the Smithian in other parts of the world (McTavish, 1973; Mosher, 1973; Goel, 1977; Buryi, 1979; Solien, 1979; Wang and Cao, 1981; Koike, 1982; Matsuda, 1983; Beyers and Orchard, 1991; Orchard, 2007b; Orchard and Krystyn, 2007; Zhao *et al*., 2007; Orchard, 2008; Beranek *et al*., 2010; Goudemand *et al*., 2012 etc.). Orchard and Krystyn (2007), Zhao *et al*. (2007) and Orchard (2010) reported that the first appearance datum of the species is an indicator of the Induan/Olenekian boundary (IOB). Furthermore, the range of the species extends to the uppermost Smithian (Orchard, 2007a; Zhao *et al*., 2007).

A significant morphological change in *Novispathodus waageni* was pointed out by Matsuda (1983), Orchard and Krystyn (2007), Zhao *et al*. (2007) and Igo (2009). Orchard and Krystyn (2007) divided the species into six morphotypes based on the form of denticles, lateral ribs, and basal cavities of abundant specimens from the Mud section, Spiti, India. According to Orchard and Krystyn (2007), the first appearance data of these morphotypes are different, and Morphotype 1 (M1), which has a prominent lateral rib, is the oldest, with a range limited to the lowermost part of the formation. M1 does not occur in the Bac Thuy Formation, which indicates that lowermost Smithian strata are not included in the formation.

Discretella discreta was first described from the Smithian ammonoid beds at Crittenden Springs, Nevada as *Ctenognathus discreta* (Müller, 1956). It has also been reported from Malaysia (Koike, 1982), South China (Duan, 1987), northeastern Vietnam (Bui, 1989), Spiti, India (Krystyn *et al*., 2007), and British Columbia (Orchard, 2008; Beranek *et al*., 2010). In particular, Krystyn *et al*. (2007) and Orchard (2007b) reported the occurrence of *D. discreta* from the *Rohillites rohilla* ammonoid Zone (=Lower Smithian) of Spiti, India, and Orchard (2008) reported that it co-occurs with the Smithian ammonoid *Euflemingites romunderi* Tozer, 1961, which indicates an Early to Middle Smithian age. Thus, *D. discreta* ranges from the Lower to the Middle Smithian, and its occurrence extends from throughout the Tethyan realm to the Panthalassan region. Hence, this world-wide species is an important indicator of Lower to Middle Smithian sediments.

Abundant specimens of *Guangxidella bransoni* occur in the middle part of the Bac Thuy Formation in association with *Conservatella conservativa* and *Discretella discreta*, and its range extends from throughout the *Urdyceras tulongensis* ammonoid beds up through the *Leyeceras* horizon of the *Owenites koeneni* ammonoid beds. *G. bransoni*, characterized by an arched element and cordiform basal cavity, has only been reported from the Panthalassan realm; Nevada (Müller, 1956), Utah (Solien, 1979), northeastern Vietnam (Bui, 1989), and South China (Zhang and Yang, 1991).

Eurygnathodus costatus is a well-known species that ranges from the Upper Dienerian to the Lower Smithian in certain parts of the world. This segminiplanate element is characteristic and its distribution is limited mainly to the Tethyan realm. However, the species has been reported from Smithian strata in British Columbia, Canada (Beyers and Orchard, 1991). In the Bac Thuy Formation, the species co-occurrs with *Flemingites rursiradiatus*, and it also coexists with flemingitid ammonoids in Spiti and South China (Orchard and Krystyn, 2007; Zhao *et al*., 2007).

Smithodus longiusculus, which has only been reported from a few worldwide locations, co-occurs with the following ammonoids and conodonts: *Arctoceras tuberculatum* (Smith, 1932) and *Furnishius triserratus* (Buryi, 1997, South Primorye); *Euflemingites romunderi* and *Neospathodus waageni* (=*Novispathodus waageni*) (Mosher, 1973, British Columbia). These taxa indicate that *S. longiusculus* ranges from the Lower to the Middle Smithian, and furthermore, its geographical occurrence is limited to the marginal region of Panthalassa.

Novispathodus pingdingshanensis *Zone*: This zone extends from the first occurrence of *Novispathodus pingdingshanenesis* to the first appearance of *Triassospathodus symmetricus*. Other co-occurring taxa include *Nv*. ex gr. *waageni*, *Nv*. sp. nov. A, *Nv*. sp. indet. A, and *Icriospathodus*? *zaksi*. The zone encompasses the *Xenoceltites variocostatus* and *Tirolites* cf. *cassianus* ammonoid beds.

Compared to the other two zones, conodonts in this zone are fewer in number and their size is smaller. Chen *et al*. (2013) reported a size reduction in conodonts around the Smithian/Spathian boundary (SSB) and suggested that the phenomenon is related to the SSB global worming event. In this study, a similar trend is also documented near the SSB in the Bac Thuy Formation.

Novispathodus pingdingshanenesis was first described by Zhao *et al*. (2007) from the West Pingdingshan section, Anfui Province, South China. Subsequently, the taxa has been reported from other Chinese localities including Anhui (Liang *et al*., 2011), Guizhou (Ji *et al*., 2011) and Guangxi (Goudemand *et al*., 2012). These authors reported only a lowermost Spathian occurrence for the species. However, in Guangxi (Goudemand *et al*., 2012) and northeastern Vietnam (this study), *Nv*. *pingdingshanensis* co-occurs with *Xenoceltites variocostatus*, which indicates a latest Smithian age. Furthermore, in this study the Spathian part of the Bac Thuy Formation also yields the mentioned species. This evidence revises the range of the species downwards such that it extends from the uppermost Smithian to the Lower Spathian.

Icriospathodus? *zaksi*, an important species for recognition of the SSB, was first described by Buryi (1979) from the upper part of the *Anasibirites nevolini* Zone (=Upper Smithian) and the lower part of the *Tirolites cassianus* Zone (=Lower Spathian) in South Primorye, Russia (Buryi, 1979). The taxa has also been reported from the southern Alps (Perri and Andraghetti, 1987, pl. 33, figs. 1–4) where it co-occurs with *Triassospathodus symmetricus* (Perri and Andraghetti, 1987, pl. 33, fig. 5), which indicates a range from the Lower to the Upper Spathian (both species were described as *Neospathodus triangularis*). According to these reports, the range of *I*.? *zaksi* extends from the uppermost Smithian to the Lower Spathian.

The form of the P_1 element of *Icriospathodus*? *zaksi* resembles that of *I. collinsoni* except for a single row of denticles. Obviously, the species exhibits a form that is ancestral to *I. collinsoni*, but their rarity in the Bac Thuy Formation makes it difficult to resolve the evolutionary process between them. However, the existence of *I*.? *zaksi* may result in a revision of conodont biostratigraphy around the SSB based on the evolutionary process of *Neospathodus* or *Novispathodus*.

Novispathodus sp. nov. A has only been reported from the Guangxi Province, South China (Goudemand *et al*., 2012) where it co-occurs with *Nv*. *pingdingshanensis* and *Nv*. *waageni*. Moreover, according to Goudemand *et al*. (2012), these species were collected from the *Xenoceltites* ammonoid Zone, which contains the latest Smithian aged ammonoid *X. variocostatus*.

Triassospathodus symmetricus *Zone*: This zone, consisting of typical Spathian species, is defined by the first appearance of *Triassospathodus symmetricus*. Co-occuring taxa include *Novispathodus pingdingshanensis*, *Nv*. *triangularis*, *T. homeri*, *Icriospathodus collin-*

soni, and *I.*? *crassatus*. The zone encompasses the *Tirolites* cf. *cassianus* and *Tirolites* sp. nov. ammonoid beds. In this study, relatively few conodonts were collected in the middle to upper parts of the zone, but the occurrence of *Nv. pingdingshanensis* at KC02-17 demonstrates that the zone is continuous.

Triassospathodus symmetricus, first reported from Jabal Safra, Oman by Orchard (1995), is described as having a symmetrical segminate element with fused and reclined denticles, and a strongly expanded subtriangular or subquadrate basal cavity, which exhibits several morphological changes (Orchard, 1995). In addition, the larger basal cavity and fewer posterior processes are different from those of *T. homeri*. Furthermore, its range extends from the Lower to the Upper Spathian (Orchard, 1995).

In the Bac Thuy Formation, *Triassospathodus symmetricus* also exhibits morphological variations of the denticulation and basal cavity. In addition, its posterior small processes gradually increase from the lowermost to the lower part of the zone (KC02-12 to KC02-15). *T. homeri* also co-occurs with *T. symmetricus* in KC02-15, which indicates rapid evolution of *Triassospathodus*. *T. symmetricus* probably evolved into *T. homeri* during early Spathian time.

Novispathodus triangularis and *Triassospathodus homeri* are well-known Spathian species and have been reported from many localities. In addition, the range of these species has been extended to the uppermost Spathian (Orchard, 2010).

The P_1 element of *Icriospathouds collinsoni* is characterized by ridge-like denticles and a developed lateral rib. Although its range is of relatively short duration, its distribution covers a wide area, extending from the Tethys to Panthalassa and also to the boreal region (Sweet *et al*., 1971; Solien, 1979; Duan, 1987; Koike, 1992; Orchard, 1995; Lucas and Orchard, 2007; Ji *et al*., 2011). These facts demonstrate that *I. collinsoni* is one of the most important index fossils for the Lower Spathian.

Correlation (by Y. Shigeta and T. Maekawa)

Based on Smithian ammonoid and conodont biostratigraphy (Fig. 37), the lowest part of the basal portion of the Bac Thuy Formation, containing the *Flemingites rursiradiatus* beds and the lower part of the *Novispathodus* ex. gr. *waageni* Zone, can be correlated with the lowermost Middle Smithian. The overlying middle and upper parts of the basal portion of the Bac Thuy Formation, characterized by the *Urdyceras tulongensis* beds and the *Leyeceras* horizon of the *Owenites koeneni* beds, are correlatable with the lower to middle Middle Smithian. The *Guodunites* horizon of the *Owenites koeneni* beds indicates that the upper lower portion of the Bac Thuy Formation is correlatable with the upper Middle Smithian.

A change in the ammonoid and conodont assemblages in middle portion of the Bac Thuy Formation, in which the *Xenoceltites variocostatus* beds and the *Novispathodus pingdingshanensis* Zone are recognized, suggests that this part is correlatable with the Upper Smithian (Fig. 37). The upper portion of the Bac Thuy Formation, yielding the Early Spathian ammonoid *Tirolites* and *Columbites* and a typical Spathian conodont *Icriospathodus collinsoni* and *Triassospathodus homeri*, can be correlated with the Lower Spathian (Fig. 37).

Age of rhyolite from the Khon Lang Formation

(by Y. Tsutsumi and T. Komatsu)

Rhyolite samples from the basal part of the Khon Lang Formation at NT01 were investigated for radiometric age analysis of zircon. Cathodoluminescence imaging reveals (Fig. 38) that the sample includes two types of zircon grains, those exhibiting core-rim structure (core-rim grains) and those having less

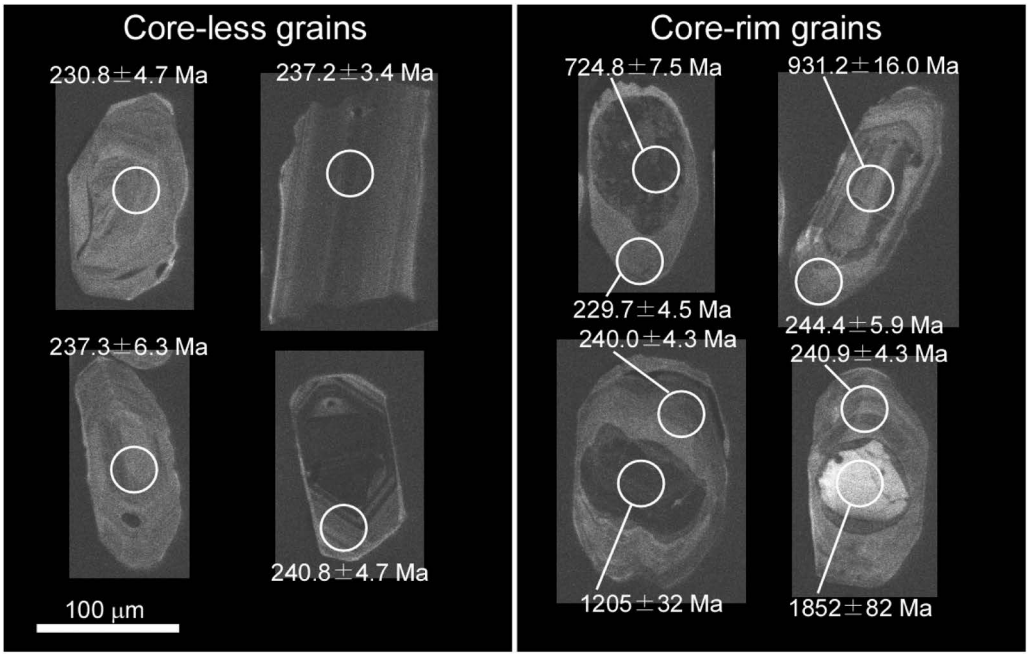

Fig. 38. Cathodoluminescence images of typical zircon grain in the sample. Circles on the images indicate the analyzed spots by LA-ICP-MS.

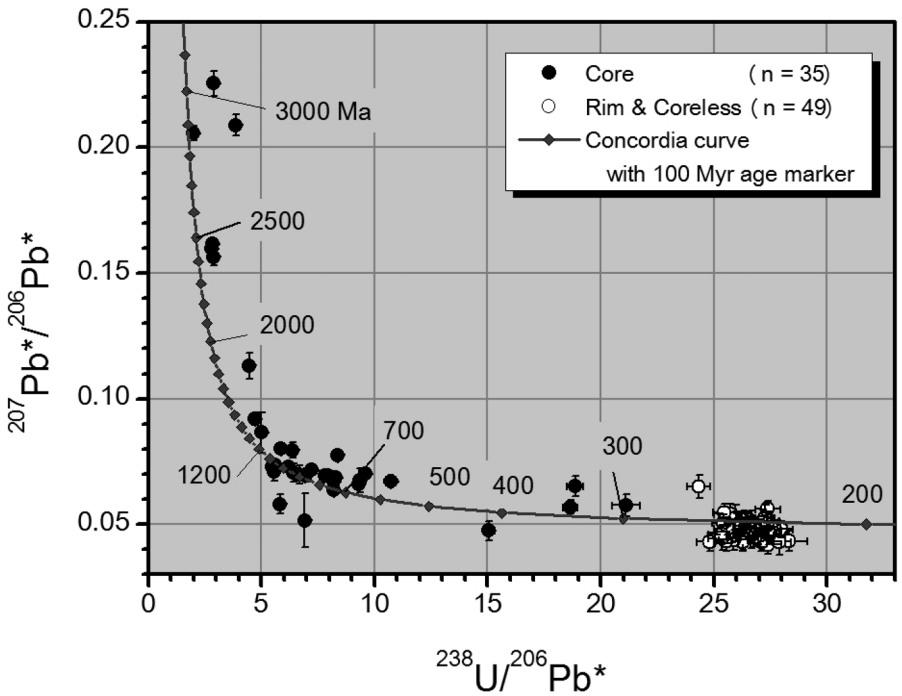

Fig. 39. Tera-Wasserberg U-Pb concordia diagram of all data from the sample. $^{207}Pb^*$ and $^{206}Pb^*$ indicate radiometric ^{207}Pb and ^{206}Pb, respectively.

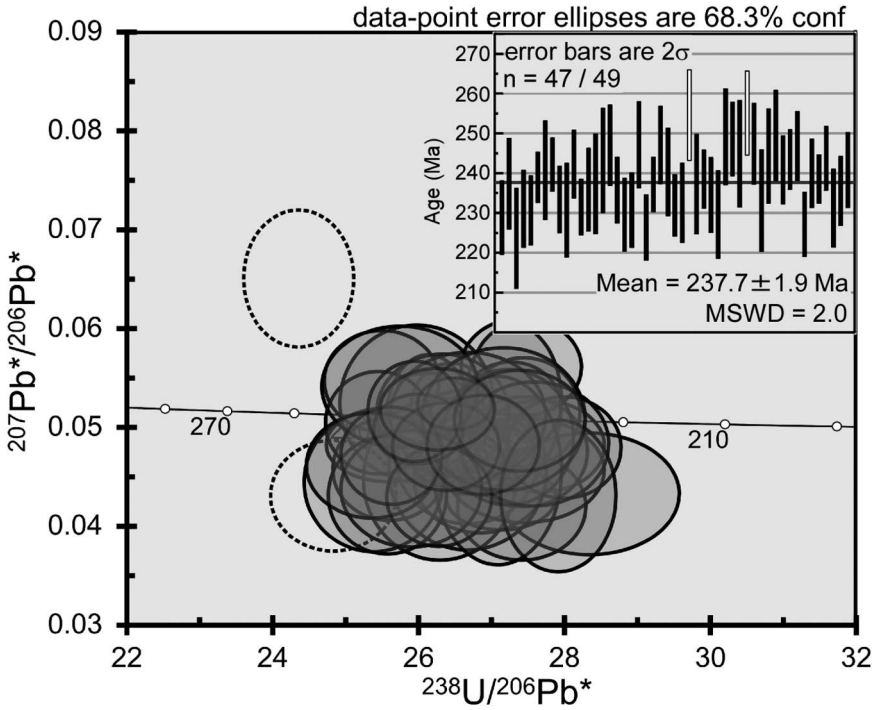

Fig. 40. Tera-Wasserberg U-Pb concordia diagrams and age distribution plot of the zircons from the sample. $^{207}Pb^*$ and $^{206}Pb^*$ indicate radiometric ^{207}Pb and ^{206}Pb, respectively.

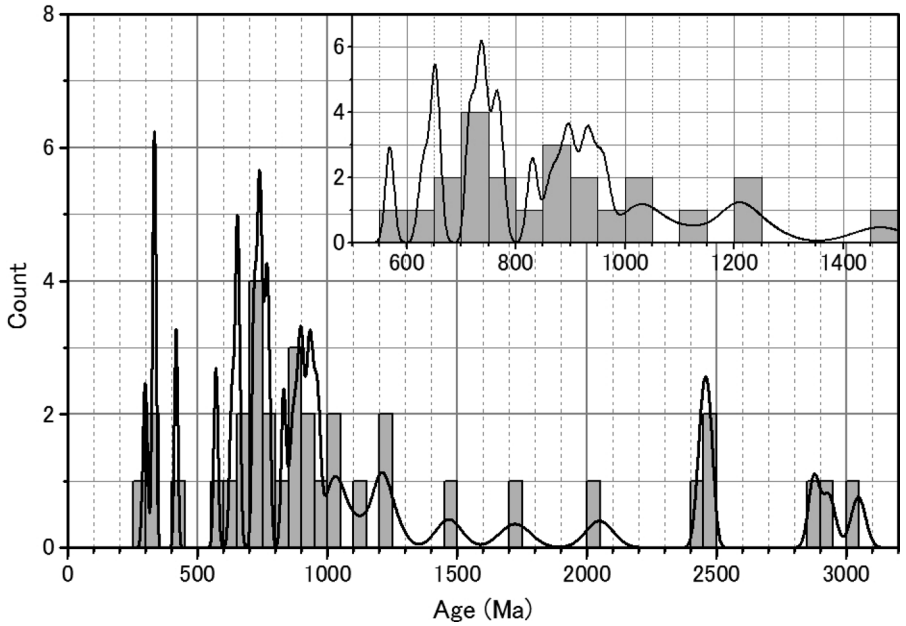

Fig. 41. Probability distribution diagram of the core ages from the grains that show core-rim structure. The $^{207}Pb^*/^{206}Pb^*$ ages for older (>1 Ga) zircons, and $^{206}Pb^*/^{238}U$ ages for younger zircons are used in this diagram. $^{207}Pb^*$ and $^{206}Pb^*$ indicate radiometric ^{207}Pb and ^{206}Pb, respectively.

core (core-less grains). The core-less grains show magmatic oscillatory zoning.

The ages of the core-less grains and rims in the core-rim grains show a concentration of ~240 Ma, but data from the cores in the core-rim grains yield older and variable ages (Fig. 39). The weighted mean age of the core-less grains and rims in the core-rim grains indicate 237.7±1.9 Ma (95% conf.; Fig. 40), which is thought to be the magmatism (eruption) age of the rhyolite. On the other hand, the cores in the core-rim grains indicate multiple ages (Fig. 41); ca. >500 Ma, 600–800 Ma, 800–1100 Ma, ~2500 Ma and ~3000 Ma. This age-distribution is analogous to the detrital zircon from the South China Craton (e.g. Xu. *et al*., 2007; Jia *et al*., 2010). In consideration of the above data, the zircon cores are thought to have originated from rocks of sedimentary-origin associated with the South China Craton, and the cores thought to be xenocrysts were captured by the rhyolitic magma from the wall and/or cap rocks when the magma rose in the surrounding rocks.

Discussion

Aspects of Smithian ammonoid fauna (by Y. Shigeta)

Because of the difficulty encountered in collecting macrofossils from the very hard limestones in the Bac Thuy Formation, a complete faunal list of Smithian ammonoids is not yet possible. However, ammonoids collected thus far and described herein clearly suggest that the Smithian ammonoid fauna in northeastern Vietnam is nearly identical to that of South China (Chao, 1959; Brayard and Bucher, 2008).

These ammonoid taxa exhibit six different geographical distribution patterns (Fig. 42). The first pattern, characterized by endemic distribution restricted to South China and northeastern Vietnam, is represented by *Ussuria kwangsiana* (Fig. 42.1), *Jinyaceras* cf. *bellum*, *Paranannites sinensis* and *Paranannites involutus* (Chao, 1959). The second pattern, consisting of numerous taxa, exhibits a relatively wide distribution in the Tethys (e.g. South China, Timor, South Tibet, Spiti, the Salt Range, Oman), and includes the following species: *Preflorianites radians* (Fig. 42.2), *Xenoceltites variocostatus*, *Pseudaspidites muthianus*, *Leyeceras rothi*, *Guodunites monneti*, *Dieneroceras*? *goudemandi*, *Flemingites rursiradiatus*, *Anaflemingites hochulii*, *Galfettites simplicitatis*, *Urdyceras tulongensis* and *Submeekoceras hsüyüchieni*. *Aspenites acutus*, the only taxon of third pattern (Fig. 42.3) is distributed in the Tethys and the eastern equatorial side of the Panthalassa (e.g. California, Nevada, Utah, Idaho). In contrast, the fourth pattern, consisting of *Juvenites sinuosus* (Fig. 42.4) also exhibits a Tethyan distribution, but its Panthalassan distribution is limited to the western middle latitude (South Promorye). *Parussuria compressa* and *Owenites koeneni* (Fig. 42.5), which are widely distributed in the low- to middle-paleolatitudinal regions in the Tethys and both sides of the Panthalassa, are members of the fifth pattern. The sixth pattern is represented by the pandemic distribution of *Pseudosageceras multilobatum* (Fig. 42.6), which occurs in the Tethys, both sides of the Panthalassa and the Boreal Realm (e.g. Arctic Canada, Spitsbergen).

Most species belonging to the first, second, and fourth distribution patterns also have related species belonging to the same genus in other low- to middle-paleolatitudinal regions. For example, *Preflorianites toulai* (Smith, 1932), *Xenoceltites youngi* Kummel and Steele, 1962, *Pseudaspidites silberlingi* Jenks *et al.*, 2010, *Galfettites lucasi* Jenks *et al.*, 2010, *Anaflemingites silberlingi* Kummel and Steele, 1962, *A. russelli* (Hyatt and Smith, 1905), *Guodunites hooveri* (Hyatt and Smith, 1905), *Submeekoceras mushbachanum* (White, 1879) and *Juvenites septentrionalis* Smith, 1932 all occur on the eastern equatorial side of the Panthalassa (western USA). Brayard *et al*. (2006, 2009) discussed the paleobiogeography

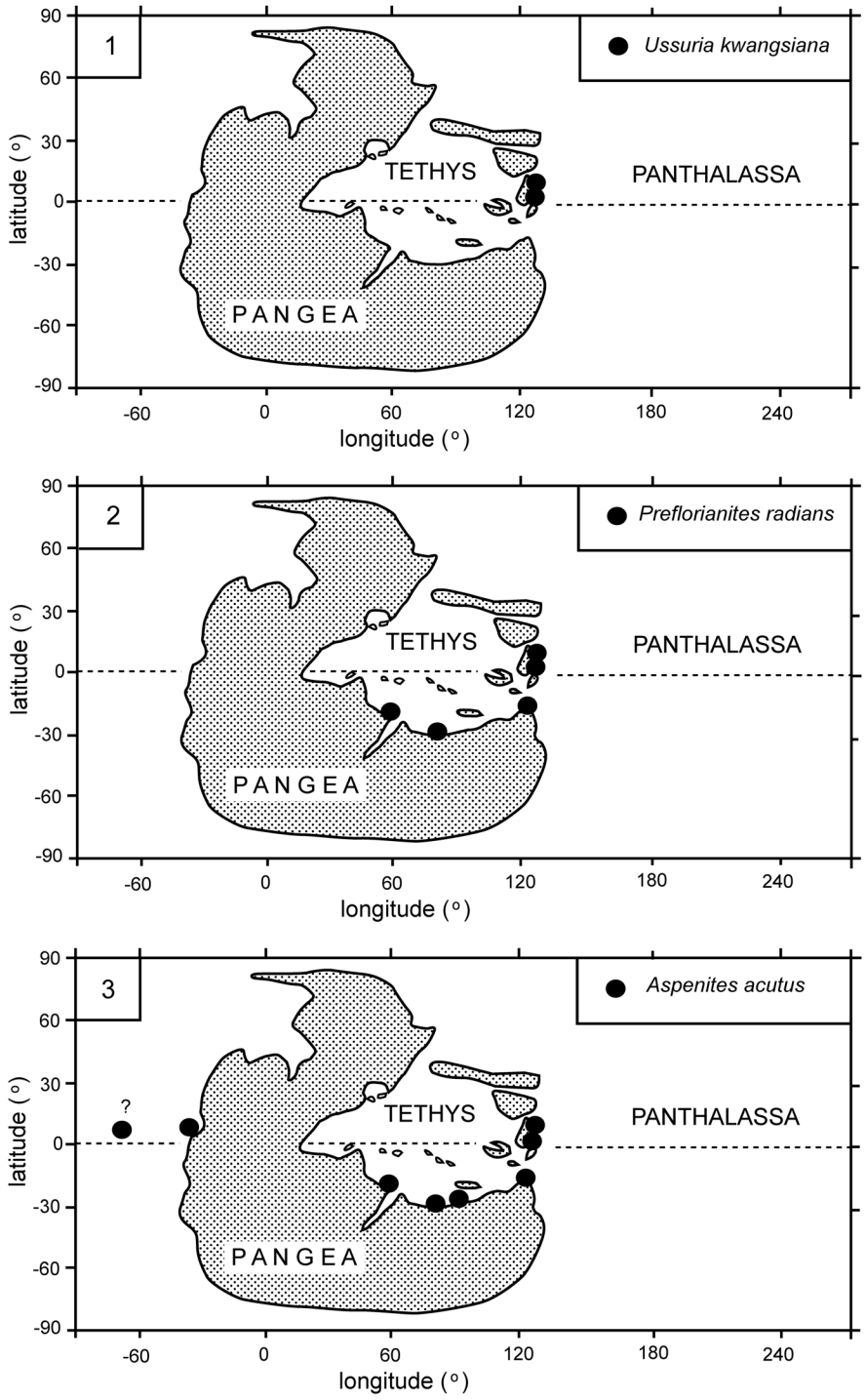

Fig. 42. Paleogeographical distribution of selected Smithian ammonoids. Paleomaps modified after Péron *et al*., 2005, Brayard *et al*., 2006 and Brayard *et al*., 2009. 1, *Ussuria kwangsiana*. 2, *Preflorianites radians*. 3, *Aspenites acutus*. 4, *Juvenites sinuosus*. 5, *Owenites koeneni*. 6, *Paseudosageceras multilobatum*.

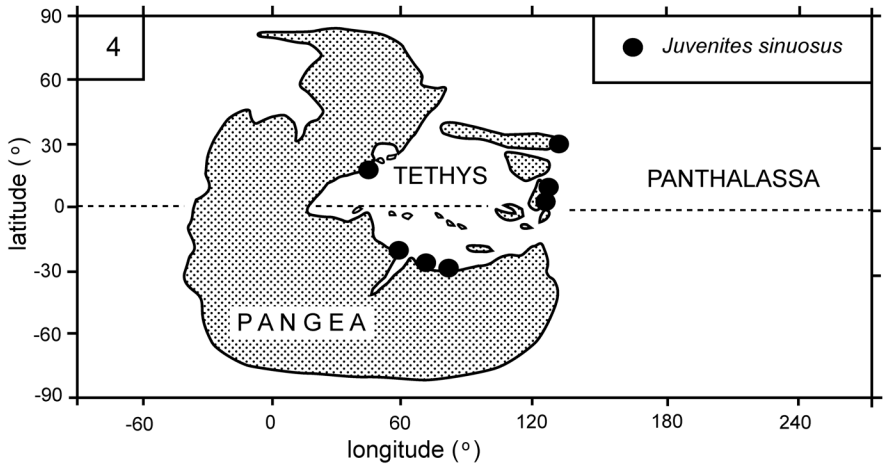
4
Juvenites sinuosus
TETHYS
PANTHALASSA
PANGEA
latitude (°)
longitude (°)
90
60
30
0
-30
-60
-90
-60
0
60
120
180
240

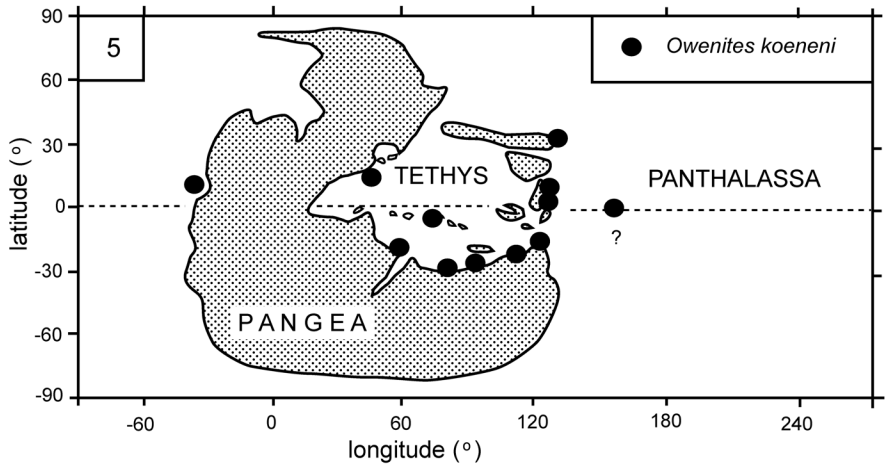
5
Owenites koeneni
TETHYS
PANTHALASSA
?
PANGEA
latitude (°)
longitude (°)
90
60
30
0
-30
-60
-90
-60
0
60
120
180
240

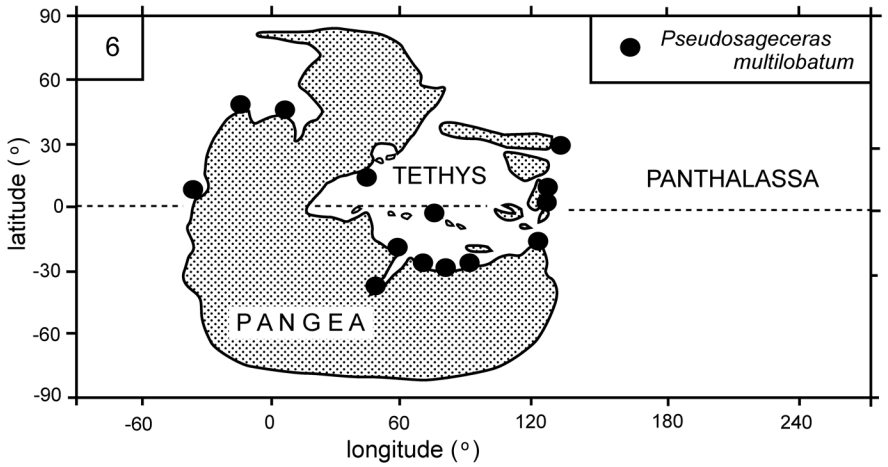
6
Pseudosageceras multilobatum
TETHYS
PANTHALASSA
PANGEA
latitude (°)
longitude (°)
90
60
30
0
-30
-60
-90
-60
0
60
120
180
240

of Smithian ammonoids from South China and concluded that the fauna exhibits strong affinities at the generic level with the low-paleolatitudinal regions (Tethys and eastern Panthalassa) and South Primorye. However, Shigeta *et al.* (2009) pointed out that the Smithian ammonoid fauna in South Primorye contains many endemic species and it actually shares very few common species with South China. Thus, faunal affinity at the generic level does not coincide with that at the specific level for Smithian ammonoids. Smithian ammonoid occurrences in the Bac Thuy Formation suggest that the fauna exhibits a very strong relationship with other Tethyan faunas, but relatively weak relationships with faunas on both sides of the Panthalassa.

Internal features in the early whorls of ammonoids (by Y. Shigeta and T. Maekawa)

Following the treatment of limestone samples from the Bac Thuy Formation with acetic acid, many well-preserved micro-ammonoid specimens free of obscuring matrix were found in the residue together with abundant conodonts. The sparry calcite filling of the phragmocones had been completely dissolved as had all of the shell material, thus leaving only insoluble thin layers (probably of organic origin) that originally covered the shell surfaces. This phenomenon permitted observation of the unique three-dimensional geometry of the internal features of the early whorls.

These early whorls consist of the initial chamber, caecum, flange, siphuncle, and septa (Fig. 43). Shaped somewhat like a rugby football, the initial chamber is separated from the succeeding whorls by the first septum (=proseptum), which is slightly convex adapically. The bulb-like beginning of the siphuncle, termed the caecum, is attached to the inside surface of the initial chamber and is located in the ventral position at the first septum. A granular structure is also visible on the inside surface of the initial chamber near the inner lip of initial chamber (=flange).

Since the mid-nineteenth century, many workers have studied the internal shell features of the early whorls of ammonoids, and it has been determined that these embryonic shells all share a number of common morphological features (Landman *et al*., 1996). The relative shape of these features as well as their size and position with respect to each other appear to be stable at higher taxonomic levels (Druschits and Khiami, 1970; Druschits and Doguzhaeva, 1974, 1981; Tanabe *et al*., 1979, 2003; Tanabe and Ohtsuka, 1985; Ohtsuka, 1986; Tanabe *et al*., 1994; Landman *et al*., 1996; Shigeta *et al*., 2001). This fact suggests that these internal shell features are strongly constrained phylogenetically, and therefore, it is possible to investigate the higher-level systematics and evolution of the ammonoids on the basis of subtle changes in these features. Shigeta *et al*. (2001) studied these early internal shell features in 40 species of the Goniatitida, Prolecanitida and Ceratitida, and discussed the origin of the Ceratitida. Shigeta and Weitschat (2004) also discussed the origin of the Ammonitina inferred from the internal shell features of some latest Triassic and Jurassic ammonoids.

Compared to Carboniferous, Permian, Jurassic and Cretaceous ammonoids, the internal shell features of Triassic ammonoids have received relatively little attention. Most previous studies, excluding that of Weitschat (1986), are based on the observation of sections polished parallel to the median section plane of matrix-filled specimens (Arkadiev and Vavilov, 1984; Vavilov, 1992; Zakharov, 1978; Shigeta and Weitschat, 2004). After dissolving the sparry calcite filling of the phragmocones with acetic acid, Weitschat (1986) then described the three-dimensional inner structures that included complex networks of cameral membranes in Middle Anisian ammonoids from Central Spitsbergen.

It is quite rare to find specimens whose phragmocones are free of interior matrix, but this preservational feature has been noted in

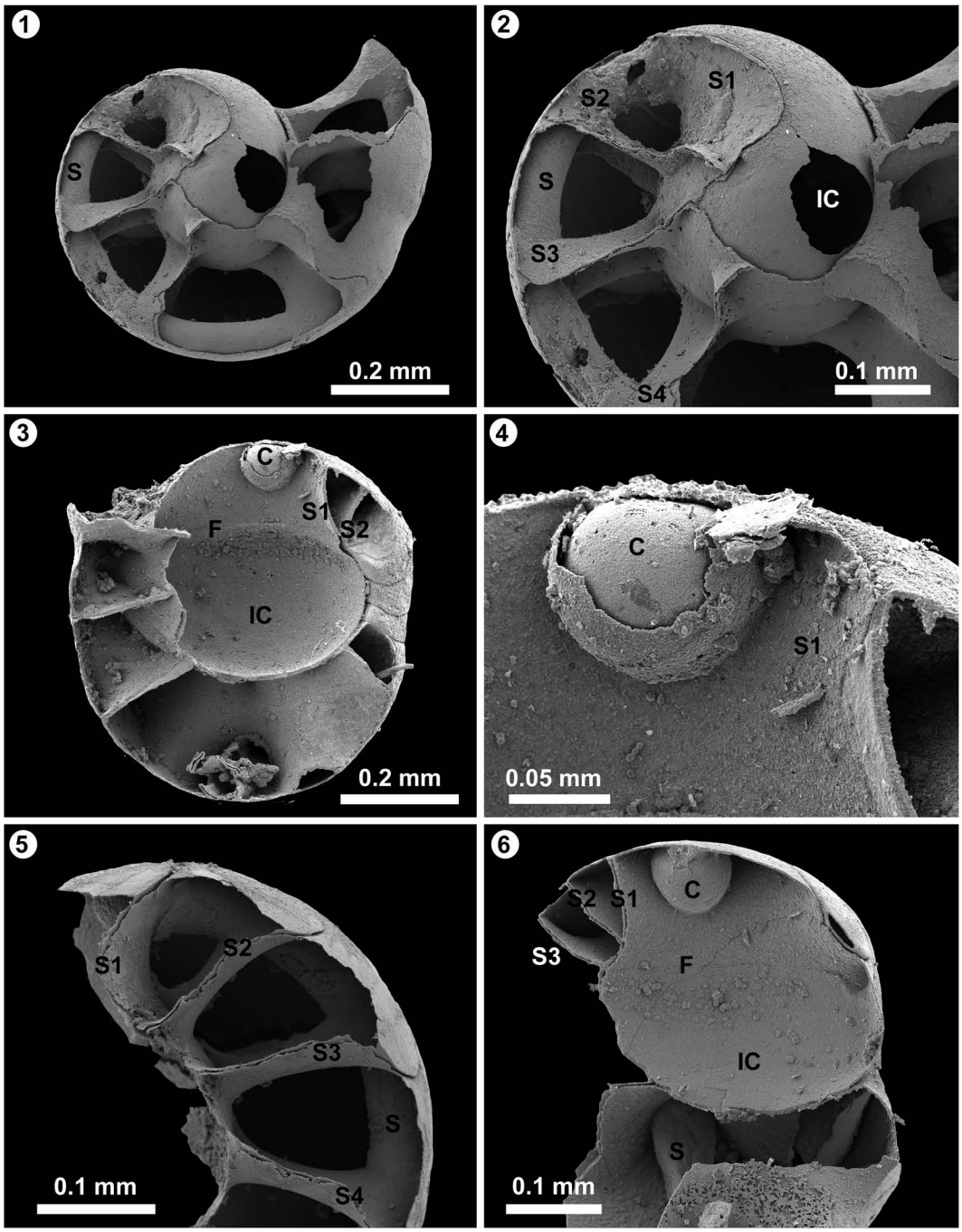

Fig. 43. Internal features in the early whorls of the Lower Triassic ammonoids from the Bac Thuy Formation in northeastern Vietnam. 1–2, NMNS PM23855, from BR01-06. 3–4, NMNS PM23856, from PK01-01. 5, NMNS PM23857, from BT02-01. 6, NMNS PM23858, from KC01-10. C: caecum, F: flange, IC: initial chamber, S: siphuncle, S1: first septum (proseptum), S2: second septum, S3: third septum, S4: fourth septum.

some Jurassic and Cretaceous ammonoids. This phenomenon permits detailed observations regarding the shape and spacing of the first few septa and associated structures in the early whorls (Landman and Bandel, 1985), and it has contributed significantly to the understanding of the sequence of embryonic development (Bandel, 1982). Furthermore, Maeda and Seilacher (1996) reported the existence of fungal "pseudomorphs" preserved in the hollow phragmocone of a Cretaceous ammonoid from Hokkaido and discussed early decay processes. Recently, Hoffmann's (2010) study of a hollow Cretaceous ammonoid from northern Kamchatka with a three-dimensional visualization method that utilized a computer tomography (CT-scan) showed a clear image of internal shell features.

Acid treatment of limestone samples from various horizons of the Bac Thuy Formation yields numerous well-preserved micro-ammonoids whose phragmocones are free of obscuring matrix. Continued studies of the internal shell features of these specimens may provide an important key for understanding the detailed microstructural relationships of their morphological features, as well help establish a clearer understanding of the higher taxonomy and evolution of Early Triassic ammonoids.

Ammonoid mode of occurrence (by Y. Shigeta and T. Komatsu)

Ammonoids are not preserved in the portion of the lower part of the Bac Thuy Formation consisting of wavy, lenticular thin flat-bedded carbonates and intraclastic limestones containing angular flat carbonate pebbles and cobbles that were deposited in a tidal flat environment, between the supratidal and intertidal zones (Komatsu *et al*., 2014). However, the cross-stratified limestones presumably deposited in an intertidal to subtidal calcareous sand-flat environment do yield rare, poorly preserved ammonoids. Various types of ammonoids occur abundantly in the alternating beds of bioclastic, oolitic, and intraclastic limestone characterized by wave ripples and low-angle cross-stratification that were deposited in a subtidal flat to storm-wave-influenced shallow marine environment. Ammonoids are also abundant in the alternating beds of bioclastic and intraclastic limestone formed by concentrated density flows as well as the marls of hemipelagic calcareous deposits. Poorly preserved ammonoids occur only rarely in the structureless intraclastic limestones that probably represent transgressive lag deposits. Ammonoids are not found in the limestone breccias formed by debris flows.

In the middle part of the Bac Thuy Formation, only *Xenoceltites variocostatus* occurs in the organic-rich dark gray bioclastic limestone and mudstone. The limestone is interpreted as a turbidity flow deposit (calciturbidite), whereas the mudstone is considered to be a hemipelagic siliciclastic deposit formed in an anoxic to dysoxic environment in a slope to marginal basin plain (Komatsu *et al*., 2014). Ammonoid shells were probably transported by turbidity flows.

In the upper part of the Bac Thuy Formation, ammonoids are preserved mainly in fine- to very-fine grained calcareous sandstone embedded in a thick and weakly laminated mudstone. The sandstone beds are typical of distal turbidites, and the mudstone accumulated from suspension under calm conditions (Komatsu *et al*., 2014). As with the middle part of the Bac Thuy Formation, ammonoid shells were probably transported by turbidity flows. The scarcity of ammonoids in the surrounding mudstone suggests that the slope to marginal basin plane was not a suitable environment in which to live. A similar mode of occurrence of ammonoids has been reported for the gravity flow deposits of the Lower Triassic Abrek section in South Primorye, Russia (Shigeta *et al*., 2009).

In summary, the ammonoid mode of occurrence in the Bac Thuy Formation suggests that while the supratidal to intertidal environ-

ment was uninhabitable, the majority of ammonoids probably lived in the subtidal flat to storm-wave-influenced shallow marine environment typical of a carbonate platform. After death their shells were transported from their biotope to the slope to marginal basin plane by gravity flow.

Smithian gastropod assemblages of the Bac Thuy Formation (by A. Kaim, A. Nützel and T. Maekawa)

All gastropods described and illustrated in this paper were removed from the limestone samples by applying acetic acid. The specimens are silicified larval and/or juvenile shells or their moulds. The preservation of the shells vary from well preserved shells with external ornamentation preserved (e.g., Figs. 125.1–125.3, 132.4–132.6, 135.4–135.6), shells where the external layer peeled off (e.g., Figs.125.7–125.12, 132.7–132.9) and specimens where only internal mould is preserved (Figs. 123.1–123.3, 130.6, 132.1–132.3, 133.4–133.9). Both the preservation and the larval/juvenile nature of the specimens cause that the detailed taxonomy (i.e., species level) is impossible.

The gastropods come from the fossiliferous limestone beds in the basal portion of the Bac Thuy Formation (BTF) exposed at Bac Thuy (sections BT01, 02), bedded limestone in the lower to middle portions of the BTF exposed along the Ky Cung River (sections KC01, 02), and the upper middle portion of the BTF (section KC02). Gastropod shells have been found in following stratigraphic levels of the Smithian though they significantly differ in number and preservation (Table 1).

Lowest Middle Smithian gastropods: Only two poorly preserved gastropods were collected from the *Flemingites rursiradiatus* beds. Specimen NMNS PM23849 from BT01-04 (Fig. 123.1–123.3) is moderately high-spired juvenile shell with deeply incised suture. The shell is poorly preserved with no external ornamentation preserved. The shell may have belonged to a caenogastropod juvenile (see e.g., *Atorcula*-type and *Ampezzopleura*-type juvenile shells it this paper). Another single poorly preserved specimen NMNS PM23848 from BT02-01 (Fig. 123.4–123.6) may belong to *Atorcula* though the preservation does not allow any precise identification.

Table 1. The number of gastropod taxa and the number of specimens in the recognized ammonoid biostratigraphic units. F: *Flemingites rursiradiatus* beds, O: *Owenites koeneni* beds, X: *Xenoceltites variocostatus* beds, F/O: beds between the *Flemingites rursiradiatus* and the *Owenites koeneni* beds.

Species	F	F/O	O	X
Worthenia sp. indet.		2		
Anomphalus sp. indet.			8	1
Abrekopsis sp. indet.			1	
Naticopsis sp. indet. A		2	7	1
Naticopsis sp. indet. B			9	
Strobeus sp. indet.			1	
Ampezzopleura sp. indet.			2	
Atorcula sp. indet.	1	10	4	
Others	1	1	4	
Total specimens	2	15	36	2
Total taxa	2	4	8	2

Lower Middle Smithian gastropods: Fifteen juvenile gastropod shells representing four taxa were obtained from beds between the *Flemingites rursiradiatus* beds and the *Owenites koeneni* beds. They are dominated by *Atorcula* sp. indet. (10 specimens) associated by *Worthenia* sp. indet. (2 specimens), *Naticopsis* sp. indet. A (2 specimens) and single poorly preserved gastropod (Fig. 127.10–127.12) that could not be matched to any other species recognized in the samples from Vietnam.

Middle to upper Middle Smithian gastropods: The *Owenites koeneni* beds provided not only the richest by number but also most diversified assemblage of gastropods: thirty-six shells are classifies in eight taxa. Most common are neritoids represented by sixteen specimens of *Naticopsis* (sp. indet. A+sp. indet. B) and single specimen of *Abrekopsis*? sp. indet. *Anomphalus*? sp. indet. (8 specimens) is also common. *Atorcula* sp. indet. (4 specimens),

Ampezzopleura sp. indet. (2 specimens), and *Strobeus* sp. indet. (1 specimen). Additional four specimens are too poorly preserved for generic identification (Figs. 130.6, 133.4–133.12).

Upper Smithian gastropods: Single specimen of *Anomphalus*? sp. and *Naticopsis* sp. indet. A were collected from the *Xenoceltites variocostatus* beds.

The shells found in the Smithian of northeasternVietnam are only larval conchs or early juveniles of taxa displaying mostly planktotrophic type of development. This is indicated by the small size of the specimens (smaller 1 mm) and the fact that the initial whorl is present in most specimens showing that the apical portions of gastropods are present. Gastropod larval fall assemblages have been reported from several Palaeozoic formations (Bockelie and Yochelson, 1979; Herholz, 1992; Nützel and Mapes, 2001; Nützel *et al*., 2007; Mapes and Nützel, 2009). Nützel and Mapes (2001) and Mapes and Nützel (2009) reported a larval fall assemblage from the Mississippian of the United States and showed that metamorphosis and growth to larger adult sizes of the larvae was impossible due to anoxic condition in bottom waters. The same is probably the case in the studied assemblages from the Early Triassic of Vietnam. The gastropods either failed to survive metamorphosis or died soon thereafter. Most likely the bottom water was dysoxic or periodically anoxic.

Most of the taxa present in the investigated samples have also been reported from other associations of Smithian or more generally Early Triassic age (see e.g. Batten and Stokes, 1986; Nützel, 2005; Nützel and Schubert, 2005; Wheeley and Twitchett, 2005; Kaim, 2009; Kaim *et al*., 2010, 2013). The only taxa not recorded before in the Early Triassic are *Anomphalus* and *Atorcula* though known from Permian and Late Triassic and therefore not surprising in the Early Triassic.

Bivalve assemblages and mode of occurrence
(by T. Komatsu, H. T. Dang and T. C. Dinh)

Bivalves are found in uppermost Smithian to lowermost Spathian marginal basin deposits consisting of thin-bedded turbidite limestone (=calciturbidite), marl and hemipelagic mudstone containing calcareous nodules. The calciturbidites are composed mainly of Tb (parallel laminated limestone), Tc (cross-laminated limestone) and Td (week parallel laminated limestone and marl) divisions. Well-preserved shells are commonly found in the calciturbidites, marls and calcareous nodules, but nearly all specimens in the hemipelagic mudstone are poorly preserved and completely flattened.

Bivalve preservation exhibits two different types in the modes of occurrence. The first type is a shell- and matrix-supported thin (1–3 cm) lenticular shell-concentration within the thin calciturbidite beds and marl layers consisting of ammonoids and bivalves such as *Crittendenia australasiatica*, *C. langsonensis*, *Leptochondria bittneri*, *Bositra limbata* and "*Pseudomonotis*" *himaica*. In Facies 8, which consists of organic-rich dark gray wackestone and hemipelagic mudstone containing marl layers (Komatsu *et al*., 2014), *C. australasiatica* is the dominant species, accounting for +80% of the bivalve assemblage from the basal parts of Tb, Tc and Td divisions of the organic-rich dark gray calciturbidites. In Facies 10, which consists of thick hemipelagic mudstone intercalated with sandstone and wackestone layers (Komatsu *et al.*, 2014), *C. australasiatica* and "*Pseudomonotis*" *himaica* are abundant in the Tc and Td divisions of the turbidite wackestone layers, respectively (Fig. 17). Furthermore, in both Facies 8 and 10 *B. limbata*, *Bositra* sp. indet. and juveniles of *Crittendenia* form small lenticular shell-concentrations 3–10 cm thick in the Td divisions of the thin turbidite layers and hemipelagic mudstone. These bivalves are commonly disarticulated and/or fragmentary, which is indicative of gravity flow transport and typical allochthonous occurrence.

The second mode of occurrence consists of shell-scattered beds in the hemipelagic mudstone overlying the calciturbidite and marl. Both articulated and disarticulated shells of *B. limbata* and *Bositra* sp. indet. are found in the hemipelagic mudstone. Some of the articulated shells are preserved in a butterfly position, and disarticulated right and left valves of the same individual are seen to occasionally overlap. Both articulated and disarticulated shells of *C. australasiatica* are also commonly found in the hemipelagic mudstones of Facies 8. These species may represent a parautochthonous assemblage.

Brief note on the radiolarian faunas of the Upper Smithian (Lower Triassic) (by O. Takahashi)

Very little has been published on the distributions and relative abundances of radiolarians in the Lower Triassic, particularly in the Induan and lower Olenekian (Smithian), as radiolarian occurrences from these times are apparently restricted and scarce, and the diversity is very low. Induan and lower Olenekian radiolarians have been recovered from the following five sections: the Dienerian (upper Induan) to lower Smithian (lower Olenekian) marly limestone beds of northwestern Turkey (Kozur *et al*., 1996a), the Induan to Olenekian chert beds of northern New Zealand (Kamata *et al*., 2007; Takemura *et al*., 2007; Hori *et al*., 2011), the Dienerian limestone beds of southern Thailand (Sashida *et al*., 1998), the Smithian chert beds of central Oregon (Blome and Reed, 1992), and the Olenekian limestone beds of southern Italy (Marsella *et al*., 1993). In addition, Sugiyama (1997) described well-preserved Early Triassic radiolarian faunas from central Japan; his *Follicucullus-Parentactinia* Assemblage Zone (TR0), which correlates with the lower part of the *Parentactinia nakatsugawaensis* assemblage of Sugiyama (1992) and the lower part of the *Stylosphaera fragilis* Zone of Bragin (1991), may be early Spathian or older in age.

The Upper Smithian radiolarian fauna from the Bac Thuy Formation presented in this study has a unique species composition and a relatively high diversity for this stratigraphic level. The fauna includes a mixture of Paleozoic- and Triassic-type radiolarians. The Paleozoic-type radiolarians are dominated by entactinarians with several species of the following genera: *Multisphaera*, *Plenoentactinia*, *Retentactinia*, and *Spongentactinia*. These genera have been reported from the Devonian and Carboniferous of western Australia (Aitchison, 1993; Won, 1997) and western Germany (Won, 1990), and from the Permian of Urals (Afanasieva, 2000; Dumitrica, 2011), but none of them have been previously reported from Mesozoic strata. Interestingly, the same type of faunas, dominated by entactinarians, have been reported in other faunas from the Lower Triassic limestone beds such as: the Dienerian to lower Smithian of Turkey (Kozur *et al*., 1996a), the Dienerian of Thailand (Sashida *et al*., 1998), and the latest Spathian to earliest Anisian of Thailand (Sashida and Igo, 1992). Moreover, all of these Early Triassic occurrences have been restricted to limestone beds in low-latitude regions along the western margin of Panthalassa (Scotese, 2002). Therefore, the radiolarian fauna described here has the biostratigraphic potential to be of Early Triassic age, and may also have paleogeographic and paleoceanographic affinities to Early Triassic low-latitude faunas along the western margin of Panthalassa.

Systematic Paleontology

Cephalopods (by Y. Shigeta and H. D. Nguyen)

Systematic descriptions basically follow the classification established by Sweet (1964) for orthocerids and Tozer (1981, 1994) for ceratitids and phylloceratids. Morphological terms are those used in the Treatise on Invertebrate Paleontology (Moore, 1957, 1964). Quantifiers used to describe the size and shape of ammonoid shell replicate those proposed by

Matsumoto (1954, p. 246) and modified by Haggart (1989, table 8.1).

Abbreviations for shell dimensions: D = shell diameter; U = umbilical diameter; H = whorl height; W = whorl width.

Institution abbreviations: CGM = Central Research Geological Prospecting Museum (CNIGR Museum), St. Petersburg; GPIBo = Goldfuss Museum (Steinmann Institute), Bonn University; GSI = Geological Survey of India, Kolkata; IPUW = Department of Palaeontology, University of Vienna, Vienna; NIGP = Nanjing Institute of Geology and Palaeontology, Chinese Academy of Sciences, Nanjing; NMNS = National Museum of Nature and Science, Tsukuba; PIMUZ = Institute and Museum of Paleontology, University of Zurich, Zurich; USNM = Smithonian National Museum of Natural History, Washington, D. C.

Class Cephalopoda Cuvier, 1795
Order Orthocerida Kuhn, 1940
Superfamily Orthoceratoidea McCoy, 1844
Family Orthoceratidae McCoy, 1844
Genus ***Trematoceras*** Eichwald, 1851

Type species: *Orthoceras elegans* Münster, 1841.

Trematoceras sp. indet.

Figs. 44, 45

Material examined: Five specimens, NMNS PM23459–23463, from NT01-04.

Description: Moderately expanding orthoconic shell with 4–5 degree adoral angle of expansion and circular whorl cross-section. Juvenile shell ornamented with fine transverse lirae, while adult body chamber exhibits very weak ribs as well as fine transverse lirae. Siphuncle located at center, with cylindrical connecting ring and short, orthochoanitic septal neck. Suture simple and straight. Cameral deposits not observed.

Discussion: Although the described specimens are very close to *Trematoceras subcampanile* (Kiparisova, 1954), they are easily distinguished by the fine transverse lirae on the juvenile shell, which contrasts with network lirae on the juvenile shell of *T. subcampanile* (Shigeta and Zakharov, 2009, Fig. 27). They differ from *T. mangishlakense* Schastlivtceva (1981) and *T. insperatum* Schastlivtceva (1988) by the smaller angle of shell expansison. The described specimens are morphologically very similar to *T. campanile* (Mojsisovics, 1882), *T. vulgare* Schastlivtceva (1981), *T. ciarum* Schastlivtceva (1986), and *T. boreale* Schastlivtceva (1986), but a definitive species assignment cannot be made due to an insufficient number of well-preserved specimens.

Occurrence: Described specimens from NT01-04 within the portion of the *Novispathodus pingdingshanensis* Zone represented by the *Xenoceltites variocostatus* beds (Upper Smithian = upper Lower Olenekian) in the Bac Thuy Formation, northeastern Vietnam.

Order Ceratitida Hyatt, 1884
Superfamily Xenodiscoidea Frech, 1902
Family Kashmiritidae Spath, 1934
Genus ***Preflorianites*** Spath, 1930

Type species: *Danubites strongi* Hyatt and Smith, 1905.

Preflorianites radians Chao, 1959

Figs. 46, 47

Xenodiscus bittneri Hyatt and Smith, 1905. Welter, 1922, p. 106, pl. 158, figs. 8–9.

Preflorianites radians Chao, 1959, p. 196, pl. 3, figs. 6–8; Brühwiler *et al*., 2012a, p. 15, pl. 1, figs. 8–9, pl. 2, figs. 1–7.

? *Glyptophiceras langsonense* Vu Khuc, 1984, p. 31, pl. 1, figs. 2–3, pl. 2, fig. 1; Vu Khuc, 1991, p. 121, pl. 45, figs. 1–3, pl. 50, fig. 3.

Pseudoceltites? *angustecostatus* (Welter, 1922). Brayard and Bucher, 2008, p. 18, pl. 3, figs. 1–7, text-fig. 19.

Preflorianites cf. *radians* Chao, 1959. Brühwiler *et al*., 2012c, p. 132, fig. 13A–E.

Holotype: NIGP 12564, figured by Chao (1959, p. 196, pl. 3, figs. 7–8), from the Owenitian (Middle Smithian) of the Tientung district (Tsoteng), western Guangxi, South

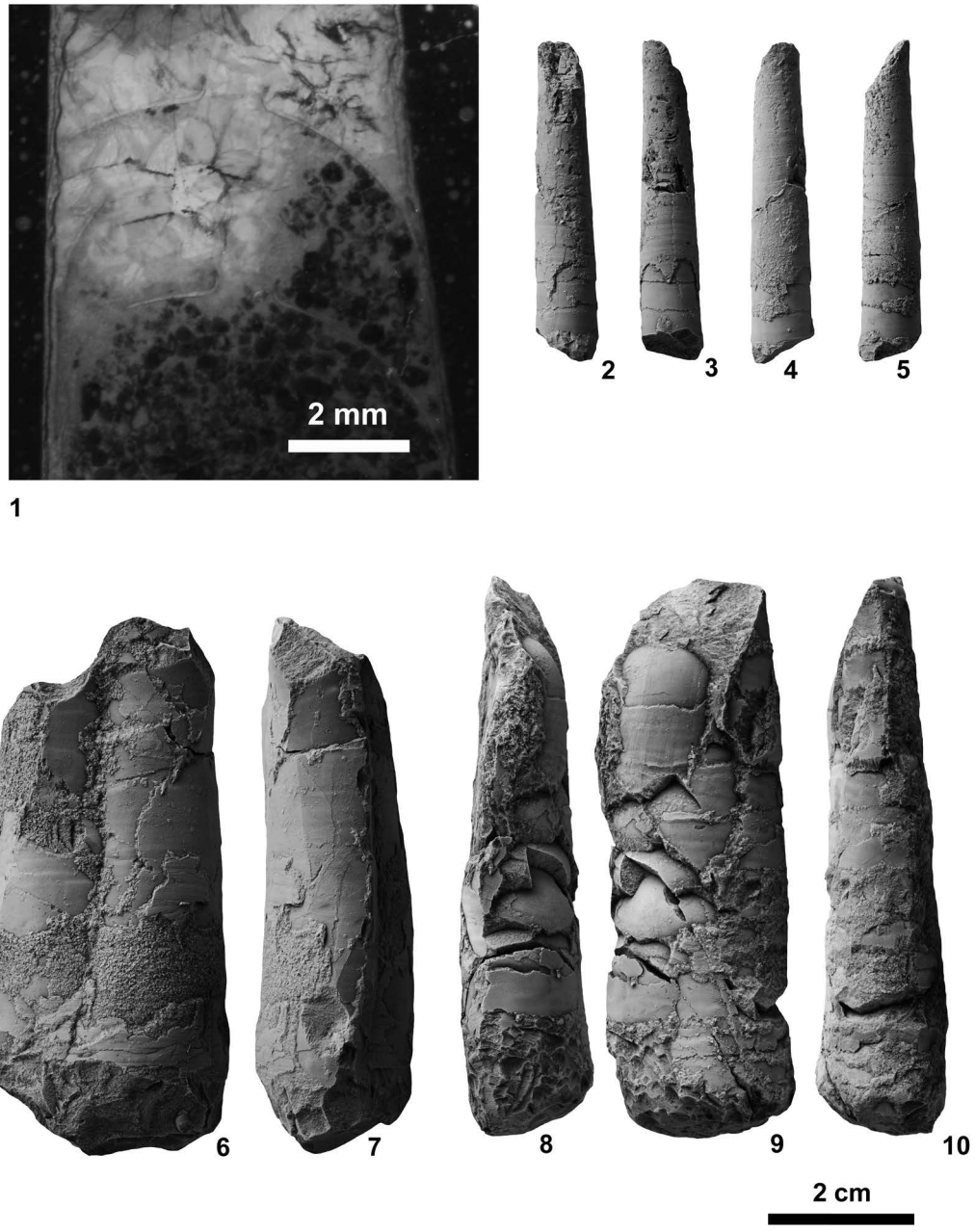

Fig. 44. *Trematoceras* sp. indet. from NT01-04. 1, NMNS PM23459. 2–5, NMNS PM23460. 6–7, NMNS PM23461. 8–10, NMNS PM23462.

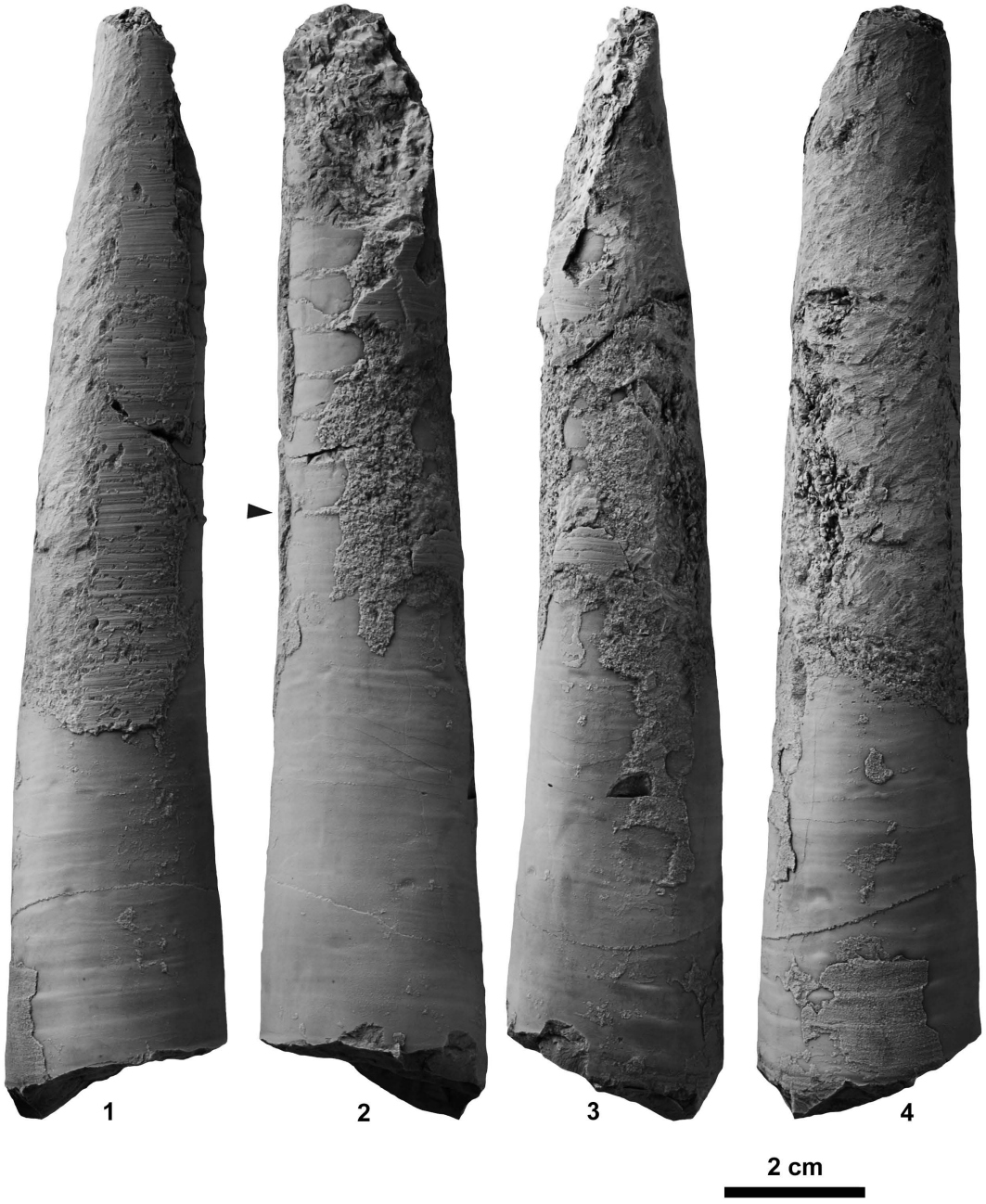

Fig. 45. *Trematoceras* sp. indet., NMNS PM23463, from NT01-04. Arrow indicates position of last septum.

China.

Material examined: Five specimens, NMNS PM23464–23468, from BT01-14, one specimen, NMNS PM23469, from BT02-03, one specimen, NMNS PM23470, from a float limestone block at BT03, one specimen, NMNS PM23471, from KC01-10, and three specimens, NMNS PM23472–23474, from KC01-13.

Description: Evolute, fairly compressed shell with elliptical whorl section, arched venter, indistinct ventral shoulders and slightly convex flanks with maximum whorl width slightly below mid-flank. Umbilicus fairly wide with moderately high, nearly vertical wall and rounded shoulders. Ornamentation consists of regularly spaced, strong, radial or slightly rursiradiate rounded ribs arising on umbilical shoulder and fading away on ventral shoulder. Suture ceratitic. First lateral saddle higher than second saddle, and third saddle lower than second saddle. First lateral lobe deep, wide with many denticulations at base, and second lateral lobe one-half depth of first lobe.

Measurements (mm):

Specimen no.	D	U	H	W	U/D	W/H
NMNS PM23466	32.0	13.0	—	—	0.41	—
NMNS PM23467	33.5	15.0	—	—	0.45	—
NMNS PM23472	39.5	17.8	12.4	10.0	0.45	0.81
NMNS PM23464	57.0	25.0	17.0	13.3	0.44	0.78
NMNS PM23465	59.2	28.5	17.0	14.0	0.48	0.82
NMNS PM23470	77.0	38.0	22.0	17.2	0.49	0.78
NMNS PM23468	79.0	42.3	—	—	0.54	—
NMNS PM23474	79.0	40.0	20.0	16.0	0.51	0.80

Discussion: The shell features of the specimens described herein match well with specimens from South China described as *Pseudoceltites*? cf. *angustecostatus* by Brayard and Bucher (2008). However, as Brühwiler *et al*. (2012a, p. 15) later indicated, these Chinaese specimens actually belong to *Preflorianites radians*.

Brühwiler *et al*. (2012a) recently described *Preflorianites radians* from exotic blocks in Oman, and illustrated the intraspecific variation in shell form and ornamentation of this species. One of their specimens, PIMUZ 27316 (Pl. 2, fig. 7), has a slightly narrower umbilicus and weaker ribs than the typical shell of this species (e.g. PIMUZ 27311, Pl. 2, fig. 1). This particular specimen is very similar to a specimen from Timor described as *Xenodiscus bittneri* by Welter (1922, pl. 158, figs. 8–9). Welter's specimen probably should be assigned to *P. radians*.

The specimen described as *Preflorianites* cf. *radians* by Brühwiler *et al*. (2012c, PIMUZ 28201) from Spiti exhibits a slightly more involute coiling than *P. radians*, but this specimen is slightly flattened. Had its shell not been deformed, its coiling would be more evolute, which would fit well within the range of variation of *P. radians*.

Specimens attributed to *Preflorianites* cf. *radians* by Brayard and Bucher (2008) from the *Flemingites rursiradiatus* beds (lowest Middle Smithian) of South China have weaker ornamentation and thicker whorls than *P. radians*. This taxon probably represents the ancestor of *P. radians* because it is otherwise very similar.

Occurrence: Described specimens from BT01-14, BT02-03, BT03, KC01-10 and KC01-13 within the portion of the *Novispathodus* ex gr. *waageni* Zone that includes the *Leyeceras* horizon of the *Owenites koeneni* beds (middle Middle Smithian = middle Lower Olenekian) in the Bac Thuy Formation, northeastern Vietnam. This species also occurs in the Middle Smithian of South China (*Owenites koeneni* beds, Brayard and Bucher, 2008), Timor (Welter, 1922), Spiti (*Truempyceras compressum* horizon, Brühwiler *et al*., 2012c), and Oman (*Owenites koeneni* fauna, Brühwiler *et al*., 2012a).

Family Xenoceltidae Spath, 1930

Genus ***Xenoceltites*** Spath, 1930

Type species: *Xenoceltites subevolutus*

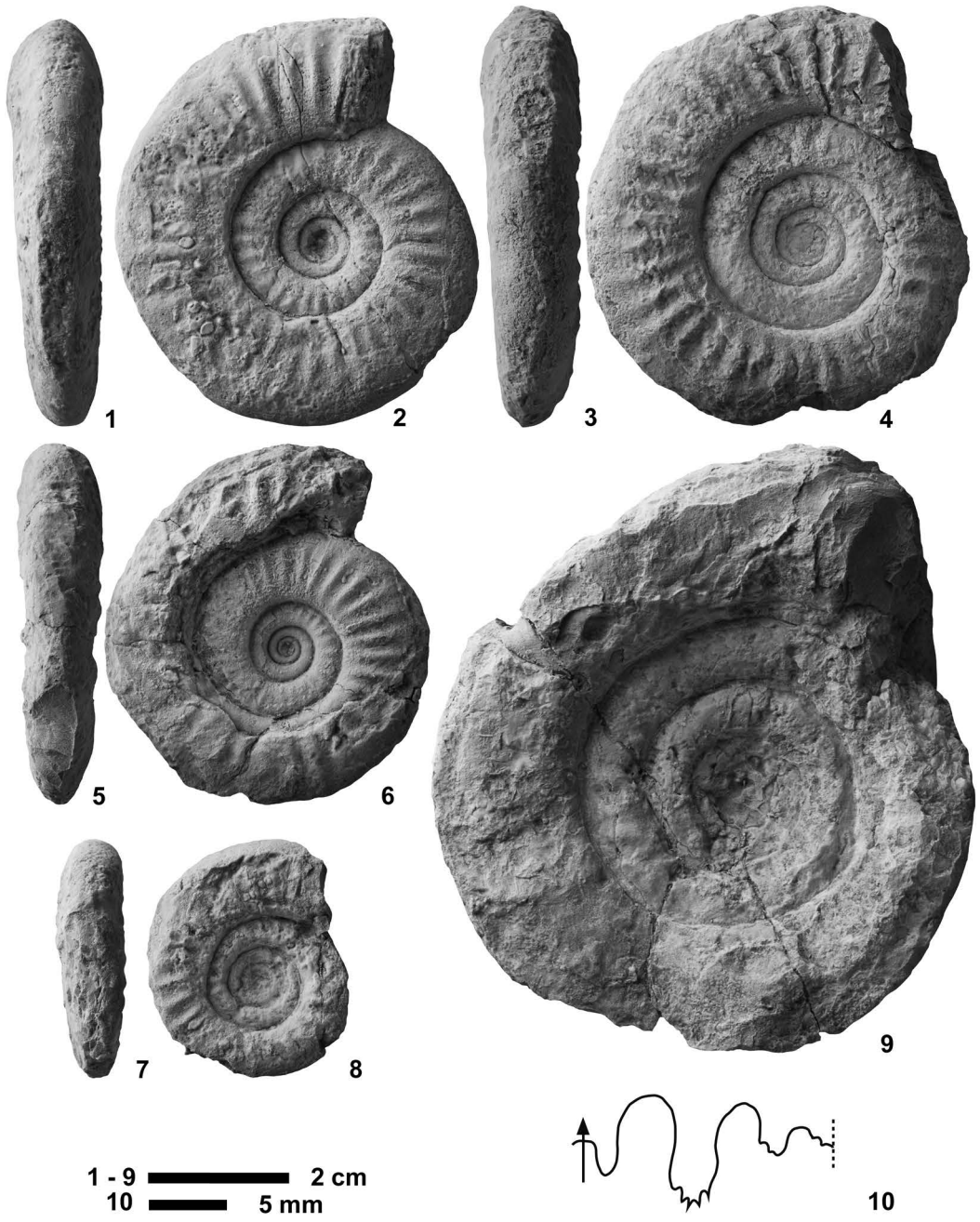

Fig. 46. *Preflorianites radians* Chao, 1959 from BT01-14. 1–2, 10, NMNS PM23464. 3–4, NMNS PM23465. 5–6, NMNS PM23466. 7–8, NMNS PM23467. 9, NMNS PM23468.

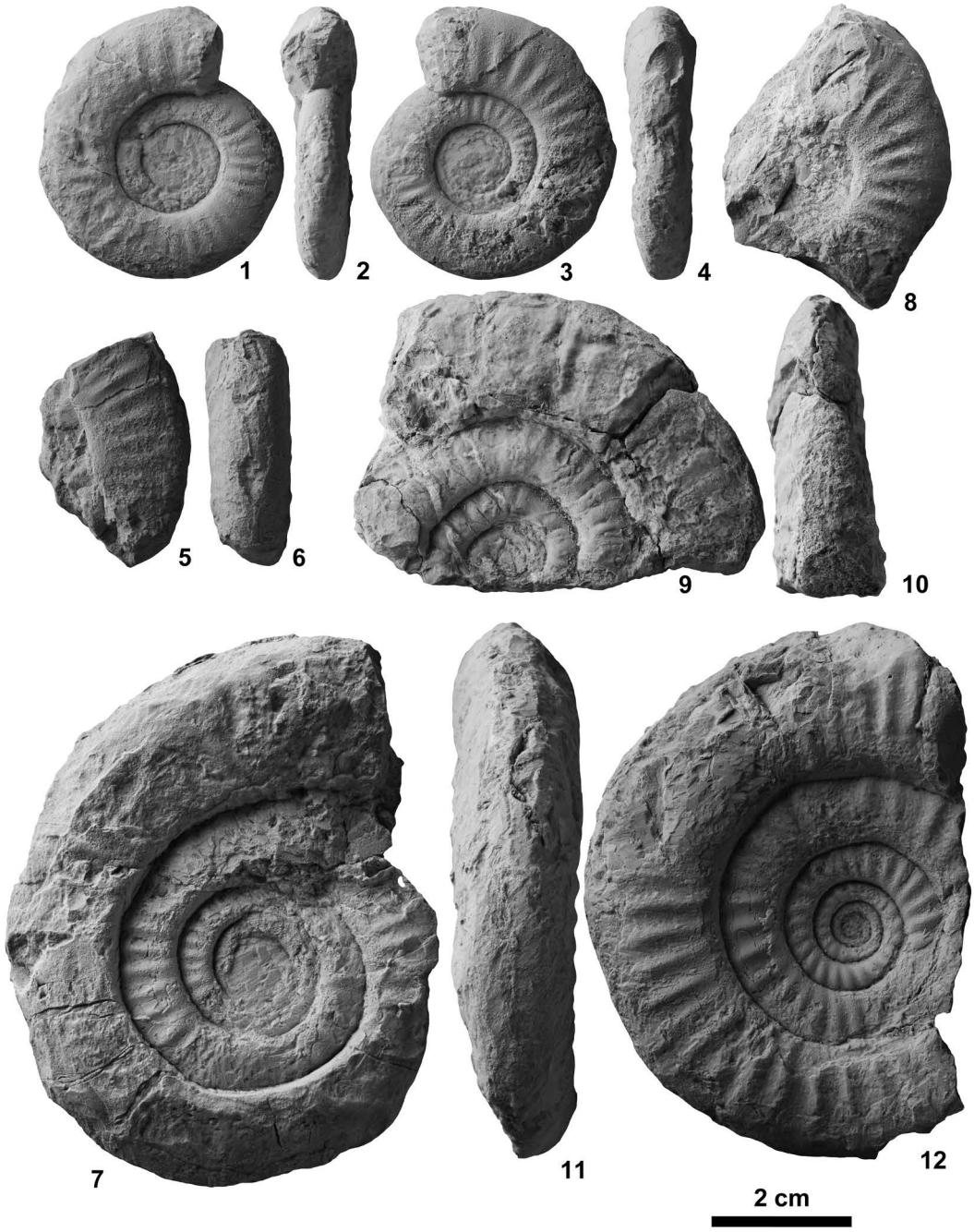

Fig. 47. *Preflorianites radians* Chao, 1959. 1–4, NMNS PM23472, from KC01-13. 5–6, NMNS PM23473, from KC01-13. 7, NMNS PM23474, from KC01-13. 8, NMNS PM23471, from KC01-10. 9–10, NMNS PM23469, from BT02-03. 11–12, NMNS PM23470, from BT03.

Spath, 1930.

Xenoceltites variocostatus Brayard and Bucher, 2008

Figs. 48–51

Xenoceltites variocostatus Brayard and Bucher, 2008, p. 21, pl. 5, figs, 1–14, pl. 6, figs. 1–6, text-fig. 21.

Xenoceltites cf. *variocostatus* Brayard and Bucher, 2008. Brühwiler *et al*., 2010, p. 411, fig. 7.1–7.2; Brühwiler *et al*., 2012b, p. 31, fig. 24A–AG; Brühwiler *et al*., 2012c, p. 134, fig. 14A–G.

Holotype: PIMUZ 25838, figured by Brayard and Bucher (2008, p. 21, pl. 5, fig. 1), from the *Anasibirites multiformis* beds in Waili, northwestern Guangxi, South China.

Material examined: One specimen, NMNS PM23483, from NT01-04, one specimen, NMNS PM23484, from NT01-05, one specimen, NMNS PM23485, from NT01-06, fourteen specimens, NMNS PM23475–23482, 23492–23497, from NT01-07, one specimen, NMNS PM23498, from NT01-09, three specimens, NMNS PM23486–23488, from KC02-10, and one specimen, NMNS PM23489, from BR01-05.

Description: Early whorls (up to 10 mm in diameter): Fairly evolute, fairly compressed to very compressed shell with elliptical whorl section, arched venter, indistinct ventral shoulders and slightly convex flanks with maximum whorl width at mid-flank. Umbilicus moderately wide with low, nearly vertical wall and rounded shoulders. Ornamentation consists of conspicuous, sinuous, prorsiradiate ribs arising at umbilical shoulder, becoming strongly projected at ventral shoulders, and crossing venter in an acute convex arch.

Middle whorls (10–50 mm in diameter): As size increase, elliptical whorl section tends to become more compressed, with narrow rounded to sub-acute venter and slightly convex flanks with maximum whorl width near mid-flank. Umbilicus varies from fairly narrow to fairly wide with low, oblique wall and rounded shoulders. Distinctive ribs gradually lose strength and become low, weak, fold-type ribs. Shell surface covered by numerous growth lines, which arise at umbilical seam, curve backwards on umbilical shoulder, become sinuous, prorsiradiate, and cross venter in broad convex arch. Suture ceratitic. First lateral saddle nearly equal to second saddle, and third saddle lower than second saddle. First lateral lobe deep, wide with many denticulations at base, and second lateral lobe nearly equal to first lobe.

Later whorls (over 50 mm in diameter): As shell grows larger, whorl section becomes even more compressed and umbilicus becomes narrower. Shell surface ornamented by growth lines as well as low, weak, fold-type ribs.

Measurements (mm):

Specimen no.	D	U	H	W	U/D	W/H
NMNS PM23489	11.7	3.4	5.0	4.0	0.29	0.80
NMNS PM23497	12.1	4.1	4.4	3.3	0.34	0.75
NMNS PM23495	12.7	5.0	4.8	4.2	0.39	0.88
NMNS PM23496	14.1	5.3	4.9	3.6	0.38	0.73
NMNS PM23485	15.3	4.8	6.2	4.0	0.31	0.65
NMNS PM23498	16.5	5.0	7.2	4.2	0.30	0.58
NMNS PM23475	22.2	9.4	7.0	5.3	0.42	0.76
NMNS PM23478	23.0	7.6	9.0	5.6	0.33	0.62
NMNS PM23483	26.0	8.0	10.3	5.4	0.31	0.52
NMNS PM23484	31.5	10.2	12.8	7.2	0.32	0.56
NMNS PM23488	37.0	10.2	15.0	6.8	0.28	0.45
NMNS PM23477	40.0	12.5	15.0	8.5	0.31	0.56
NMNS PM23482	46.0	15.4	17.8	10.0	0.33	0.56
NMNS PM23479	49.0	15.7	19.0	11.0	0.32	0.58
NMNS PM23481	49.3	15.2	19.0	11.2	0.31	0.59
NMNS PM23480	50.0	17.0	17.5	10.5	0.34	0.60
NMNS PM23487	59.0	14.3	25.4	12.3	0.24	0.48
NMNS PM23486	68.0	20.6	28.0	14.3	0.30	0.51

Discussion: NMNS PM23475 has a very similar shell morphology to the type specimens of *Xenoceltites variocostatus*, but most specimens described herein exhibit a slightly narrower umbilicus at comparable shell sizes. Because the other shell features are very similar to those of the types, our specimens are considered to be assignable to *X. variocostatus*. Close scrutiny of the type specimens together with the Vietnam specimens reveals that this species displays a wide range of intra-

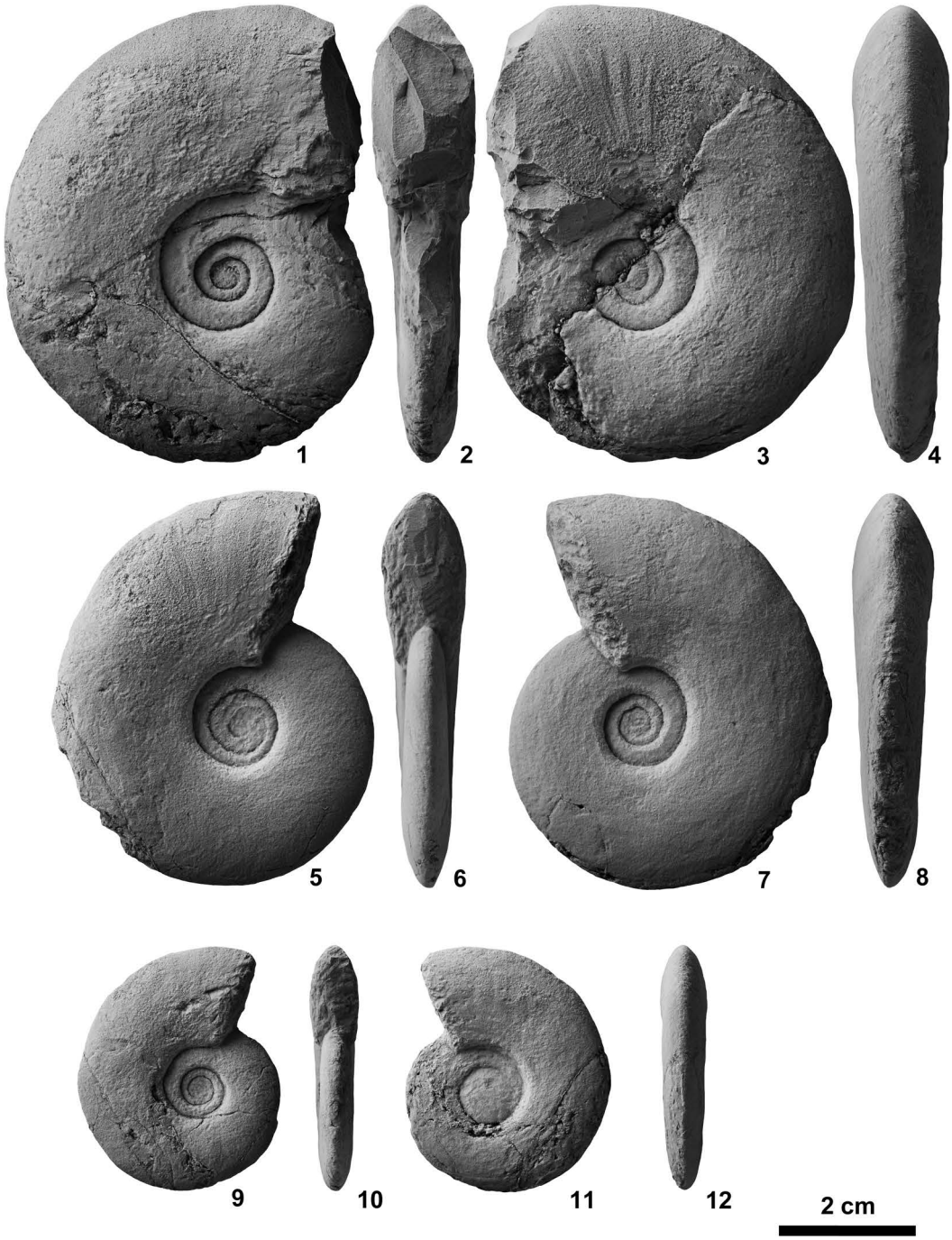

Fig. 48. *Xenoceltites variocostatus* Brayard and Bucher, 2008 from KC02-10. 1–4, NMNS PM23486. 5–8, NMNS PM23487. 9–12, NMNS PM23488.

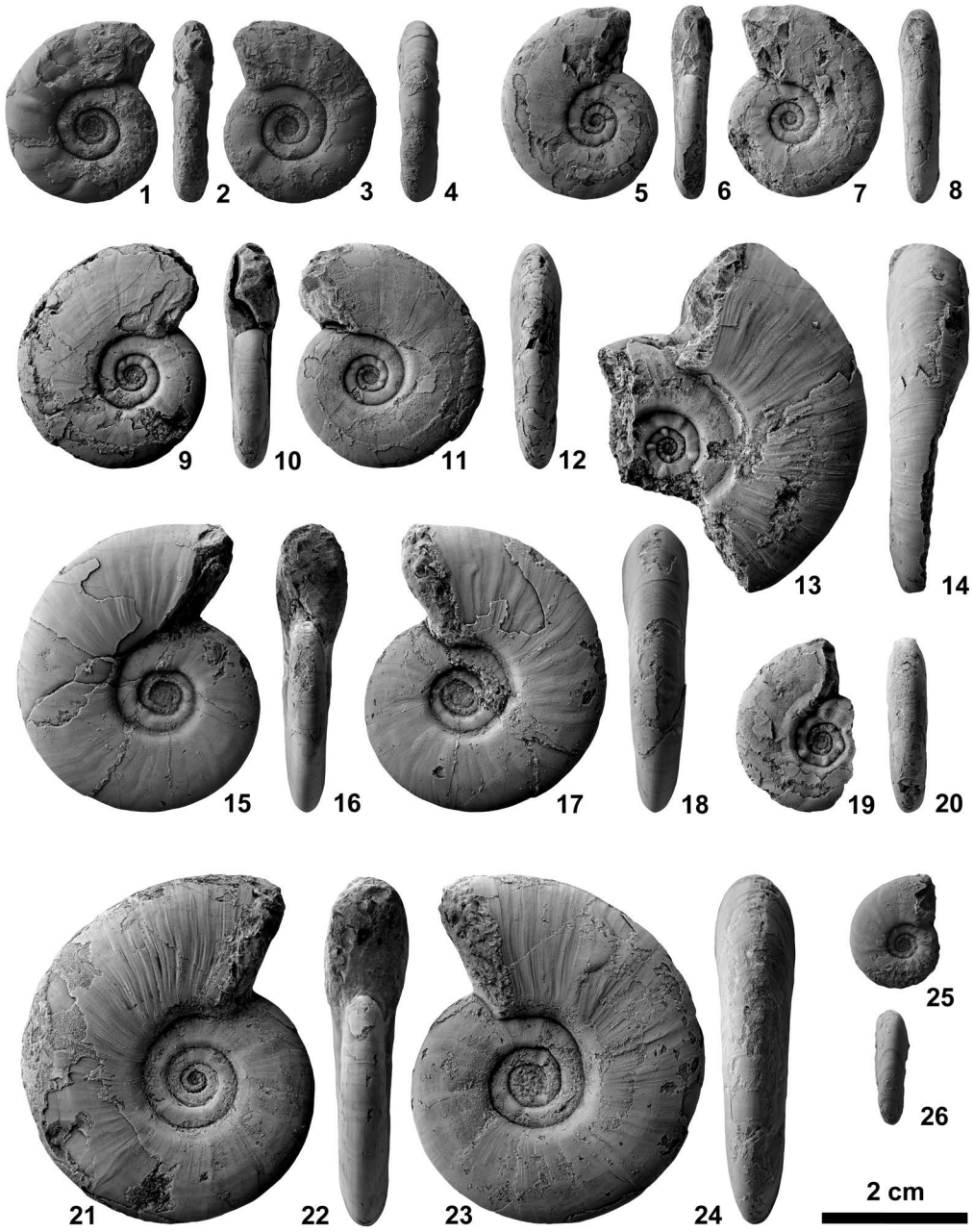

Fig. 49. *Xenoceltites variocostatus* Brayard and Bucher, 2008. 1–4, NMNS PM23475, from NT01-07. 5–8, NMNS PM23483, from NT01-04. 9–12, NMNS PM23484, from NT01-05. 13–14, NMNS PM23476, from NT01-07. 15–18, NMNS PM23477, from NT01-07. 19–20, NMNS PM23478, from NT01-07. 21–24, NMNS PM23479, from NT01-07. 25–26, NMNS PM23485, from NT01-06.

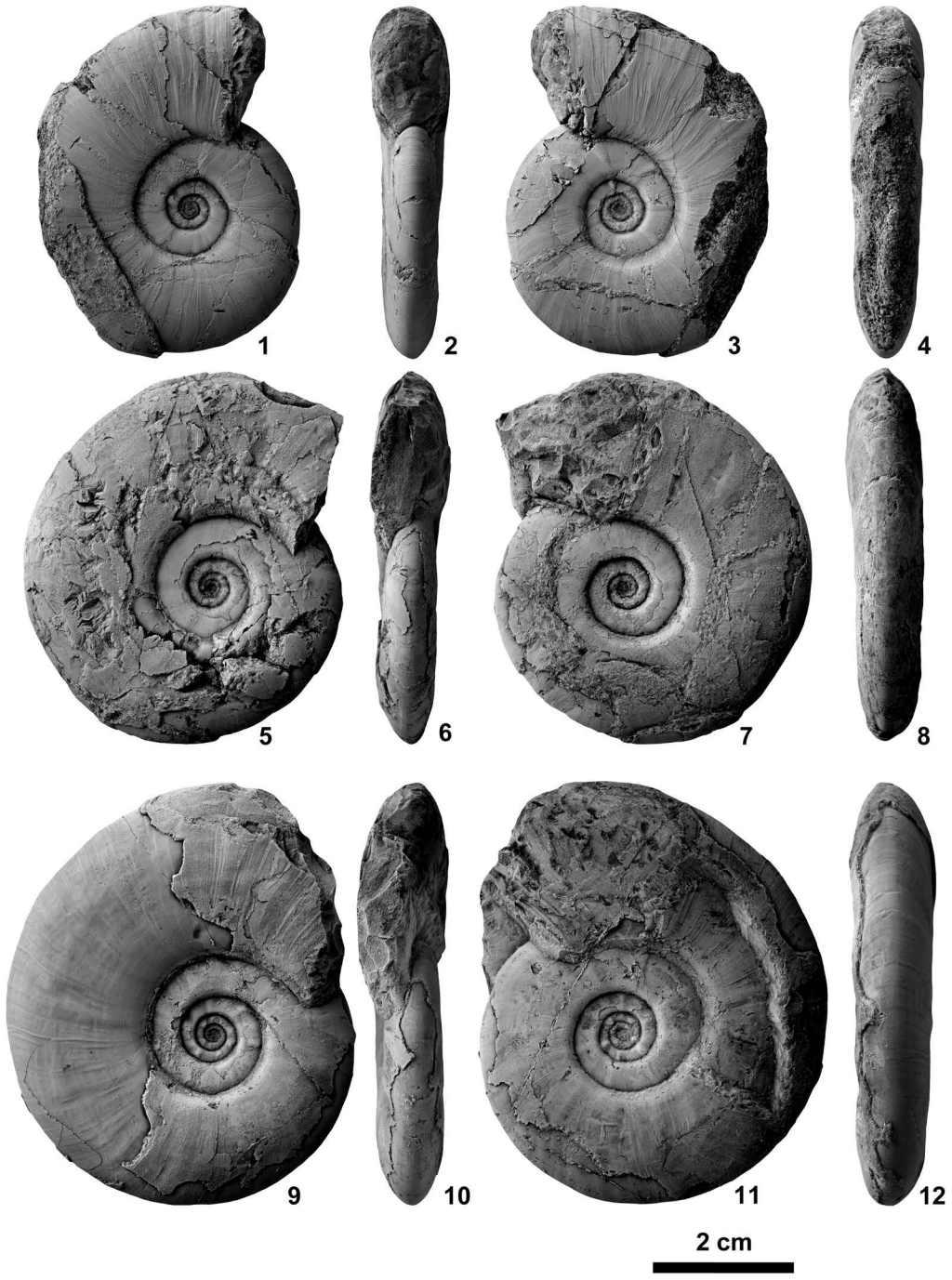

Fig. 50. *Xenoceltites variocostatus* Brayard and Bucher, 2008 from NT01-07. 1–4, NMNS PM23480. 5–8, NMNS PM23481. 9–12, NMNS PM23482.

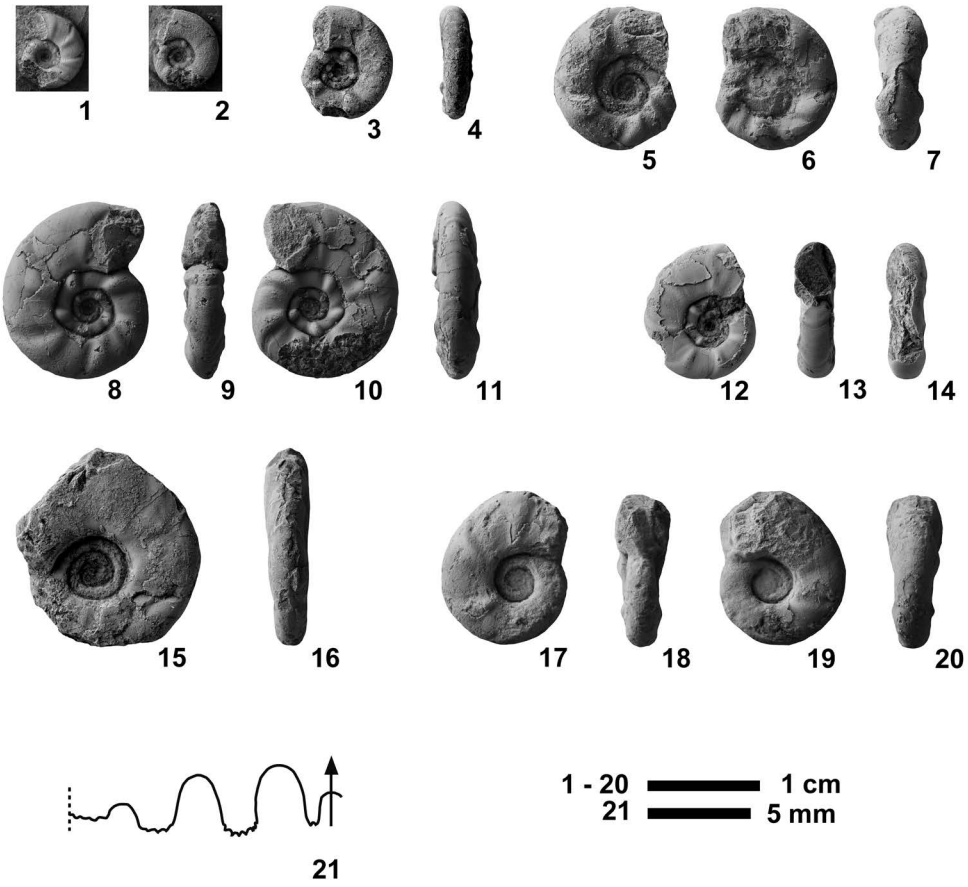

Fig. 51. *Xenoceltites variocostatus* Brayard and Bucher, 2008. 1, NMNS PM23492, from NT01-07. 2, NMNS PM23493, from NT01-07. 3–4, NMNS PM23494, from NT01-07. 5–7, NMNS PM23495, from NT01-07. 8–11, NMNS PM23496, from NT01-07. 12–14, NMNS PM2497, from NT01-07. 15–16, NMNS PM23498, from NT01-09. 17–20, NMNS PM23489, from BR01-05. 21, NMNS PM23484, from NT01-05.

specific variation with respect to umbilical diameter.

Specimens described as *Xenoceltites* cf. *variocostatus* by Brühwiler *et al*. (2010) from South Tibet, Brühwiler *et al*. (2012b) from the Salt Range and Brühwiler *et al*. (2012c) from Spiti all have slightly thinner whorls than the types, but otherwise are very similar. This variation almost certainly should be included within the intraspecific variation of *X. variocostatus.*

Xenoceltites compressus Chao, 1959 from the Middle Smithian of South China is very close to *X. variocostatus*, but differs by its slightly phylloid saddles. It possibly should be assigned to *Subflemingites* Spath, 1934.

Occurrence: Described specimens from NT01-04 to NT01-07, NT01-09, KC02-10 and BR01-05 within the portion of the *Novispathodus pingdingshanensis* Zone represented by the *Xenoceltites variocostatus* beds (Upper Smithian=upper Lower Olenekian) in the Bac Thuy Formation, northeastern Vietnam. This species also occurs in the Upper Smithian in South China (*Anasibirites multiformis* beds, Brayard and Bucher, 2008), South Tibet (*Glyptophiceras sinuatum* beds, Brühwiler *et al*., 2010), Spiti (*Subvishnuites posterus* beds, Brühwiler *et al*., 2012c) and the Salt Range (*Glyptophiceras sinuatum* beds, Brühwiler *et*

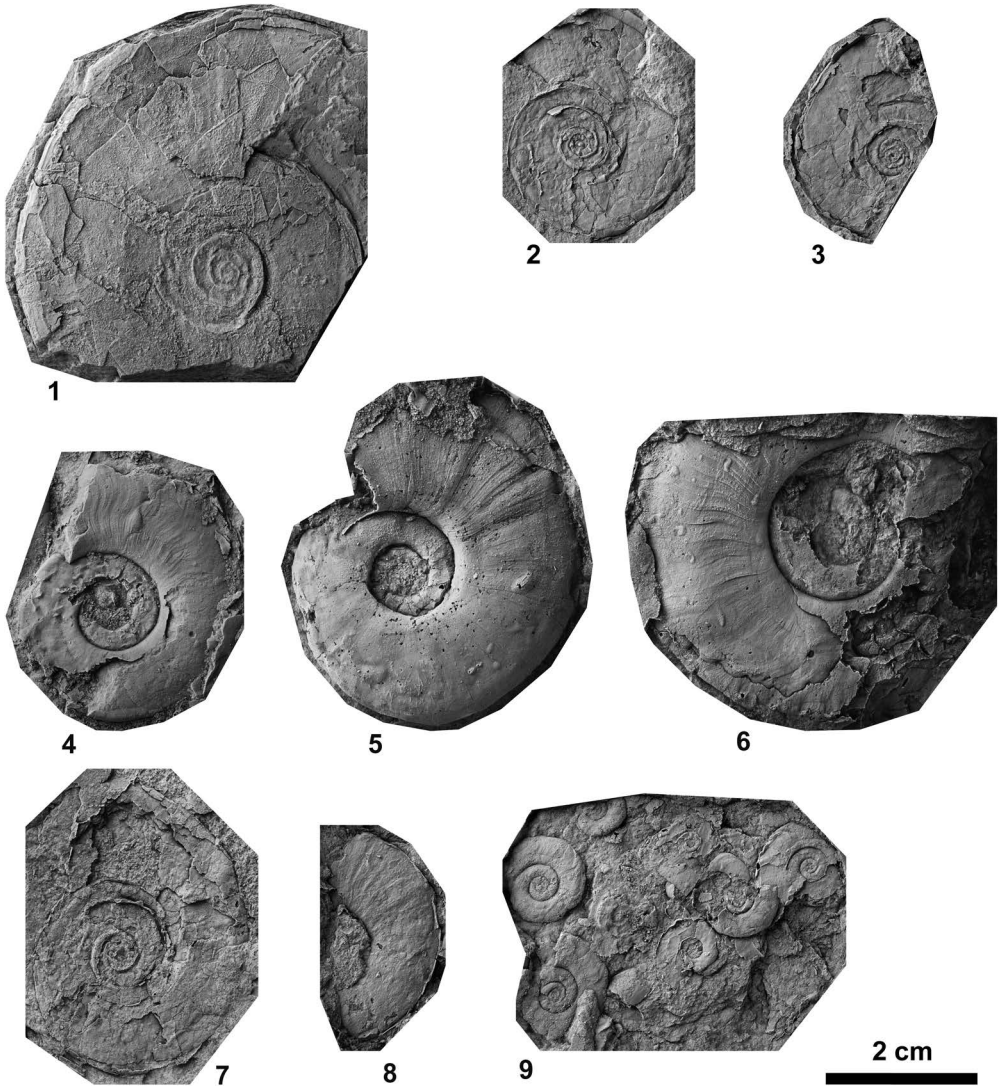

Fig. 52. *Xenoceltites*? sp. indet. 1, NMNS PM23640, from KC02-11. 2, NMNS PM23641, from KC02-11. 3, NMNS PM23642, from KC02-11. 4–8, rubber casts of outer molds. 4, NMNS PM23643, from KC02-15. 5, NMNS PM23644, from KC02-15. 6, NMNS PM23645, from KC02-14. 7, NMNS PM23761, from KC02-12. 8, NMNS PM23490, from BT02-05. 9, NMNS PM23491, from BT02-05.

al., 2012b).

Xenoceltites? sp. indet.

Fig. 52

Material examined: Two specimens, NMNS PM23490–23491, from BT02-05, three specimens, NMNS PM23640–23642, from KC02-11, one specimen, NMNS PM23761, from KC02-12, and three specimens, NMNS PM23643–23645, from KC02-15.

Description: Fairly evolute, very compressed shell with elliptical whorl section, rounded to subacute venter, indistinct ventral shoulders, and slightly convex flanks with maximum whorl width at mid-flank. Umbilicus moderately wide with low, nearly vertical wall and rounded shoulders. Ornamentation consists of low, weak, fold-type ribs. Suture not visible.

Discussion: Assignment of these specimens to *Xenoceltites* is uncertain because of their poor preservation and is based only on the similarity of their morphology with *Xenoceltites*.

Occurrence: Described specimens from KC02-11 within the portion of the *Novispathodus pingdingshanensis* Zone that includes the *Tirolites* cf. *cassianus* beds (lowest Lower Spathian = lowest Upper Olenekian), and those form KC02-12 and KC02-15 within the portion of the *Triasssospathodus symmetricus* Zone that includes the *Tirolites* cf. *cassianus* beds (lowest Lower Spathian = lowest Upper Olenekian) and *Tirolites* sp. nov. beds (Lower Spathian = lower Upper Olenekian) and from BT02-05, whose horizon probably lies within the the *Tirolites* cf. *cassianus* beds in the Bac Thuy Formation, northeastern Vietnam.

Superfamily Meekoceratoidea Waagen, 1895
Family Proptychitidae Waagen, 1895
Genus ***Pseudaspidites*** Spath, 1934

Type species: *Aspidites muthianus* Kraft and Diener, 1909.

Pseudaspidites muthianus (Krafft and Diener, 1909)

Figs. 53–56

Aspidites muthianus Krafft and Diener, 1909, p. 59, pl. 6, fig. 5, pl. 15, figs. 1–2.
Clypeoceras lenticulare Chao, 1959, p. 225, pl. 12, figs. 3–5, text-fig. 19b.
Clypeoceras kwangiense Chao, 1959, p. 226, pl. 17, figs. 1–2, text-fig. 19a.
Pseudaspidites lolouensis Chao, 1959, p. 229, pl. 13, figs. 17–21, text-figs. 20a, 21a.
Pseudaspidites kwangsianus Chao, 1959, p. 230, pl. 12, figs. 6–8, text-fig. 21d.
Pseudaspidites simplex Chao, 1959, p. 231, pl. 13, figs. 6–13, pl. 45, figs. 5–7, text-figs. 20b, 21b.
Pseudaspidites stenosellatus Chao, 1959, p. 231, pl. 13, figs. 4–5, pl. 45, fig. 8, text-fig. 21c.
Pseudaspidites aberrans Chao, 1959, p. 232, pl. 13, figs. 14–15, text-fig. 20d.
Pseudaspidites longisellatus Chao, 1959, p. 232, pl. 13, figs. 1–3, text-fig. 20c.
Proptychites hemialis var. *involutus* Chao, 1959, p. 237, pl. 15, figs. 13–16, text-fig. 24d.
Proptychites markhami Chao, 1959, p. 239, pl. 15, figs. 3–5, text-fig. 23c.
Proptychites sinensis Chao, 1959, p. 240, pl. 16, figs. 5–6, pl. 17, figs. 14–16, text-fig. 22c.
Proptychites angusellatus Chao, 1959, p. 240, pl. 15, figs. 1–2.
Proptychites aff. *trilobatus* Waagen, 1895. Chao, 1959, p. 241, pl. 16, figs. 11–12, text-fig. 24c.
Proptychites latilobatus Chao, 1959, p. 243, pl. 16, figs. 1–2, pl. 19, figs. 4–5.
Proptychites abnormalis Chao, 1959, p. 243, pl. 16, figs. 3–4.
Proptychites sp. A. Chao, 1959, p. 243, pl. 15, figs. 9–12.
Ussuriceras sp. Chao, 1959, p. 247, pl. 19, fig. 1.
Pseudohedenstroemia magna Chao, 1959, p. 265, pl. 41, figs. 13–16, pl. 45, figs. 1–2, text-fig. 32b.
Pseudaspidites muthianus (Krafft and Diener, 1909). Brayard and Bucher, 2008, p. 33, pl. 10, figs. 1–10, pl.

→

Fig. 53. *Pseudaspidites muthianus* (Krafft and Diener, 1909). 1–2, NMNS PM23505, from BT01-11. 3–4, NMNS PM23503, from BT01-05.

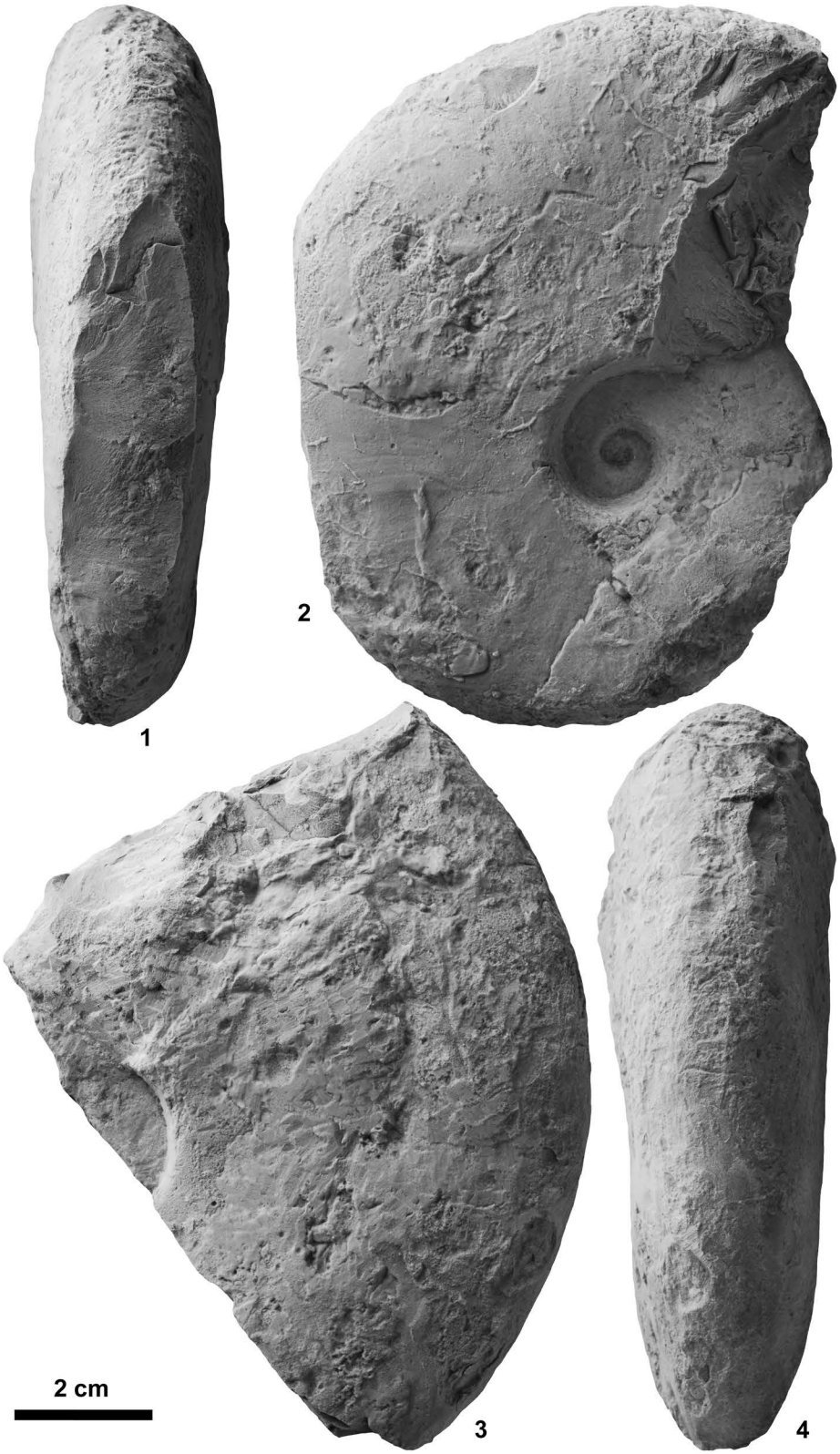
1
2
3
4
2 cm

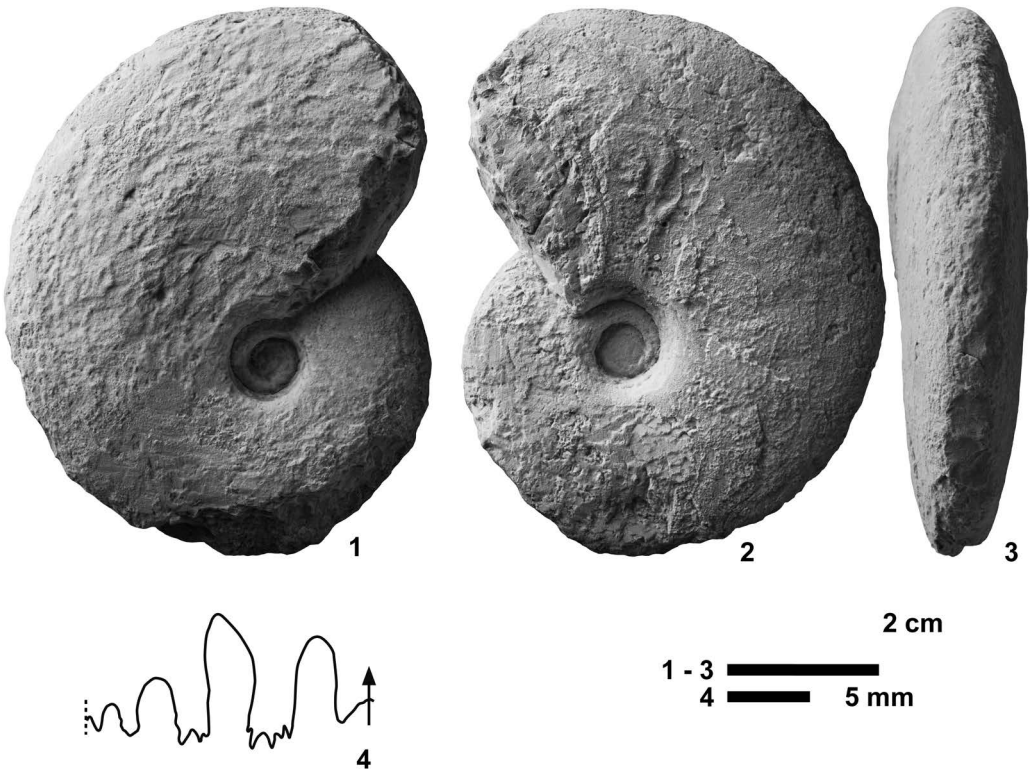

Fig. 54. 1–4, *Pseudaspidites muthianus* (Krafft and Diener, 1909), NMNS PM23504, from BT01-09.

11, figs. 1–4, text-fig. 31; Brühwiler *et al*., 2012c, p. 136, figs. 14M–R.

Pseudaspidites sp. Brühwiler *et al*., 2010, p. 413, fig. 7.11a-e.

non *Pseudaspidites* cf. *muthianus* (Krafft and Diener, 1909). Brühwiler *et al*., 2012a, p. 17, pl. 3, figs. 3–5.

Pseudaspidites cf. *muthianus* (Krafft and Diener, 1909). Brühwiler *et al*., 2012b, p. 53, figs. 37A–B, I.

Lectotype: Specimen designated by Spath (1934, p. 163), is GSI 9404, original of Krafft and Diener (1909, p. 59, pl. 6, fig. 5) from the "*Hedenstroemia*" beds at Mud, Spiti area, northwest Himalayan region.

Material examined: Three specimens, NMNS PM23499–23501, from BT01-03, one specimen, NMNS PM23502, from BT01-04, one specimen, NMNS PM23503, from BT01-05, one specimen, NMNS PM23504, from BT01-09, and one specimen, NMNS PM23505, from BT01-11.

Description: Very involute, very compressed shell with elliptical whorl section, arched venter (juveniles) or subtabulate venter (mature), indistinct ventral shoulders, and slightly convex flanks with maximum whorl width at mid-flank. Narrow umbilicus with moderately high, vertical wall and rounded shoulders. Ornamentation consists of weak radial folds. Suture ceratitic. Lateral saddle elongated, and second saddle slanted slightly toward umbilicus. First lateral lobe deep, wide with many denticulations at base, and second lateral lobe about two thirds depth of first lobe.

Measurements (mm):

Specimen no.	D	U	H	W	U/D	W/H
NMNS PM23500	61.0	7.8	31.7	16.5	0.13	0.52

→

Fig. 55. 1–4, *Pseudaspidites muthianus* (Krafft and Diener, 1909), NMNS PM23499, from BT01-03.


1
2
4
3
2 cm

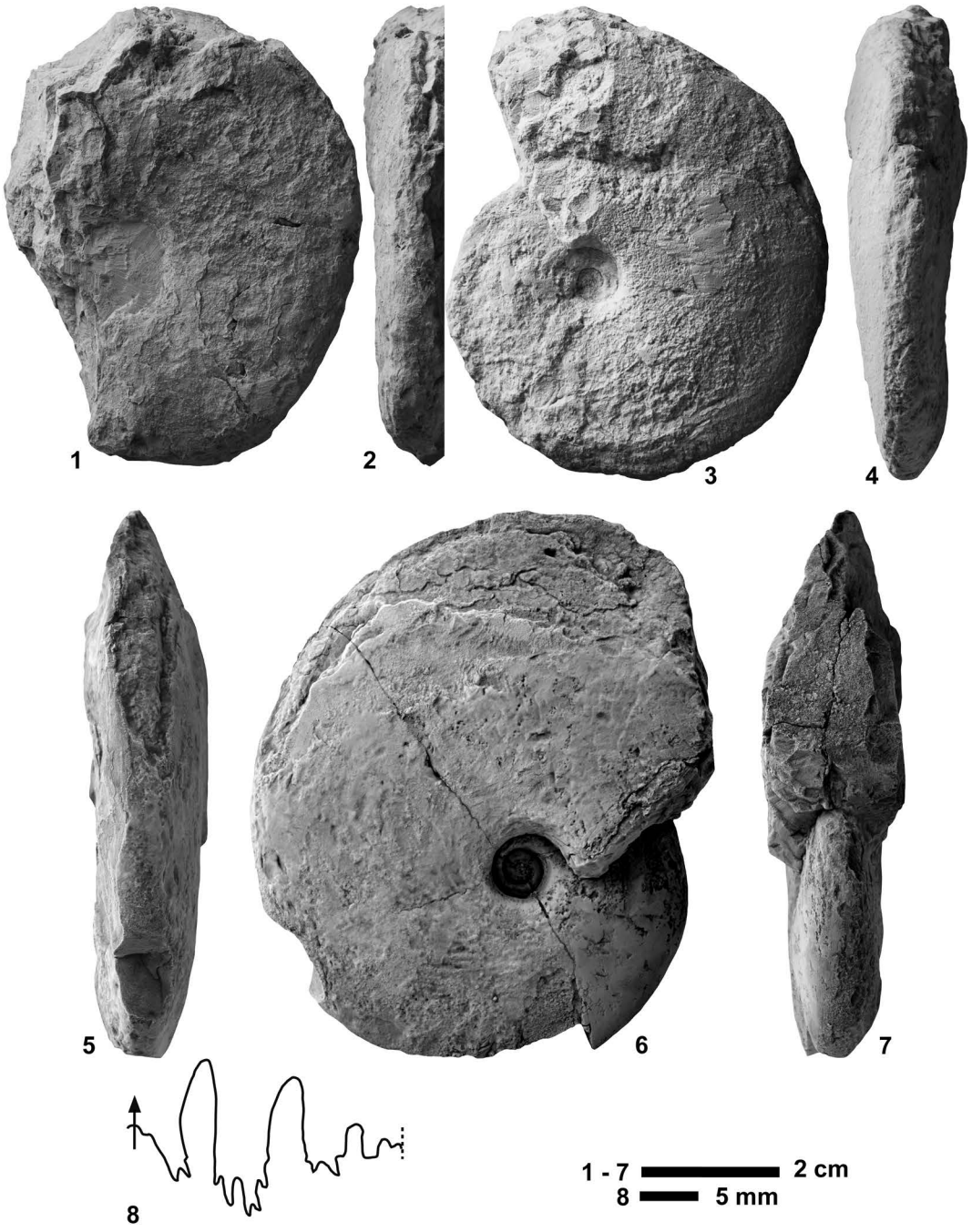

Fig. 56. *Pseudaspidites muthianus* (Krafft and Diener, 1909). 1–2, NMNS PM234502, from BT01-04. 3–4, NMNS PM23500, from BT01-03. 5–8, NMNS PM23501, from BT01-03.

NMNS PM23504	73.0	10.1	40.0	19.2	0.14	0.48
NMNS PM23501	78.0	8.5	—	—	0.11	—
NMNS PM23499	87.0	12.0	46.5	20.5	0.14	0.44
NMNS PM23505	105.5	17.0	52.0	28.0	0.16	0.54
NMNS PM23503	—	—	64.0	33.0	—	0.52

Discussion: Brayard and Bucher (2008) discussed and illustrated the intraspecific variation of *Pseudaspidites muthianus* from South China and synonymized many species described by Chao (1959). we agree with their analysis. According to this demonstrated range of intraspecific variation, a specimen described as *Pseudaspidites* sp. by Brühwiler *et al*. (2010) from South Tibet should be included within the intraspecific variation of *P. muthianus*. A specimen from the Salt Range described as *P.* cf. *muthianus* by Brühwiler *et al*. (2012b) is more evolute than specimens of *P. muthianus* of comparative size from South China and Spiti. This particular specimen may represent an evolute variant as stated by Brühwiler *et al*. (2012b, p. 53), because it otherwise is very similar. In contrast, specimens described as *P.* cf. *muthianus* by Brühwiler *et al*. (2012a) from exotic blocks in Oman have a subammonitic suture that is very similar to that of Ussuritid ammonoids. These specimens probably should be assigned to Ussuritids.

Smith (1932) described three specimens from Idaho as *Clypeoceras muthianum*, and Kummel and Steele (1962) later erected *Pseudaspidites wheeleri* based on these three specimens (Smith, 1932, pl. 27, figs. 1, 2). This species differs from *P. muthianus* by its much more involute coiling.

Occurrence: Described specimens from BT01-03, BT01-04, BT01-05, BT01-09 and BT01-11 within the portion of the *Novispathodus* ex gr. *waageni* Zone that includes the *Flemingites rursiradiatus* beds (lowest Middle Smithian = middle Lower Olenekian) and *Urdyceras tulongensis* beds (lower Middle Smithian = middle Lower Olenekian) in the Bac Thuy Formation, northeastern Vietnam. This species also occurs in the Middle Smithian in South China (*Flemingites rursiradiatus* beds and *Owenites koeneni* beds, Brayard and Bucher, 2008), South Tibet (*Brayardites compressus* beds, Brühwiler *et al*., 2010), Spiti (*Brayardites compressus* beds and *Escarguelites spitiensis* horizon, Brühwiler *et al*., 2012c), and the Salt Range (*Radioceras evolvens* beds, Brühwiler *et al*., 2012b).

Genus ***Leyeceras*** Brayard and Bucher, 2008

Type species: *Leyeceras rothi* Brayard and Bucher, 2008.

Leyeceras rothi Brayard and Bucher, 2008

Figs. 57–62

Leyeceras rothi Brayard and Bucher, 2008, p. 39, pl. 14, figs. 1–3.

? *Leyeceras* cf. *rothi* Brayard and Bucher, 2008. Brühwiler *et al*., 2012a, p. 18, pl. 5, figs. 1–5, pl. 6, figs. 1–3.

Holotype: PIMUZ 25964, figured by Brayard and Bucher (2008, p. 39, pl. 14, fig. 3), from the *Owenites koeneni* beds in Jinya, northwestern Guangxi, South China.

Material examined: Two specimens, NMNS PM23518–23519, from BT02-03, one specimen, NMNS PM23520, from a float limestone block at PK01, one specimen, NMNS PM23521, from KC01-11, two specimens, NMNS PM23514, 23522, from KC01-13, and one specimen, NMNS PM23523, from a float limestone block at BT02.

Description: Moderately evolute, very compressed shell with elliptical whorl section, arched or subtabulate venter, indistinct ventral shoulders, and slightly convex flanks with maximum whorl width near mid-flank. Fairly narrow umbilicus with moderately high, vertical wall and rounded shoulders. Ornamentation consists only of radial lirae. Suture ceratitic. Lateral saddle elongated, and second saddle slanted slightly toward umbilicus. First lateral lobe deep, wide with many denticulations at base, and second lateral lobe about two thirds depth of first lobe.

Measurements (mm):

Specimen no.	D	U	H	W	U/D	W/H

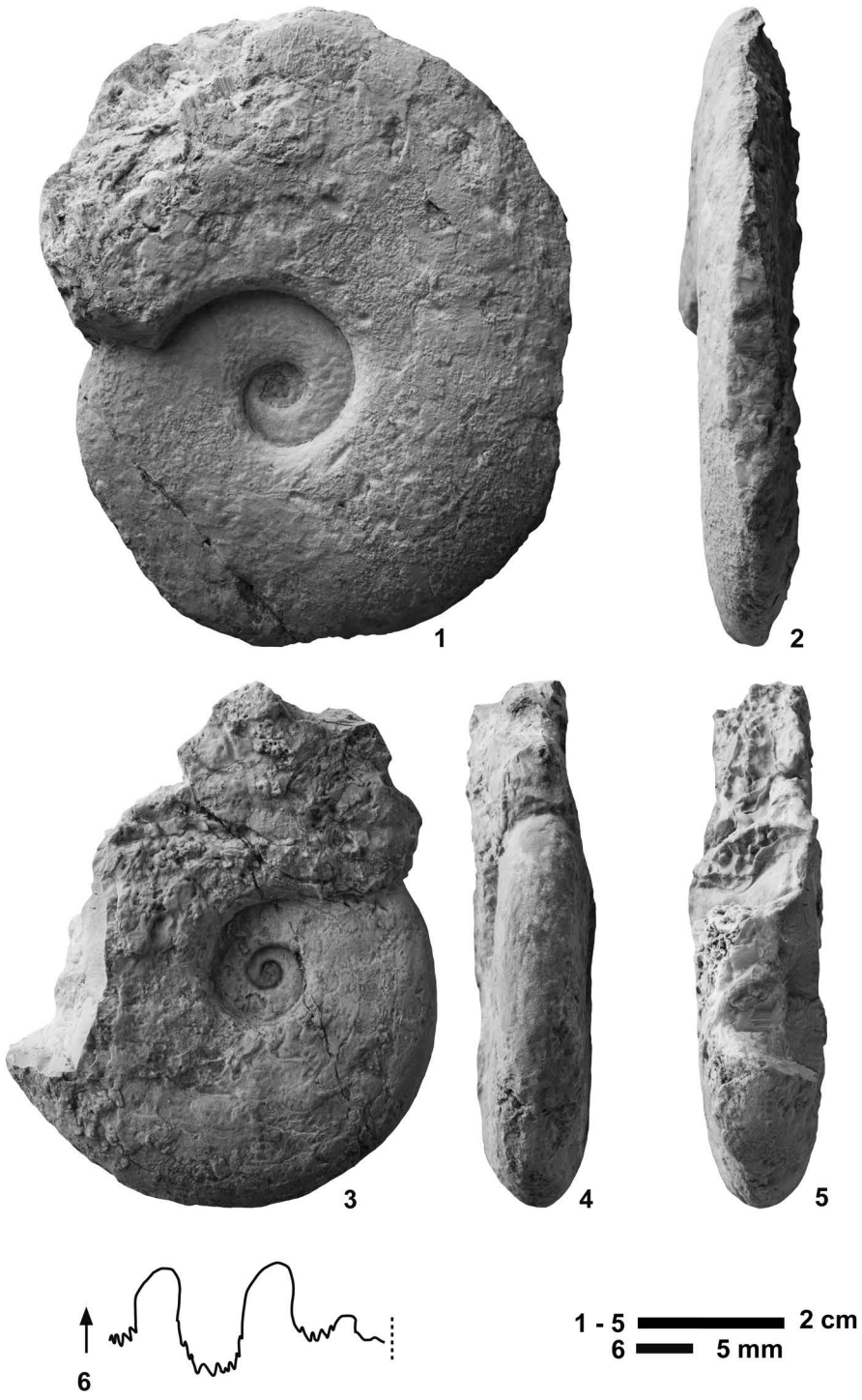

Fig. 57. *Leyeceras rothi* Brayard and Bucher, 2008, from BT02-03. 1–2, NMNS PM23518. 3–6, NMNS PM23519.

Fig. 58. *Leyeceras rothi* Brayard and Bucher, 2008, NMNS PM23523, from a float limestone block at BT02.

Fig. 59. *Leyeceras rothi* Brayard and Bucher, 2008, NMNS PM23523, from a float limestone block at BT02.

Fig. 60. *Leyeceras rothi* Brayard and Bucher, 2008, NMNS PM23523, from a float limestone block at BT02.

Fig. 61. *Leyeceras rothi* Brayard and Bucher, 2008, from KC01-13. 1–2, NMNS PM23522. 3–5, NMNS PM23514.

Fig. 62. *Leyeceras rothi* Brayard and Bucher, 2008. 1–2, NMNS PM23520, from a float limestone block at PK01. 3–4, NMNS PM23521, from KC01-11.

NMNS PM23519	61.0	12.8	31.0	17.0	0.21	0.55
NMNS PM23518	89.0	20.2	40.0	—	0.23	—
NMNS PM23520	94.0	21.7	43.0	10.5	0.23	0.48
NMNS PM23521	100.2	23.0	46.0	—	0.23	—
NMNS PM23522	138.5	28.8	68.4	29.0	0.21	0.42
NMNS PM23523	163.0	39.5	75.0	31.0	0.24	0.41

Discussion: Specimens described as *Leyeceras* cf. *rothi* by Brühwiler *et al*. (2012a) from Oman have more convex flanks than the type specimens of *L. rothi* from South China, but otherwise are very similar. They may be conspecific with *L*. *rothi*.

Occurrence: Described specimens from BT02-03, KC01-11 and KC01-13 within the portion of the *Novispathodus* ex gr. *waageni* Zone that includes the *Leyeceras* horizon of the *Owenites koeneni* beds (middle Middle Smithian=middle Lower Olenekian) in the Bac Thuy Formation, northeastern Vietnam. This species also occurs in the Middle Smithian in South China (*Owenites koeneni* beds, Brayard and Bucher, 2008).

Genus ***Guodunites*** Brayard and Bucher, 2008

Type species: *Guodunites monneti* Brayard and Bucher, 2008.

Guodunites monneti
Brayard and Bucher, 2008
Fig. 63

Guodunites monneti Brayard and Bucher, 2008, p. 83, pl. 44, figs. 1–2; Brayard *et al*., 2009, p. 473, pl. 1, figs. 1–14, text-fig. 3A–C; Brühwiler *et al*., 2012a, p. 19, pl. 7, figs. 1–5.

? *Guodunites* cf. *monneti* Brayard and Bucher, 2008. Jenks *et al*., 2010, p. 10, figs. 6A–D, 7.

Guodunites cf. *monneti* Brayard and Bucher, 2008. Jenks *et al*., 2010, p. 10, fig. 6E–H.

Holotype: PIMUZ 26193, figured by Brayard and Bucher (2008, p. 83, pl. 44, fig. 1), from the *Owenites koeneni* beds in Jinya, northwestern Guangxi, South China.

Material examined: Three specimens, NMNS PM23515–23517, from KC02-02.

Description: Fairly involute, very compressed shell with narrowly rounded venter, indistinct ventral shoulders, and slightly convex flanks with maximum whorl width near mid-flank. Umbilicus fairly narrow with gently inclined wall. Ornamentation consists of distinct, fine strigation on flanks disappearing on venter as well as slightly biconcave growth lines that become strongly projected on ventral shoulders. Suture line not well preserved.

Measurements (mm):

Specimen no.	D	U	H	W	U/D	W/H
NMNS PM23515	29.2	7.7	13.4	7.3	0.26	0.54
NMNS PM23516	59.1	11.4	27.3	12.0	0.19	0.44

Discussion: Jenks *et al*. (2010) described four medium-sized specimens as *Guodunites* cf. *monneti* from western USA. One specimen (Jenks *et al*., 2010, fig. 6E–H) is nearly identical to *G. monneti* from Oman and South China and is clearly conspecific with *G. monneti*. However, the other three specimens have a much wider umbilicus (U/D: 0.25–0.27, Jenks *et al*., 2010, table 4) than *G. monneti* (U/D: 0.18–0.20, Brayard *et al*., 2009, table 1). They may belong to a more evolute form of *G. monneti.*

A poorly preserved specimen described as *Owenites slavini* (Popov, 1962) by Kummel and Erben (1968, p. 124, pl. 21, figs. 3–4; GPIBo. 24) from Afghanistan is characterized as having a very compressed shell with a narrowly rounded venter and slightly convex flanks ornamentated by strigation. The specimen is somewhat similar to *Guodunites monneti* as stated by Brayard *et al*. (2009, p. 476), but differs by stronger strigation covering its flanks and venter. *G. monneti* has fine strigation on its flanks, but it disappears on the venter. Kummel and Erben's (1968) specimen is not conspecific with *G. monneti.*

Occurrence: Described specimen from KC02-02 within the portion of the *Novispathodus* ex gr. *waageni* Zone that includes the *Guodunites* horizon of the *Owenites koeneni* beds (upper Middle Smithian=middle Lower Olenekian) in the Bac Thuy Formation, northeastern Vietnam. This species also occurs in the Middle Smithian in South China (*Owenites*

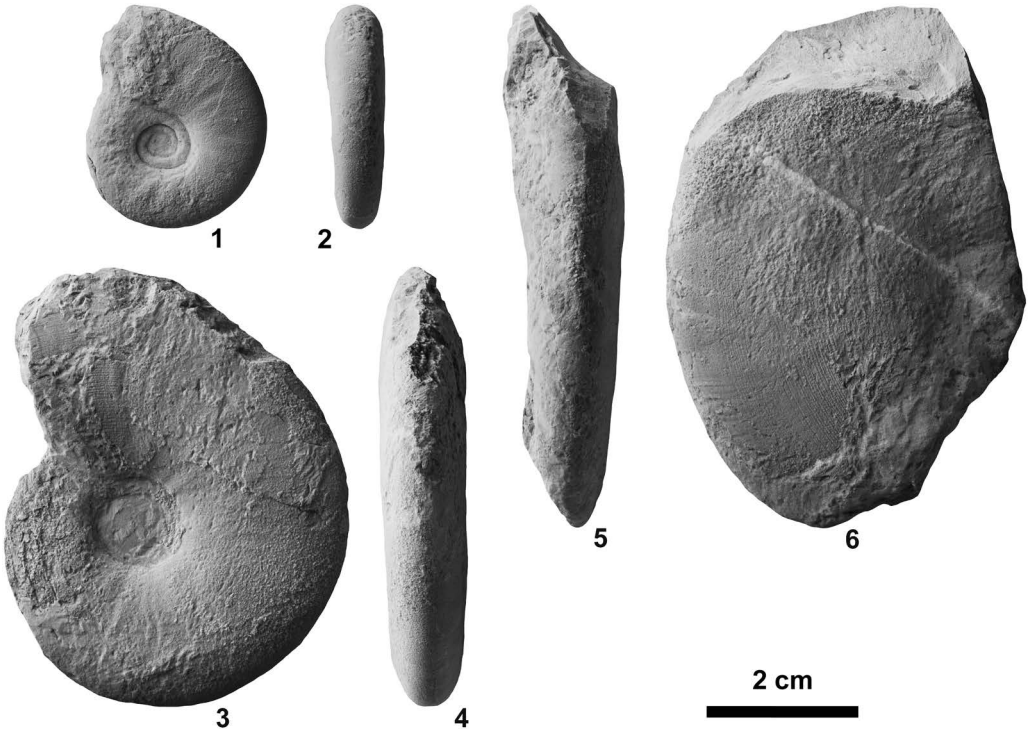

Fig. 63. *Guodunites monneti* Brayard and Bucher, 2008, from KC02-02. 1–2, NMNS PM23515. 3–4, NMNS PM23516. 5–6, NMNS PM23517.

koeneni beds, Brayard and Bucher, 2008), Oman (*Owenites koeneni* fauna, Brühwiler *et al*., 2012a), and western USA (*Meekoceras gracilitatis* Zone, Jenks *et al*., 2010).

Family Dieneroceratidae Spath, 1934
Genus ***Dieneroceras*** Spath, 1934

Type species: *Ophiceras dieneri* Hyatt and Smith, 1905.

Dieneroceras? ***goudemandi*** (Brayard and Bucher, 2008)

Figs. 64–66

?*Dieneroceras tientungense* Chao, 1959, p. 192, pl. 2, figs. 5–6, 8–10, 29.

?*Dieneroceras*? *vermiforme* Chao, 1959, p. 192, pl. 2, figs. 14–16, 28, text-fig. 7b.

?*Dieneroceras ovale* Chao, 1959, p. 192, pl. 2, figs. 11–13, text-fig. 7a.

Pseudoflemingites goudemandi Brayard and Bucher, 2008, p. 49, pl. 22, figs. 1–5, text-fig. 44.

Pseudoflemingites goudemandi Brayard and Bucher, 2008. Brühwiler *et al*., 2012a, p. 24, pl. 14, figs. 4–5.

Holotype: PIMUZ 26004, figured by Brayard and Bucher (2008, p. 49, pl. 22, fig. 2), from the *Owenites koeneni* beds in Jinya, northwestern Guangxi, South China.

Material examined: one specimen, NMNS PM23546, from KC01-01, one specimen, NMNS PM23547, from KC01-10, one specimen, NMNS PM23548, from KC01-11, six specimens, NMNS PM23549–23554, from KC01-13, one specimen, NMNS PM23555, from KC02-02, three specimens, NMNS PM23556–23558, from BT02-03, and two specimens, NMNS PM23559–23560, from BT01-14.

Description: Very evolute, fairly compressed shell with elliptical whorl section, subtabulate venter, slightly rounded shoulders,

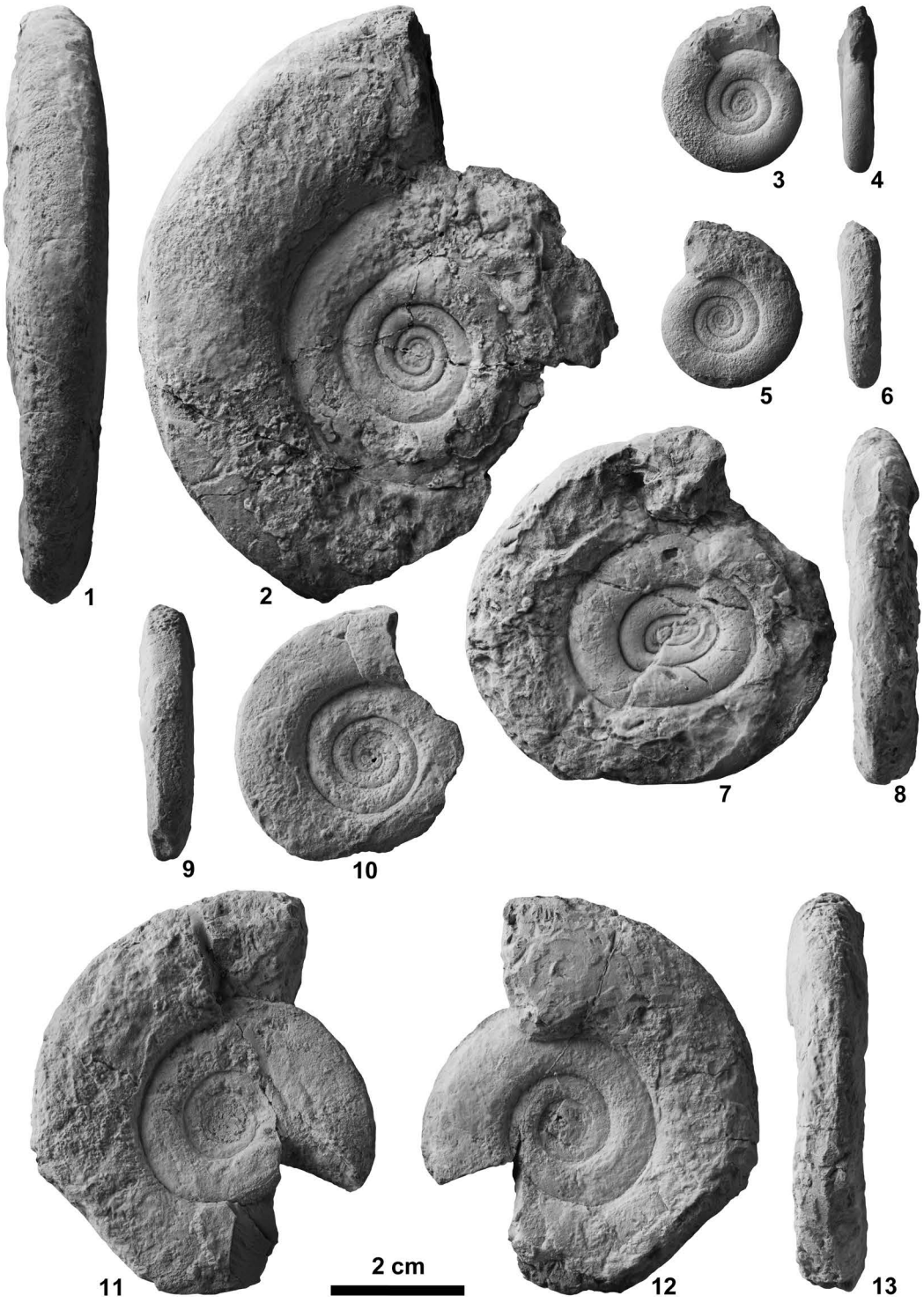

Fig. 64. *Dieneroceras*? *goudemandi* (Brayard and Bucher, 2008). 1–2, NMNS PM23556, from BT02-03. 3–6, NMNS PM23557, from BT02-03. 7–8, NMNS PM23558, from BT02-03. 9–10, NMNS PM23559, from BT01-14. 11–13, NMNS PM23560, from BT01-14.

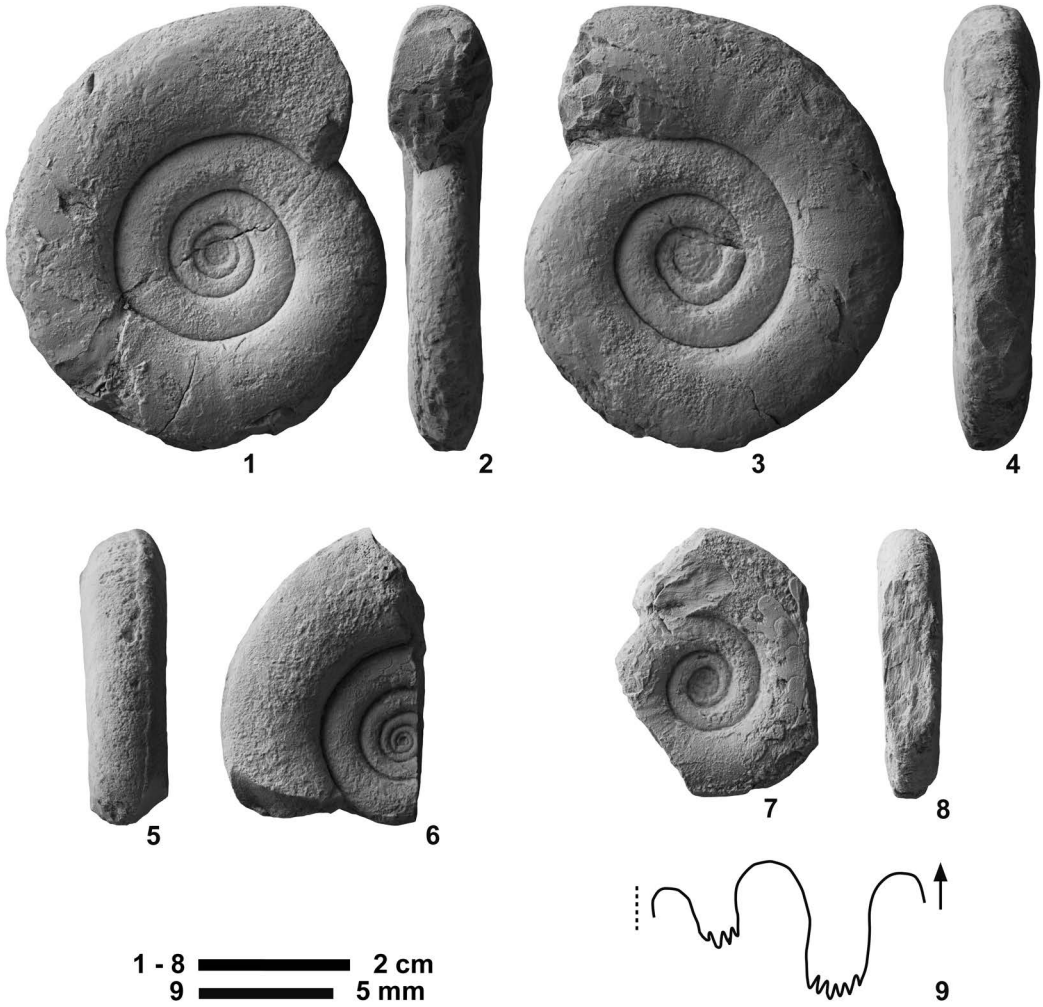

Fig. 65. *Dieneroceras*? *goudemandi* (Brayard and Bucher, 2008), from KC01-13. 1–4, NMNS PM23552. 5–6, NMNS PM23553. 7–9, NMNS PM23554.

and slightly convex flanks with maximum whorl width at mid-flank. Umbilicus fairly wide with low, nearly vertical wall and rounded shoulders. Surface smooth or ornamented with weak radial folds. Suture ceratitic. First lateral saddle nearly equal to second saddle, and third saddle lower than second saddle. First lateral lobe deep, wide with many denticulations at base, and second lateral lobe half depth of first lobe.

Measurements (mm):

Specimen no.	D	U	H	W	U/D	W/H
NMNS PM23557	23.0	10.7	7.1	6.0	0.47	0.85
NMNS PM23549	25.0	11.4	6.8	4.4	0.46	0.65
NMNS PM23553	25.8	12.3	8.3	7.4	0.48	0.89
NMNS PM23555	26.9	13.7	7.3	6.6	0.51	0.90
NMNS PM23550	30.2	13.8	9.5	6.7	0.46	0.72
NMNS PM23546	32.6	14.0	11.0	—	0.43	—
NMNS PM23554	35.3	15.1	11.1	8.3	0.43	0.75
NMNS PM23559	39.0	19.2	11.1	8.0	0.49	0.72
NMNS PM23547	52.5	25.6	16.0	—	0.49	—
NMNS PM23558	54.0	25.9	15.3	11.0	0.48	0.72
NMNS PM23560	55.6	23.8	18.0	11.2	0.43	0.62
NMNS PM23552	60.1	28.0	17.7	12.8	0.47	0.72
NMNS PM23551	73.8	34.3	21.2	14.0	0.46	0.66

Fig. 66. *Dieneroceras*? *goudemandi* (Brayard and Bucher, 2008). 1, NMNS PM23546, from KC01-01. 2–3, NMNS PM23547, from KC01-10. 4–5, NMNS PM23548, from KC01-11. 6–7, NMNS PM23549, from KC01-13. 8–9, NMNS PM23550, from KC01-13. 10–11, NMNS PM23551, from KC01-13. 12–13, NMNS PM23555, from KC02-02.

NMNS PM23556	91.0	43.1	28.0	15.3	0.47	0.55

Discussion: Brayard and Bucher (2008) attributed this species to *Pseudoflemingites* Spath, 1930, but their specimens' elliptical whorl section, subtabulate venter and slightly rounded ventral shoulders do not agree well with the diagnostic characters of *Pseudoflemingites,* which has a narrowly rounded venter and indistinct shoulders. Even though the overall shell morphology of this species is similar to that of *Dieneroceras*, the smooth shell surface differs from *Dieneroceras*, which is characterized by fine strigation. Therefore, the assignment to this genus is questionable.

Chao (1959) described three new species, *Dieneroceras tientungense*, *D.*? *vermiforme*, and *D. ovale*, from the middle Smithian (Owenitan) of South China. Their shells, which are less than 4 cm in diameter, are very similar to the inner whorls of the type specimens of *Pseudoflemingites goudemandi* Brayard and Bucher, 2008. Ultimately, they may be shown to be conspecific with this taxon, but further taxonomic studies are necessary to confirm this attribution.

Occurrence: Described specimen from KC01-01, KC01-010, KC01-11, KC01-13, KC02-02, BT02-03 and BT01-14 within the portion of the *Novispathodus* ex gr. *waageni* Zone that includes the *Owenites koeneni* beds (middle to upper Middle Smithian = middle Lower Olenekian) in the Bac Thuy Formation, northeastern Vietnam. This species also occurs in the Middle Smithian in South China (*Owenites koeneni* beds, Brayard and Bucher, 2008) and Oman (*Owenites koeneni* fauna, Brühwiler *et al*., 2012a).

Family Flemingitidae Hyatt, 1900

Genus ***Flemingites*** Waagen, 1895

Type species: *Ceratites flemingianus* de Koninck, 1863.

Flemingites rursiradiatus Chao, 1959

Figs. 67, 68.1

?*Flemingites evolutus* Chao, 1959, p. 204, pl. 7, figs. 13–14, pl. 8, figs. 5–6, text-fig. 12c.

?*Flemingites nalilingensis* Chao, 1959, p. 205, pl. 6, figs. 6–7, text-fig. 12d.

Flemingites rursiradiatus Chao, 1959, p. 205, pl. 6, figs. 1–5, 8–10, text-fig. 13; Brayard and Bucher, 2008, p. 44, pl. 18, figs. 1–7, pl. 9, figs. 1–3, text-fig. 39; Brühwiler *et al*., 2012a, p. 20, pl. 12, figs. 1–5.

Flemingites ellipticus Chao, 1959, p. 206, pl. 4, figs. 5–7, 10–12, text-fig. 12a.

?*Flemingites ellipticus* var. *kaohwaiensis* Chao, 1959, p. 207, pl. 4, figs. 8–9.

Flemingites kwangsiensis Chao, 1959, p. 208, pl. 8, fig. 8.

Flemingites cf. *rursiradiatus* Chao, 1959. Vu Khuc, 1984, p. 34, pl. 1, figs. 4–5; Vu Khuc, 1991, p. 122, pl. 46, figs. 2–3.

Flemingites aff. *flemingianus* (de Koninck, 1863). Vu Khuc, 1984, p. 34, pl. 3, fig. 2; Vu Khuc, 1991, p. 122, pl. 46, fig. 1.

Flemingites flemingianus (de Koninck, 1863). Brayard and Bucher, 2008, p. 44, pl. 17, figs. 1–5, text-fig. 38.

Holotype: NIGP 12174, figured by Chao (1959, p. 205, pl. 6, figs. 8–10), from the Flemingitan (lower Smithian) in the Linglo district (Lolou), western Guangxi, South China.

Material examined: Five specimens, NMNS PM23506–23509, 23513 from BT01-03, one specimen, NMNS PM23510, from BT01-05 and one specimen, NMNS PM23511, from BT02-01.

Description: Very evolute, fairly compressed shell with elliptical to subquadratic whorl section, subtabulate venter, rounded ventral shoulders, and slightly convex flanks with maximum whorl width at mid-flank. Umbilicus fairly wide with moderately high, nearly vertical wall and rounded shoulders. Ornamentation consists of conspicuous, dense strigation covering entire shell and variable strength, radial to conspicuous rursiradiate ribs arising on umbilical shoulder and fading away on ventral shoulder. Suture not preserved.

Measurements (mm):

Specimen no.	D	U	H	W	U/D	W/H
NMNS PM23513	21.0	10.1	13.0	10.0	0.41	0.77

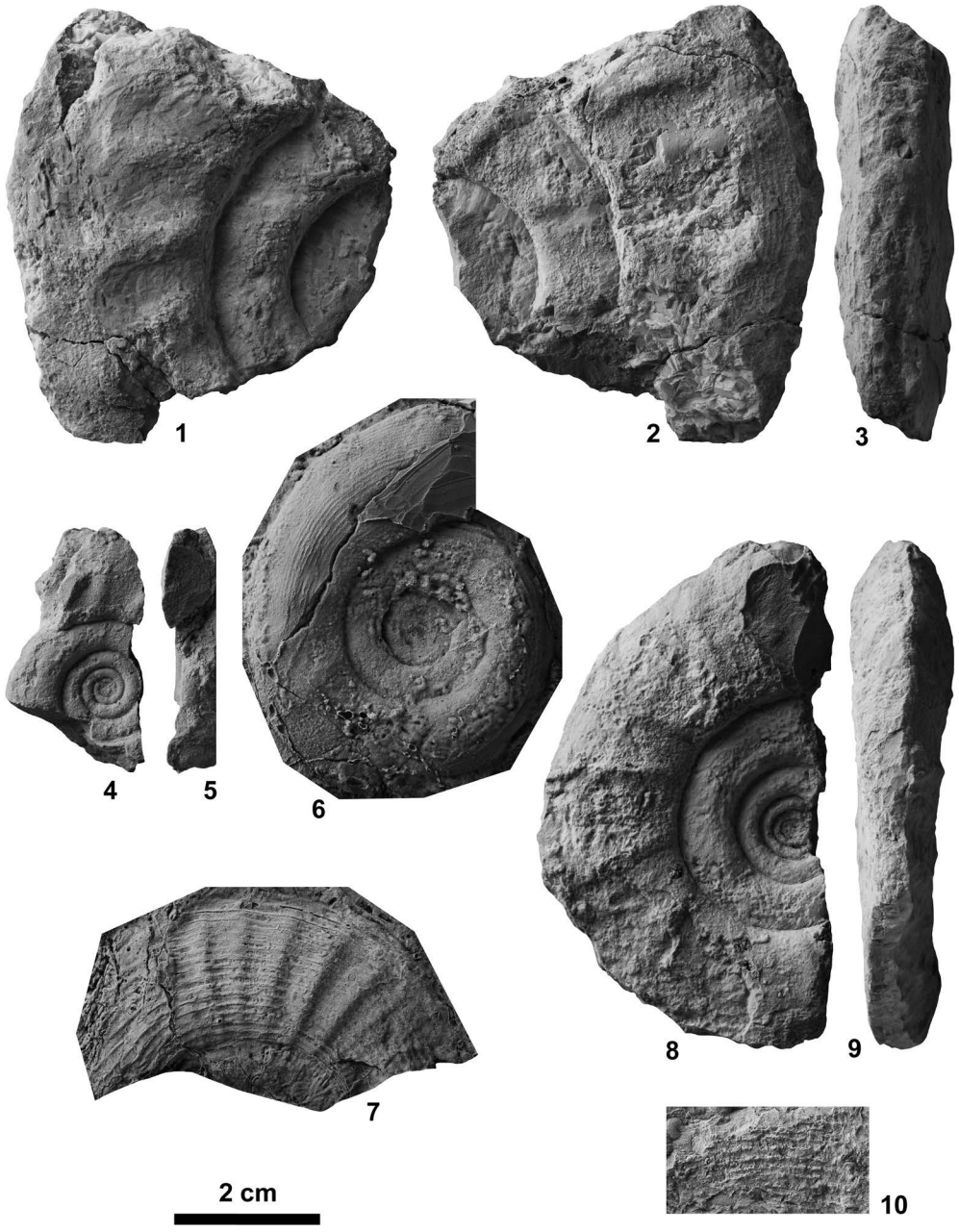

Fig. 67. *Flemingites rursiradiatus* Chao, 1959. 1–3, NMNS PM23511, from BT02-01. 4–5, NMNS PM23513, from BT01-03. 6, NMNS PM23506 (rubber cast of outer mold), from BT01-03. 7, NMNS PM23509 (rubber cast of outer mold), from BT01-03. 8–9, NMNS PM23508, from BT01-03. 10, NMNS PM23510, from BT01-05.

Fig. 68. 1, *Flemingites rursiradiatus* Chao, 1959, NMNS PM23507, from BT01-03. 2, *Euflemingites* sp. indet., NMNS PM23512 (rubber cast of outer mold), from a float limestone block at BT02.

NMNS PM23506	47.0	19.5	7.3	6.1	0.48	0.84
NMNS PM23508	69.5	31.0	20.5	14.5	0.45	0.71
NMNS PM23507	85.0	39.0	—	—	0.46	—
NMNS PM23511	—	—	31.0	17.0	—	0.55

Discussion: Brayard and Bucher (2008) collected many specimens assignable to *Flemingites* from a 3 m thick limestone bed in the Luolou Formation, South China and identified them as *Flemingites rursiradiatus*, *F. flemingianus* and *F. radiates*. Brühwiler *et al*. (2012b, p. 68) later pointed out that specimens described as *F. flemingianus* by Brayard and Bucher (2008) differ from that taxon by their more evolute coiling and lower whorl height at comparable size, and stated that they may represent a weakly ribbed variant of *F. rursiradiatus*. Specimens assigned to *F. rursiradiatus* by Brayard and Bucher (2008) exhibit a wide range of intraspecific variation and they include forms very similar to the types of *F. ellipticus* and *F. kwangsiensis* erected by Chao (1959). This evidence suggests that these two species of Chao are conspecific. Chao's other species, *F. evolutus*, *F. nalilingensis* and *F. ellipticus* var. *kaohwaiensis* are also very similar to juveniles of *F. rursiradiatus*, but it is questionable whether they are conspecific because their ornamentation is poorly preserved.

Occurrence: Described specimens from BT01-03, BT01-05 and BT02-01 within the portion of the *Novispathodus* ex gr. *waageni* Zone that includes the *Flemingites rursiradiatus* beds (lowest Middle Smithian = middle Lower Olenekian) in the Bac Thuy Formation, northeastern Vietnam. This species also occurs in the lowest Middle Smithian in South China (*Flemingites rursiradiatus* beds, Brayard and Bucher, 2008) and Oman (*Flemingites rursiradiatus* fauna, Brühwiler *et al*., 2012a).

Genus ***Euflemingites*** Spath, 1934

Type species: *Flemingites guyerdetiformis* Welter, 1922.

Euflemingites sp. indet.

Fig. 68.2

Material examined: One specimen, NMNS PM23512, from a float limestone block at BT02.

Description: Moderately evolute, very compressed shell with rounded venter, indistinct ventral shoulders, and gently convex flanks forming an elliptical whorl section with maximum whorl width at mid-flank. Umbilicus fairly narrow with moderately high, vertical wall and rounded shoulders. Ornamentation consists of conspicuous, dense strigation covering entire shell. Spiral ridges number about 25 between umbilical shoulders and mid-line of venter. Suture not preserved.

Discussion: The described specimen is very similar to *Euflemingites tsotengensis* Chao, 1959 from South China, *E. guyerdetiformis* (Welter, 1922) from Timor, *E. prynadai* (Kiparisova, 1947) from South Primorye and *E. cirratus* (White, 1879) from western USA, but the fragmental nature of the specimen precludes a definitive species assignment.

Occurrence: Described specimen was found in a float limestone block at BT02. Although the exact horizon from which the block originated is uncertain, judging from the locality where it was found, it certainly came from a limestone bed (Middle Smithian) in the Bac Thuy Formation, northeastern Vietnam.

Genus ***Anaflemingites*** Kummel and Steele, 1962

Type species: *Anaflemingites silberlingi* Kummel and Steele, 1962.

Anaflemingites hochulii Brayard and Bucher, 2008

Figs. 69–72

Anaflemingites hochulii Brayard and Bucher, 2008, p. 51, pl. 23, figs. 3–6, text-fig. 45.

Subflemingites involutus (Welter, 1922). Brühwiler *et al*., 2012a, p. 23, pl. 13, figs. 1–3.

Holotype: PIMUZ 26020, figured by Brayard and Bucher (2008, p. 51, pl. 24, fig. 5), from the *Owenites koeneni* beds in Jinya, northwestern Guangxi, South China.

Material examined: Three specimens, NMNS PM23773–23775, from float limestone blocks at BT02 and five specimens, NMNS PM23776–23780, from KC01-13.

Description: Moderate to fairly evolute, very compressed shell with elliptical whorl section, rounded venter, indistinct ventral shoulders, and slightly convex flanks with maximum whorl width at mid-flank. Umbilicus moderately wide with low, gently sloped wall and rounded shoulders. Ornamentation on juvenile whorls consists of sinuous growth lines and weak strigation near venter. Suture ceratitic. First lateral saddle lower than second saddle. First and second lateral lobes deep, wide with many denticulations at base.

Measurements (mm):

Specimen no.	D	U	H	W	U/D	W/H
NMNS PM23774	33.8	11.2	13.5	8.7	0.33	0.64
NMNS PM23773	43.0	14.8	16.2	10.9	0.34	0.67
NMNS PM23775	60.2	18.8	28.2	13.2	0.31	0.47
NMNS PM23776	82.2	25.6	34.0	14.0	0.31	0.41
NMNS PM23780	151.3	51.9	58.3	21.7	0.34	0.37

Discussion: Specimens described as *Subflemingites involutus* (Welter, 1922) by Brühwiler *et al*. (2012a) from Oman are very similar to *Anaflemingites hochulii*, and are clearly conspecific. *A. silberlingi* Kummel and Steele, 1962 from western USA is also very close to *A. hochulii*, but differs by the fine strigation that covers its entire shell (Jenks *et al*., 2010).

Occurrence: Described specimens from KC01-13 within the portion of the *Novispathodus* ex gr. *waageni* Zone that includes the *Leyeceras* horizon of the *Owenites koeneni* beds (middle Middle Smithian = middle Lower Olenekian) in the Bac Thuy Formation, northeastern Vietnam. This species also occurs in the Middle Smithian in South China (*Owenites koeneni* beds, Brayard and Bucher, 2008) and Oman (*Owenites koeneni* fauna, Brühwiler *et al*., 2012a).

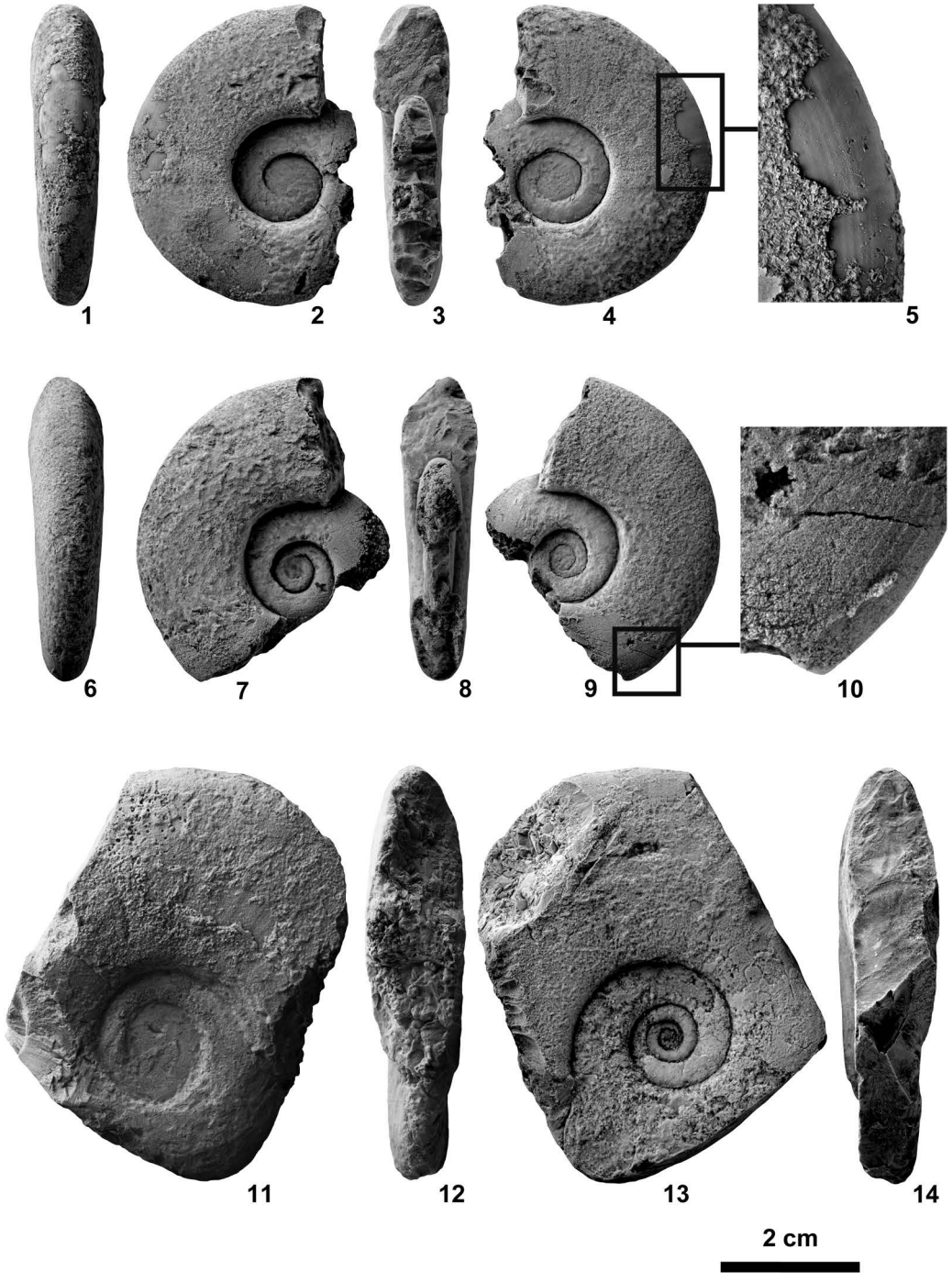

Fig. 69. *Anaflemingites hochulii* Brayard and Bucher, 2008, from float limestone blocks at BT02. 1–5, NMNS PM23773. 6–10, NMNS PM23774. 11–14, NMNS PM23775.

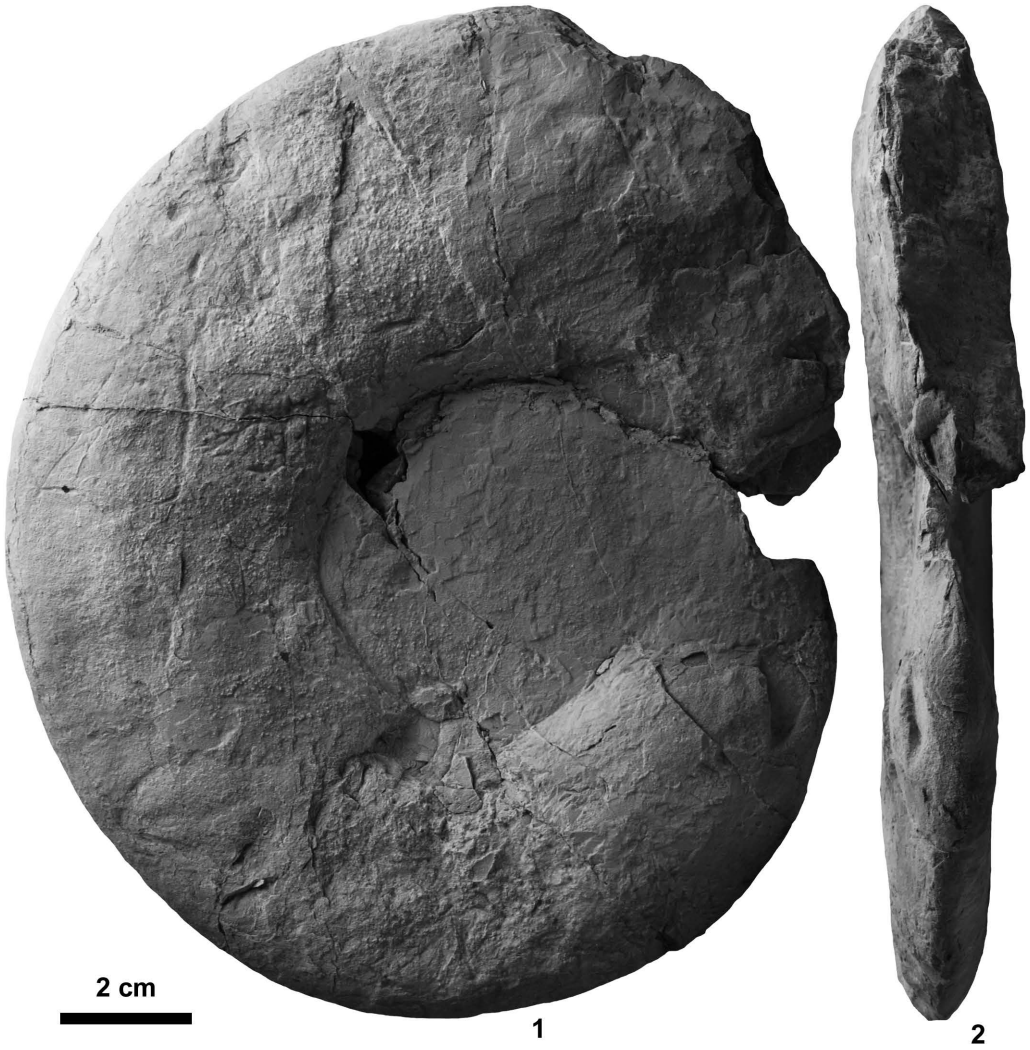

Fig. 70. *Anaflemingites hochulii* Brayard and Bucher, 2008. NMNS PM23780, from KC01-13.

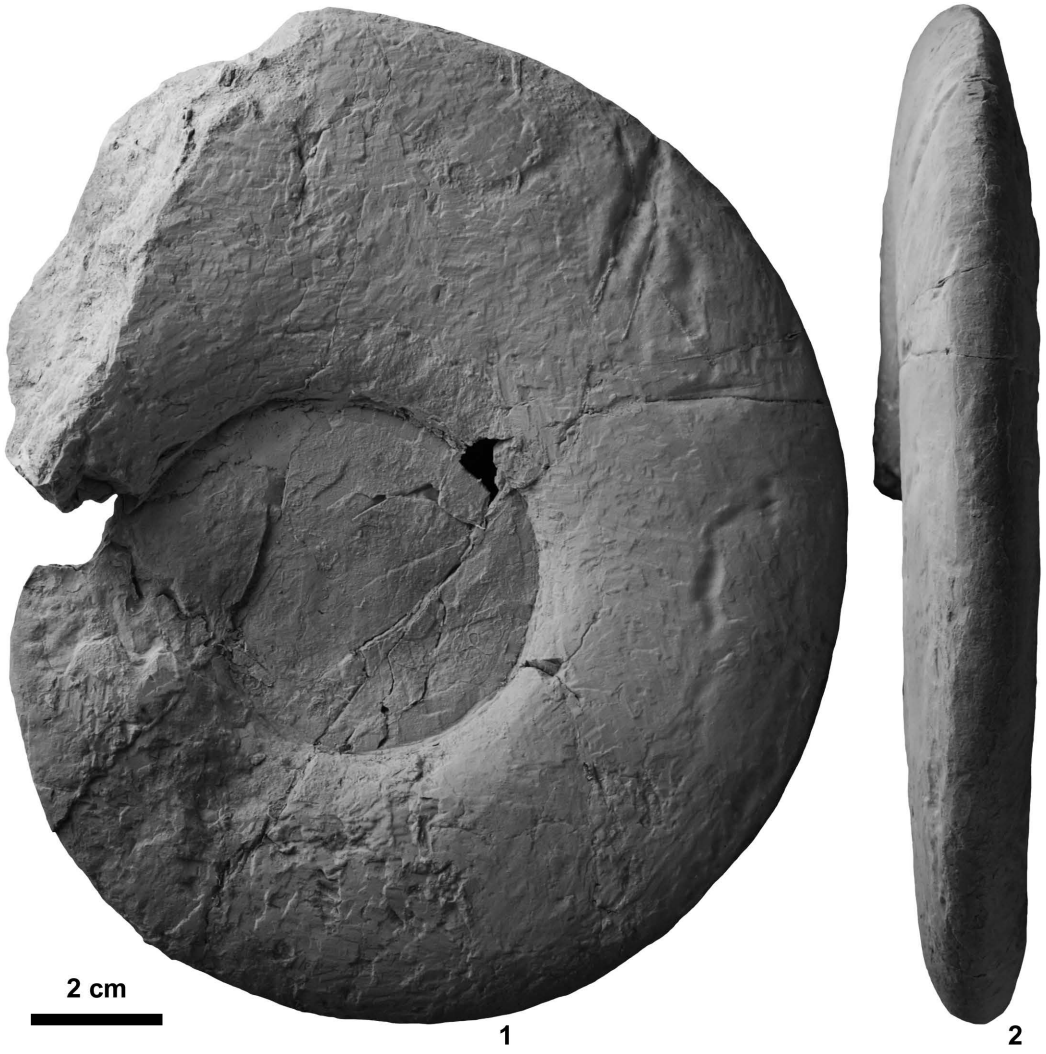

Fig. 71. *Anaflemingites hochulii* Brayard and Bucher, 2008. NMNS PM23780, from KC01-13.

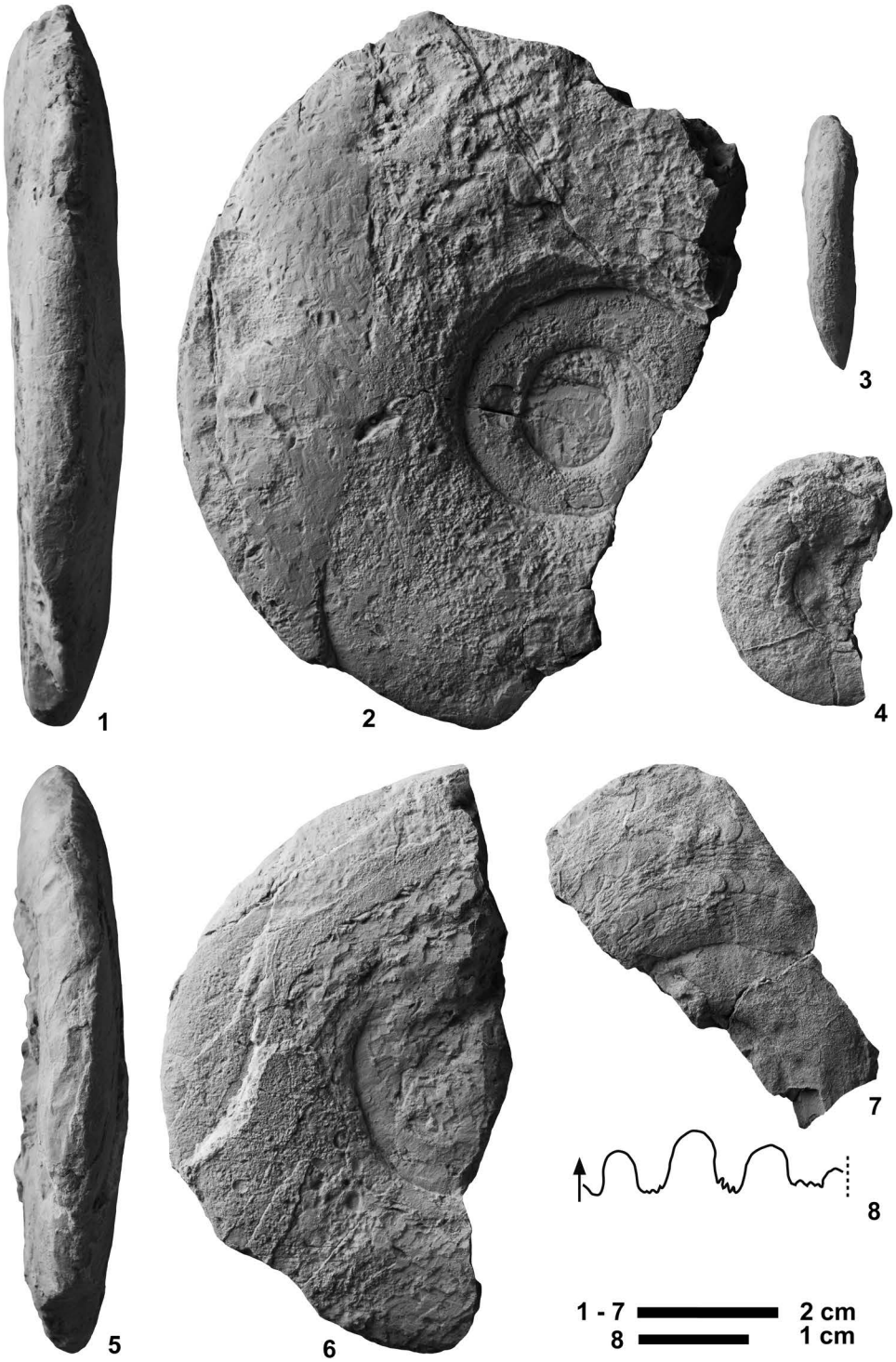

Fig. 72. *Anaflemingites hochulii* Brayard and Bucher, 2008, from KC01-13. 1–2, NMNS PM23776. 3–4, NMNS PM23777. 5–6, NMNS PM23778. 7–8, NMNS PM23779.

Family Galfettitidae Brühwiler *et al*., 2010
Genus ***Galfettites*** Brayard and Bucher, 2008

Type species: *Galfettites simplicitatis* Brayard and Bucher, 2008.

Revised diagnosis: Laterally compressed Galfettitidae with flat, parallel flanks and narrow tabulate venter.

Discussion: Brayard and Bucher (2008) described the venter of the type species of this genus, *Galfettites simplicitatis* as narrowly curved to subtabulate. However, the ventral part of their type specimens is poorly preserved. Recently, Brühwiler *et al*. (2012a) studied and illustrated many well-preserved specimens assignable to *Galfettites* from Oman and stated that the taxon's venter is tabulate. Jenks *et al*. (2010) earlier reported that specimens referable to *Galfettites* from Nevada also have a tabulate venter. Therefore, the original diagnosis of the genus with regard to its venter is revised from a "narrowly curved venter" to a "narrow tabulate venter". *Meekoceras wanneri* Welter, 1922, matches well with the revised diagnosis and is herein assigned to *Galfettites*.

Galfettites simplicitatis
Bryard and Bucher, 2008
Figs. 73, 74

? *Meekoceras wanneri* Welter, 1922,p. 129, pl. 164, figs. 17–18, pl. 165, figs. 18–19.
Galfettites simplicitatis Brayard and Bucher, 2008, p. 48, pl. 21, figs. 1–2, text-fig. 43; Brühwiler *et al*., 2012a, p. 26, pl. 15, figs. 1–4, pl. 16, fig. 1.

Holotype: PIMUZ 26002, figured by Brayard and Bucher (2008, p. 48, pl. 21, fig. 2), from the *Owenites koeneni* beds in Jinya, northwestern Guangxi, South China.

Material examined: One specimen, NMNS PM23781, from a float limestone block at BT02 and two specimens, NMNS PM23782–23783, from BT01-09.

Description: Very evolute, very compressed shell with angular ventral shoulders, and flat parallel flanks for two-thirds of flank, then gradually converging toward tabulate venter. Umbilicus moderately wide with low, nearly vertical wall and rounded shoulders. Ornamentation consists of low, broad, prorsiradiate ribs visible on outer flank. Suture ceratitic with subphylloid saddles. First lateral saddle equal but narrower than second saddle, and third saddle lower. First lateral lobe deep, wide with many denticulations at base, and second lateral lobe half depth of first lobe.

Measurements (mm):

Specimen no.	D	U	H	W	U/D	W/H
NMNS PM23783	41.7	15.1	—	—	0.36	—
NMNS PM23781	93.1	37.5	34.0	15.0	0.40	0.44

Discussion: Brühwiler *et al*. (2012a) previously recognized the similarity in shape of "*Meekoceras*" *wanneri* Welter, 1922 from Timor and *G. simplicitatis*, but they hesitated to synonymize them because the suture line of "*M*." *wanneri* is unknown. However, these similarities in shell morphology and ornamentation provide convincing evidence that the two taxa are almost certainly conspecific.

Occurrence: Described specimens from BT01-09 within the portion of the *Novispathodus* ex gr. *waageni* Zone that includes the *Urdyceras tulongensis* beds (lower Middle Smithian=middle Lower Olenekian) in the Bac Thuy Formation, northeastern Vietnam. This species also occurs in the Middle Smithian in South China (*Owenites koeneni* beds, Brayard and Bucher, 2008) and Oman (*Owenites koeneni* fauna, Brühwiler *et al*., 2012a).

Genus ***Urdyceras*** Brayard and Bucher, 2008

Type species: *Urdyceras insolitus* Brayard and Bucher, 2008.

Urdyceras tulongensis Brühwiler *et al*., 2010
Fig. 75

Urdyceras tulongensis Brühwiler *et al*., 2010, p. 416, fig. 10.5–10.11.

Holotype: PIMUZ 27644, figured by Brühwiler *et al*. (2010, p. 416, fig. 10.6), from the *Brayardites compressus* beds (lower Mid-

Fig. 73. *Galfettites simplicitatis* Brayard and Bucher, 2008. 1–2, NMNS PM23781, from a float limestone block at BT02. 3–5, NMNS PM23782, from BT01-09. 6–7, NMNS PM23783, from BT01-09.

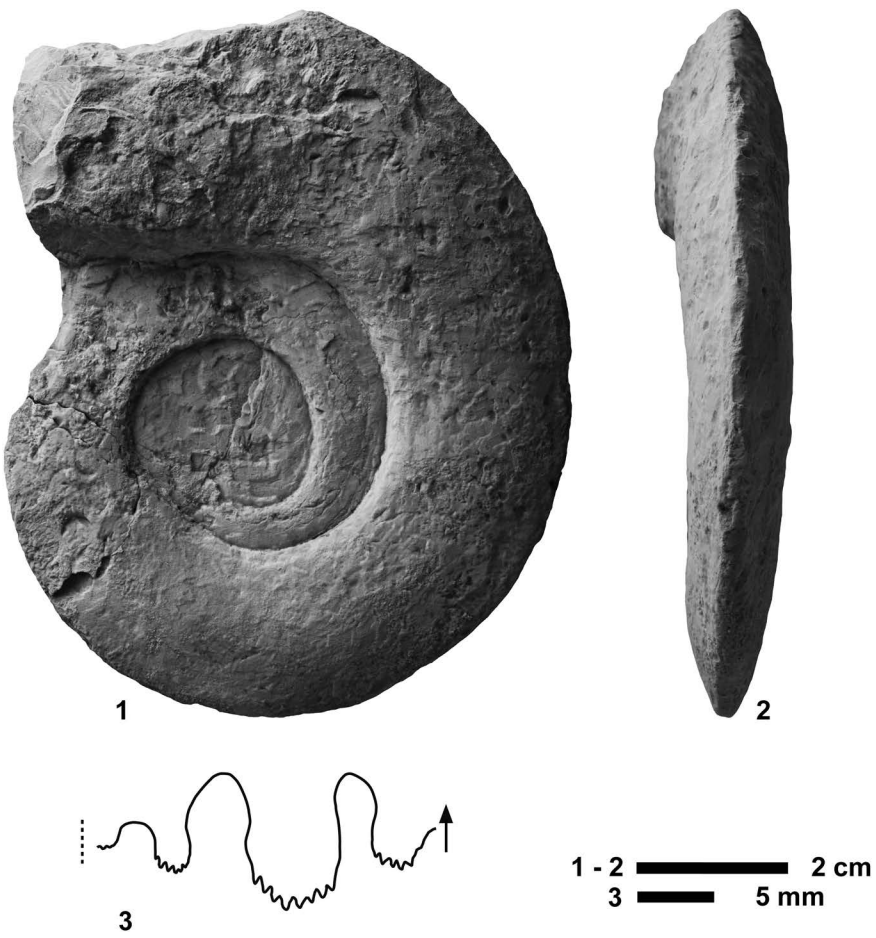

Fig. 74. *Galfettites simplicitatis* Brayard and Bucher, 2008. NMNS PM23781, from BT02-02.

dle Smithian) in Tulong, South Tibet.

Material examined: Four specimens, NMNS PM23785–23788, from BT01-09 and one specimen, NMNS PM23784, from BT02-02.

Description: Moderately evolute, fairly compressed shell with subrectangular whorl section, tabulate venter, angular ventral shoulders, and slightly convex flanks with maximum whorl width near umbilical shoulder. Umbilicus moderately wide with moderately high, nearly vertical wall and rounded shoulders. Ornamentation consists of strong, radial or slightly rursiradiate ribs arising on umbilical shoulder and fading away on ventral shoulder. Suture ceratitic. First lateral saddle lower and narrower than second saddle, and third saddle lower than second saddle. First lateral lobe deep, wide with many denticulations at base, and second lateral lobe half depth of first lobe.

Measurements (mm):

Specimen no.	D	U	H	W	U/D	W/H
NMNS PM23784	22.0	8.2	8.4	6.0	0.37	0.71
NMNS PM23785	25.7	10.0	8.8	7.6	0.39	0.86
NMNS PM23788	33.4	11.0	13.0	9.8	0.33	0.75
NMNS PM23786	43.0	16.7	15.7	11.9	0.39	0.79
NMNS PM23787	74.0	23.0	34.0	22.0	0.31	0.65

Discussion: The described specimens have stronger radial ribs and a wider umbilicus than the holotype of *Urdyceras tulongensis*, but

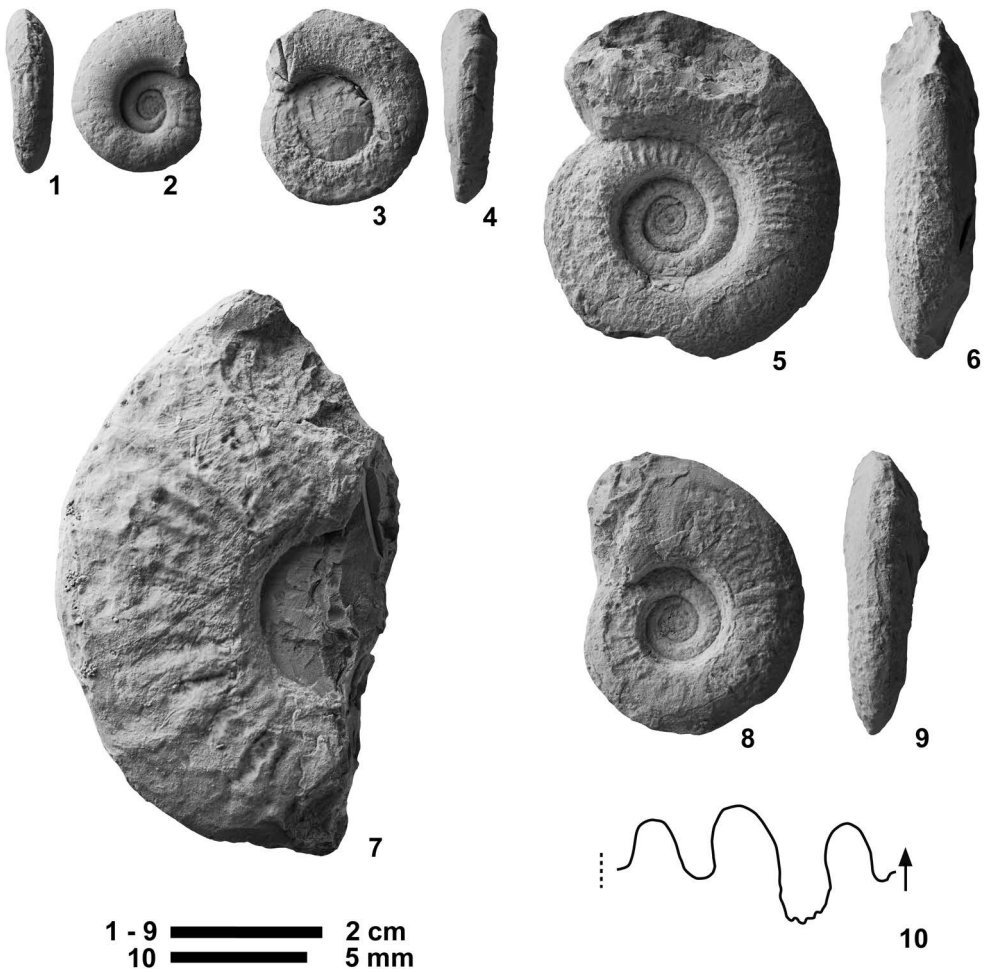

Fig. 75. *Urdyceras tulongensis* Brühwiler *et al*., 2010. 1–2, NMNS PM23784, from BT02-02. 3–10, from BT01-09. 3–4, NMNS PM23785. 5–6, NMNS PM23786. 7, NMNS PM23787. 8–10, NMNS PM23788.

they are very similar to two of the paratypes (i.e. PIMUZ 27643, 27646; Brühwiler *et al*., 2010, fig. 10.5, 10.8), which have strong ribs on their inner flanks and a moderately wide umbilicus. Therefore, the described specimens are considered to fit well within the intraspecific variation of *U. tulongensis*.

The shell diameters of the type specimens of *Urdyceras tulongensis* are less than 40 mm. In contrast, NMNS PM23787 is a partial whorl section more than 74 mm in diameter that shares many similarities with *U. tulongensis*, such as a tabulate venter and radial ribs. This evidence suggests that this particular specimen is probably an adult shell of *U. tulongensis*.

Occurrence: Described specimens from BT01-09 and BT02-02 within the portion of the *Novispathodus* ex gr. *waageni* Zone that includes the *Urdyceras tulongensis* beds (lower Middle Smithian = middle Lower Olenekian) in the Bac Thuy Formation, northeastern Vietnam. This species also occurs at the lower Middle Smithian (*Brayardites compressus* beds) in South Tibet (Brühwiler *et al*., 2010).

Family Arctoceratidae Arthaber, 1911
Genus ***Submeekoceras*** Spath, 1934

Type species: *Meekoceras mushbachanum* White, 1879.

Submeekoceras hsüyüchieni (Chao, 1959)

Figs. 76–78

? *Prionolobus ophionus* var. *involutus* Chao, 1959, p. 201, pl. 9, figs. 11–15, text-fig. 11b.
Prionolobus hsüyüchieni Chao, 1959, p. 202, pl. 9, figs. 9–10, text-fig. 11c.
Paranorites ovalis Chao, 1959, p. 217, pl. 9, figs. 16–19, text-fig. 16b.
Paranorites linguisellatus Chao, 1959, p. 218, pl. 10, figs. 1–2, text-fig. 16c.
Paranorites aff. *linguisellatus* Chao, 1959, p. 218, pl. 10, figs. 3–4.
Meekoceras lativentrosum Chao, 1959, p. 309, pl. 38, figs. 15–18, text-fig. 43a.
Meekoceras densistriatum Chao, 1959, p. 310, pl. 38, figs. 1–3, 19, text-fig. 43b.
Meekoceras yukiangense Chao, 1959, p. 311, pl. 39, figs. 1–7, 13, text-fig. 44a.
Meekoceras kaohwaiense Chao, 1959, p. 311, pl. 40, figs. 16–18, text-fig. 44b.
Meekoceras pulchriforme Chao, 1959, p. 313, pl. 40, figs. 14–15, text-fig. 44c.
Meekoceras (*Submeekoceras*) *subquadratum* Chao, 1959, p. 317, pl. 14, figs. 1–5, pl. 39, figs. 8–9, text-fig. 45c.
Meekoceras (*Submeekoceras*) *quadratum* Chao, 1959, p. 318, pl. 39, figs. 10–11, 22–23.
Meekoceras (*Submeekoceras*) sp. indet. Chao, 1959, p. 319, pl. 40, fig. 20.
Meekoceras (*Submeekoceras*) *lolouense* Chao, 1959, p. 320, pl. 10, figs. 7–8, text-fig. 45d.
Meekoceras (*Submeekoceras*) *longiseptatum* Chao, 1959, p. 321, pl. 10, figs. 5–6, text-fig. 46c.
Arctoceras mushbachanum (White, 1879). Kummel and Erben, 1968, p. 131, pl. 21, figs. 1–2.
Submeekoceras mushbachanum (White, 1879). Brayard and Bucher, 2008, p. 52, pl. 16, fig. 4, pl. 26, figs. 1–9, text-fig. 46; Brühwiler *et al*., 2012a, p. 30, pl. 17, figs. 1–3.

Holotype: NIGP 12119, figured by Chao (1959, p. 202, pl. 9, figs. 9–10), from the *Flemingites* bed in the Linglo district (Lolou), western Guangxi, South China.

Material examined: Five specimens, NMNS PM23624–23628, from BT01-03, two specimens, NMNS PM23629–23630, from BT01-09, one specimen, NMNS PM23631, from KC01-01, and three specimens, NMNS PM23632–23634, from float limestone blocks at BT02.

Description: Moderately evolute, very compressed shell with elliptical whorl section, arched venter, indistinct ventral shoulders, and slightly convex flanks with maximum whorl width near mid-flank. Fairly narrow umbilicus with moderately high, vertical wall and rounded shoulders. Ornamentation consists of sinuous growth lines and weak, fold-type ribs. Suture ceratitic. First and second lateral saddles narrowly elongated. First lateral lobe deep, wide with many denticulations at base, and second lateral lobe about two thirds depth of first lobe.

Measurements (mm):

Specimen no.	D	U	H	W	U/D	W/H
NMNS PM23629	35.4	7.5	16.2	7.2	0.21	0.44
NMNS PM23630	38.6	11.3	16.3	7.7	0.29	0.47
NMNS PM23626	51.0	11.3	23.0	12.5	0.22	0.54
NMNS PM23624	51.5	14.4	21.9	12.5	0.28	0.57
NMNS PM23625	53.9	12.6	22.5	12.1	0.23	0.54
NMNS PM23628	—	17.3	36.0	19.7	—	0.55
NMNS PM23632	70.3	20.3	28.3	13.0	0.29	0.46
NMNS PM23633	77.2	21.1	33.0	18.7	0.27	0.57
NMNS PM23634	—	28.1	40.8	22.6	—	0.55

Discussion: Even though Chao (1959) first assigned this species to *Prionolobus* Waagen, 1895, its shell morphology, which is similar to Arctoceratidae without umbilical tubercles, clearly suggests that it belongs to *Submeekoceras*. This species is very close to type species of the genus, *S. mushbachanum* (White, 1879), but the latter has a more involute shell with a narrower umbilicus. Specimens attributed to *S. mushbachanum* by Brayard and Bucher (2008) from South China are characterized by a more evolute shell with a wider umbilicus than the type specimen of *S. mushbachanum* and other illustrated specimens described by Smith (1932) from western USA. They are herein assigned to *S. hsüyüchieni*. Similar specimens were described as compris-

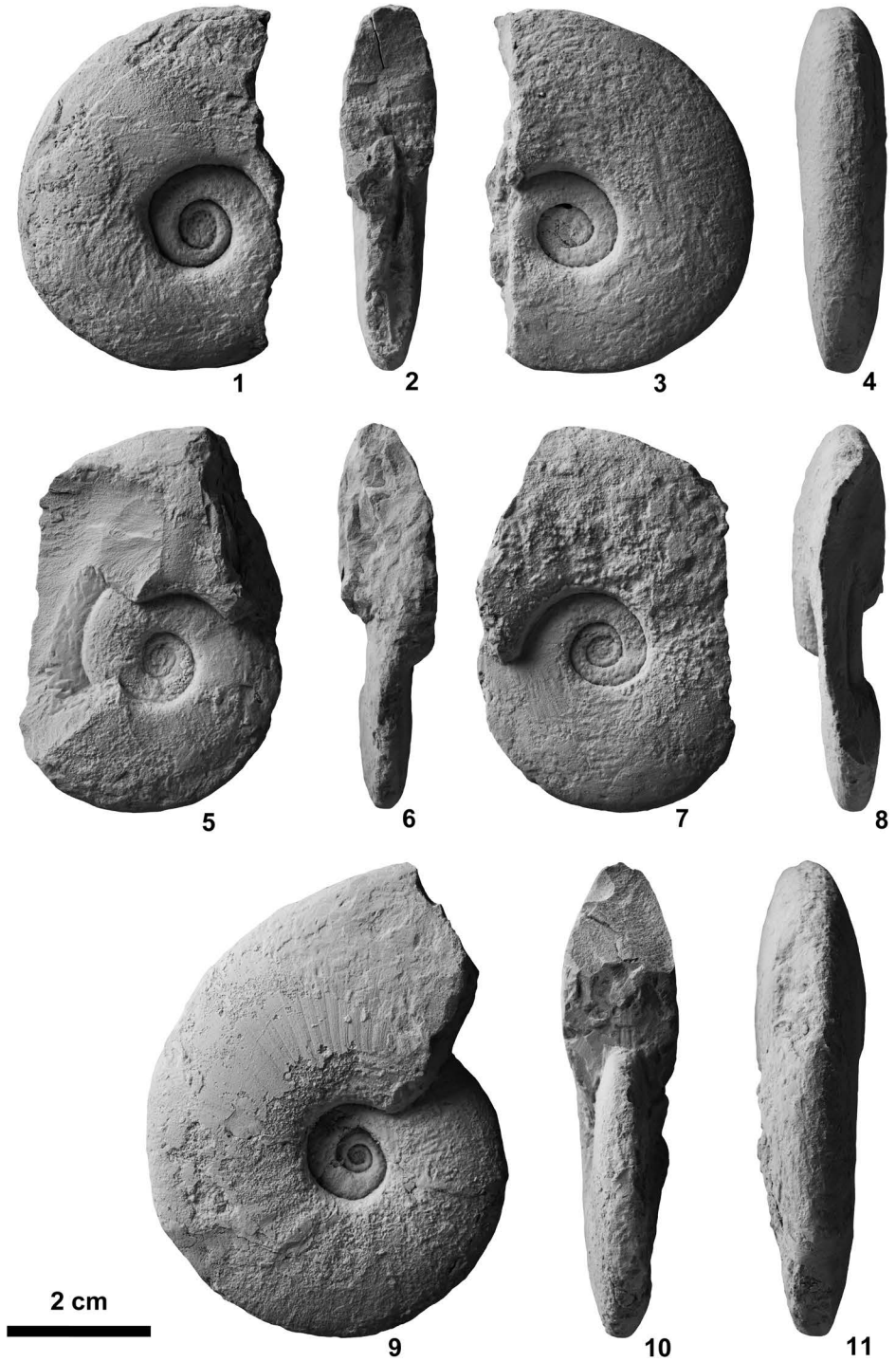

Fig. 76. *Submeekoceras hsüyüchieni* (Chao, 1959), from BT01-03. 1–4, NMNS PM23624. 5–8, NMNS PM23625. 9–11, NMNS PM23626.

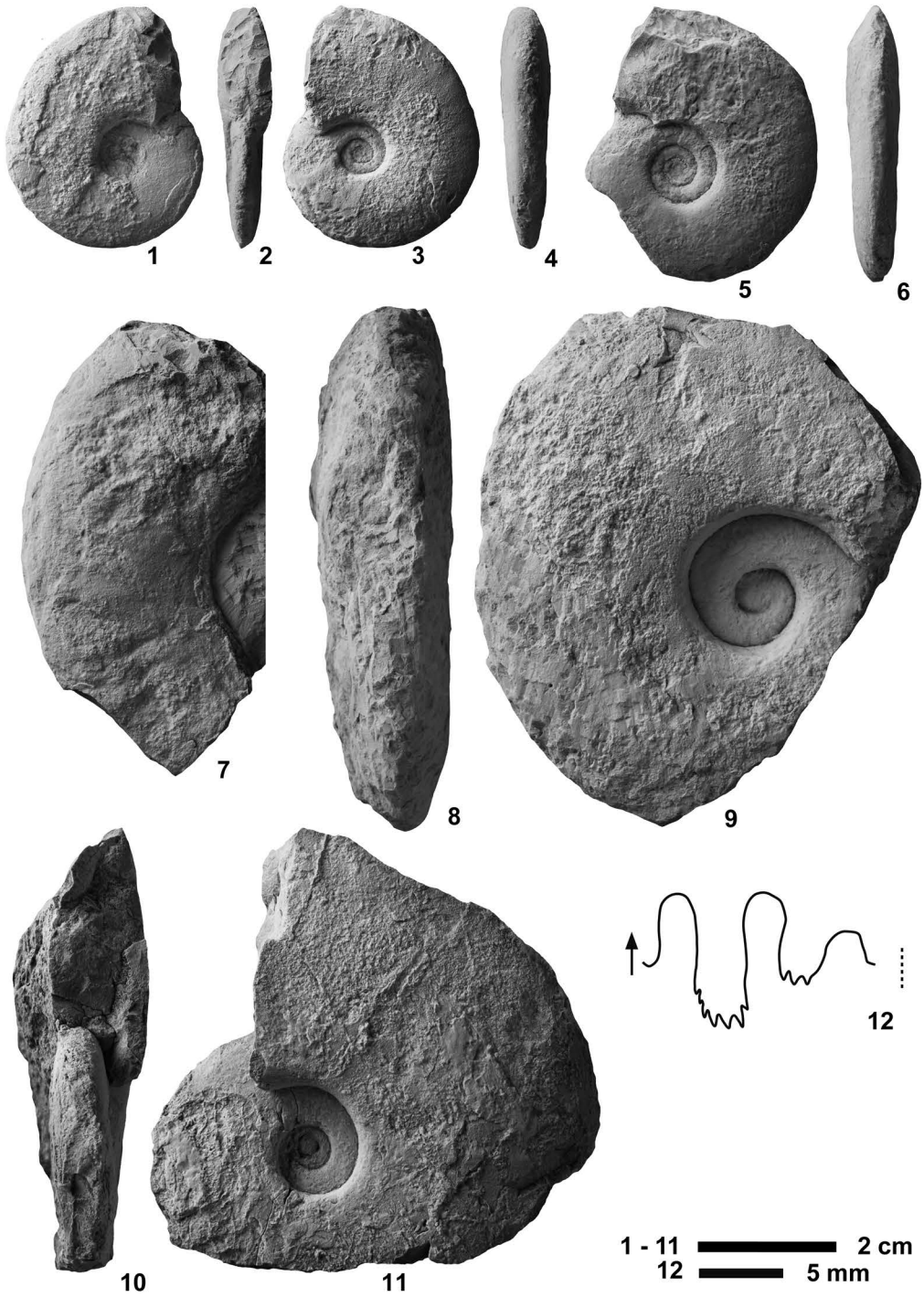

Fig. 77. *Submeekoceras hsüyüchieni* (Chao, 1959). 1–4, NMNS PM23629, from BT01-09. 5–6, NMNS PM23630, from BT01-09. 7, NMNS PM23627, from BT01-03. 8–9, NMNS PM23628 from BT01-03. 10–12, NMNS PM23631, from KC01-01.

Fig. 78. *Submeekoceras hsüyüchieni* (Chao, 1959), from float limestone blocks at BT02. 1–2, NMNS PM23632. 3–4, NMNS PM23633. 5–6, NMNS PM23634.

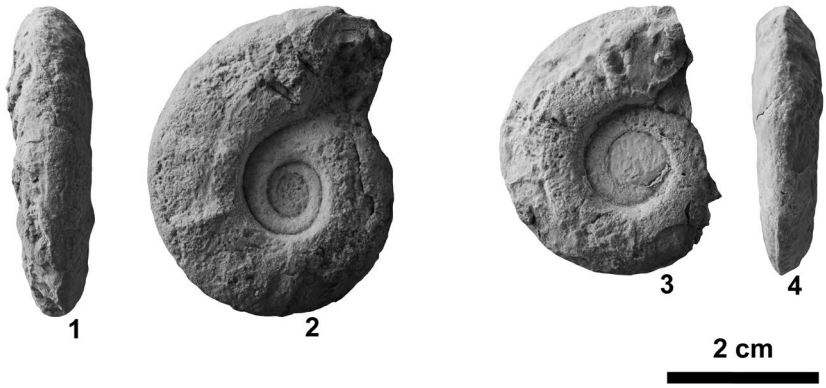

Fig. 79. *Nammalites* sp. indet., from BT02-03. 1–2, NMNS PM23524. 3–4, NMNS PM23525.

ing several different species by Chao (1959, see above synonymy list), but they probably fit within the interspecific variation of a single species because their morphological differences are insignificant. *Prionolobus ophionus* var. *involutus* Chao, 1959 is somewhat similar to *Submeekoceras hsüyüchieni*, but it is unclear if they are conspecific because the type specimen of the former species is very small (diameter ~30 mm) and its preservation is quite poor.

Occurrence: Described specimens from BT01-03, BT01-09 and KC01-01 within the portion of the *Novispathodus* ex gr. *waageni* Zone that includes the *Flemingites rursiradiatus* beds (lowest Middle Smithian = middle Lower Olenekian) and *Urdyceras tulongensis* beds (lower Middle Smithian = middle Lower Olenekian) in the Bac Thuy Formation, northeastern Vietnam. This species also occurs in the Middle Smithian in South China (*Flemingites rursiradiatus* beds and *Owenites koeneni* beds, Brayard and Bucher, 2008), Afganistan (Kummel and Erben, 1968), and Oman (*Flemingites rursiradiatus* fauna and *Owenites koeneni* fauna, Brühwiler *et al*., 2012a).

Genus *Nammalites* Brühwiler *et al*., 2010

Type species: *Nammalites pilatoides* (Guex, 1978).

Nammalites sp. indet.

Fig. 79

Material examined: Two specimens, NMNS PM23524–23525, from BT02-03.

Description: Moderately evolute, fairly compressed shell with rounded venter, indistinct ventral shoulders, and slightly convex flanks with maximum whorl width near umbilical shoulder. Umbilicus moderately wide with moderately high, nearly vertical wall and rounded shoulders. Ornamentation consists of distant, rursiradiate ribs that develop elongated bullar near umbilicus and fade out toward venter. Suture not well preserved.

Measurements (mm):

Specimen no.	D	U	H	W	U/D	W/H
NMNS PM23524	40.0	13.4	15.0	11.0	0.34	0.73
NMNS PM23524	34.8	12.5	12.6	9.0	0.36	0.71

Discussion: Even though the present specimens are poorly preserved, their distinctive features enable me to assign them with reasonable confidence to the genus *Nammalites*. They differ from *Nammalites pilatoides* (Guex, 1978) by their wider umbilicus; this feature in combination with their poor preservation precludes a definitive species assignment.

Occurrence: Described specimens from BT02-03 within the portion of the *Novispathodus* ex gr. *waageni* Zone that includes the *Owenites koeneni* beds (Middle Smithian =

middle Lower Olenekian) in the Bac Thuy Formation, northeastern Vietnam.

Family Ussuridae Spath, 1930
Genus ***Ussuria*** Diener, 1895

Type species: *Ussuria schamarae* Diener, 1895.

Ussuria kwangsiana Chao, 1959
Fig. 80

Ussuria kwangsiana Chao, 1959, p. 258, pl. 31, figs. 8–10, pl. 8, text-fig. 30a; Brayard and Bucher, 2008, p. 54, pl. 27, figs. 1–3, text-fig. 47.
Ussuria pakungiana Chao, 1959, p. 258, pl. 31, figs. 1–3, pl. 8, text-fig 30c, d.
Ussuria longilobata Chao, 1959, p. 259, pl. 31, figs. 4–7, pl. 8, text-fig 30b.
Ussuria lenticularis Vu Khuc, 1984, p. 79, pl. 6, fig. 5, text-fig. 14; Vu Khuc, 1991, p. 140, pl. 47, fig. 4, text-fig. 4–1.

Holotype: NIGP 12321, figured by Chao (1959, p. 258, pl. 31, figs. 8–10), from the Owenitan (middle Smithian) in the Tiengno district (Pakung), western Guangxi, South China.

Material examined: One specimen, NMNS PM23526, from BT02-02 and one specimen, NMNS PM23527, from BT01-09.

Description: Very involute, very compressed oxycone with narrowly rounded venter and gently convex flanks with maximum width near umbilicus. Umbilicus very narrow with high, perpendicular wall and rounded shoulders. Shell surface smooth. Suture subammonitic, with distinctly phylloid saddles and strongly indented lobes.

Measurements (mm):

Specimen no.	D	U	H	W	U/D	W/H
NMNS PM23527	42.1	3.8	24.5	10.6	0.09	0.43
NMNS PM23526	69.0	4.7	41.2	17.7	0.07	0.43

Discussion: Chao (1959) erected *Ussuria pakungiana* and *U. longilobata* from the same locality as *U. kwangsiana* in South China. They are differentiated from *U. kwangsiana* only by small differences in their suture line, but otherwise are very similar. These two taxa probably represent juvenile whorls of *U. kwangsiana* and the difference in suture line is interpreted to simply be the result of intraspecific variation or ontogenetic variation. According to Brayard and Bucher (2008), *U. kwangsiana* has a nearly occluded umbilicus. *U. lenticularis* Vu Khuc, 1984 from the Bac Thuy Formationis is very similar to the described specimens and probably should be synonymized with *U. kwangsiana.*

Occurrence: Described specimens from BT01-09 and BT02-02 within the portion of the *Novispathodus* ex gr. *waageni* Zone that includes the *Urdyceras tulongensis* beds (lower Middle Smithian = middle Lower Olenekian) in the Bac Thuy Formation, northeastern Vietnam. This species also occurs in the Middle Smithian (*Owenites koeneni* beds) in South China (Brayard and Bucher, 2008).

Genus ***Parussuria*** Spath, 1930

Type species: *Ussuria compressa* Hyatt and Smith, 1905.

Parussuria compressa
(Hyatt and Smith, 1905)
Figs. 81, 82

Ussuria compressa Hyatt and Smith, 1905, p. 89, pl. 3, figs. 6–11.
Sturia compressa (Hyatt and Smith, 1905). Smith, 1932, p. 93, pl. 3, figs. 6–11.
Parussuria compressa (Hyatt and Smith, 1905). Spath, 1934, fig. 66c–d; Kummel and Steele, 1962, p. 690, pl. 99, fig. 23, pl. 102, fig. 11; Shevyrev, 1995, p. 37, pl. 4, fig. 6, text-fig. 16; Brayard and Bucher, 2008, p. 56, pl. 12, fig. 17; Brühwiler *et al*., 2012a, p. 31, pl. 18, figs. 8–14; Brayard *et al*., 2013, p. 191, fig. 57a–f.
Metussuria spathi Chao, 1959, p. 261, pl. 21, fig. 3, pl. 31, fig. 13.
Parussuria semenovi Zakharov, 1968, p. 59, pl. 5, fig. 4, text-fig. 8e.

Holotype: USNM 75250, figured by Hyatt and Smith (1905, p. 89, pl. 3, figs. 6–7), from the *Meekoceras* beds (middle Smithian) in the Inyo Range, California, western USA.

Material examined: One specimen, NMNS

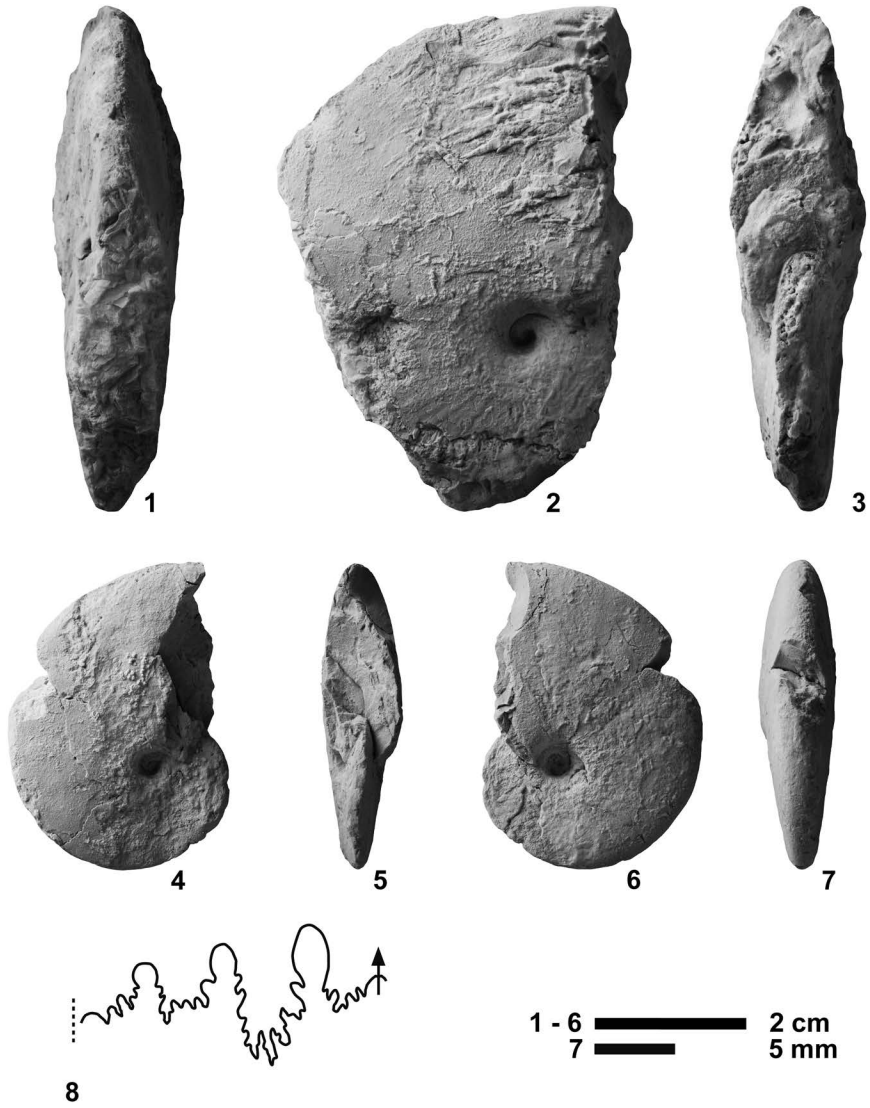

Fig. 80. *Ussuria kwangsiana* Chao, 1959. 1–3, NMNS PM23526, from BT02–02. 4–8, NMNS PM23527, from BT01-09.

PM23528, from BT02-03 and four specimens, NMNS PM23529–23532, from KC01-13.

Description: Very involute, very compressed oxycone with very narrowly rounded venter and gently convex flanks with maximum width near umbilicus. Flanks gradually convergent to venter. Umbilicus occluded with low, oblique wall and rounded shoulders. Shell surface smooth. Suture subammonitic, with deeply divided, phylloid saddles and strongly indented lobes.

Measurements (mm):

Specimen no.	D	U	H	W	W/H
NMNS PM23529	40.6	0.0	27.1	11.6	0.43
NMNS PM23530	44.6	0.0	29.0	13.2	0.46
NMNS PM23531	—	0.0	35.3	15.0	0.42
NMNS PM23528	72.4	0.0	50.0	18.0	0.36
NMNS PM23532	—	0.0	55.4	18.9	0.34

Discussion: *Metussuria spathi* Chao, 1959 from South China has a subammonitic suture

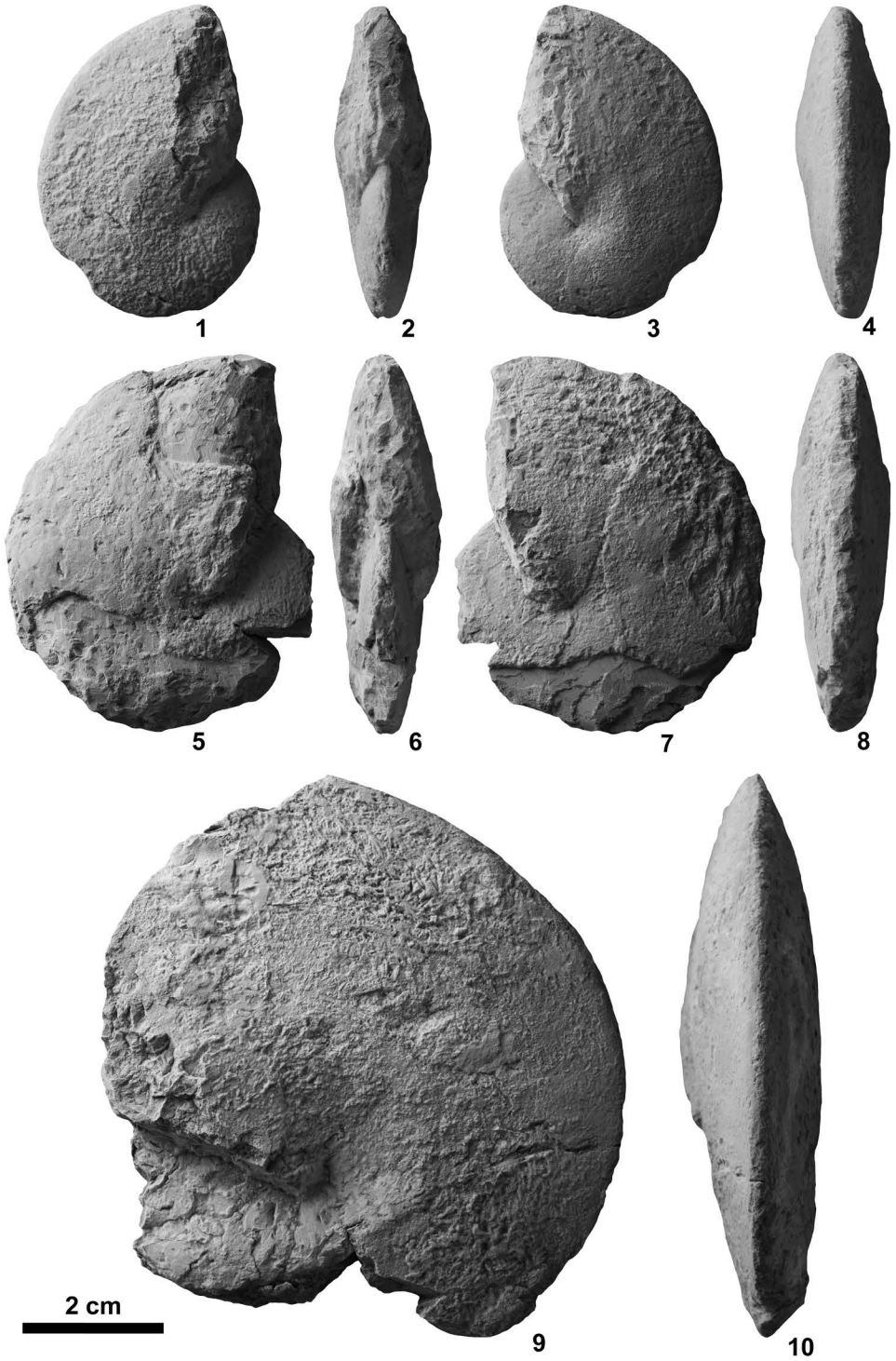

Fig. 81. *Parussuria compressa* (Hyatt and Smith, 1905) from KC01-13. 1–4, NMNS PM23530. 5–8, NMNS PM23531. 9–10, NMNS PM23532.

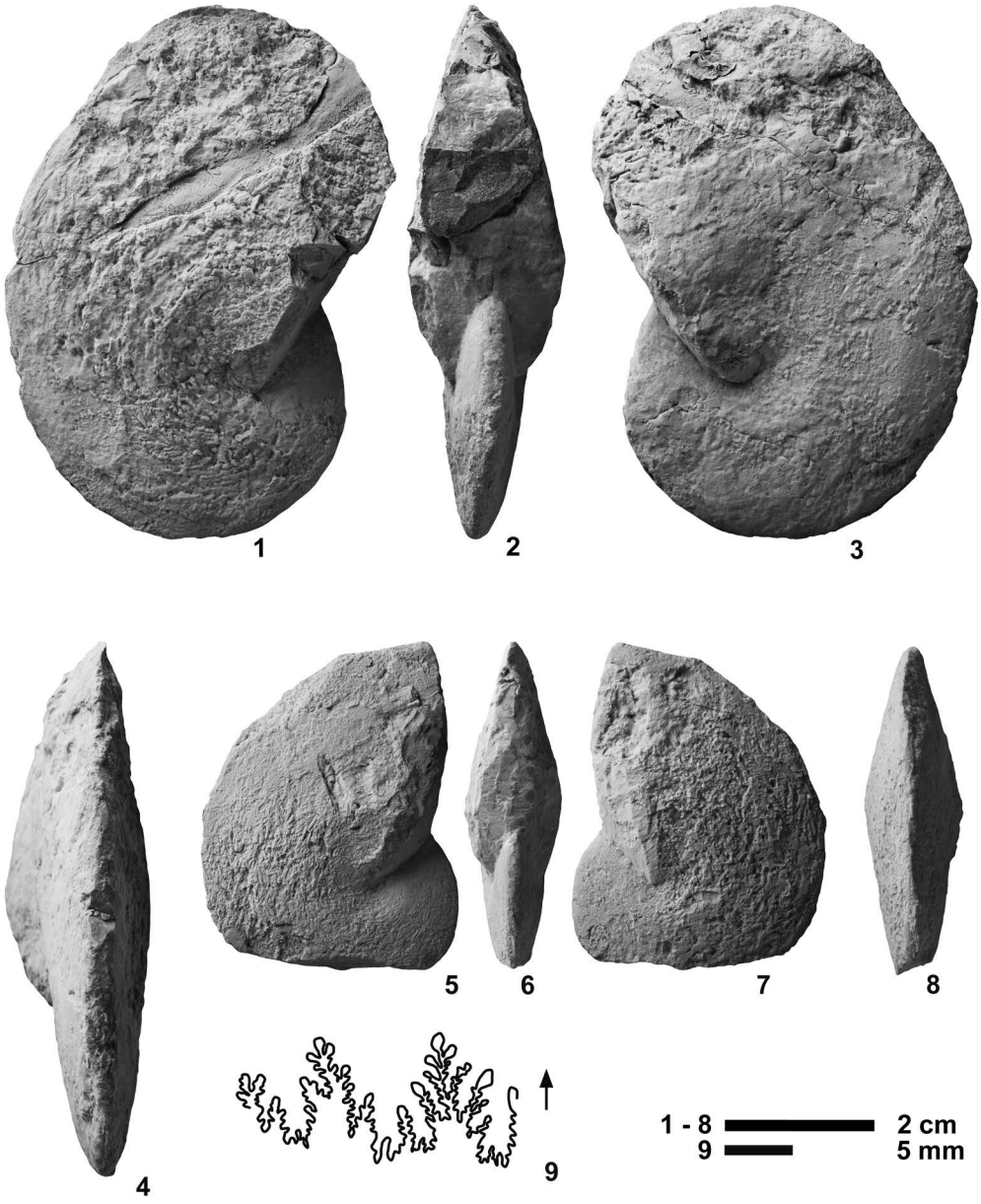

Fig. 82. *Parussuria compressa* (Hyatt and Smith, 1905). 1–4, NMNS PM23528, from BT02-03. 5–9, NMNS PM23529, from KC01-12.

line with deeply divided, phylloid saddles and strongly indented lobes. This evidence clearly suggests that this species should be assigned to *Parussuria*. Furthermore, its shell morphology does not exhibit any significant differences from *Parussuria compressa* and is herein considered as a synonym. *P. semenovi* Zakharov, 1968 from South Primorye, whose suture line and shell morphology is very similar, is also probably conspecific with *P. compressa*.

Occurrence: Described specimens from BT02-03 and KC01-13 within the portion of the *Novispathodus* ex gr. *waageni* Zone that includes the *Leyeceras* horizon of the *Owenites koeneni* beds (middle Middle Smithian=middle Lower Olenekian) in the Bac Thuy Formation, northeastern Vietnam. This species also occurs in the Middle Smithian in South China (*Owenites koeneni* beds, Brayard and Bucher, 2008), Oman (*Owenites koeneni* fauna, Brühwiler *et al*., 2012a), northwestern Caucasus (*Owenites-Dieneroceras* beds, Shevyrev, 1995), western USA (*Meekoceras gracilitatis* Zone, Kummel and Steele, 1962; *Owenites* beds, Brayard *et al*., 2013) and South Primorye (*Owenites koeneni* Zone, Zakharov, 1968).

Family Melagathiceratidae Tozer, 1971

Genus ***Jinyaceras*** Brayard and Bucher, 2008

Type species: *Jinyaceras bellum* Brayard and Bucher, 2008.

Jinyaceras cf. ***bellum***

Brayard and Bucher, 2008

Fig. 83.1–83.15

cf. *Jinyaceras bellum* Brayard and Bucher, 2008, p. 31, pl. 9, figs. 1–19, text-figs. 29.

Material examined: Two specimens, NMNS PM23539–23540, from BT01-03, one specimen, NMNS PM23541, from BT01-09, one specimen, NMNS PM23542, from BT02-02, and one specimen, NMNS PM23543, from a float limestone block at BT02.

Description: Moderately involute, fairly depressed shell with broadly arched venter, rounded ventral shoulders, and slightly convex flanks gradually converging from umbilical shoulders to venter. Umbilicus fairly narrow with moderately high, nearly vertical wall and rounded shoulders. Ornamentation consists of distant, prorsiradiate constrictions that become weaker on venter. Suture not well preserved.

Measurements (mm):

Specimen no.	D	U	H	W	U/D	W/H
NMNS PM23542	14.4	3.4	6.0	8.3	0.24	1.38
NMNS PM23543	14.6	4.5	5.7	6.6	0.31	1.16
NMNS PM23541	14.7	3.9	6.4	6.6	0.27	1.03
NMNS PM23539	14.7	4.2	5.7	7.1	0.29	1.25
NMNS PM23540	19.8	4.8	5.5	6.8	0.24	1.23

Discussion: The described specimens are very similar to *Jinyaceras bellum* from South China, but their poor preservation prevents a definitive species assignment. Chao (1959) attributed two new species to *Kashmirites* Diener, 1913, *K. prorsiradiatus* and *K. varians*, and also described two specimens as *K. subarmatus* Diener, 1913, all of which are very close to *J. bellum.* They may be conspecific, but further taxonomic studies are necessary to confirm the synonymy.

Occurrence: Described specimens from BT01-03, BT01-09 and BT02-02 within the portion of the *Novispathodus* ex gr. *waageni* Zone that includes the *Flemingites rursiradiatus* beds (lowest Middle Smithian=middle Lower Olenekian) and *Urdyceras tulongensis* beds (lower Middle Smithian=middle Lower Olenekian) in the Bac Thuy Formation, northeastern Vietnam. *Jinyaceras bellum* occurs in the Middle Smithian in South China (*Flemingites rursiradiatus* beds and *Owenites koeneni* beds, Brayard and Bucher, 2008).

Jinyaceras? sp. indet.

Fig. 83.16–83.19

Material examined: One specimen, NMNS PM23544, from BT02-02 and one specimen, NMNS PM23545, from BT01-09.

Description: Moderately involute shell with equal whorl height and width. Venter

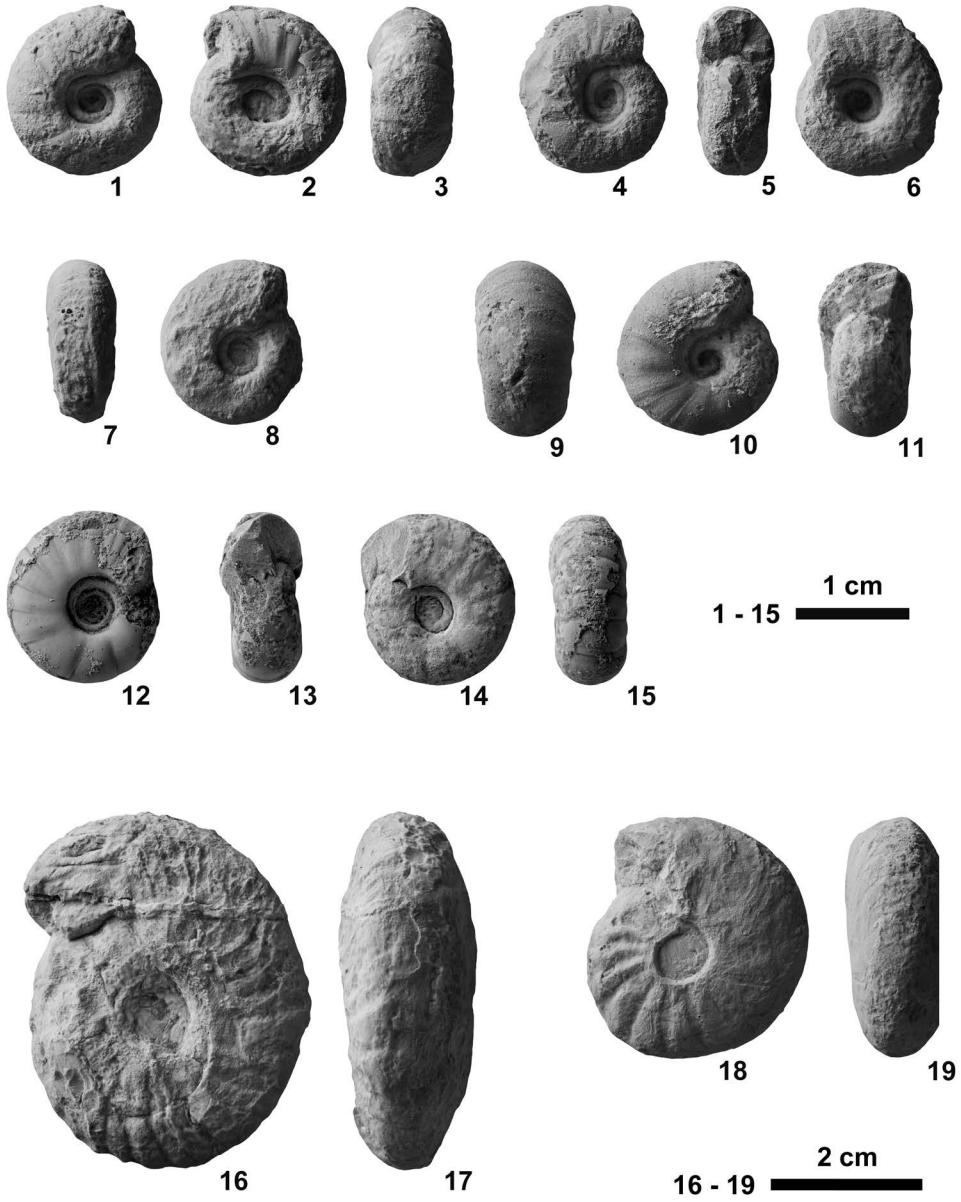

Fig. 83. 1–15, *Jinyaceras* cf. *bellum* Brayard and Bucher, 2008. 1–3, NMNS PM23539, from BT01-03. 4–6, NMNS PM23540, from BT01-03. 7–8, NMNS PM23541, from BT01-09. 9–11, NMNS PM23542, from BT02-02. 12–15, NMNS PM23543, from a float limestone block at BT02. 16–19, *Jinyaceras*? sp. indet. 16–17, NMNS PM23544, from BT02-02. 18–19, NMNS PM23545, from BT01-09.

broadly arched with rounded shoulders and slightly convex flanks with maximum whorl width near umbilicus. Umbilicus fairly narrow with moderately high, nearly vertical wall and rounded shoulders. Ornamentation consists of distant, prorsiradiate constrictions. Suture not well preserved.

Measurements (mm):

Specimen no.	D	U	H	W	U/D	W/H
NMNS PM23545	31.8	7.0	14.2	14.5	0.22	1.02
NMNS PM23544	46.0	10.5	20.0	18.0	0.23	0.90

Discussion: The assignment of the described specimens to *Jinyaceras* is uncertain and is based only on the similarity of their morphology with *Jinyaceras*. However, these specimens are larger than specimens assigned to *Jinyaceras* by previous authors (Brayard and Bucher, 2008; Brühwiler *et al*., 2010, 2012a, 2012c).

Occurrence: Described specimens from BT01-09 and BT02-02 within the portion of the *Novispathodus* ex gr. *waageni* Zone that includes the *Urdyceras tulongensis* beds (lower Middle Smithian=middle Lower Olenekian) in the Bac Thuy Formation, northeastern Vietnam.

Genus ***Juvenites*** Smith, 1927

Type species: *Juvenites kraffti* Smith, 1927.

Juvenites sinuosus (Kiparisova, 1947)

Fig. 84

Nannites sinuosus Kiparisova, 1947, p. 141, pl. 27, figs. 7–8.

Nannites sinuosus var. *pressula* Kiparisova, 1947, p.141, pl. 27, fig. 6, text-fig. 27.

Juvenites kwangsianus Chao, 1959, p. 287, pl. 26, figs. 6–8.

Juvenites medius (Diener, 1909). Chao, 1959, p. 288, pl. 25, figs. 11–20.

Juvenites septentrionalis Smith, 1932. Chao, 1959, p. 289, pl. 25, figs. 6–10.

Juvenites orientalis Chao, 1959, p. 290, pl. 26, figs. 3–5.

Juvenites sp. A. Chao, 1959, p. 290, pl. 25, figs. 21–22.

Juvenites sp. B. Chao, 1959, p. 291, pl. 25, figs. 23–27.

Anasibirites simplex Chao, 1959, p. 327, pl. 40, figs. 7–9.

Juvenites sp. Kummel and Sakagami, 1960, p. 8, pl. 1, fig. 2.

Nannites cf. *septentrionalis* (Smith, 1932). Kiparisova, 1961, p. 132, pl. 27, fig. 13.

Nannites aff. *sinuosus* Kiparisova, 1947. Kiparisova, 1961, p. 133, pl. 27, fig. 12, text-fig. 100.

Nannites simplex (Chao, 1959). Zakharov, 1968, p. 117, pl. 22, figs. 3–7.

Juvenites sinuosus (Kiparisova, 1947). Shevyrev, 1995, p. 23, pl. 1, fig. 1–2.

Juvenites procurvus Brayard and Bucher, 2008, p. 32, pl. 22, figs. 6–12, text-figs. 30; Brühwiler *et al*., 2012a, p. 41, pl. 22, figs. 10–11; Brühwiler *et al*., 2012c, p. 163, fig. 37AK–AP.

Juvenites cf. *thermarum* (Smith, 1927). Brühwiler *et al*., 2012a, p. 39, pl. 22, figs. 1–9.

Juvenites sp. Brühwiler *et al*., 2012b, p. 105, fig. 89AN–AX.

Holotype: CGM 43/6259, figured by Kiparisova (1947, p. 141, pl. 27, fig. 8), from the middle Smithian (*Owenites-Dieneroceras* beds) in northwestern Caucasus.

Material examined: One specimen, NMNS PM23533, from KC01-03 and five specimens, NMNS PM23534–23538, from KC01-13.

Description: Fairly involute, very depressed shell with semicircular whorl section and convex flanks gradually converging from abruptly rounded umbilical shoulders to arched venter. Umbilicus moderately wide with moderately high, nearly vertical wall and abruptly rounded shoulders. Ornamentation consists of distant, forward projected constrictions, becoming denser on mature body chamber. Suture not well preserved.

Measurements (mm):

Specimen no.	D	U	H	W	U/D	W/H
NMNS PM23538	12.8	4.1	4.8	8.4	0.32	1.75
NMNS PM23535	16.0	4.9	6.5	11.3	0.31	1.73
NMNS PM23537	17.0	5.2	6.6	10.5	0.31	1.59
NMNS PM23536	17.7	5.7	6.4	9.5	0.32	1.48
NMNS PM23533	18.2	6.2	6.3	10.3	0.34	1.63
NMNS PM23534	18.8	6.4	7.0	10.4	0.34	1.49

Discussion: Countless specimens referable to the genus *Juvenites* are known not only from eastern Panthalassa (western USA), but also from the Tethys (northwestern Caucasus, Oman, Spiti, the Salt Range, South China) and

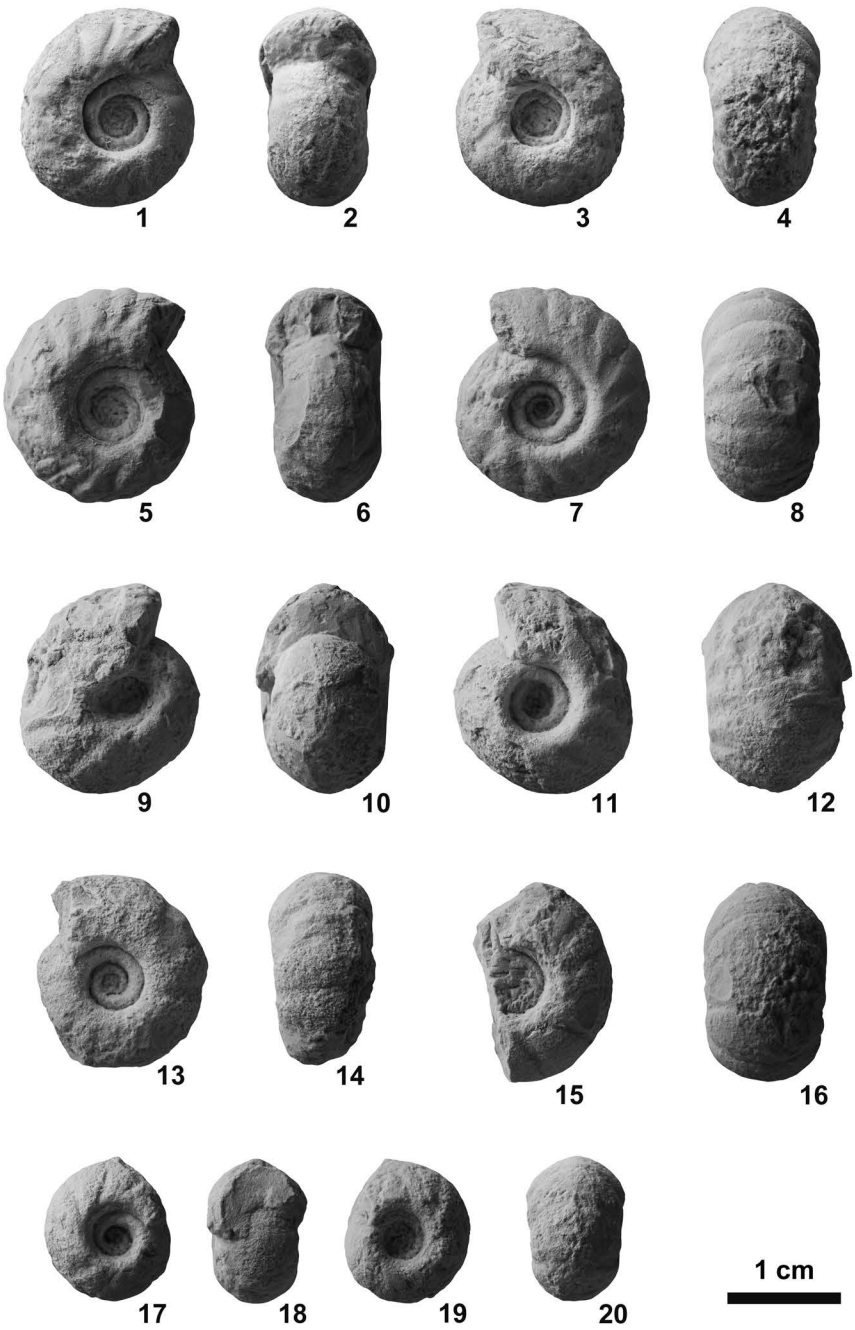

Fig. 84. *Juvenites sinuosus* (Kiparisova, 1947). 1–4, NMNS PM23533, from KC01-03. 5–8, NMNS PM23534, from KC01-13. 9–12, NMNS PM23536, from KC01-13. 13–14, NMNS PM23535, from KC01-13. 15–16, NMNS PM23537, from KC01-13. 17–20, NMNS PM23538, from KC01-13.

western Panthalassa (South Primorye). Many different species have been erected based only on slight differences in shell shape and suture line, but the intraspecific variation of each species is not yet that well understood.

Brayard and Bucher (2008) recently erected *Juvenites procurvus* based on seven specimens from South China ranging from juvenile to mature stages. Some of these specimens are very similar to other species previously described from the Tethys and western Panthalassa. For example, PIMUZ 26010 (Brayard and Bucher, 2008, pl. 22, fig. 8, holotype) is quite similar to the holotype of *J. sinuosus* (Kiparisova, 1947, pl. 27, fig. 8), and PIMUZ 26009 (Brayard and Bucher, 2008, pl. 22, fig. 7) is very close to holotype of *J. kwangsianus* (Chao, 1959, pl. 26, figs. 6–7). In addition, PIMUZ 26012 (Brayard and Bucher, 2008, pl. 22, fig. 10) is similar to holotype of *J. orientalis* (Chao, 1959, pl. 26, figs. 3–4). These very close similarities strongly suggest that the previously described species from the Tethys and western Panthalassa synonymized above probably fall within the intraspecific or ontogenetic variation *J. sinuosus*.

Occurrence: Described specimens from KC01-03 and KC01-13 within the portion of the *Novispathodus* ex gr. *waageni* Zone that includes the *Leyeceras* horizon of the *Owenites koeneni* beds (middle Middle Smithian=middle Lower Olenekian) in the Bac Thuy Formation, northeastern Vietnam. This species also occurs in the Middle Smithian in South China (*Owenites koeneni* beds, Brayard and Bucher, 2008), Spiti (*Pseudoceltites multiplicatus* beds, Brühwiler *et al*., 2012c), the Salt Range (*Brayardites compressus* beds, Brühwiler *et al*., 2012b), Oman (*Owenites koeneni* fauna, Brühwiler *et al*., 2012a), northwestern Caucasus (*Owenites-Dieneroceras* beds, Shevyrev, 1995), and South Primorye (*Owenites koeneni* Zone, Zakharov, 1968).

Genus ***Paranannites*** Hyatt and Smith, 1905

Type species: *Paranannites aspenensis* Hyatt and Smith, 1905.

Paranannites sinensis (Chao, 1959)

Figs. 85–87

Prosphingites sinensis Chao, 1959, p. 297, pl. 25, figs. 1–5, pl. 27, figs. 1–17, text-fig. 40a–c.

Paranannites spathi (Frebold, 1930). Brayard and Bucher, 2008, p. 63, pl. 35, figs. 10–19, text-fig. 55.

Juvenites cf. *spathi* (Frebold, 1930). Brühwiler *et al.* (2012c), p. 161, pl. 37A–O.

Lectotype: Specimen NIGP 12587, figured by Chao (1959, p. 297, pl. 27, figs. 16–17) from the Owenitan (middle Smithian) in the Tientung district (Kaoyunling), western Guangxi, South China, here designated.

Material examined: Three specimens, NMNS PM23564–23566, from KC01-07, one specimen, NMNS PM23567, from KC01-10, seven specimens, NMNS PM23568–23574, from BT02-02, and three specimens, NMNS PM23561–23563, from a float limestone block at BT02.

Description: Fairly involute, fairly depressed shell characterized by subtrigonal whorl section with narrowly rounded to subangular venter and convex flanks gradually converging from umbilical shoulders to venter. Maximum whorl width occurs on umbilical shoulders. Umbilicus fairly narrow with high, vertical wall and abruptly rounded shoulders. Ornamentation consists of variable strength, prorsiradiate constrictions. Suture not well preserved.

Measurements (mm):

Specimen no.	D	U	H	W	U/D	W/H
NMNS PM23565	19.6	5.2	7.8	11.6	0.27	1.48
NMNS PM23567	26.0	5.7	10.5	—	0.21	—
NMNS PM23563	30.0	5.6	13.4	18.4	0.19	1.37
NMNS PM23569	32.0	6.1	15.0	18.0	0.19	1.20
NMNS PM23570	33.8	5.5	15.7	18.0	0.16	1.15
NMNS PM23561	38.7	7.4	18.9	24.1	0.19	1.28
NMNS PM23571	38.7	8.4	16.0	23.5	0.22	1.47
NMNS PM23562	40.3	8.8	15.0	19.5	0.22	1.30
NMNS PM23573	42.0	10.1	18.5	27.0	0.24	1.46

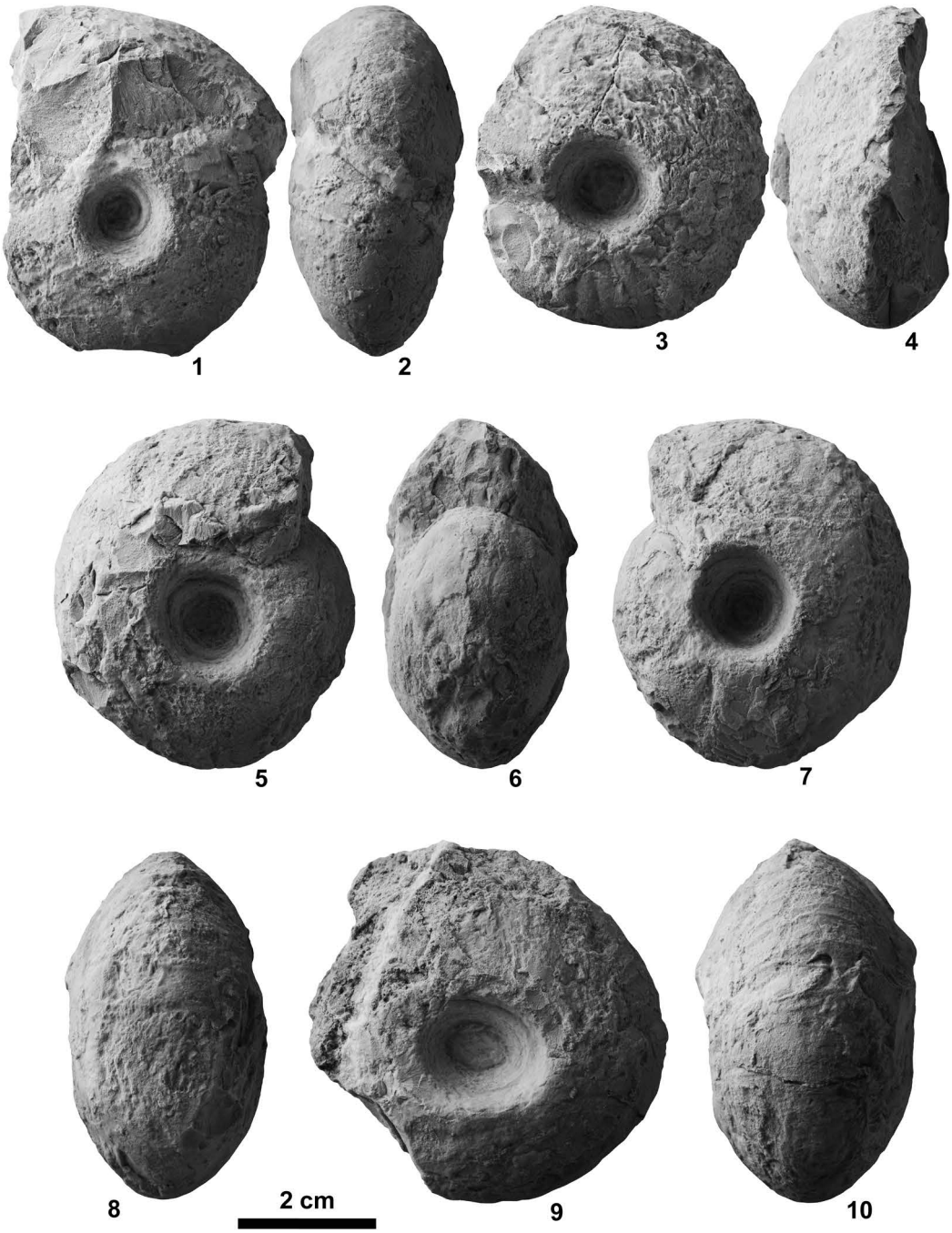

Fig. 85. *Paranannites sinensis* (Chao, 1959) from BT02-02. 1–2, NMNS PM23571. 3–4, NMNS PM23572. 5–7, NMNS PM23573. 8–10, NMNS PM23574.

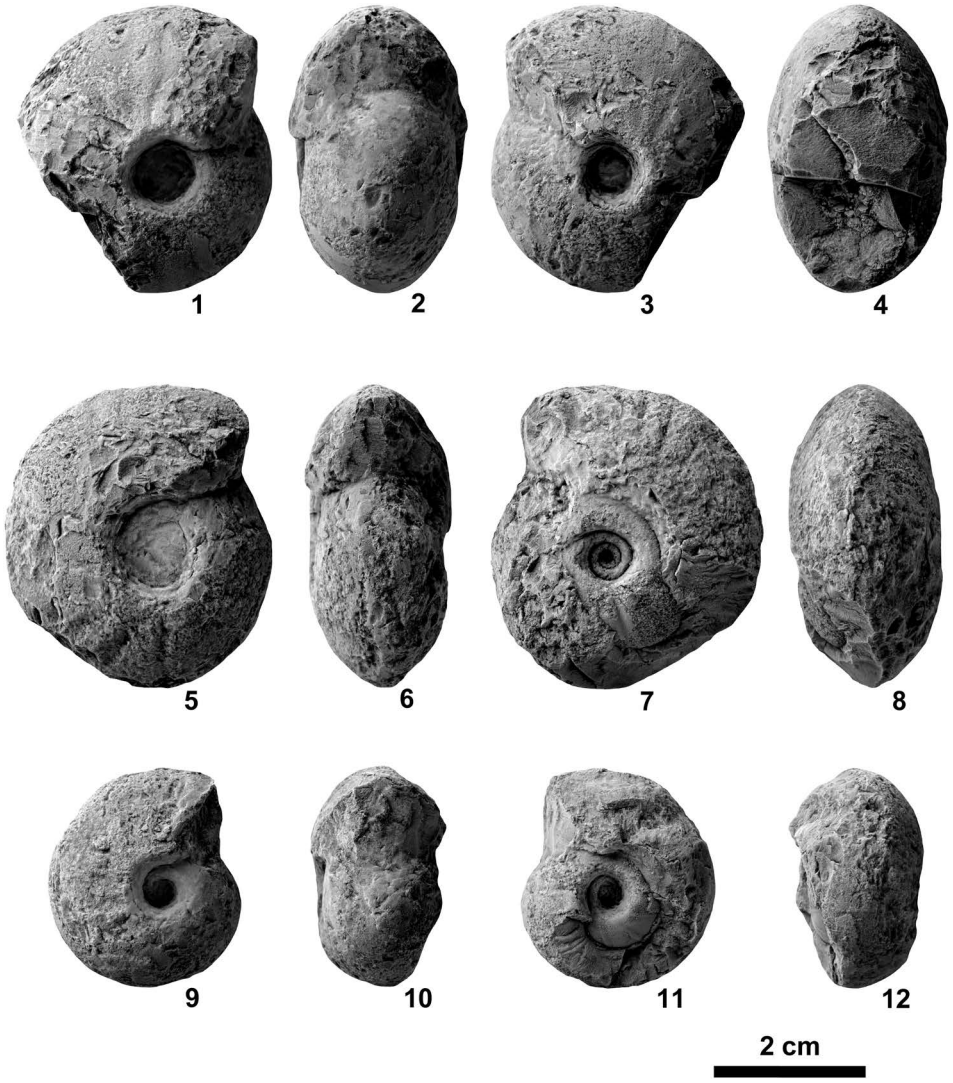

Fig. 86. *Paranannites sinensis* (Chao, 1959) from a float limestone block at BT02. 1–4, NMNS PM23561. 5–8, NMNS PM23562. 9–12, NMNS PM23563.

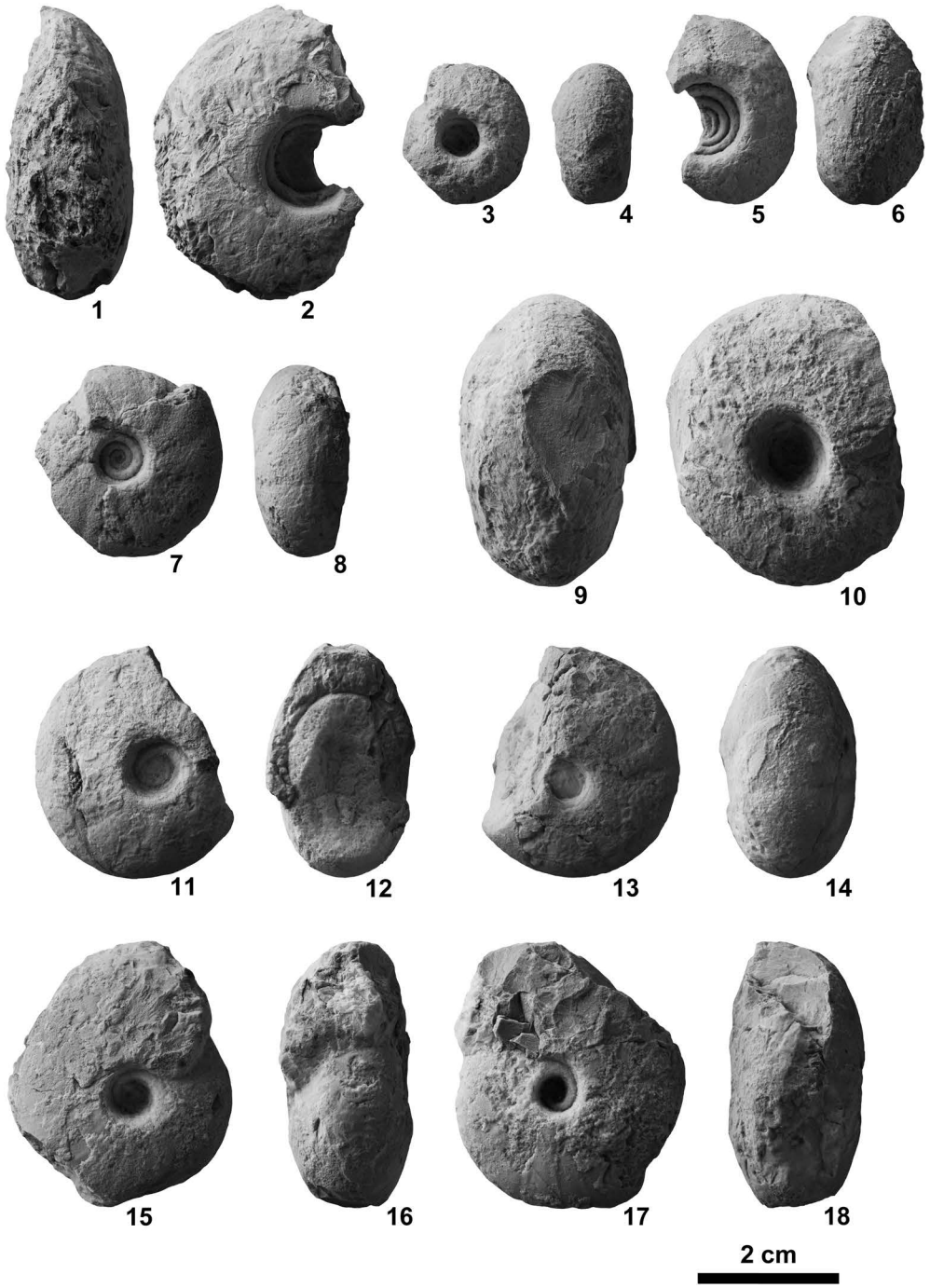

Fig. 87. *Paranannites sinensis* (Chao, 1959). 1–2, NMNS PM23564, from KC01-07. 3–4, NMNS PM23565, from KC01-07. 5–6, NMNS PM23566, from KC01-07. 7–8, NMNS PM23567, from KC01-10. 9–10, NMNS PM23568, from BT02-02. 11–14, NMNS PM23569, from BT02-02. 15–18, NMNS PM23570, from BT02-02.

NMNS PM23572	47.3	9.3	22.5	—	0.20	—
NMNS PM23574	51.0	13.1	18.5	27.6	0.26	1.49

Discussion: *Paranannites sinensis* is very close to *P. spathi* (Frebold, 1930) from the Spathian (Upper Olenekian) of Spitsbergen, but differs by its variable strength constrictions. In contrast, *P. spathi* is ornamented with distant, fine ribs. Specimens described as *P. spathi* from Arctic Canada by Tozer (1961, 1994) and South Tibet by Brühwiler *et al*. (2010) are somewhat similar to *P. sinensis*, but their venters are more rounded. The same observation holds true for specimens from Spiti attributed to *Juvenites* cf. *spathi* by Brühwiler *et al.* (2012c).

Occurrence: Described specimens from BT02-02, KC01-07 and KC01-10 within the portion of the *Novispathodus* ex gr. *waageni* Zone that includes the *Urdyceras tulongensis* beds (lower Middle Smithian=middle Lower Olenekian) and the *Leyeceras* horizon of *Owenites koeneni* beds (middle Middle Smithian=middle Lower Olenekian) in the Bac Thuy Formation, northeastern Vietnam. This species also occurs in the Middle Smithian (*Owenites koeneni* beds) in South China (Brayard and Bucher, 2008).

Paranannites involutus (Chao, 1959)

Fig. 88.1–88.4

Prosphingites involutus Chao, 1959, p. 297, pl. 28, figs. 1–11, text-fig. 39c.

"*Paranannites*" *ovum* Brayard and Bucher, 2008, p. 65, pl. 34, figs. 4–5.

Holotype: NIGP 12575, figured by Chao (1959, p. 297, pl. 28, fig. 1–2), from the Owenitian (middle Smithian) in the Tientung district (Tsoteng), western Guangxi, South China.

Material examined: two specimens, NMNS PM2357–23578, from a float limestone block at PK01.

Description: Involute, very depressed shell with broadly rounded venter and convex flanks gradually converging from umbilical shoulders to venter. Maximum whorl width occurs on umbilical shoulders. Umbilicus fairly narrow with high, vertical wall and abruptly rounded shoulders. Shell surface smooth. Suture not well preserved.

Measurements (mm):

Specimen no.	D	U	H	W	U/D	W/H
NMNS PM23578	29.6	6.8	11.4	23.0	0.23	2.02
NMNS PM23577	36.5	6.2	16.3	29.5	0.17	1.81

Discussion: Two specimens (PIMUZ 26090, 26091) described as "*Paranannites*" *ovum* by Brayard and Bucher (2008, pl. 34, figs. 4–5), which are characterized by a more depressed shell than the type specimens, are very similar to *P. involutus* and are probably conspecific.

Occurrence: Described specimens from PK01 within the portion of the *Novispathodus* ex gr. *waageni* Zone that includes the *Owenites koeneni* beds (middle to upper Middle Smithian=middle Lower Olenekian) in the Bac Thuy Formation, northeastern Vietnam. This species also occurs in the middle Smithian (Owenitian) in South China (Chao, 1959).

Paranannites sp. indet.

Fig. 88.5–88.12

Material examined: One specimen, NMNS PM23772, from BT01-09, one specimen, NMNS PM23575, from BT01-11, and one specimen, NMNS PM23576, from a float limestone block at BT02.

Description: Very involute, fairly compressed shell characterized by a subelliptical whorl section with rounded venter and convex flanks gradually converging from umbilical shoulders to venter. Maximum whorl width occurs near umbilical shoulders. Umbilicus narrow with moderately high, vertical wall and abruptly rounded shoulders. Ornamentation consists of weak, forward projected constrictions. Suture not well preserved.

Measurements (mm):

Specimen no.	D	U	H	W	U/D	W/H
NMNS PM23772	27.0	3.8	13.7	13.3	0.14	0.97

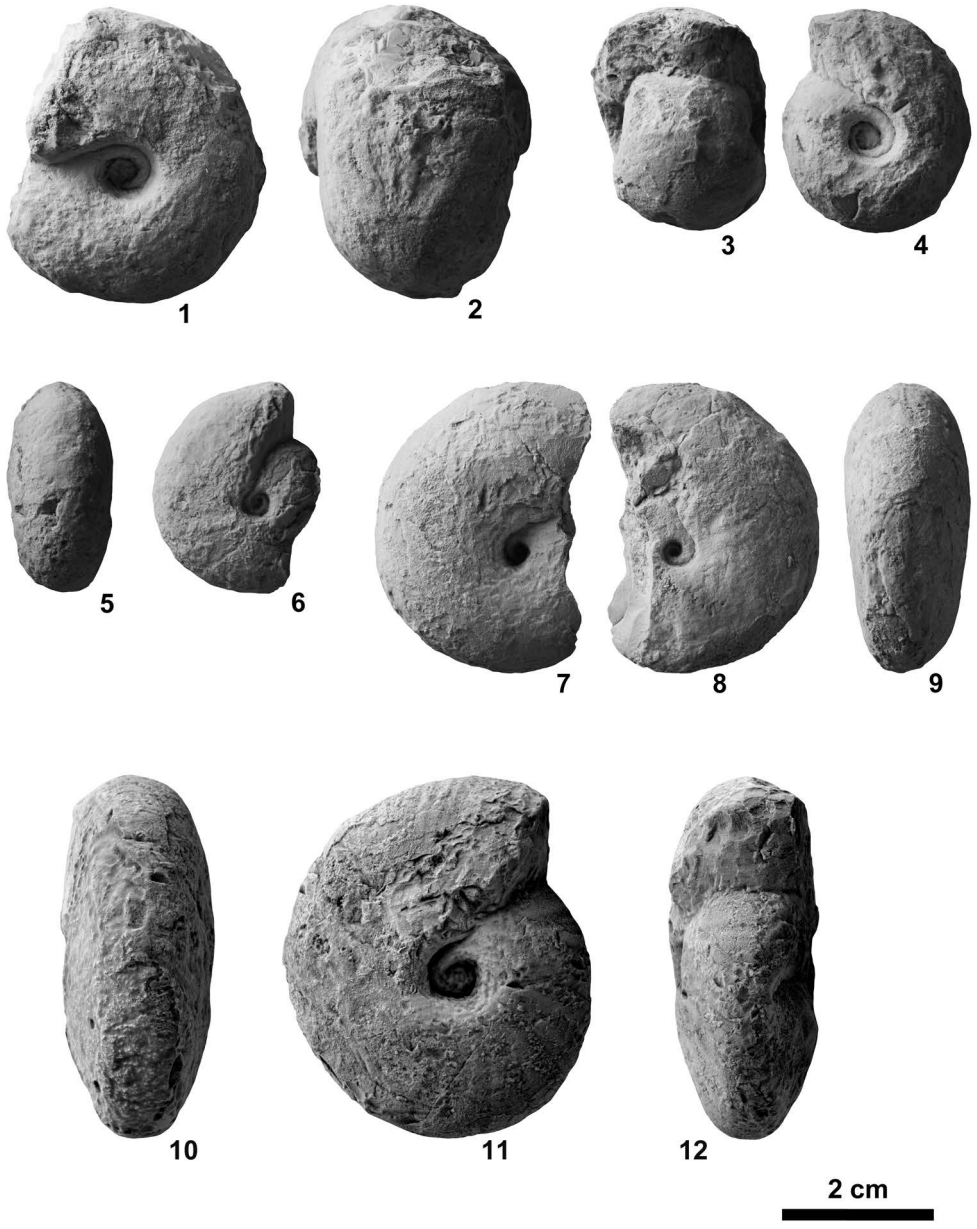

Fig. 88. 1–4, *Paranannites involutus* (Chao, 1959) from PK01. 1–2, NMNS PM23577. 3–4, NMNS PM23578. 5–12, *Paranannites* sp. indet. 5–6, NMNS PM23772, from BT01-09. 7–9, NMNS PM23575, from BT01-11. 10–12, NMNS PM23576, from a float limestone block at BT02.

NMNS PM23575	37.9	4.2	19.0	16.4	0.11	0.86
NMNS PM23576	47.5	7.4	21.7	19.6	0.16	0.90

Discussion: The described specimens are somewhat similar to *Paranannites aspenensis* Hyatt and Smith (1905, p. 81) from western USA in that they exhibit a fairly compressed shell with a narrow umbilicus, but the number of available specimens is insufficient to make a definitive species assignment.

Occurrence: Described specimens from BT01-09 and BT01-11 within the portion of the *Novispathodus* ex gr. *waageni* Zone that includes the *Urdyceras tulongensis* beds (lower Middle Smithian＝middle Lower Olenekian) in the Bac Thuy Formation, northeastern Vietnam.

Genus ***Owenites*** Hyatt and Smith, 1905

Type species: *Owenites koeneni* Hyatt and Smith, 1905.

Owenites koeneni Hyatt and Smith, 1905

Figs. 89–96

Owenites koeneni Hyatt and Smith, 1905, p. 83, pl. 10, figs. 1–22; Smith, 1932, p. 100, pl. 10, figs. 1–22; Spath, 1934, p. 185, text-fig. 57a–c; Kummel and Steele, 1962, p. 674, pl. 101, figs. 3–7, text-figs. 9–10; Popov, 1962, p. 44, pl. 6, fig. 6; Kuenzi, 1965, p. 374, pl. 53, figs. 1–6, text-figs. 3d, 6; Hada, 1966, pl. 4, figs. 2–4; Kummel and Erben, 1968, p. 121, pl. 19, figs. 10–15; Zakharov, 1968, p. 94, pl. 18, figs. 1–3, text-figs. 21, 24a–c; Collignon, 1973, p. 139, pl. 4, figs. 2–3; Bando, 1981, p. 158, pl. 17, fig. 7; Shevyrev, 1990, p. 118, pl. 1, fig. 5; Shevyrev, 1995, p. 51, pl. 5, figs. 1–3; Brayard and Bucher, 2008, p. 67, pl. 36, figs. 1–8, text-fig. 58; Brühwiler *et al*., 2010, p. 426, fig. 15.9; Brühwiler *et al*., 2012a, p. 43, pl. 25, figs. 1–6; Brühwiler *et al*., 2012c, p. 155, fig. 35AH–AJ; Brayard *et al*., 2013, p. 204, fig. 74a–i.

Owenites egrediens Welter, 1922, p. 151, pl. 168, figs. 22–26, text-figs. 14–18; Smith, 1932, p. 100, pl. 52, figs. 6–8; Spath, 1934, p. 186, text-figs. 56, 57d–f.

Owenites zitteli Smith, 1932, p. 101, pl.52, figs. 1–5.

Owenites aff. *egrediens* Welter, 1922. Kiparisova, 1947, p. 139, pl. 32, figs. 1–3.

Kingites shimizui Sakagami, 1955, p. 138, pl. 2, fig. 2.

Owenites pakungensis Chao, 1959, p. 248, pl. 21, figs. 6–8, text-fig. 26a.

Owenites pakungensis var. *compressus* Chao, 1959, p. 248, pl. 21, figs. 4–5.

Owenites costatus Chao, 1959, p. 249, pl. 22, figs. 10–18, 22–23, text-fig. 26c.

Owenites costatus var. *lenticuluris* Chao, 1959, p. 249, pl. 22, figs. 7–9, text-fig. 26d.

Pseudowenites oxynotus Chao, 1959, p. 252, pl. 23, figs. 1–16, text-fig. 27a–d; Vu Khuc, 1984, p. 82, pl. 7, figs. 3–4; Vu Khuc, 1991, p. 142, pl. 52, figs. 4–5.

Owenites shimizui (Sakagami, 1955). Kummel and Sakagami, 1960, p. 6, pl. 5, figs. 5–6.

Owenites cf. *koeneni* Hyatt and Smith, 1905. Kummel, 1959, p. 441, figs. 2–4.

Owenites carinatus Shevyrev, 1968, p. 189, pl. 16, fig. 1; Vu Khuc, 1984, p. 81, pl. 6, figs. 1–4, text-fig. 16; Vu Khuc, 1991, p. 142, pl. 52, figs. 2–3, pl. 53, figs. 1–2, text-fig. 4.4.

? *Owenites* cf. *koeneni* Hyatt and Smith, 1905. Nichols and Silberling, 1979, pl. 1, figs. 17–18.

Holotype: USNM 75261, figured by Hyatt and Smith (1905, p. 83, pl. 10, figs. 1–4), from the *Meekoceras* beds (middle Smithian) in Inyo Range, California, western USA.

Material examined: One specimen, NMNS PM23579, from KC01-07, two specimens, NMNS PM23580–23581, from KC01-10, two specimens, NMNS PM23582–23583, from KC01-11, one specimen, twenty one specimens, NMNS PM23603–23623 from KC01-13, NMNS PM23584, from KC02-02, five specimens, NMNS PM23589–23593, from BT01-14, nine specimens, NMNS PM23594–23602, from BT02-03, one specimen, NMNS PM23584, from BT02-04, one specimen, NMNS PM23586, from a float limestone block at BT03, one specimen, NMNS PM23587, from PK01-01, and one specimen, NMNS PM23588, from PK01-02.

Description: During earlier growth stages, very involute, fairly compressed shell characterized by lenticular whorl section with angular venter and convex flanks gradually converging from umbilical shoulders to venter. Maximum whorl width occurs near umbilical shoulders. Umbilicus very narrow with moderately high, oblique wall and rounded shoulders. Ornamentation consists of weak, forward projected folds. As growth proceeds, whorl

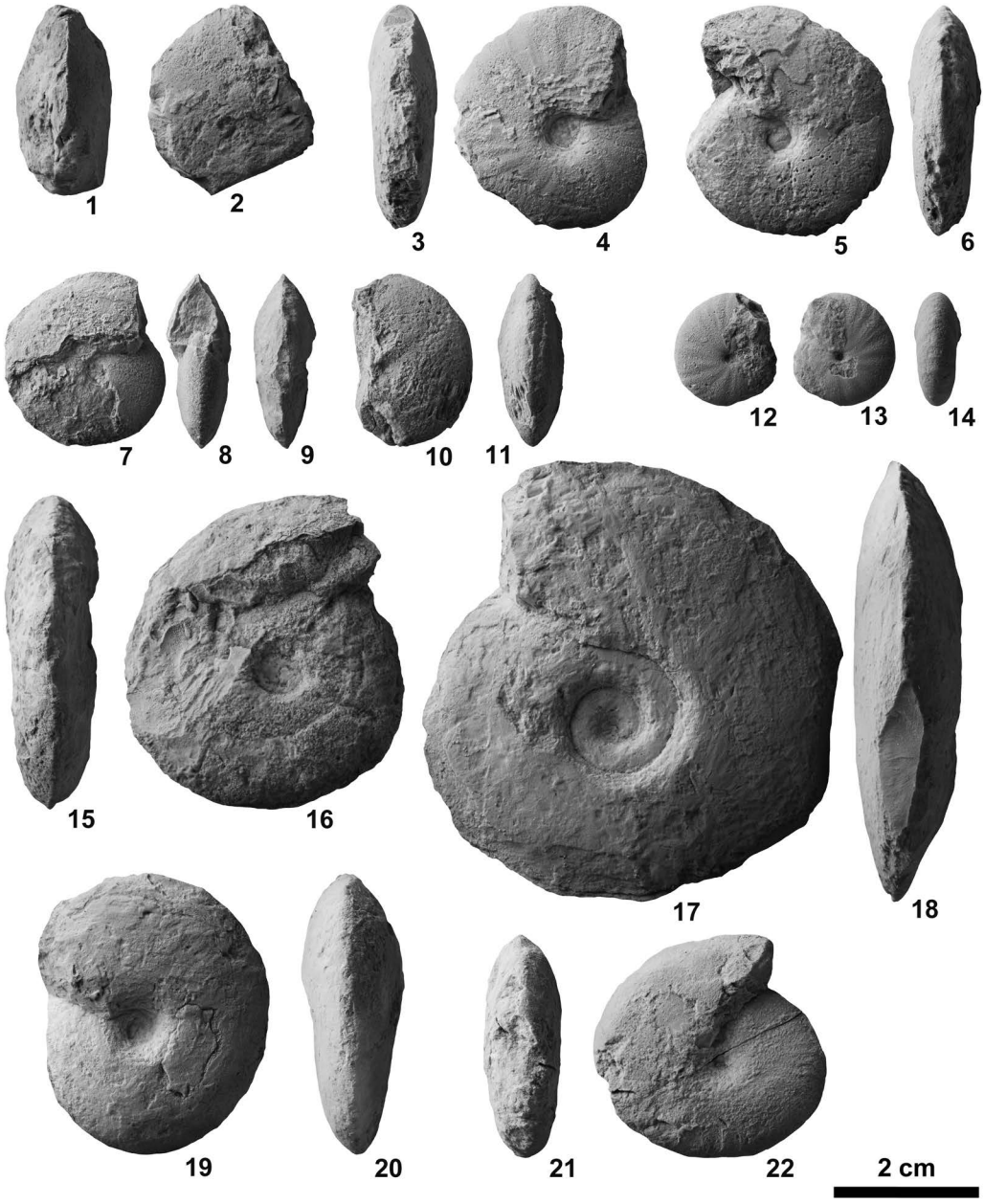

Fig. 89. *Owenites koeneni* Hyatt and Smith, 1905. 1–2, NMNS PM23579, from KC01-07. 3–4, NMNS PM23580, from KC01-10. 5–6, NMNS PM23581, from KC01-10. 7–9, NMNS PM23582, from KC01-11. 10–11, NMNS PM23583, from KC01-13. 12–14, NMNS PM23584, from KC02-02. 15–16, NMNS PM23585, from BT02-04. 17–18, NMNS PM23586, from BT03. 19–20, NMNS PM23587, from PK01-01. 21–22, NMNS PM23588, from PK01-02.

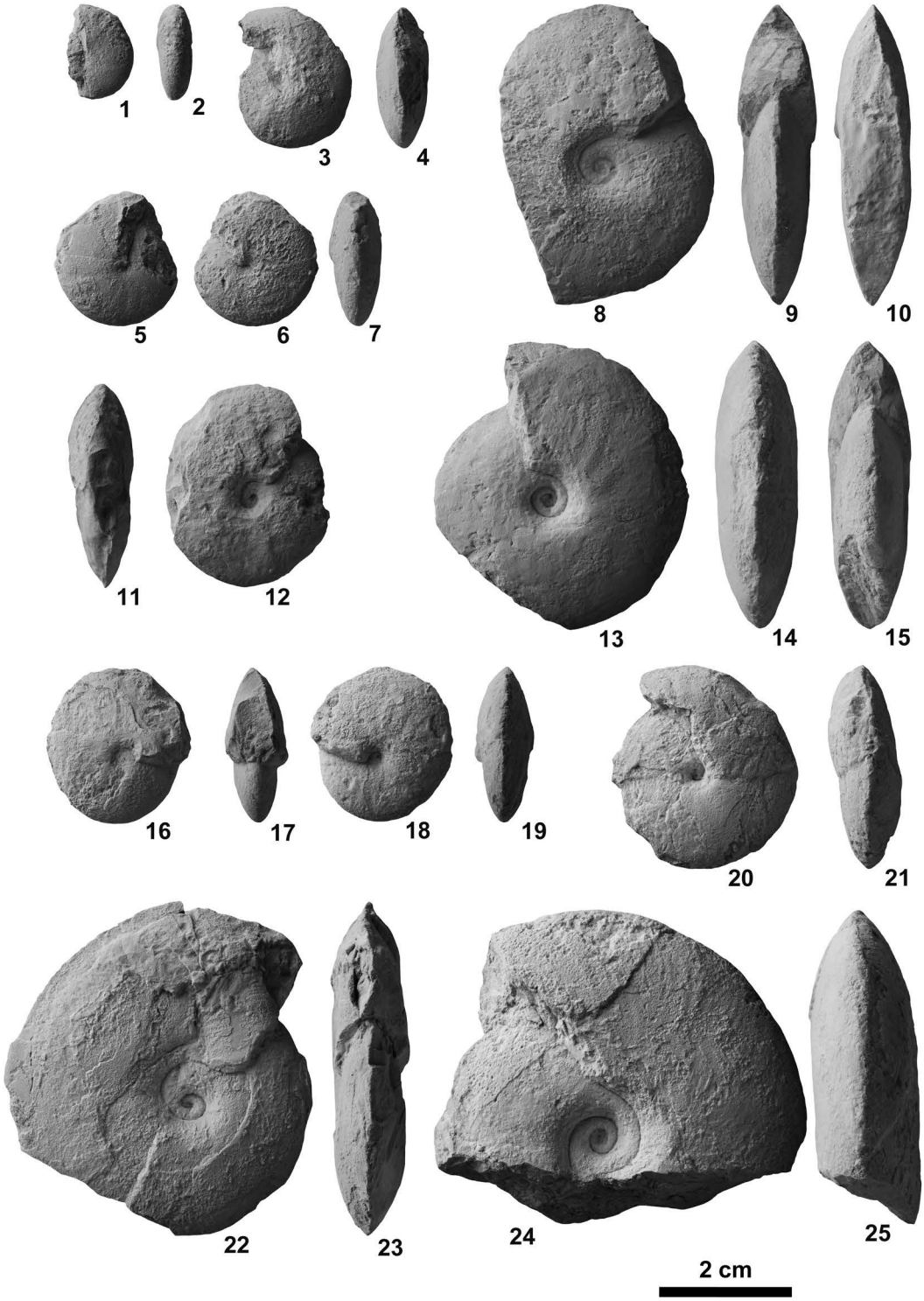

Fig. 90. *Owenites koeneni* Hyatt and Smith, 1905, from KC01-13. 1–2, NMNS PM23603. 3–4, NMNS PM23604. 5–7, NMNS PM23605. 8–10, NMNS PM23606. 11–12, NMNS PM23607. 13–15, NMNS PM23608. 16–19, NMNS PM23609. 20–21, NMNS PM23610. 22–23, NMNS PM23611. 24–25, NMNS PM23612.

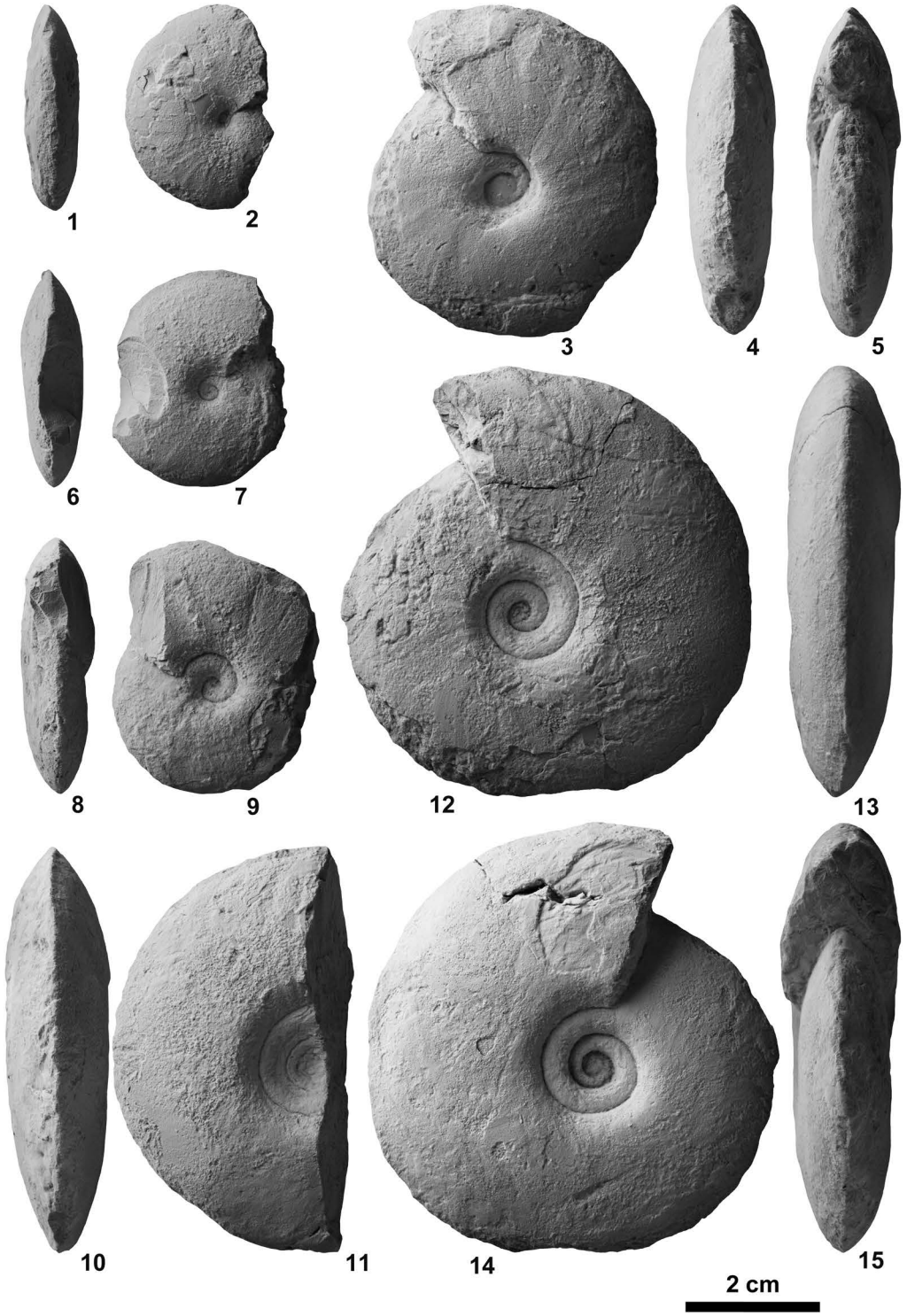

Fig. 91. *Owenites koeneni* Hyatt and Smith, 1905, from KC01-13. 1–2, NMNS PM23613. 3–5, NMNS PM23614. 6–7, NMNS PM23615. 8–9, NMNS PM23616. 10–11, NMNS PM23617. 12–15, NMNS PM23618.

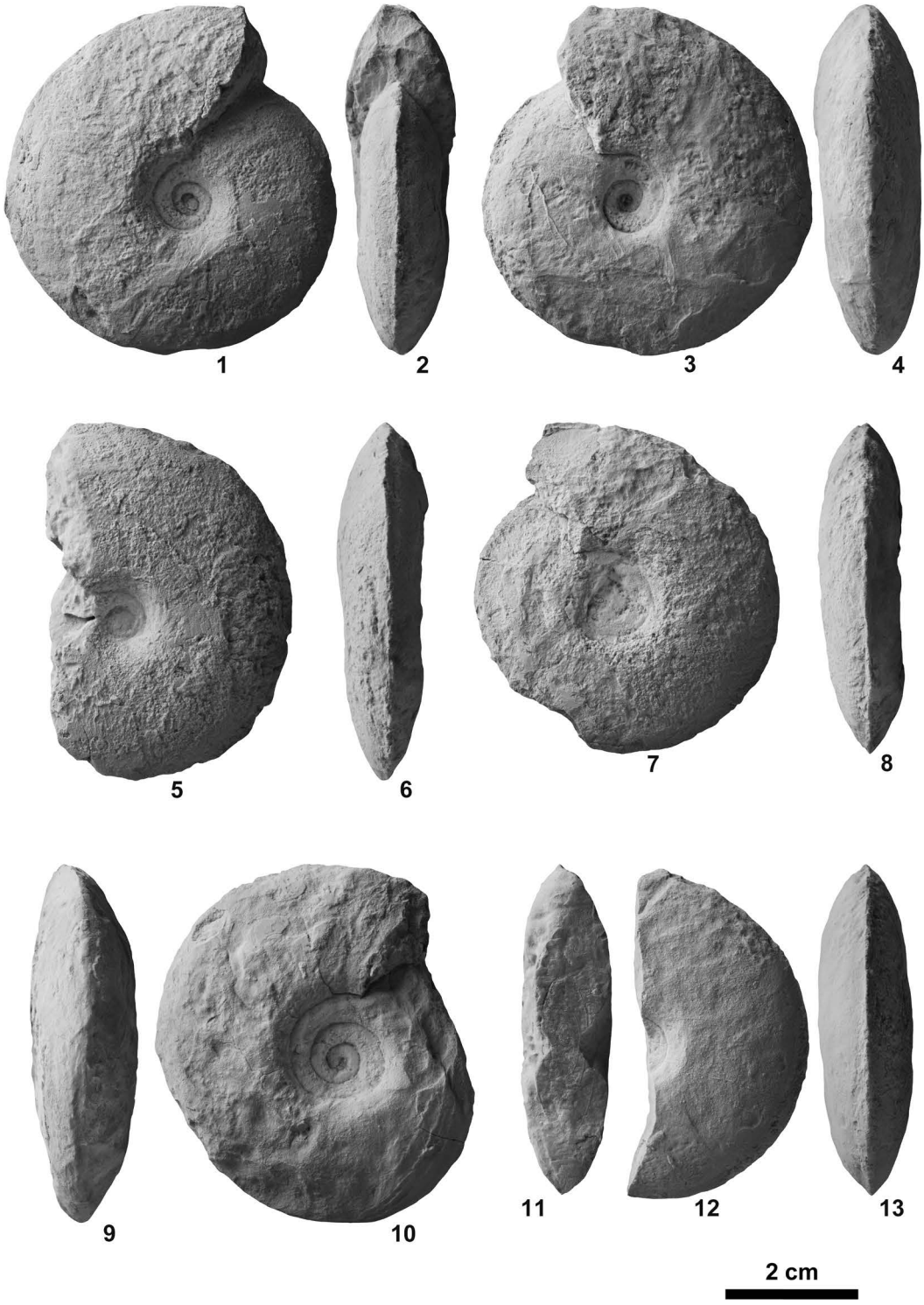

Fig. 92. *Owenites koeneni* Hyatt and Smith, 1905, from KC01-13. 1–4, NMNS PM23619. 5–6, NMNS PM23620. 7–8, NMNS PM23621. 9–10, NMNS PM23622. 11–13, NMNS PM23623.

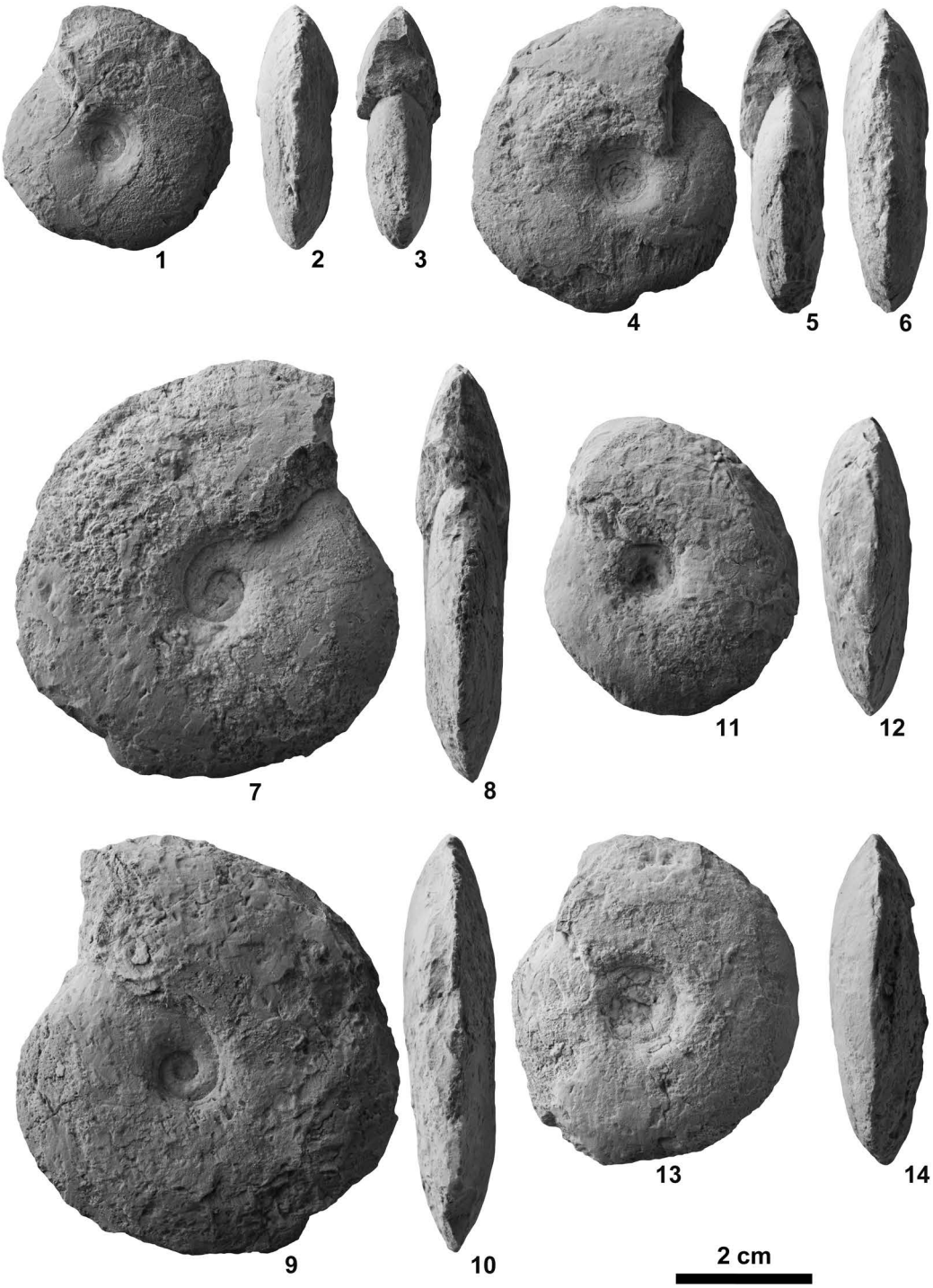

Fig. 93. *Owenites koeneni* Hyatt and Smith, 1905, from BT01-14. 1–3, NMNS PM23589. 4–6, NMNS PM23590. 7–10, NMNS PM23591. 11–12, NMNS PM23592. 13–14, NMNS PM23593.

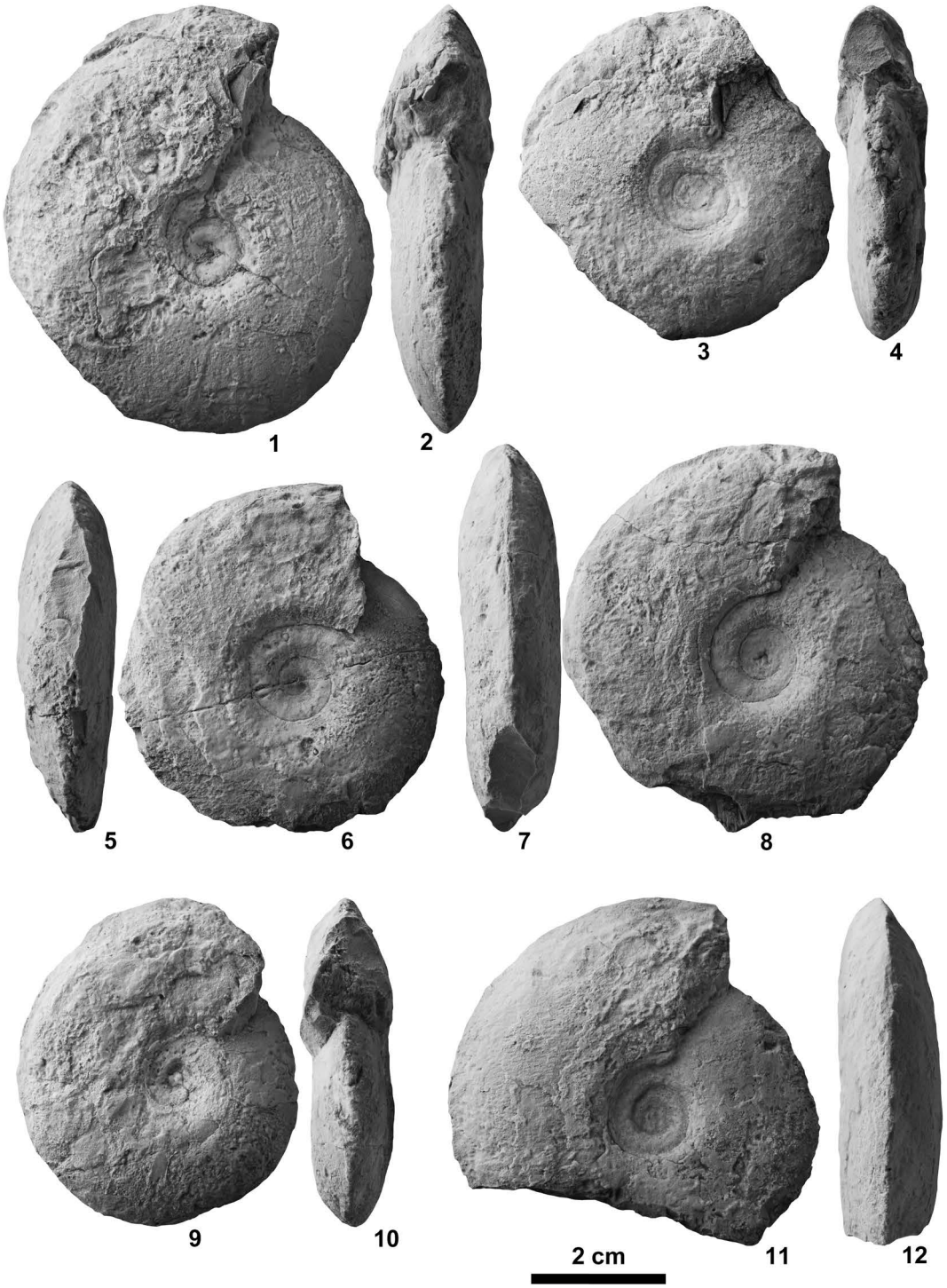

Fig. 94. *Owenites koeneni* Hyatt and Smith, 1905, from BT02-03. 1–2, NMNS PM23594. 3–4, NMNS PM23595. 5–6, NMNS PM23596. 7–8, NMNS PM23597. 9–10, NMNS PM23598. 11–12, NMNS PM23599.

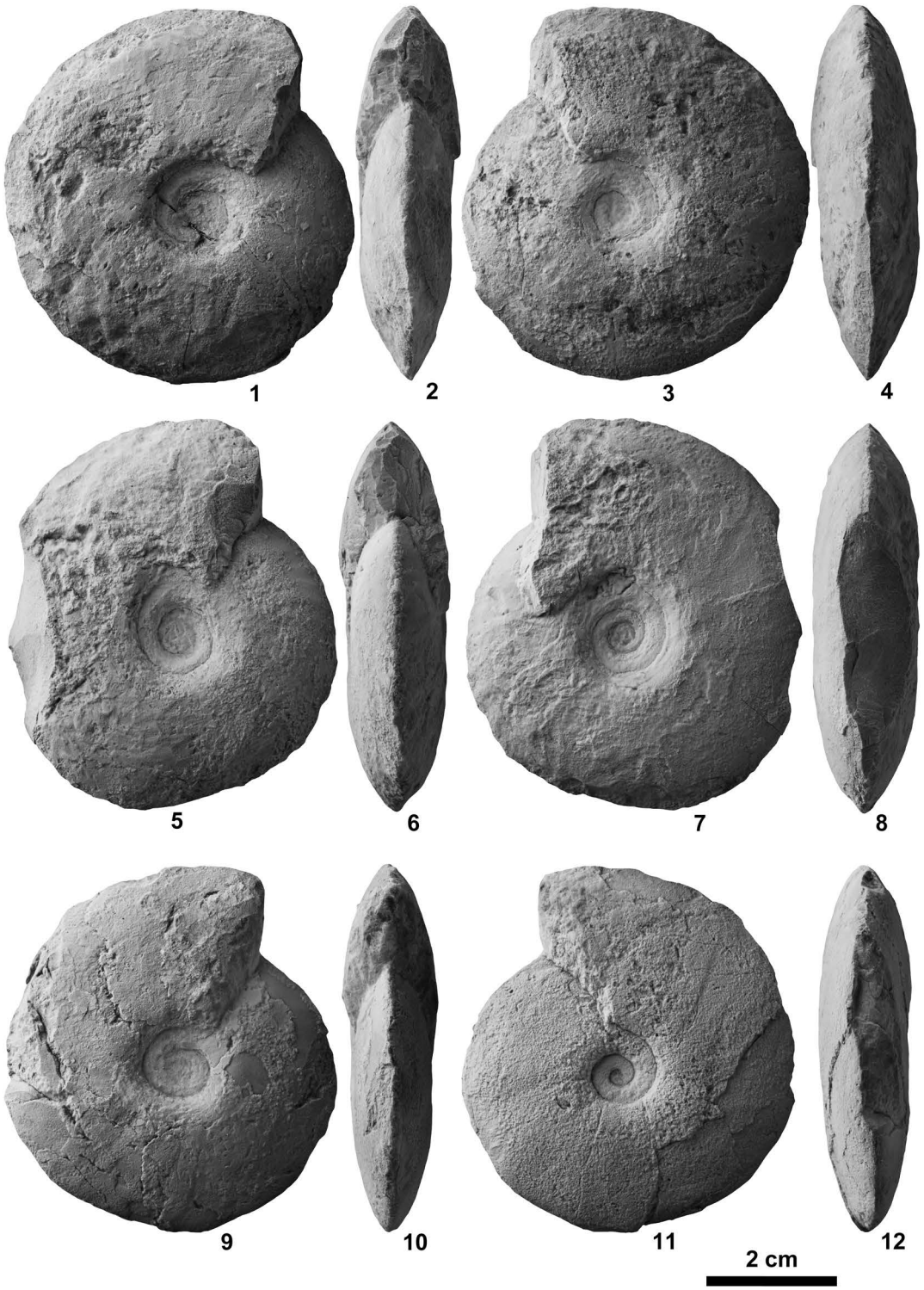

Fig. 95. *Owenites koeneni* Hyatt and Smith, 1905, from BT02-03. 1–4, NMNS PM23600. 5–8, NMNS PM23601. 9–12, NMNS PM23602.

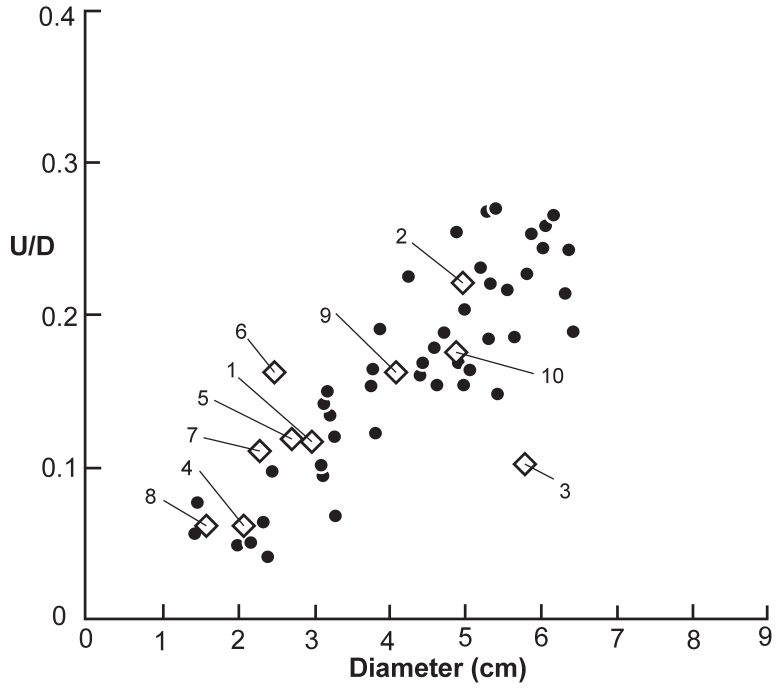
U/D
Diameter (cm)
0.4
0.3
0.2
0.1
0
0 1 2 3 4 5 6 7 8 9
1
2
3
4
5
6
7
8
9
10

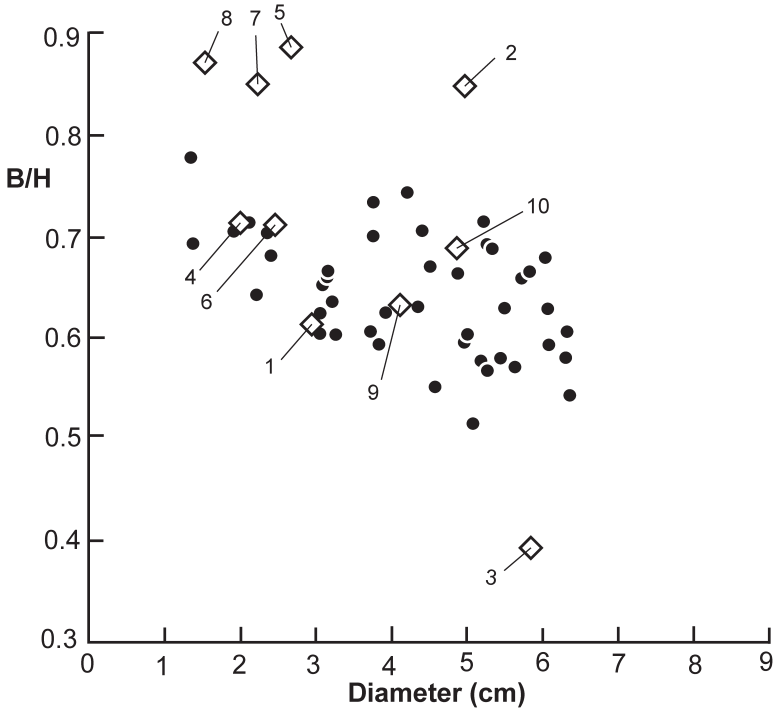
B/H
Diameter (cm)
0.9
0.8
0.7
0.6
0.5
0.4
0.3
0 1 2 3 4 5 6 7 8 9
1
2
3
4
5
6
7
8
9
10

section tends to become more compressed, and umbilical width becomes wider. Suture not well preserved.

Measurements (mm):

Specimen no.	D	U	H	W	U/D	W/H
NMNS PM23584	14.2	1.1	7.9	5.7	0.08	0.78
NMNS PM23603	14.3	0.8	7.9	5.6	0.06	0.70
NMNS PM23605	19.9	1.0	10.6	7.5	0.05	0.71
NMNS PM23604	21.6	1.1	10.9	7.8	0.05	0.71
NMNS PM23609	23.0	1.5	12.9	8.3	0.07	0.64
NMNS PM23583	24.0	1.0	13.0	9.2	0.04	0.71
NMNS PM23582	24.5	2.4	12.9	8.8	0.10	0.68
NMNS PM23607	31.0	4.5	15.1	9.5	0.15	0.63
NMNS PM23613	31.0	3.1	15.7	9.5	0.10	0.61
NMNS PM23610	31.1	3.0	15.0	10.0	0.10	0.66
NMNS PM23580	31.2	4.5	15.3	10.0	0.14	0.65
NMNS PM23581	32.3	4.4	15.3	10.2	0.14	0.67
NMNS PM23588	32.8	2.2	16.7	10.6	0.07	0.63
NMNS PM23615	32.9	4.0	16.0	9.6	0.12	0.60
NMNS PM23585	37.2	5.7	18.2	11.1	0.15	0.61
NMNS PM23589	37.8	6.3	17.4	12.2	0.17	0.70
NMNS PM23587	38.0	4.7	19.1	14.0	0.12	0.73
NMNS PM23616	38.5	7.4	17.1	10.2	0.19	0.60
NMNS PM23593	42.4	9.7	17.9	13.3	0.23	0.74
NMNS PM23607	43.9	7.1	19.9	12.6	0.16	0.63
NMNS PM23592	44.3	7.4	19.0	13.4	0.17	0.71
NMNS PM23590	45.7	8.2	21.0	13.1	0.18	0.67
NMNS PM23606	46.0	7.0	20.1	11.1	0.15	0.55
NMNS PM23595	49.0	12.4	21.0	14.0	0.25	0.67
NMNS PM23614	49.5	8.4	22.0	13.8	0.17	0.63
NMNS PM23598	50.0	10.2	21.2	12.7	0.20	0.60
NMNS PM23623	50.0	7.8	23.2	14.0	0.16	0.60
NMNS PM23611	50.4	8.3	23.0	11.8	0.16	0.51
NMNS PM23621	52.0	12.1	21.6	12.5	0.23	0.58
NMNS PM23622	52.5	14.2	20.2	14.5	0.27	0.72
NMNS PM23596	53.0	14.3	21.2	14.7	0.27	0.69
NMNS PM23599	53.0	11.8	23.0	13.1	0.22	0.57
NMNS PM23619	53.0	9.9	23.4	16.2	0.19	0.69
NMNS PM23620	54.4	8.1	25.0	14.5	0.15	0.58
NMNS PM23612	55.4	12.9	23.8	15.0	0.23	0.63
NMNS PM23602	56.7	10.5	25.7	14.7	0.19	0.57
NMNS PM23600	58.0	13.2	24.3	16.1	0.23	0.66
NMNS PM23597	58.7	14.8	22.6	15.0	0.25	0.66
NMNS PM23601	60.5	14.8	24.8	16.9	0.24	0.68
NMNS PM23617	60.7	15.8	24.9	15.7	0.26	0.63
NMNS PM23586	61.4	16.2	25.3	15.1	0.26	0.60
NMNS PM23594	63.5	13.6	28.8	17.5	0.21	0.61
NMNS PM23618	63.6	15.4	27.8	16.2	0.24	0.58
NMNS PM23591	64.2	12.1	25.7	14.0	0.19	0.54

Discussion: Morphologically, the described specimens are highly variable and include shell forms ranging from fairly compressed to very compressed with an umbilicus that varies from very narrow to fairly narrow. Shell form ratios (U/D, W/H) of the holotypes of *Owenites koeneni* Hyatt and Smith, 1905*, Kingites shimizui* Sakagami, 1955, *O. pakungensis* Chao, 1959, *O. pakungensis* var. *compressus* Chao, 1959, *O. costatus* Chao, 1959, *O. costatus* var. *lenticuluris* Chao, 1959, *Pseudowenites oxynotus* Chao, 1959, and *O. carinatus* Shevyrev, 1968 for the most part are included within the variation of the described specimens (Fig. 89). This evidence strongly suggests that these type specimens merely represent the variants of a single species, and hence, they should be synonymized with *O. koeneni,* the first described taxon of these various species.

The holotype of *Owenites zitteli* Smith, 1932 has a more compressed shell with a narrower umbilicus than these specimens, but according to Kummel and Steele (1962), it probably is a more compressed variant of *O. koeneni.* The lectotype of *O. egrediens* Welter, 1922 has a more depressed shell, but otherwise is very similar to *O. koeneni.* It probably represents a more depressed variant of *O. koeneni.* Similar depressed forms are known

←Fig. 96. Scatter diagrams of umbilical diameter/shell diameter (U/D) versus shell diameter (D) and whorl width/whorl height (W/H) versus shell diameter (D) for *Owenites koeneni* Hyatt and Smith, 1905 from the Bac Thuy Formation, northeastern Vietnam (black circles) and ten selected type specimens referable to *Owenites*. Numbered squares correspond as follows. 1: *Owenites koeneni* (holotype), 2: *O. egrediens* Welter, 1922 (lectotype), 3: *O. zitteli* Smith, 1932 (holotype), 4: *Kingites shimizui* Sakagami, 1955 (holotype), 5: *O. pakungensis* Chao, 1959 (holotype), 6: *O. pakungensis* var. *compressus* Chao, 1959 (holotype), 7: *O. costatus* Chao, 1959 (holotype), 8: *O. costatus* var. *lenticuluris* Chao, 1959 (holotype), 9: *Pseudowenites oxynotus* Chao, 1959 (holotype), 10: *O. carinatus* Shevyrev, 1968 (holotype). Most of the type specimen shell form ratios fit well within those of the specimens from the Bac Thuy Formation.

from Tulong (Brühwiler *et al*., 2010) and Oman (Brühwiler *et al*., 2012a) and they too, have been assigned to *O. koeneni*. Nichols and Silberling (1979) described a specimen as *Owenites* cf. *koeneni* from South-central Alaska, but their generic assignment is questionable because its ventral view is not shown.

Occurrence: Described specimens from KC01-07, KC01-10, KC01-11, KC01-13, KC02-02, BT01-14, BT02-03, BT02-04, BT03, PK01-01 and PK01-02 within the portion of the *Novispathodus* ex gr. *waageni* Zone that includes the *Leyeceras* and *Guodunites* horizons of the *Owenites koeneni* beds (middle to upper Middle Smithian = middle Lower Olenekian) in the Bac Thuy Formation, northeastern Vietnam. This species also occurs in the Middle Smithian in South China (*Owenites koeneni* beds, Brayard and Bucher, 2008; Chao, 1959), Malaya (Hada, 1966), Timor (Welter, 1922), South Tibet (*Pseudoceltites multiplicatus* beds and *Nyalamites angustecostatus* beds, Brühwiler *et al*., 2010), Spiti (*Nyalamites angustecostatus* beds, Brühwiler *et al*., 2012c), Kashmir (*Owenites-Kashmirites* Zone, Bando, 1981), Afganistan (Kummel and Erben, 1968; Collignon, 1973), Oman (*Owenites koeneni* fauna, Brühwiler *et al*., 2012a), northwestern Caucasus (Shevyrev, 1968, 1990, 1995), New Zealand (Kummel, 1959), Japan (Kummel and Sakagami, 1960), South Primorye (*Owenites koeneni* Zone, Zakharov, 1968), and western USA (*Meekoceras gracilitatis* Zone, Kummel and Steele, 1962, Kuenzi, 1965; *Owenites* beds, Brayard *et al*., 2013).

Superfamily Sageceratoidea Hyatt, 1884
Family Aspenitidae Spath, 1934
Genus ***Aspenites*** Hyatt and Smith, 1905

Type species: *Aspenites acutus* Hyatt and Smith, 1905.

Aspenites acutus Hyatt and Smith, 1905
Fig. 97

Aspenites acutus Hyatt and Smith, 1905, p. 96, pl. 2, figs. 9–13, pl. 3, figs. 1–5; Smith, 1932, p. 86, pl. 2, figs. 9–13, pl. 3, figs. 1–5, pl. 30, figs. 1–26, pl. 60, figs. 4–6; Chao, 1959, p. 269, pl. 35, figs. 12–18, 23, text-figs. 34a; Kummel and Steele, 1962, p. 692, pl. 99, figs. 16–17; Nichols and Silberling, 1979, pl. 1, figs. 12–14; Brayard and Bucher, 2008, p. 77, pl. 42, figs. 1–9, text-fig. 67; Brühwiler *et al*., 2010, p. 429, fig. 16.12, 16.13; Brühwiler *et al*., 2012a, p. 48, pl. 26, figs. 1–2; Brühwiler *et al*., 2012c, p. 166, fig. 41A–M; Brayard *et al*., 2013, p. 212, fig. 81a–j.

Aspenites laevis Welter, 1922, p. 99, pl. 155, figs. 4–5; Smith, 1932, p. 86, pl. 28, figs. 28–33; Chao, 1959, p. 270, pl. 35, figs. 9–11, text-fig. 34b.

Aspenites obtusus Smith, 1932, p. 86, pl. 31, figs. 8–10.

Hemiaspenites obtusus (Smith, 1932). Kummel and Steele, 1962, p. 666, pl. 99, fig. 18.

Aspenites cf. *acutus* Hyatt and Smith, 1905. Nichols and Silberling, 1979, pl. 1, figs. 15–16.

Holotype: USNM 75249, figured by Hyatt and Smith (1905, p. 96, pl. 3, figs. 1–2), from the *Meekoceras* beds (middle Smithian) in the Inyo Range, California, western USA.

Material examined: One specimen, NMNS PM23635, from BT01-09 and one specimen, NMNS PM23636, from KC01-13.

Description: Very involute, very compressed oxycone with acutely keeled venter and slightly convex flanks with maximum width at mid-flank. Umbilicus occluded. Shell surface smooth or ornamented with radial folds. Suture ceratitic with many adventitious elements.

Measurements (mm):

Specimen no.	D	U	H	W	U/D	W/H
NMNS PM23636	30.7	0.0	18.8	5.6	0.0	0.18
NMNS PM23635	48.8	0.0	30.0	—	0.0	—

Discussion: *Aspenites laevis* Welter, 1922 and *A. obtusus* Smith, 1932 were synonymized with *A. acutus* by Brayard and Bucher (2008, p. 77), and we agree with their interpretation. *Hedenstroemia acuta* Kraft and Diner, 1909 from Spiti is somewhat similar to *A. acutus*, but differs by its suture line, which has lateral lobes with many denticulations at the base and wide lateral saddles.

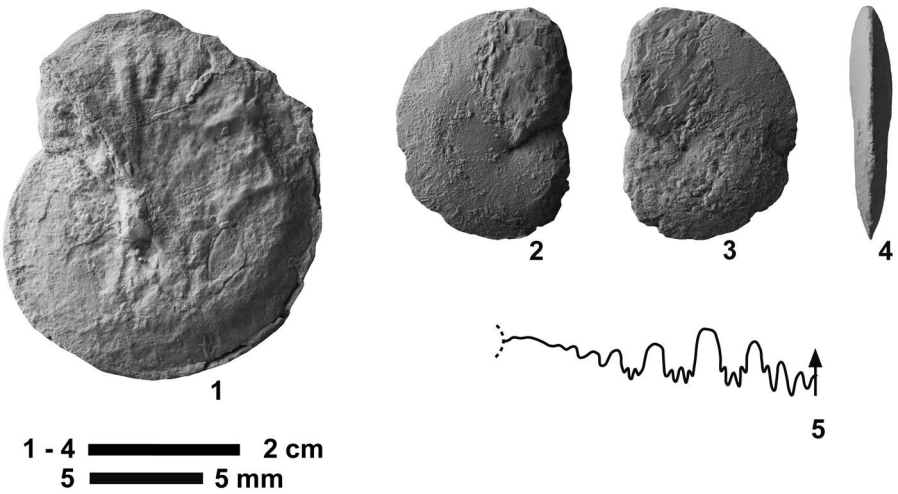

Fig. 97. *Aspenites acutus* Hyatt and Smith, 1905. 1, NMNS PM23635, from BT01-09. 2–5, NMNS PM23636, from KC01-13.

Occurrence: Described specimens from BT01-09 and KC01-03 within the portion of the *Novispathodus* ex gr. *waageni* Zone that includes the *Urdyceras tulongensis* beds (lower Middle Smithian=middle Lower Olenekian) and *Leyeceras* horizon of the *Owenites koeneni* beds (middle Middle Smithian=middle Lower Olenekian) in the Bac Thuy Formation, northeastern Vietnam. This species also occurs in the Middle Smithian in South China (*Flemingites rursiradiatus* beds and *Owenites koeneni* beds, Brayard and Bucher, 2008), Timor (Welter, 1922), South Tibet (*Brayardites compressus* beds, Brühwiler *et al*., 2010), Spiti (*Brayardites compressus* beds, Brühwiler *et al*., 2012c), Oman (*Rohilites omanensis* fauna, *Nammalites pilatoides* fauna, and *Owenites koeneni* fauna, Brühwiler *et al*., 2012a), South-central Alaska (Nichols and Silberling, 1979) and western USA (*Meekoceras gracilitatis* Zone, Kummel and Steele, 1962; *Owenites* beds, Brayard *et al*., 2013).

Family Hedenstroemiidae Hyatt, 1884
Genus ***Pseudosageceras*** Diener, 1895

Type species: *Pseudosageceras* sp. indet. Diener, 1895.

Pseudosageceras multilobatum
Noetling, 1905a

Figs. 98, 99

Pseudosageceras sp. indet. Diener, 1895, p. 28, pl. 1, fig. 8.

Pseudosageceras multilobatum Noetling, 1905a, p. 181, pls. 19–27; Noetling, 1905b, pl. 23, fig. 4, pl. 25, fig. 1, pl. 26, fig. 3; Krafft and Diener, 1909, p. 145, pl. 21, fig. 5; Welter, 1922, p. 94, fig. 3; Smith, 1932, p. 87, pl. 4, figs. 1–3, pl. 5, figs. 1–6, pl. 25, figs. 7–16, pl. 60, fig. 32, pl. 63, figs. 1–6; Collignon, 1933, p. 56, pl. 11, fig. 2; Spath, 1934, p. 54, text-fig. 6a; Kiparisova,1947, p. 127, pl. 25, figs. 3–4; Chao, 1959, p. 183, pl. 1, figs. 9, 12; Kummel, 1966, p. 388, pl. 1, figs. 11–12; Hada, 1966, pl. 4, fig. 6; Kummel and Erben, 1968, p. 112, pl. 19, fig. 9; Shevyrev, 1968, p. 79, pl. 1, figs. 1–2; Collignon, 1973, p. 5, pl. 1, fig. 1; Weitschat and Lehmann, 1978, p. 75, pl. 10, fig. 2; Vu Khuc, 1984, p. 26, pl. 1, fig. 1, text-fig. 1; Pakistani-Japanese Research Group, 1985, pl. 12, figs. 5–7; Vu Khuc, 1991, p. 119, pl. 45, figs. 5–6, text-fig. 2.2; Tozer, 1994, p. 83, pl. 18, fig. 1, text-fig. 17; Brayard and Bucher, 2008, p. 70, pl. 37, figs. 1–5; Shigeta and Zakharov, in Shigeta *et al*., 2009, p. 140, figs. 129–130; Brühwiler *et al*., 2010, p. 429, fig. 16.14; Brühwiler *et al*., 2012a, p. 47, pl. 26, fig. 4; Brühwiler *et al*., 2012c, p. 109, fig. 95A–N; Brayard *et al*., 2013, p. 208, fig. 77a–f.

non *Pseudosageceras multilobatum* Noetling, 1905a. Kummel and Steele, 1962, p. 701, pl. 102, figs. 1–2.

Lectotype: Designated by Spath (1934, p.

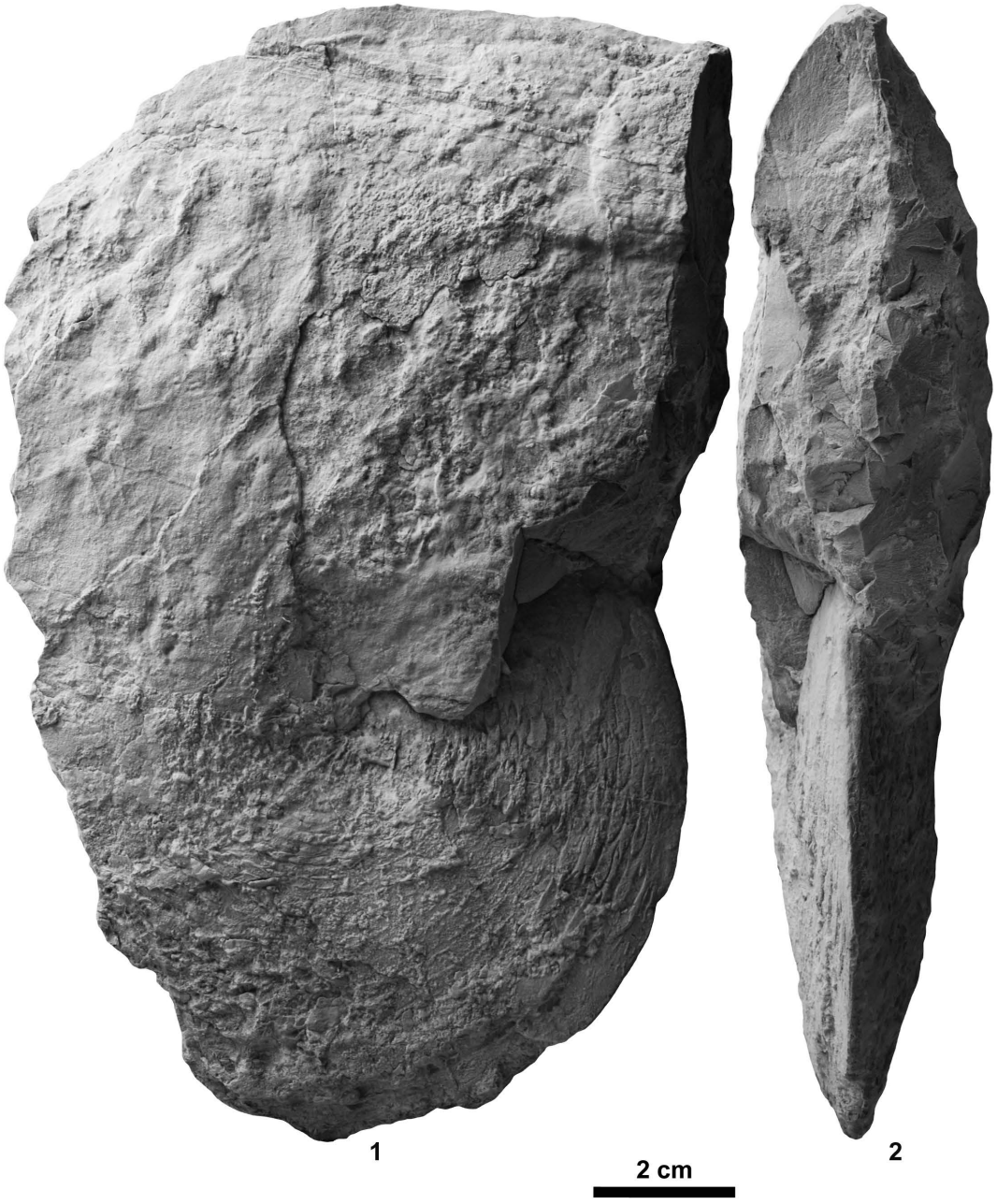

Fig. 98. *Pseudosageceras multilobatum* Noetling, 1905, from BT02-02. 1–2, NMNS PM23638.

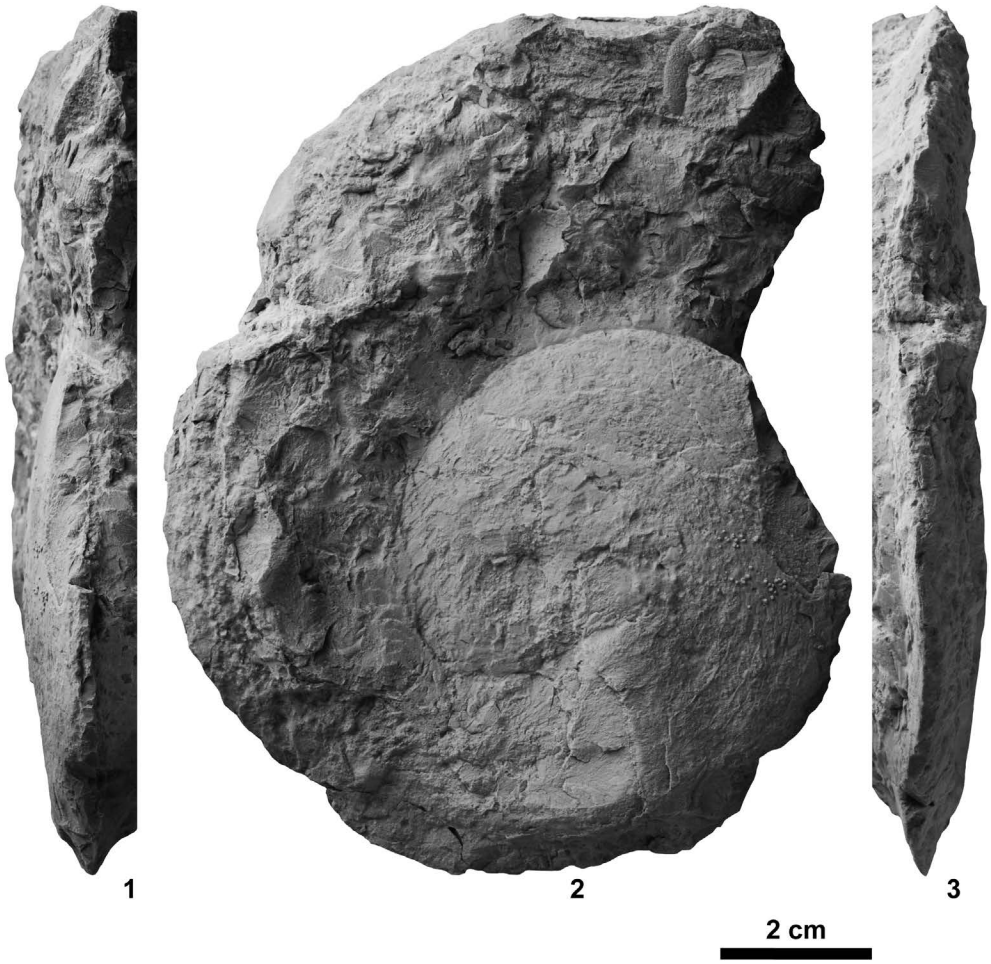

Fig. 99. *Pseudosageceras multilobatum* Noetling, 1905, from BT01-14. 1–3, NMNS PM23637.

54), is original of Noetling (1905a, p. 181, pl. 19, fig. 1, pl. 24, fig. 12) from the Ceratite Marls of the Salt Range, Pakistan.

Material examined: One specimen, NMNS PM23637, from BT01-14 and one specimen, NMNS PM23638, from BT02-02.

Description: Very involute, very compressed oxycone with very narrow, bicarinate venter and weakly convex flanks, gently convergent from occluded umbilicus to venter. Shell surface smooth. Suture ceratitic with many adventitious elements.

Discussion: The specimen described as *Pseudosageceras multilobatum* by Kummel and Steele (1962, pl. 102, figs. 1–2) from Nevada is characterized by an acutely keeled venter and wider lobes and saddles than *Pseudosageceras*. It probably should be assigned to *Aspenites*. As earlier reported by Shigeta and Zakharov (in Shigeta *et al.*, 2009), the specimen described as *Pseudosageceras* sp. by Diener (1895) from South Primorye is only a partial phragmocone, but it displays the same shell shape and suture as *P. multilobatum*, and thus, is probably conspecific.

Occurrence: Described specimens from BT02-02 and BT01-14 within the portion of the *Novispathodus* ex gr. *waageni* Zone that includes the *Urdyceras tulongensis* beds (lower Middle Smithian = middle Lower Ole-

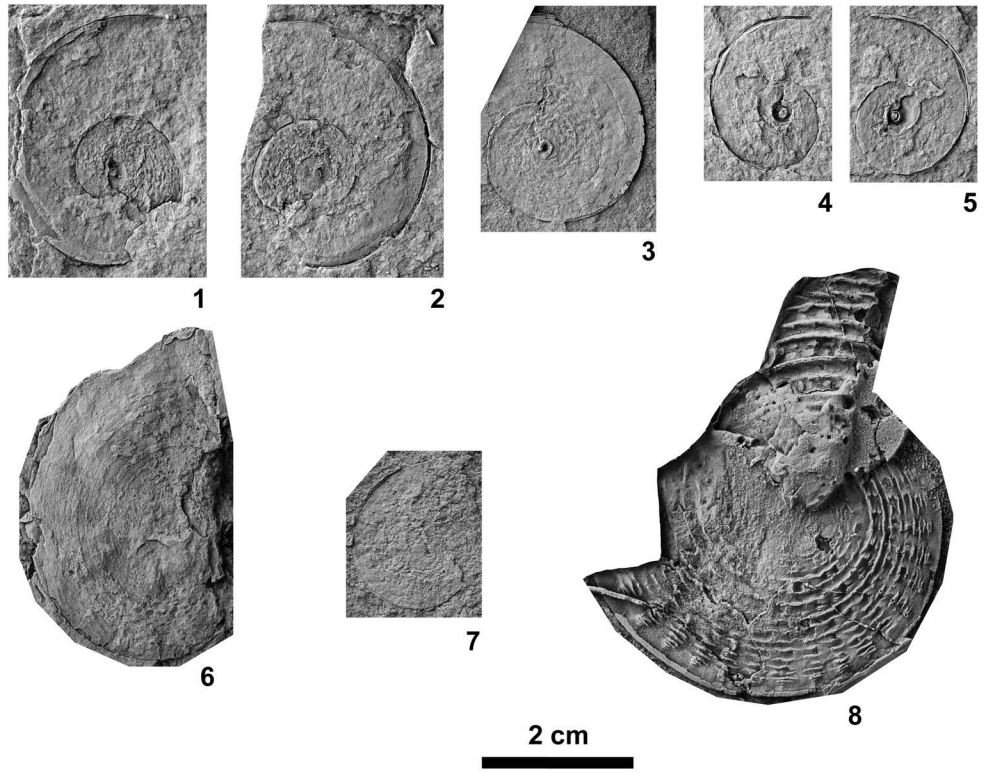

Fig. 100. *Pseudosageceras* sp. indet. 1–6, from KC02-11. 1–2, NMNS PM23648. 3, NMNS PM23649 (rubber cast of outer mold). 4–5, NMNS PM23650. 6, NMNS PM23651. 7, NMNS PM23760, from KC02-13. 8, NMNS PM23652 (rubber cast of outer mold), from KC02-15.

nekian) and the *Leyeceras* horizon of the *Owenites koeneni* beds (middle Middle Smithian=middle Lower Olenekian) in the Bac Thuy Formation, northeastern Vietnam. This taxon, which is probably the most cosmopolitan species of the Early Triassic, occurs in the Smithian in South China (Chao, 1959; Brayard and Bucher, 2008), Malaya (Hada, 1966), Timor (Welter, 1922), South Tibet (Brühwiler *et al*., 2010), Spiti (Krafft and Diener, 1909), Afganistan (Kummel and Erben, 1968; Collignon, 1973), Salt Range (Kummel, 1966; Brühwiler *et al*., 2012b), Madagascar (Collignon, 1933), Oman (Brühwiler *et al*., 2012a), northwestern Caucasus (Shevyrev, 1968), South Primorye (Kiparisova, 1961), western USA (Hyatt and Smith, 1905, Smith, 1932, Brayard *et al*., 2013), Arctic Canada (Tozer, 1994) and Spitsbergen (Weitschat and Lehmann, 1978).

Pseudosageceras sp. indet.

Fig. 100

Material examined: Four specimens, NMNS PM23648–23651, from KC02-11, one specimen, NMNS PM23760, from KC02-13 and one specimen, NMNS PM23652, from KC02-15.

Description: Very involute, very compressed shell with very narrow, bicarinate venter. Umbilicus occluded. Suture ceratitic with many adventitious elements.

Discussion: The described specimens are very similar to *Pseudosageceras multilobatum* Noetling, 1905, but a definitive assignment in not possible because of their poor preservation.

Occurrence: Described specimen from KC02-11 within the portion of the *Novispathodus pingdingshanensis* Zone represented by the *Tirolites* cf. *cassianus* beds (lowest Lower Spathian = lowest Upper Olenekian), those from KC02-13 and KC02-15 within the portion of the *Triassospathodus symmetricus* Zone represented by the *Tirolites* cf. *cassianus* beds (lowest Lower Spathian = lowest Upper Olenekian) and *Tirolites* sp. nov. beds (Lower Spathian = lower Upper Olenekian) in the Bac Thuy Formation, northeastern Vietnam.

Superfamily Dinaritoidea Mojsisovics, 1882
Family Tirolitidae Mojisisovics, 1882
Genus ***Tirolites*** Mojsisovics, 1879

Type species: *Tirolites idrianus* Hauer, 1865.

Tirolites cf. ***cassianus*** (Quenstedt, 1849)

Fig. 101

cf. *Ceratites cassianus* Quenstedt, 1849, p. 231, pl. 18, fig. 11.
cf. *Tirolites spinosus* Mojsisovics, 1882, p. 70, pl. 2, fig. 2.
cf. *Tirolites darwini* Mojsisovics, 1882. Kittl, 1903, p. 60, pl. 11, figs. 1–2.
cf. *Tirolites spinosior* Kittl, 1903, p. 62, pl. 11, fig. 5.
cf. *Tirolites toulai* Kittl, 1903, p. 64, pl. 11, fig. 11.

Material examined: Four specimens, NMNS PM23662–23665, from KC02-11, two specimens, NMNS PM23762–23763, from KC02-12, and two specimens, NMNS PM23765–23766, from KC02-13.

Description: Very evolute, very compressed shell with arched venter, rounded ventral shoulders, and slightly convex flanks. Umbilicus fairly wide with moderately high, gently inclined wall. Ornamentation consists of spiny tubercles on ventrolateral shoulders as well as strong radial ribs on early to middle growth stages. Ribs decrease in strength and become much finer, while ventrolateral tubercles exhibit attenuation in strength and finally disappear on mature body chamber. Suture not preserved.

Measurements (mm):

Specimen no.	D	U	H	W	U/D	W/H
NMNS PM23662	39.2	16.2	14.0	—	0.41	—
NMNS PM23665	57.0	24.0	21.5	—	0.42	—
NMNS PM23663	59.0	26.5	20.8	—	0.43	—
NMNS PM23664	89.0	37.0	32.0	—	0.42	—

Discussion: Even though the present specimens are significantly deformed and crushed, their distinctive ornamentation and shell shape enable me to identify them with reasonable confidence as *Tirolites cassianus*. Specimen NMNS PM23664 is very close to specimens described as *T. spinosus* by Mojsisovics (1882, pl. 2, fig. 2), *T. darwini* Mojsisovics, 1882 by Kittl (1903, pl. 11, figs. 1–2), *T. spinosior* by Kittl (1903, pl. 11, fig. 5), and *T. toulai* by Kittl (1903, pl. 11, fig. 11). These species were synonymized with *T. cassianus* by Kummel (1969).

Occurrence: Described specimens from KC02-11 within the portion of the *Novispathodus pingdingshanensis* Zone represented by the *Tirolites* cf. *cassianus* beds (lowest Lower Spathian = lowest Upper Olenekian), and those of KC02-12 and KC02-13 within the portion of the *Triassospathodus symmetricus* Zone represented by the *Tirolites* cf. *cassianus* beds (lowest Lower Spathian = lowest Upper Olenekian) in the Bac Thuy Formation, northeastern Vietnam. *Tirolites cassianus* occurs in the lowest Lower Spathian in the Alps (Werfen Formation), Dalmatia and associated regions (Mojsisovics, 1882; Kittl, 1903; Krystyn, 1974; Posenato, 1992), and Mangyshlak (Shevyrev, 1968).

Tirolites sp. nov.

Figs. 102–113

Material examined: Seven specimens, NMNS PM23666–23672, from KC02-14, twenty specimens, NMNS PM23673–23690, 23768–23769, from KC02-15, two specimen, NMNS PM23770–23771, from KC02-16, four specimen, NMNS PM23695–23698, from KC02-18, two specimens, NMNS PM23691–

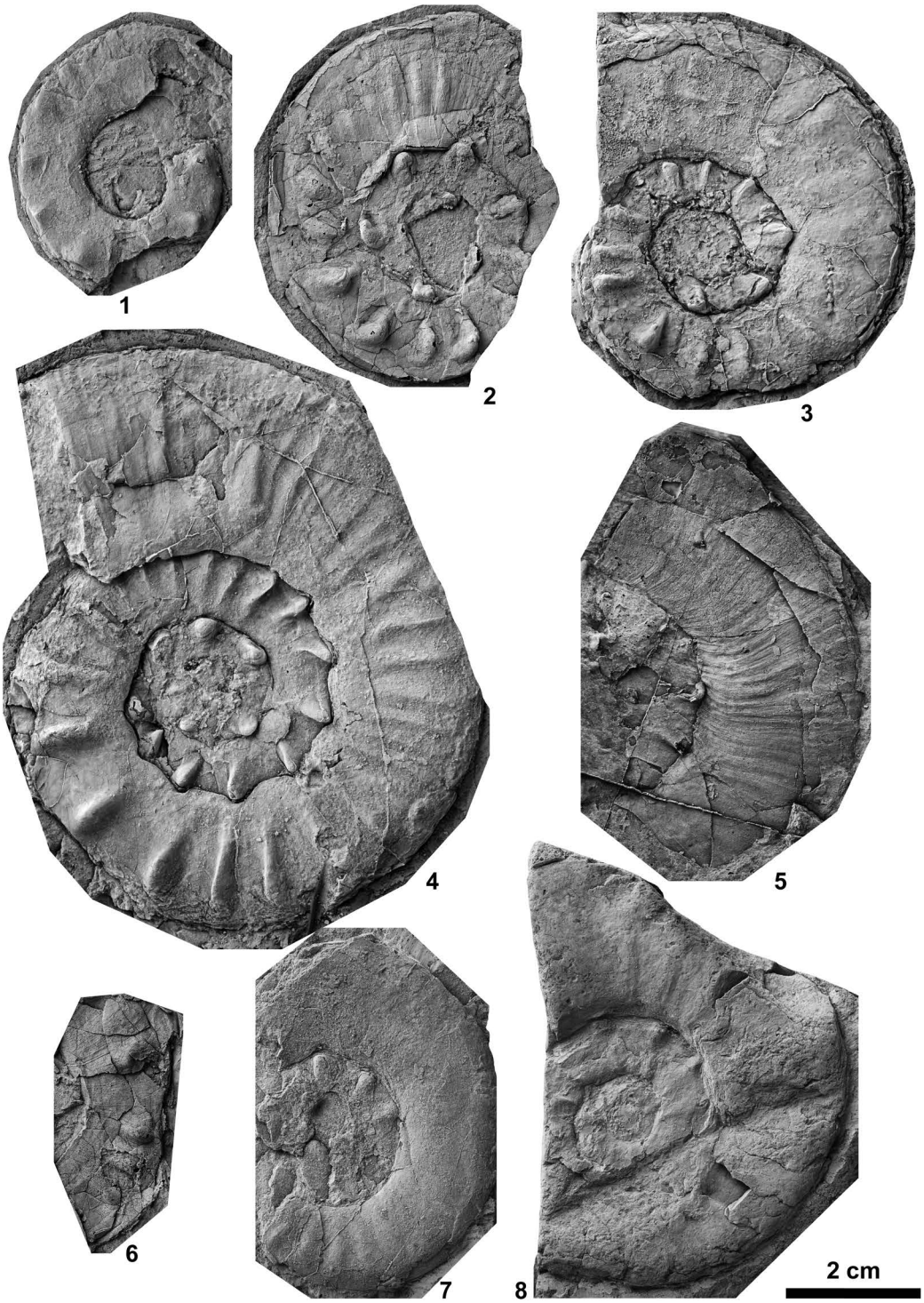

Fig. 101. *Tirolites* cf. *cassianus* (Quenstedt, 1849). 1–4, from KC02-11. 1, NMNS PM23662. 2, NMNS PM23665 (rubber cast of outer mold). 3, NMNS PM23663. 4, NMNS PM23664. 5–6, from KC02-12. 5, NMNS PM23762 (rubber cast of outer mold). 6, NMNS PN23763 (rubber cast of outer mold). 7–8, from KC02-13. 7, NMNS PM23765. 8, NMNS PM23766.

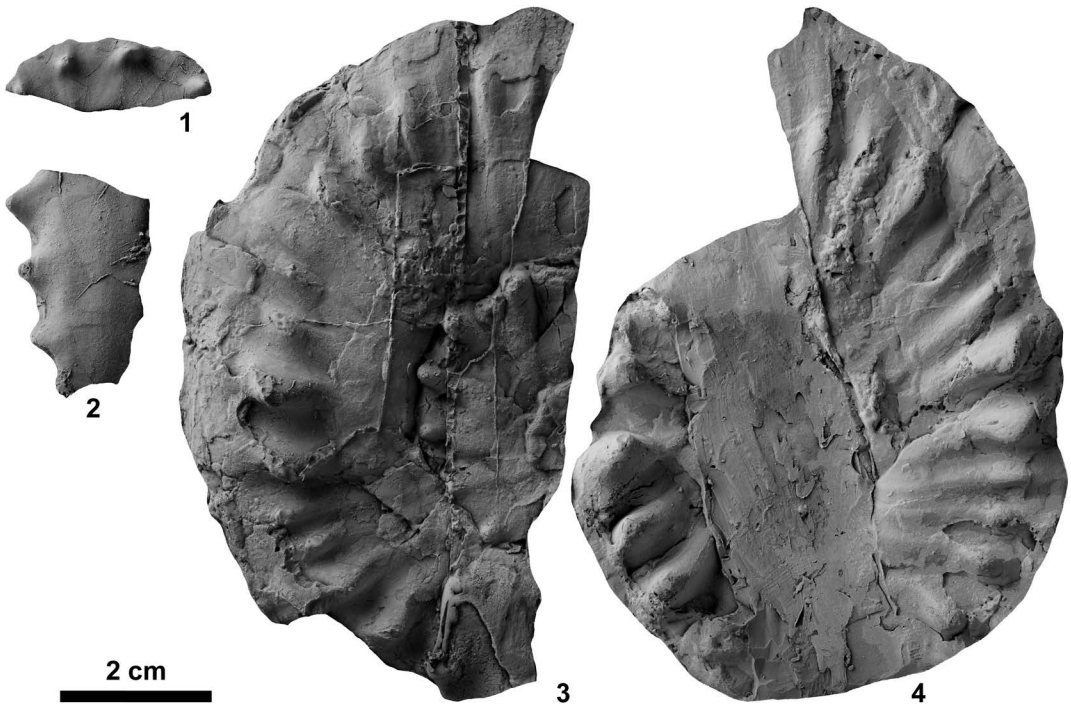

Fig. 102. *Tirolites* sp. nov. 1–4, from NT01-10. 1, NMNS PM23764. 2, NMNS PM23693. 3–4, NMNS PM23694 (rubber casts of outer molds).

23692, from BT02-06, and three specimens, NMNS PM23693–23694, 23764, from NT01-10.

Description: Fairly evolute, very compressed shell with rectangular whorl section, broadly rounded or nearly tabulate venter, rounded ventral shoulders, and slightly convex flanks with maximum whorl width near ventral shoulder. Umbilicus moderately wide with moderately high, gently inclined wall. Ornamentation consists of large, spiny tubercles on ventrolateral shoulders as well as variable strength, slightly sinuous, prorsiradiate ribs that arise on or slightly above umbilical shoulder and culminate in the large tubercles on the ventral shoulder. Ribs and ventrolateral tubercles abruptly disappear on mature body chamber, but weaker tubercles may rarely re-occur. Suture not preserved.

Measurements (mm):

Specimen no.	D	U	H	W	U/D	W/H
NMNS PM23678	62.4	21.0	25.0	—	0.34	—
NMNS PM23668	65.0	20.5	25.0	—	0.32	—
NMNS PM23666	72.0	24.0	28.0	—	0.33	—
NMNS PM23676	72.5	24.0	30.5	—	0.33	—
NMNS PM23679	74.0	23.5	28.0	—	0.32	—
NMNS PM23770	74.0	25.6	29.0	—	0.35	—
NMNS PM23684	75.5	25.6	30.0	—	0.34	—
NMNS PM23695	76.0	25.0	27.0	—	0.33	—
NMNS PM23670	78.0	25.0	31.5	—	0.32	—
NMNS PM23683	79.0	26.3	31.7	—	0.33	—
NMNS PM23771	79.0	28.0	—	—	0.35	—
NMNS PM23685	80.5	27.0	32.0	—	0.34	—
NMNS PM23769	82.5	31.0	30.0	—	0.38	—
NMNS PM23677	84.0	26.4	34.0	—	0.31	—
NMNS PM23768	87.0	31.0	31.0	—	0.36	—
NMNS PM23687	90.5	30.4	35.5	—	0.34	—

Discussion: The described specimens differ from *Tirolites cassianus* (Quenstedt, 1849) by their more involute shell, narrower umbilicus and nearly smooth mature body chamber, and they likely represent a new species. However, we hesitate to propose a new specific

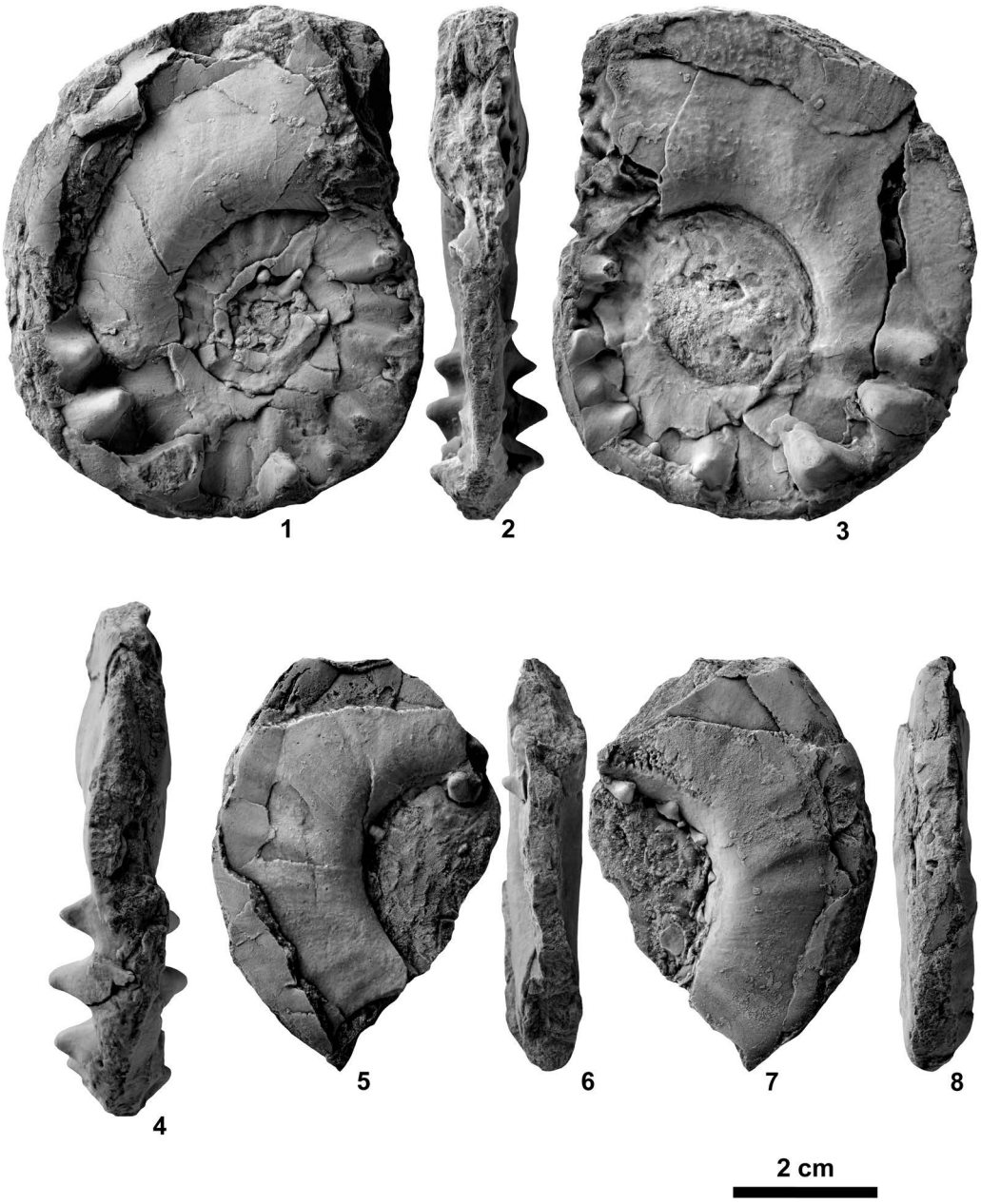

Fig. 103. *Tirolites* sp. nov., from KC02-14. 1–4, NMNS PM23666. 5–8, NMNS PM23667.

Fig. 104. *Tirolites* sp. nov., from KC02-14. 1–4, NMNS PM23668. 5, NMNS PM23669.

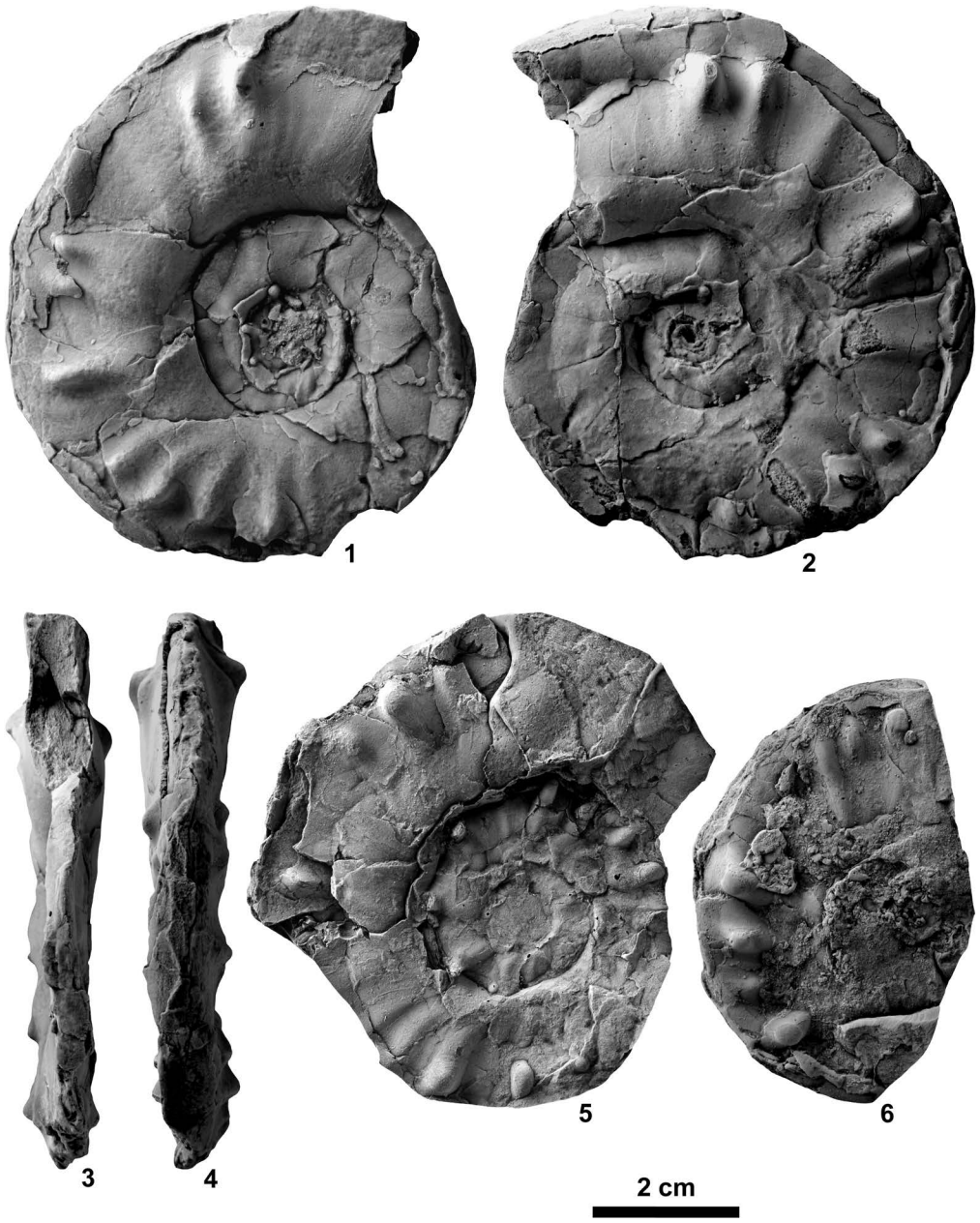

Fig. 105. *Tirolites* sp. nov., from KC02-4. 1–4, NMNS PM23670. 5, NMNS PM23671 (rubber cast of outer mold). 6, NMNS PM23672 (rubber cast of outer mold).

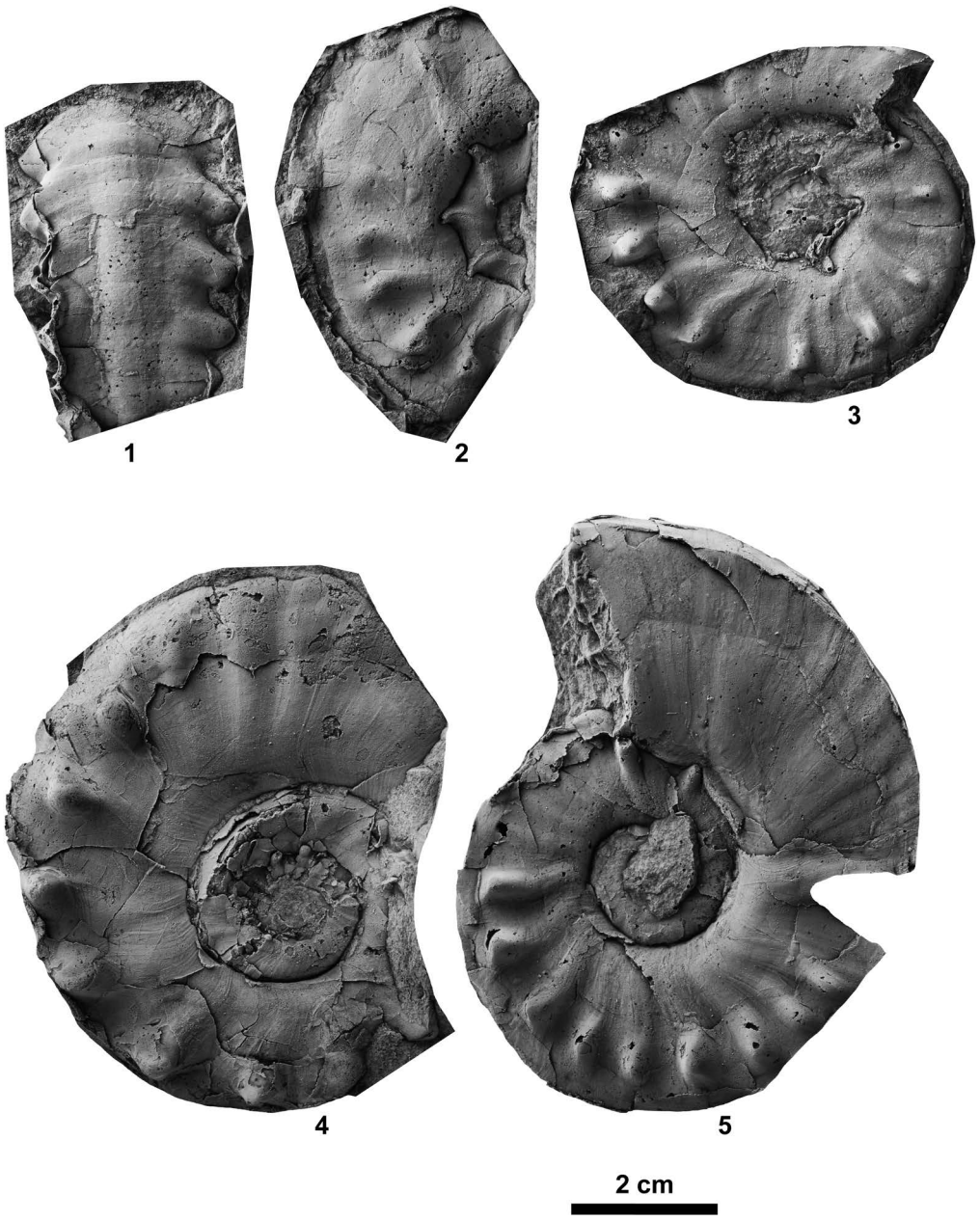

Fig. 106. *Tirolites* sp. nov., from KC02-15. 1, NMNS PM23673. 2, NMNS PM23674. 3, NMNS PM23675. 4, NMNS PM23676. 5, NMNS PM23677. All specimens are rubber casts of the outer molds.

Fig. 107. *Tirolites* sp. nov., from KC02-15. 1, NMNS PM23678. 2, NMNS PM23679. 3, NMNS PM23680. 4, NMNS PM23681.

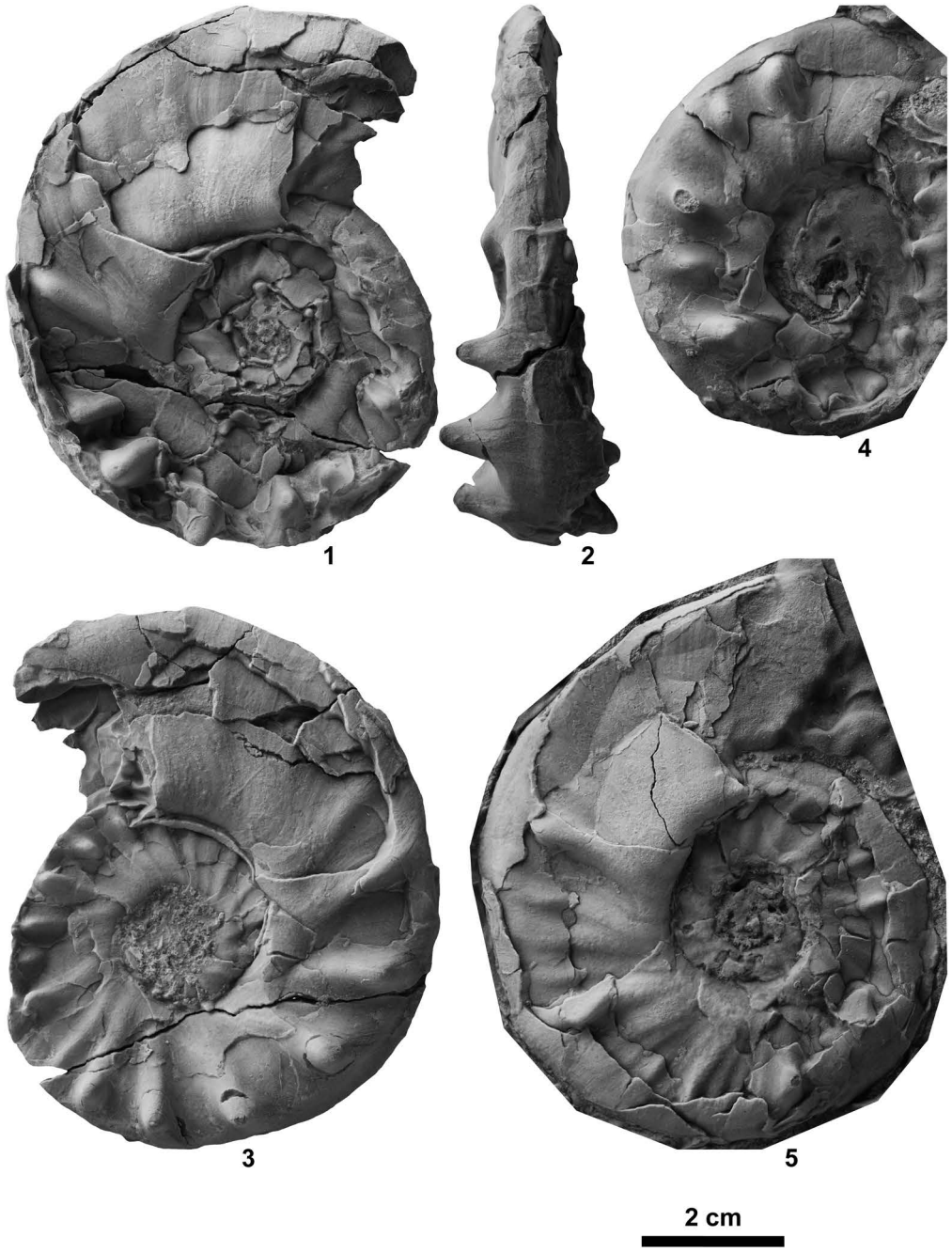

Fig. 108. *Tirolites* sp. nov., from KC02-15. 1–3, NMNS PM23684. 4, NMNS PM23682. 5, NMNS PM23683.

Fig. 109. *Tirolites* sp. nov., from KC02-15. 1–4, NMNS PM23685. 5–8, NMNS PM23686.

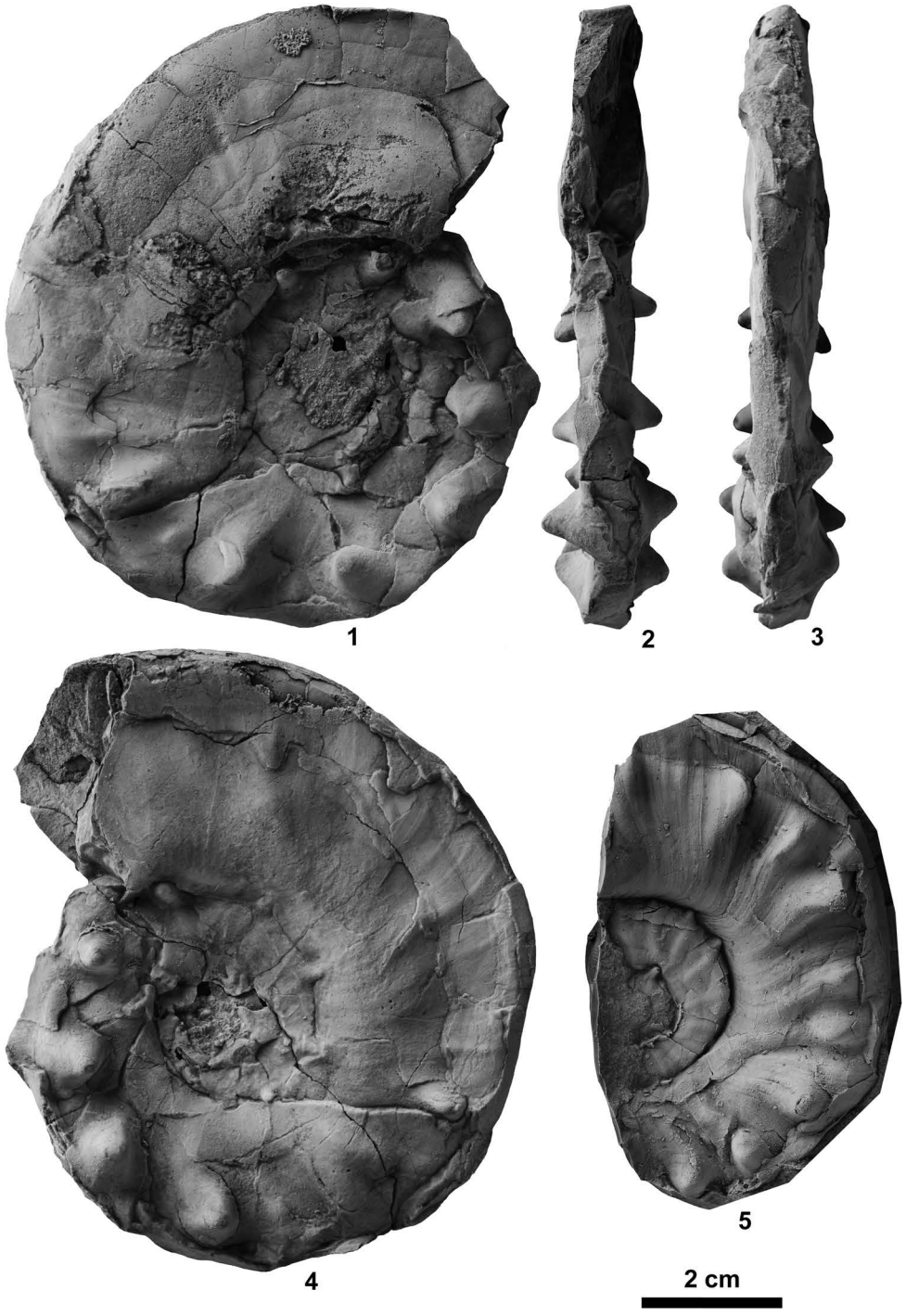

Fig. 110. *Tirolites* sp. nov., from KC02-15. 1–4, NMNS PM23687. 5, NMNS PM23688 (rubber cast of outer mold).

Fig. 111. *Tirolites* sp. nov., from KC02-15. 1–4, NMNS PM23690. 5, NMNS PM23689 (rubber cast of outer mold).

Fig. 112. *Tirolites* sp. nov. 1–2, from KC02-15. 1, NMNS PM23768. 2, NMNS PM23769. 3–4, from KC02-16. 3, NMNS PM23770 (rubber cast of outer mold). 4, NMNS PM23771 (rubber cast of outer mold).

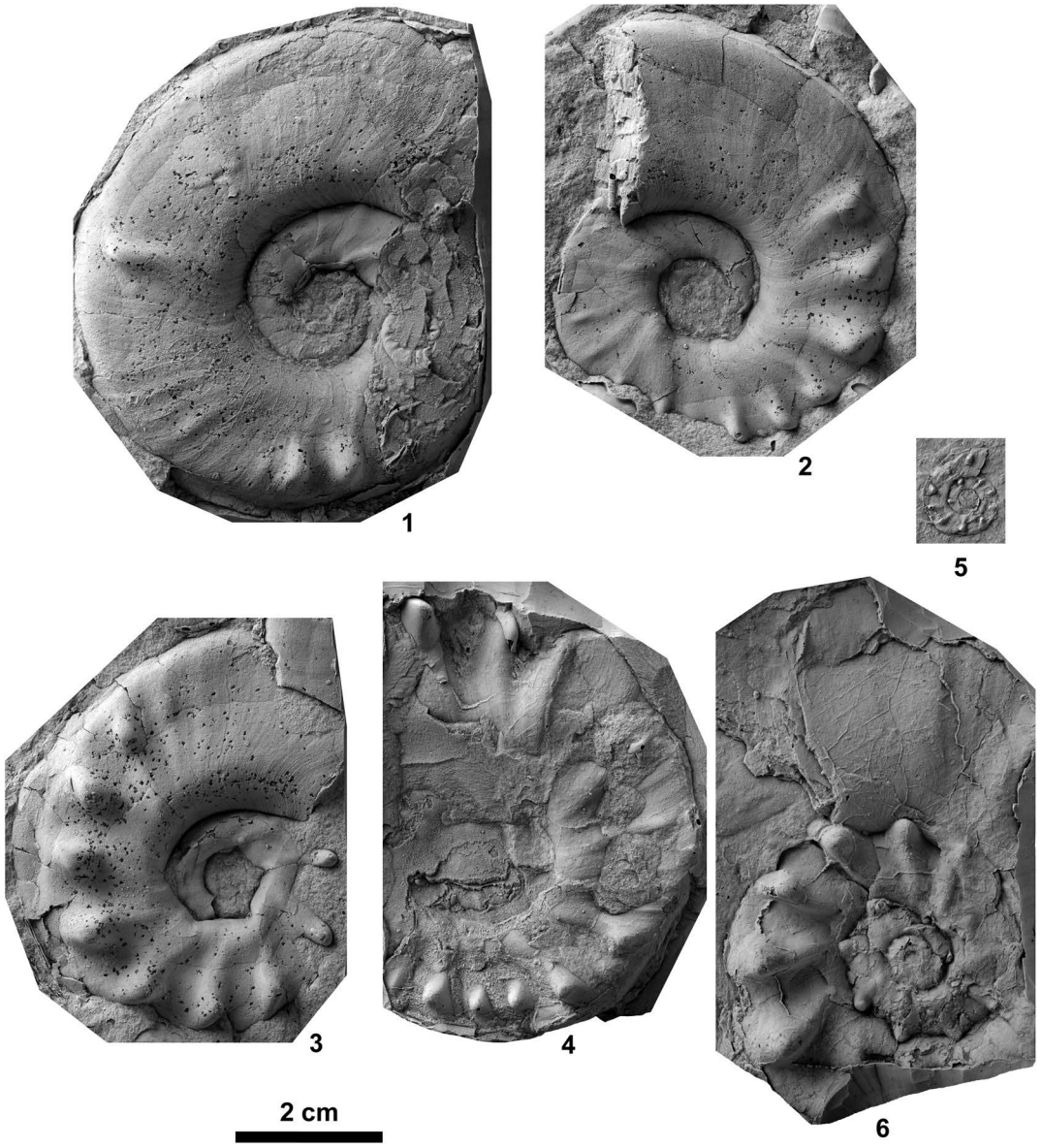

Fig. 113. *Tirolites* sp. nov. 1–4, from KC02-18. 1, NMNS PM23695. 2, NMNS PM23696. 3, NMNS PM23697. 4, NMNS PM23698. 5–6, from BT02-06. 5, NMNS PM23692. 6, NMNS PM23691. All specimens are rubber casts of outer molds.

name because the specimens are poorly preserved and the suture line is unknown.

Occurrence: Described specimens from KC02-14, KC02-15 and KC02-16 within the portion of the *Triassospathodus symmetricus* Zone represented by the *Tirolites* sp. nov. beds (Lower Spathian = lower Upper Olenekian), and those from BT02-06, KC02-18 and NT01-10 within the *Tirolites* sp. nov. beds (Lower Spathian = lower Upper Olenekian) in the Bac Thuy Formation, northeastern Vietnam.

Family Columbitidae Spath, 1934

Genus ***Columbites*** Hyatt and Smith, 1905

Type species: *Columbites parisianus* Hyatt and Smith, 1905.

Columbites sp. indet.

Fig. 114

Material examined: Six specimens, NMNS PM23699–23704, from KC02-14, four specimens, NMNS PM23705–23708, from KC02-15, one specimen, NMNS PM23709, from KC02-18, two specimens, NMNS PM23710–23711, from BT02-06, one specimen, NMNS PM23712, from BR01-08, three specimens, NMNS PM23713–23715, from NT01-10, one specimen, NMNS PM23716, from NT01-11, and one specimen, NMNS PM23716, from NT01-12.

Description: Very evolute, fairly depressed shell with quadratic whorl section, broadly rounded venter, rounded ventral shoulders, and slightly convex flanks. Umbilicus wide with moderately high, gently inclined wall. Ornamentation consists of strong radial ribs that arise on umbilical shoulder and project forward prominently on outer flanks, thus creating impression of tubercles and sinus on ventral shoulders. Ribs continue across venter adorally and are associated with parallel and deep, but variable strength constrictions. Suture not preserved.

Discussion: The described specimens are more or less laterally crushed – they may simply be juvenile forms of an undetermined species of *Columbites*. Although they appear to be somewhat similar to *Columbites parisianus* Hyatt and Smith, 1905, their poor preservation precludes a definitive species assignment.

Occurrence: Described specimens from KC02-14 and KC02-15 within the portion of the *Triassospathodus symmetricus* Zone represented by the *Tirolites* sp. nov. beds (Lower Spathian = lower Upper Olenekian), and those from KC02-18, BT02-06, BR01-08, NT01-10, NT01-11 and NT01-12 within the *Tirolites* sp. nov. beds (Lower Spathian = lower Upper Olenekian) in the Bac Thuy Formation, northeastern Vietnam.

Genus ***Yvesgalleticeras*** Guex *et al*., 2005

Type species: *Preflorianites montpelierensis* Kummel, 1969.

Yvesgalleticeras? sp. indet.

Fig. 115

Material examined: Five specimens, NMNS PM23718–23722, from BT02-06, one specimen, NMNS PM23723, from BT02-07, one specimen, NMNS PM23724, from BT02-08, one specimen, NMNS PM23725, from KC02-15, and one specimen, NMNS PM23726, from KC02-18.

Description: Very evolute, fairly compressed shell with elliptical whorl section, rounded venter, rounded ventral shoulders, and slightly convex flanks with maximum whorl width near mid-flank. Umbilicus wide with low, gently inclined wall. Ornamentation consists of radial to slightly concave ribs. Suture not preserved.

Discussion: The assignment of the specimens to *Yvesgalleticeras* is uncertain because of their poor preservation and lack of suture lines, and is based only on the similarity of their morphology with *Yvesgalleticeras*. In particular, they are somewhat similar to inner whorls of *Yvesgalleticeras montpelierense* (Kummel, 1969) from western USA (Guex *et*

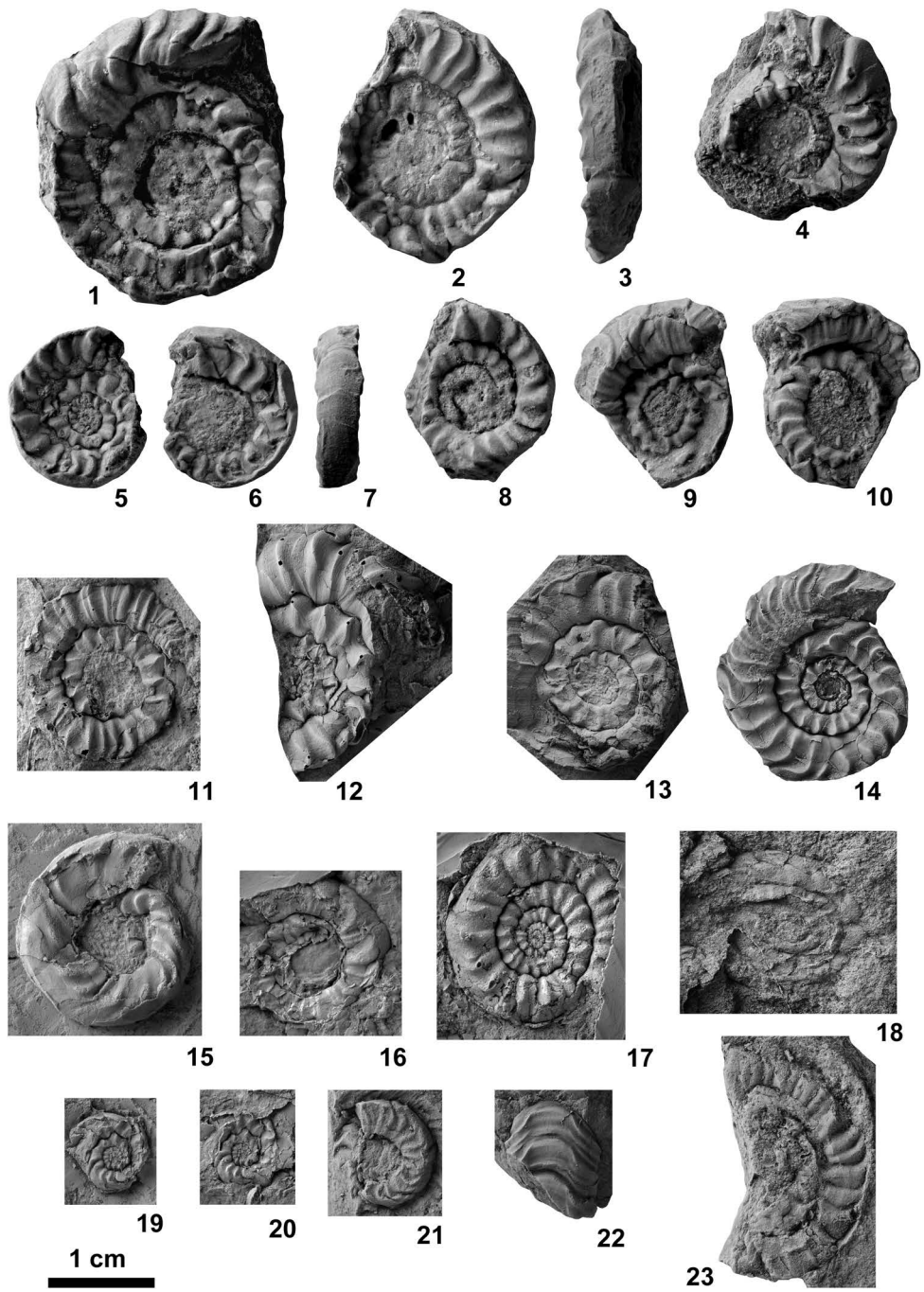

Fig. 114. *Columbites* sp. indet. 1–10, from KC02-14. 1, NMNS PM23699. 2–3, NMNS PM23700. 4, NMNS PM23701. 5–7, NMNS PM23702. 8, NMNS PM23703. 9–10, NMNS PM23704. 11–13, rubber casts of outer molds from KC02-15. 11, NMNS PM23705. 12, NMNS PM23706. 13, NMNS PM23707. 14, NMNS PM23708, from KC02-14. 15, NMNS PM23709, from KC02-18. 16–17, rubber casts of outer molds from BT02-06. 16, NMNS PM23710. 17, NMNS PM23711. 18, NMNS PM23712 (rubber cast of outer mold), from BR01-08. 19–21, from NT01-10. 19, NMNS PM23713. 20, NMNS PM23714 (rubber cast of outer mold). 21, NMNS PM23715. 22, NMNS PM23716, from NT01-11. 23, NMNS PM23717, from NT01-12.

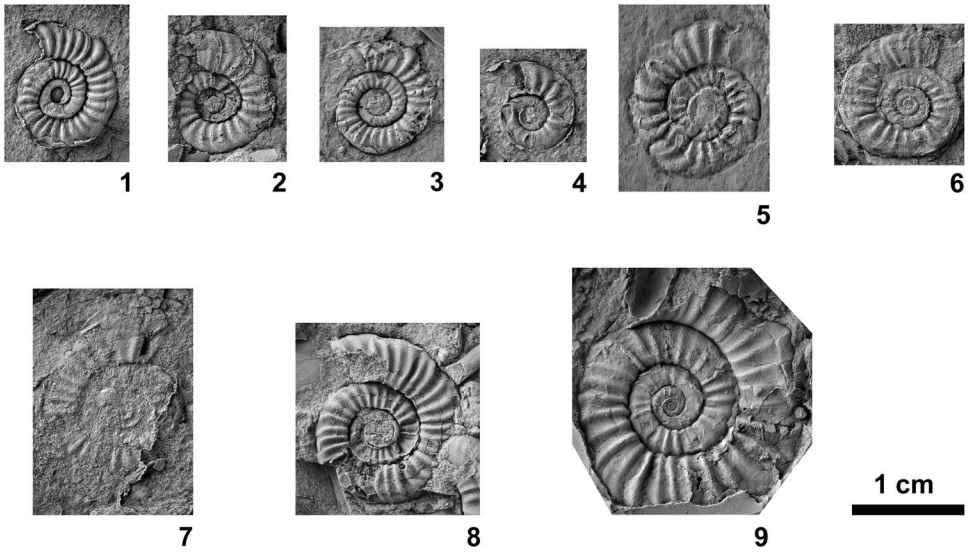

Fig. 115. *Yvesgalleticeras*? sp. indet. 1–5, from BT02-06. 1, NMNS PM23718. 2, NMNS PM23719. 3, NMNS PM23720. 4, NMNS PM23721. 5, NMNS PM23722. 6, NMNS PM23723, from BT02-07. 7, NMNS PM23724, from BT02-08. 8, NMNS PM23725, from KC02-15. 9, NMNS PM23726, from KC02-18. All specimens except for NMNS PM23725 are rubber casts of outer molds.

al., 2010).

Occurrence: Described specimens from KC02-15 within the portion of the *Triassospathodus symmetricus* Zone represented by the *Tirolites* sp. nov. beds (Lower Spathian = lower Upper Olenekian), and those from KC02-18, BT02-06, BT02-07 and BT02-08 within the *Tirolites* sp. nov. beds (Lower Spathian = lower Upper Olenekian) in the Bac Thuy Formation, northeastern Vietnam.

Superfamily Megaphyllitoidea Mojsisovics, 1896

Family Procarnitidae Chao, 1959

Genus ***Procarnites*** Arthaber, 1911

Type species: *Parapopanoceras kokeni* Arthaber, 1908.

Procarnites? sp. indet.

Fig. 116

Material examined: Three specimens, NMNS PM23653–23655, from KC02-14.

Description: Fairly involute, very compressed shell with subelliptical whorl section, narrow rounded venter, indistinct ventral shoulders, and slightly convex flanks with maximum whorl width at mid-flank. Umbilicus fairly narrow with moderately high, vertical wall and abruptly rounded shoulders. Ornamentation consists of sigmoidal growth lines strongly projected forwards on outer flank and low, weak folds. Suture ceratitic with subphylloid saddles. First lateral saddle lower than second saddle, and third saddle only slightly lower than second saddle. First lateral lobe deep, wide with many denticulations at base, and second lateral lobe narrower and shallower than first lobe.

Measurements (mm):

Specimen no.	D	U	H	W	U/D	W/H
NMNS PM23654	40.9	9.7	17.7	9.2	0.34	0.52

Discussion: The assignment of the specimens to *Procarnites* is uncertain because of their poor preservation and is based only the similarity of their shell morphology and suture line with *Procarnites*. They are somewhat similar to specimen (IPUW 1911-4-11) de-

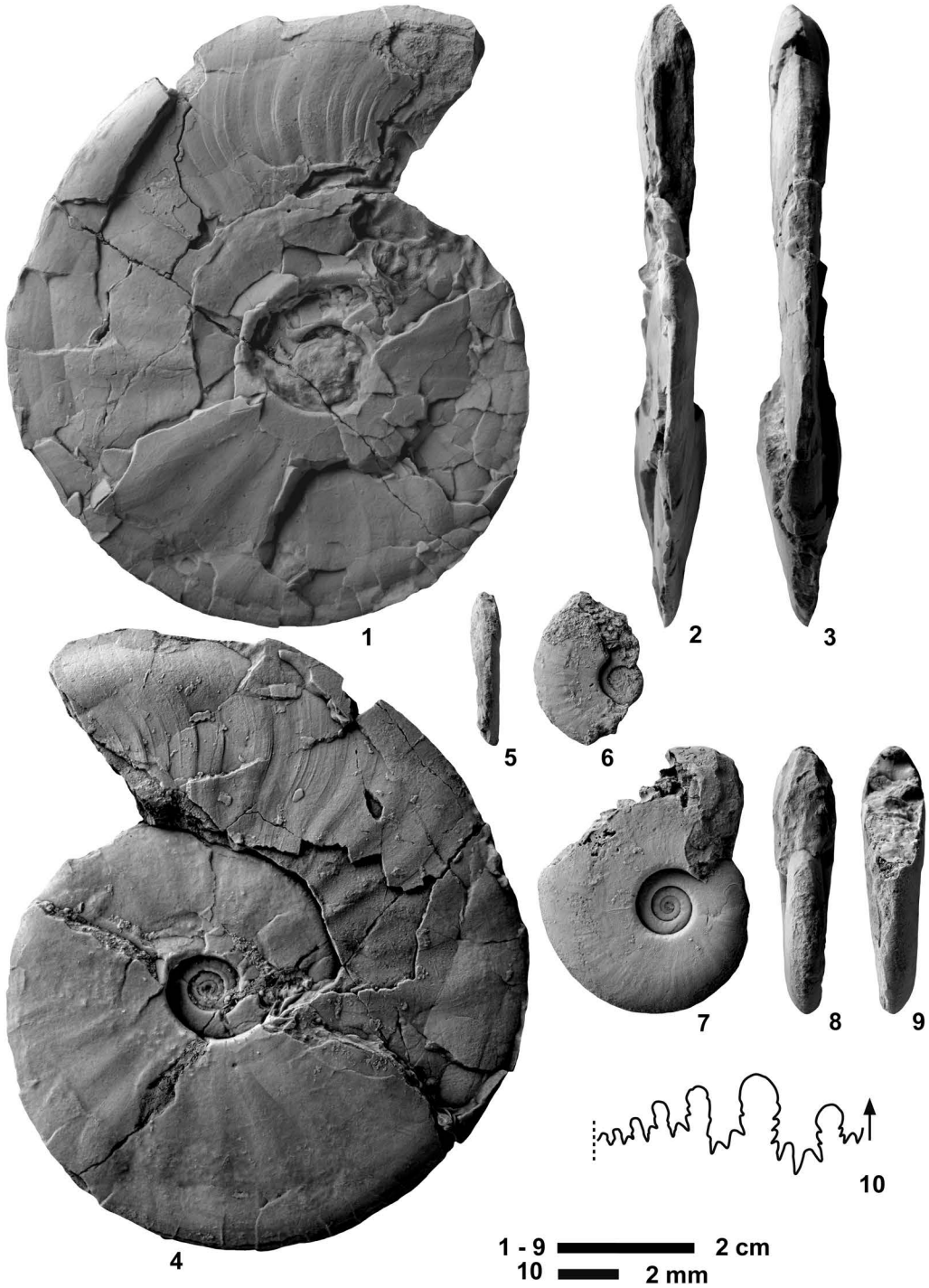

Fig. 116. *Procarnites*? sp. indet., from KC02-14. 1–4, NMNS PM23653. 5–6, NMNS PM23654. 7–10, NMNS PM23655.

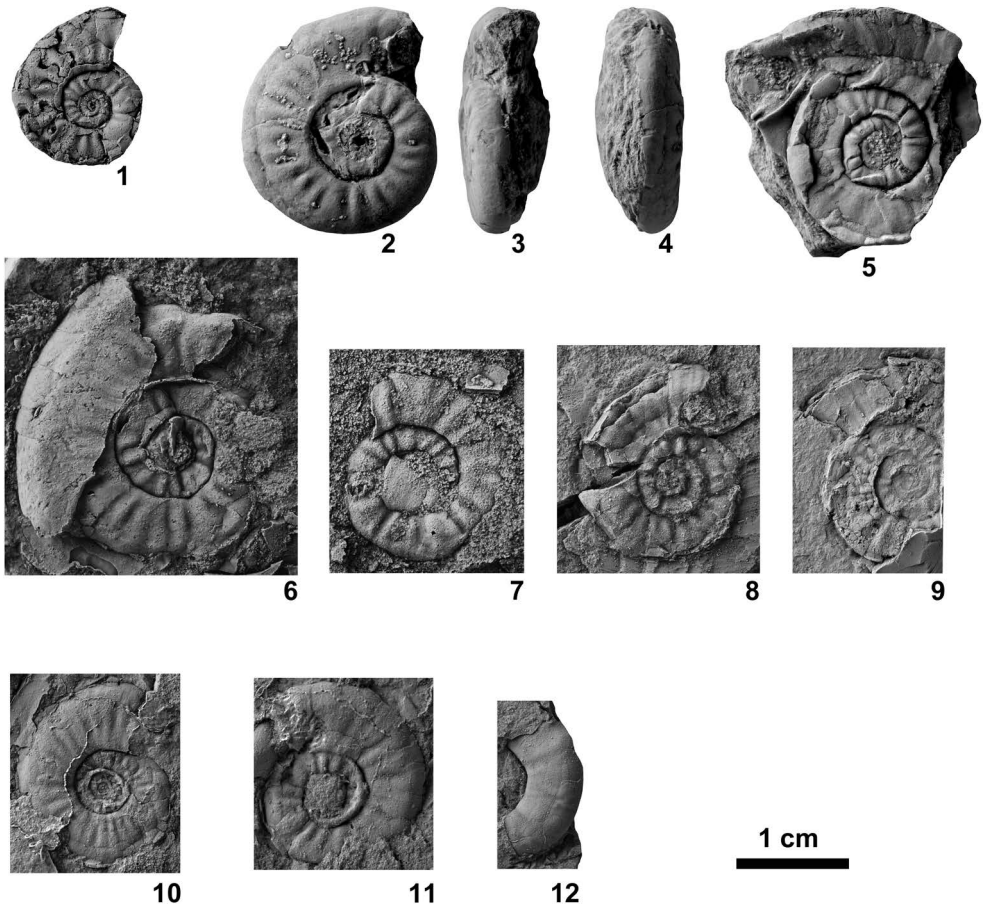

Fig. 117. *Eodanubites*? sp. indet. 1–5, from KC02-14. 1, NMNS PM23727 (rubber cast of outer mold). 2–4, NMNS PM23728. 5, NMNS PM23729. 6–7, from KC02-15. 6, NMNS PM23730 (rubber cast of outer mold). 7, NMNS PM23731 (rubber cast of outer mold). 8, NMNS PM23732, from KC02-19. 9, NMNS PM23733 (rubber cast of outer mold), from BT02-08. 10–12, from NT01-08. 10, NMNS PM23734 (rubber cast of outer mold). 11, NMNS PM23735 (rubber cast of outer mold). 12, NMNS PM23736.

scribed as *Procarnites kokeni* (Arthaber, 1908) by Arthaber (1911, pl. 18, fig. 5) in that it has a slender shell form.

Occurrence: Described specimen from KC02-14 within the portion of the *Triassospathodus symmetricus* Zone represented by the *Tirolites* sp. nov. beds (Lower Spathian= lower Upper Olenekian) in the Bac Thuy Formation, northeastern Vietnam.

Superfamily Ceratitaceae Mojsisovics, 1879
Family Danubitidae Spath, 1951
Genus ***Eodanubites*** Wang, 1978

Type species: *Eodanubites xinyuanensis* Wang, 1978.

Eodanubites? sp. indet.
Figs. 117, 118

Material examined: Three specimens, NMNS PM23727–23729, from KC02-14, two specimens, NMNS PM23730–23731, from KC02-15, one specimen, NMNS PM23732,

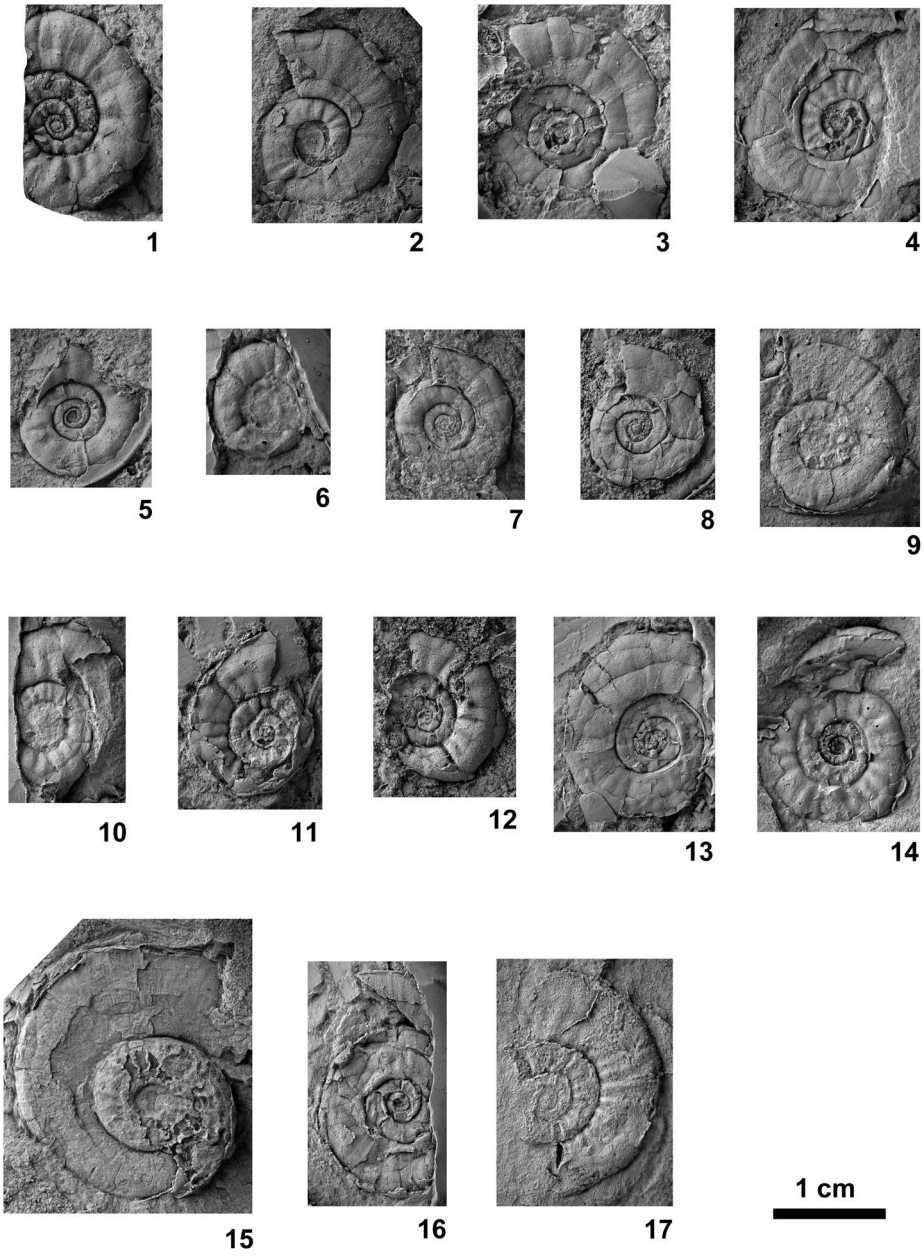

Fig. 118. *Eodanubites*? sp. indet., from BT02-06. 1, NMNS PM23737. 2, NMNS PM23738. 3, NMNS PM23739. 4, NMNS PM23740. 5, NMNS PM23741. 6, NMNS PM23742. 7, NMNS PM23743. 8, NMNS PM23744. 9, NMNS PM23745. 10, NMNS PM23746. 11, NMNS PM23747. 12, NMNS PM23748. 13, NMNS PM23749. 14, NMNS PM23750. 15, NMNS PM23751. 16, NMNS PM23752. 17, NMNS PM23753. All specimens are rubber casts of outer molds.

from KC02-19, seventeen specimens, NMNS PM23737–23753, from BT02-06, one specimen, NMNS PM23733, from BT02-08, and three specimens, NMNS PM23734–23736, from NT01-10.

Description: Fairly evolute, fairly compressed shell with elliptical whorl section, rounded venter, rounded ventral shoulders, and slightly convex flanks with maximum whorl width near mid-flank. Umbilicus fairly wide with low, vertical wall and rounded shoulders. Ornamentation consists of strong, radial or slightly rursiradiate rounded ribs arising on umbilical shoulder, becoming most prominent at mid-flank and weakening at ventral shoulder. Suture not preserved.

Discussion: Assignment of the specimens to *Eodanubites* is uncertain because of their poor preservation and lack of suture lines, and is based only on the similarity of their morphology with *Eodanubites.* They are somewhat similar to *Eodanubites* (*Dumitricaceras*) *judae* (Guex *et al.,* 2005) from western USA (Guex *et al*., 2010).

Occurrence: Described specimens from KC02-14 and KC02-15 within the portion of the *Triassospathodus symmetricus* Zone represented by the *Tirolites* sp. nov. beds (Lower Spathian = lower Upper Olenekian), and those from KC02-19, BT02-06, BT02-08 and NT01-10 within the *Tirolites* sp. nov. beds (Lower Spathian = lower Upper Olenekian) in the Bac Thuy Formation, northeastern Vietnam.

Order Phylloceratida Zittel, 1884
Superfamily Ussuritoidea Hyatt, 1900
Family Palaeophyllitidae Popov, in Luppov and Drushchits, 1958

Genus ***Goudemandites*** Brühwiler *et al*., 2012a

Type species: *Goudemandites sinensis* Brühwiler *et al*., 2012a.

Gaudemandites langsonensis
Shigeta and Nguyen sp. nov.
Fig. 119

Eophyllites sp. nov. Tong *et al*., 2004, p. 201, pl. 2, figs. 16–17.

Type specimen: Holotype, NMNS PM23639, consists of the phragmocone and most of the body chamber, which begins at a diameter of about 60 mm and occupies nearly two-thirds of the outer whorl. Specimen was collected from KC02-14.

Diagnosis: Moderatory evolute *Goudemandites* with subtrapezoidal whorl section, ornamented with slightly biconcave, fine lirae and very weak, radial plications.

Etymology: Named after Lang Son City, northeastern Vietnam.

Description: Moderately evolute, fairly compressed shell with subtrapezoidal whorl section, broadly rounded venter, rounded ventral shoulders, and slightly convex flanks with maximum whorl width near umbilical shoulder. Umbilicus moderately wide with moderately high, vertical wall and rounded shoulders. Ornamentation consists of very weak, radial plications, as well as slightly biconcave, fine lirae. Suture ceratitic with subphylloid saddles. First lateral saddle nearly equal to second saddle, and third saddle even lower. First lateral lobe deep, wide with many denticulations at base, and second lateral lobe about two thirds depth of first lobe.

Measurements (mm):

Specimen no.	D	U	H	W	U/D	W/H
NMNS PM23639	60.0	18.9	26.5	22.7	0.32	0.86

Comparison: *Gaudemandites langsonensis* sp. nov. is close to *G. sinensis* Brühwiler *et al*., 2012a from the Middle Smithian in South China and Oman, but differs by its subtrapezoidal whorl section and ornamentation consisting of very weak, radial plications. Specimens described as *Eophyllites* sp. nov. by Tong *et al*. (2004, pl. 2, figs. 16) from the *Columbites-Tirolites* Zone in East China are very similar to *G. langsonensis* and are probably

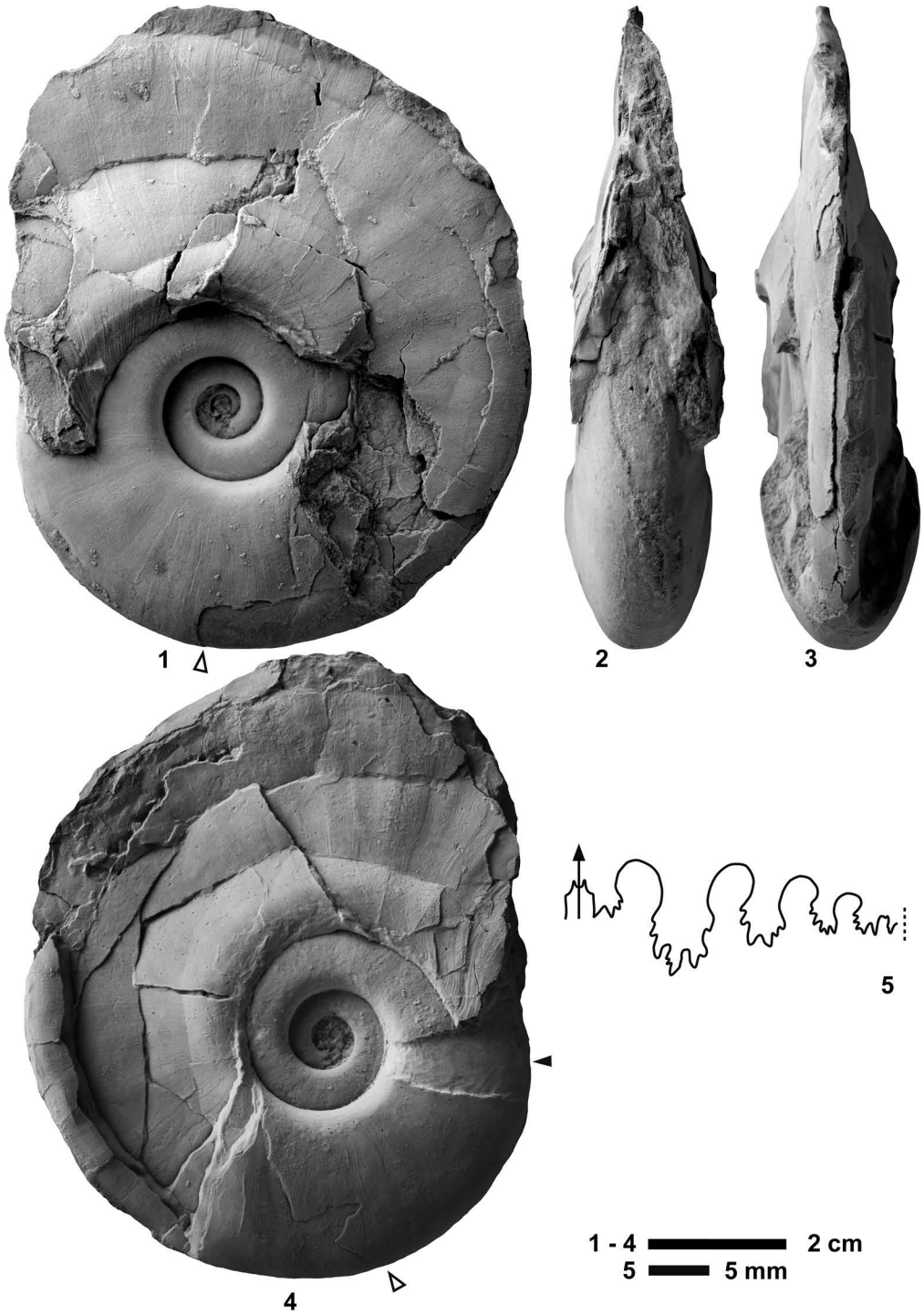

Fig. 119. *Gaudemandites langsonensis* Shigeta and Nguyen sp. nov., from KC02-14. 1–5, NMNS PM23639, holotype. White arrows indicate shell breakage. Suture line drawn at position indicated by black arrow.

conspecific.

Remarks: A major sub-lethal shell break and repair scar are visible on the shell of the holotype. Its outer flank and ventral portion were severly damaged and nearly one-sixth of the outer whorl was lost.

Occurrence: Described specimen from KC02-14 within the portion of the *Triassospathodus symmetricus* Zone represented by the *Tirolites* sp. nov. beds (Lower Spathian=lower Upper Olenekian) in the Bac Thuy Formation, northeastern Vietnam. This species also occurs in the Lower Spathian (*Columbites-Tirolites* Zone in Tong *et al*., 2004) in East China.

Incertae sedis

Genus gen. indet. A

Fig. 120.1–120.3

Material examined: One specimen, NMNS PM23754, from BT02-04.

Description: Moderately evolute, fairly compressed shell with elliptical whorl section, arched venter, rounded ventral shoulders, and slightly convex flanks with maximum whorl width near mid-flank. Umbilicus fairly narrow with moderately high, vertical wall and rounded shoulders. Ornamentation consists of sigmoidal ribs, more pronounced near venter. Suture not visible.

Occurrence: Described specimen from BT02-04 within the portion of the *Novispathodus* ex gr. *waageni* Zone that includes the *Leyeceras* horizon of the *Owenites koeneni* beds (middle Middle Smithian=middle lower Olenekian) in the Bac Thuy Formation, northeastern Vietnam.

Genus gen. indet. B

Fig. 120.4–120.5

Material examined: One specimen, NMNS PM23755, from BT01-09.

Description: Very evolute, very compressed shell with narrow tabulate venter, rounded ventral shoulders, and convex flanks with maximum whorl width near mid-flank. Umbilicus fairly wide with moderately high, oblique wall and rounded shoulders. Shell surface smooth. Suture not visible.

Occurrence: Described specimens from BT01-09 within the portion of the *Novispathodus* ex gr. *waageni* Zone that includes the *Urdyceras tulongensis* beds (lower Middle Smithian=middle Lower Olenekian) in the Bac Thuy Formation, northeastern Vietnam.

Genus gen. indet. C

Fig. 121.1–121.2

Material examined: One specimen, NMNS PM23756, from KC01-10.

Description: Involute, fairly compressed shell with tabulate or subtabulate venter, angular ventral shoulders, and slightly convex flanks with maximum whorl width near mid-flank. Umbilicus narrow. Ornamentation consists of dense, concave,fine and projected ribs. Suture not visible.

Occurrence: Described specimen from KC01-10 within the portion of the *Novispathodus* ex gr. *waageni* Zone that includes the *Leyeceras* horizon of the *Owenites koeneni* beds (middle Middle Smithian=middle Lower Olenekian) in the Bac Thuy Formation, northeastern Vietnam.

Genus gen. indet. D

Fig. 121.3–121.4

Material examined: One specimen, NMNS PM23757, from NT01-10.

Description: Fairly evolute, very compressed shell with subelliptical whorl section, arched venter, rounded ventral shoulders, and flat, subparallel flanks. Umbilicus moderately wide with moderately high, oblique wall. Ornamentation consists of dense, sigmoidal fine ribs strongly projected forwards on outer flank. Suture not preserved.

Occurrence: Described specimen from NT01-10 within the *Tirolites* sp. nov. beds (Lower Spathian=lower Upper Olenekian) in

Fig. 120. 1–3, Genus gen. indet. A, NMNS PM23754, from BT02-04. 4–5, Genus gen. indet. B, NMNS PM23755, from BT01-09.

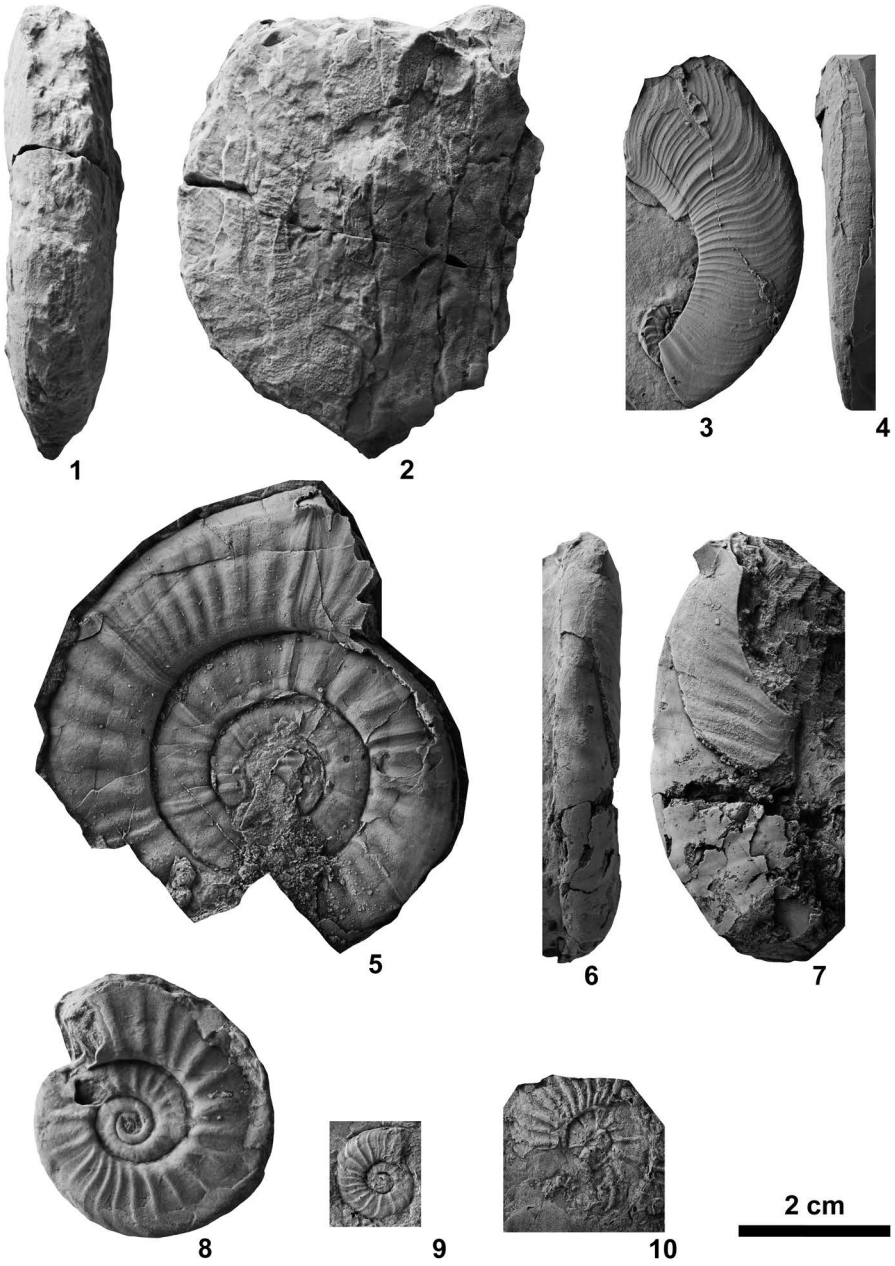

Fig. 121. 1–2, Genus gen. indet. C, NMNS PM23756, from KC01-10. 3–4, Genus gen. indet. D, NMNS PM23757 (rubber cast of outer mold), from NT01-10. 5–7, Genus gen. indet. E. 5, NMNS PM23758 (rubber cast of outer mold), from KC02-15. 6–7, NMNS PM23759, from KC02-14. 8–10, Genus gen. indet. F. 8, NMNS PM23767, from KC02-16. 9, NMNS PM23646 (rubber cast of outer mold), from a float mudstone block at KC02. 10, NMNS PM23647 (rubber cast of outer mold), from a float mudstone block at KC02.

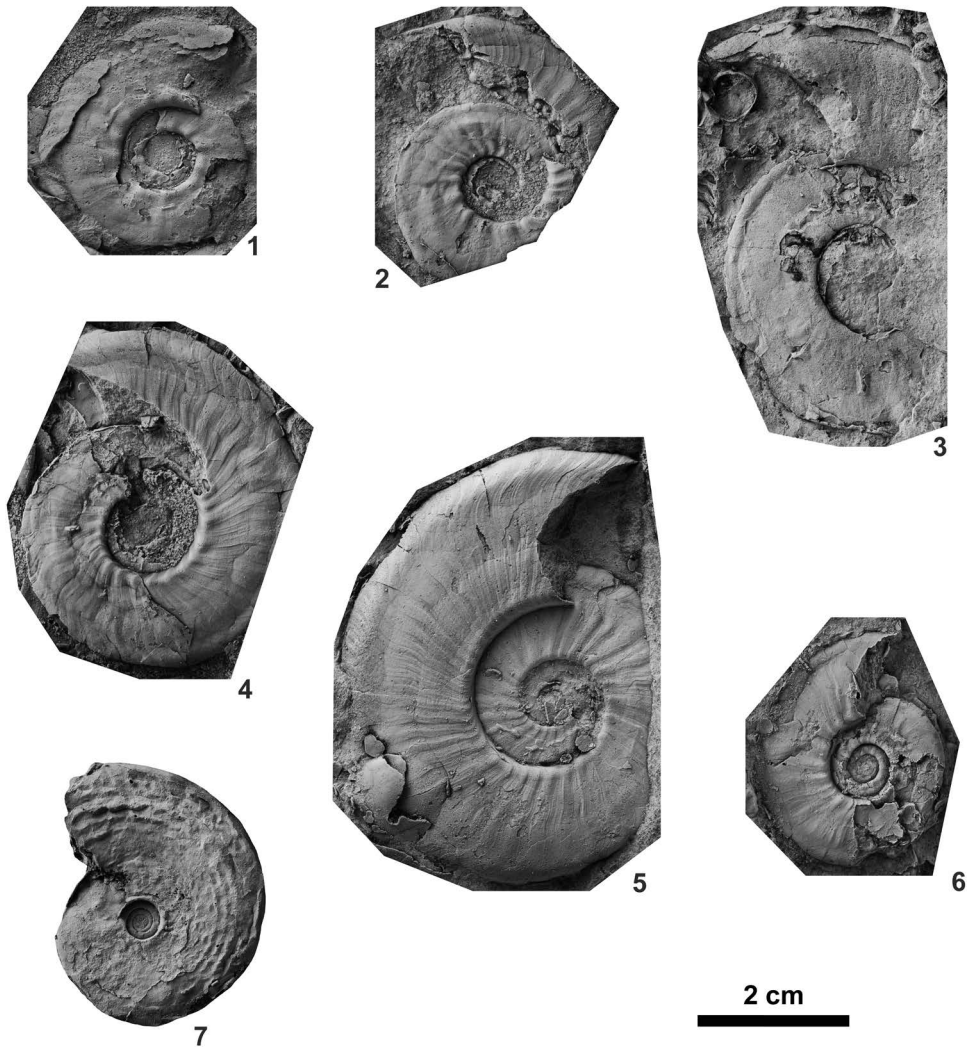

Fig. 122. 1–6, Genus gen. indet. G, from KC02-14. 1, NMNS PM23656. 2, NMNS PM23657. 3, NMNS PM23658. 4, NMNS PM23659. 5, NMNS PM23660. 6, NMNS PM23661. All specimens are rubber casts of outer molds.7, Genus gen. indet. H, NMNS PM23789 (rubber cast of outer mold), from KC02-16.

the Bac Thuy Formation, northeastern Vietnam.

Genus gen. indet. E

Fig. 121.5–121.7

Material examined: One specimen, NMNS PM23759, from KC02-14 and one specimen, NMNS PM23758, from KC02-15.

Description: Very evolute, very compressed shell with elliptical whorl section, arched venter, rounded ventral shoulders, and slightly convex flanks with maximum whorl width near mid-flank. Umbilicus wide with low, vertical wall and rounded shoulders. Ornamentation consists of periodic major ribs with parabolic nodes on ventrolateral margin and radial rounded ribs, arising on umbilical shoulder, becoming most prominent at mid-flank and weakening at ventral shoulder. Suture not preserved.

Occurrence: Described specimen from

KC02-14 and KC02-15 within the portion of the *Triassospathodus symmetricus* Zone represented by the *Tirolites* sp. beds (Lower Spathian = lower Upper Olenekian) in the Bac Thuy Formation, northeastern Vietnam.

Genus gen. indet. F

Fig. 121.8–121.10

Material examined: Two specimens, NMNS PM23646–23647, from float mudstone blocks in KC02 and one specimen, NMNS PM23767, from KC02-16.

Description: Moderately evolute, very compressed shell with slightly convex flanks with maximum whorl width near mid-flank. Umbilicus moderately wide with low, vertical wall and rounded shoulders. Ornamentation consists of strong, sigmoidal ribs. Suture not preserved.

Occurrence: Described specimens from KC02-16 within the portion of the *Triassospathodus symmetricus* Zone represented by the *Tirolites* sp. nov. beds (Lower Spathian = lower Upper Olenekian), and those from float mudstone blocks probably derived from the mudstone within the *Tirolites* sp. nov. beds (Lower Spathian = lower Upper Olenekian) in the Bac Thuy Formation, northeastern Vietnam.

Genus gen. indet. G

Fig. 122.1–122.6

Material examined: Six specimens, NMNS PM23656–23661, from KC02-15.

Description: Fairly evolute, very compressed shell with subelliptical whorl section, arched venter, rounded ventral shoulders, and flat, subparallel flanks. Umbilicus moderately wide with moderately high, vertical wall and abruptly rounded shoulders. Ornamentation consists of sigmoidal growth lines that form umbilical bullae and rib-like plications, becoming strongly projected forwards on outer flank. Suture not preserved.

Measurements (mm):

Specimen no.	D	U	H	W	U/D	W/H
NMNS PM23657	24.6	8.2	9.6	—	0.33	—
NMNS PM23656	32.0	11.8	12.5	—	0.37	—
NMNS PM23661	33.0	11.3	11.8	—	0.34	—
NMNS PM23659	45.0	14.5	19.2	—	0.32	—
NMNS PM23660	57.0	21.0	20.2	—	0.37	—

Occurrence: Described specimen from KC02-15 within the portion of the *Triassospathodus symmetricus* Zone represented by the *Tirolites* sp. nov. beds (Lower Spathian = lower Upper Olenekian) in the Bac Thuy Formation, northeastern Vietnam.

Genus gen. indet. H

Fig. 122.7

Material examined: One specimen, NMNS PM23789, from KC02-16.

Description: Very involute, very compressed shell with narrow rounded venter, rounded ventral shoulders, and slightly convex flanks with maximum whorl width near mid-flank. Umbilicus narrow with low, vertical wall and abruptly rounded shoulders. Suture with probably subphylloid saddles partly visible.

Measurements (mm):

Specimen no.	D	U	H	W	U/D	W/H
NMNS PM23789	35.0	5.0	18.6	—	0.14	—

Occurrence: Described specimen from KC02-16 within the portion of the *Triassospathodus symmetricus* Zone represented by the *Tirolites* sp. nov. beds (Lower Spathian = lower Upper Olenekian) in the Bac Thuy Formation, northeastern Vietnam.

Gastropods (by A. Kaim, A. Nützel and T. Maekawa)

Systematic descriptions basically follow the classification by Bouchet *et al.* (2005). Morphological terms are those used in the Treatise on Invertebrate Paleontology (Cox, 1960) and the glossary of malacological terms by Arnold (1965).

The present material consists entirely of small specimens (smaller 1 mm) and repre-

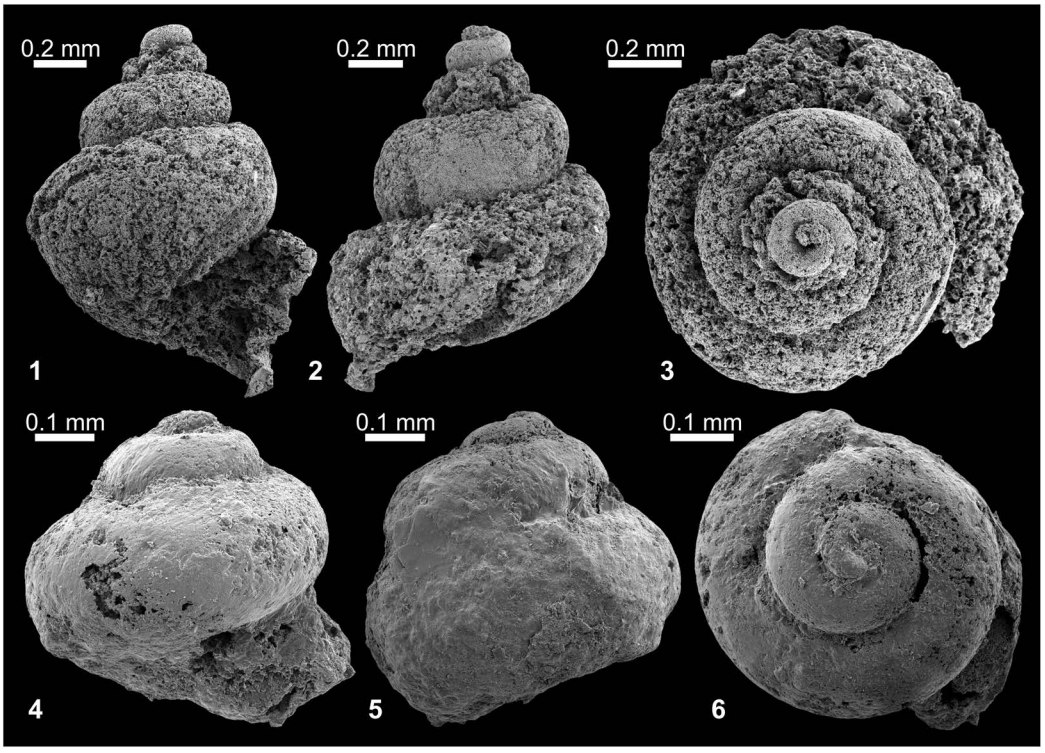

Fig. 123. Gastropods from the lowest Middle Smithian. 1–3, unidentified caenogastropod, NMNS PM23849, from BT01-04. 4–6, ?*Atorcula* sp. indet., NMNS PM23848, from BT02-01.

sents protoconchs and/or early juveniles. The specimens are silicified and most are internal moulds so that the ornament is rarely preserved. For these reasons, open nomenclature must be used and all generic assignments are tentative. However, it is possible to characterize various different forms.

Institution abbreviation: NMNS = National Museum of Nature and Science, Tsukuba

Class Gastropoda Cuvier, 1795
Order Vetigastropoda Salvini-Plawen, 1980
Superfamily Trochonematoidea von Zittel, 1895
Family Lophospiridae Wenz, 1938
Genus ***Worthenia*** de Koninck, 1883

Type species: *Turbo tabulatus* Conrad, 1835.

Worthenia? sp. indet.
Fig. 124.1–124.6

Material examined: One juvenile specimen, NMNS PM23800, from BT01-06 and one specimen, NMNS PM23801, from KC01-04.

Description: Shell from sample BT01-06 (Fig. 124.1–124.3) relatively well preserved consisting of 3.5 round convex turbiniform whorls with deep sutures and covered with granular micro-ornament. Small umbilicus present. Aperture circular. Demarcation between larval shell and teleoconch not visible. Selenizone not yet developed.

Discussion: This shell is most likely a juvenile of a *Worthenia*-like gastropod. Bandel (2009) argues that the Triassic species of *Worthenia* should be classified as *Pseudoschizogonium* Kutassy, 1937 (with the Late Tri-

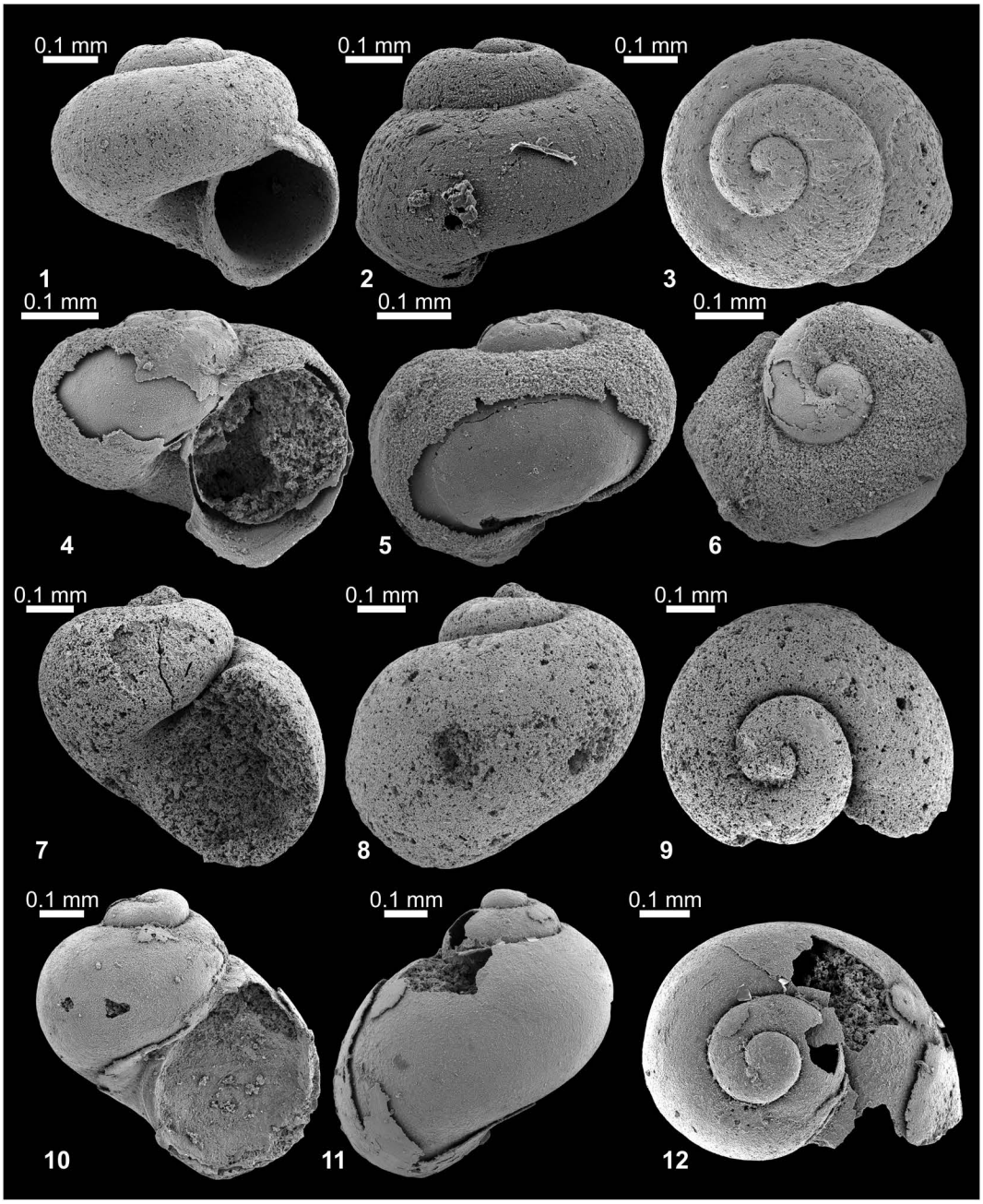

Fig. 124. Gastropods from the lower Middle Smithian. 1–6, *Worthenia*? sp. indet. 1–3, NMNS PM23800, from BT01-06. 4–6, NMNS PM23801, from KC01-04. 7–12, *Naticopsis* sp. indet. A. 7–9, NMNS PM23812, from BT01-06. 10–12, NMNS PM23813, from BT01-07.

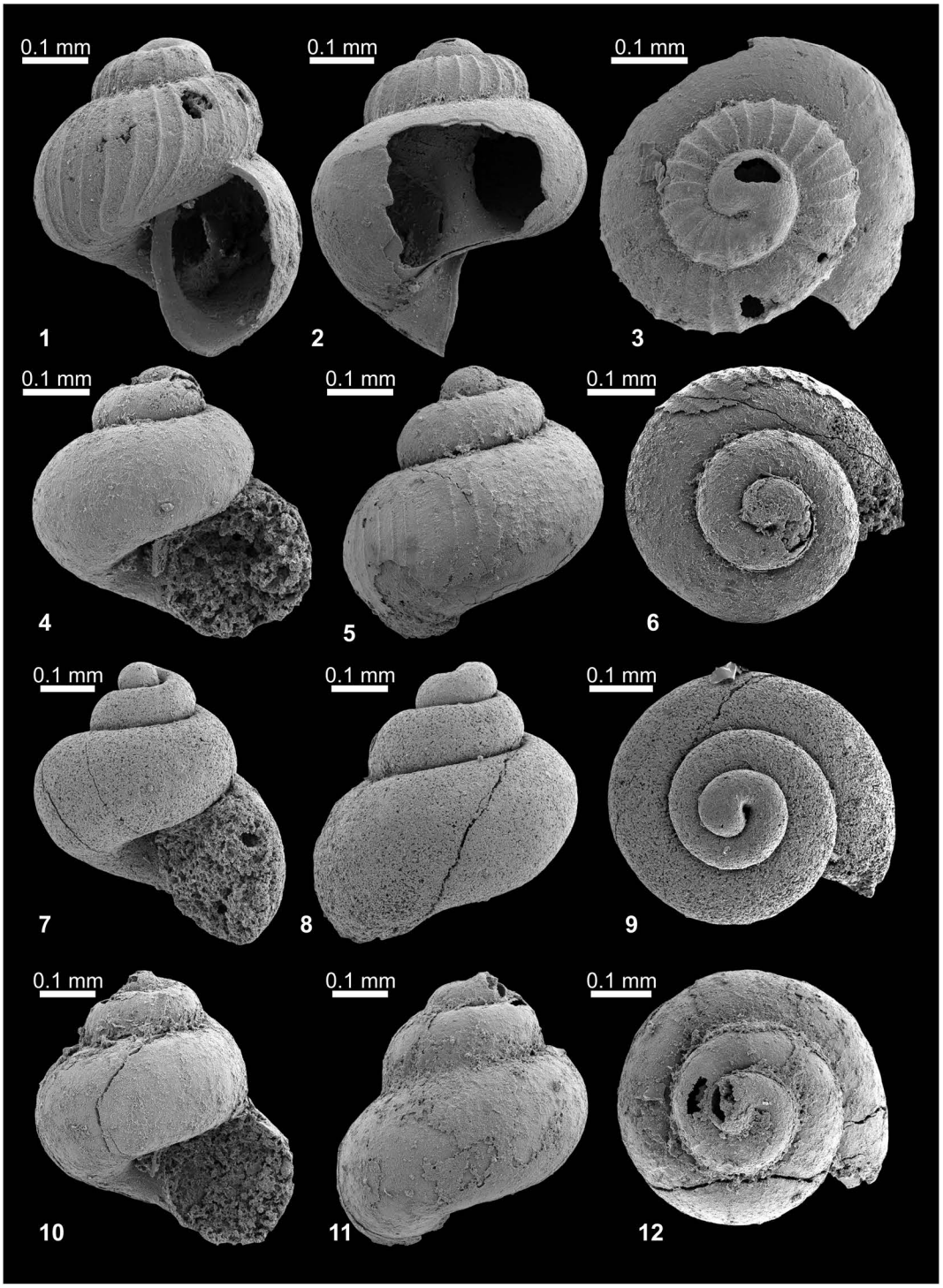

Fig. 125. Gastropods from the lower Middle Smithian. *Atorcula* sp. indet. 1–3, NMNS PM23840, from KC01-04. 4–6, NMNS PM23834, from BT01-07. 7–9, NMNS PM23835, from BT01-07. 10–12, NMNS PM23836, from BT01-07.

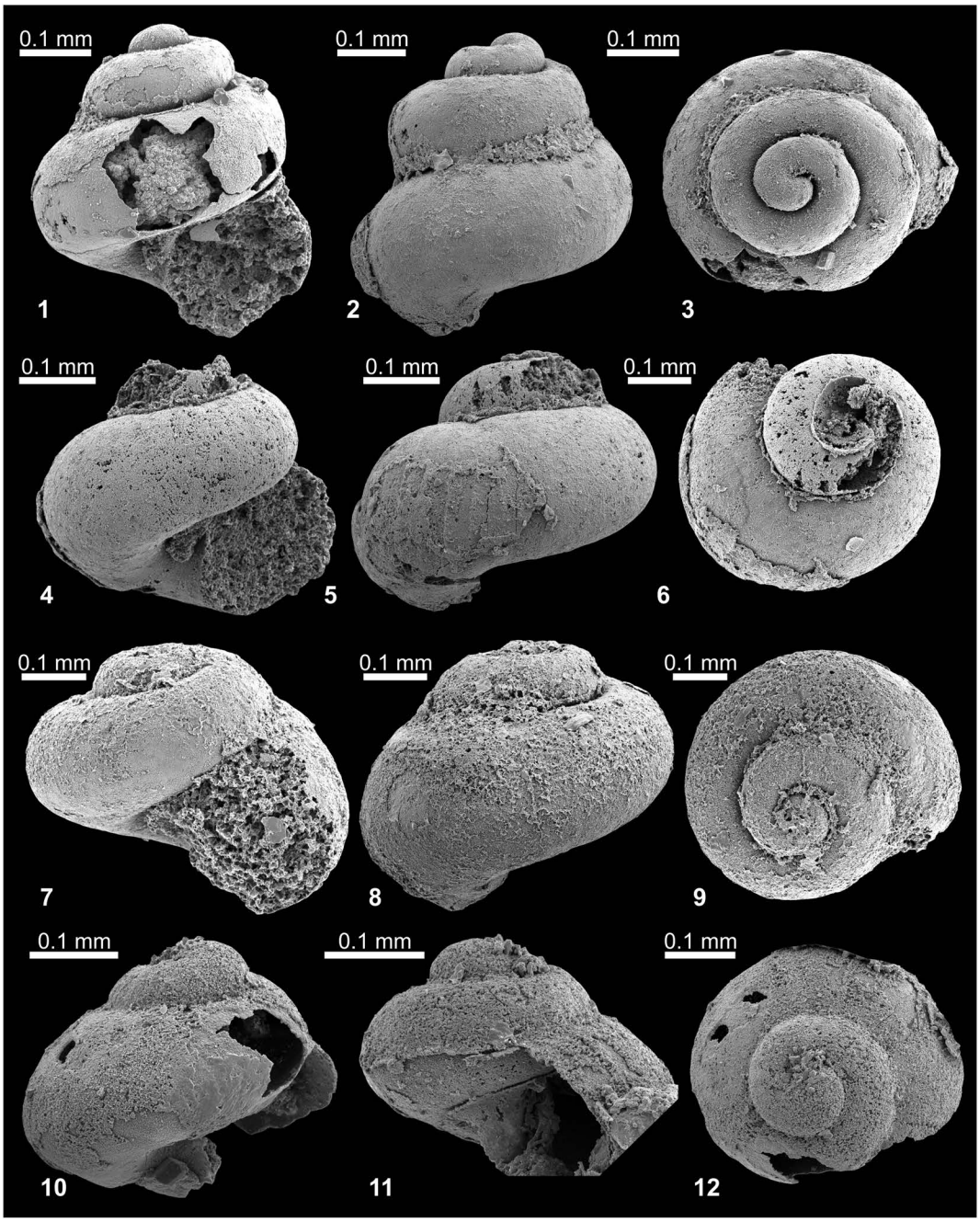

Fig. 126. Gastropods from the lower Middle Smithian. *Atorcula* sp. indet. 1–3, NMNS PM23837, from BT01-07. 4–6, NMNS PM23838, from BT01-07. 7–9, NMNS PM23839, from BT01-07. 10–12, NMNS PM23841, from KC01-04.

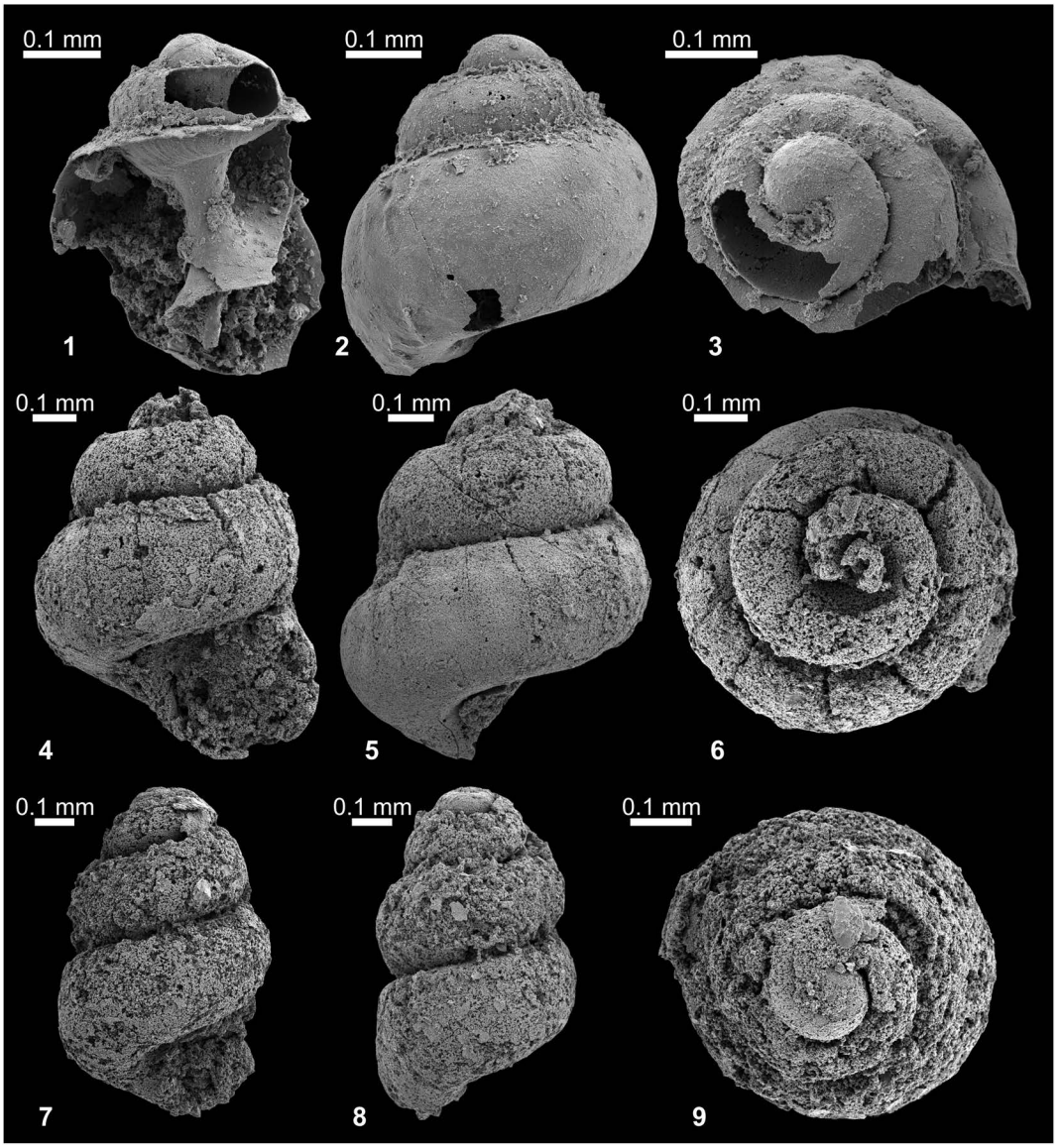

Fig. 127. Gastropods from the lower Middle Smithian. 1–6, *Atorcula* sp. indet. 1–3, NMNS PM23842, from KC01-04. 4–6, NMNS PM23843, from BT01-06. 7–9, unidentified caenogastropod, NMNS PM23850, from BT01-06.

assic type species *Pseudoschizogonium turriculatum* Kutassy, 1937) rather than *Worthenia* (having the Carboniferous type species). The problem of *Pseudoschizogonium* vs. *Worthenia* needs further research in our opinion as some Triassic species (including our specimens from Vietnam) are more reminiscent of the Carboniferous type species of *Worthenia* than the Late Triassic type species of *Pseudoschizogonium*. The Early Triassic species of *Worthenia* were previously reported from Utah, USA (Batten and Stokes, 1986), Oman (Wheeley and Twitchett, 2005), and South Primorye, Russia (Kaim, 2009). Some additional reports from Greenland (Spath, 1930, 1935) and China (Pan, 1982; Zhan, 1995) require review. Unpublished micrographs of early whorls of *Worthenia* from the Smithian Sinbad Limestone closely resemble the present specimens from Vietnam. In these species, the slit develops late during ontogeny.

Occurrence: Described specimen collected from BT01-06 and KC01-04 within the *Novispathodus* ex gr. *waageni* Zone in the Bac Thuy Formation, northeastern Vietnam. BT01-06 is located between the *Flemingites rursiradiatus* beds (lowest Middle Smithian=middle Lower Olenekian) and the *Urdyceras tulongensis* beds (lower Middle Smithian=middle Lower Olenekian). KC01-04 is located beneath the *Owenites koeneni* beds (middle Middle Smithian=middle Lower Olenekian).

Superfamily Trochoidea Rafinesque, 1815
Family Turbinidae Rafinesque, 1815
Subfamily Anomphalinae Wenz, 1938
Genus ***Anomphalus*** Meek and Worthen, 1867

Type species: *Anomphalus rotulus* Meek and Worthen, 1867.

Anomphalus? sp. indet.
Figs. 128.4–128.12, 134

Material examined: One specimen, NMNS PM23802, from BT01-15, two specimens, NMNS PM23803–23804, from KC02-02, five specimens, NMNS PM23805–23809, from KC02-03, and one specimen, NMNS PM23810, from KC02-10.

Description: All available specimens juveniles of about two whorls or less. Shells low-spired, rotelliform with convex whorls. Shell surface smooth. Initial whorl orthostrophic. Protoconch/teleoconch demarcation not visible. Umbilicus well developed. Aperture circular.

Discussion: The shells under consideration are poorly preserved juveniles of rather simple morphology. The low rotelliform shells with orthostrophic protoconch are characteristic for small vetigastropods of turbinid affinity. Such shells in the Paleozoic and Triassic (see e.g., Haas, 1953; Bandel, 1993; Nützel and Nakazawa, 2012) are classified in the family Anomphalidae (here downranked to subfamily). We follow this identification in preliminarily classifying our shells from Vietnam as *Anomphalus*? sp. indet.

Occurrence: Described specimens from BT01-15, KC02-02 and KC02-03 within the *Novispathodus* ex gr. *waageni* Zone that includes the *Leyeceras* and the *Guodunites* horizons of the *Owenites koeneni* beds (middle to upper Middle Smithian=middle Lower Olenekian), and those from KC02–10 within the portion of the *Novispathodus pingdingshanensis* Zone represented by the *Xenoceltites variocostatus* beds (Upper Smithian=upper Lower Olenekian) in the Bac Thuy Formation, northeastern Vietnam.

Order Neritimorpha Koken, 1896
Superfamily Neritoidea Rafinesque, 1815
Family Naticopsidae Waagen, 1880
Genus ***Abrekopsis*** Kaim, 2009

Type species: *Naticopsis* (*Naticopsis*) *depressispirus* Batten and Stokes, 1986.

Abrekopsis? sp. indet.
Fig. 128.13–128.15

Material examined: One specimen, NMNS

PM23811, from BT02-03.

Description: Juvenile neritoid shell with flattened upper whorl surface and whorls embracing above periphery. Shell surface densely covered with fine orthoclinal lirae probably reflecting some selective erosional feature of external shell layer. Aperture drop-shaped. Small umbilicus present.

Discussion: The shell resembles *Abrekopsis depressispirus* (Batten and Stokes, 1986) from the Early Triassic of Russia (Kaim, 2009) and the United States (Batten and Stokes, 1986), however, it is juvenile and poorly preserved; the diagnostic protoconch is also preserved and it may actually belong also to some other neritoid gastropod. The suture is reduced in the earliest whorls and this may indicate that this neritimorph resorbed the inner shell walls as is typical for modern Neritidae.

Occurrence: Described specimen from BT02-03 within the portion of the *Novispathodus* ex gr. *waageni* Zone represented by the *Leyeceras* horizon of the *Owenites koeneni* beds (middle Middle Smithian = middle Lower Olenekian) in the Bac Thuy Formation, northeastern Vietnam.

Genus ***Naticopsis*** McCoy, 1844

Type species: *Naticopsis phillipsii* McCoy, 1844.

Naticopsis sp. indet. A

Figs. 124.7–124.12, 130.7–130.12, 131, 132.1–132.3, 135.1–135.3

Material examined: One specimen, NMNS PM23812, from BT01-06, one specimen, NMNS PM23813, from BT01-07, two specimens, NMNS PM23814–23815, from BT01-15, four specimens, NMNS PM23816–23819, from BT02-03, one specimen, NMNS PM23820, from KC01-12, and one specimen, NMNS PM23821, from KC02-10.

Description: Juvenile relatively high-spired naticopsid shell with shallow but sharply incised suture and bulbous initial whorl. Aperture drop-shaped.

Discussion: The shells under considerations are similar to *Naticopsis utahensis* Batten and Stokes, 1986 from Early Triassic of Utah (Batten and Stokes, 1986). Similar species have also been reported from the Early Triassic of China (Kaim *et al.,* 2010) and Pakistan (Kaim *et al.*, 2013), however, the juvenile nature of our material discourages us from attributing the *Naticopsis* sp. indet. A to any formally named species.

Occurrence: Described specimens collected from BT01-06, BT01-07, BT01-15, BT02-03 and KC01-12 within the *Novispathodus* ex gr. *waageni* Zone in the Bac Thuy Formation, northeastern Vietnam. BT01-06 and BT01-07 are located between the *Flemingites rursiradiatus* beds (lowest Middle Smithian = middle Lower Olenekian) and the *Urdyceras tulongensis* beds (lower Middle Smithian = middle Lower Olenekian). BT01-15, BT02-03 and KC01-12 are located the *Leyeceras* horizon of the *Owenites koeneni* beds (middle Middle Smithian = middle Lower Olenekian), and those from KC02-10 within the portion of the *Novispathodus pingdingshanensis* Zone represented by the *Xenoceltites variocostatus* beds (Upper Smithian = upper Lower Olenekian) in the Bac Thuy Formation, northeastern Vietnam.

Naticopsis sp. indet. B

Figs. 129, 130.1–130.5

Material examined: Five specimens, NMNS PM23822–23826, from BT02-03, three specimens, NMNS PM23827–23829, from BT01-14, and one specimen, NMNS PM23830, from KC01-13.

Description: Juvenile relatively low-spired naticopsid shell with slightly flattened upper whorl surface and shallow but sharply incised suture and bulbous initial whorl. Aperture rectangular with rounded corners.

Discussion: *Naticopsis* sp. indet. B differs from *Naticopsis* sp. indet. A in having polygo-

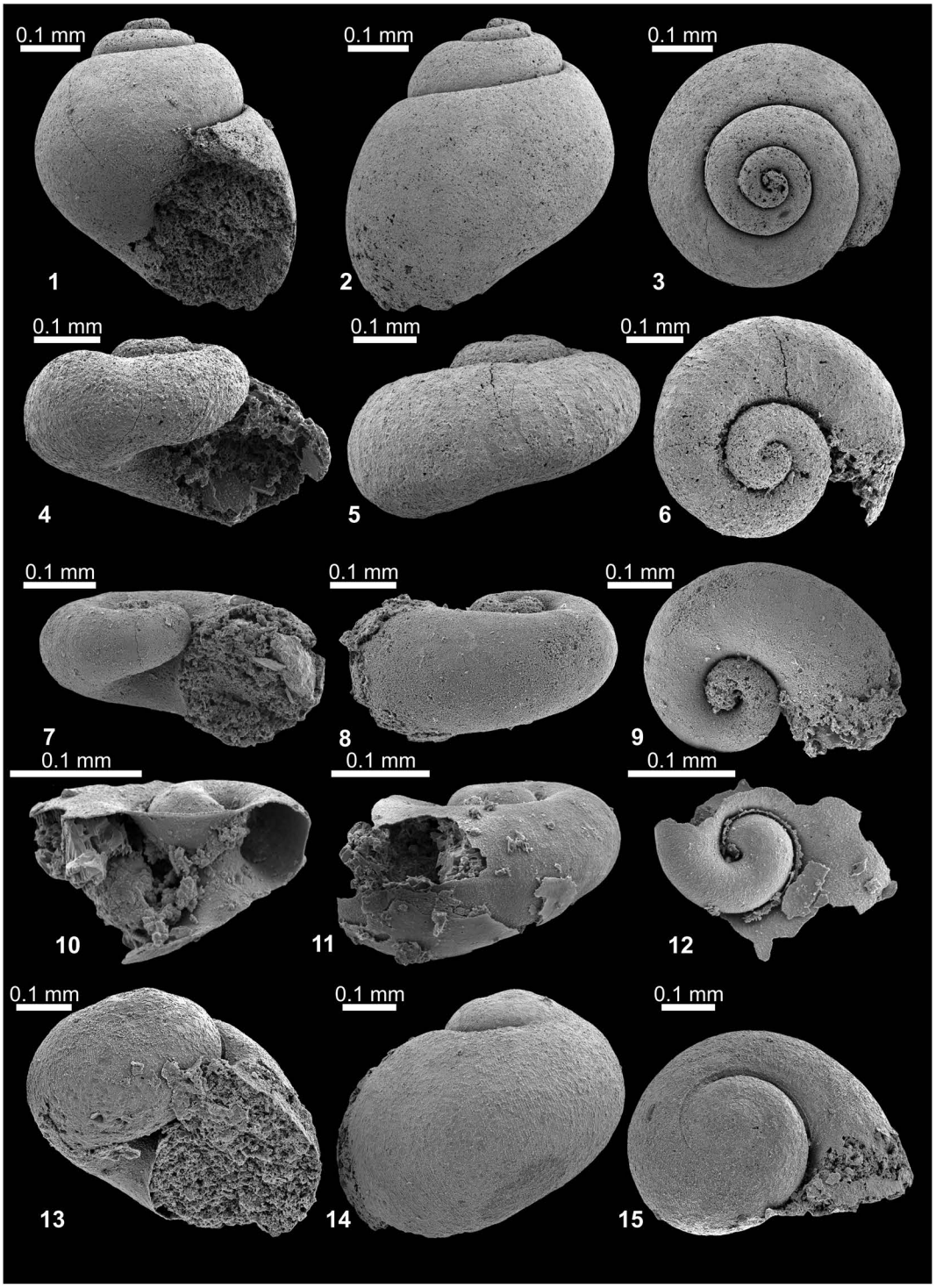

Fig. 128. Gastropods from the middle to upper Middle Smithian. 1–3, *Strobeus* sp. indet., NMNS PM23831, from BT01-15. 4–12, *Anomphalus*? sp. indet. 4–6, NMNS PM23802, from BT01-15. 7–9, NMNS PM23803, from KC02-02. 10–12, NMNS PM23804, from KC02-02. 13–15, *Abrekopsis*? sp. indet., NMNS PM23811, from BT02-03.

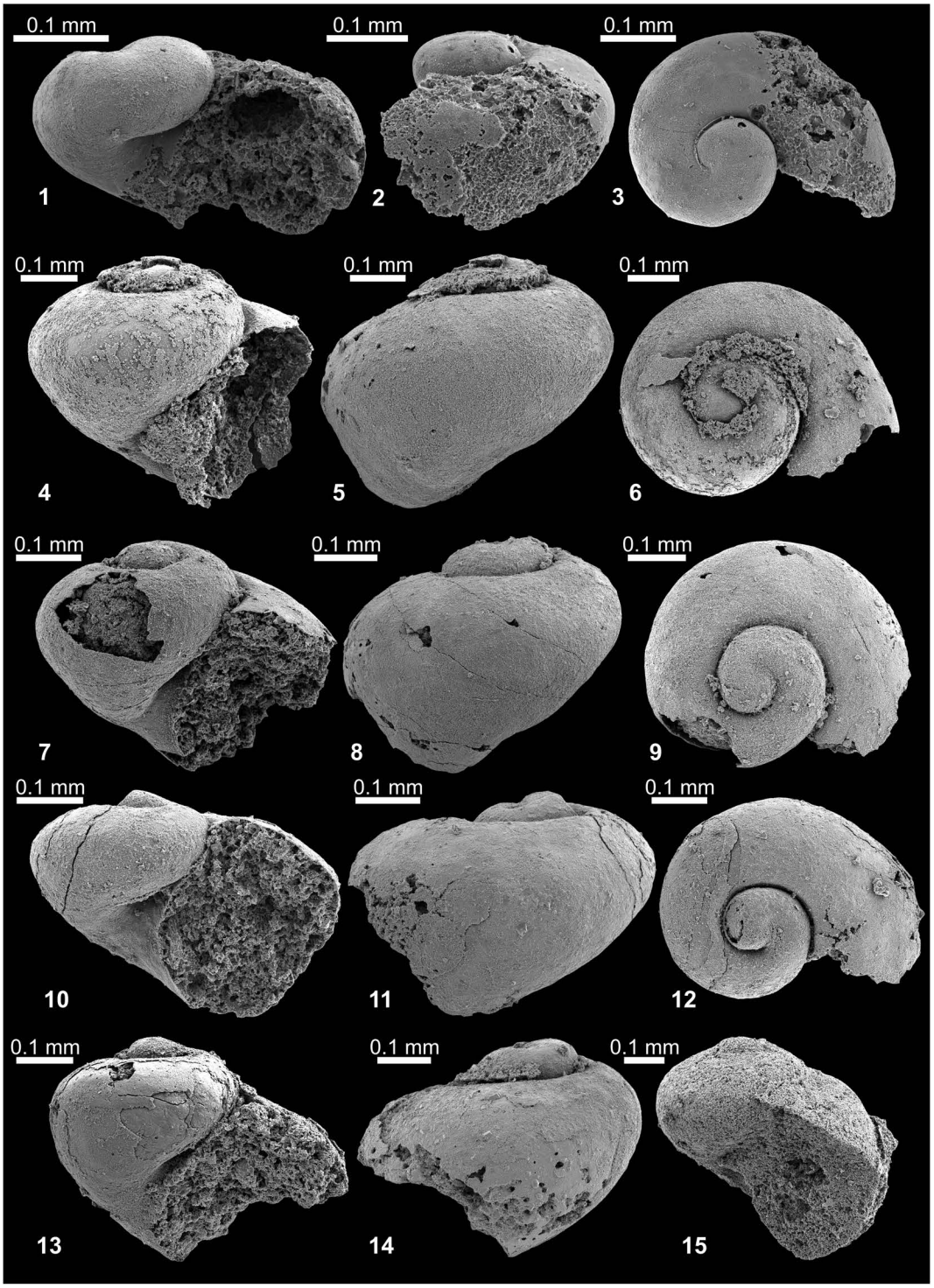

Fig. 129. Gastropods from the middle to upper Middle Smithian. *Naticopsis* sp. indet. B. 1–3, NMNS PM23830, from KC01-13. 4–6, NMNS PM23822, from BT02-03. 7–9, NMNS PM23823, from BT02-03. 10–12, NMNS PM23824, from BT02-03. 13–14, NMNS PM23827, from BT01-14. 15, NMNS PM23828, from BT01-14.

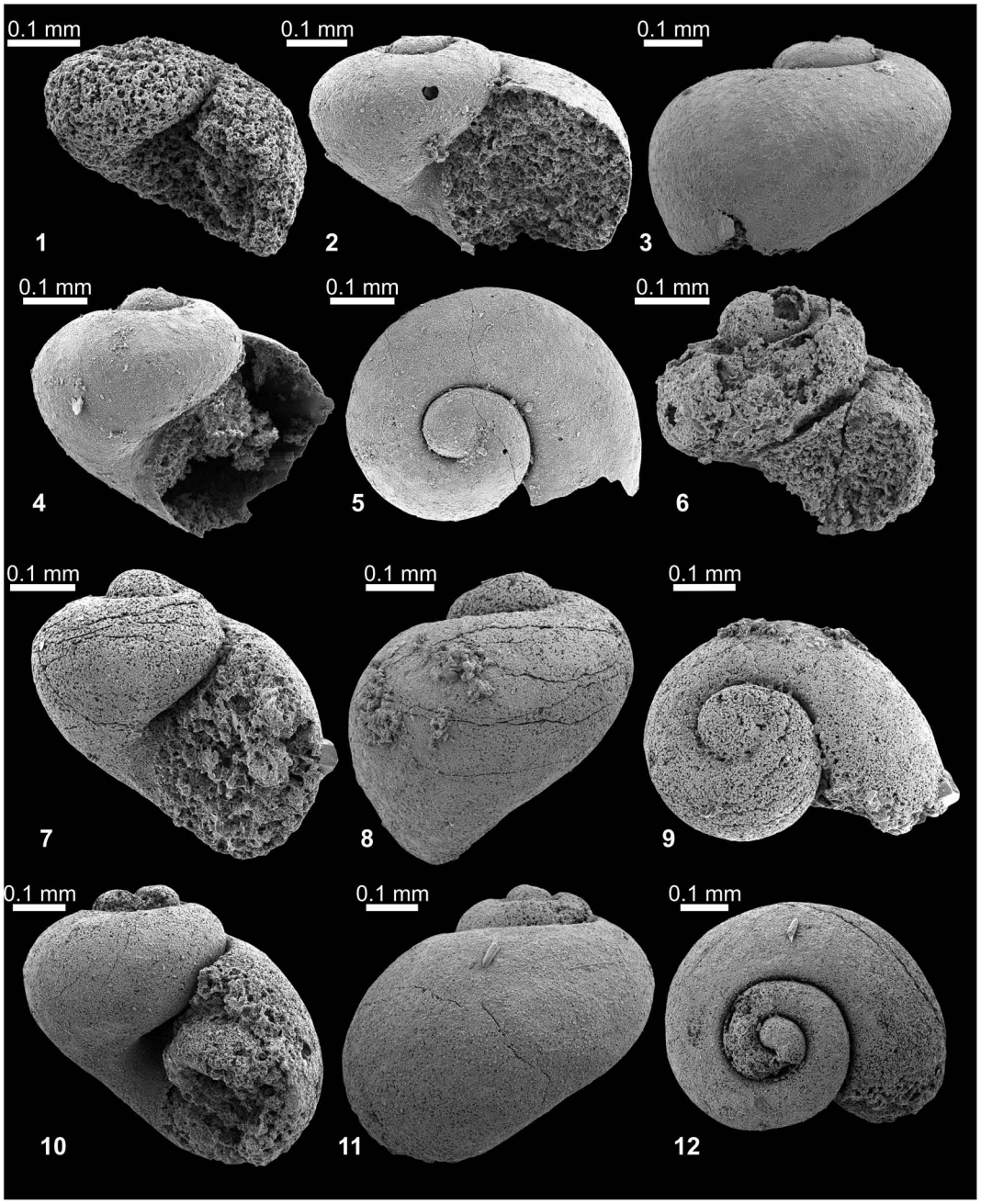

Fig. 130. Gastropods from the middle to upper Middle Smithian. 1–5, *Naticopsis* sp. indet. B. 1, NMNS PM23829, from BT01-14. 2–3, NMNS PM23825, from BT02-03. 4–5, NMNS PM23826, from BT02-03. 6, unidentified gastropod, NMNS PM23851, from KC01-12. 7–12, *Naticopsis* sp. indet. A. 7–9, NMNS PM23814, from BT01-15. 10–12, NMNS PM23815, from BT01-15.

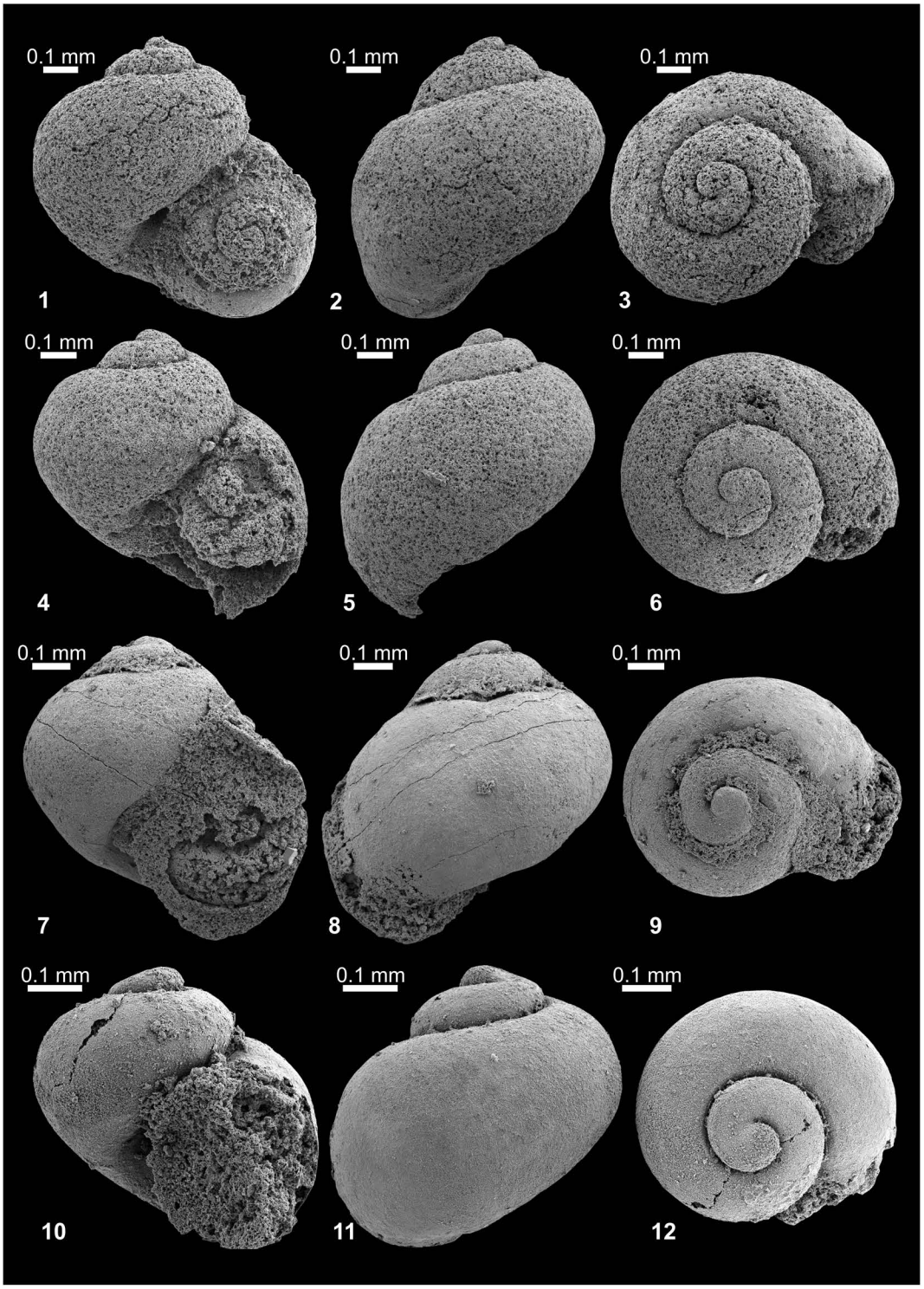

Fig. 131. Gastropods from the upper Middle Smithian. *Naticopsis* sp. indet. A, from BT02-03. 1–3, NMNS PM23816. 4–6, NMNS PM23817. 7–9, NMNS PM23818. 10–12, NMNS PM23819.

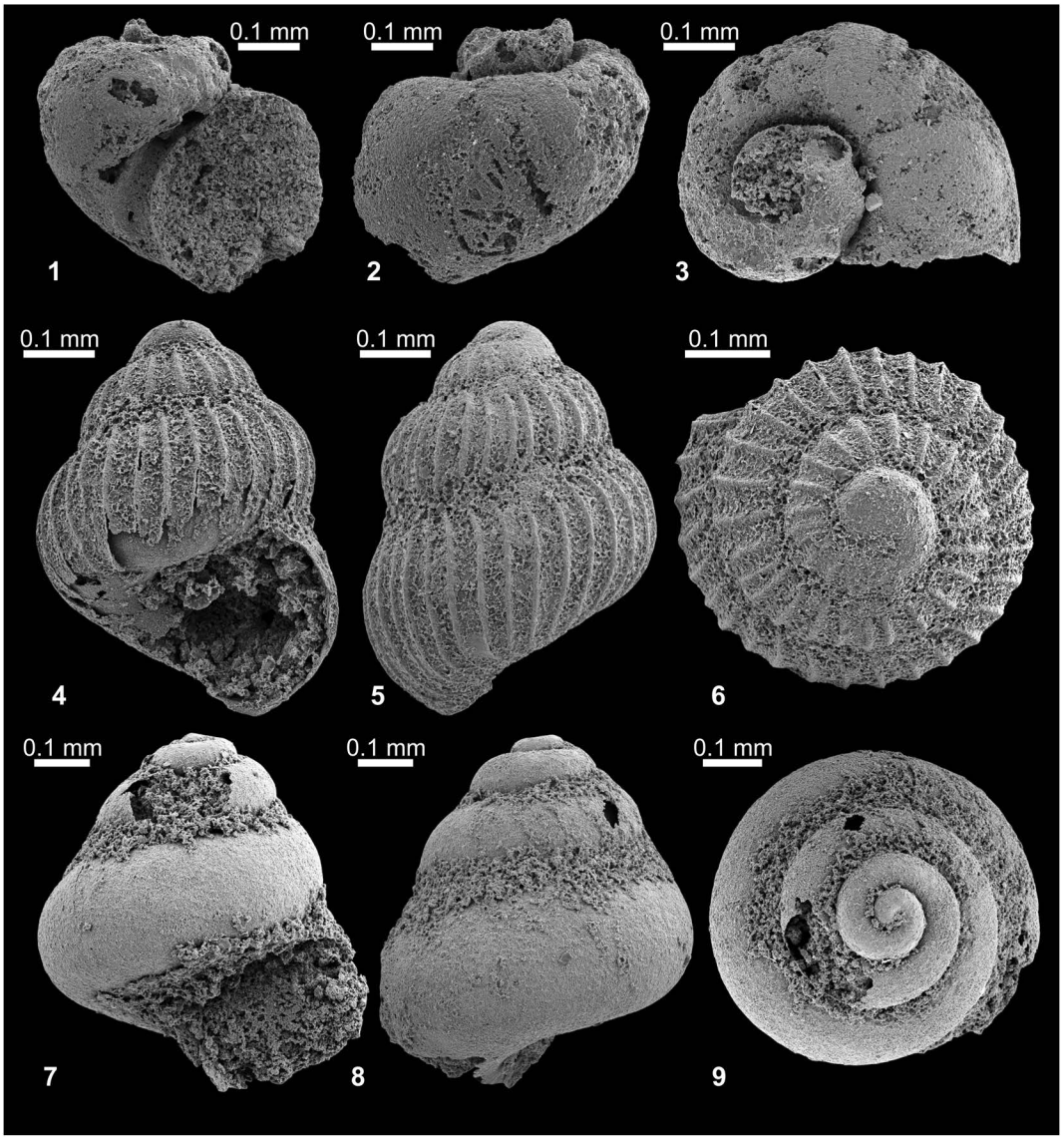

Fig. 132. Gastropods from the middle to upper Middle Smithian. 1–3, *Naticopsis* sp. indet. A, NMNS PM23820, from KC01-12. 4–9, *Ampezzopleura* sp. indet., from BT02-03. 4–6, NMNS PM23832. 7–9, NMNS PM23833.

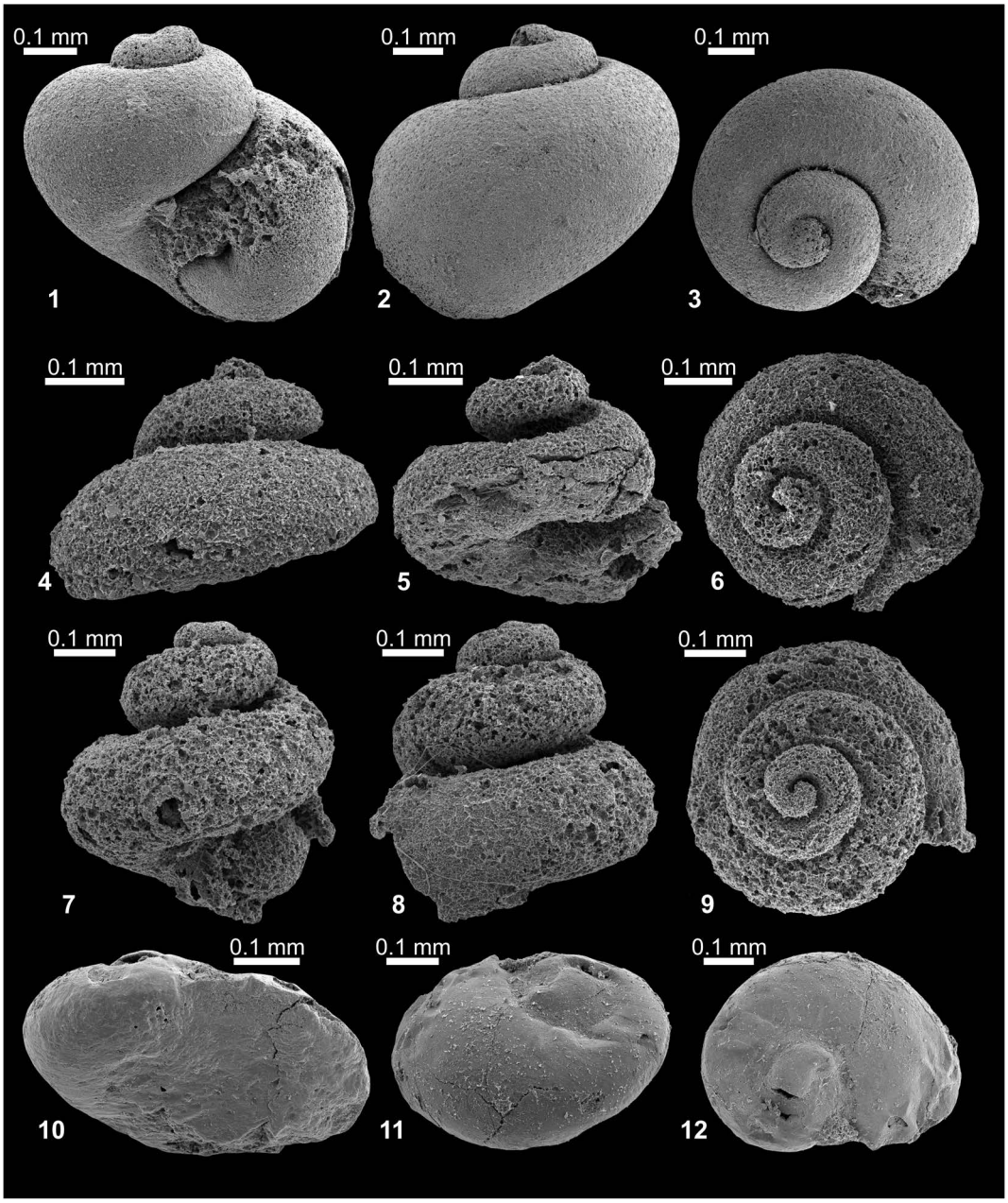

Fig. 133. Gastropods from the middle Middle Smithian. 1–3, *Atorcula* sp. indet., NMNS PM23844, from BT01-15. 4–9, unidentified caenogastropods, from KC01-13. 4–6, NMNS PM23852. 7–9, NMNS PM23853. 10–12, unidentified ?gastropod, NMNS PM23854, from KC01-13.

→

Fig. 134. Gastropods from the upper Middle and Upper Smithian. *Anomphalus*? sp. indet. 1–15, from KC02-03, 1–3, NMNS PM23805. 4–6, NMNS PM23806. 7–9, NMNS PM23807. 10–12, NMNS PM23808. 13–15, NMNS PM23809. 16–18, NMNS PM23810, from KC02-10.

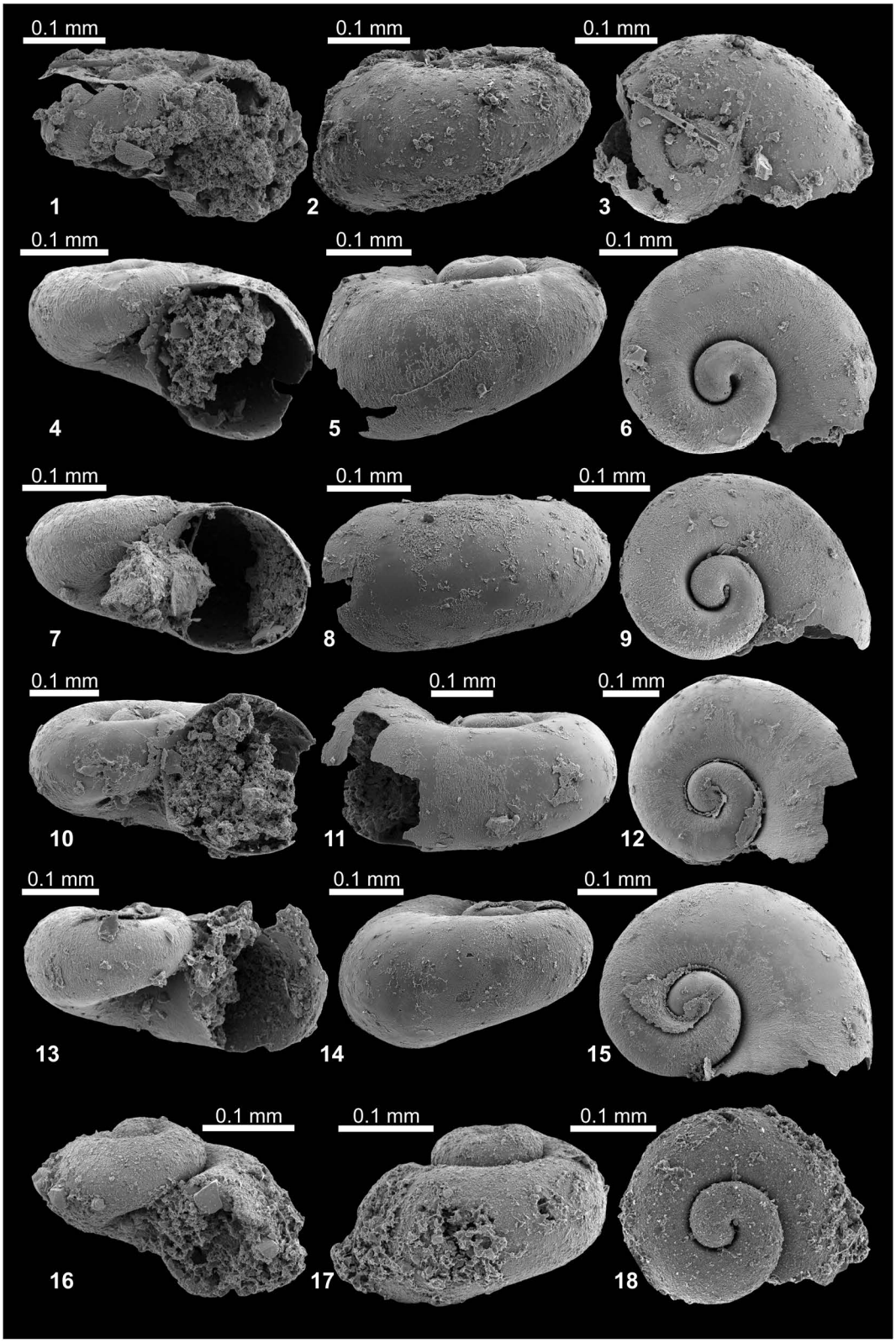
0.1 mm
1
0.1 mm
2
0.1 mm
3
0.1 mm
4
0.1 mm
5
0.1 mm
6
0.1 mm
7
0.1 mm
8
0.1 mm
9
0.1 mm
10
0.1 mm
11
0.1 mm
12
0.1 mm
13
0.1 mm
14
0.1 mm
15
0.1 mm
16
0.1 mm
17
0.1 mm
18

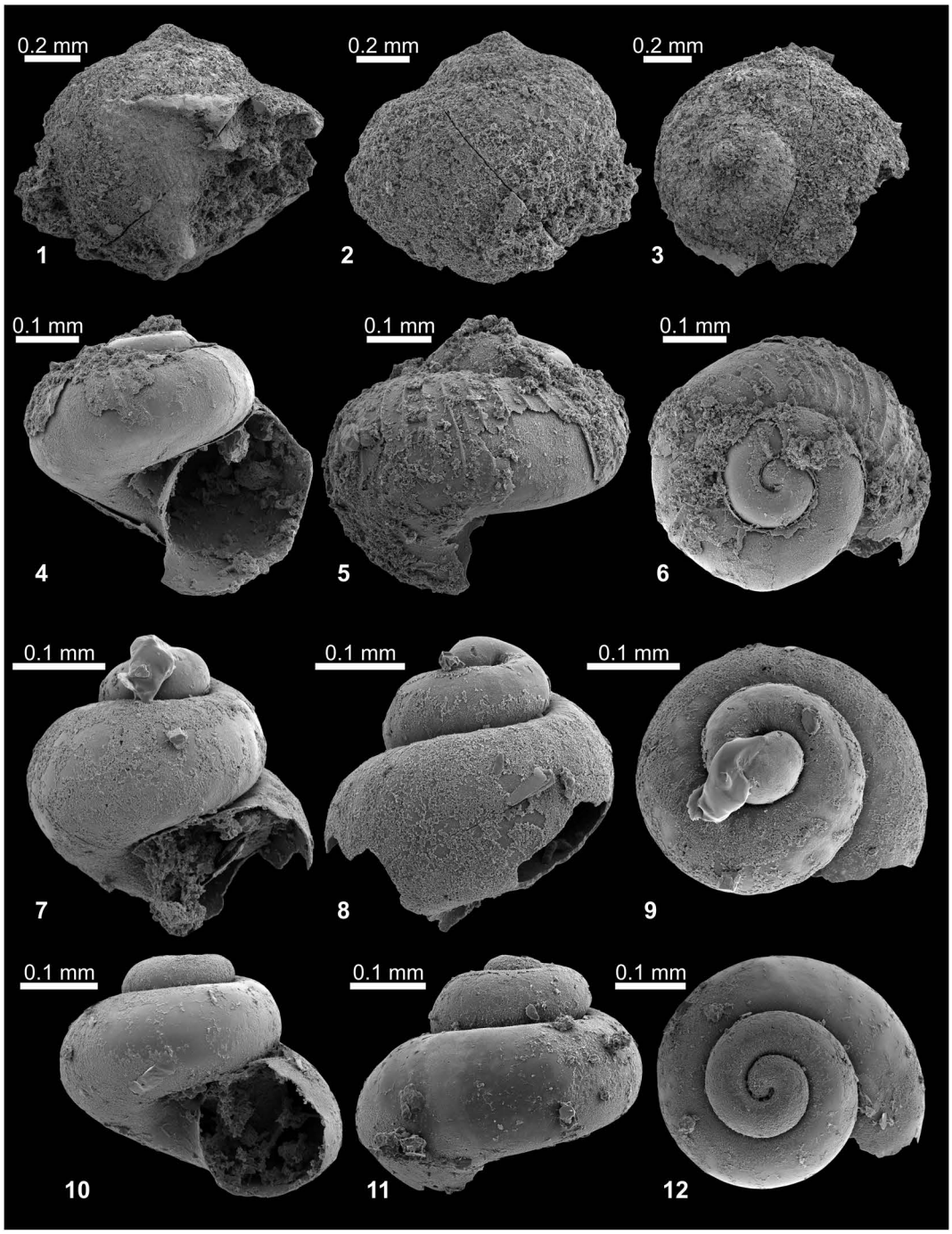

Fig. 135. Gastropods from the upper Middle and Upper Smithian. 1–3, *Naticopsis* sp. indet. A, NMNS PM23821, from KC02-10. 4–12, *Atorcula* sp. indet., from KC02-03. 4–6, NMNS PM23845. 7–9, NMNS PM23846. 10–12, NMNS PM23847.

nal aperture rather than drop-shaped, more flattened upper whorl surface, and a lower shell profile. The gross shell morphology of *Naticopsis* sp. indet. B is similar to *Abrekopsis depressispirus* (Batten and Stokes, 1986) but the initial whorl is bulbous (naticopsid) and not flattened as in *Abrekopsis* (see Kaim, 2009). All shells are early juveniles and we refrain from identifying them to a species level.

Occurrence: Described specimens from BT01-14, BT02-03 and KC01-13 within the portion of the *Novispathodus* ex gr. *waageni* Zone represented by the *Leyeceras* horizon of the *Owenites koeneni* beds (middle Middle Smithian=middle Lower Olenekian) in the Bac Thuy Formation, northeastern Vietnam.

Order Caenogastropoda Cox, 1960
Superfamily Acteoninoidea Cossmann, 1895
Family Soleniscidae Knight, 1931
Genus ***Strobeus*** de Koninck, 1881

Type species: *Strobeus ventricosus* de Koninck, 1881.

Strobeus sp. indet.
Fig. 128.1–128.3

Material examined: One specimen, NMNS PM23831, from BT01-15.

Description: Shell of globular fusiform shape with 3.5 juvenile whorls preserved. Initial whorl corroded. Demarcation between protoconch and teleoconch not discernible. Shell surface smooth. Suture moderately impressed, flanks evenly convex with no shoulder or ramp. No clear demarcation between flank and base. Growth lines not discernible.

Discussion: The shell under consideration is similar to early whorls of *Strobeus pakistanensis* Kaim, Nützel, Hautmann, and Bucher, 2013 from the Smithian of Pakistan (Kaim *et al*., 2013) though we refrain from including the shells from Vietnam to the latter species because of its juvenile nature. Other Early Triassic *Strobeus* are known from the Smithian of Utah (Batten and Stokes, 1986; Nützel, 2005), Dienerian of Russia (Kaim, 2009), and from Griesbachian of Oman (Wheeley and Twitchett, 2005).

Occurrence: Described specimen from BT01-15 within the portion of the *Novispathodus* ex gr. *waageni* Zone within or above the *Owenites koeneni* beds (middle Middle Smithian=middle Lower Olenekian) in the Bac Thuy Formation, northeastern Vietnam.

Superfamily Zygopleuroidea Wenz, 1938
Family Zygopleuridae Wenz, 1938
Subfamily Ampezzopleurinae Nützel, 1998
Genus ***Ampezzopleura*** Bandel, 1991

Type species: *Ampezzopleura tenuis* Bandel, 1991.

Ampezzopleura sp. indet.
Fig. 132.4–132.9.

Material examined: Two specimens, NMNS PM23832–23833, from BT02-03.

Description: Protoconch 1 smooth, slightly bulbous, and composed of about one whorl. Protoconch 2 composed of 2.5 whorls ornamented by 30 axial ribs per whorl; axial ribs straight opisthocline to slightly sigmoidal, continuous from suture to suture. Teleoconch not present, either not developed or not preserved.

Discussion: The specimen NMNS PM23832 is a well preserved larval shell of *Ampezzopleura*. The specimen NMNS PM23833 is classified to *Ampezzopleura* only conditionally as its external surface is eroded away and the identification is based solely on gross shell morphology. We refrain from putting any species name on the larval shell alone. A single species of this genus was identified from the Early Triassic, *Ampezzopleura rugosa* (Batten and Stokes, 1986) has been reported from the Smithian of Utah, United States (Nützel and Schulbert, 2005).

Occurrence: Described specimen from BT02-03 within the portion of the *Novispathodus* ex gr. *waageni* Zone represented by the

Leyeceras horizon of the *Owenites koeneni* beds (middle Middle Smithian = middle Lower Olenekian) in the Bac Thuy Formation, northeastern Vietnam.

Family Protorculidae Bandel 1991
Genus ***Atorcula*** Nützel, 1998

Type species: *Melania canalifera* zu Münster, 1841 sensu Kittl, 1894.

Atorcula sp. indet.
Figs. 123.4–123.6, 125, 126, 127.1–127.6, 133.1–133.3, 135.4–135.12

Material examined: Six specimens, NMNS PM23834–23839, from BT01-07, three specimens, NMNS PM23840–23842, from KC01-04, one specimen, NMNS PM23843, from BT01-06, one specimen, NMNS PM23844, from BT01-15, three specimens, NMNS PM23845–23847, from KC02-03, and one specimen, NMNS PM23848, from BT02-01.

Description: Protoconch 1 smooth and composed of about one whorl. Protoconch 2 composed of about 1.5–2 whorls ornamented by about 30 axial ribs; axial ribs opisthocyrt, slightly more incurved in abapical shell portion, and continuous from suture to suture. Teleoconch smooth, whorls convex and sutures deeply incised. Aperture circular.

Discussion: *Atorcula* unites protorculid gastropods characterised by an axially-ribbed protoconch followed by smooth high-spired shells; the present taxon differs from the type species in being relatively low and in having convex whorls and incised suture. Most of the shells from Vietnam, which we attributed to this genus have the outermost ornamented shell layer eroded away. Nevertheless, in a number of specimens the protoconch ornamentation is partially or wholly preserved (e.g., Figs. 125.1–125.6, 126.5, 135.4–135.6).

Occurrence: Described specimens from BT01-06, BT01-07, BT01-15, BT02-01, KC01-04 and KC02-03 within the *Novispathodus* ex gr. *waageni* Zone in the Bac Thuy Formation, northeastern Vietnam. BT02-01 is represented by the *Flemingites rursiradiatus* beds (lowest Middle Smithian = middle Lower Olenekian). BT01-06 and BT01-07 are located between the *Flemingites rursiradiatus* beds and the *Urdyceras tulongensis* beds (lower Middle Smithian = middle Lower Olenekian). KC01-04 is located beneath the *Owenites koeneni* beds (middle Middle Smithian = middle Lower Olenekian). BT01-15 is represented by the *Leyeceras* horizon of the *Owenites koeneni* beds. KC02-03 is located above the *Guodunites* horizon of the *Owenites koeneni* beds. *Atorcula* is known from the Late Triassic (Nützel 1998); it also resembles some *Omphaloptycha* species from the Early Triassic which have been reported from Utah (Batten and Stokes, 1986) and Russia (Kaim, 2009).

Bivalves (by T. Komatsu, H. T. Dang and T. C. Dinh)

Systematic descriptions basically follow the classification established by Newell (1938) and Moore (1969).

Abbreviations for shell dimensions: RV = right valve; LV = left valve; H = shell height; L = shell length; T = shell thickness.

Institution abbreviations: KMSP = Faculty of Science, Kumamoto University.

Class Bivalvia Linné, 1758
Order Pterioida Newell, 1965
Superfamily Posidonioidea Frech, 1909
Family Posidoniidae Frech, 1909
Genus ***Bositra*** de Gregorio, 1886

Type species: *Posidonia ornati* Quenstedt, 1856.

Remarks: Emended diagnoses of *Posidonia* Bronn, 1828 and *Bositra* were described by Waller and Stanley (2005). According to Waller and Stanley (2005), the characteristics of the right anterior auricle and byssal sinus of

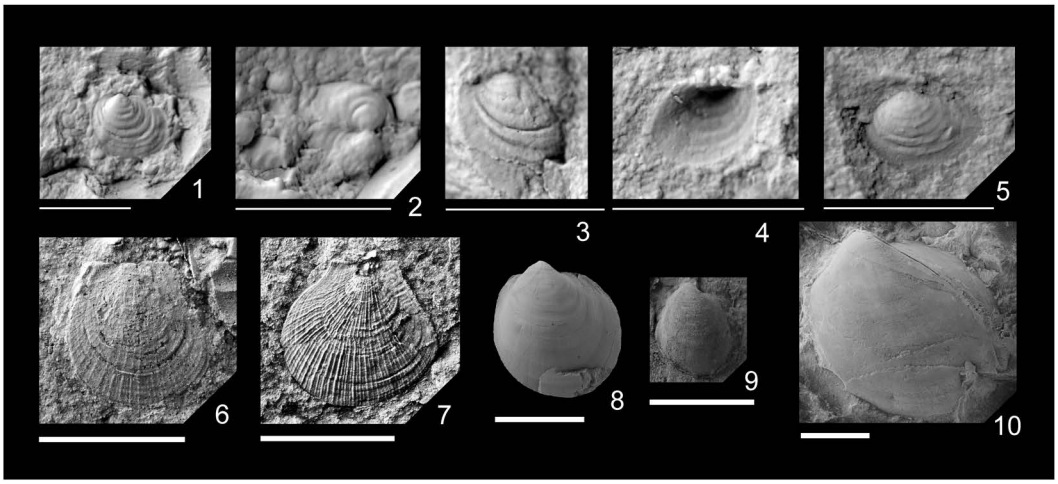

Fig. 136. 1–4, *Bositra limbata* (Guo, 1985). 1, KMSP-5131, from KC02-15, external cast of left valve. 2, KMSP-5132, from NT01-12, external cast of articulated valves. 3, KMSP-5133, from NT01-07, external cast of incomplete left valve. 4, KMSP-5134, from KC02-14, internal cast of left valve. 5, *Bositra* sp. indet, KMSP-5135, from KC02-03, external cast of left valve. 6–7, *Leptochondria bittneri* (Kiparisova, 1938) from KC02-14. 6, KMSP-5136, external cast of left valve. 7, KMSP-5137, external cast of left valve. 8–10, *Crittendenia langsonensis* Komatsu and Dang, 2013. 8, KMSP-5117 (paratype), from KC02-08, left valve. 9, KMSP-5120, from NT01-04, left valve. 10, KMSP-5119 (holotype), from NT01-09, left valve. Thick scale bars indicate 1 cm. Thin scale bars 5 mm.

Posidonia are more in line with placement near the Pterineidae rather than the Pteriopectinidae. *Bositra* has a single adductor muscle scar and an alivincular ligament. In contrast, *Posidonia* is characterized by a duplivincular ligament system and anisomyarian adductor musculature. The Triassic "*Posidonia*" is placed in *Bositra* and is common in early Mesozoic offshore sediments (Waller and Stanley, 2005).

Bositra limbata (Guo, 1985)

Fig. 136.1–136.4

Posidonia limbata Guo, 1985, pl. 15, figs. 1, 2.

Types: Type specimens figured by Guo (1985, pl. 15, figs. 1, 2) from the Middle Triassic Baifeng Formation, Jiuzhai, Funing, Yunnan, South China.

Material examined: Disarticulated left valves and articulated valves (KMSP-5131–5134) collected from dark gray and greenish gray laminated mudstones and marls in NT01 and KC02. KMSP-5131 and 5134 are moderately well preserved.

Description: Shell small for genus, equivalve, suborbicular to transversely oval in outline, shell length greater than shell height; test very thin; moderately convex valves, dorsal margin short and straight, ventral margins rounded, umbo not prominent but inflated, situated slightly anterior to the middle, auricles lacking; shell surface (except for umbonal area) covered with broad concentric ribs, fine lamellae and undulations; umbonal area covered with coarse concentric folds and undulations; byssal notch lacking; ligament and adductor muscle impressions unknown.

Measurements (*in mm*):

Specimen no.	H	L	T	Remarks
KMSP-5131	3.2	4.0	—	LV
KMSP-5134	1.9+	2.3	—	LV

Discussion: *Bositra limbata* has been described as *Posidonia limbata* from the Middle Triassic Baifeng Formation, Jiuzhai, Funing, Yunnan, South China (Guo, 1985). Guo (1985) described the umbonal area and ornamentation of this species in detail, reporting

that the early stage of the shell is much more inflated than the surrounding tissue, which is like "a gypsy-hat margin". Fine broad concentric lamellae are rarely found on the fold.

In Vietnam, "*Posidonia*", are commonly reported from the Middle Triassic (Vu Khuc *et al.*, 1991), although almost all species of these Triassic "*Posidonia*" probably belonged to *Bositra*. These Middle Triassic Vietnamese "*Posidonia*" are ornamented by many clear concentric ribs and have never been reported from the Lower Triassic.

Occurrence: Described specimens from NT01-07 and KC02-09 within the *Novispathodus pingdingshanensis* Zone represented by the *Xenoceltites variocostatus* beds (upper Smithian=upper Lower Olenekian), and those from BR01-06 between the *Xenoceltites variocostatus* beds and *Tirolites* sp. nov. beds (lower Spathian=lower Upper Olenekian), and those from KC02-14 and KC02-15 within the *Triassospathodus symmetricus* Zone represented by the *Tirolites* sp. nov. beds, and those from NT01-11, NT01-12 and BR01-08 within the *Tirolites* sp. nov. beds in the Bac Thuy Formation, northeastern Vietnam. They co-occur with *Crittendenia australasiatica*, *Crittendenia langsonensis*, *Leptochondria bittneri*, and "*Pseudomonotis" himaica*. This species also occurs in the Middle Triassic Baifeng Formation, Yunnan, South China (Guo, 1985).

Bositra sp. indet.

Fig. 136.5

Material examined: Poorly preserved disarticulated left valve (KMSP-5135) collected from greenish gray laminated mudstone.

Description: Shell small and suborbicular to elongately ovate; shell length greater than shell height; test very thin; moderately convex valve; dorsal margin short and straight; ventral margins rounded; umbo not prominent but inflated, situated a little anterior to middle; auricles lacking; shell surface covered with fine weak concentric ribs and undulations; umbonal area smooth; byssal notch lacking; ligament and adductor muscle impressions unknown.

Measurements (*in mm*):

Specimen no.	H	L	T	Remarks
KMSP-5135	2.0	3.0	—	LV

Discussion: This species is characterized by an elongately ovate shell ornamented with weak concentric ribs. In contrast, *B. limbata* is suborbicular to transversely oval in outline and is characterized by broad concentric ribs.

Occurrence: Described specimen from KC02-03 within the portion of the *Novispathodus* ex gr. *waageni* Zone above the *Guodunites* horizon of the *Owenites koeneni* beds (upper Middle Smithian=middle Lower Olenekian) in the Bac Thuy Formation, northeastern Vietnam.

Order Pterioida Newell, 1965
Superfamily Pterinopectinacea Newell, 1938
Family Pterinopectinidae Newell, 1938
Subfamily Claraiinae Gavrilova, 1996
Genus ***Crittendenia*** Newell and Boyd, 1995

Type species: *Crittendenia kummeli* Newell and Boyd, 1995.

Crittendenia australasiatica
(Krumbeck, 1924)

Fig. 137

Pseudomonotis australasiatica Krumbeck, 1924, pl. 8, figs. 8–10.
Pseudomonotis subconvexa Krumbeck, 1924, pl. 8, fig. 12a, b.
Claraia australasiatica (Krumbeck, 1924). Kiparisova, 1938, pl. 3, figs. 8, 9a, b, 10.
Crittendenia australasiatica (Krumbeck, 1924). Komatsu and Dang, 2013, figs. 4.1–4.18, 4.24, 4.26–4.28.

Types: Type specimens sketched by Krumbeck (1924, pl. 8, figs. 8–10) from the Lower Triassic, Timor, Indonesia.

Material examined: Abundant well-preserved left valves and several right valves collected from calcareous nodules and limestone beds (KMSP-5100–5115, 5122–5124). Over-

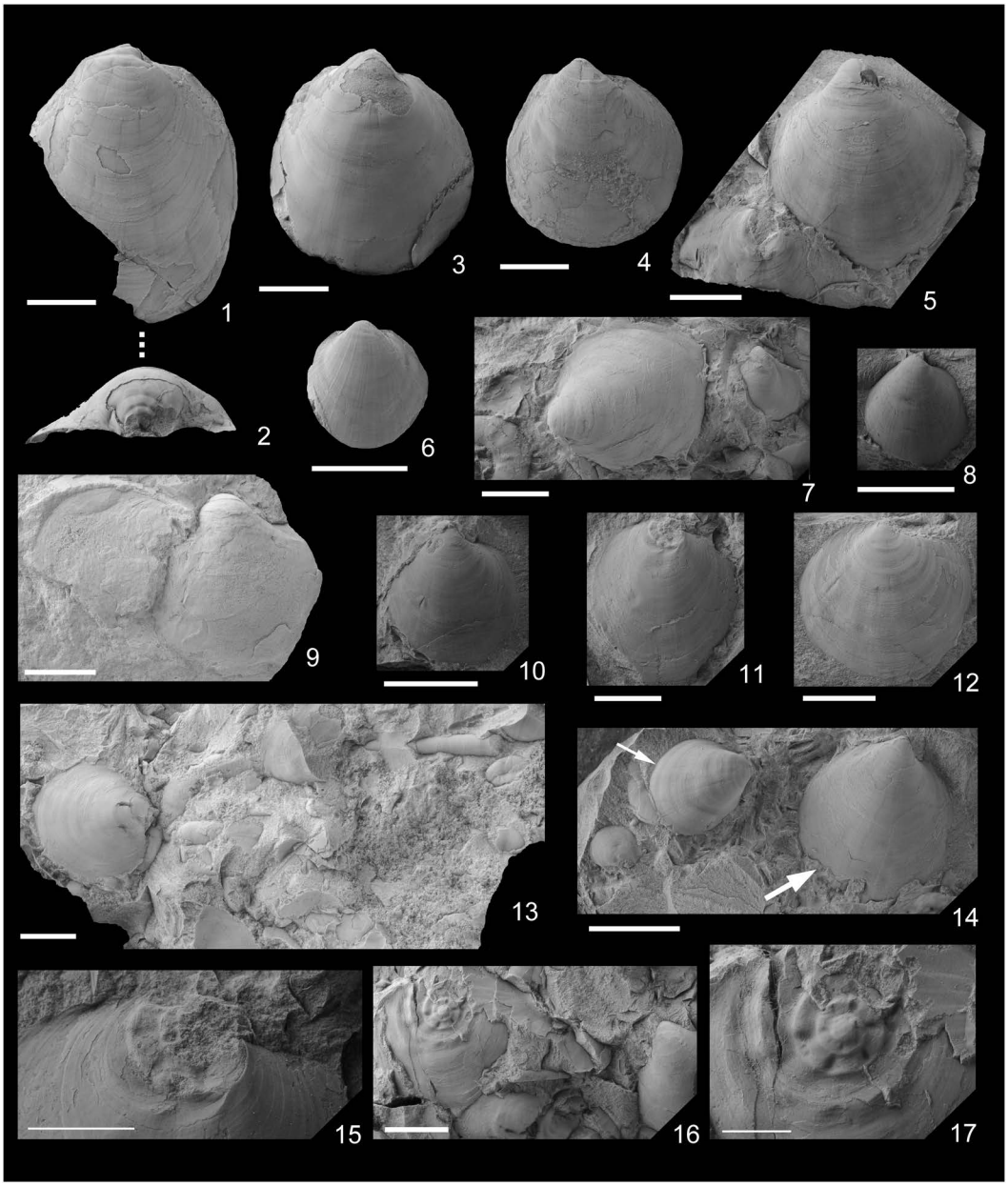

Fig. 137. *Crittendenia australasiatica* (Krumbeck, 1924). 1, KMSP-5110, from NT01-09, external view of left valve. 2, Dorsal view of KMSP-5110, umbonal showing imprint of ammonoid (*Xenoceltites variocostatus* Brayard and Bucher, 2008). 3, KMSP-5111, from NT01-09, left valve. 4, KMSP-5101, from NT01-09, left valve, 5, KMSP-5126 (left valve) and KMSP-5122 (right valve), from KC02-08, KMSP-5122 (lower) showing irregular attachment cicatrix on right valve. 6, KMSP-5105, from NT01-04, left valve. 7, KMSP-5127, from NT01-04, left valve. 8, KMSP-5128, from BR01-04, left valve. 9, KMSP-5116, from NT01-07, right and left valves, showing anterior auricle of right valve. 10, KMSP-5129, from KC02-06, left valve. 11, KMSP-5123, from NT01-04, right valve. 12, KMSP-5114, from NT01-05, right valve. 13, KMSP-5113, from NT02-04, modes of occurrence of *C. australasiatica* and ammonoid shells. 14, *Crittendenia langsonensis* Komatsu and Dang, 2013 (small arrow), KMSP-5125, and *C. australasiatica* (large arrow), KMSP-5108, from NT01-07, left valves. 15, KMSP-5123, umbonal area showing imprint of ammonoid (*X. variocostatus*) umbilicus on right valve. 16, KMSP-5124, from NT01-07, modes of occurrence of *C. australasiatica* and ammonoid shells. 17, KMSP-5124, umbonal area showing imprint of ammonoid (*X. variocostatus*) umbilicus on right valve. Thick scale bars indicate 1 cm. Thin scale bars 5 mm.

lapping solitary right and left valves found in a calcareous nodule (KMSP-5116; Fig. 137. 9).

Description: Shell moderate in size for genus, inequivalve, orbicular or suborbicular in outline; length and height of shells subequal, or height slightly greater than length; test very thin; hinge line straight and moderately long for genus; strongly convex left valve, orthocline; anterior wing small without sinus, posterior wing also small and indistinguishable; ventral margins rounded, umbo protruded above hinge line, situated mostly central; umbonal angle about 90 to 120 degrees; shell surface of left valve moderately smooth except for very weak concentric growthlines, irregularly faint radial threads, and ribs occasionally showing growth stop; slightly inflated right valve ornamented with irregularly, very weak radials and growthlines, posterior wing not differentiated, anterior auricle small for genus, surface of auricle smooth, narrow and moderately deep byssal notch conspicuous; dorsal area of right valve and umbonal area of left valve occasionally imprinted by the reflecting substrate, for example, an ammonoid umbilicus.

Measurements (*in mm*):

Specimen no.	H	L	T	Remarks
KMSP-5100	33.1	34.4	11.8	LV
KMSP-5101	28.9	31.2	8.8	LV
KMSP-5102	26.1	26.2	8.5	LV
KMSP-5111	29.1	32.0	9.5	LV
KMSP-5113	22.4	20.7	3.7	RV
KMSP-5114	23.6	22.1	4.4	RV
KMSP-5128	12.1+	11.2	3.1	LV

Discussion: *Crittendenia australasiatica* has been described as *Pseudomonotis australasiatica* on the basis of the left valve from the Lower Triassic Timor, Indonesia (Krumbeck, 1924). Komatsu *et al*. (2013) recently reported some well-preserved right and left valves of this species from NT01-03 to NT01-07 within the *Xenoceltites variocostatus* beds in the Bac Thuy Formation; they described right valves and juveniles of this species in detail.

The described specimens show an important diagnostic characteristic for the genus. Small attachment imprints are clearly marked on the umbonal area of the left valve and near the byssal notch of the right valve (Fig. 137.15–137.17). Some of the imprints of the attachments are coiled impressions of ammonoid umbilicus of *Xenoceltites variocostatus* (Fig. 137.2, 137.15–137.17). Newell and Boyd (1995) described *Crittendenia kummeli* specimens characterized by a coiled negative impression of an ammonoid umbilicus from the *Meekoceras* zone of the Thaynes Formation, northeast Nevada, USA.

Occurrence: Described specimens from KC02-06, KC02-07 and BR01-01 to BR01-04, below the *Xenoceltites variocostatus* beds (Upper Smithian = upper Lower Olenekian), and those from BT02-05, KC02-10, KC02-11, NT01-01 to NT01-07, NT01-09 and BR01-05 within the *Novispathodus pingdingshanensis* Zone that includes the *Xenoceltites variocostatus* beds and *Tirolites* cf. *cassianus* beds, and those from KC02-12 to KC02-17 within the *Triassospathodus symmetricus* Zone that includes the *Tirolites* cf. *cassianus* beds (lowest Lower Spathian = lowest Upper Olenekian) and *Tirolites* sp. nov. beds (Lower Spathian = lower Upper Olenelian), and those from BR01-06 and BR01-07 between the *Xenoceltites variocostatus* beds and *Tirolites* sp. nov. beds, and those from BT02-07, BT02-08, KC02-18, NT01-10 to NT01-12, and BR01-08 within the *Tirolites* sp. nov. beds in the Bac Thuy Formation, northeastern Vietnam. This species also occurs in the Lower Triassic in Timor, Indonesia (Krumbeck, 1924) and the upper Smithian to lower Spathian on Russky Island, South Primorye, Russia (Kiparisova, 1938).

Crittendenia langsonensis Komatsu and Dang, 2013

Figs. 136.8–136.10, 137.14

Crittendenia langsonensis Komatsu and Dang, 2013, figs. 4.19–4.24, 10.

Holotype: Holotype KMSP-5119, figured by Komatsu and Dang (2013, fig. 4.21) from NT01-06 within the *Xenoceltites variocostatus* beds in the Bac Thuy Formation.

Material examined: Holotype (KMSP-5119), paratypes (KMSP-5117, 5118, 5120) from NT01-04, 07, and 09, and one specimen from KC02-08.

Descriptions: Shells of average size for genus, inequivalve and inequilateral, prosocline, suborbicular in outline, slightly longer than high; test very thin; surface ornamented with growth lines and irregularly faint threads and radials occasionally representing growth stop; hinge line moderately long and straight; left valve inflated, strongly prosogyrous umbo protruded above hinge line, situated about 1/3 to 2/5 of the way from the anterior margin; umbonal angle about 95 to 105 degrees; obtuse anterior left wing very small without sinus; posterior left wing inconspicuous, ventral margins rounded; right valve gently convex, non-protruded umbo; right spatulate small anterior auricle ornamented with fine clear ribs parallel to the anterior auricle end; byssal sinus; hinge unknown.

Measurements (*in mm*):

Specimen no.	H	L	T	Remarks
KMSP-5119	27.5+	28.6	7.8	LV (Holotype)
KMSP-5117	12.7	13.5	5.0	LV (Paratype)
KMSP-5120	8.9	9.6	3.5	LV (Paratype)
KMSP-5125	12.1	10.9	4.9	LV

Discussion: *Crittendenia langsonensis* is characterized as a prosocline species and is ornamented with faint radial threads on the left valve. Prosocline species are not common in this genus. Olenekian (upper Smithian?/Spathian) *C. nammalensis* (Nakazawa, 1996) characterized as typical prosocline shells described by Waterhouse (2000) are reported from the Langpo Member, Gungdang Formation, Manang, Nepal and the Sungjar Formation, the Salt Range, Pakistan. However, only poorly preserved *C. nammalensis* are figured and sketched by Waterhouse (2000).

Occurrence: Described specimens from KC02-08 and NT01-05 to NT01-09 within the portion of the *Novispathodus pingdingshanensis* Zone represented by the *Xenoceltites variocostatus* beds (Upper Smithian = upper Lower Olenekian) in the Bac Thuy Formation, northeastern Vietnam.

Superfamily Pseudomonotoidea Newell, 1938
Family Leptochondriidae Newell and Boyd, 1995
Genus ***Leptochondria*** Bittner, 1891

Type species: *Pecten* (*Leptochondria*) *aeolicus* Bittner, 1891.

Leptochondria bittneri (Kiparisova, 1938)
Fig. 136.6–136.7

Pseudomonotis cf. *multiformis* Bittner, 1899, p.10, pl. 2, figs. 11–14.
Pecten (*Velopecten*) *bittneri* Kiparisova, 1938, p. 289, pl. 4, figs. 5–9, 11, 13.

Holotype: Right valve, figured by Kiparisova (1938, p. 289, pl. 4, fig. 13), from the Lower Triassic, Russky Island, South Primorye, Russia.

Material examined: Disarticulated left valves collected from dark gray and greenish gray laminated shales (KMSP-5136, 5137). Almost all specimens moderately well preserved.

Description: Left valve moderate in size for genus, suborbicular in outline, moderately inflated; test very thin; dorsal margin short and straight, ventral margins well rounded, umbo slightly projecting above dorsal margin, situated central; anterior and posterior auricles right-angled to obtuse, indistinctly delimited from disk; shell surface ornamented with fine radial ribs and concentric lamellae, close-set radial ribs, intercalating in two or three ranks; about 15 to 20 first-order ribs slightly prominent, weaker ribs separated by first-order ribs, first- and second-order ribs rarely bifurcated; concentric fine lamellae irregularly spaced on marginal ventral surface; hinge and internal structures unknown, right valve not collected.

Measurements (*mm*):

Specimen no.	H	L	T	Remarks
KMSP-5136	8.1	8.0	—	LV
KMSP-5137	10.7	11.1	—	LV

Discussion: The ornamentations of *Leptochondria bittneri* are more or less variable. According to Kiparisova (1938, pl. 4, figs. 5–9, 11, 13), the shell surface is irregularly covered by concentric lamellae and very fine concentric ribs. Furthermore, the number, sequence, and strength of the radial ribs are quite variable. In addition, third-order radial ribs and concentric erect lamellae are not found on some Russian specimens (e.g. fig. 9, pl. 4 in Kiparisova, 1938). Vietnamese specimens are similar to specimens of Kiparisova (1938, pl. 4, figs. 5–7).

Leptochondria bittneri resembles *L. minima* (Kiparisova, 1938) described from the Induan Lazurnaya Formation and Induan to Olenekian (Smithian) Zhitkov Formation by Kiparisova (1938). *L. minima* is also characterized by variable shell ornamentations. However, the primary ribs of *L. bittneri* are much stronger than those of *L. minima* (Kumagae and Nakazawa, 2009). In addition, *L. bittneri* is distinguished from *L. minima*, which is characterized by very fine numerous radial ribs.

Leptochondria cf. *bittneri* reported from the Lower Triassic Daye Formation, Guizhou, South China, by Gu (1976) and the Guizhou Bureau of Geology and Mineral Resources (1987) is very similar to *L. bittneri*. However, we cannot confirm, because the umbonal area of the specimen figured by Gu (1976, pl. 29, fig. 4) is poorly preserved.

Occurrence: Described specimens from NT01-07 to NT01-09 within the *Novispathodus pingdingshanensis* Zone represented by the *Xenoceltites variocostatus* beds (upper Smithian=upper Lower Olenekian), and those from KC02-14 within the *Triassospathodus symmetricus* Zone represented by the *Tirolites* sp. nov. beds (Lower Spathian=lower Upper Olenekian), and those from BR01-07 between the *Xenoceltites variocostatus* beds and *Tirolites* sp. nov. beds in the Bac Thuy Formation, northeastern Vietnam. This species also occurs in the Lower Triassic Tobizin Formation in South Primorye, Russia (Bittner, 1899; Kiparisova, 1938).

Conodonts (by T. Maekawa and H. Igo)

Terminology for the orientation of elements has largely been modified by intensive analysis of multielement reconstruction of conodont animals (e.g., Purnell *et al*., 2000). All specimens described herein are discrete P elements; hence, the orientation terms proposed by Orchard (1995, 2005) are utilized, and the superageneric classification proposed by Orchard (2005, 2007a) and Sweet (1988) has also been adopted.

Institution abbreviation: MPC=Micropaleontology Collection, National Museum of Nature and Science, Tsukuba.

Order Ozarkodinida Dzik, 1976
Superfamily Gondolelloidea (Lindström, 1970)
Family Gondolellidae Lindström, 1970
Subfamily Mullerinae Orchard, 2005
Genus ***Conservatella*** Orchard, 2005

Type species: *Ctenognathus conservativa* Müller, 1956.

Conservatella conservativa (Müller, 1956)

Figs. 138–140, 141.1–141.6

Ctenognathus conservativa Müller, 1956, p. 821, pl. 95, fig. 25.
Neospathodus conservativa (Müller, 1956). Buryi, 1979, p. 50, pl. 9, fig. 1.
Neospathodus conservativus (Müller, 1956). Sweet *et al*., 1971, pl. 1, fig. 10; Solien, 1979, p. 303, pl. 3, figs. 5–6.
multielement apparatuses, *Conservatella* aff. *conservativa* (Müller, 1956). Orchard, 2005, p. 81, text-fig. 7.
Conservatella conservativa (Müller, 1956). Orchard, 2008, p. 402, figs. 8.20–8.21.

Material examined: Three specimens, MPC25067–25069, from BT01-03, two specimens, MPC25070, 25071, from BT01-04, one specimen, MPC25072, from BT01-06, four specimens, MPC25073–25076 from BT01-07,

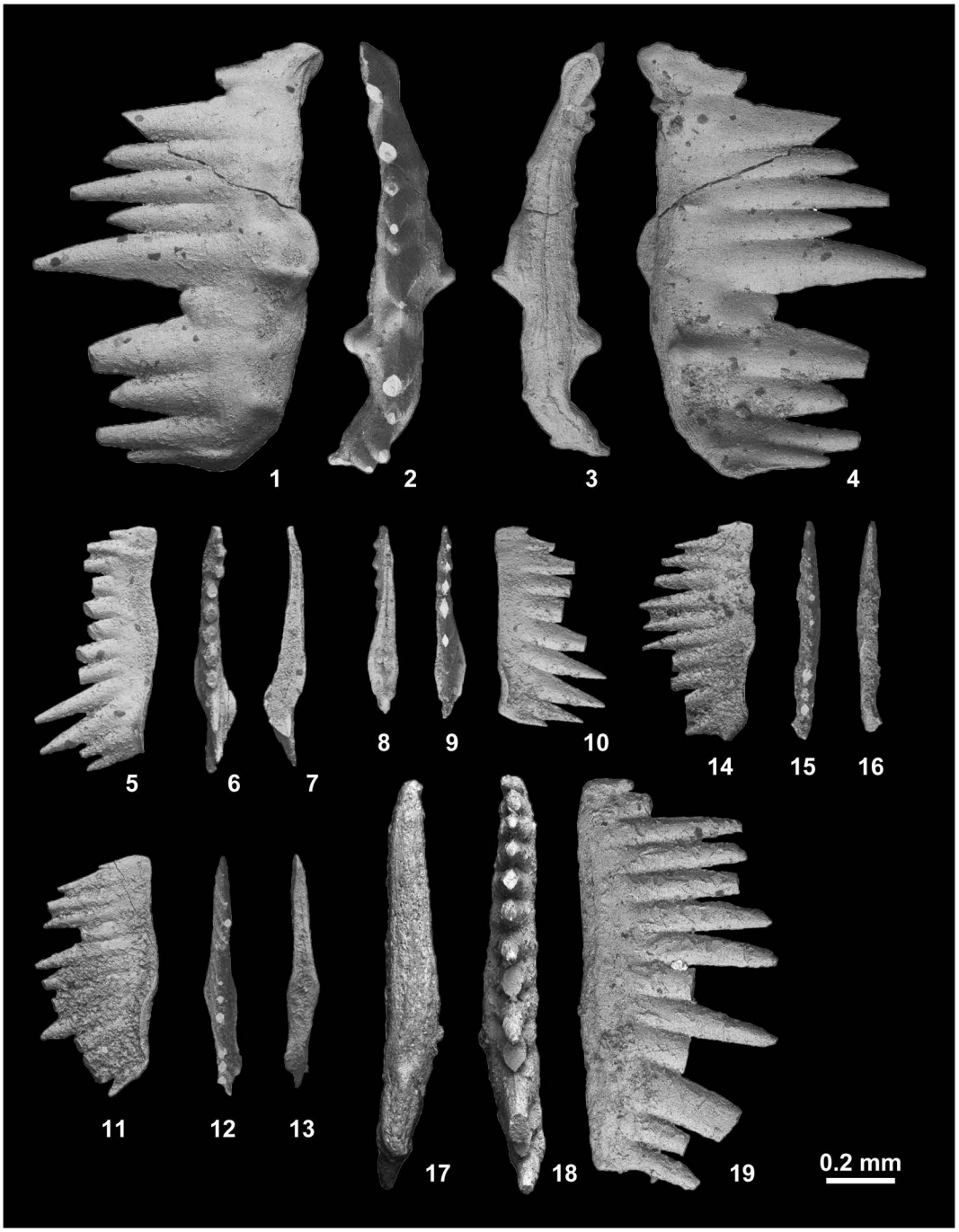

Fig. 138. *Conservatella conservativa* (Müller, 1956). 1–4, MPC25067, from BT01-03. 5–7, MPC25068, from BT01-03. 8–10, MPC25069, from BT01-03. 11–13, MPC25070, from BT01-04. 14–16, MPC25071, from BT01-04. 17–19, MPC25072, from BT01-06.

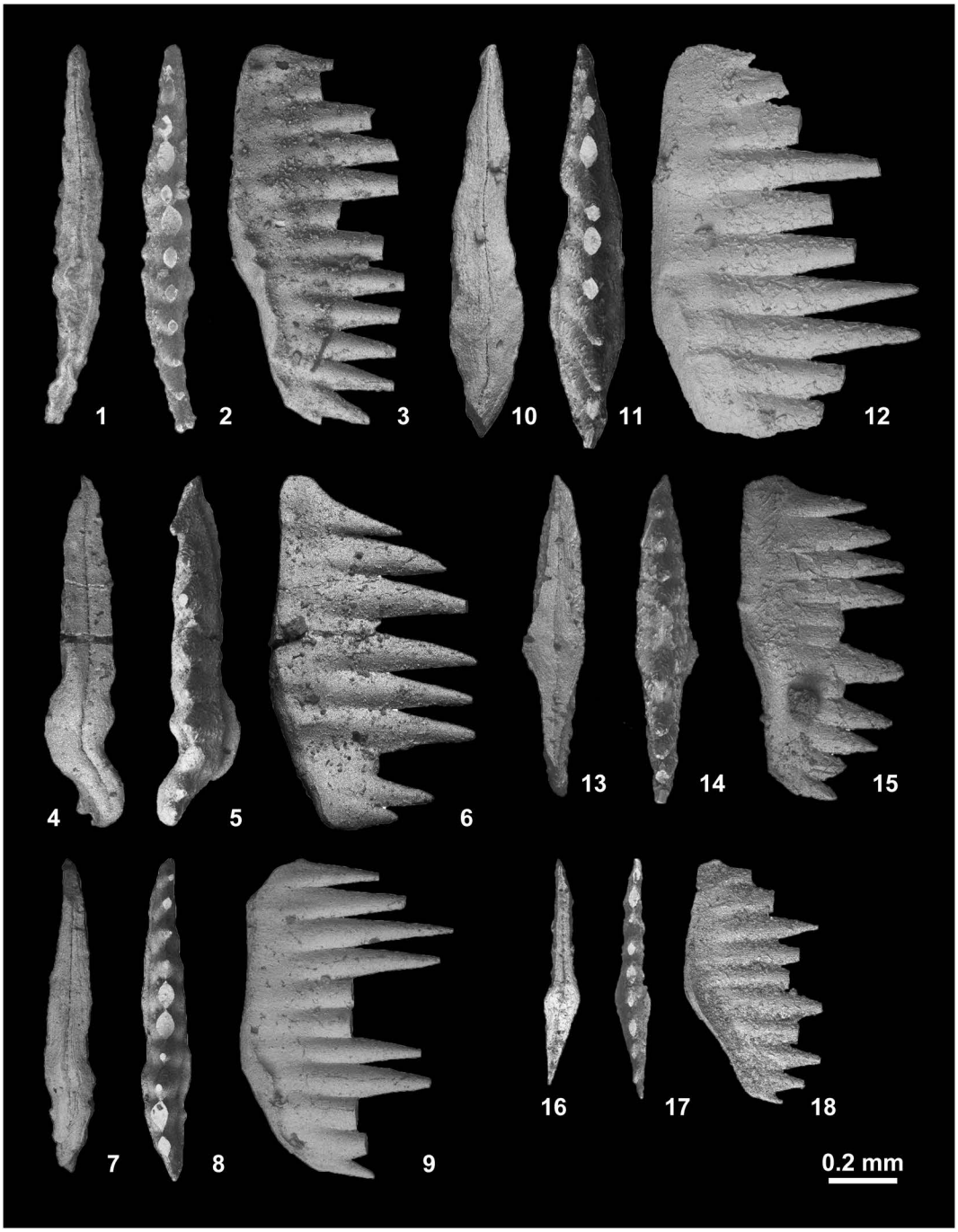

Fig. 139. *Conservatella conservativa* (Müller, 1956). 1–3, MPC25073, from BT01-07. 4–6, MPC25074, from BT01-07. 7–9, MPC25075, from BT01-07. 10–12, MPC25076, from BT01-07. 13–15, MPC25077, from BT01-10. 16–18, MPC25078, from BT01-10.

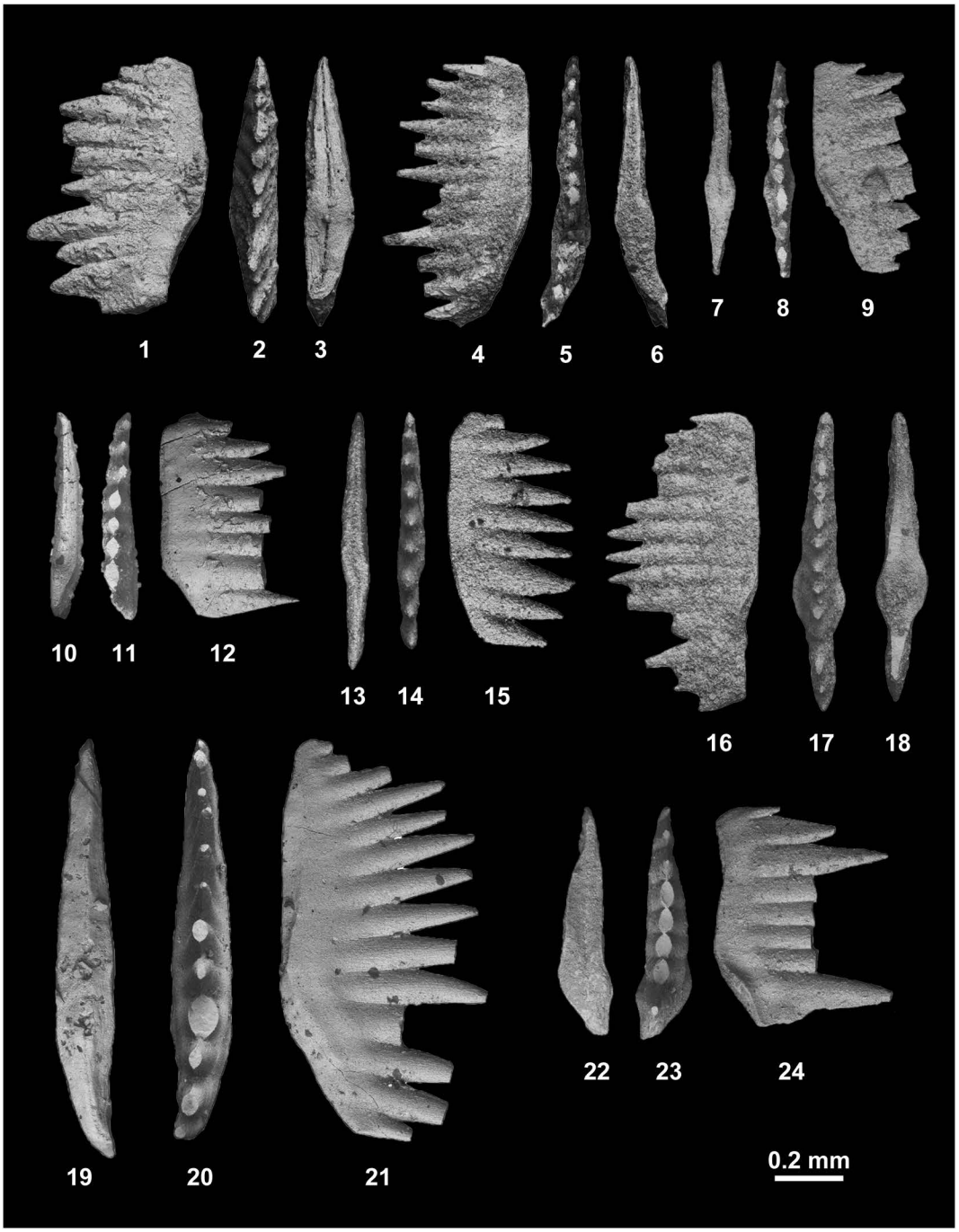

Fig. 140. *Conservatella conservativa* (Müller, 1956). 1–3, MPC25079, from BT01-10. 4–6, MPC25080, from BT01-10. 7–9, MPC25081, from BT01-12. 10–12, MPC25082, from BT01-14. 13–15, MPC25083, from BT02-01. 16–18, MPC25084, from BT02-01. 19–21, MPC25085, from BT02-02. 22–24, MPC25086, from BT02-02.

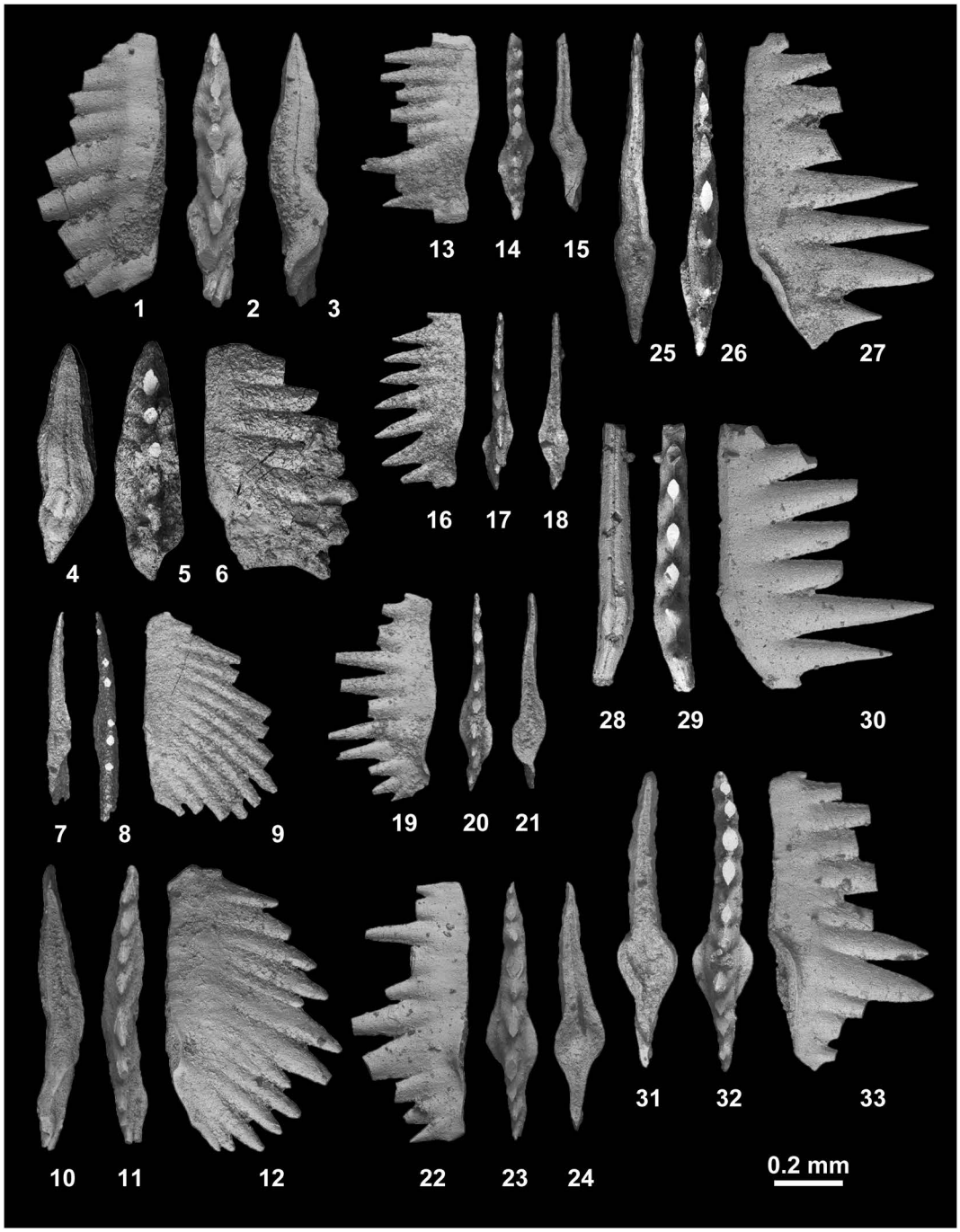

Fig. 141. 1–6, *Conservatella conservativa* (Müller, 1956). 1–3, MPC25087, from BT02-02. 4–6, MPC25088, from BT03-01. 7–12, *Conservatella* sp. indet. A. 7–9, MPC25089, from BT01-03. 10–12, MPC25090, from BT01-04. 13–33, *Discretella discreta* (Müller, 1956). 13–15, MPC25091, from BT01-03. 16–18, MPC25092, from BT01-03. 19–21, MPC25093, from BT01-03. 22–24, MPC25094, from BT01-04. 25–27, MPC25095, from BT01-06. 28–30, MPC25096, from BT01-06. 31–33, MPC25097, from BT01-06.

four specimens, MPC25077–25080, from BT01-10, one specimen, MPC25081, from BT01-12, one specimen, MPC25082, from BT01-14, two specimens, MPC25083, 25084, from BT02-01, three specimens, MPC25085–25087, from BT02-02, and one specimen, MPC25088, from BT03-01.

Description: Laterally compressed, rectangular or rhombic segminate elements 0.59–1.26 mm in length, average 0.85 mm; 0.31–0.85 mm in height, average 0.49 mm; length to height ratio 1.2–2.2, average 1.7 for twenty-two specimens. Pointed spine-like denticles vary in number from 7 to 14, average 11, straight or slightly reclined posteriorly, discrete in upper two-thirds, fused in lower one-third. Basal margin straight or slightly upturned in anterior and upturned 5–40 degrees, average 18 degrees at middle to one-third posterior margin. Triangular, non-expanded, flat or slightly convex basal cavity posteriorly extended. Anterior groove continues to posterior end. Some elements curved left or right side posteriorly.

Remarks: The Bac Thuy Formation includes many well preserved specimens of *Conservatella conservativa* (Müller, 1956) that exhibit denticles and a groove at different growth stages. The length of the denticule and the upturned position of the basal part of the element are variable, but they share some common features including slightly fused denticles and a non-expanded and non-concave basal cavity, features that are recognized only in this species. Smaller specimens (MPC25068–25071, 25078, etc.), in contrast to larger ones with typical form (MPC25067, 25072–25076, etc.), are probably juveniles, and have fused short denticles. These features are different from juvenile specimens of *Discretella discreta* (Müller, 1956), whose denticles are more discrete and fewer in number.

Occurrence: Described specimens from BT01-03, BT01-04, BT01-06, BT01-07, BT01-10, BT01-12, BT01-14, BT02-01, BT02-02 and BT03-01 within the portion of the *Novispathodus* ex gr. *waageni* Zone that includes the *Flemingites rursiradiatus* beds (lowest Middle Smithian = middle Lower Olenekian), *Urdyceras tulongensis* beds (lower Middle Smithian = middle Lower Olenekian) and *Leyeceras* horizon of the *Owenites koeneni* beds (middle Middle Smithian = middle Lower Olenekian) in the Bac Thuy Formation, northeastern Vietnam. This species also occurs in the Middle Smithian in Nevada (*Meekoceras* beds, Müller, 1956; Sweet *et al*., 1971), Utah (*Furnishius* Zone to *Parachirognathus* Zone, Solien, 1979), South Primorye, Russia (*Parachirognathus-Furnishius* Zone, Buryi, 1979), Jabra Safra, Oman (Orchard, 2005), and Canadian Arctic (*Euflemingites romunderi* Zone, Orchard, 2008).

Conservatella sp. indet. A

Fig. 141.7–141.12

Material examined: One specimen, MPC25089, from BT01-03, and one specimen, MPC25090, from BT01-04.

Description: Two laterally compressed segminate elements 0.61–0.84 mm in length; 0.39–0.52 mm in height; length to height ratio 1.6. Strongly reclined and fused denticles total 13 and 14 in number. Cusp situated at middle to posterior part with two posterior small denticles. Basal margin straight in anterior and slightly upturned in posterior. Non-expanded basal cavity extended posteriorly. Anterior shallow groove extends to basal pit.

Remarks: The laterally compressed element with fused denticles suggests that the described specimens belong to the genus *Conservatella*. However, their extremely reclined and fused denticles are different from those of the type species of the genus, *C. conservativa* (Müller, 1956). They probably represent an unknown species of *Conservatella*.

Occurrence: Described specimens from BT01-03 and BT01-04 within the portion of the *Novispathodus* ex gr. *waageni* Zone represented by the *Flemingites rursiradiatus* beds

(lowest Middle Smithian = middle Lower Olenekian) in the Bac Thuy Formation, northeastern Vietnam.

Genus ***Discretella*** Orchard, 2005

Type species: *Ctenognathus discreta* Müller, 1956.

Discretella discreta (Müller, 1956)

Figs. 141.13–141.33, 142–145, 146.1–146.30

Ctenognathus discreta Müller, 1956, p. 821, pl. 95, fig. 28.
Neospathodus conservativus (Müller, 1956). Koike, 1982, p. 36, pl. 6, figs. 12–14.
Neospathodus discretus (Müller, 1956). Tian *et al*., 1983, p. 376, pl. 95, fig. 1.
Neospathodus aff. *cristagalli* (Huckriede, 1958). Bui, 1989, p. 404, pl. 30, fig. 1.
multielement apparatuses, *Discretella* sp. A, Orchard, 2005, p. 83, text-fig. 8.
Discretella discreta (Müller, 1956). Orchard, 2008, p. 402, figs. 8.18–8.19; Beranek *et al*., 2010, figs. 6.18, 6.19.

Material examined: Three specimens, MPC25091–25093, from BT01-03, one specimen, MPC25094, from BT01-04, three specimens, MPC25095–25097, from BT01-06, four specimens, MPC25098–25101, from BT01-07, five specimens, MPC25102–25106, from BT01-10, one specimen, MPC25107, from BT01-12, two specimens, MPC25108, 25109, from BT01-14, seven specimens, MPC25110–25116, from BT02-01, four specimens, MPC25117–25120 from BT02-02, one specimen, MPC25121, from BT02-03, two specimens, MPC25122, 25123, from BT03-01, one specimen, MPC25124, from KC01-01, three specimens, MPC25125–25127, from KC01-04, two specimens, MPC25128, 25129, from KC01-05, four specimens, MPC25130-25133, from KC01-11, four specimens, MPC25134–25137, from KC01-12, two specimens, MPC25138, 25139, from KC01-13, one specimen, MPC25140, from KC02-02, and two specimens, MPC25141, 25142, from PK01-02.

Description: Long and slender segminate elements 0.35–1.36 mm in length, average 0.77 mm; 0.27–0.72 mm in height, average 0.42 mm; length to height ratio 1.1–2.4, average 1.7 for fifty-two specimens. General profile of element rectangular, highest point situated at posterior one-third to posterior margin. Lower margin of element almost straight to slightly undulated and posterior part upturned in some specimens. Discrete denticles vary in number from 4 to 13, average 8, sub-erect or reclined posteriorly. Cusp situated above basal cavity and bears one to three small denticles at posterior end. Sub-rounded and posteriorly elongated basal cavity with a thin pit. Anterior groove continues to posterior end.

Remarks: The Bac Thuy Formation includes many well preserved specimens of *Discretella discreta* (Müller, 1956), and two morphotypes (A and B) are also recognized. Morphotype A (MPC25097, 25101, 25103, etc.) is characterized by a higher cusp with two or three small posterior denticles and a rounded basal cavity. The posterior part of the lower margin is downturned. Morphotype A is identical to the typical form of *D. discreta* described by Müller (1956) from Nevada. Morphotype B (MPC25095, 25096, 25100, etc.) can be distinguished by its triangular larger denticle and upturned posterior margin.

Occurrence: Described specimens from BT01-03, BT01-04, BT01-06, BT01-07, BT01-10, BT01-12, BT01-14, BT02-01, BT02-02, BT02-03, BT03-01, KC01-01, KC01-04, KC01-05, KC01-11, KC01-12, KC01-13, KC02-02 and PK01-02 within the portion of the *Novispathodus* ex gr. *waageni* Zone that includes the *Flemingites rursiradiatus* beds (lowest Middle Smithian = middle Lower Olenekian), *Urdyceras tulongensis* beds (lower Middle Smithian = middle Lower Olenekian) and *Owenites koeneni* beds (middle Middle Smithian = middle Lower Olenekian) in the Bac Thuy Formation, northeastern Vietnam. This species also occurs in the Middle Smithian in Nevada (*Meekoceras* beds, Müller, 1956), Gunong Keriang, West Malaysia (Koike, 1982), Tibet (Tian *et al*.,

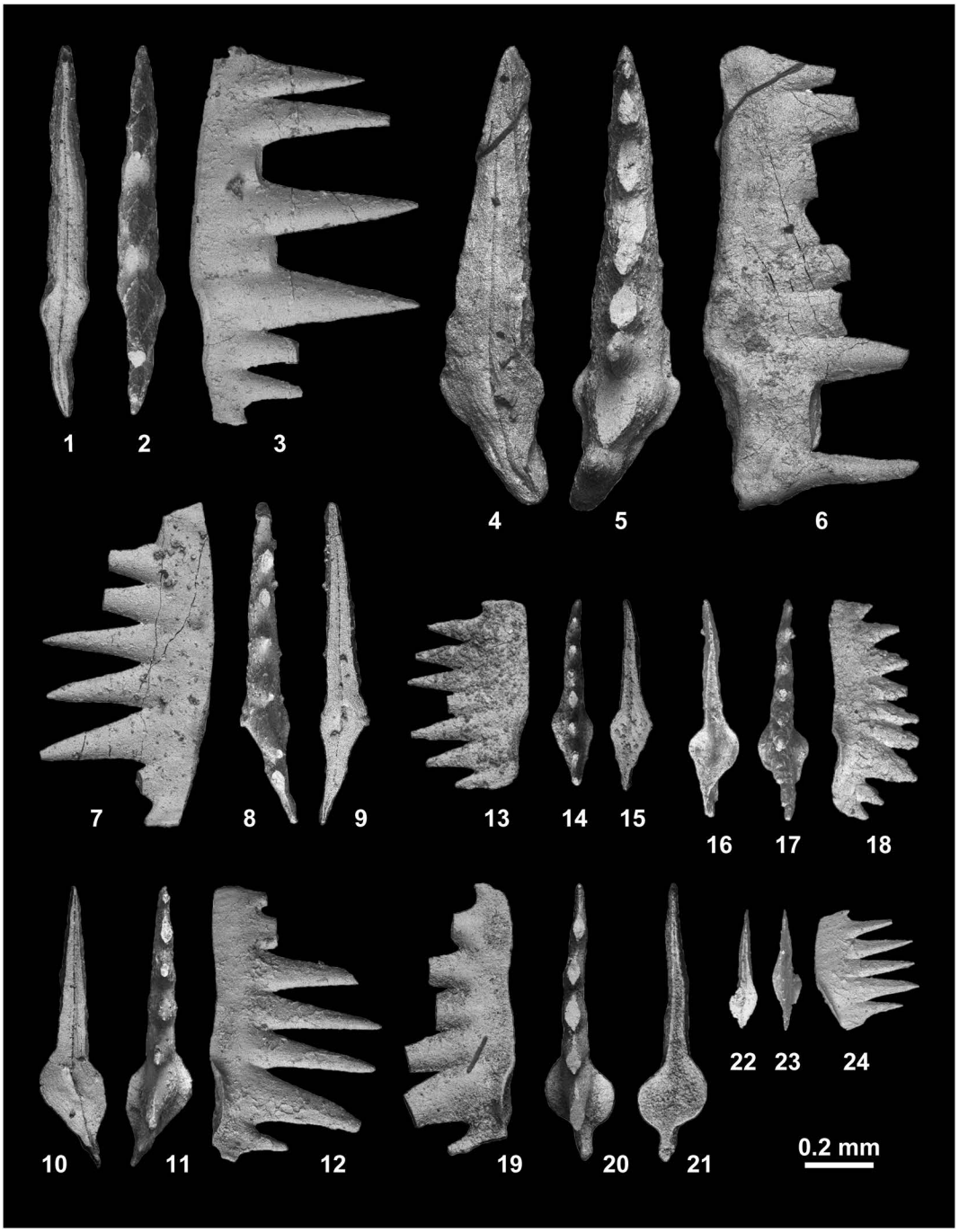

Fig. 142. *Discretella discreta* (Müller, 1956). 1–3, MPC25098, from BT01-07. 4–6, MPC25099, from BT01-07. 7–9, MPC25100, from BT01-07. 10–12, MPC25101, from BT01-07. 13–15, MPC25102, from BT01-10. 16–18, MPC25103, from BT01-10. 19–21, MPC25104, from BT01-10. 22–24, MPC25105, from BT01-10.

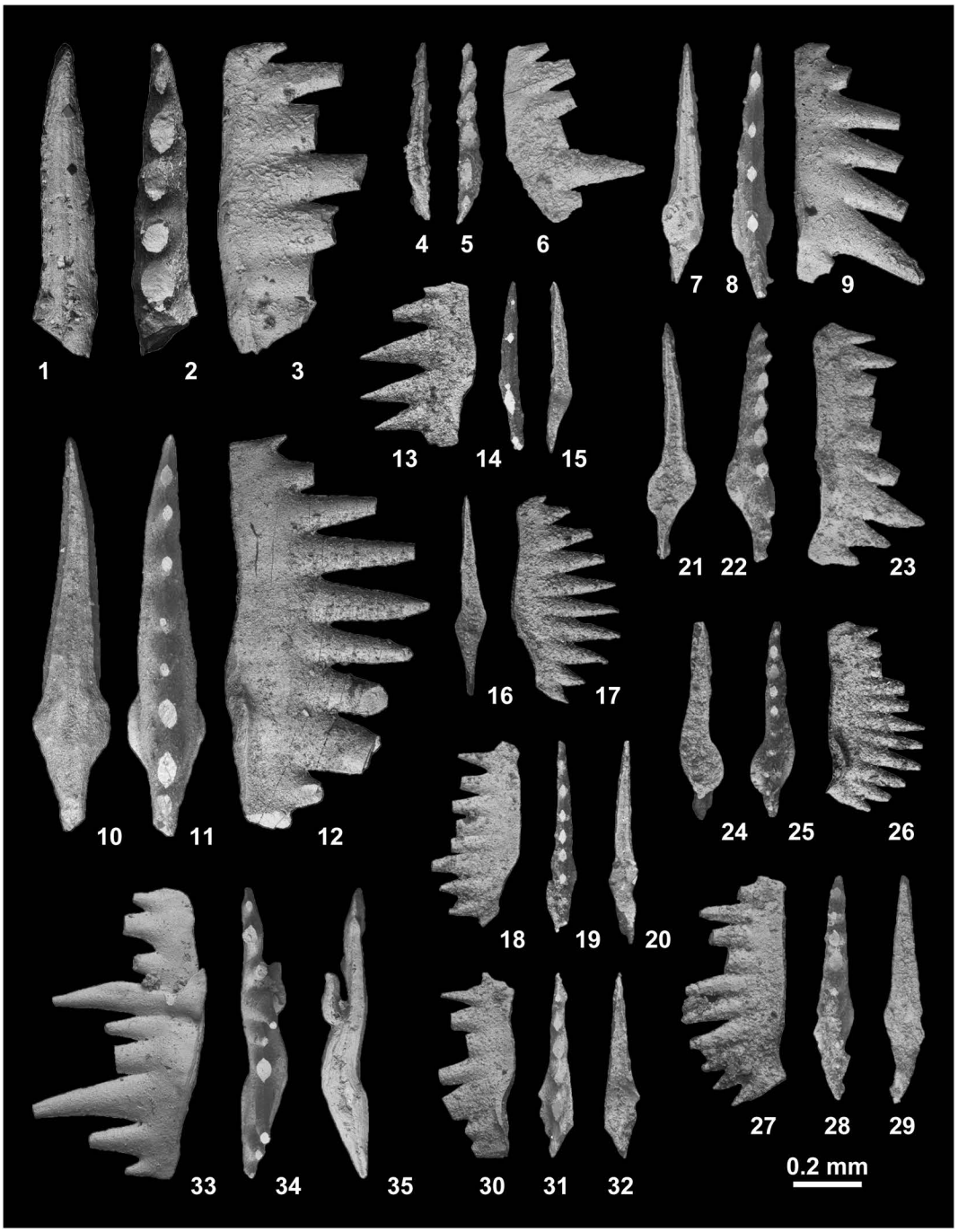

Fig. 143. *Discretella discreta* (Müller, 1956). 1–3, MPC25106, from BT01-10. 4–6, MPC25107, from BT01-12. 7–9, MPC25108, from BT01-14. 10–12, MPC25109, from BT01-14. 13–15, MPC25110, from BT02-01. 16–17, MPC25111, from BT02-01. 18–20, MPC25112, from BT02-01. 21–23, MPC25113, from BT02-01. 24–26, MPC25114, from BT02-01. 27–29, MPC25115, from BT02-01. 30–32, MPC25116, from BT02-01. 33–35, MPC25117, from BT02-02.

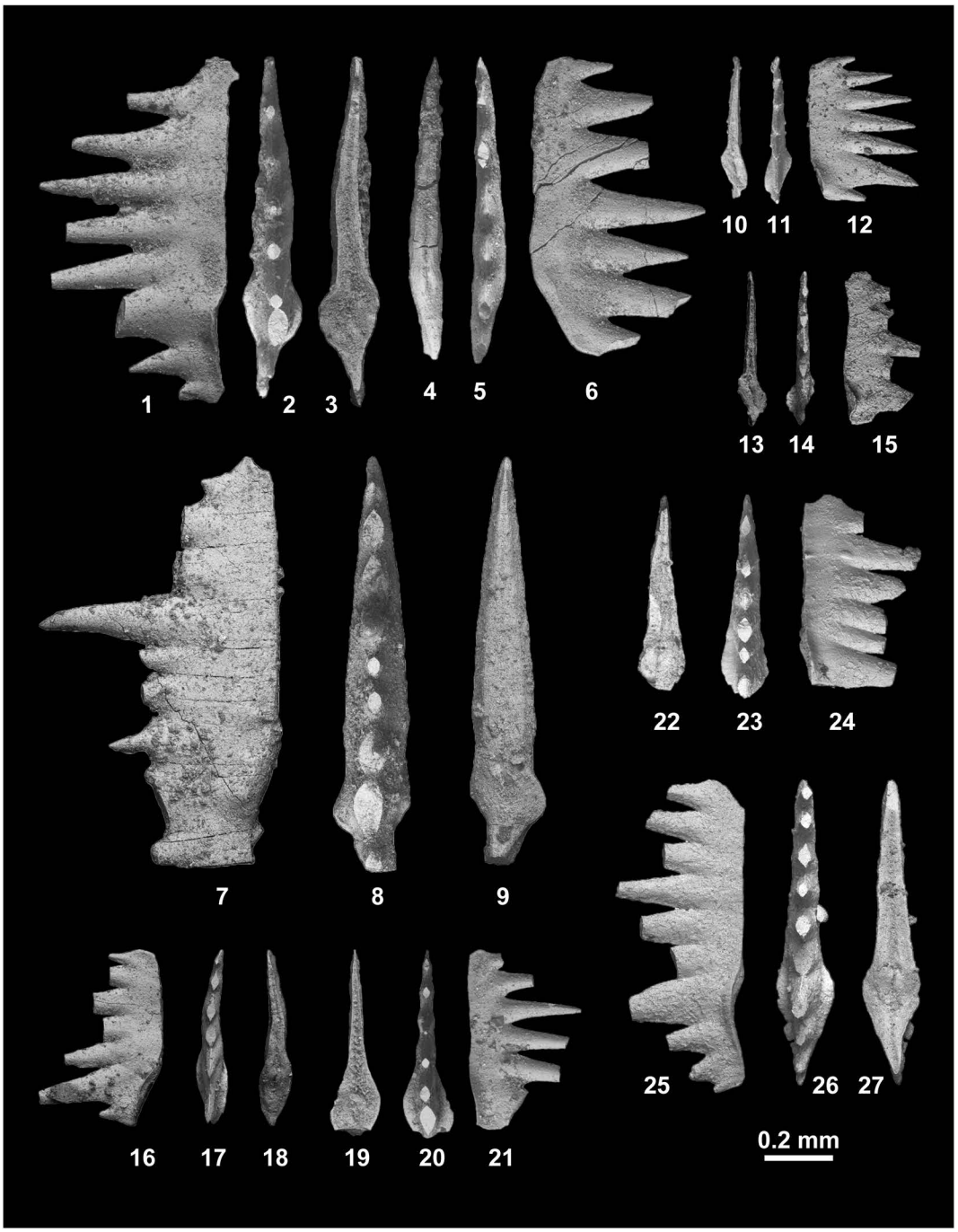

Fig. 144. *Discretella discreta* (Müller, 1956). 1–3, MPC25118, from BT02-02. 4–6, MPC25119, from BT02-02. 7–9, MPC25120, from BT02-02. 10–12, MPC25121, from BT02-03. 13–15, MPC25122, from BT03-01. 16–18, MPC25123, from BT03-01. 19–21, MPC25124, from KC01-01. 22–24, MPC25125, from KC01-04. 25–27, MPC25126, from KC01-04.

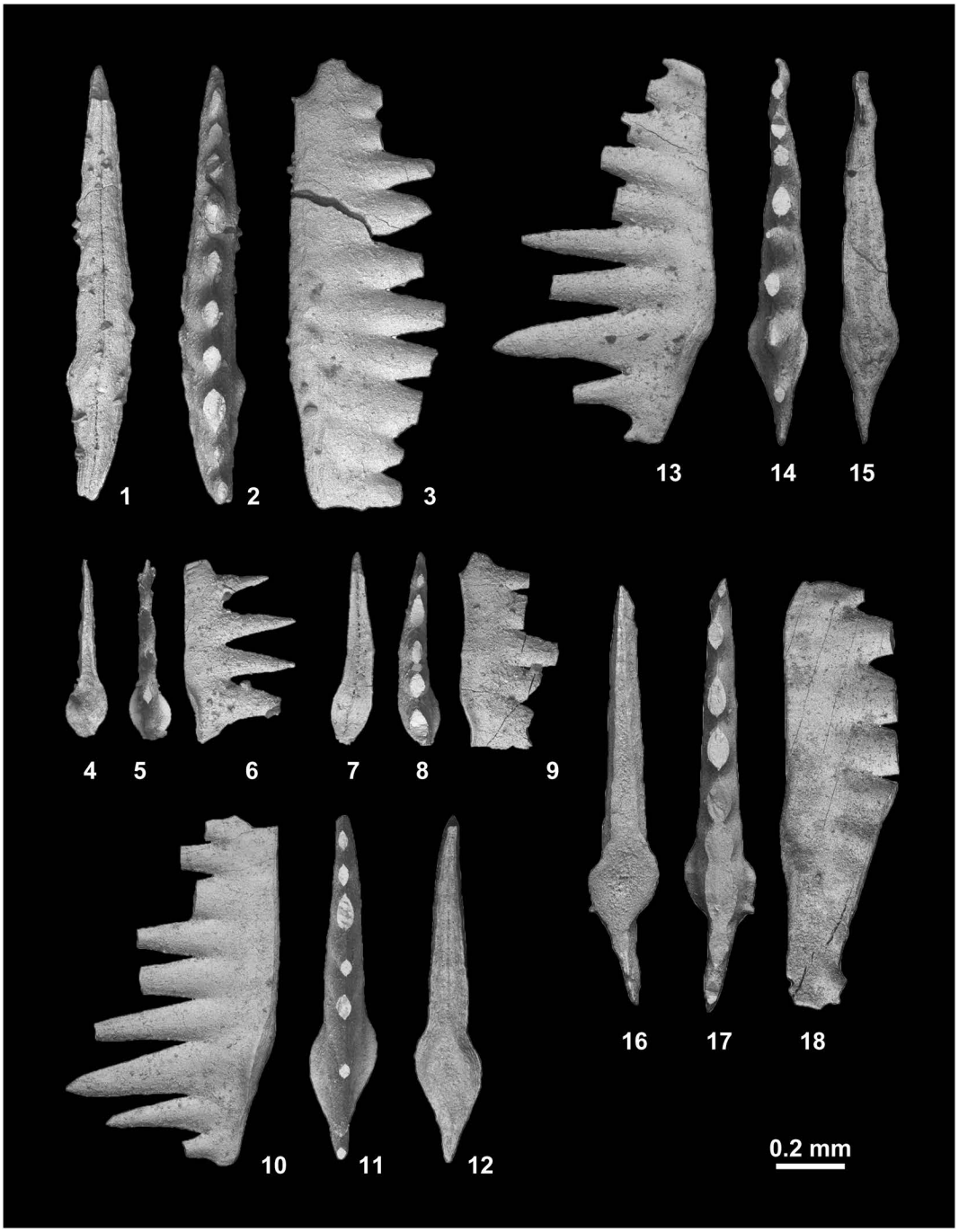

Fig. 145. *Discretella discreta* (Müller, 1956). 1–3, MPC25127, from KC01-04. 4–6, MPC25128, from KC01-05. 7–9, MPC25129, from KC01-05. 10–12, MPC25130, from KC01-11. 13–15, MPC25131, from KC01-11. 16–18, MPC25132, from KC01-11.

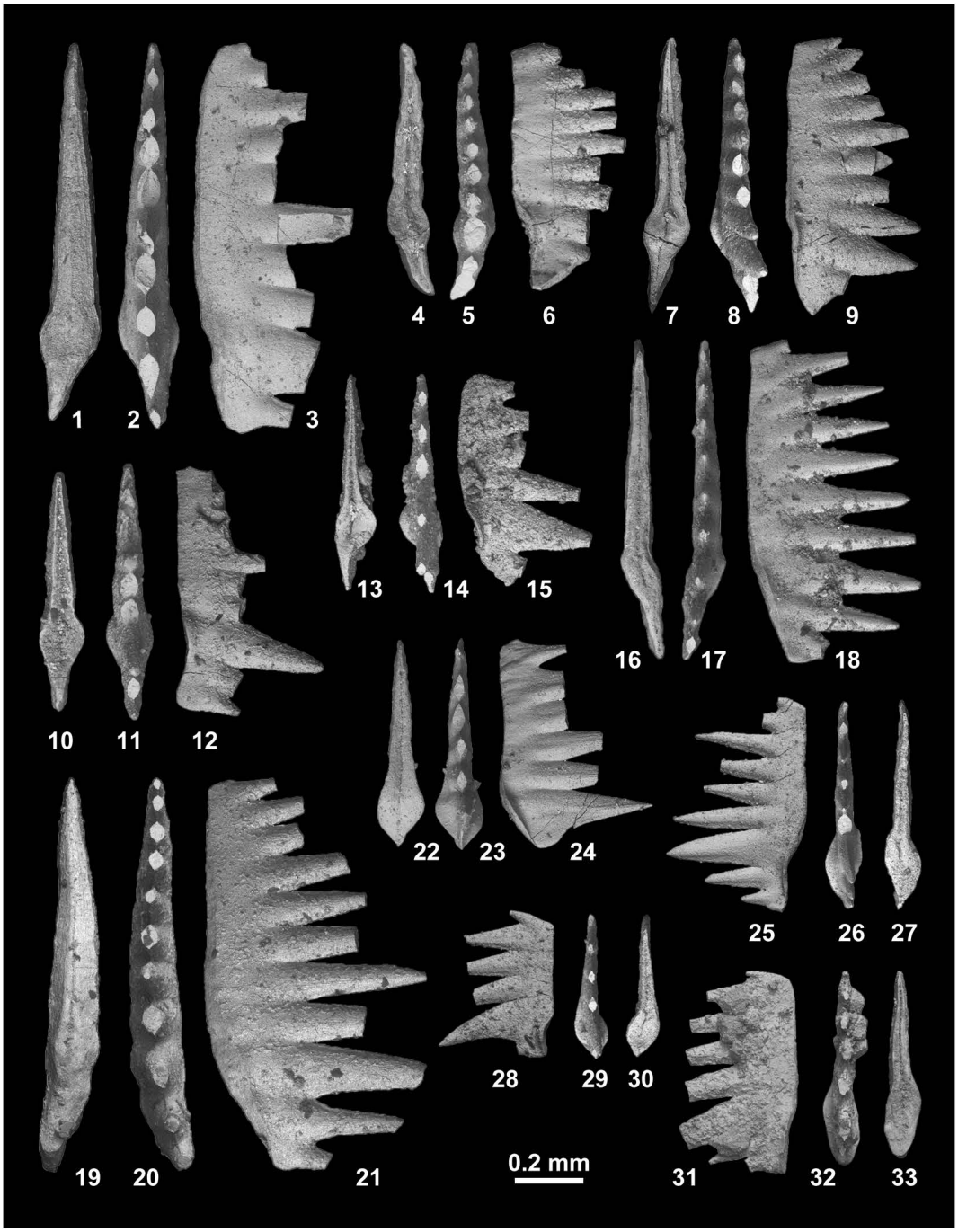

Fig. 146. 1–30, *Discretella discreta* (Müller, 1956). 1–3, MPC25133, from KC01-11. 4–6, MPC25134, from KC01-12. 7–9, MPC25135, from KC01-12. 10–12, MPC25136, from KC01-12. 13–15, MPC25137, from KC01-12. 16–18, MPC25138, from KC01-13. 19–21, MPC25139, from KC01-13. 22–24, MPC25140, from KC02-02. 25–27, MPC25141, from PK01-02. 28–30, MPC21542, from PK01-02. 31–33, *Discretella robustus* (Wang and Wang, 1976), MPC25143, from BT01-03.

1983), Jabal Safra, Oman (Orchard, 2005), British Columbia, Canada (Beranek *et al*, 2010), and Canadian Arctic (*Euflemingites romunderi* Zone, Orchard, 2008).

Discretella robustus (Wang and Wang, 1976)

Figs. 146.31–146.33, 147–150

?*Ctenognathus discreta* Müller, 1956, p. 821, pl. 95, fig. 24.

Cratognathodus robustus Wang and Wang, 1976, p. 397, pl. 3, figs. 21–25.

Cratognathodus robustus Wang and Z. H. Wang, 1976. Tian *et al*., 1983, p. 347, pl. 88, figs. 8, 9.

Neospathodus discreta (Müller, 1956). Buryi, 1979, p. 52, pl. 7, figs. 2–6.

Guangxidella? *robustus* (Wang and Wang, 1976). Orchard, 2007a, fig. 1.

Material examined: Two specimens, MPC25143, 25144, from BT01-03, four specimens, MPC25145–25148, from BT01-04, six specimens, MPC25149–25154, from BT01-06, one specimen, MPC25155, from BT01-07, four specimens, MPC25156–25159, from BT01-10, one specimen, MPC25160, from BT01-12, five specimens, MPC25161–25165, from BT01-14, four specimens, MPC25166–25169, from BT01-15, two specimens, MPC25170, 25171, from BT02-01, eight specimens, MPC25172–25179, from BT02-02, two specimens, MPC25180, 25181, from BT02-03, two specimens, MPC25182, 25183, from KC01-01, two specimens, MPC25184, 25185, from KC01-10, and one specimen, MPC25186, from KC02-03.

Description: Segminate elements 0.43–1.69 mm in length, average 0.64 mm; 0.26–0.91 mm in height, average 0.41 mm; length to height ratio 1.0–2.4, average 1.6 for forty-four specimens. General profile of element triangular or trapezoidal, highest point situated at posterior one-third to posterior margin. Lower margin of element almost straight, posterior part downturned in those specimens whose lower margins are bowed. Almost discrete denticles vary in number from 4 to 13, average 8, sub-erect or gradually reclined posteriorly. Cusp longer and two times larger than other denticles, bears one to 4 small denticles at posterior end. Element shows sigmoidal shape in lower view. Flared basal cavity sub-rounded and concave with a thin pit. Anterior groove continues to posterior end.

Remarks: Typical elements of *Discretella robustus* (Wang and Wang, 1976) have a strongly reclined large posterior cusp with two or three small posterior denticles, exhibits a sigmoidal shape in the lower view, and differs from those of typical *D. discreta* (Müller, 1956). *Ctenognathus discreta* (Müller, 1956, pl. 98, fig. 24) is somewhat similar to *D. robustus*, but it is questionable whether they are conspecific because the cusp of *C. discreta* is broken and the lower view is not illustrated.

Occurrence: Described specimens from BT01-03, BT01-04, BT01-06, BT01-07, BT01-10, BT01-12, BT01-14, BT01-15, BT02-01, BT02-01, BT02-03, KC01-01, KC01-10 and KC02-03 within the portion of the *Novispathodus* ex gr. *waageni* Zone that includes the *Flemingites rursiradiatus* beds (lowest Middle Smithian = middle Lower Olenekian), *Urdyceras tulongensis* beds (lower Middle Smithian = middle Lower Olenekian) and *Owenites koeneni* beds (middle Middle Smithian = middle Lower Olenekian) in the Bac Thuy Formation, northeastern Vietnam. This species also occurs in the Middle Smithian in Nevada (*Meekoceras* beds, Müller, 1956), Qomolangma, Tibet (Wang and Wang, 1976; Tian *et al*., 1983), and South Primorye, Russia (*Parachirognathus-Furnishius* Zone, Buryi, 1979).

Discretella sp. indet. A

Fig. 151.1–151.18

Discretella discreta (Müller, 1956). Bondarenko *et al*., 2013, p. 60, figs. 7.1, 7.2.

Material examined: Two specimens, MPC25187, 25188, from BT02-02, one specimen, MPC25189, from KC01-10, two specimens, MPC25190, 25191, from KC02-02, and

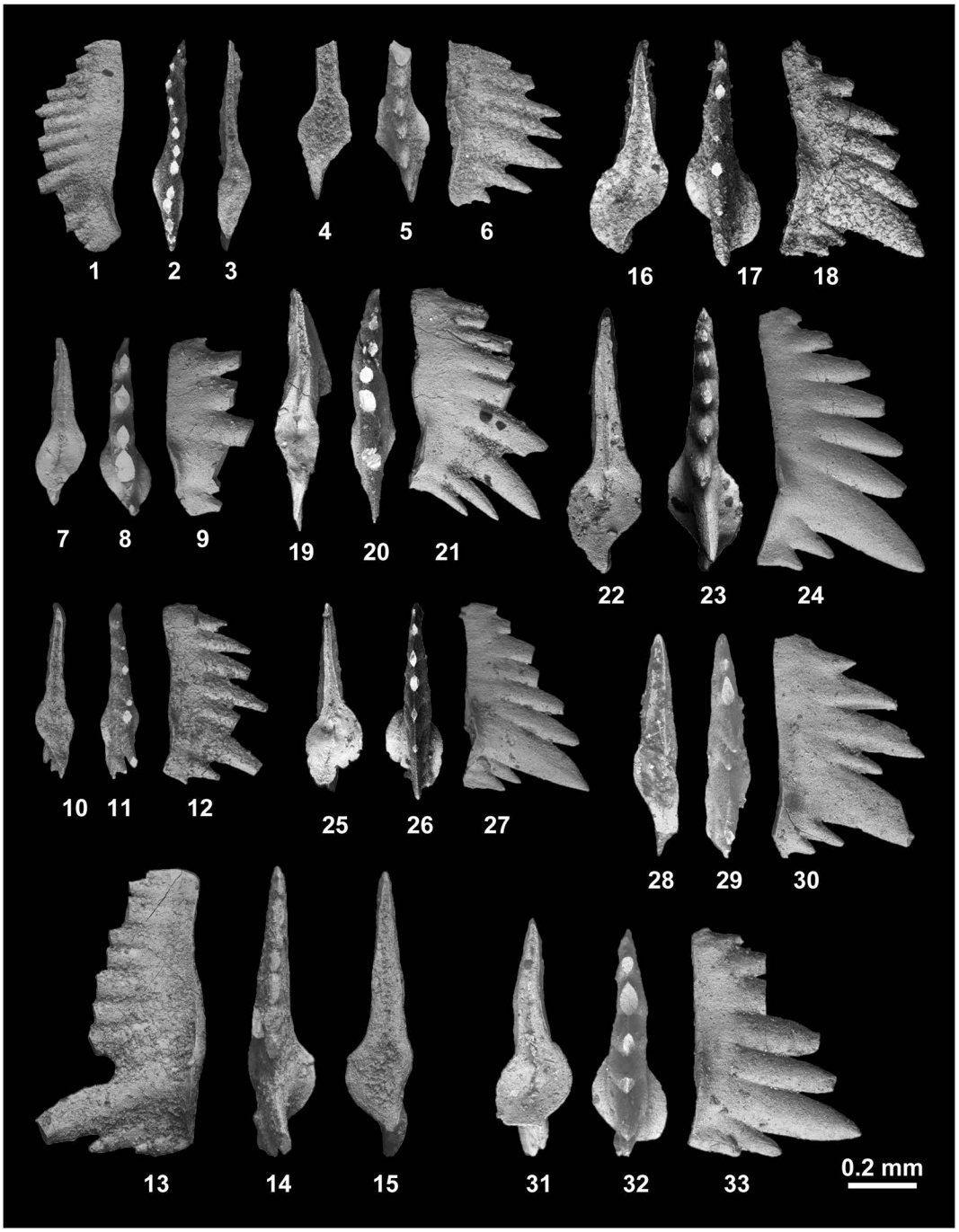

Fig. 147. *Discretella robustus* (Wang and Wang, 1976). 1–3, MPC25144, from BT01-03. 4–6, MPC25145, from BT01-04. 7–9, MPC25146, from BT01-04. 10–12, MPC25147, from BT01-04. 13–15, MPC25148, from BT01-04. 16–18, MPC25149, from BT01-06. 19–21, MPC25150, from BT01-06. 22–24, MPC25151, from BT01-06. 25–27, MPC25152, from BT01-06. 28–30, MPC25153, from BT01-06. 31–33, MPC25154, from BT01-06.

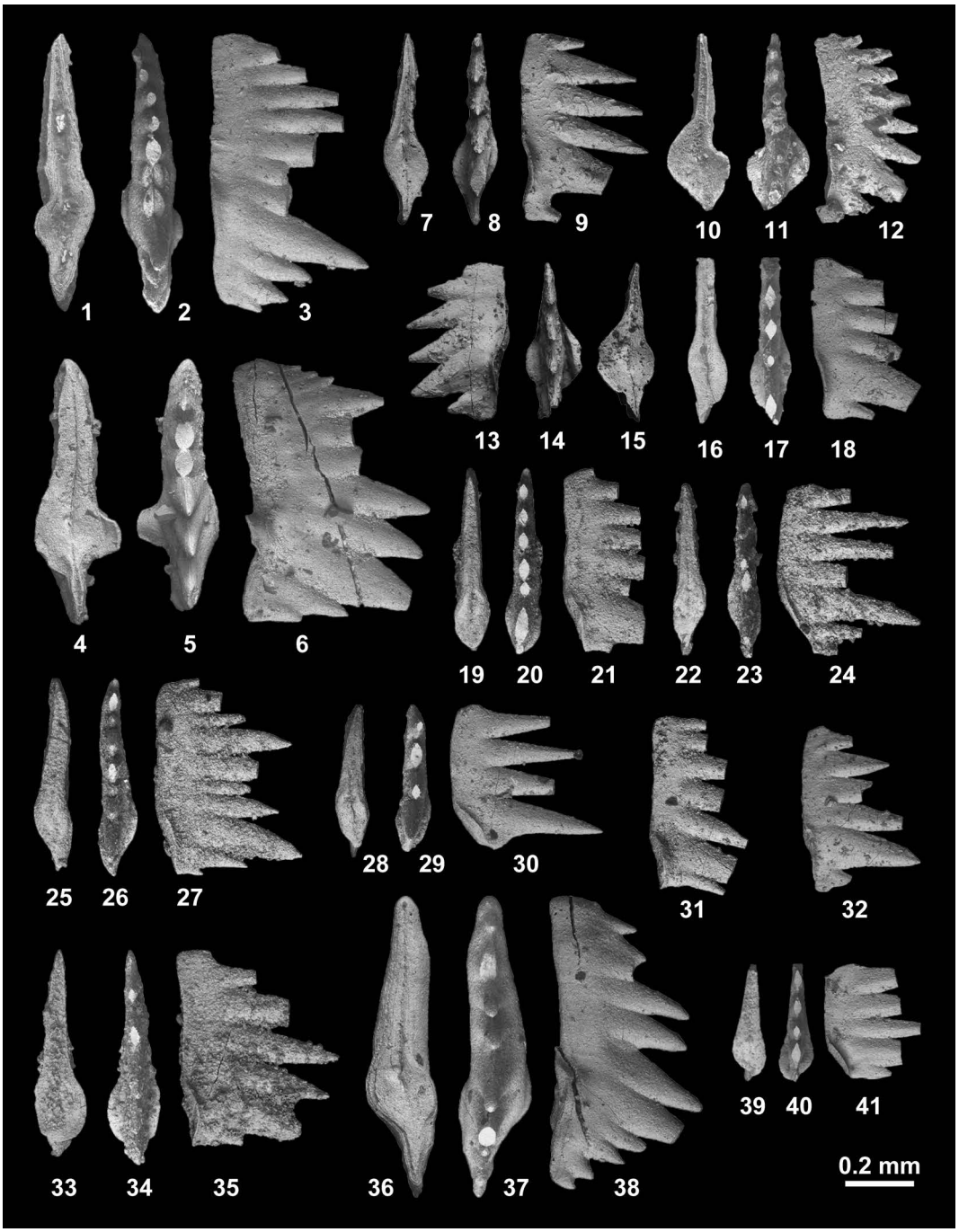

Fig. 148. *Discretella robustus* (Wang and Wang, 1976). 1–3, MPC25155, from BT01-07. 4–6, MPC25156, from BT01-10. 7–9, MPC25157, from BT01-10. 10–12, MPC25158, from BT01-10. 13–15, MPC25159, from BT01-10. 16–18, MPC25160, from BT01-12. 19–21, MPC25161, from BT01-14. 22–24, MPC25162, from BT01-14. 25–27, MPC25163, from BT01-14. 28–30, MPC25164, from BT01-14. 31, MPC25165, from BT01-14. 32, MPC25166, from BT01-15. 33–35, MPC25167, from BT01-15. 36–38, MPC25168, from BT01-15. 39–41, MPC25169, from BT01-15.

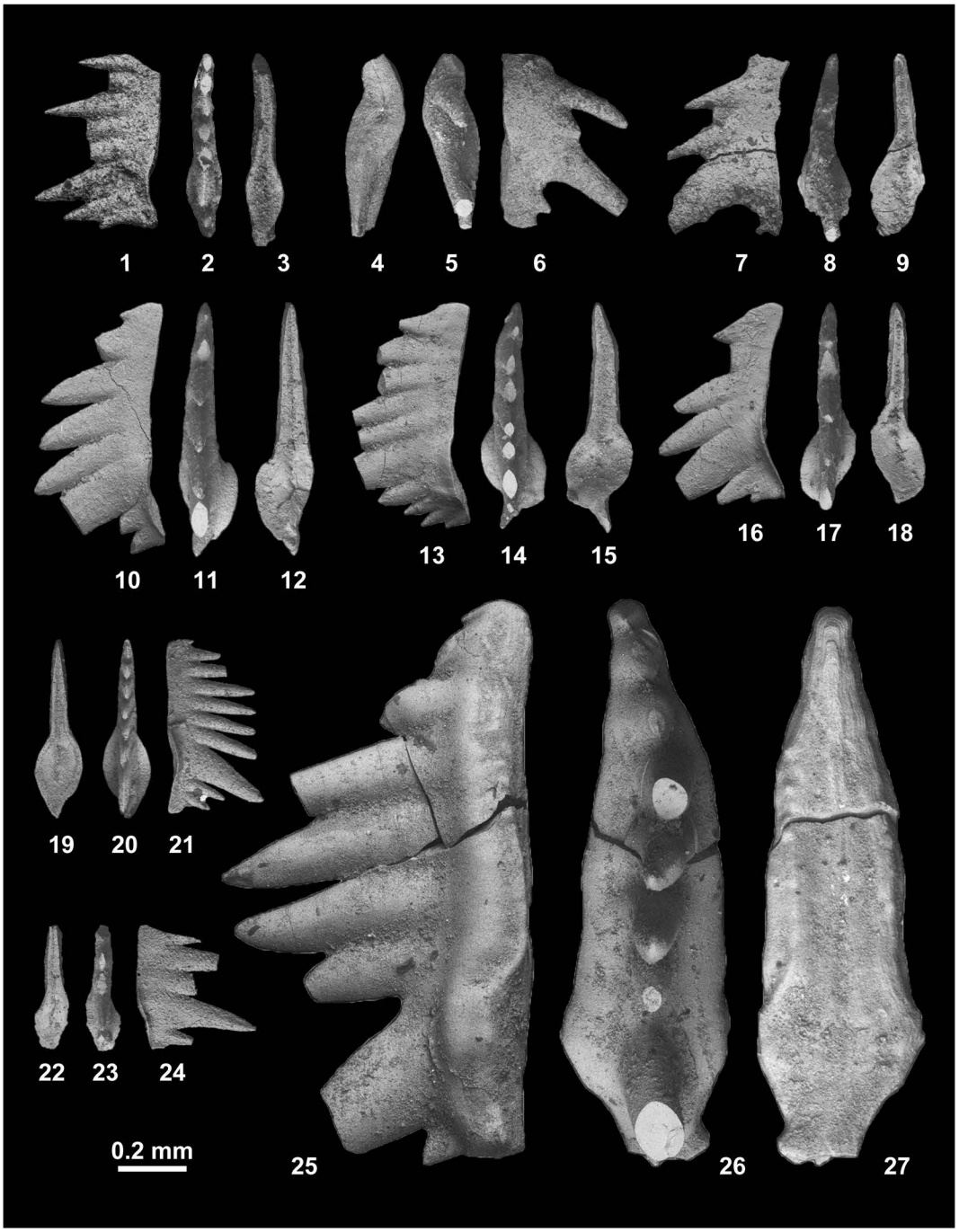

Fig. 149. *Discretella robustus* (Wang and Wang, 1976). 1–3, MPC25170, from BT02-01. 4–6, MPC25171, from BT02-01. 7–9, MPC25172, from BT02-02. 10–12, MPC25173, from BT02-02. 13–15, MPC25174, from BT02-02. 16–18, MPC25175, from BT02-02. 19–21, MPC25176, from BT02-02. 22–24, MPC25177, from BT02-02. 25–27, MPC25178, from BT02-02.

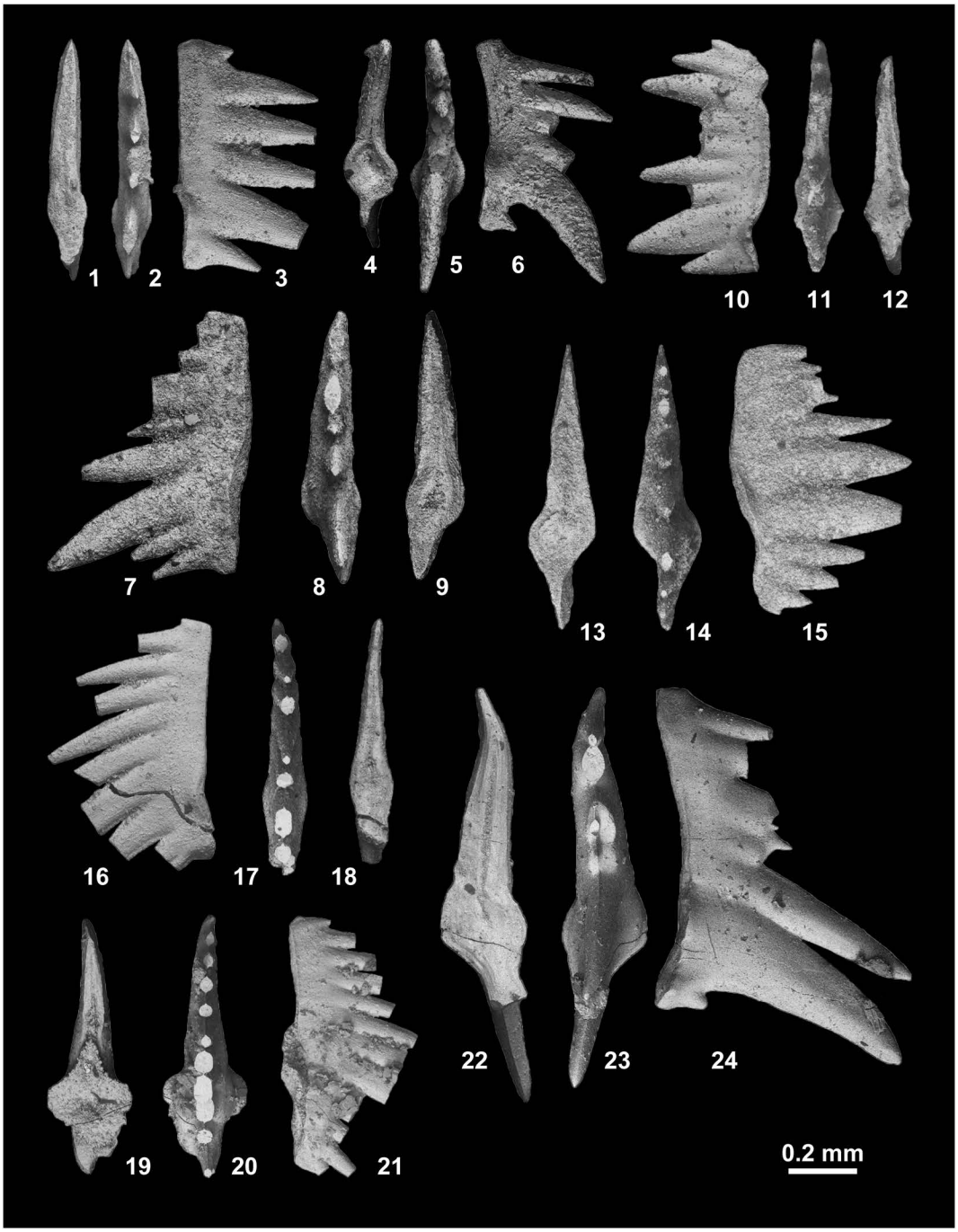

Fig. 150. *Discretella robustus* (Wang and Wang, 1976). 1–3, MPC25179, from BT02-02. 4–6, MPC25180, from BT02-03. 7–9, MPC25181, from BT02-03. 10–12, MPC25182, from KC01-01. 13–15, MPC25183, from KC01-01. 16–18, MPC25184, from KC01-10. 19–21, MPC25185, from KC01-10. 22–24, MPC25186, from KC02-03.

one specimen, MPC25192, from KC02-03.

Description: Triangular segminate elements 0.43–0.73 mm in length, average 0.57 mm; 0.31–0.58 mm in height, average 0.49 mm; length to height ratio 0.7–1.4, average 1.2 for six specimens. Discrete, triangular denticles vary in number from 3 to 5, average 4, revealing showing gradual size increase posteriorly. Largest denticle twice the size of others, and strongly inclined posteriorly. Small, triangular marginal process situated at posterior end. Lower margin generally straight or weakly upturned in anterior part, and downturned or slightly deflected upward in posterior part. Element exhibits sigmoidal shape in lower view. Sub-rounded basal cavity elongated posteriorly. Shallow furrow extends from basal pit to anterior end.

Remarks: The described specimens are triangular in lateral view and sigmoidal in lower view. These features indicate a close phylogenetic relationship with *Discretella robustus* (Wang and Wang, 1976). The first appearance of *D.* sp. indet. A occurs higher than that of *D. robustus* in the Bac Thuy Formation. This evidence suggests that *D.* sp. A probably evolved from *D. robustus* during early Middle Smithian time.

The number of denticles on the described specimens apparently decreases with younger-aged taxa. Specimens from the *Urdyceras tulongensis* beds have five denticles, but those from the *Owenites koeneni* beds bear only four denticles. The size of the cusp also gradually increases in younger-aged taxa.

Specimens described as *Discretella discreta* (Müller, 1956) from South Primorye, Russia by Bondarenko *et al*. (2013, p. 60, Fig. 7.1, 7.2) are identical to *D.* sp. indet. A.

Occurrence: Described specimens from BT02-02, KC01-10, KC02-02 and KC02-03 within the portion of the *Novispathodus* ex gr. *waageni* Zone that includes the *Urdyceras tulongensis* beds (lower Middle Smithian = middle Lower Olenekian) and the *Leyeceras* and the *Guodunites* horizons of the *Owenites koeneni* beds (middle to upper Middle Smithian = middle Lower Olenekian) in the Bac Thuy Formation, northeastern Vietnam. This species also occurs in the *Anasibirites nevolini* Zone (Upper Smithian) in South Primorye, Russia (Bondarenko *et al.*, 2013).

Discretella sp. indet. B

Fig. 151.19–151.24

Material examined: Two specimens, MPC25193, 25194, from BT01-03.

Description: Two laterally compressed segminate elements 0.53–0.56 mm in length; 0.32–0.36 mm in height; length to height ratio 1.6–1.7. Laterally compressed, erect spine-like denticles total 9 and 11 in number. Cusp situated in middle part of element. Denticle size gradually decreases both anteriorly and posteriorly. Basal margin shows biangular shape in lateral view. Anterior part of elements appears sigmoidal or straight in lower view. Basal cavity sub-rounded and elongated posteriorly. Shallow groove extends from basal pit to anterior end.

Remarks: Described specimens have completely discrete denticles and a sub-rounded basal cavity. These features are common in *Discretella discreta* (Müller, 1956). However, the biangular lateral shape of the element is similar to that of *Conservatella conservativa* (Müller, 1956). Thus, this feature indicates that these specimens are probably ancestoral to *C. conservativa*.

Occurrence: Described specimens from BT01-03 within the portion of the *Novispathodus* ex gr. *waageni* Zone in the *Flemingites rursiradiatus* beds (lowest Middle Smithian = middle Lower Olenekian) in the Bac Thuy Formation, northeastern Vietnam.

Discretella sp. indet. C

Fig. 151.25–151.28

Material examined: One specimen, MPC25195, from BT01-07.

Description: Anterior branched segminate

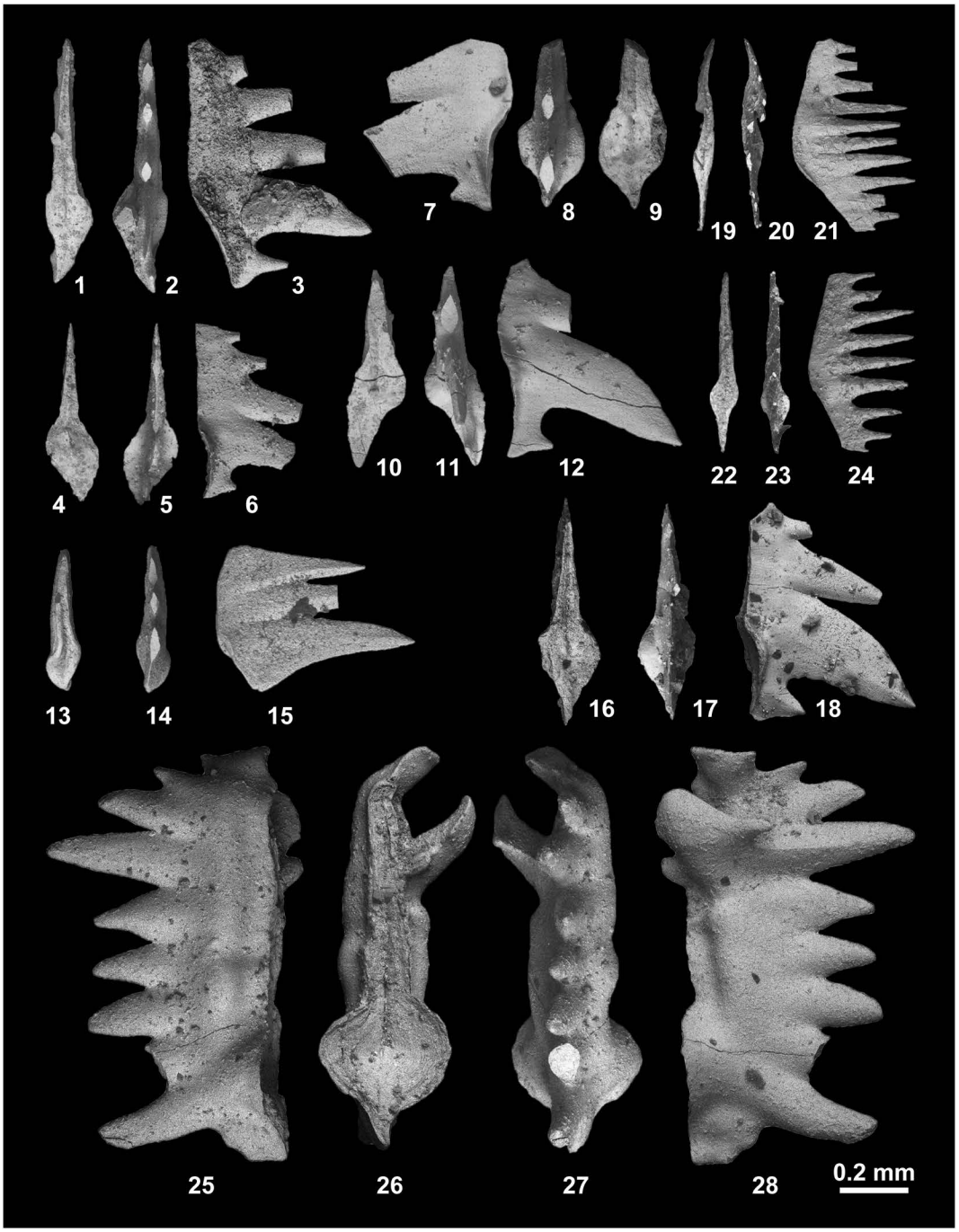

Fig. 151. 1–18, *Discretella* sp. indet. A. 1–3, MPC25187, from BT02-02. 4–6, MPC25188, from BT02-02. 7–9, MPC25189, from KC01-10. 10–12, MPC25190, from KC02-02. 13–15, MPC25191, from KC02-02. 16–18, MPC25192, from KC02-03. 19–24, *Discretella* sp. indet. B from BT01-03. 19–21, MPC25193. 22–24, MPC25194. 25–28, *Discretella* sp. indet. C, MPC25195, from BT01-07.

element 1.23 mm in length; 0.68 mm in height; length to height ratio 1.8. Upper edge consists of node-like robust discrete denticles, with cusp situated in one-third of anterior and posterior (posterior cusp lost). Denticles total 11 in number, including two small, barely remaining posterior denticles. Denticle size decreases from cusp anteriorly and posteriorly, and same in middle part. Lower margin straight. Prominent lateral rib developed. Anterior margin turns 60 degrees to the left in upper view. Branch cusp extends in parallel with anterior margin from left side of anterior one-third, and then turns anteriorly in upper view. Rounded basal cavity situated in posterior with a deep pit in lower view. Broad, deep furrow extends anteriorly and branched at anterior one-third.

Remarks: The discrete denticles, including the small posterior ones and the rounded basal cavity suggest that the described specimen belongs to the genus *Discretella*, but no definitive assignment can be made.

Occurrence: Specimen from BT01-07 within the portion of the *Novispathodus* ex gr. *waageni* Zone between the *Flemingites rursiradiatus* beds (lowest Middle Smithian = middle Lower Olenekian) and *Urdyceras tulongensis* beds (lower Middle Smithian = middle Lower Olenekian) in the Bac Thuy Formation, northeastern Vietnam.

Discretella sp. indet. D

Fig. 152.1–152.6

Material examined: Two specimens, MPC25196, 25197, from BT01-07.

Description: Two segminate elements 1.0–1.36 mm in length; 0.51–0.67 mm in height; length to height ratio 2.0. General profile of element triangular, slightly bowed lower edge. Upper edge bears several pointed denticles, including one larger posterior cusp with one or two small processes. Cusp three times larger than other denticles, with two pronged ends. Denticles total 9 in number. Lower edge straight in anterior, downturned in posterior below cusp. Aboral surface broad with rounded basal cavity below cusp. Groove extended to both anterior and posterior ends through basal pit.

Remarks: The described specimens differ from other species of *Discretella* in having two pronged cusps and an arched basal margin. However, a definitive species assignment cannot be made due to an insufficient number of specimens. Their lateral profiles are somewhat similar to that of *Guangxidella bransoni* (Müller, 1956), except for the small posterior processes.

Occurrence: Described specimens from BT01-07 within the portion of the *Novispathodus* ex gr. *waageni* Zone between the *Flemingites rursiradiatus* beds (lowest Middle Smithian = middle Lower Olenekian) and *Urdyceras tulongensis* beds (lower Middle Smithian = middle Lower Olenekian) in the Bac Thuy Formation, northeastern Vietnam.

Discretella sp. indet. E

Fig. 152.7–152.9

Material examined: One specimen, MPC25198, from BT01-10.

Remarks: The described specimen lacks the anterior part, but it differs from other species of *Discretella* in having a rectangular shaped element, small pole-like denticles, and a triangular shaped posterior cusp.

Occurrence: Specimen from BT01-10 within the portion of the *Novispathodus* ex gr. *waageni* Zone between the *Urdyceras tulongensis* beds (lower Middle Smithian = middle Lower Olenekian) and *Leyceras* horizon of the *Owenites koeneni* beds (middle Middle Smithian = middle Lower Olenekian) in the Bac Thuy Formation, northeastern Vietnam.

Discretella sp. indet. F

Fig. 152.10–152.12

Material examined: One specimen, MPC25199, from BT01-15.

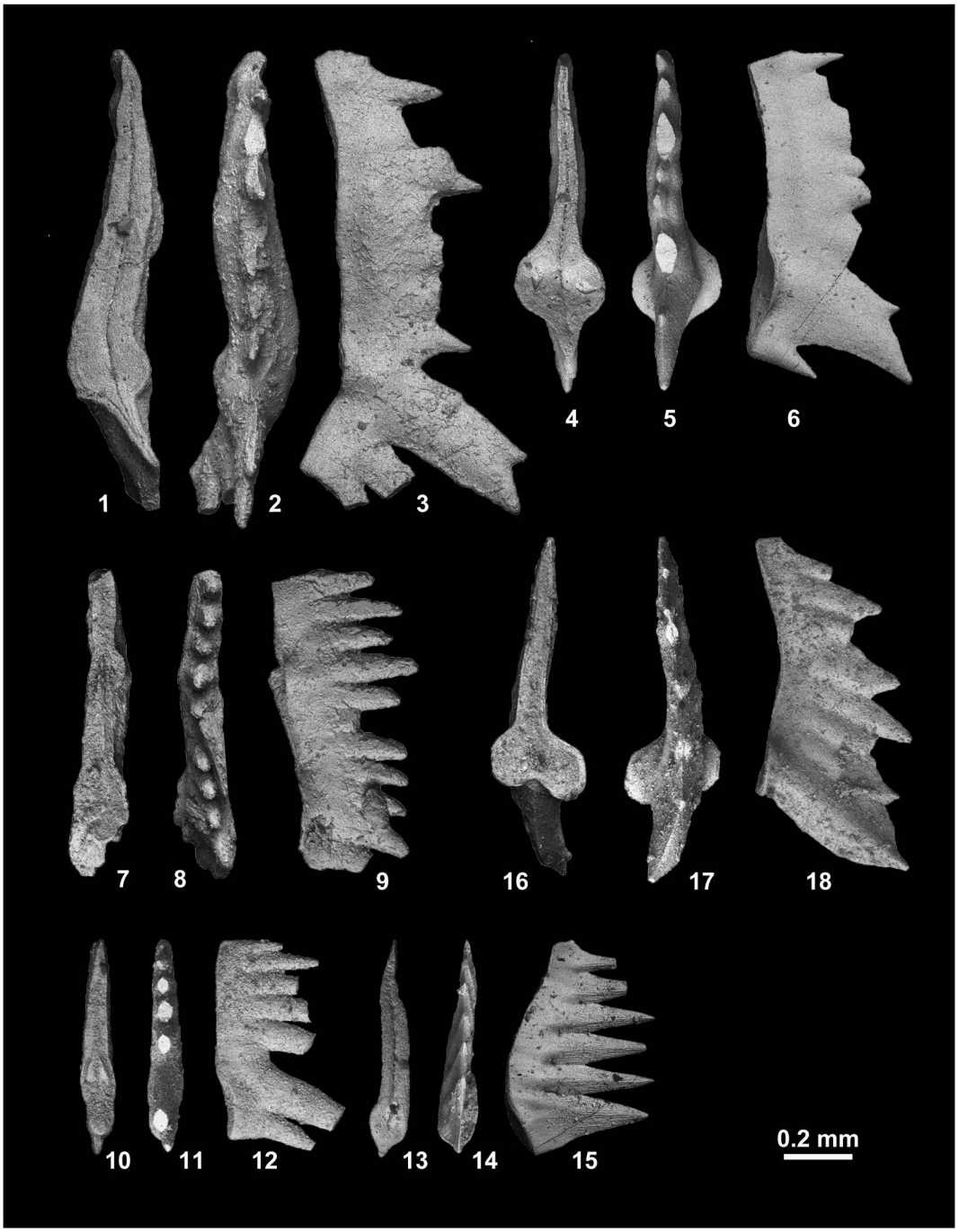

Fig. 152. 1–6, *Discretella* sp. indet. D from BT01-07. 1–3, MPC25196. 4–6, MPC25197. 7–9, *Discretella* sp. indet. E, MPC25198, from BT01-10. 10–12, *Discretella* sp. indet. F, MPC25199, from BT01-15. 13–15, *Discretella* sp. indet. G, MPC25200, from KC02-02. 16–18, *Guangxidella bransoni* (Müller, 1956), MPC25201, from BT01-06.

Remarks: The lateral profile of this specimen is similar to that of *Discretella robustus* (Wang and Wang, 1976), but it differs by having a space in front of the cusp and a non-expanded basal cavity.

Occurrence: Specimen from BT01-15 within the portion of the *Novispathodus* ex gr. *waageni* Zone above the *Leyeceras* horizon of the *Owenites koeneni* beds (middle Middle Smithian = middle Lower Olenekian) in the Bac Thuy Formation, northeastern Vietnam.

Discretella sp. indet. G

Fig. 152.13–152.15

Material examined: One specimen, MPC25200, from KC02-02.

Description: Laterally compressed segminate element 0.63 mm in length; 0.44 mm height; length to height ratio 1.4. Erect denticles total 6 in number. Lower margin upturned in anterior two-thirds and posterior one-third. Rounded basal cavity slightly wider than the width of element. Shallow groove extends from basal pit to anterior end.

Remarks: The described specimen is distinguished from other species of *Discretella* by the strongly upturned anterior lower margin, straight denticles and small basal cavity.

Occurrence: Described specimen from KC02-02 within the portion of the *Novispathodus* ex gr. *waageni* Zone represented by the *Guodunites* horizon of the *Owenites koeneni* beds (upper Middle Smithian = middle Lower Olenekian) in the Bac Thuy Formation, northeastern Vietnam.

Genus ***Gunagxidella*** Zhang and Yang, 1991

Type species: *Neoprioniodus bransoni* Müller, 1956.

Guangxidella bransoni (Müller, 1956)

Figs. 152.16–125.18, 153–159, 160.1–160.4

Neoprioniodus bransoni Müller, 1956, p. 829, pl. 95, figs. 19–21.

Neoprioniodus bicuspidatus Müller, 1956, p. 828, pl. 95, figs. 16–17.

Neospathodus bicuspidatus (Müller, 1956). Solien, 1979, p. 302, pl. 3, figs. 2–3.

Ozarkordina gigantea Bui, 1989, p. 409, pl. 31, figs. 10, 14.

multielement apparatuses, *Guangxidella typica* Zhang and Yang, 1991, p. 33, pl. 1, figs. 1a-b, 2a-b.

Material examined: Three specimens, MPC25201–25203, from BT01-06, four specimens, MPC25204–25207, from BT01-10, two specimens, MPC25208, 25209, from BT01-14, seven specimens, MPC25210–25216, from BT01-15, six specimens, MPC25217–25222, from BT02-02, ten specimens, MPC25223–25232, from BT02-03, eight specimens, MPC25233–25240, from BT03-01, six specimens, MPC25241–25246, from KC01-07, two specimens, MPC25247, 25248, from KC01-10, and nine specimens, MPC25249–25257, from PK01-02.

Description: Bowed segminate elements 0.43–1.45 mm in length, average 0.76 mm; 0.25–0.78 mm in height, average 0.40 mm; length to height ratio 1.3–2.6, average 1.9 for fifty-seven specimens. Bowed carina bears pointed denticles in upper part and more or less in concave lower part. Spine and node-like denticles vary in number from 5 to 12, average 8. Most denticles almost entirely discrete in small specimens, but fused over half of the length in large specimens. Denticle size increases posteriorly. Cusp situated in posterior end, and is two to three times larger than others. Sub-rounded or rectangular, cordiform-like basal cavity branches at posterior end. Width of basal cavity two times width of element. Deep furrow extends from basal pit to anterior end.

Remarks: The described specimens show a wide range of intraspecific variation in the form of denticles and basal cavity. However, all specimens share features characterized by the bow-like lateral form and cusp situated in the posterior end. They also include forms (MPC25202, 25211, 25214, etc.) that are very similar to the holotype of *Guangxidella bran-*

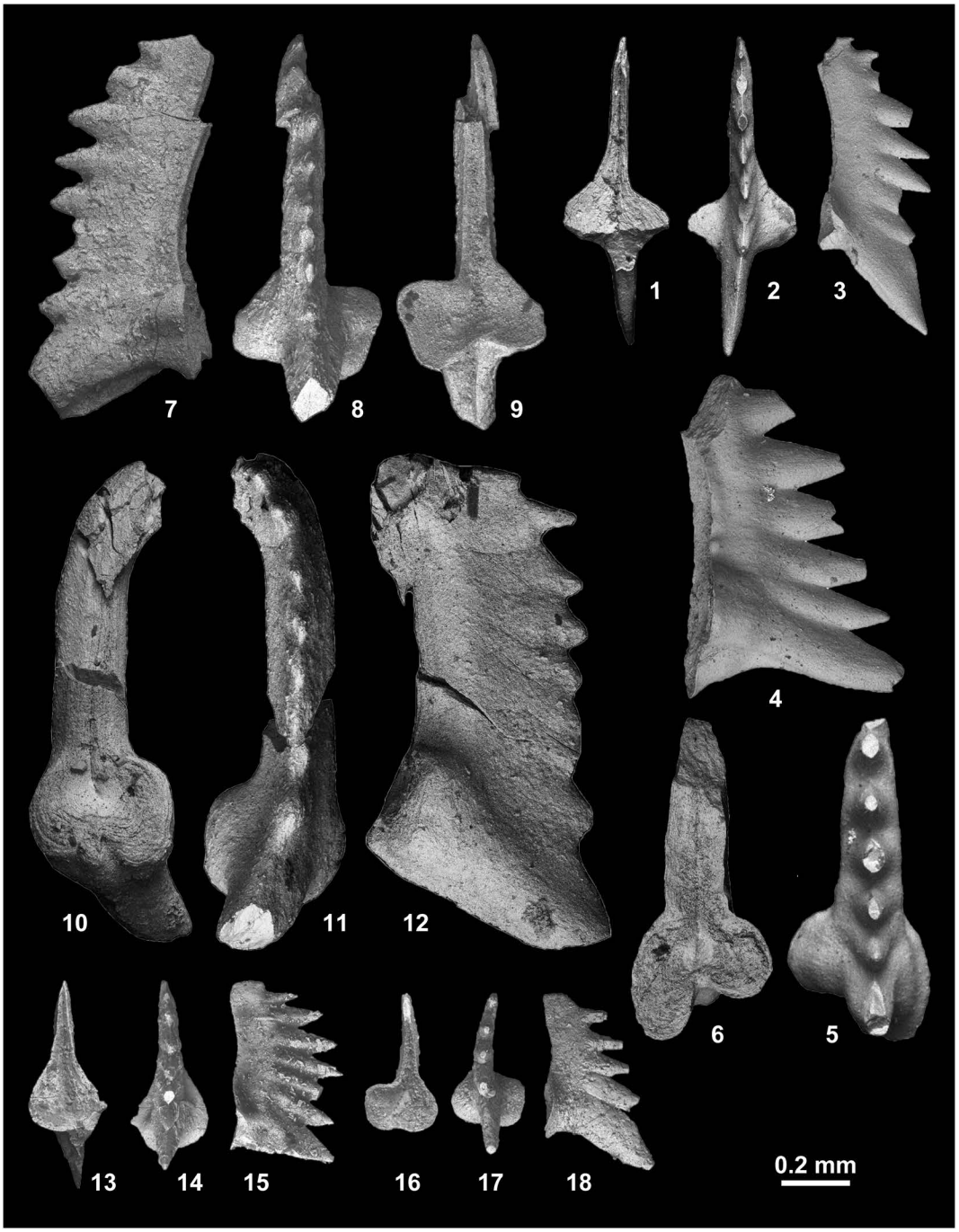

Fig. 153. *Guangxidella bransoni* (Müller, 1956). 1–3, MPC25202, from BT01-06. 4–6, MPC25203, from BT01-06. 7–9, MPC25204, from BT01-10. 10–12, MPC25205, from BT01-10. 13–15, MPC25206, from BT01-10. 16–18, MPC25207, from BT01-10.

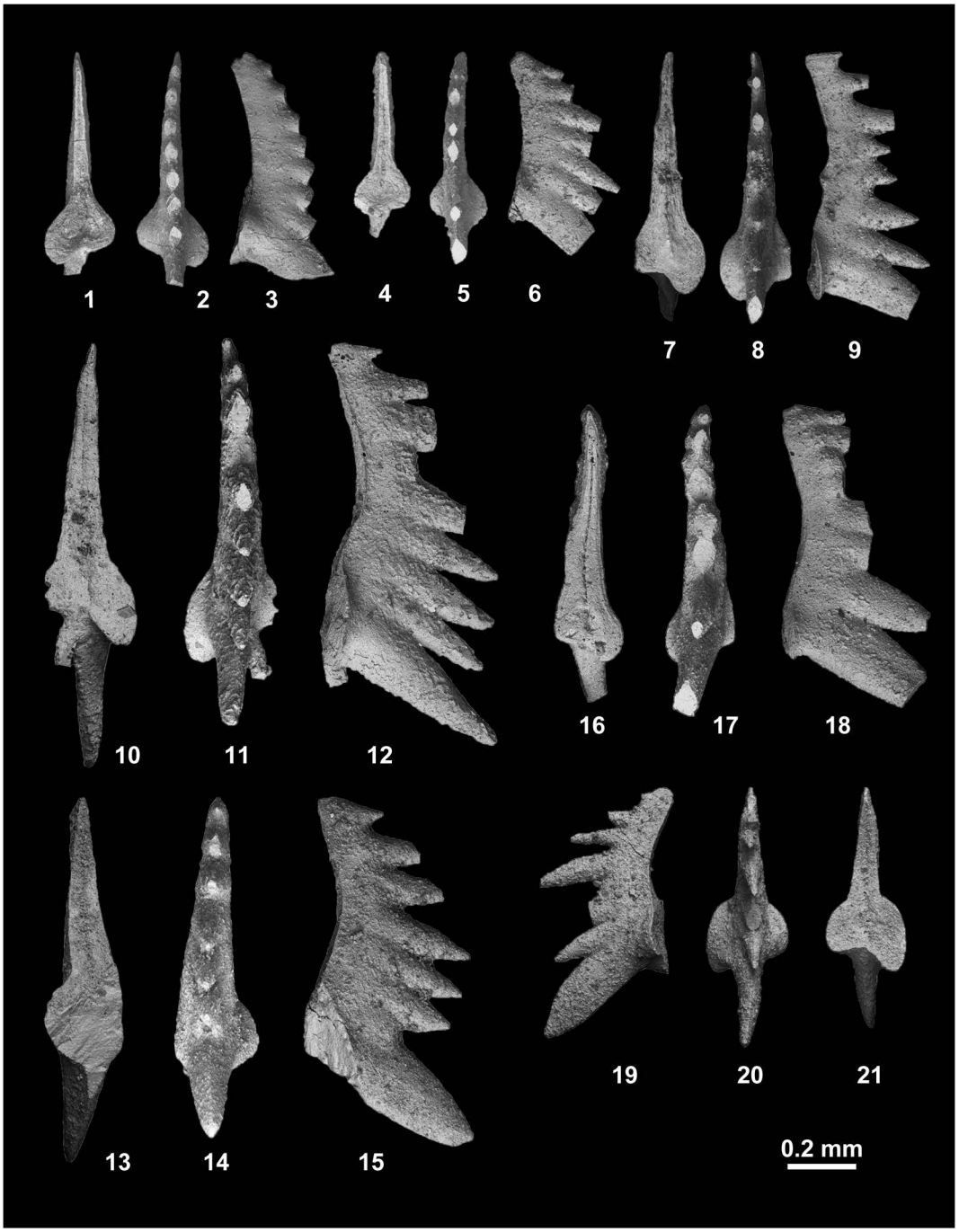

Fig. 154. *Guangxidella bransoni* (Müller, 1956). 1–3, MPC25208, from BT01-14. 4–6, MPC25209, from BT01-14. 7–9, MPC25210, from BT01-15. 10–12, MPC25211, from BT01-15. 13–15, MPC25212, from BT01-15. 16–18, MPC25213, from BT01-15. 19–21, MPC25214, from BT01-15.

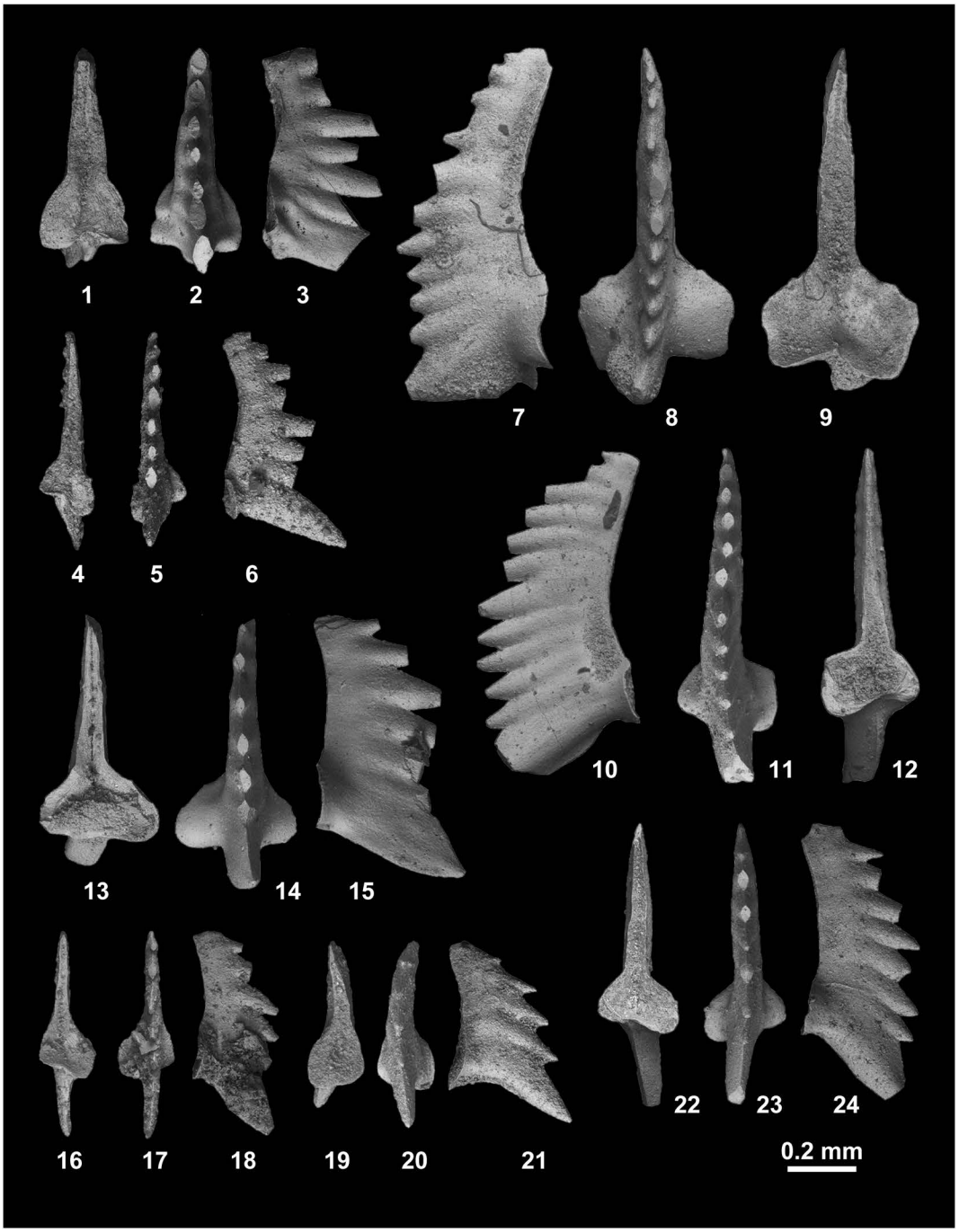

Fig. 155. *Guangxidella bransoni* (Müller, 1956). 1–3, MPC25215, from BT01-15. 4–6, MPC25216, from BT01-15. 7–9, MPC25217, from BT02-02. 10–12, MPC25218, from BT02-02. 13–15, MPC25219, from BT02-02. 16–18, MPC25220, from BT02-02. 19–21, MPC25221, from BT02-02. 22–24, MPC25222, from BT02-02.

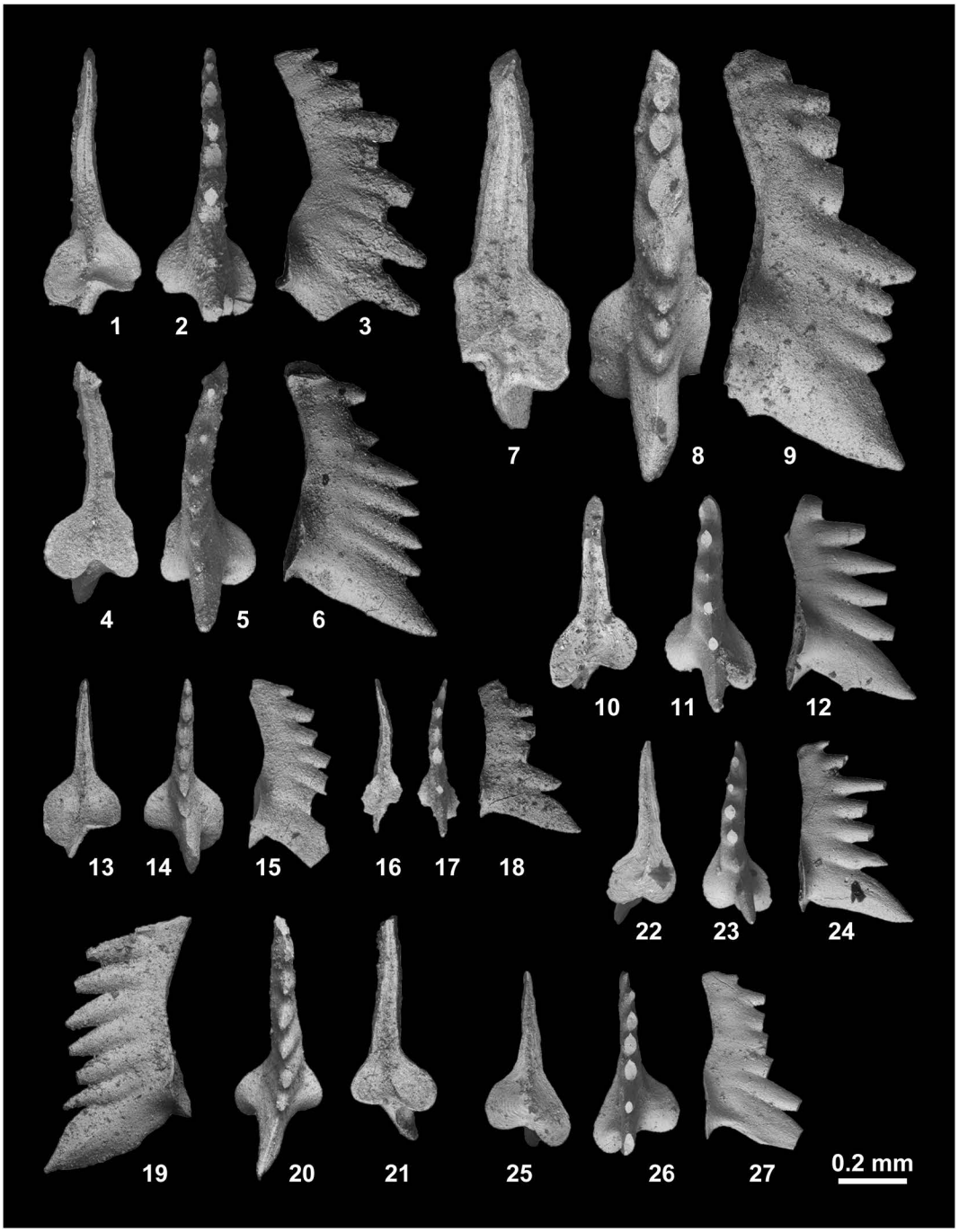

Fig. 156. *Guangxidella bransoni* (Müller, 1956) from BT02-03. 1–3, MPC25223. 4–6, MPC25224. 7–9, MPC25225. 10–12, MPC25226. 13–15, MPC25227. 16–18, MPC25228. 19–21, MPC25229. 22–24, MPC25230. 25–27, MPC23231.

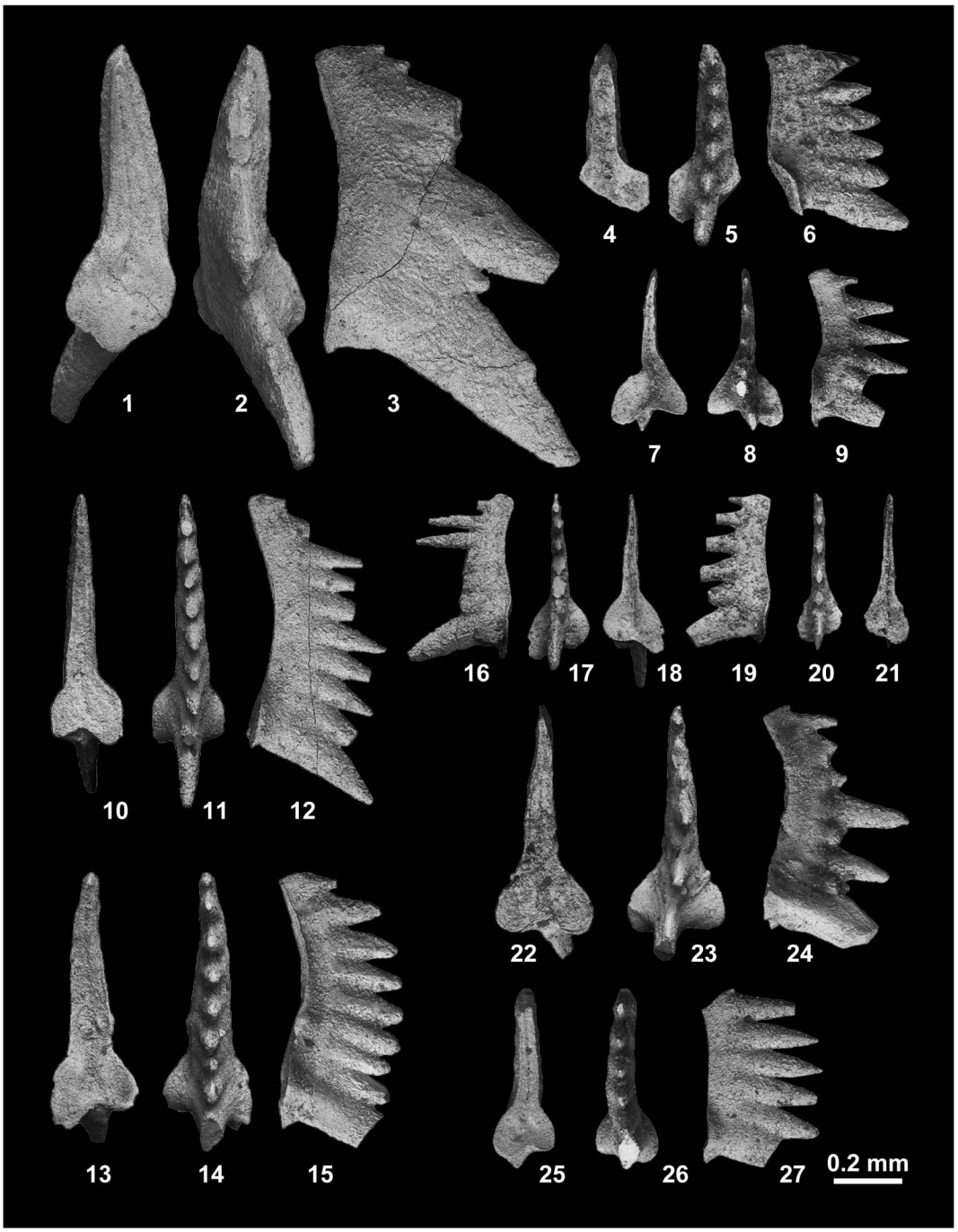

Fig. 157. *Guangxidella bransoni* (Müller, 1956). 1–3, MPC25232, from BT02-03. 4–6, MPC25233, from BT03-01. 7–9, MPC25234, from BT03-01. 10–12, MPC25235, from BT03-01. 13–15, MPC25236, from BT03-01. 16–18, MPC25237, from BT03-01. 19–21, MPC25238, from BT03-01. 22–24, MPC25239, from BT03-01. 25–27, MPC25240, from BT03-01.

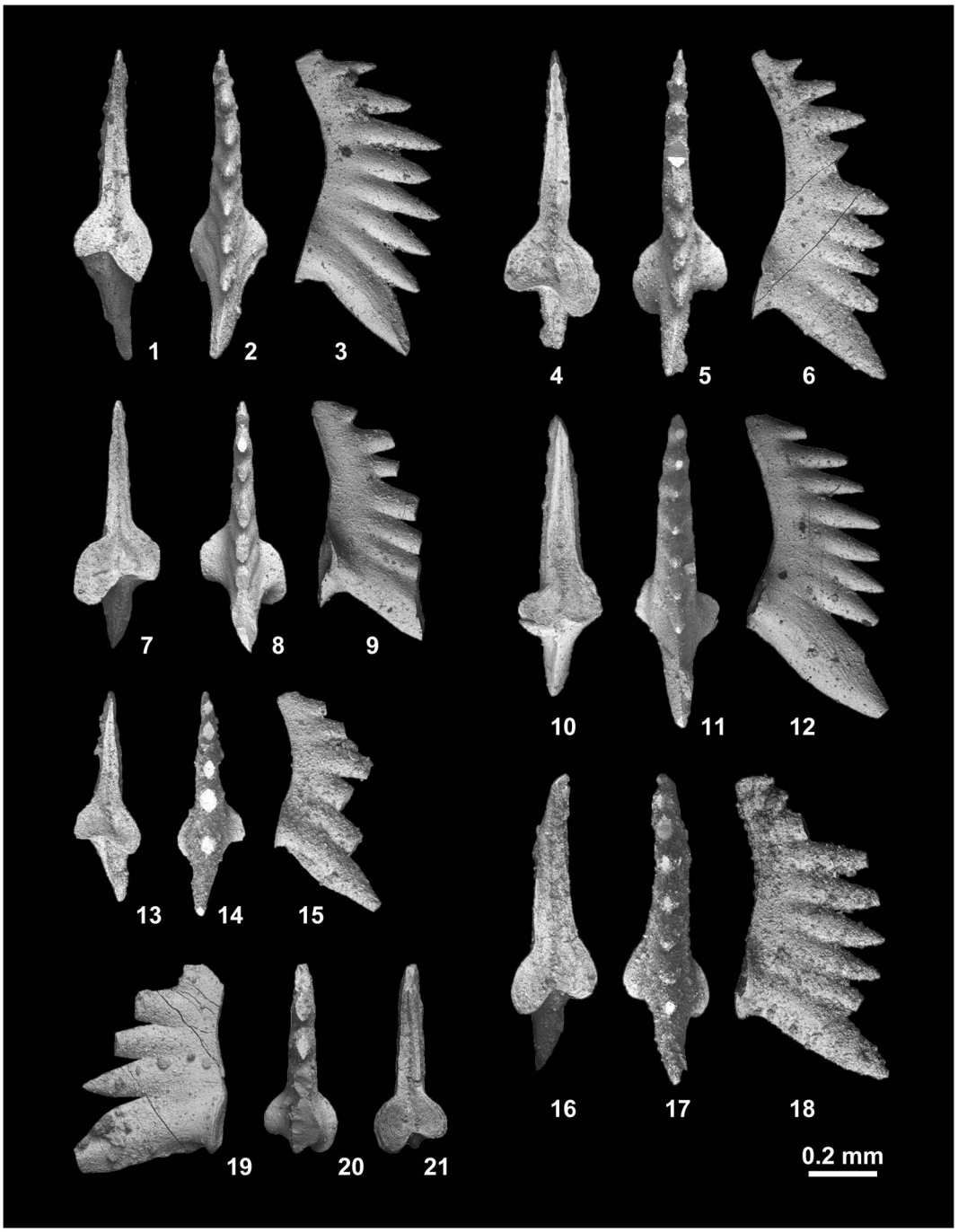

Fig. 158. *Guangxidella bransoni* (Müller, 1956). 1–3, MPC25241, from KC01-07. 4–6, MPC25242, from KC01-07. 7–9, MPC25243, from KC01-07. 10–12, MPC25244, from KC01-07. 13–15, MPC25245, from KC01-07. 16–18, MPC25246, from KC01-07. 19–21, MPC25247, from KC01-10.

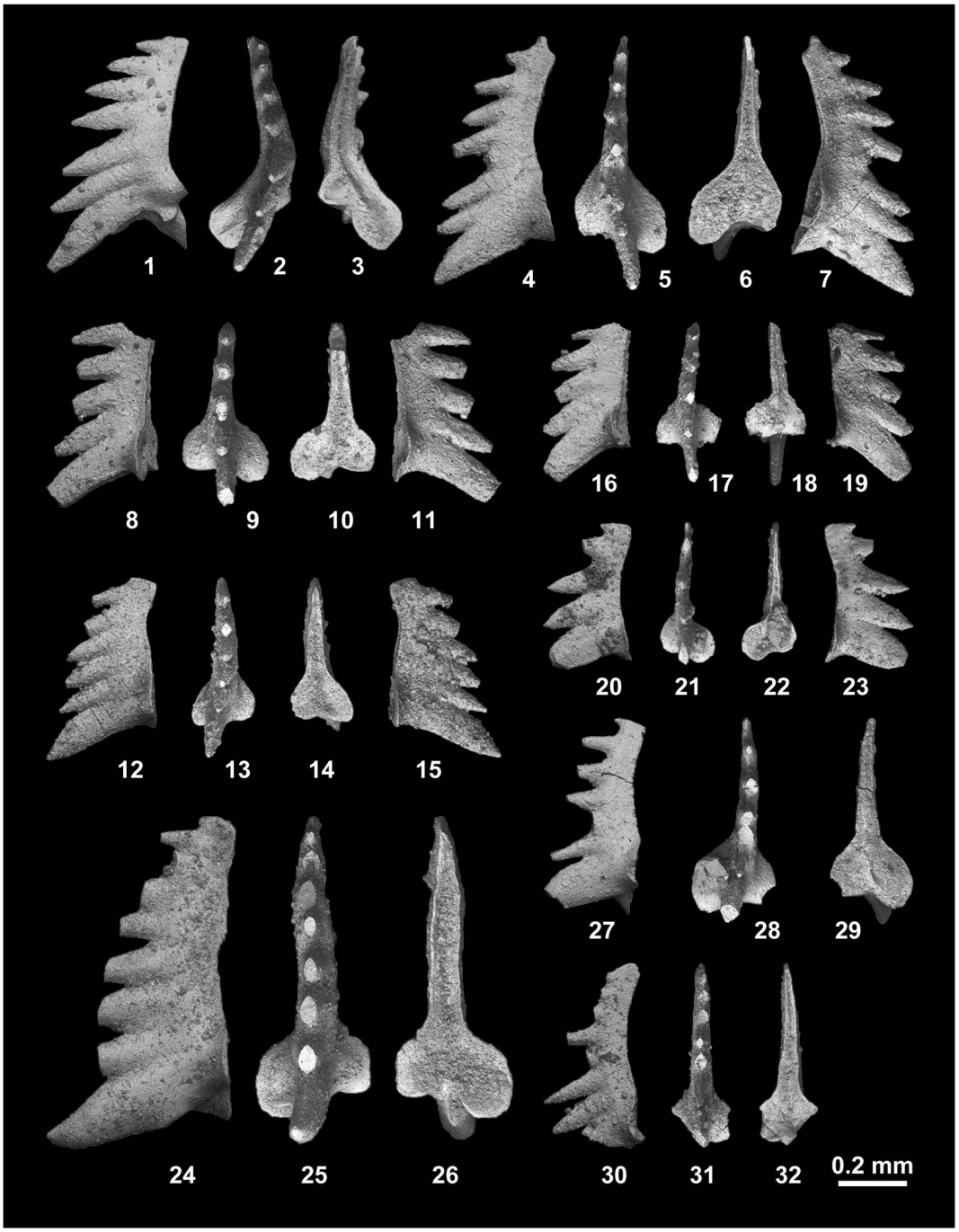

Fig. 159. *Guangxidella bransoni* (Müller, 1956). 1–3, MPC25248, from KC01-10. 4–7, MPC25249, from PK01-02. 8–11, MPC25250, from PK01-02. 12–15, MPC25251, from PK01-02. 16–19, MPC25252, from PK01-02. 20–23, MPC25253, from PK01-02. 24–26, MPC25254, from PK01-02. 27–29, MPC25255, from PK01-02. 30–32, MPC25256, from PK01-02.

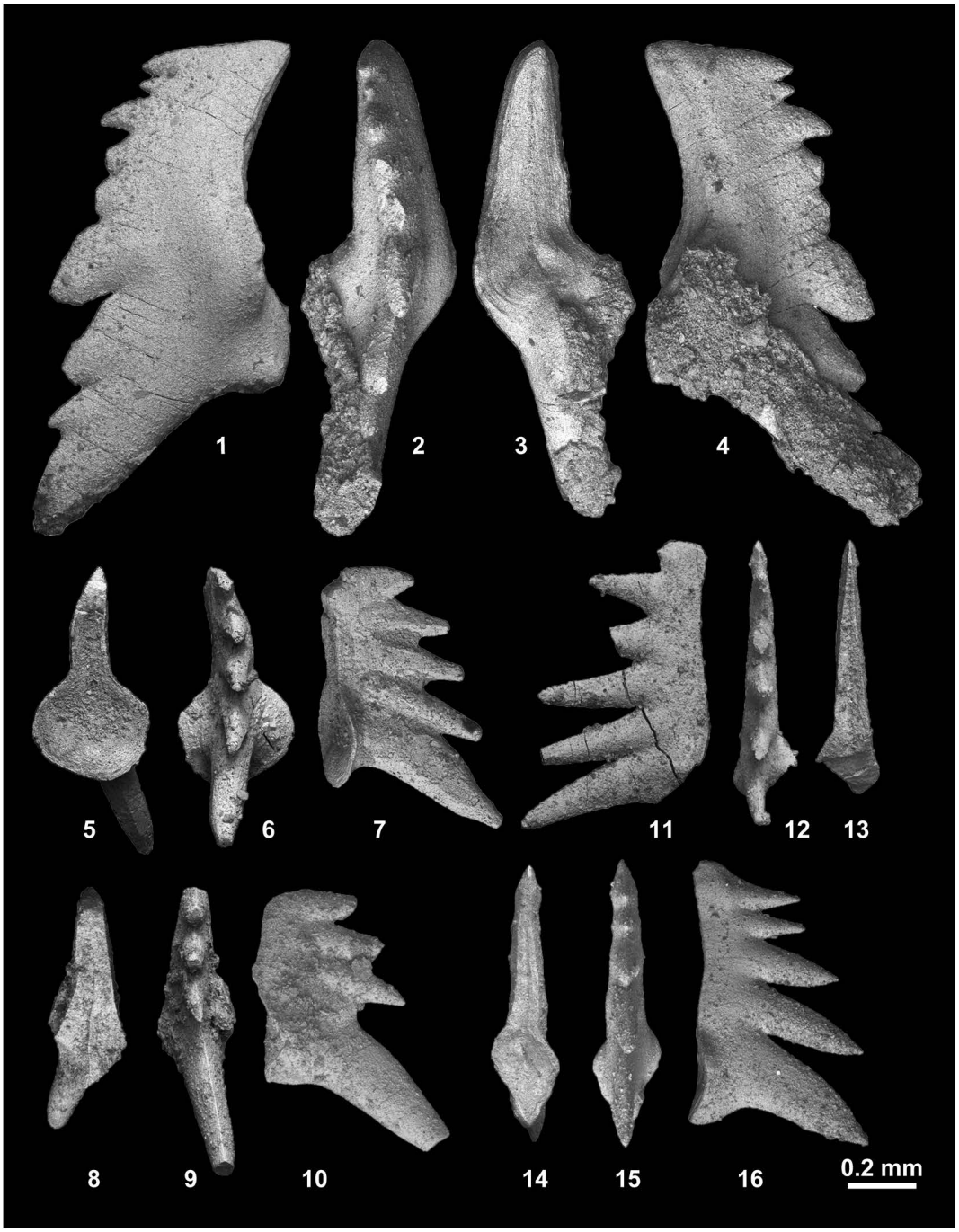

Fig. 160. 1–4, *Guangxidella bransoni* (Müller, 1956), MPC25257, from PK01-02. 5–10, *Guangxidella* sp. indet. A from BT01-06. 5–7, MPC25258. 8–10, MPC25259. 11–16, *Guangxidella* sp. indet. B. 11–13, MPC25260, from BT02-02. 14–16, MPC25261, from KC01-07.

soni (Müller, 1956, pl. 95, figs. 20, 21).

Occurrence: Described specimens from BT01-06, BT01-10, BT01-14, BT01-15, BT02-02, BT02-03, BT03-01, KC01-07, KC01-10 and PK01-02 within the portion of the *Novispathodus* ex gr. *waageni* Zone that includes the *Urdyceras tulongensis* beds (lower Middle Smithian=middle Lower Olenekian) and the *Leyeceras* horizon of the *Owenites koeneni* beds (middle Middle Smithian=middle Lower Olenekian) in the Bac Thuy Formation, northeastern Vietnam. This species also occurs in the Middle Smithian at Crittenden Springs, Nevada (*Meekoceras* beds, Müller, 1956), the Luolou Formation, Guangxi, China (*Neospathodus waageni* Zone, Zhang and Yang, 1991), the Thaynes Formation, Utah (*Parachirognathus* Zone, Solien, 1979) and the Taho limestone, Southwest Japan (unpublished).

Guangxidella sp. indet. A

Fig. 160.5–160.10

Material examined: Two specimens, MPC25258, 25259, from BT01-06.

Description: Two triangular segminate elements 0.76 mm in length; 0.54–0.56 mm in height; length to height ratio 1.4. Robust denticles total 4 and 5 in number, reclined posteriorly. Cusp situated in posterior end, three times larger than other denticles. Rounded basal cavity expanded in posterior end. Shallow groove extends from basal pit to anterior end.

Remarks: The described specimens are very similar to the juvenile form of *Guangxidella bransoni* (Müller, 1956), but differ in having a larger element size, robust denticles and a rounded basal cavity.

Occurrence: Described specimens from BT01-06 within the portion of the *Novispathodus* ex gr. *waageni* Zone between the *Flemingites rursiradiatus* beds (lowest Middle Smithian=middle Lower Olenekian) and *Urdyceras tulongensis* beds (lower Middle Smithian=middle Lower Olenekian) in the Bac Thuy Formation, northeastern Vietnam.

Guangxidella sp. indet. B

Figs. 160.11–160.16, 161.1–161.3

Material examined: One specimen, MPC25260, from BT02-02, one specimen, MPC25261, from KC01-07, and one specimen MPC25262, from KC01-11.

Description: Three triangular segminate elements 0.63–0.84 mm in length, average 0.77 mm; 0.43–0.55 mm in height, average 0.50 mm; length to height ratio 1.5–1.6. Lower margin slightly concave and down-turned posteriorly. Completely discrete and pointed denticles total 5 to 6 in number. Denticle size and inclination gradually increases posteriorly. Cusp situated in posterior end. Sub-rounded basal cavity extends posteriorly. Shallow furrow runs from basal pit to anterior end.

Remarks: The described specimens differ from *Guangxidella bransoni* (Müller, 1956) by slightly bowed elements with quite discrete denticles and non-branched basal cavity, and from *Guangxidella* sp. indet. A. by a smaller basal cavity and slender lateral form.

Occurrence: Described specimens from BT02-02, KC01-07 and KC01-11 within the portion of the *Novispathodus* ex gr. *waageni* Zone that includes the *Urdyceras tulongensis* beds (lower Middle Smithian=middle Lower Olenekian) and the *Leyeceras* horizon of the *Owenites koeneni* beds (middle Middle Smithian=middle Lower Olenekian) in the Bac Thuy Formation, northeastern Vietnam.

Subfamily Neogondolellinae Hirsch, 1994

Genus ***Eurygnathodus*** Staesche, 1964

Type species: *Eurygnathodus costatus* Staesche, 1964.

Eurygnathodus costatus Staesche, 1964

Fig. 161.4–161.6

Eurygnathodus costatus Staesche, 1964, p. 269, pl. 28, figs. 1–6; Budurov and Pantic, 1973, p. 51, pl. pl. 1,

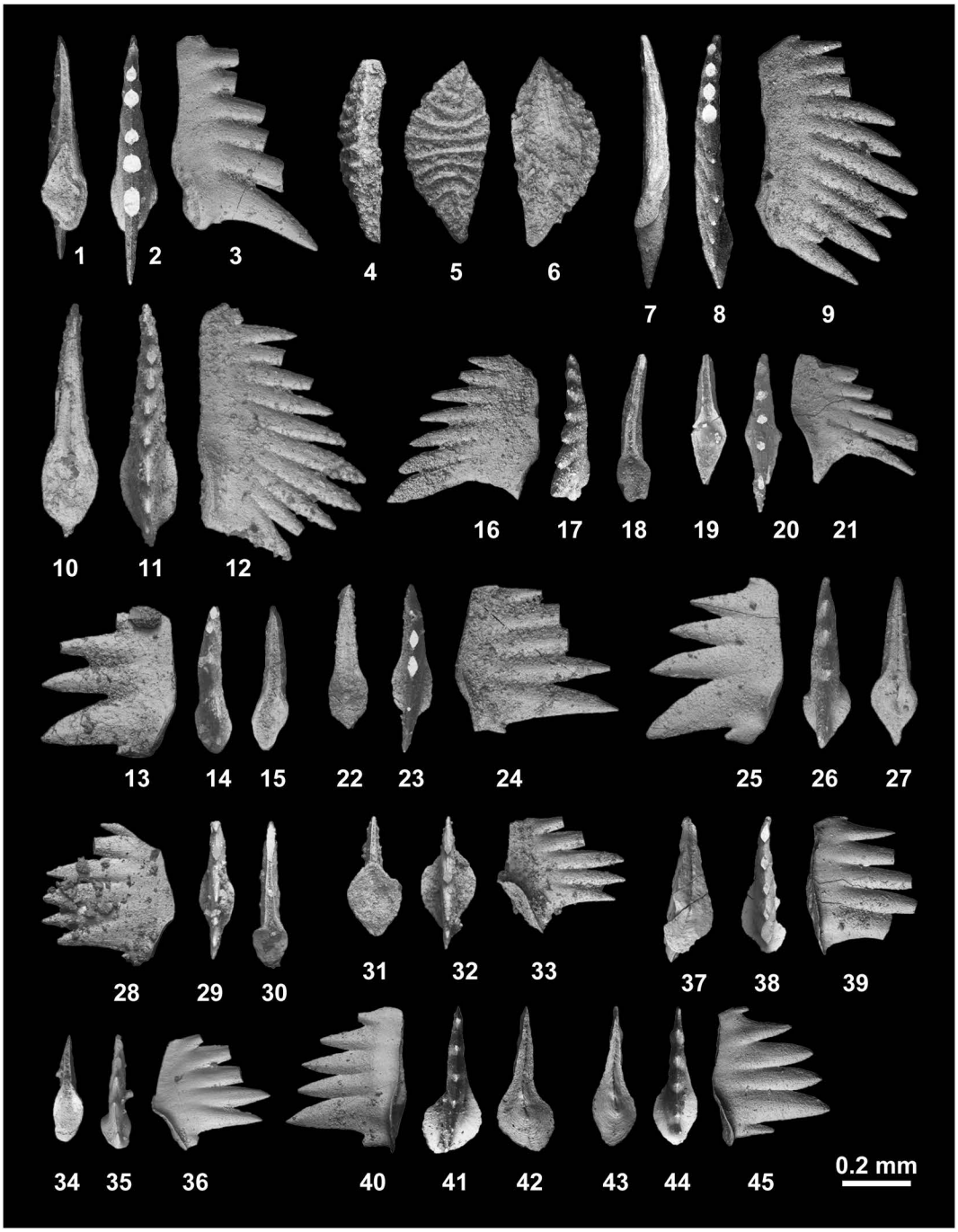

Fig. 161. 1–3, *Guangxidella* sp. indet. B, MPC25262, from KC01-11. 4–6, *Eurygnathodus costatus* Staesche, 1964, MPC25263, from BT01-03. 7–9, *Neospathodus* aff. *concavus* Zhao and Orchard, 2007, MPC25264, from BT01-07. 10–12, *Neospathodus cristagalli* (Huckriede, 1958), MPC25265, from BT01-04. 13–45, *Neospathodus dieneri* Sweet, 1970a. 13–15, MPC25266, from BT01-04. 16–18, MPC25267, from BT01-07. 19–21, MPC25268, from BT01-07. 22–24, MPC25269, from BT02-02. 25–27, MPC25270, from KC01-01. 28–30, MPC25271, from KC01-13. 31–33, MPC25272, from KC01-13. 34–36, MPC25273, from KC01-13. 37–39, MPC25274, from KC02-02. 40–42, MPC25275, from KC02-02. 43–45, MPC25276, from KC02-02.

figs. 1–15; Igo, 2009, p. 183, figs. 152.23–152.24; Orchard, 2010, figs. 5.9, 5.10.

Platyvillosus costatus (Staesche, 1964). Goel, 1977, p. 1098, pl. 2, figs. 15–21; Wang and Cao, 1981, p. 371, pl. 2, figs. 1–4, 28, 29, 30, 33; Koike, 1982, p. 44, pl. 5, figs. 1–9; Tian *et al*., 1983, p. 391, pl. 81, fig. 2; Matsuda, 1984, p. 128, pl. 6, figs. 6–10; Duan, 1987, pl. 3, fig. 4; Koike, 1988, pl. 1, figs. 1–57, pl. 2, figs. 1–37; Bui, 1989, p. 411, pl. 31, figs. 7–9; Beyers and Orchard, 1991, pl. 5, fig. 10; Cao and Wang, 1993, pl. 56, fig. 16; Wang and Zhong, 1994, p. 404, pl.1, figs. 15, 23.

Material examined: One specimen, MPC25263, from BT01-03.

Description: Dextral segminiplanete element; outline of platform ellipsoidal with sharply pointed anterior and posterior ends; length 0.53 mm; width 0.25 mm; length to width ratio 2.1. Upper surface of the platform bears 10 transverse ridge-like denticles, denticle form straight in middle part and curved convexly toward center in middle to both anterior and posterior parts. Element exhibits slightly bowed lateral form. Basal cavity narrow, sub-rounded. Groove runs from basal pit to anterior end.

Remarks: Koike (1988) demonstrated morphological variation in the ornamentation of *Platyvillosus costatus* (Staesche, 1964) (=*Eurygnathodus costatus* Staesche, 1964) based on abundant specimens from the Taho limestone, Southwest Japan. He recognized four morphotypes (Central form, Morphotype α, β, γ, σ) and fifteen forms (A–O) based on the ornamentation on the platform. Central form (=Form A) is characterized by transverse ridges covering the entire width of the platform. This form is identical to the holotype of this species (Staesche, 1964, pl. 28, figs. 1–4). Morphotype α has nodose denticles and is subdivided into three forms (Form B, C, D). Morphotype β exhibits a size increase of denticles in the axial region and includes three forms (Form E, F, G). Morphotype γ represents a tendency toward development of increasingly prominent nodose to ridge-like denticulation and consists of four forms (Form H, I, J, K). Morphotype σ shows a tendency to decrease in oral ornamentation and includes four forms (Form L, M, N, O).

The described specimen has conspicuous ridge-like denticles, which extend the entire width of the platform. This feature matches well with Form A of Koike (1988). Bui (1989) described some specimens of *Eurygnathodus costatus* from the Bac Thuy Formation, one of which (Bui, 1989, pl. 31, fig. 7) is identical to Form A and a second type with weak ridge-like denticles (Bui, 1989, pl. 31, figs. 8, 9), is very similar to Form L of Morphotype σ.

Occurrence: Specimen from BT01-03 within the portion of the *Novispathodus* ex gr. *waageni* Zone in the *Flemingites rursiradiatus* beds (lowest Middle Smithian=middle Lower Olenekian) in the Bac Thuy Formation, northeastern Vietnam. This species also occurs in Lower Triassic formations in South Tirol (Staesche, 1964), Spiti, India (Goel, 1977; Orchard and Krystyn, 2007; Orchard, 2010), Kashmir, India (Matsuda, 1984), South China (Wang and Cao, 1981; Wang and Zhong, 1994), Malaysia (Koike, 1982), Southwest Japan (Koike, 1988), British Columbia, Canada (*Neogonlodella milleri* Zone, Beyers and Orchard, 1991), South Primorye, Russia (*Neospathodus dieneri-Ns. pakistanensis* Zone and *Neospathodus* ex gr. *waageni-Ns. novaehollandiae* Zone, Shigeta *et al*., 2009). According to Orchard and Krystyn (2007) and Shigeta *et al.* (2009), this species ranges from the Upper Dienerian to the Smithian.

Genus ***Neospathodus*** Mosher, 1968

Type species: *Spathognathodus cristagalli* Huckriede, 1968.

Neospathodus aff. ***concavus*** Zhao and Orchard, 2007

Fig. 161.7–161.9

aff. *Neospathodus concavus* Zhao and Orchard, 2007, in Zhao *et al*., 2007, p. 35, pl. 1, figs. 1A–C; Orchard and Krystyn, 2007, fig. 4; Igo, 2009, p. 184–185, fig.

154.13.

Material examined: One specimen, MPC25264, from BT01-07.

Description: Bowed segminate element 0.73 mm in length; 0.48 mm in height; length to height ratio 1.5. Pole-like pointed denticles total 12 in number. Lower part of element straight anteriorly and downturned at posterior margin. Non-expanded basal cavity convex to aboral surface. Groove extends to anterior end.

Remarks: The described specimen is similar to *Neospathodus concavus* Zhao and Orchard, 2007 in having a bowed element, but differs by a convex, non-expanded basal cavity. *Ns. concavus* has an arched blade, a concave, expanded and rounded basal cavity, and a prominent lateral rib.

Occurrence: Described specimen from BT01-07 within a portion of the *Novispathodus* ex gr. *waageni* Zone between the *Flemingites rursiradiatus* beds (lowest Middle Smithian = middle Lower Olenekian) and *Urdyceras tulongensis* beds (lower Middle Smithian = middle Lower Olenekian) in the Bac Thuy Formation, northeastern Vietnam. This species also occurs in the Upper Dienerian (upper Upper Induan, *Neospathodus cristagalli* Zone with *Gyronites frequens* Zone) in the Mikin Formation at the Mud Section, Spiti, India (Orchard and Krystyn, 2007), in the Lower Smithian (lower Lower Olenekian) in Anhui Province, South China (*Neospathodus waageni eowaageni* Subzone to *Neospathodus waageni waageni* Subzone with *Flemingites-Euflemeingites* Zone, Zhao *et al.*, 2007) and South Primorye (*Neospathodus* ex gr. *waageni-Ns. novaehollandiae* Zone with *Clypeoceras timorense* Zone, Shigeta *et al*., 2009).

Neospathodus cristagalli (Huckriede, 1958)

Fig. 161.10–161.12

Spathognathodus cristagalli Huckriede, 1958, p. 161, pl. 10, fig. 14, 15.

Neospathodus cristagalli (Huckriede, 1958). Sweet, 1970a, p. 9, pl. 1, figs. 18, 21; Sweet, 1970b, p. 246, pl. 1, figs. 14, 15; Mosher, 1973, p. 170, pl. 20, fig. 4; Matsuda, 1982, p. 92, pl. 3, figs. 1–12; Tian *et al.*, 1983, p. 375, pl. 80, figs. 2a, 2b; Orchard and Krystyn, 2007, pl. 1, fig. 5.

multielement apparatuses, *Neospathodus* cf. *cristagalli* (Huckriede, 1958). Orchard, 2005, p. 88, text-fig. 14.

Material examined: One specimen, MPC25265, from BT01-04

Description: Laterally compressed blade-like element 0.75 mm in length; 0.48 mm in height; length to height ratio 1.6, with arched upper edge. Basal margin straight anteriorly and slightly turned upward in the posterior one-third. Reclined broad denticles, 12 in number, lower part fused and upper part discrete, highest point situated in posterior one-third of element. Triangular shaped large process situated at posterior end. Basal cavity oblong, with deep pit, and groove extends from pit to anterior end.

Remarks: The described specimen has a terminal triangular denticle at the posterior end, which is a diagnostic feature of *Neospathodus cristagalli* (Huckriede, 1958). The lateral form of the element and the ratio of the fused part of the denticles of the described specimen are similar to those of the holotype (Huckriede, 1958, pl. 10, fig. 15) and specimens described by various authors (e.g. Sweet, 1970a, b; Matsuda, 1982; Tian *et al*., 1983).

Occurrence: Described specimen from BT01-04 within the portion of the *Novispathodus* ex gr. *waageni* Zone in the *Flemingites rursiradiatus* beds (lowest Middle Smithian = middle Lower Olenekian) in the Bac Thuy Formation, northeastern Vietnam. This species also ranges from the Upper Dienerian (upper Upper Induan) to the Smithian (Lower Olenekian) in the Salt Range, Pakistan (Huckriede, 1958; Sweet, 1970a, b), British Columbia, Canada (*Vavilovites sverdrupi* Zone, Mosher, 1973), Kashmir, India (Matsuda, 1982), Tibet (Tian *et al*., 1983), and the Mikin Formation at the Mud Section, Spiti, India (*Neospathodus cristagalli* Zone to *Neospathodus waageni* sensu stricto Zone with *Gyronites frequens*

Zone, *Meekophiceras*? *vercherei* beds, and *Rohillites rohilla* Zone, Krystyn *et al*., 2007; Orchard, 2007b; Orchard and Krystyn, 2007).

Neospathodus dieneri Sweet, 1970a

Figs. 161.13–161.45, 162, 163, 164.1–164.6

Neospathodus dieneri Sweet, 1970a, p. 9, pl. 1, fig. 17; Sweet, 1970b, p. 249, pl. 1, figs. 1, 4; McTavish, 1973, p. 293, pl. 2, figs. 3, 6; Birkenmajer and Trammer, 1975, pl. 1, fig. 4; Buryi, 1979, p. 52, pl. 7. fig. 7; Wang and Cao, 1981, pl. 2, figs. 24, 25; Matsuda, 1982, p. 90, pl. 2, figs. 1–11; Koike, 1982, p. 37, pl. 6, figs. 15–21, 25; Beyers and Orchard, 1991, pl. 5, fig. 4; Wang and Zhong, 1994, p. 400, pl. 1, figs. 18; Zhao and Orchard (in Zhao *et al.*, 2007), p. 35, pl. 1, figs. 12A, B, 9A, B, C, 11A, B, C; Orchard and Krystyn, 2007, figs. 3, 6, 7; Igo , 2009, p. 186, 188, figs. 151.6–151.16, 152.8, 152.9; Beranek *et al*., 2010, figs. 6.20, 6.21.

Material examined: One specimen, MPC25266, from BT01-04, two specimens, MPC25267, 25268, from BT01-07, one specimen, MPC25269, from BT02-02, one specimen, MPC25270, from KC01-01, three specimens, MPC25271–25273, from KC01-11, forty specimens, MPC25274–25313, from KC02-02, and one specimen, MPC25314, from KC02-03.

Description: Sub-triangular or sub-square segminate elements 0.32–0.55 mm in length, average 0.41 mm; 0.32–0.55 mm in height, average 0.38 mm; length to height ratio 0.7–1.6, average 1.1 for forty-nine specimens. Denticles erect or slightly reclined posteriorly, and vary in number from 4 to 9, average 6. Cusp situated at posterior end. Some specimens have small posterior denticle. Lower margin of element straight and slightly upturned or concave anteriorly, and upturned posteriorly. Rounded or sub-rounded basal cavity extends one-fourth to one-half the length of the element and is slightly or strongly concave. Groove runs from basal pit to anterior end.

Remarks: Zhao *et al.* (2007) recognized three morphotypes in *Neospathodus dieneri* Sweet, 1970a. Morphotype 1 has the longest posterior terminal cusp, which is broader in width than the other morphotypes. Morphotype 2 is characterized by a penultimate denticle as large as the terminal cusp. Morphotype 3 has an additional posterior denticle, which is broader in width and shorter in length than the other denticles. These morphotypes occur continuously in ascending order from the Upper Dienerian to the Smithian part of the Yinkeng Formation in the West Pingingshan Section, South China (Zhao *et al.*, 2007). Specimens from the Bac Thuy Formation include all morphotypes of Zhao *et al.* (2007), and their ranges are equal.

Occurrence: Described specimens from BT01-04, BT01-07, BT02-02, KC01-01, KC01-11, KC02-02 and KC02-03 within the portion of the *Novispathodus* ex gr. *waageni* Zone that includes the *Flemingites rursiradiatus* beds (lowest Middle Smithian = middle Lower Olenekian), *Urdyceras tulongensis* beds (lower Middle Smithian = middle Lower Olenekian) and the *Leyeceras* and *Guodunites* horizons of the *Owenites koeneni* beds (middle to upper Middle Smithian = middle Lower Olenekian) in the Bac Thuy Formation, northeastern Vietnam. This species also ranges from the Dienerian (Upper Induan) to the Smithian (Lower Olenekian) in the Salt Range, West Pakistan (Zone 3 to middle part of Zone 7, Sweet, 1970a, b), Australia (McTavish, 1973), Svalbard (Birkenmajer and Trammer, 1975; Hatlebarg and Clark, 1984), Spiti, India (Goel, 1977; Orchard and Krystyn, 2007), South Primorye, Russia (*Neospathodus dieneri*-*Ns. pakistanensis* Zone with *Clypeoceras spitiense* "bed" and lower part of *Paranorites varians* Zone, Shigeta *et al.*, 2009), South China (*Neospathodus dieneri* M1 Zone to lower part of *Neospathodus waageni waageni* Subzone with upper part of *Ophiceras*-*Lytophiceras* Zone, *Prionolobus*-*Gyronites* Zone, and lower part of *Fleminigites*-*Euflemingites* Zone, Wang and Cao, 1981; Zhao *et al*., 2007), Kashmir, India (Matsuda, 1982), Malaysia (Koike, 1982), and British Columbia, Canada (Beyers and Orchard, 1991; Beranek *et al*., 2010). *Ns. dieneri*

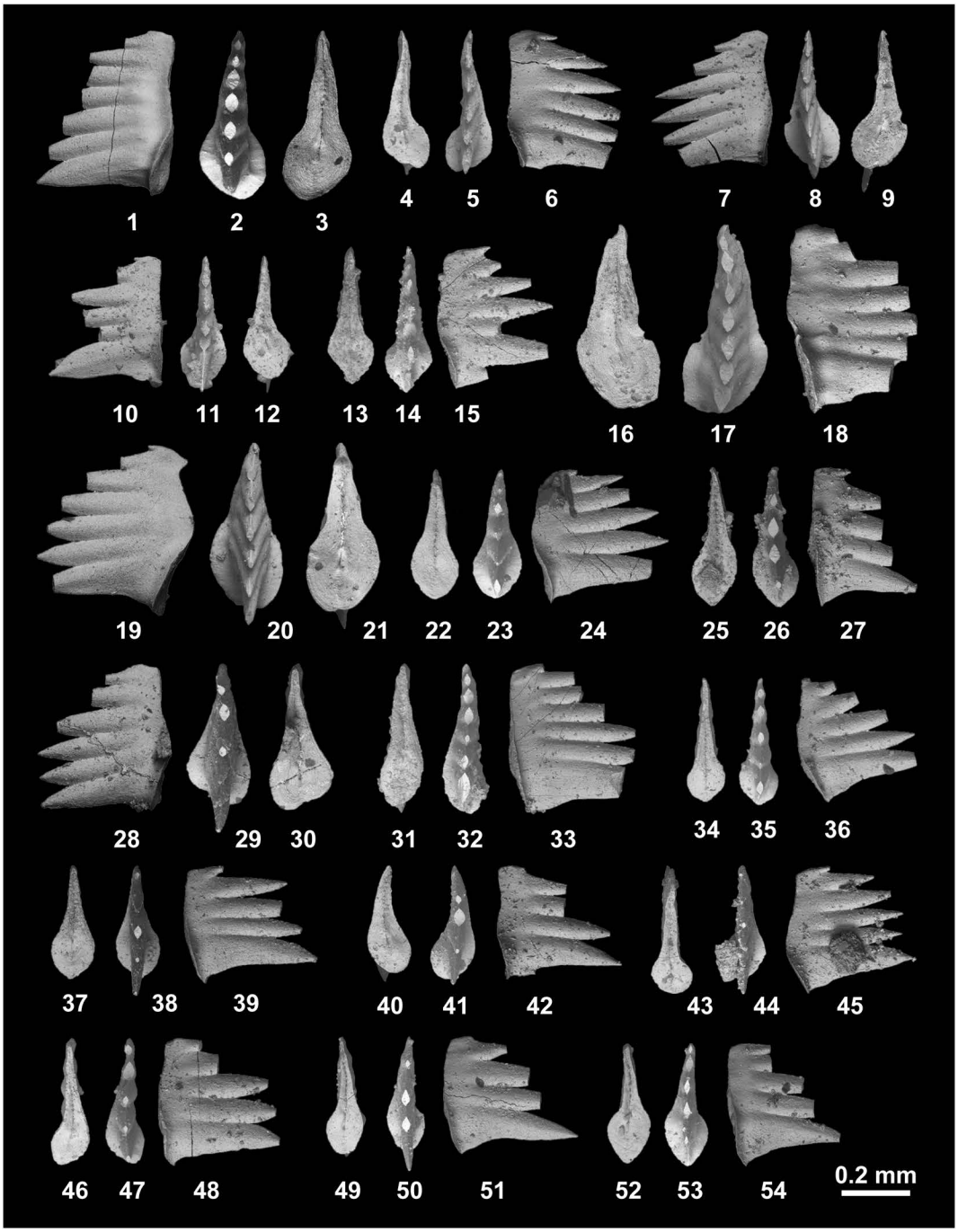

Fig. 162. *Neospathodus dieneri* Sweet, 1970a from KC02-02. 1–3, MPC25277. 4–6, MPC25278. 7–9, MPC25279. 10–12, MPC25280. 13–15, MPC25281. 16–18, MPC25282. 19–21, MPC25283. 22–24, MPC25284. 25–27, MPC25285. 28–30, MPC25286. 31–33, MPC25287. 34–36, MPC25288. 37–39, MPC25289. 40–42, MPC25290. 43–45, MPC25291. 46–48, MPC25292. 49–51, MPC25293. 52–54, MPC25294.

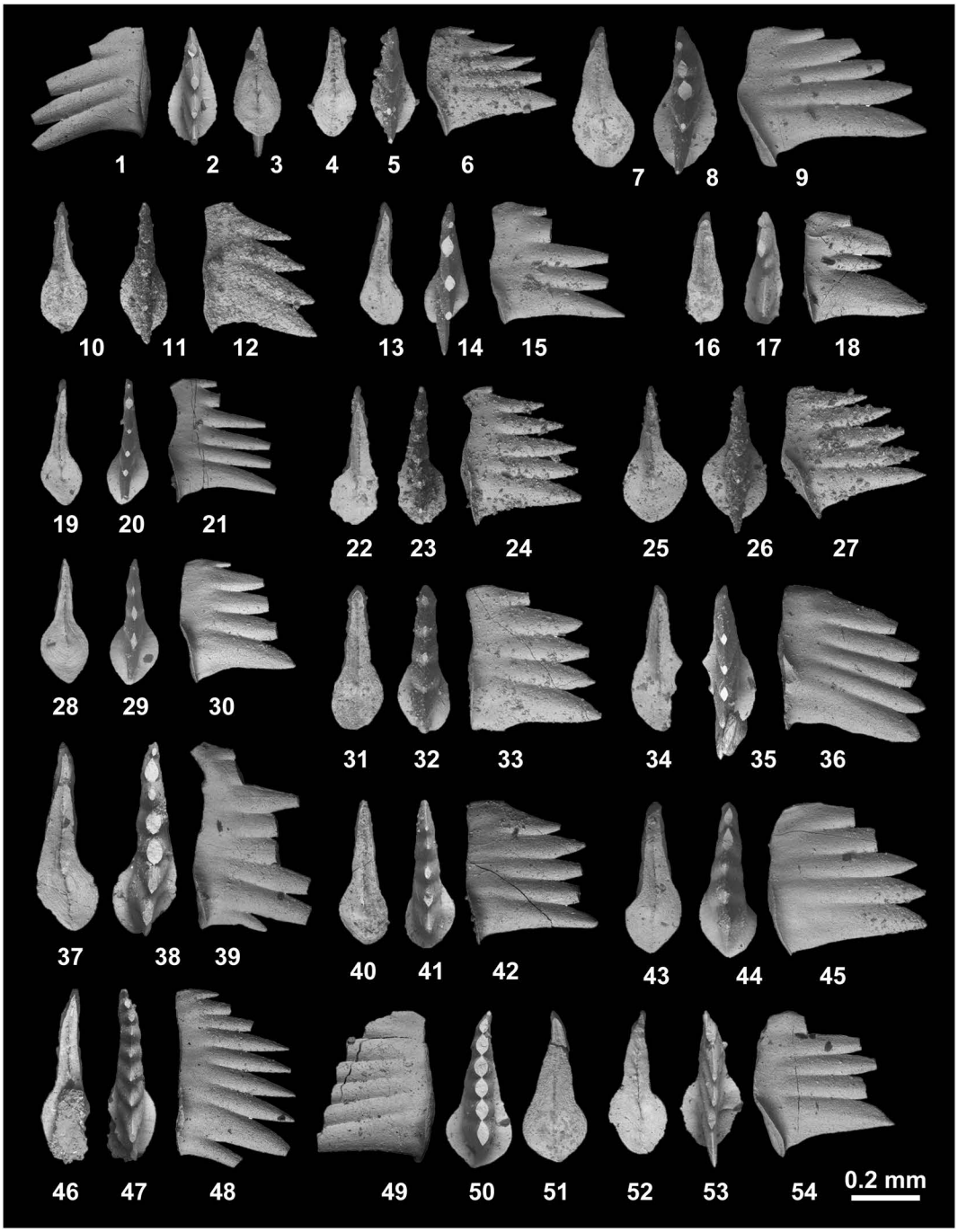

Fig. 163. *Neospathodus dieneri* Sweet, 1970a from KC02-02. 1–3, MPC25295. 4–6, MPC25296. 7–9, MPC25297. 10–12, MPC25298. 13–15, MPC25299. 16–18, MPC25300. 19–21, MPC25301. 22–24, MPC25302. 25–27, MPC25303. 28–30, MPC25304. 31–33, MPC25305. 34–36, MPC25306. 37–39, MPC25307. 40–42, MPC25308. 43–45, MPC25309. 46–48, MPC25310. 49–51, MPC25311. 52–54, MPC25312.

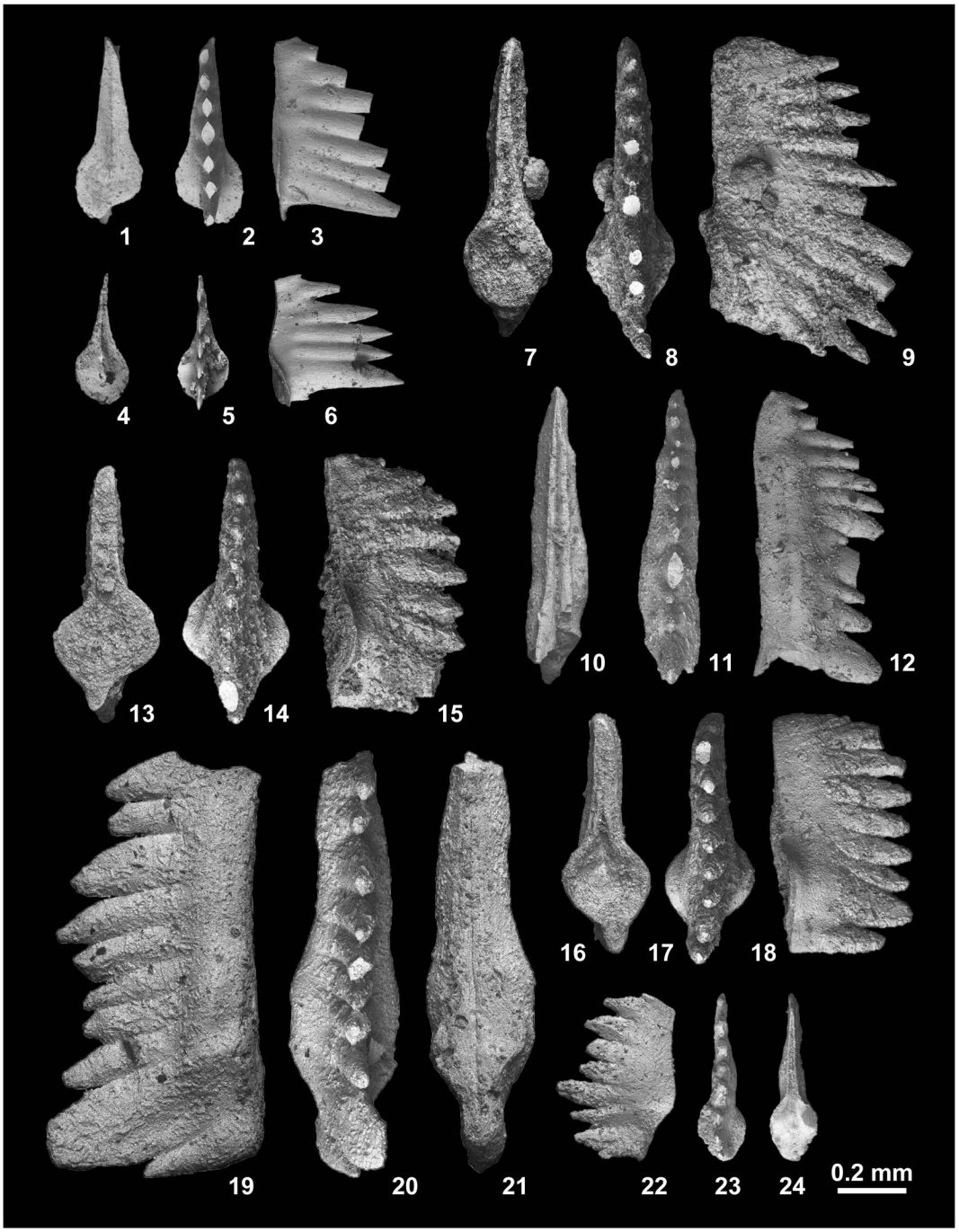

Fig. 164. 1–6, *Neospathodus dieneri* Sweet, 1970a. 1–3, MPC25313, from KC02-02. 4–6, MPC25314, from KC02-03. 7–24, *Neospathodus novaehollandiae* McTavish, 1973. 7–9, MPC25315, from BT01-03. 10–12, MPC25316, from BT01-07. 13–15, MPC25317, from BT01-10. 16–18, MPC25318, from BT01-10. 19–21, MPC25319, from BT01-10. 22–24, MPC25320, from BT01-10.

attains its maximum abundance at KC02-02 in the Bac Thuy Formation. A similar phenomenon is also reported from the *Ns. w. waageni* Subzone in the Yinkeng Formation, South China (Zhao *et al.*, 2007).

Neospathodus novaehollandiae McTavish, 1973

Figs. 164.7–164.24, 165.1–165.3

Neospathodus novaehollandiae McTavish, 1973, p. 294, figs. 4, 5, 14, 16–23; Goel, 1977, p. 1091, pl. 1, figs. 1, 2; Beyers and Orchard, 1991, pl. 5, fig. 7; Orchard, 2007b, figs. 15–18, 27, 28; Igo, 2009, p. 188, 190, figs. 153.8–153.14, 154.7–154.11, 155.1–155.11.

Material examined: One specimen, MPC25315, from BT01-03, one specimen, MPC25316, from BT01-07, four specimens, MPC25317–25320, from BT01-10, and one specimen, MPC25321, from KC01-05.

Description: Blade-like large elements 0.49–1.25 mm in length, average 0.86 mm; 0.35–0.64 mm in height, average 0.48 mm; length to height ratio 1.4–2.0, average 1.8 for seven specimens. Robust, broad, pole-like and fused denticles vary in number from 8 to 12, average 10, sub-erect or reclined posteriorly. Upper edge forms arched or straight outline. Cusp, situated in nearby posterior end, bears one to three small posterior denticles. Some specimens have a cusp twice as long as other denticles. Prominent lateral rib at middle and lower parts of element. Lower margin straight in larger element, and straight anteriorly and upturned in posterior one-third in smaller specimen (MPC25320). Rounded basal cavity expanded in posterior one-third of element. Deep furrow extends from both anterior and posterior ends.

Remarks: The element of *Neospathodus novaehollandiae* Mctavish, 1973 resembles that of *Ns. pakistanensis* Sweet, 1970b, but previous authors have already pointed out that *Ns. novaehollandiae* has a larger element, a stronger lateral rib, and a straighter lower margin than *Ns. pakistanensis*. These features enable us to distinguish the mentioned species.

Occurrence: Described specimens from BT01-03, BT01-10 and KC01-05 within the portion of the *Novispathodus* ex gr. *waageni* Zone that includes the *Flemingites rursiradiatus* beds (lowest Middle Smithian = middle Lower Olenekian) and *Urdyceras tulongensis* beds (lower Middle Smithian = middle Lower Olenekian) in the Bac Thuy Formation, northeastern Vietnam. This species also occurs in the Smithian (Lower Olenekian) in West Australia (McTavish, 1973), Spiti, India (Goel, 1977; Orchard, 2007b), British Columbia, Canada (Beyers and Orchard, 1991), and South Primorye, Russia (*Neospathodus* ex gr. *waageni-Ns. novaehollandiae* Zone with *Clypeoceras timorense* Zone and *Radioprionites abrekensis* "bed", Shigeta *et al*., 2009).

Neospathodus pakistanensis Sweet, 1970b

Fig. 165.4–165.24

Neospathodus pakistanensis Sweet, 1970b, p. 254, pl. 1, figs. 16, 17; McTavish, 1973, p. 295, pl. 1, figs. 1, 2; Buryi, 1979, p. 57, pl. 9. fig. 2; Wang and Cao, 1981, p. 367, pl. 2, fig. 27; Matsuda, 1983, p. 87, pl. 1, figs. 1–5; Tian *et al*., 1983, p. 379, pl. 81, fig. 3; Hatlebarg and Clark, 1984, pl. 1, fig. 5; Beyers and Orchard, 1991, pl. 5, fig. 2; Cao and Wang, 1993, pl. 56, fig. 14; Orchard, 2007b, figs. 19, 20, 23–26; Orchard and Krystyn, 2007, figs. 19, 20; Orchard, 2008, p. 407, figs. 8.11, 8.12; Igo, 2009, p. 190, 192, figs. 151.18–151.26, 152.1–152.7, 152.10–152.13, 152.20–152.21, 153.1–153.7, 154.1–154.6; Beranek *et al*., 2010, figs. 6.31–6.33.

Neospathodus homeri (Bender, 1970). Bui, 1989, p. 402, pl. 31, fig. 16.

Material examined: Five specimens, MPC25322–25326, from BT01-03, one specimen, MPC25327, from BT01-04, and one specimen, MPC25328, from BT01-06.

Description: Blade-like elements 0.51–0.75 mm in length, average 0.60 mm; 0.36–0.47 mm in height, average 0.35 mm; length to height ratio 1.4–2.1, average 1.7 for seven specimens. Upper edge of element straight or arched, highest point located at posterior one-third, lower edge generally straight or upward at anterior end, posterior part of lower margin

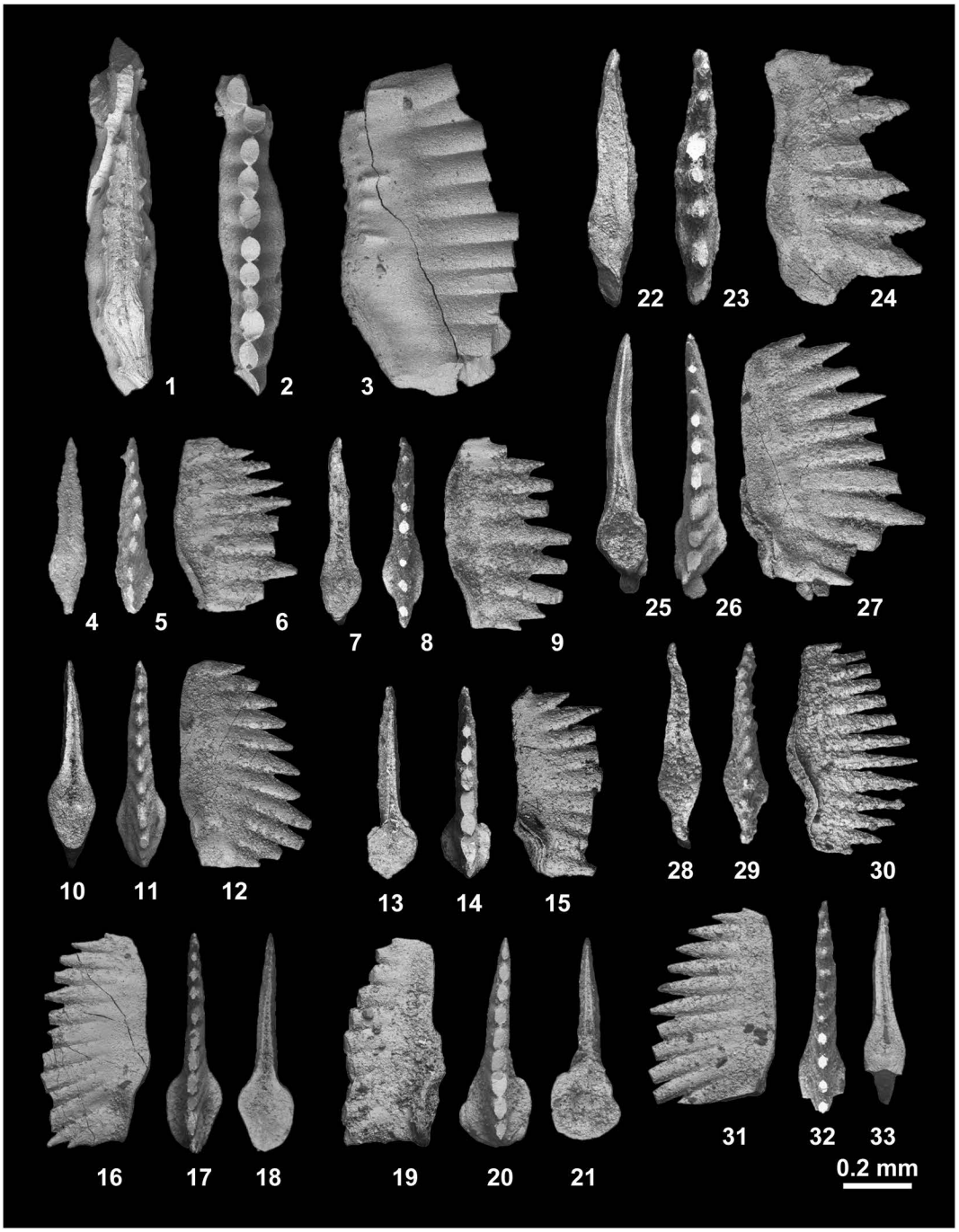

Fig. 165. 1–3, *Neospathodus novaehollandiae* McTavish, 1973, MPC25321, from KC01-05. 4–24, *Neospathodus pakistanensis* Sweet, 1970b. 4–6, MPC25322, from BT01-03. 7–9, MPC25323, from BT01-03. 10–12, MPC25324, from BT01-03. 13–15, MPC25325, from BT01-03. 16–18, MPC25326, from BT01-03. 19–21, MPC25327, from BT01-04. 22–24, MPC25328, from BT01-06. 25–33, *Neospathodus posterolongatus* Zhao and Orchard, 2007 from BT01-03. 25–27, MPC25329. 28–30, MPC25330. 31–33, MPC25331.

slightly deflected upward or slightly downturned posteriorly. Spine-like denticles vary in number from 9 to 13, average 10, erect or reclined posteriorly. Cusp bears two posterior small denticles. Rounded or sub-rounded basal cavity situated in posterior one-third. Groove extends from basal pit to anterior end.

Remarks: *Neospathodus pakistanensis* Sweet, 1970b is characterized by its blade-like element, sub-rounded basal cavity, several posterior small denticles, and a strongly downturned posterior lower margin. Although the described specimens have a slightly upturned lower posterior margin, they share many features with *Ns. pakistanensis*.

Occurrence: Described specimens from BT01-03, BT04 and BT01-06 within the portion of the *Novispathodus* ex gr. *waageni* Zone that includes the *Flemingites rursiradiatus* beds (lowest Middle Smithian = lower Lower Olenekian) in the Bac Thuy Formation, northeastern Vietnam. This species also ranges from the Upper Dienerian (upper Upper Induan) to Lower Smithian (lower Lower Olenekian) in the Salt Range, Pakistan (Zone 6, Sweet, 1970b), West Australia (McTavish, 1973), South Primorye (Buryi, 1979; *Neospathodus dieneri-Ns. pakistanensis* Zone and *Neospathodus* ex gr. *waageni-Ns. novaehollandiae* Zone with *Clypeoceras spitienze* "bed", *Paranorites varians* Zone, and *Clypeoceras timorenze* Zone, Shigeta *et al*., 2009), South China (Wang and Cao, 1981; Cao and Wang, 1993), Kashmir, India (Matsuda, 1983), Tibet (Tian *et al*., 1983), and the Mikin Formation at the Mud Section, Spiti, India (Krystyn *et al*., 2007; Orchard, 2007b; Orchard and Krystyn, 2007).

Neospathodus posterolongatus Zhao and Orchard, 2007

Figs. 165.25–165.33, 166.1–166.18

Neospathodus waageni subsp. B Zhao, 2004, p. 42, fig. 2.
Neospathodus posterolongatus Zhao and Orchard, in Zhao *et al*., 2007, p. 36, pl. 1, figs. 2A, B. C; Orchard, 2007b, figs. 1–6; Orchard, 2008, p. 407, figs. 8.3, 8.4; Beranek *et al*., 2010, figs. 6.24, 6.25.

Material examined: Four specimens, MPC25329–25332, from BT01-03, three specimens, MPC25333–25335, from BT01-04, and two specimens, MPC25336, 25337, from KC01-01.

Description: Blade-like elements 0.53–0.78 mm in length, average 0.64 mm; 0.35–0.54 mm in height, average 0.43 mm; length to height ratio 1.3–1.9, average 1.5 for nine specimens. Arched upper edge bears needle-like denticles that vary in number from 10 to 13, average 12, discrete in upper half, reclined anteriorly in anterior part, erect or inclined posteriorly in center and posterior parts, denticle size decreases both anteriorly and posteriorly. Cusp situated in posterior one-third. Lower edge straight and slightly upturned in anterior end. Ellipsoidal basal cavity extended to posterior with shallow pit. Groove runs from basal pit to anterior end.

Remarks: *Neospathodus posterolongatus* Zhao and Orchard, 2007 is distinguishable from the typical *Ns. waageni* Sweet, 1970b by the posterior elongation of the basal cavity and the presence of small secondary posterior denticles (Zhao and Orchard, 2007).

Occurrence: Described specimens from BT01-03, BT01-4, and KC01-01 within the portion of the *Novispathodus* ex gr. *waageni* Zone that includes the *Flemingites rursiradiatus* beds (lowest Middle Smithian = middle Lower Olenekian) in the Bac Thuy Formation, northeastern Vietnam.

The first appearance datum (FAD) of *Neospathodus posterolongatus* in the Yingkeng Formation at the West Pingdingshan Section, South China is situated 3 cm below the FAD of the ammonoids *Flemingites* and *Euflemingites*, which indicates the Induan/Olenekian Boundary (IOB) of this formation. This evidence suggests that *Ns. posterolongatus* may have age diagnostic potential for the IOB (Zhao *et al*., 2007). In addition, this species co-occurs with *Ns*. ex gr. *waageni* Morphotype 1, whose

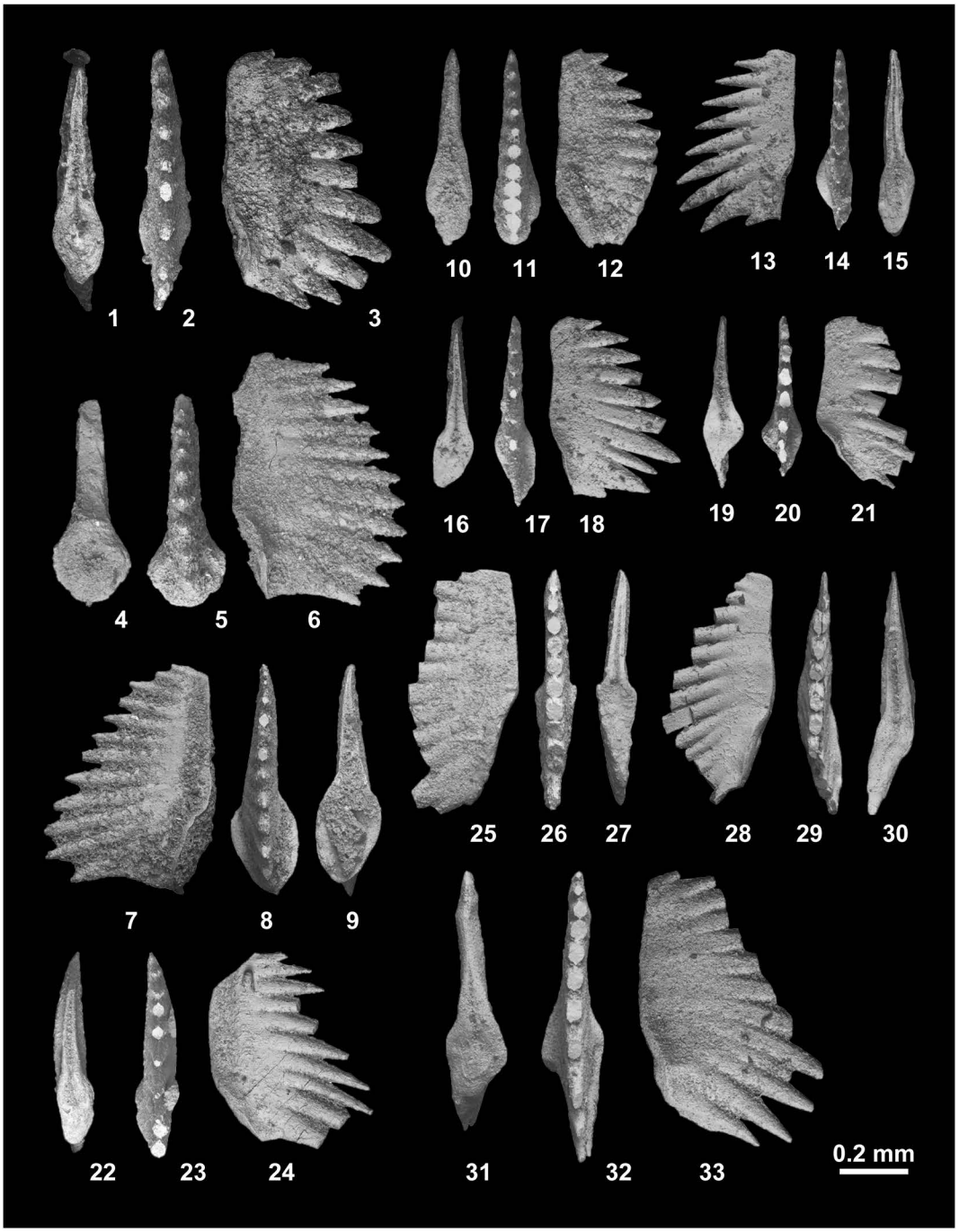

Fig. 166. 1–18, *Neospathodus posterolongatus* Zhao and Orchard, 2007. 1–3, MPC25332, from BT01-03. 4–6, MPC25333, from BT01-04. 7–9, MPC25334, from BT01-04. 10–12, MPC25335, from BT01-04. 13–15, MPC25336, from KC01-01. 16–18, MPC25337, from KC01-01. 19–33, *Neospathodus spitiensis* Goel, 1977. 19–21, MPC25338, from BT01-03. 22–24, MPC25339, from BT01-03. 25–27, MPC25340, from BT01-03. 28–30, MPC25341, from BT01-03. 31–33, MPC25342, from BT01-04.

FAD defines the IOB in the Mianwali Formation of Spiti, India (Krystyn *et al*., 2007; Orchard and Krystyn, 2007).

This species also ranges from the Upper Dienerian (upper Upper Induan) to Lower Smithian (lower Lower Olenekian) in the Yingkeng Formation, South China (*Neospathodus waageni eowaageni* Subzone and lower part of *Neospathodus waageni waageni* Subzone with uppermost part of *Prionolobus-Gyronites* Zone and lower part of *Flemingites-Euflemingites* Zone, Zhao *et al.*, 2007), the Mikin Formation in the Mud section, Spiti, India (*Neospathodus waageni* sensu lato Zone and *Neospathodus waageni* sensu stricto Zone with *Rohillites rohilla* Zone, Krystyn *et al*., 2007; Orchard, 2007b), in British Columbia, Canada (Beranek *et al*., 2010), and the Canadian Arctic (*Euflemingites romunderi* Zone, Orchard, 2008).

Neospathodus spitiensis Goel, 1977

Figs. 166.19–166.33, 167–169, 170.1–170.6

Neospathodus spitiensis Goel, 1977, p. 1094, pl. 1, figs. 14–18; Duan, 1987, pl. 2, fig. 19; Orchard and Krystyn, 2007, figs. 23, 24; Igo, 2009, p. 194, figs. 156.1–156.6, 156.21–156.22.

Neospathodus homeri (Bender, 1970). Bui, 1989, p. 402, pl. 31, fig. 15.

Material examined: Four specimens, MPC25338–25341, from BT01-03, two specimens, MPC25342, 25343, from BT01-04, nineteen specimens, MPC25344–25362, from BT01-07, five specimens, MPC25363–25367, from BT01-10, two specimens, MPC25368, 25369, from BT01-12, one specimen, MPC25370, from BT02-01, one specimen, MPC25371, from KC01-01, three specimens, MPC25372–25374, from KC01-04, two specimens, MPC25375, 25376, from KC01-05, and one specimen, MPC25377, from KC01-06.

Description: Laterally compressed segminate elements 0.38–0.81 mm in length, average 0.60 mm; 0.35–0.60 mm in height, average 0.45 mm; length to height ratio 0.9–2.2, average 1.3 for forty specimens. Upper part of element arched and consists of laterally compressed, fairly discrete denticles. Denticles vary in number from 8 to 13, average 10, suberect or reclined anteriorly, gradually inclined to posterior end. Cusp situated in posterior one-third with 2 to 4 small posterior denticles. Some specimens have a large triangular shaped process at posterior end. Basal margin straight or almost upturned in anterior part, and upturned 10–40 degrees in posterior part. Anterior part occupies more than half of element. Sub-triangular or sub-rounded basal cavity unexpanded in general, and gradually narrows toward posterior end. Groove extends from anterior end to posterior end.

Remarks: *Neospathodus spitiensis* Goel, 1977 is characterized by its arched element with mostly discrete denticles, upturned basal margin of posterior one-third to half, and narrow triangular shaped basal cavity, which extends posteriorly (Goel, 1977; Orchard and Krystyn, 2007). Igo (2009) reported that some specimens of this species have a posteriorly extended elliptical basal cavity. The described specimens exhibit a wide range of intraspecific variation in basal cavity form and denticulation, but they also include similar forms reported by previous authors. Some specimens have a large triangular process, which has never been reported.

Occurrence: Described specimens from BT01-03, BT01-04, BT01-07, BT01-10, BT01-12, BT02-01, KC01-01, KC01-04, KC01-05 and KC01-06 within the portion of the *Novispathodus* ex gr. *waageni* Zone that includes the *Flemingites rursiradiatus* beds (lowest Middle Smithian = middle Lower Olenekian) and *Urdyceras tulongensis* beds (lower Middle Smithian = middle Lower Olenekian) in the Bac Thuy Formation, northeastern Vietnam. This species also occurs in the Lower Smithian (lower Lower Olenekian) in Spiti, India (Goel, 1977; Krystyn *et al*., 2007; Orchard and Krystyn, 2007), South China (Duan, 1987; Zhao *et al*., 2007), and South Primorye, Russia (Igo, 2009).

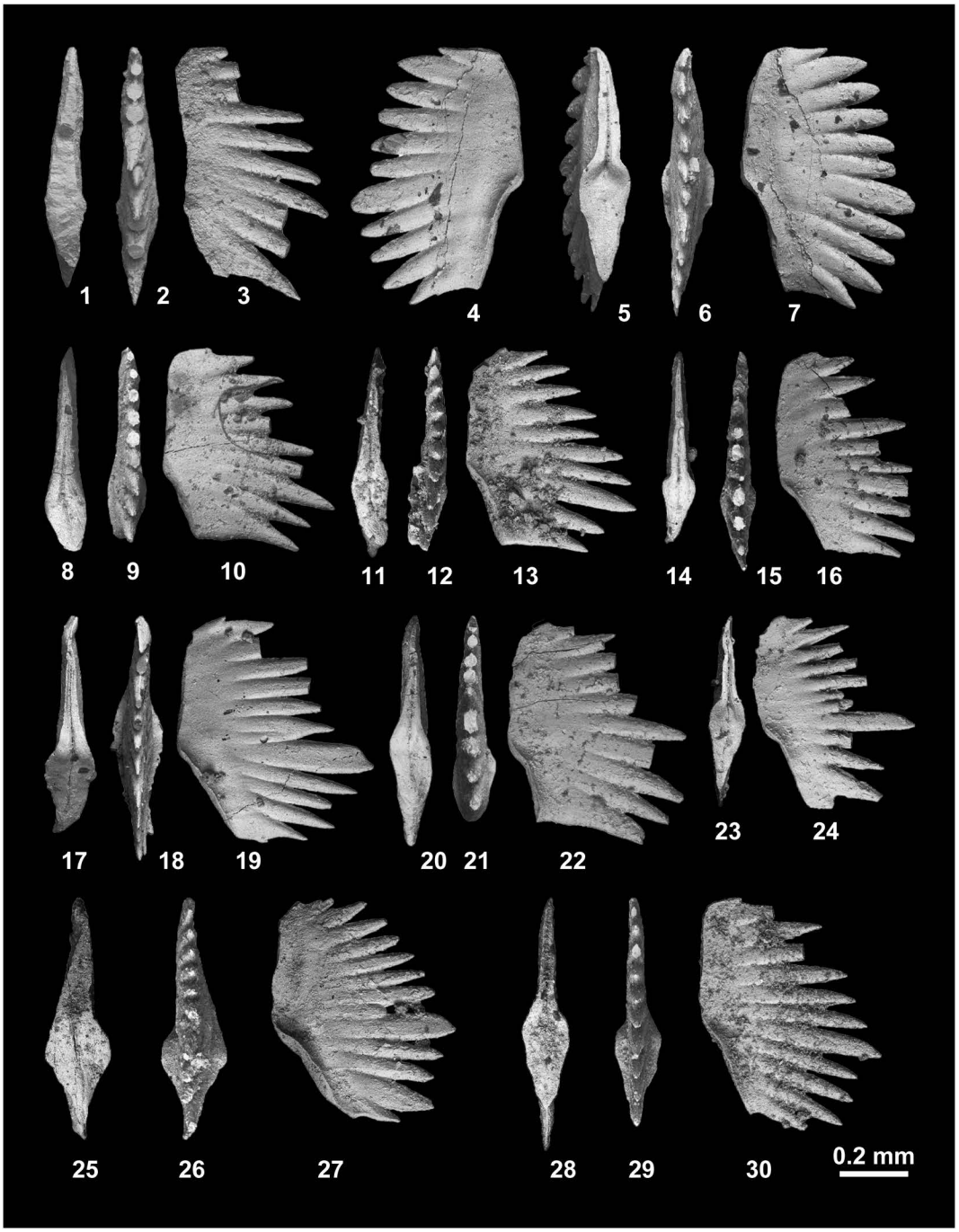

Fig. 167. *Neospathodus spitiensis* Goel, 1977. 1–3, MPC25343, from BT01-04. 4–7, MPC25344, from BT01-07. 8–10, MPC25345, from BT01-07. 11–13, MPC25346, from BT01-07. 14–16, MPC25347, from BT01-07. 17–19, MPC25348, from BT01-07. 20–22, MPC25349, from BT01-07. 23–24, MPC25350, from BT01-07. 25–27, MPC25351, from BT01-07. 28–30, MPC25352, from BT01-07.

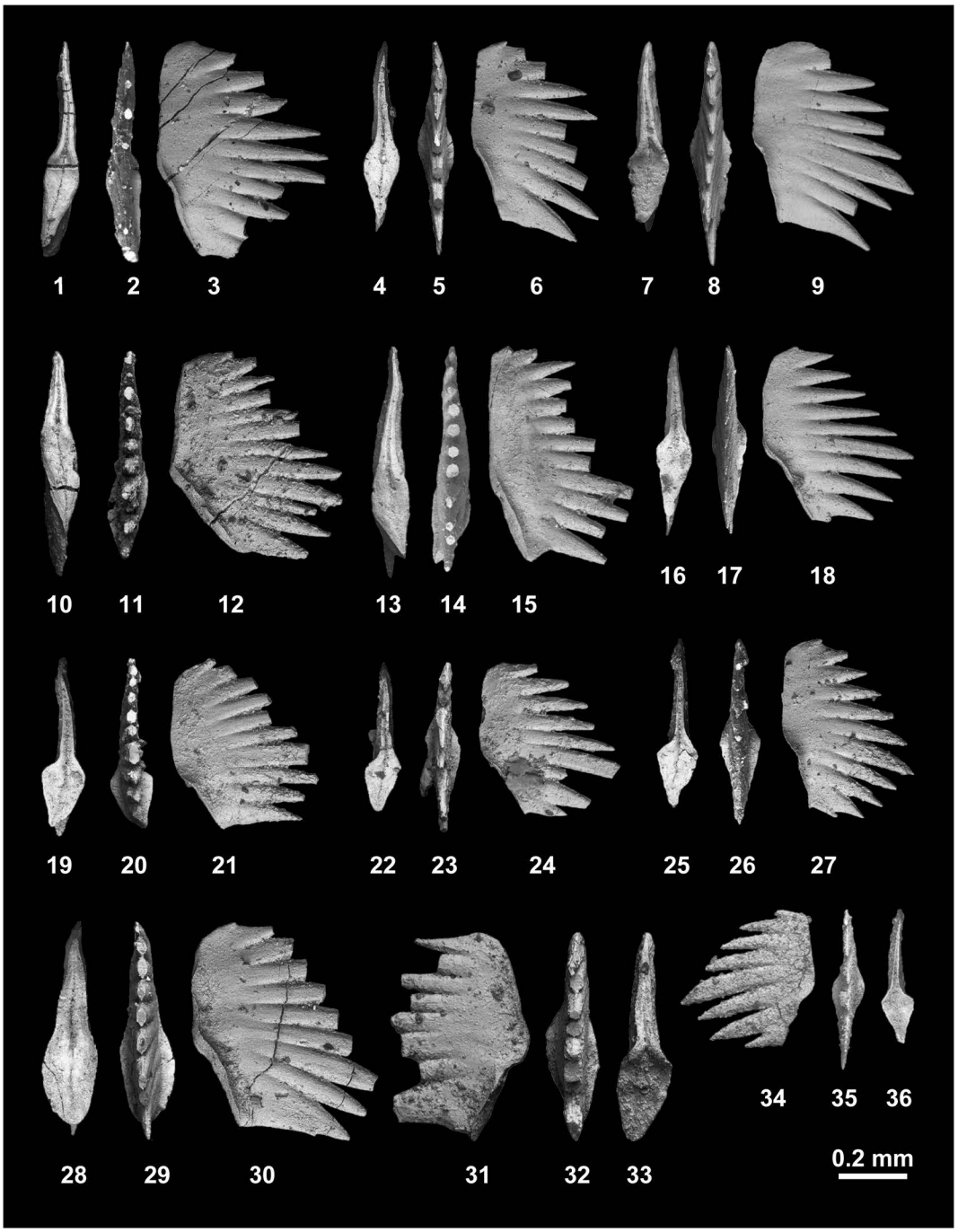

Fig. 168. *Neospathodus spitiensis* Goel, 1977. 1–3, MPC25353, from BT01-07. 4–6, MPC25354, from BT01-07. 7–9, MPC25355, from BT01-07. 10–12, MPC25356, from BT01-07. 13–15, MPC25357, from BT01-07. 16–18, MPC25358, from BT01-07. 19–21, MPC25359, from BT01-07. 22–24, MPC25360, from BT01-07. 25–27, MPC25361, from BT01-07. 28–30, MPC25362, from BT01-07. 31–33, MPC25363, from BT01-10. 34–36, MPC25364, from BT01-10.

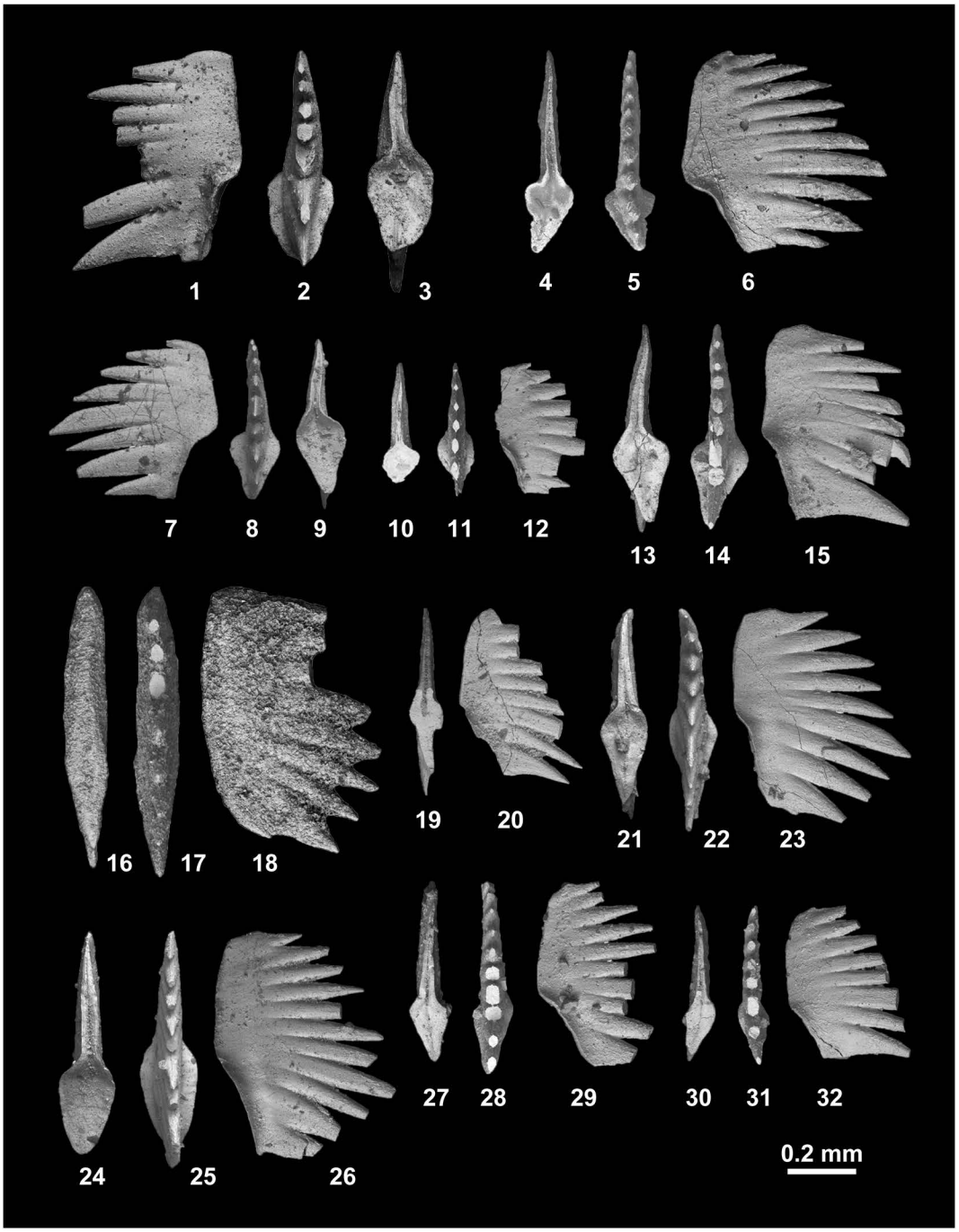

Fig. 169. *Neospathodus spitiensis* Goel, 1977. 1–3, MPC25365, from BT01-10. 4–6, MPC25366, from BT01-10. 7–9, MPC25367, from BT01-10. 10–12, MPC25368, from BT01-12. 13–15, MPC25369, from BT01-12. 16–18, MPC25370, from BT02-01. 19–20, MPC25371, from KC01-01. 21–23, MPC25372, from KC01-04. 24–26, MPC25373, from KC01-04. 27–29, MPC25374, from KC01-04. 30–32, MPC25375, from KC01-05.

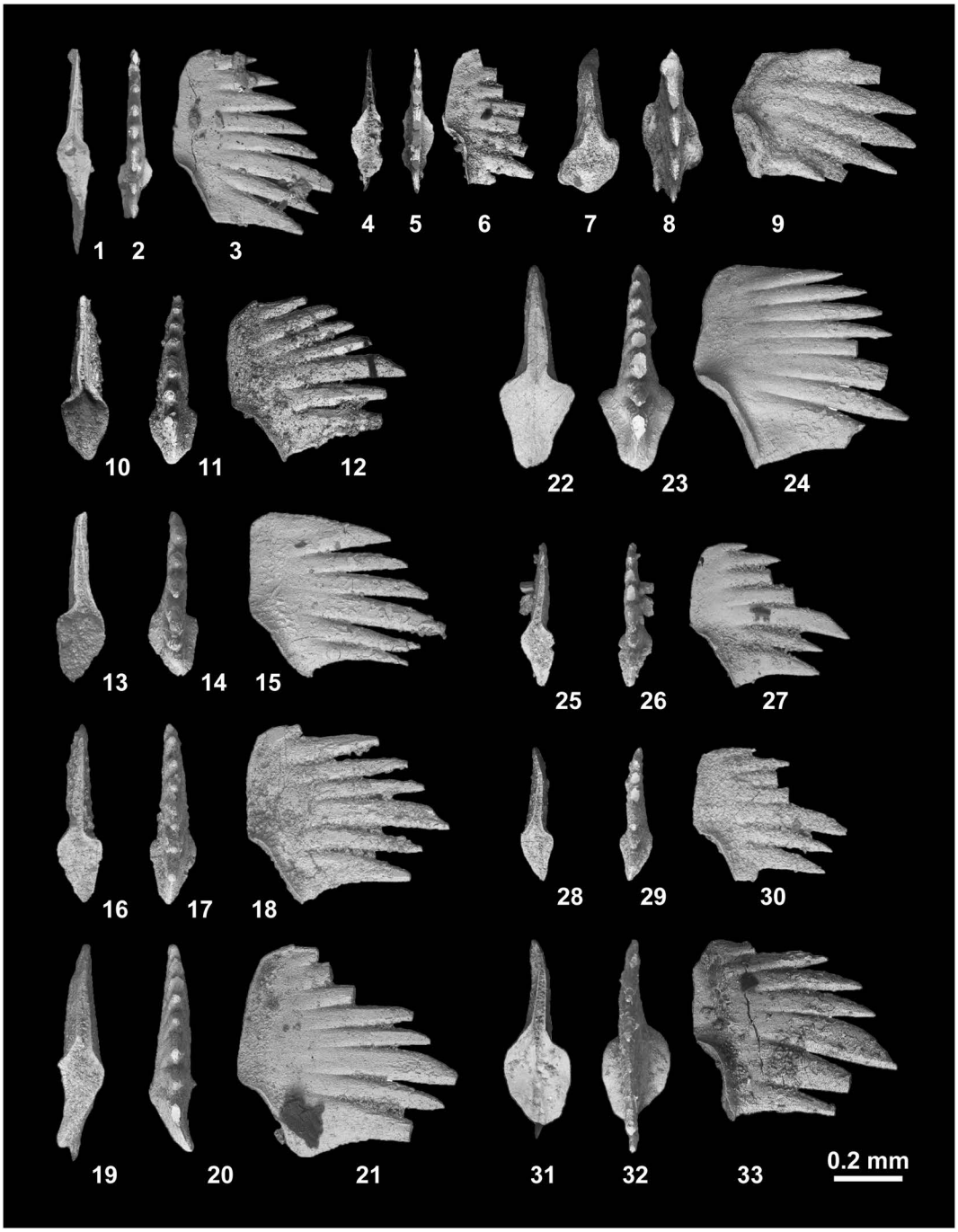

Fig. 170. 1–6, *Neospathodus spitiensis* Goel, 1977. 1–3, MPC25376, from KC01-05. 4–6, MPC25377, from KC01-06. 7–33, *Neospathodus* sp. indet. A. 7–9, MPC25378, from BT01-03. 10–12, MPC25379, from BT01-06. 13–15, MPC25380, from BT01-10. 16–18, MPC25381, from BT01-10. 19–21, MPC25382, from BT01-12. 22–24, MPC25383, from BT01-12. 25–27, MPC25384, from BT01-12. 28–30, MPC25385, from BT01-14. 31–33, MPC25386, from KC01-13.

The first appearance datum of this species is located in bed 15 of the Muth section in Spiti (Orchard and Krystyn, 2007; Krystyn *et al.*, 2007) and bed 26 of the West Pingdingshang section in Anhui Province, South China (Zhao *et al*., 2007), both of which correspond to the *Flemingites-Euflemingites* Zone of the Smithian (Orchard and Krystyn, 2007; Orchard, 2010).

Neospathodus sp. indet. A

Fig. 170.7–170.33

Material examined: One specimen, MPC25378, from BT01-03, one specimen, MPC25379, from BT01-06, two specimens, MPC25380, 25381, from BT01-10, three specimens, MPC25382–25384, from BT01-12, one specimen, MPC25385, from BT01-14, and one specimen, MPC25286, from KC01-13.

Description: Segminate elements 0.39–0.62 mm in length, average 0.50 mm; 0.45–0.65 mm in height, average 0.56 mm; length to height ratio 0.7–0.9, average 0.9 for nine specimens. Lateral profile of elements exhibits chevron-like form, with arched upper edge. Reclined slender denticles vary in number from 6 to 9, average 7. Cusp situated in center of element, size twice as large as other denticles. Large terminal process exhibits a triangular shape. Lower edge straight or almost upturned in anterior half, and upturned 15–40 degrees in posterior half. Outline of expanded basal cavity triangular. Anterior furrow extends to basal pit.

Remarks: The described specimen is very close to *Neospathodus spitiensis* Goel, 1977 in having a triangular terminal process at the posterior end and a triangular basal cavity, whose height is greater than its length, but differs by its vertical long element and a slightly fewer number of denticles.

Occurrence: Described specimens from BT01-03, BT01-06, BT01-10, BT01-12, BT01-14 and KC01-13 within the portion of the *Novispathodus* ex gr. *waageni* Zone that includes the *Flemingites rursiradiatus* beds (lowest Middle Smithian = middle Lower Olenekian), *Urdyceras tulongensis* beds (lower Middle Smithian = middle Lower Olenekian) and *Leyeceras* horizon of the *Owenites koeneni* beds (middle Middle Smithian = middle Lower Olenekian) in the Bac Thuy Formation, northeastern Vietnam.

Neospathodus sp. indet. B

Fig. 171.1–171.3

Material examined: One specimen, MPC25387, from BT01-04.

Description: Blade-like segminate element 0.77 mm in length; 0.48 mm in height; length to height ratio 1.6. Lateral form of element rectangular with arched upper edge and slightly bowed lower edge. Pointed slender denticles total 10 in number, discrete in upper half and fused in lower half, gradually reclined posteriorly. Large-sized terminal cusp triangular in shape. Elliptical basal cavity situated at posterior end. Narrow groove extends to anterior end.

Remarks: The described specimen is very close to *Neospathodus pakistanensis* Sweet, 1970b in having a rectangular lateral shape and elliptical basal cavity, but differs by its triangular shaped terminal cusp.

Occurrence: Described specimen from BT01-04 within the portion of the *Novispathodus* ex gr. *waageni* Zone represented by the *Flemingites rursiradiatus* beds (lowest Middle Smithian = middle Lower Olenekian) in the Bac Thuy Formation, northeastern Vietnam.

Neospathodus sp. indet. C

Fig. 171.4–171.6

Material examined: One specimen, MPC25388, from KC01-11.

Remarks: The specimen is characterized by its strongly reclined, laterally compressed denticles, which are discrete in the upper two-thirds. The form in lower view is slightly sigmoidal, and the width of the element is longer

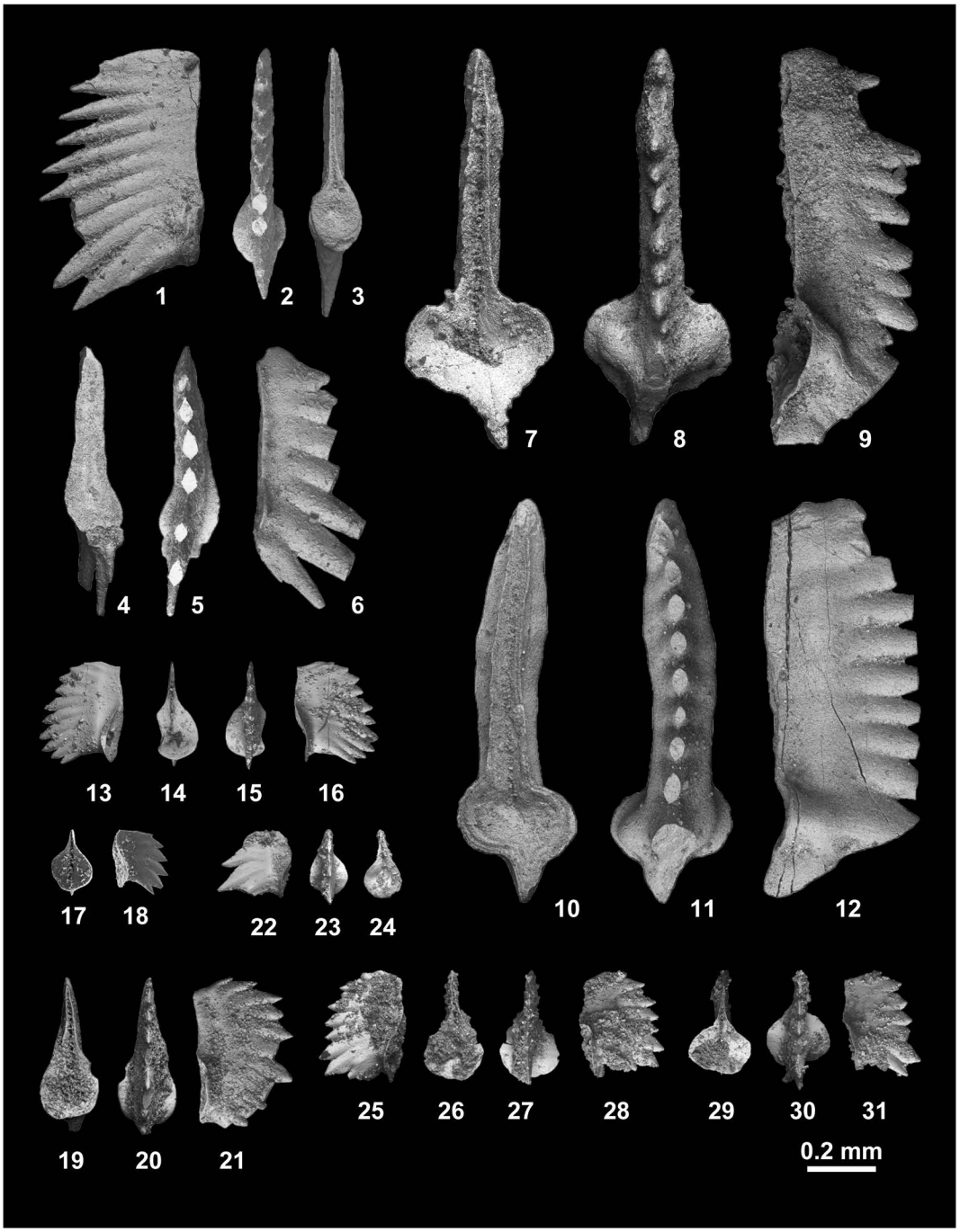

Fig. 171. 1–3, *Neospathodus* sp. indet. B, MPC25387, from BT01-04. 4–6, *Neospathodus* sp. indet. C, MPC25388, from KC01-11. 7–12, *Smithodus longiusculus* (Buryi, 1979). 7–9, MPC25389, from BT01-07. 10–12, MPC25390, from KC01-01. 13–31, *Novispathodus pingdingshanensis* (Zhao and Orchard, 2007). 13–16, MPC25391, from KC02-08. 17–18, MPC25392, from KC02-10. 19–21, MPC25393, from KC02-12. 22–24, MPC25394, from KC01-17. 25–28, MPC25395, from NT01-07. 29–31, MPC25396, from NT01-07.

than other species of *Neospathouds*. It is close to *Ns.* sp. nov. S by Orchard (2008), but differs by its lack of the terminal largest cusp and the rhomboidal outline of its basal cavity.

Occurrence: Described specimen from KC01-11 within the portion of the *Novispathodus* ex gr. *waageni* Zone represented by the *Leyeceras* horizon of the *Owenites koeneni* beds (middle Middle Smithian = middle Lower Olenekian) in the Bac Thuy Formation, northeastern Vietnam.

Genus ***Smithodus*** Budurov, Buryi and Sudar, 1988

Type species: *Neospathodus longiusculus* Buryi, 1979.

Smithodus longiusculus (Buryi, 1979)

Fig. 171.7–171.12

Anchignathodus sp. A, Mosher, 1973, p. 152, pl. 17, fig. 1.
Neospathodus longiusculus Buryi, 1979, p. 58, pl. 12, fig. 1, pl. 13, fig. 1, pl. 14, fig. 1.
Smithodus longiusculus (Buryi, 1979). Buryi, 1997, pl. 1, figs. 1, 2; Orchard, 2007a, fig. 2.

Material examined: One specimen, MPC25389, from BT01-07, and one specimen, MPC25390, from KC01-01.

Description: Two rectangular blade-like elements 1.16–1.17 mm in length; 0.45–0.46 mm in height; length to height ratio 2.5–2.6. Long, straight, and thin blade bears short node-like denticles totaling 12 and 15 in number, erect or reclined posteriorly. Cusp situated near posterior end. Basal margin straight, slightly upturned in anterior end, downturned in posterior one-fourth. Specimen (MPC25390) has prominent lateral rib. Wide, large, sub-rounded basal cavity situated below cusp, extends to posterior end, strongly concave. Deep broad furrow extends from anterior end to posterior end.

Occurrence: Described specimens collected from BT01-07 and KC01-01 within the *Novispathodus* ex gr. *waageni* Zone in the Bac Thuy Formation, northeastern Vietnam. BT01-07 is located between the *Flemingites rursiradiatus* beds (lowest Middle Smithian = middle Lower Olenekian) and *Urdyceras tulongensis* beds (lower Middle Smithian = middle Lower Olenekian). KC01-01 is located beneath the *Owenites koeneni* beds (middle Middle Smithian = middle Lower Olenekian). Mosher (1973) reported the occurrence of *Smithodus longiusculus* in the *Euflemingites romunderi* Zone (Middle Smithian) in Canada, and Buryi (1979) described the species from the *Anasibirites nevolini* Zone (Upper Smithian). Thus, this species ranges from the middle to Upper Smithian.

Subfamily Novispathodinae Orchard, 2005

Genus ***Novispathodus*** Orchard, 2005

Type species: *Novispathodus abruptus* (Orchard, 1995).

Novispathodus pingdingshanensis (Zhao and Orchard, 2007)

Fig. 171.13–171.31

Neospathodus pingdingshanensis Zhao and Orchard, 2007, in Zhao *et al*., 2007, p. 36, pl. 1, figs. 4A, B, C; Ji *et al.*, 2011, figs. 4.7–4.9; Liang *et al*., 2011, figs. 1–3.
multielement apparatuses, *Novispathodus pingdingshanensis* (Zhao and Orchard, 2007). Goudemand and Orchard (in Goudemand *et al*., 2012), p. 1030, figs. 2B, F, I, J, M, Q, AD, 3T, U, 6.

Material examined: One specimen, MPC25391, from KC02-08, one specimen, 25392, from KC02-10, one specimen, MPC25393, from KC02-12, one specimen, MPC25394, from KC02-17, and two specimens, MPC25395, 25396, from NT01-07.

Description: Small segminate elements 0.19–0.44 mm in length, average 0.30 mm; 0.17–0.29 mm in height, average 0.24 mm; length to height ratio 1.1–1.5, average 1.2 for six specimens. Arched upper edge bears mostly fused, triangular-shaped denticles, varying in number from 4 to 12, average 8, reclined posteriorly. Cusp situated in posterior one-

third with a few small posterior denticles. Basal margin straight or upturned in anterior. Large broadly expanded oval or sub-rounded basal cavity upturned on inner margin, flat to downturned on outer margin, and occupying more than half of basal margin with deep pit. Groove extends to anterior end.

Remarks: The described specimens include the juveniles (MPC25392, MPC25394), whose sizes are one-half of the others. However, the feature whereby the large basal cavity exceeds more than half of the length of element is common in all specimens.

Occurrence: Described specimens from KC02-08, KC02-10 and NT01-07 within the portion of the *Novispathodus pingdingshanensis* Zone represented by the *Xenoceltites variocostatus* beds (Upper Smithian=upper Lower Olenekian), and those from KC02-12 and KC02-17 within the portion of the *Triassospathodus symmetricus* Zone that includes the *Tirolites* cf. *cassianus* beds (lowest Lower Spathian=lowest Upper Olenekian) and *Tirolites* sp. nov. beds (Lower Spathian=lower Upper Olenekian) in the Bac Thuy Formation, northeastern Vietnam. This species also occurs in South China (Zhao *et al*., 2007; Ji *et al*., 2011; Liang *et al*., 2011; Goudemand *et al*., 2012).

Zhao and Orchard (in Zhao *et al*, 2007) originally described this species as *Neospathodus* from Chaohu, Anhui Province, South China and defined the *Ns. pingdingshanensis* (=*Novispathodus pingdingshanensis*) Zone in the Yinkeng Formation (Zhao *et al*., 2007). The zone extends from just above the *Ns. waageni* Zone to the base of the *Ns. homeri* Zone. Previous authors (Zhao *et al*., 2007; Liang *et al*., 2011) have suggested that *Nv. pingdingshanensis* is a zonal-index taxon for the lowermost Lower Spathian based on the evidence that ammonoids defining the base of the Spathian co-occur with this species. However, the species also occurs with *Xenoceltites variocostatus*, which is an index ammonoid for the Upper Smithian (Goudemand *et al*., 2012 and this study) in South China and northeastern Vietnam. This fact suggests that the FAD of *Nv. pingdingshanensis* occurs in the Upper Smithian.

Novispathodus triangularis (Bender, 1970)

Figs. 172, 173, 174.1–174.30

Neospathodus cristagalli (Huckriede, 1958). Mosher, 1968, p. 930, pl. 115, fig. 2.

Spathognathodus triangularis Bender, 1970, p. 530, pl. 5, figs. 22a, b.

Neospathodus biangularis Z. H. Wang and Cao, 1981, p. 367, pl. 2, figs. 22, 23; Wang and Cao, 1993, pl. 56, fig. 15.

Neospathodus triangularis (Bender, 1970). Sweet, 1970b, p. 253, pl. 1, figs. 7, 8; Goel, 1977, p. 1097, pl. 2, figs. 12, 13; Solien, 1979, p. 304, pl. 3, fig. 7; Koike, 1981, pl. 1, fig. 6; Duan *et al*., 1983, p. 380, pl. 97, figs. 3a, b; Matsuda, 1983, pp. 93–94, pl. 3, figs. 5–9; Wang and Zhong, 1994, pl. 1, figs. 1, 2, 6, 10; Orchard, 1995, p. 116, 118, figs. 3.–3.4; Lucas and Orchard, 2007, figs. 10–12; Ji *et al*., 2011, figs. 3.7, 3.11.

Neospathodus curtatus Orchard, 1995, p. 119, figs. 3.8–3.13.

Material examined: One specimen, MPC25397, from KC02-14, and thirty-four specimens, MPC25398–25431, from KC02-15.

Description: P_1 element: Trapezoidal-shaped, small segminate elements 0.37–0.57 mm in length, average 0.45 mm; 0.27–0.38 mm in height, average 0.33 mm; 0.16–0.35 mm, average 0.22 mm in width; length to height ratio 1.2–1.7, average 1.4 for thirty-three specimens. Arched upper edge bears erect or radial, small, fused, spine-like denticles varying in number from 10 to 14, average 12. Cusp situated from center to posterior of element. Denticle size gradually decreases from cusp to both anterior and posterior ends. Lower edge consists of straight or concave anterior part and strongly downturned posterior margin. Sub-triangular or sub-quadrangular, strongly concave basal cavity occupies posterior one-third to one-half length of element. Groove extends from basal pit to anterior end.

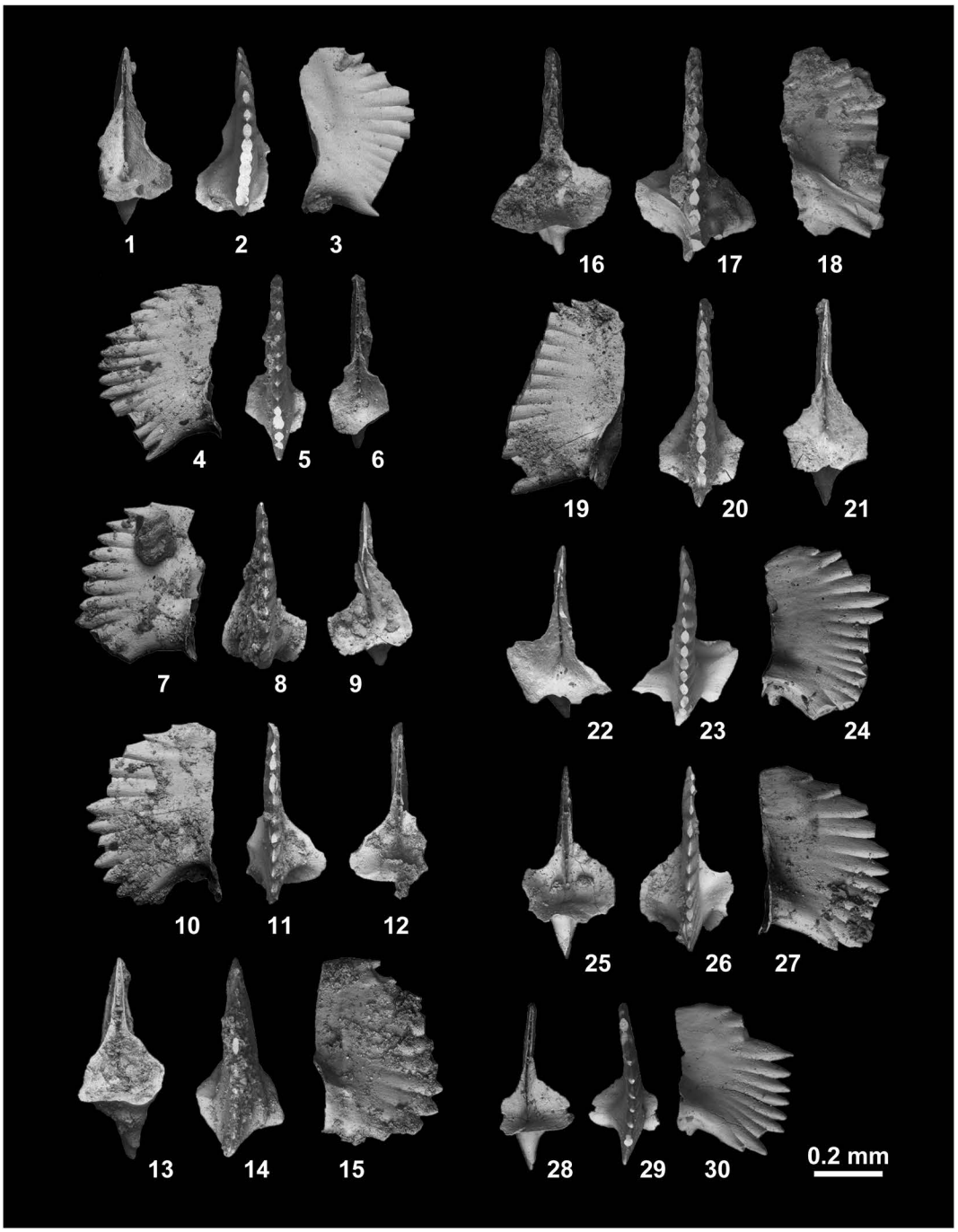

Fig. 172. *Novispathodus triangularis* (Bender, 1970), P_1 element. 1–3, MPC25397, from KC02-14. 4–6, MPC25398, from KC02-15. 7–9, MPC25399, from KC02-15. 10–12, MPC25400, from KC02-15. 13–15, MPC25401, from KC02-15. 16–18, MPC25402, from KC02-15. 19–21, MPC25403, from KC02-15. 22–24, MPC25404, from KC02-15. 25–27, MPC25405, from KC02-15. 28–30, MPC25406, from KC02-15.

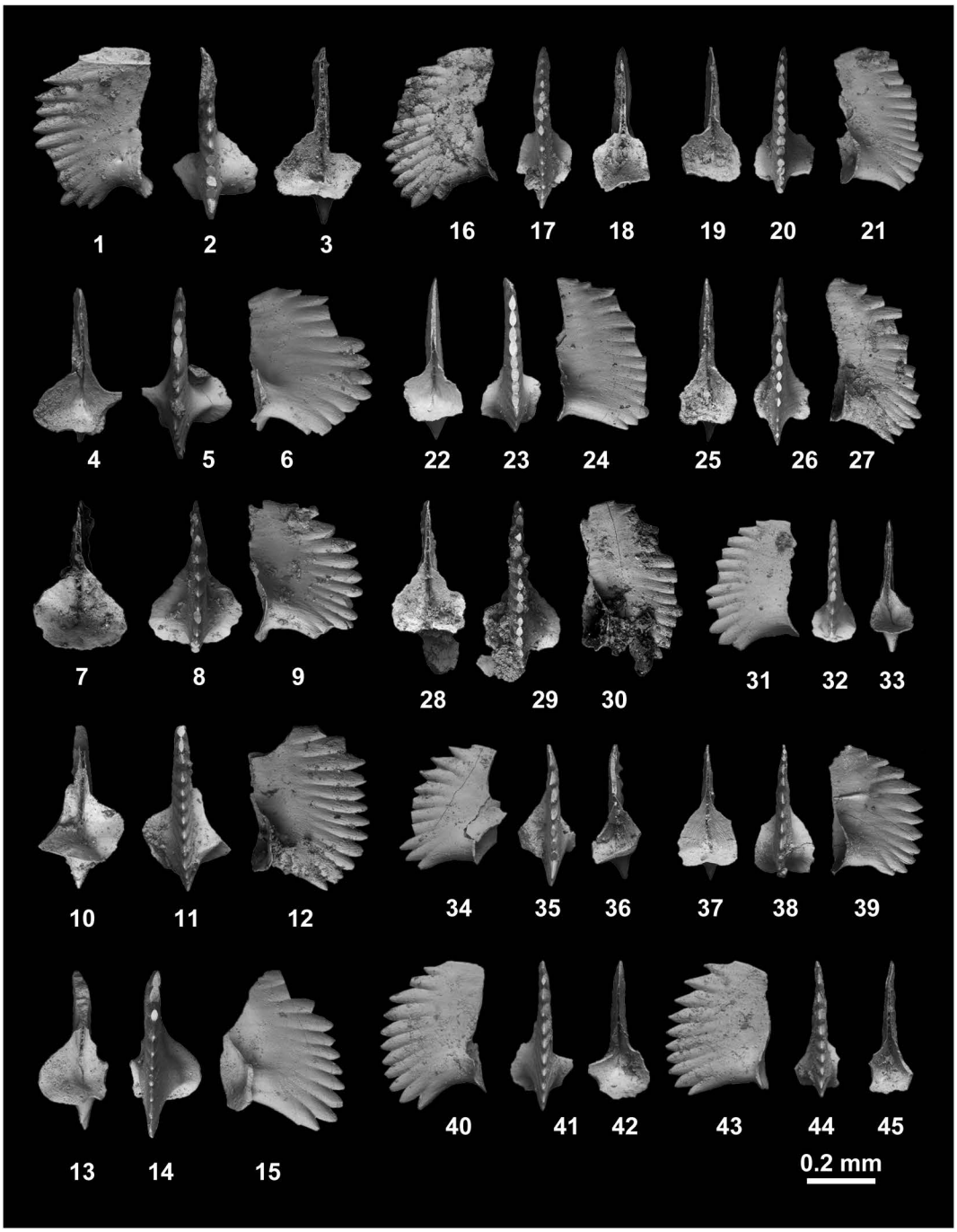

Fig. 173. *Novispathodus triangularis* (Bender, 1970), P_1 element, from KC02-15. 1–3, MPC25407. 4–6, MPC25408. 7–9, MPC25409. 10–12, MPC25410. 13–15, MPC25411. 16–18, MPC25412. 19–21, MPC25413. 22–24, MPC25414. 25–27, MPC25415. 28–30, MPC25416. 31–33, MPC25417. 34–36, MPC25418. 37–39, MPC25419. 40–42, MPC25420. 43–45, MPC25421.

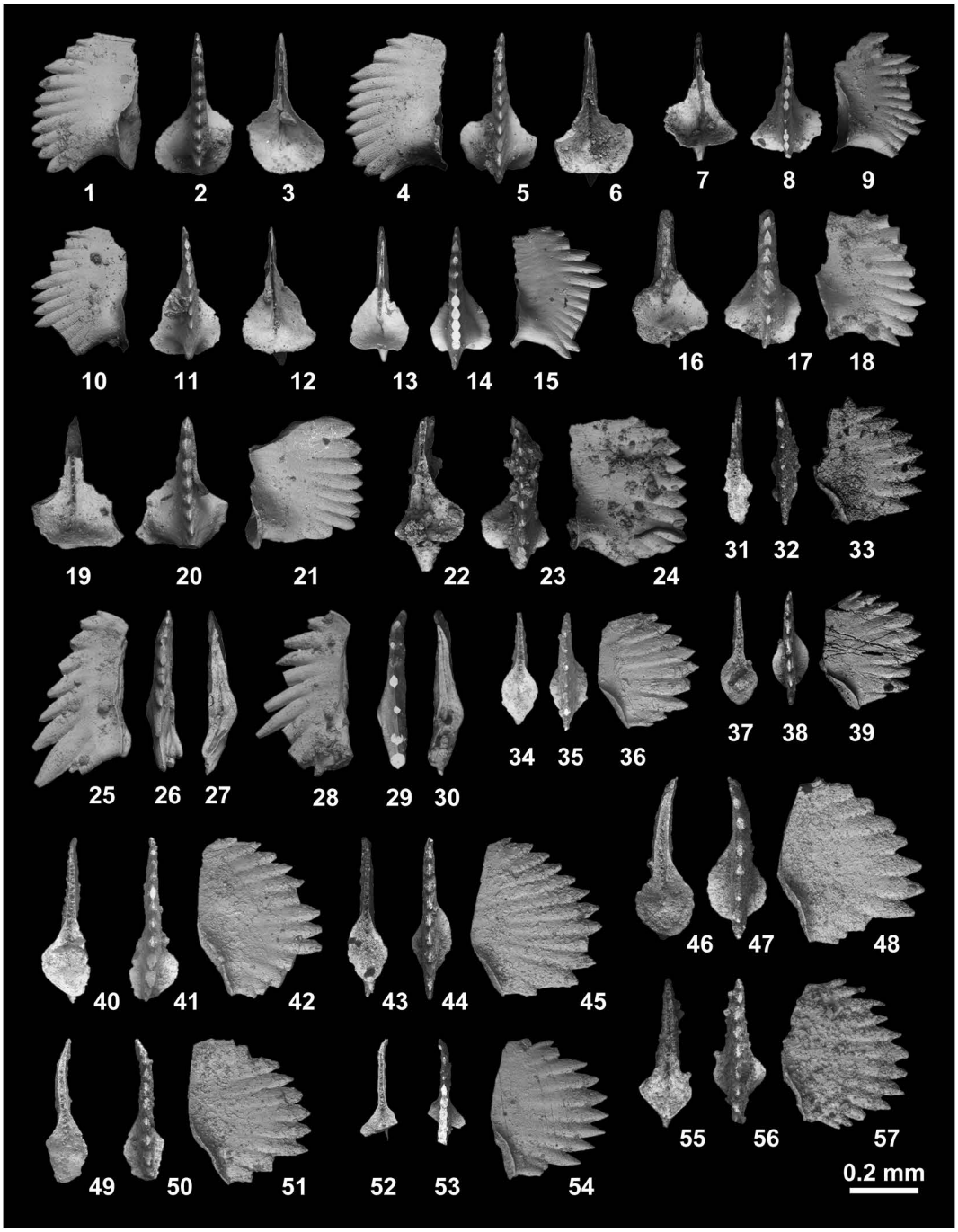

Fig. 174. 1–30, *Novispathodus triangularis* (Bender, 1970) from KC02-15. 1–3, P_1 element, MPC25422. 4–6, P_1 element, MPC25423. 7–9, P_1 element, MPC25424. 10–12, P_1 element, MPC25425. 13–15, P_1 element, MPC25426. 16–18, P_1 element, MPC25427. 19–21, P_1 element, MPC25428. 22–24, P_1 element, MPC25429. 25–27, P_2 element, MPC25430. 28–30, P_2 element, MPC25431. 31–57, *Novispathodus* ex gr. *waageni* (Sweet, 1970b) from BT01–03. 31–33, MPC25432. 34–36, MPC25433. 37–39, MPC25434. 40–42, MPC25435. 43–45, MPC25436. 46–48, MPC25437. 49–51, MPC25438. 52–54, MPC25439. 55–57, MPC25440.

P_2 element: Two laterally compressed, triangular-shaped segminate elements 0.49–0.52 mm in length; 0.29 mm in height; length to height ratio 1.7–1.8. Broad denticles total 10 in number. Size and inclination of denticles gradually increase toward posterior end. Posterior terminal cusp bears 1 or 2 small denticles. Basal margin of element bowed. Aboral surface concave, and slightly expanded around basal pit. Groove extends from anterior end to posterior end.

Remarks: Some of the described specimens (MPC25398, 25407, 25414, etc.) have 2 to 4 small posterior processes, and hence, are close to *Neospathodus curtatus* Orchard, 1995, which is probably one of the morphological variants of *Novispathodus triangularis* (Bender, 1970). The P_2 elements of the described specimens show that the denticulation gradually increases in size and inclination. They are close to the P_2 elements of *Nv. abruptus* Orchard (2005), but the number of denticles is fewer.

Occurrence: Described specimens from KC02-14 and KC02-15 within the portion of the *Triasssospathodus symmetricus* Zone represented by the *Tirolites* sp. nov. beds (Lower Spathian = lower Upper Olenekian) in the Bac Thuy Formation, northeastern Vietnam. This species occurs in the lowermost Lower Spathian in the Salt Range (Sweet, 1970b) and western USA (Sweet *et al.*, 1971), and its range extends to the uppermost Spathian (Orchard, 2010). This species is also known from Nevada (Mosher, 1968; Lucus and Orchard, 2007), Chios, Greek (Bender, 1970), Spiti, India (Goel, 1977), Southwest Japan (Koike, 1981), South China (Wang and Cao, 1981; Wang and Zhong, 1994), and Oman (Orchard, 1995).

Novispathodus ex gr. ***waageni*** (Sweet, 1970b)

Figs. 174.31–174.57, 175–180, 181.1–181.31

Neospathodus waageni Sweet, 1970b, p. 260, pl. 1, figs. 11, 12; McTavish, 1973, p. 300, pl. 2, figs. 11, 22. 25–28; Mosher, 1973, p. 172, pl. 20, fig. 5; Goel, 1977, p. 1094, pl. 2, figs. 1–4; Solien, 1979, p. 304, pl. 3, fig. 9; Buryi, 1979, p. 56, pl. 7, figs. 8, 9; Wang and Cao, 1981, pl. 2, fig. 26; Koike, 1982, p. 39, pl. 6, figs. 24–27; Matsuda, 1983, p. 88, pl. 1, figs. 6–10, pl. 2, figs. 1–7; Duan, 1987, pl. 2, figs. 7; Cao and Wang, 1993, p. 261, pl. 56, figs. 5, 11; Wang and Zhong, 1994, p. 402, pl. 1, figs. 12, 13; Nakrem *et al.*, 2008, figs. 5.7, 5.8, 5.11, 5.14; Orchard, 2008, p. 40, figs. 8.1, 8.2, 8.8, 8.9; Beranek *et al*., 2010, figs. 6.22, 6.23.

Neospathodus waageni waageni Sweet, 1970b. Zhao and Orchard (in Zhao *et al*., 2007), p. 36, pl. 1, figs. 10A, B.

Neospathodus waageni eowaageni Zhao and Orchard, 2007, in Zhao *et al.*, 2007, p. 36, pl. 1, figs. 5A, B.

Neospathodus ex gr. *waageni* (Sweet, 1970b). Orchard and Krystyn, 2007, figs. 8–18; Igo, 2009, p. 194, figs. 152.14–152.19, 156.7–156.19.

Novispathodus waageni (Sweet, 1970b). Goudemand and Orchard (in Goudemand *et al*., 2012), p. 1031, figs. 3D, E, H, N, S, T.

Material examined: Twenty-three specimens, MPC25432–25454, from BT01-03, nine specimens, MPC25455–25463, from BT01-04, seven specimens, MPC25464–25470, from BT01-06, six specimens, MPC25471–25476, from BT01-07, eighteen specimens, MPC25477–25494, from BT01-10, eight specimens, MPC25495–25502, from BT01-12, six specimens, MPC25503–25508, from BT02-01, two specimens, MPC25509, 25510, from BT02–02, three specimens, MPC25511–25513, from KC01-01, nine specimens, MPC25514–25522, from KC01-04, one specimen, MPC25523, from KC01-05, four specimens, MPC25524–25527, from KC01-06, two specimens, MPC25528, 25529, from KC01-08, two specimens, MPC25530, 25531, from KC01-11, two specimens, MPC25532, 25533, from KC01-12, two specimens, MPC25534, 25535, from KC01-13, and one specimen, MPC25536, from KC02-08.

Description: Laterally compressed arched elements 0.30–0.78 mm in length, average 0.49 mm; 0.27–0. 60 mm in height, average 0.41 mm; length to height ratio 0.9–1.8, average 1.2 for one hundred-five specimens. Arched upper edge bears sharp pointed denti-

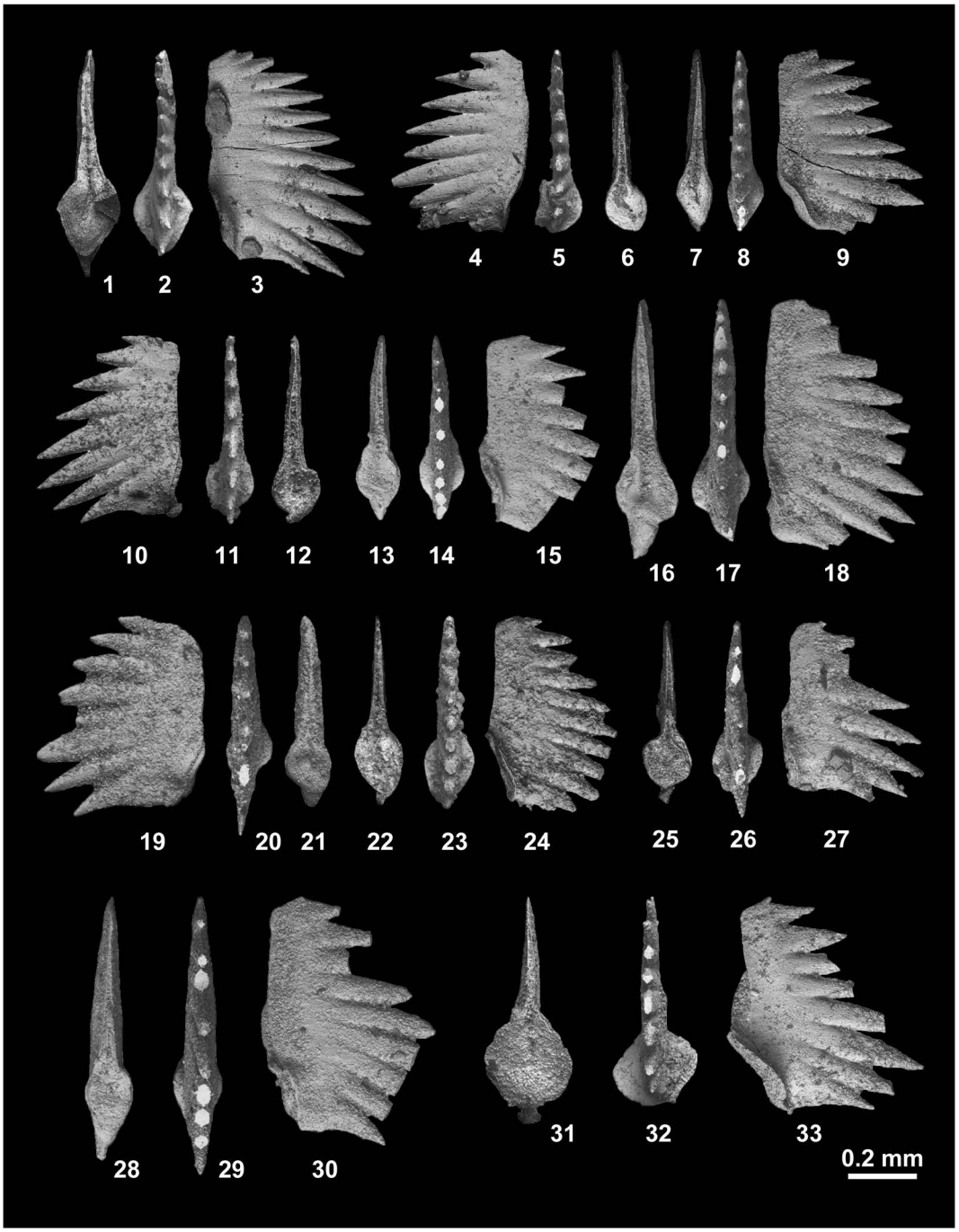

Fig. 175. *Novispathodus* ex gr. *waageni* (Sweet, 1970b) from BT01-03. 1–3, MPC25441. 4–6, MPC25442. 7–9, MPC25443. 10–12, MPC25444. 13–15, MPC25445. 16–18, MPC25446. 19–21, MPC25447. 22–24, MPC25448. 25–27, MPC25449. 28–30, MPC25450. 31–33, MPC25451.

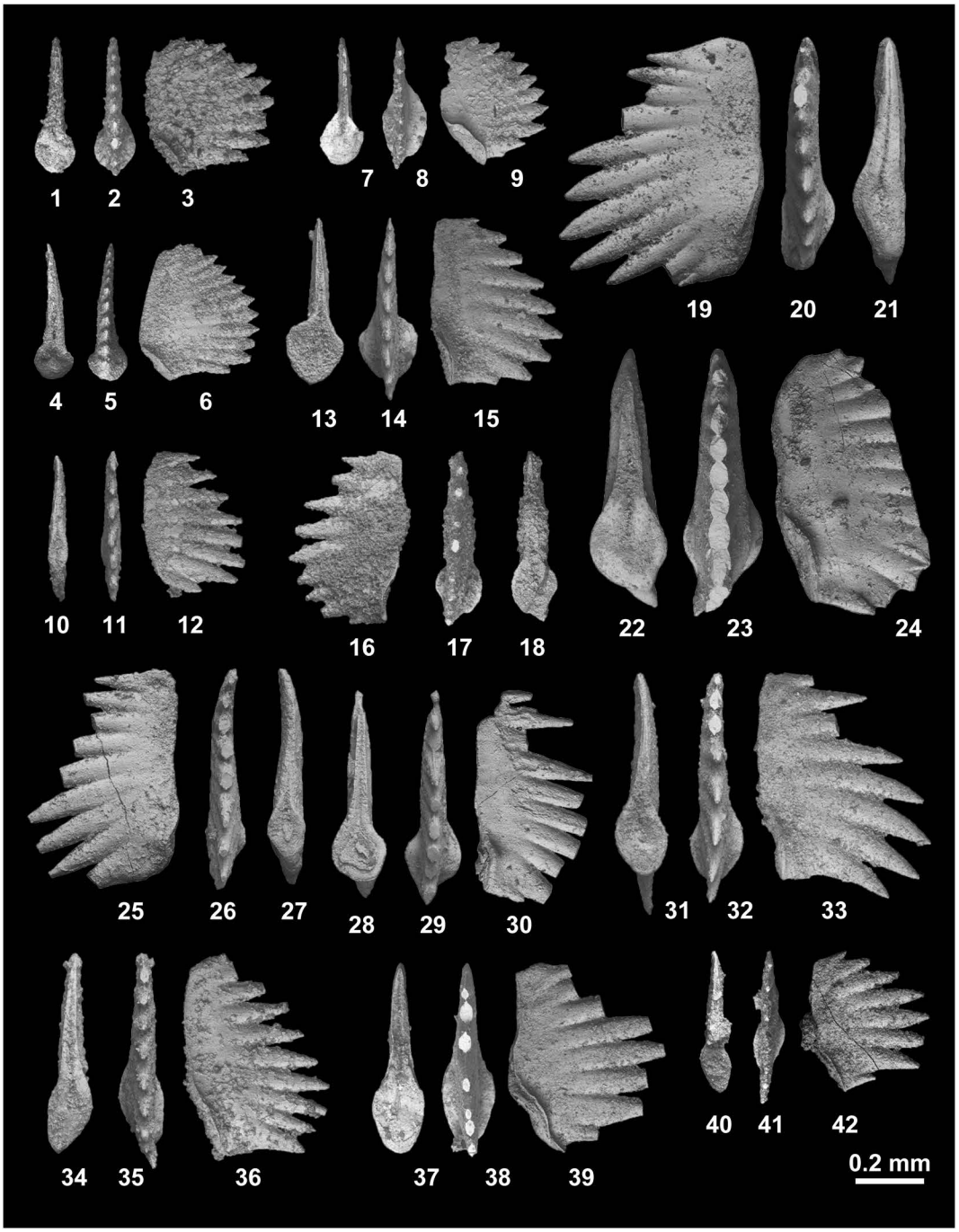

Fig. 176. *Novispathodus* ex gr. *waageni* (Sweet, 1970b). 1–3, MPC25452, from BT01-03. 4–6, MPC25453, from BT01-03. 7–9, MPC25454, from BT01-03. 10–12, MPC25455, from BT01-04. 13–15, MPC25456, from BT01-04. 16–18, MPC25457, from BT01-04. 19–21, MPC25458, from BT01-04. 22–24, MPC25459, from BT01-04. 25–27, MPC25460, from BT01-04. 28–30, MPC25461, from BT01-04. 31–33, MPC25462, from BT01-04. 34–36, MPC25463, from BT01-04. 37–39, MPC25464, from BT01-06. 40–42, MPC25465, from BT01-06.

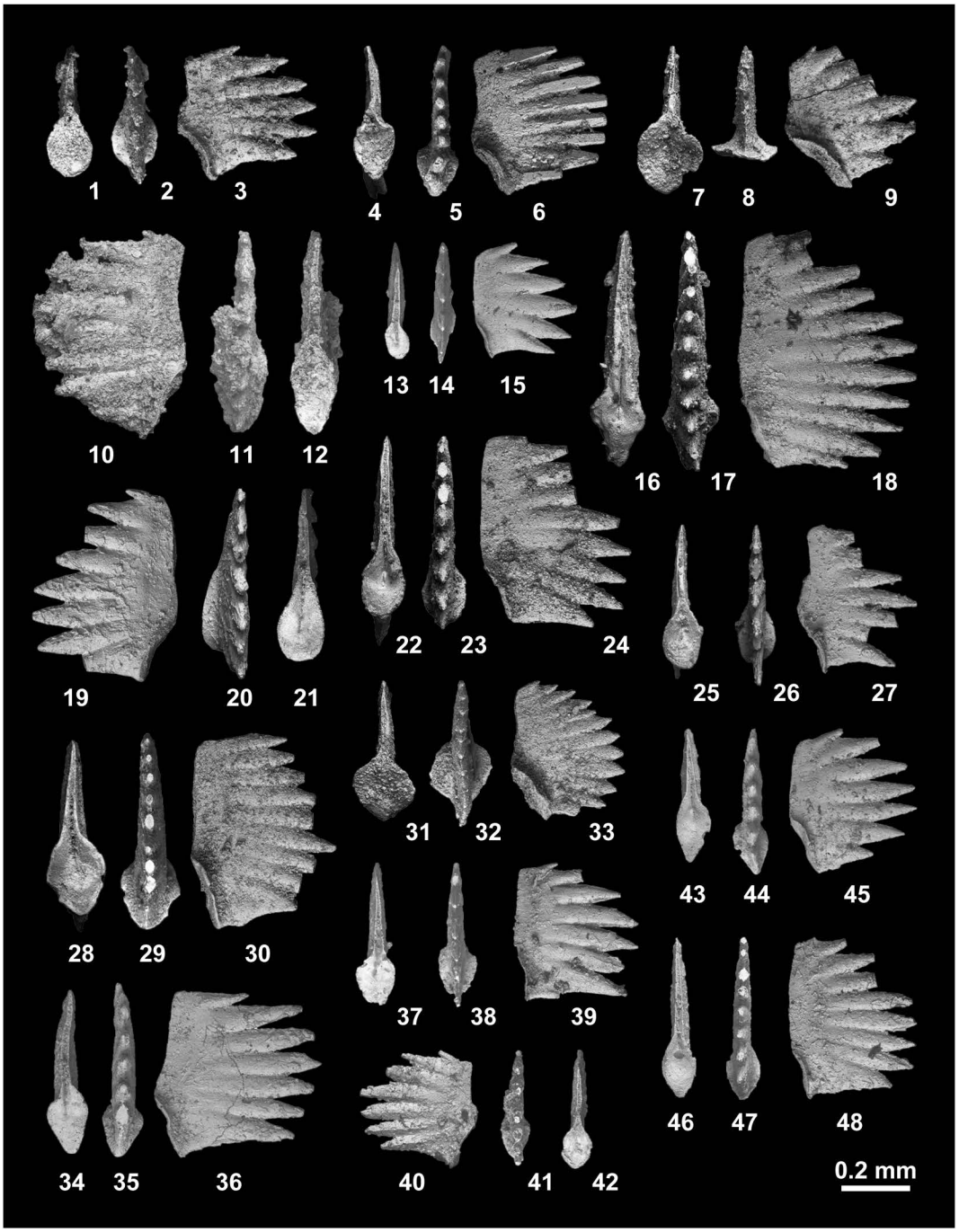

Fig. 177. *Novispathodus* ex gr. *waageni* (Sweet, 1970b). 1–3, MPC25466, from BT01-06. 4–6, MPC25467, from BT01-06. 7–9, MPC25468, from BT01-06. 10–12, MPC25469, from BT01-06. 13–15, MPC25470, from BT01-06. 16–18, MPC25471, from BT01-07. 19–21, MPC25472, from BT01-07. 22–24, MPC25473, from BT01-07. 25–27, MPC25474, from BT01-07. 28–30, MPC25475, from BT01-07. 31–33, MPC25476, from BT01-07. 34–36, MPC25477, from BT01-10. 37–39, MPC25478, from BT01-10. 40–42, MPC25479, from BT01-10. 43–45, MPC25480, from BT01-10. 46–48, MPC25481, from BT01-10.

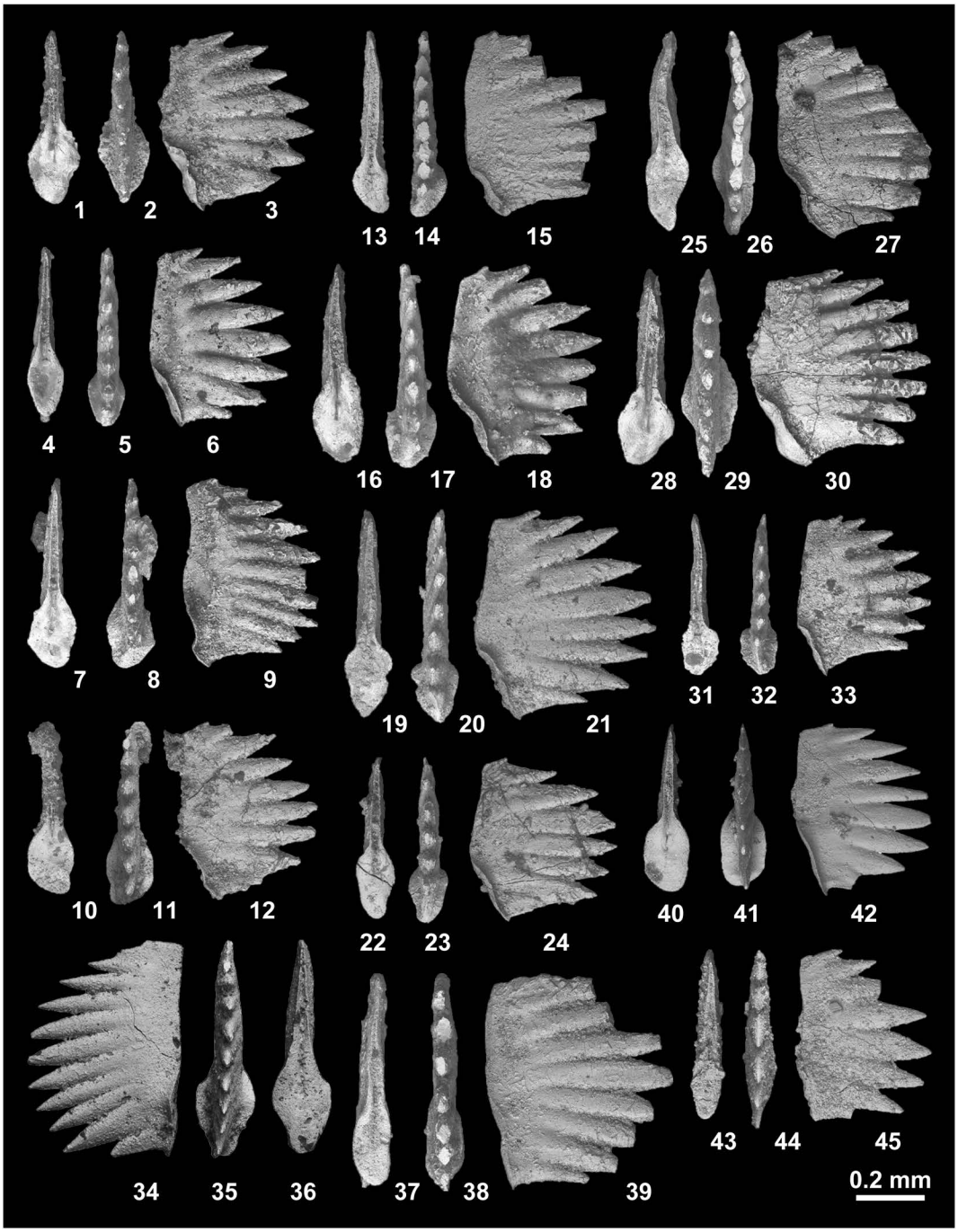

Fig. 178. *Novispathodus* ex gr. *waageni* (Sweet, 1970b). 1–3, MPC25482, from BT01-10. 4–6, MPC25483, from BT01-10. 7–9, MPC25484, from BT01-10. 10–12, MPC25485, from BT01-10. 13–15, MPC25486, from BT01-10. 16–18, MPC25487, from BT01-10. 19–21, MPC25488, from BT01-10. 22–24, MPC25489, from BT01-10. 25–27, MPC25490, from BT01-10. 28–30, MPC25491, from BT01-10. 31–33, MPC25492, from BT01-10. 34–36, MPC25493, from BT01-10. 37–39, MPC25494, from BT01-10. 40–42, MPC25495, from BT01-12. 43–45, MPC25496, from BT01-12.

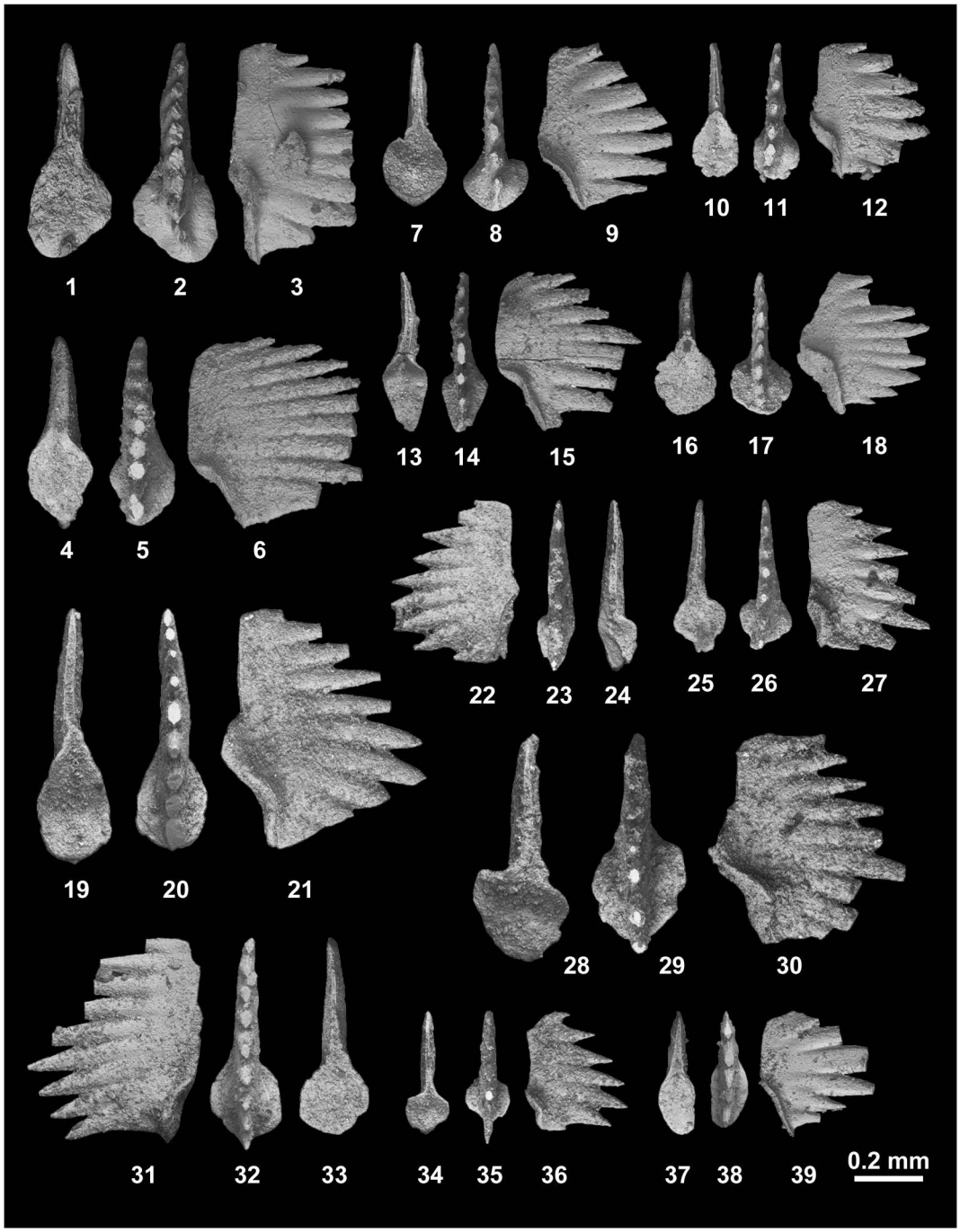

Fig. 179. *Novispathodus* ex gr. *waageni* (Sweet, 1970b). 1–3, MPC25497, from BT01-12. 4–6, MPC25498, from BT01-12. 7–9, MPC25499, from BT01-12. 10–12, MPC25500, from BT01-12. 13–15, MPC25501, from BT01-12. 16–18, MPC25502, from BT01-12. 19–21, MPC25503, from BT02-01. 22–24, MPC25504, from BT02-01. 25–27, MPC25505, from BT02-01. 28–30, MPC25506, from BT02-01. 31–33, MPC25507, from BT02-01. 34–36, MPC25508, from BT02-01. 37–39, MPC25509, from BT02-02.

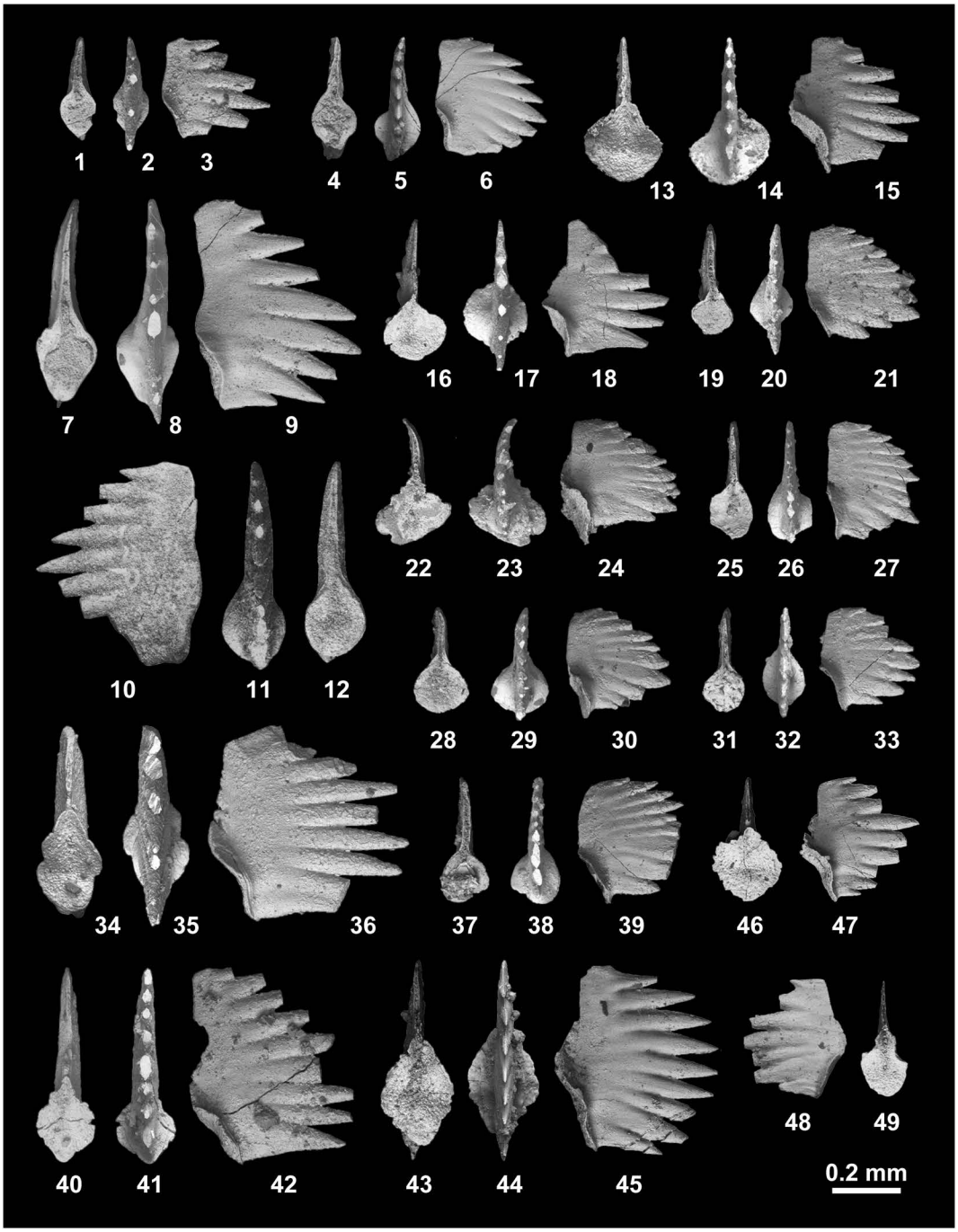

Fig. 180. *Novispathodus* ex gr. *waageni* (Sweet, 1970b). 1–3, MPC25510, from BT02-02. 4–6, MPC25511, from KC01-01. 7–9, MPC25512, from KC01-01. 10–12, MPC25513, from KC01-01. 13–15, MPC25514, from KC01-04. 16–18, MPC25515, from KC01-04. 19–21, MPC25516, from KC01-04. 22–24, MPC25517, from KC01-04. 25–27, MPC25518, from KC01-04. 28–30, MPC25519, from KC01-04. 31–33, MPC25520, from KC01-04. 34–36, MPC25521, from KC01-04. 37–39, MPC25522, from KC01-04. 40–42, MPC25523, from KC01-05. 43–45, MPC25524, from KC01-06. 46–47, MPC25525, from KC01-06. 48–49, MPC25526, from KC01-06.

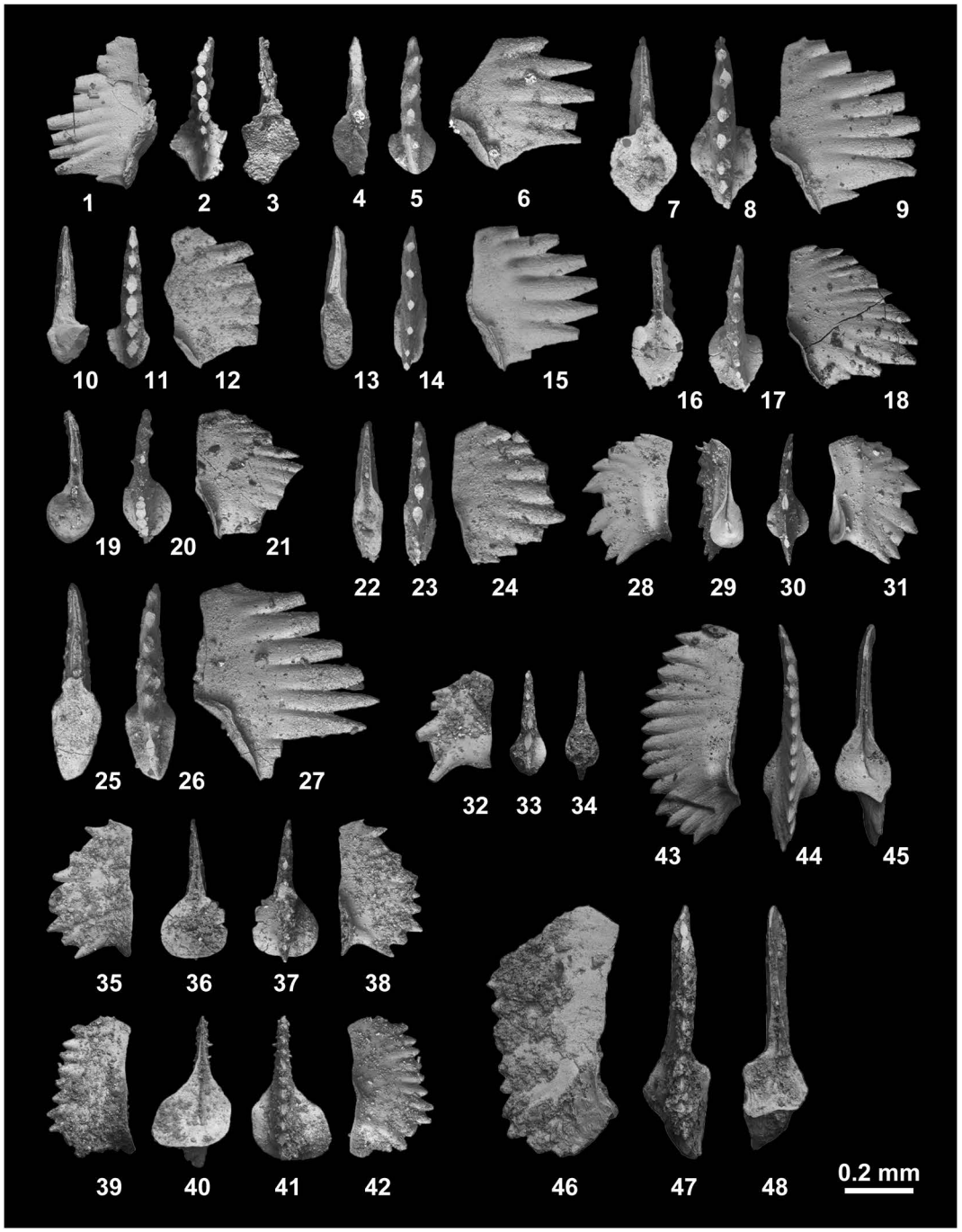

Fig. 181. 1–31, *Novispathodus* ex gr. *waageni* (Sweet, 1970b). 1–3, MPC25527, from KC01-06. 4–6, MPC25528, from KC01-08. 7–9, MPC25529, from KC01-08. 10–12, MPC25530, from KC01-11. 13–15, MPC25531, from KC01-11. 16–18, MPC25532, from KC01-12. 19–21, MPC25533, from KC01-12. 22–24, MPC25534, from KC01-13. 25–27, MPC25535, from KC01-13. 28–31, MPC25536, from KC02-08. 32–38, *Novispathodus* sp. nov. A Goudemand and Orchard, 2012. 32–34, MPC25537, from KC02-08. 35–38, MPC25538, from NT01-07. 39–42, *Novispathodus* sp. indet. A, MPC25539, from NT01-07. 43–48, *Triassospathodus homeri* (Bender, 1970) from KC02-15. 43–45, MPC25540. 46–48, MPC25541.

cles, varying in number from 6 to 13, average 9, discrete in upper one-third to one-half, suberect or reclined posteriorly, some specimens have 1 to 3 small posterior denticles. Lower edge straight or curved slightly upward anteriorly, posterior margin upturned about 5–40 degrees. Rounded or sub-rounded basal cavity expanded at posterior end, occupies one-fourth to one-half of length of element, and is slightly concave. Groove extends from basal pit to anterior end.

Remarks: Following Sweet's (1970b) first description of *Novispathodus waageni* from the Salt Range as *Neospathodus waageni*, Zhao *et al*. (2007) subdivided it into three subspecies: *Ns*. *waageni waageni*, *Ns*. *w. eowaageni*, and *Ns*. *posterolongatus*, based on many specimens collected from the West Pingdingshan section. Furthermore, Orchard and Krystyn (2007) recognized six morphotypes including two subspecies (*Ns*. *w. waageni* and *Ns*. *w. eowaageni*), based on specimens found at Spiti, India. Morphotype 1 is characterized by the developed platform flange in the lateral side of the element. Morphotype 2 is the same as the holotype (=*Ns*. *w. waageni*). Morphotype 3 is relatively small with a length to height ratio of about 1.1 and is the same as *Ns*. *w. eowaageni*. Morphotype 4 has a few small denticles at the posterior end of the element. Morphotype 5 has a large triangular shaped terminal cusp. Morphotype 6 has denticles spreading in a radial fashion from the base.

The described specimens contain Morphotypes 2, 3, 4, 5 and 6, with Morphotypes 4 and 5 being relatively abundant. Specimen (MPC25536) from KC02-08 within the *Nv*. *pingdingshanensis* Zone is smaller than the others and has an undulating basal margin. The size of basal cavity is smaller than that of *Nv*. *pingdingshanensis* (Zhao and Orchard, 2007).

Occurrence: Described specimens from BT01-03, BT01-04, BT01-06, BT01-07, BT01-10, BT01-12, BT02-01, BT02-02, KC01-01, KC01-04, KC01-05, KC01-06, KC01-08, KC01-11, KC01-12 and KC01-13 within the portion of the *Novispathodus* ex gr. *waageni* Zone that includes the *Flemingites rursiradiatus* beds, *Urdyceras tulongensis* beds and *Owenites koeneni* beds (lowest to middle Middle Smithian = middle Lower Olenekian), and KC02-08 within the portion of the *Novispathodus pingdingshanensis* Zone represented by the *Xenoceltites variocostatus* beds (Upper Smithian = upper Lower Olenekian) in the Bac Thuy Formation, northeastern Vietnam.

Novispathodus waageni is a well-known Smithian species throughout the world, and its FAD defines the IOB (Orchard, 2007a, b; Orchard and Krystyn, 2007; Zhao *et al*., 2007; Shigeta *et al*., 2009; Orchard, 2010). According to Zhao *et al.* (2007) and Goudemand *et al*. (2012), *Nv*. *waageni* occurs in the uppermost Smithian with *Nv*. *pingdingshanensis*. Therefore, *Nv*. *waageni* ranges throughout the entire Smithian.

Novispathodus sp. nov. A Goudemand and Orchard, 2012

Fig. 181.32–181.38

Novispathodus sp. nov. A Goudemand and Orchard, in Goudemand *et al*., 2012, p.1031 figs. 2A, R, Z.

Material examined: One specimen, MPC25537, from KC02-08, and one specimen, MPC25538, from NT01-07.

Description: Segminate elements 0.34–0.41 mm in length; 0.24–0.25 mm in height; length to height ratio 1.4–1.6 for two specimens, with arched upper edge. Highest point situated near posterior end. Lower margin of element almost straight. Mostly fused and pointed denticles total 7 and 10 in number, sub-erect or reclined posteriorly. Large basal cavity rounded and slightly concave. Groove extends from basal pit to anterior end.

Remarks: The described specimens including juvenile (MPC25537) are characterized by a straight lower margin and mostly fused and pointed denticles, which are reclined posteri-

orly. The basal cavity is smaller than that of *Novispathodus pingdingshanensis* (Zhao and Orchard, 2007). These features match well with specimens of *Nv.* sp. nov. A described by Goudemand and Orchard (in Goudemand *et al*., 2012) from South China.

Occurrence: Described specimens from KC02-08 and NT01-07 within the portion of the *Novispathodus pingdingshanensis* Zone represented by the *Xenoceltites variocostatus* beds (Upper Smithian=upper Lower Olenekian) in the Bac Thuy Formation, northeastern Vietnam. This species also occurs in the lowest Spathian part of the Tsoteng section, Guangxi, South China (Goudemand *et al*., 2012).

Novispathodus sp. indet. A

Fig. 181.39–181.42

Material examined: One specimen, MPC25539, from NT01-07.

Description: Small segminate element 0.41 mm in length; 0.25 mm in height; length to height ratio 1.6, with arched upper edge. Node-like short denticles total 12 in number, sub-erect or reclined posteriorly. Smallest terminal process strongly reclined posteriorly. Highest point situated above basal cavity. Lower margin of element slightly bowed. Asymmetrical sub-triangular basal cavity occupies posterior half of element. Thin furrow extends from basal pit to anterior end.

Remarks: The described segminate element has a few small posterior denticles, which are straight or reclined posteriorly and a large basal cavity. These distinctive features enable it to be assigned with reasonable confidence to the genus *Novispathodus*. The lateral view resembles *Icriospathodus*? *crassatus* (Orchard, 1995) and *I*.? *zaksi* (Buryi, 1979), but these species have a more robust denticulation and an expanded lateral rib.

Occurrence: Described specimen from NT01-07 within the portion of the *Novispathodus pingdingshanensis* Zone in the *Xenoceltites variocostatus* beds (Upper Smithian=upper Lower Olenekian) in the Bac Thuy Formation, northeastern Vietnam.

Genus ***Triassospathodus*** Kozur, 1998

Type species: *Spathognathodus homeri* Bender, 1970.

Triassospathodus homeri (Bender, 1970)

Fig. 181.43–181.48

Spathognathodus homeri Bender, 1970, p. 528, pl. 5, figs. 16a, b, c.

Neospathodus homeri (Bender, 1970). Sweet, 1970b, p. 245, pl. 1, figs. 2, 3, 9, 10; Matsuda, 1983, p. 94, pl. 5, figs. 2a, b; Wang and Zhong, 1994, p. 400–401, pl. 1, fig. 27; Orchard, 1995, p. 115, figs. 2.1–2.3, 2.7–2.9, 2.14–2.17, 2.20, 2.21.

multielement apparatuses, *Triassospathodus homeri* (Bender, 1970). Orchard, 2005, p. 93, text-fig. 19.

Triassospathodus ex gr. *homeri* (Bender, 1970). Lucas and Orchard, 2007, figs. 7.8, 7.9; Orchard *et al*., 2007a, figs. 5.5, 5.6; Orchard *et al*., 2007b, figs. 6.10–6.12; Orchrad, 2010, figs. 7.15, 7.16.

Material examined: Two specimens, MPC25540, 25541, from KC02-15.

Description: Two slender blade-like elements 0.64–0.74 mm in length; 0.30–0.39 mm in height; length to height ratio 1.9–2.1. Arched upper edge bears triangular-shaped fused denticles totaling 11 and 16 in number, including 3 or 4 posterior small terminal processes, gradually reclined posteriorly. Cusp situated in middle part of element. Basal margin straight in anterior two-thirds, downturned in posterior one-third. Sub-rounded basal cavity elongated and curved laterally at terminal end. Narrow groove extends from basal pit to anterior end.

Remarks: *Triassospathodus homeri* (Bender, 1970) is one of the well-known characteristic species of the Spathian. According to Orchard (1995), the diagnostic features of the taxon include the posteriorly elongated elliptical basal cavity and the presence of several small posterior processes. In contrast, *T. symmetricus* (Orchard, 1995) lacks small posterior

denticles and the asymmetrical basal cavity, which is slightly elongated posteriorly. In the Bac Thuy Formation, the FAD of *T. homeri* at KC02-15 occurs above the FAD of *T. symmetricus* at KC02-12. This evidence suggests that *T. homeri* evolved from *T. symmetricus* during earliest Spathian time.

Occurrence: Described specimens from KC02-15 within the portion of the *Triassospathodus symmetricus* Zone represented by the *Tirolites* sp. nov. beds (Lower Spathian=lower Upper Olenekian) in the Bac Thuy Formation, northeastern Vietnam. This species also occurs in the Spathian (Upper Olenekian) in Chios (Bender, 1970), Desli Caira, North Dobrogea, Romania (Orchard *et al*., 2007a), the Salt Range, Pakistan (Sweet, 1970), Kashmir, India (Matsuda, 1983), Jabal Safra, Oman (Orchard, 1995), Southern Jiangsu, China (Duan, 1987), and Guizhou, South China (Orchard *et al*., 2007b).

Triassospathodus symmetricus (Orchard, 1995)

Figs. 182–185, 186.1–186.3

Neospathodus cristagalli (Huckriede, 1958). Mosher, 1968, p. 930, pl. 115, fig. 1

Neospathodus triangularis (Bender, 1970). Sweet, 1970b, pp. 253–254, pl. 1, figs. 7, 8; Perri and Andraghetti, 1987, p. 311, pl. 33, figs. 5a, b, c.

Neospathodus homeri (Bender, 1970). Mosher, 1973, p. 171, pl. 20, fig. 14; Goel, 1977, p. 1097, pl. 2, figs. 10, 11; Duan, 1987, pl. 2, figs. 8, 9; Cao and Wang, 1993, pl. 56, figs. 1, 2; Ji *et al*., 2011, p. 220, figs. 3.9a, b. c.

Neospathodus ex gr. *homeri* (Bender, 1970). Orchard, 1994, pl. 1, figs. 11, 15–18.

Neospathodus symmetricus Orchard, 1995, p. 120, figs. 2.6, 2.10–2.13, 2.18; Koike, 2004, p. 137, figs. 6.34–6.38; Ji *et al*., 2011, figs. 3.5a, b, c.

Material examined: Two specimens, MPC25542, 25543, from KC02-12, three specimens, MPC25544–25546, from KC02-14, and forty-three specimens, MPC25547–25589, from KC02-15.

Description: Laterally compressed blade-like elements 0.41–0.87 mm in length, average 0.61 mm; 0.22–0.41 mm in height, average 0.33 mm; length to height ratio 1.6–2.7, average 1.9 for forty-eight specimens. Straight or arcuate upper edge bears sub-traingular, pointed and fused denticles varying in number from 10 to 18, average 13, erect and gradually reclined posteriorly. Basal margin slightly or strongly bowed. Some specimens have posterior small denticles above terminal basal cavity. Several elements have a well-developed lateral rib in middle part of element. Basal cavity concave, and exhibits various shapes: circular, elliptical, sub-triangular, square, cordiform. Narrow furrow extends to anterior end.

Remarks: The described specimens from KC02-15 display a wide range of intraspecific variation in the form of their denticulation, basal cavities, and basal margins.

Occurrence: Described specimens from KC02-12, KC02-14 and KC02-15 within the portion of the *Triassospathodus symmetricus* Zone that includes the *Tirolites* cf. *cassianus* beds (lowest Lower Spathian=lowest Upper Olenekian) and *Tirolites* sp. nov. beds (Lower Spathian=lower Upper Olenekian) in the Bac Thuy Formation, northeastern Vietnam.

This species also occurs in the Spathian in the Salt Range, Pakistan (Zone 9, Sweet, 1970b), the Werfen Formation, southern Alps, Italy (Perri and Andraghetti, 1987), British Columbia, Canada (*Keyserlingites subrobustus* Zone, Mosher, 1973 and Orchard, 1994), Spiti, India (Goel, 1977), the Prida Formation, Nevada (*Subcolumbites* beds and *Neopopanoceras hangi* Zone, Orchard, 1994), the Luolou Formation, Qingyan Section, Guizhou, South China (*Neospathodus homeri* Zone, Ji *et al*., 2011), and the Taho limestone, Southwest Japan (Koike, 2004).

The FAD of *Triassospathodus symmetricus* occurs in the lowest Spathian, but its last appearance datum (LAD) is unknown. The exact range of this taxon must be clarified with respect to its occurrence in other Spathian aged formations and detailed descriptions of co-occurring species must be included.

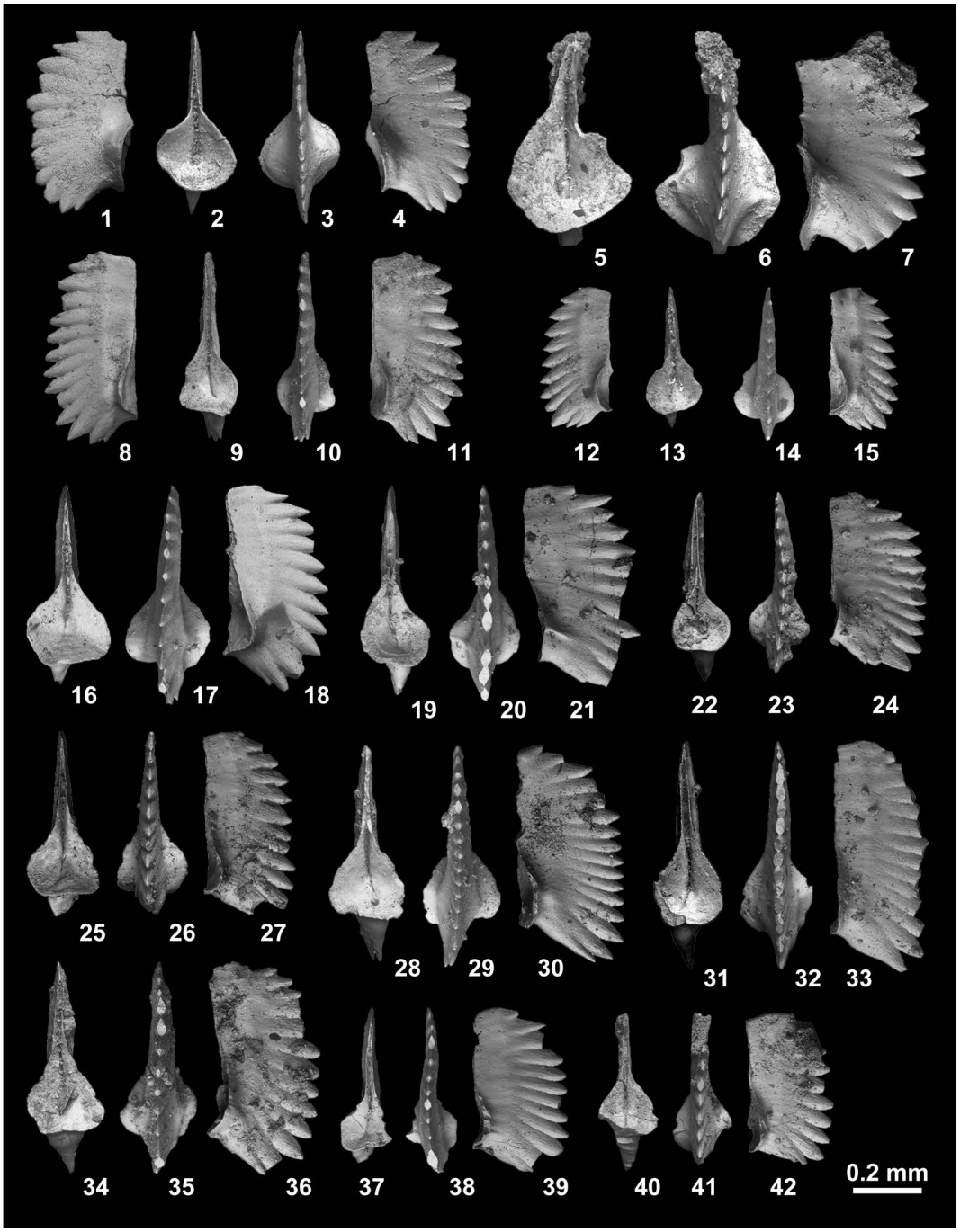

Fig. 182. *Triassospathodus symmetricus* (Orchard, 1995). 1–4, MPC25542, from KC02-12. 5–7, MPC25543, from KC02-12. 8–11, MPC25544, from KC02-14. 12–15, MPC25545, from KC02-14. 16–18, MPC25546, from KC02-14. 19–21, MPC25547, from KC02-15. 22–24, MPC25548, from KC02-15. 25–27, MPC25549, from KC02-15. 28–30, MPC25550, from KC02-15. 31–33, MPC25551, from KC02-15. 34–36, MPC25552, from KC02-15. 37–39, MPC25553, from KC02-15. 40–42, MPC25554, from KC02-15.

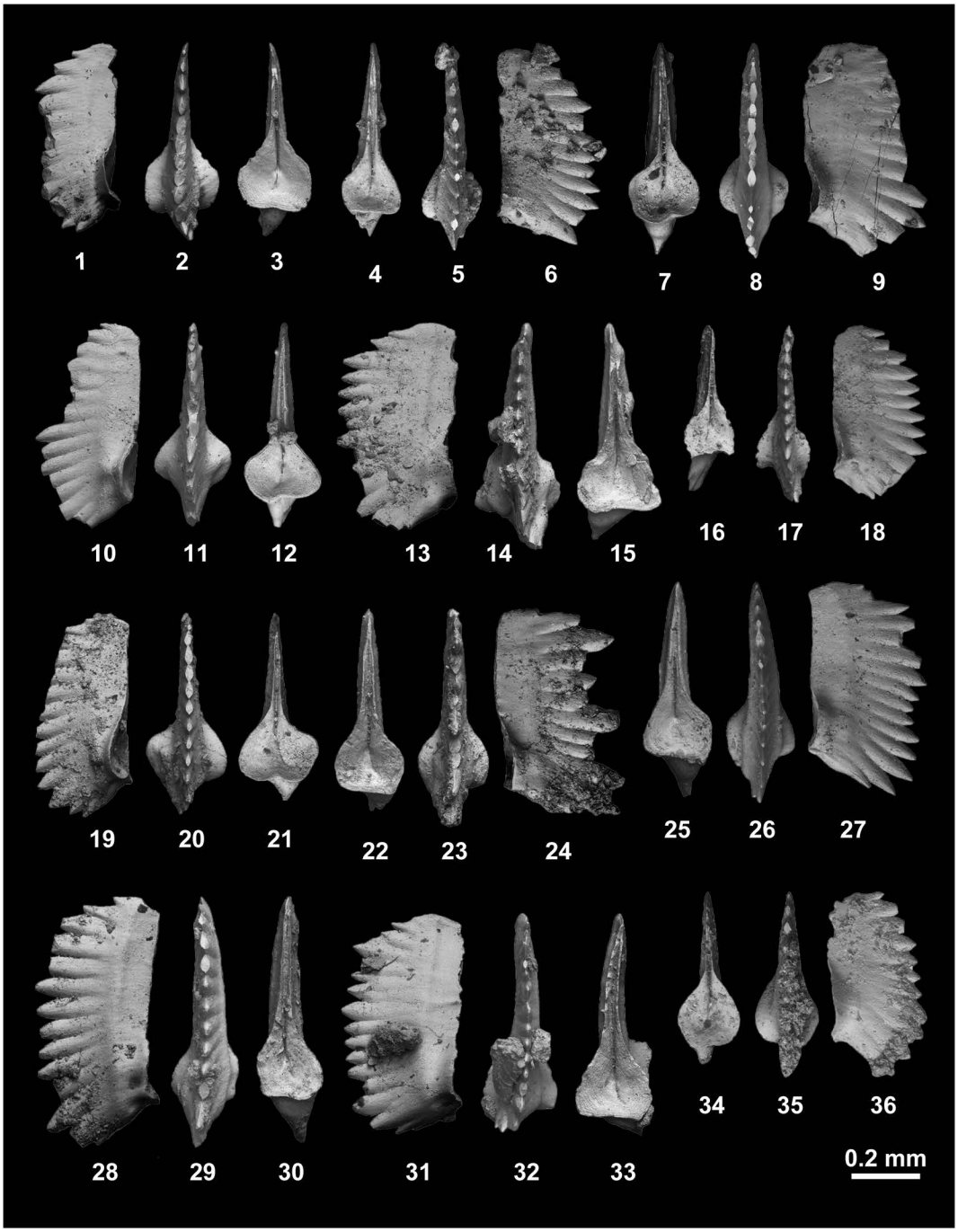

Fig. 183. *Triassospathodus symmetricus* (Orchard, 1995) from KC02-15. 1–3, MPC25555. 4–6, MPC25556. 7–9, MPC25557. 10–12, MPC25558. 13–15, MPC25559. 16–18, MPC25560. 19–21, MPC25561. 22–24, MPC25562. 25–27, MPC25563. 28–30, MPC25564. 31–33, MPC25565. 34–36, MPC25566.

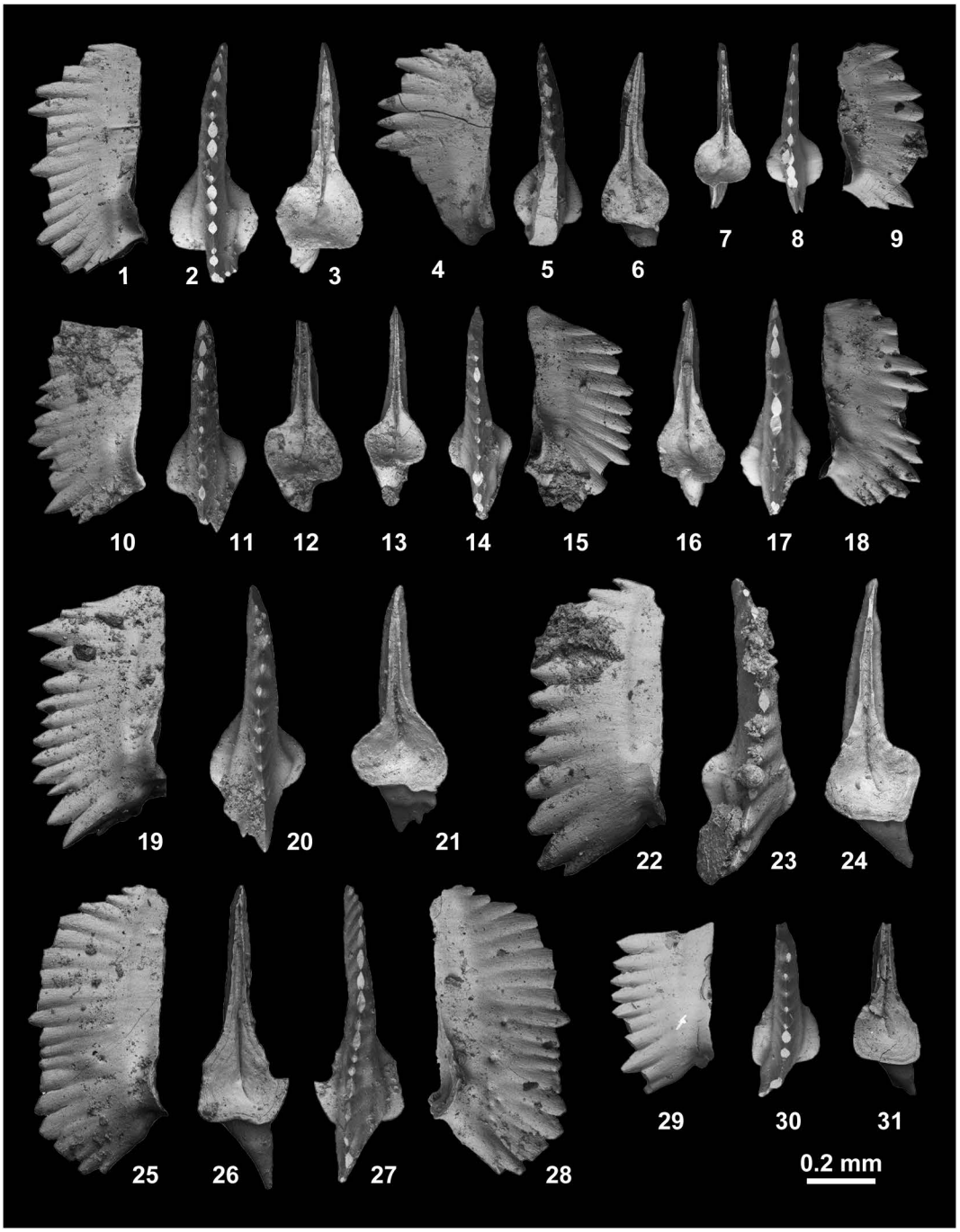

Fig. 184. *Triassospathodus symmetricus* (Orchard, 1995) from KC02-15. 1–3, MPC25567. 4–6, MPC25568. 7–9, MPC25569. 10–12, MPC25570. 13–15, MPC25571. 16–18, MPC25572. 19–21, MPC25573. 22–24, MPC25574. 25–28, MPC25575. 29–31, MPC25576.

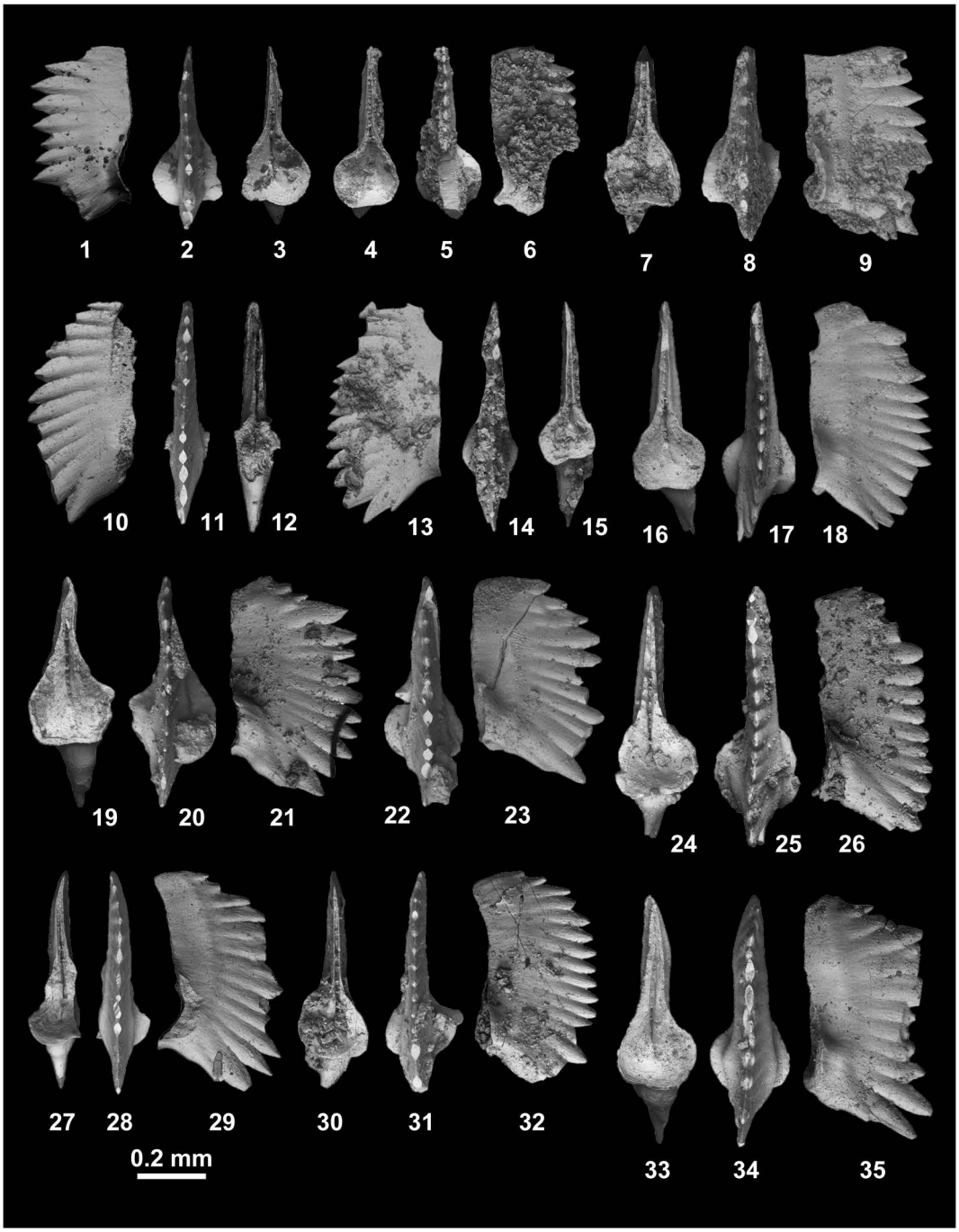

Fig. 185. *Triassospathodus symmetricus* (Orchard, 1995) from KC02-15. 1–3, MPC25577. 4–6, MPC25578. 7–9, MPC25579. 10–12, MPC25580. 13–15, MPC25581. 16–18, MPC25582. 19–21, MPC25583. 22–23, MPC25584. 24–26, MPC25585. 27–29, MPC25586. 30–32, MPC25587. 33–35, MPC25588.

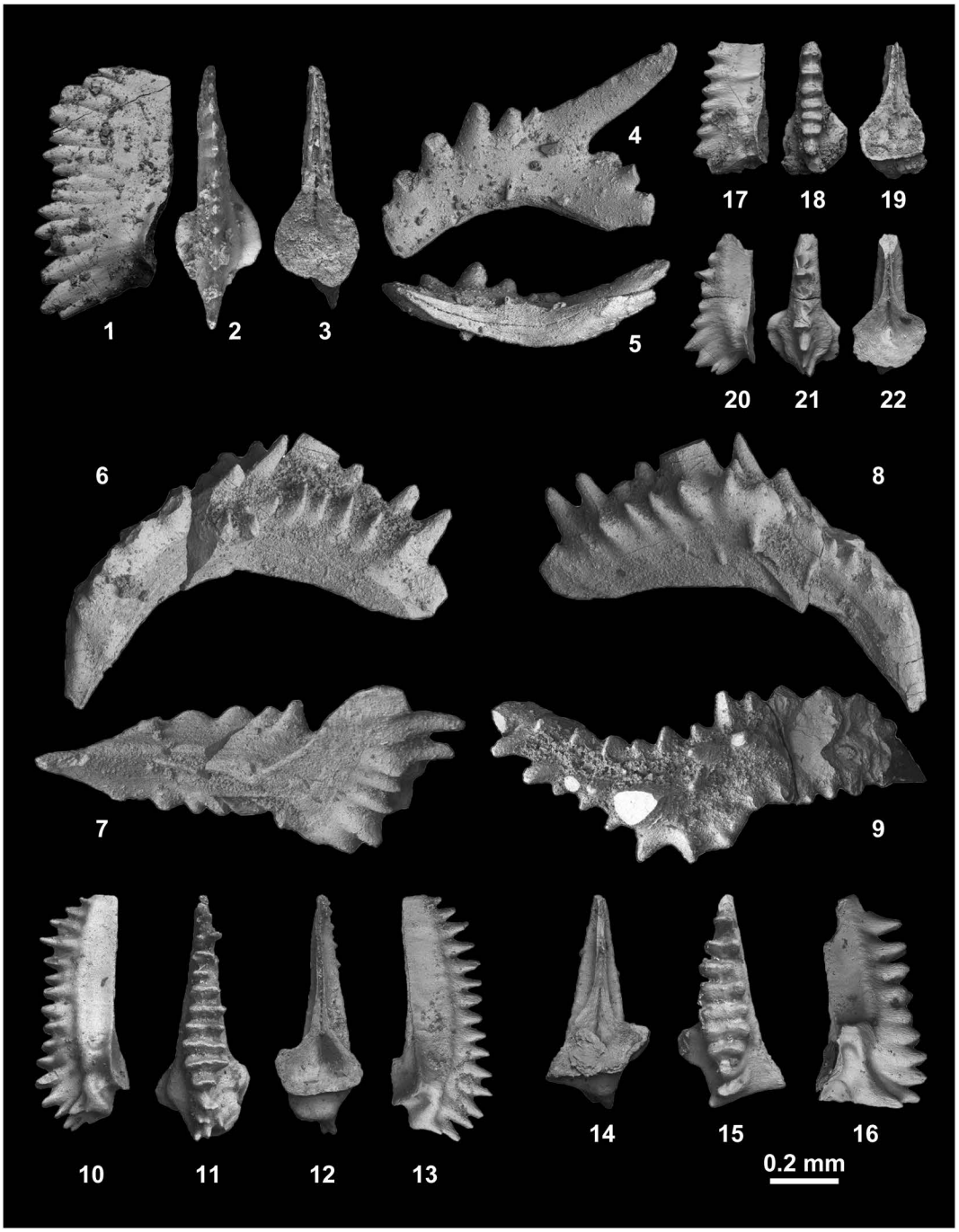

Fig. 186. 1–3, *Triassospathodus symmetricus* (Orchard, 1995), MPC25589, from KC02-15. 4–5, *Hadrodontina*? sp. indet. A, MPC25590, from BT01-07. 6–9, *Hadrodontina*? sp. indet. B, MPC25591, from BT02-02. 10–22, *Icriospathodus collinsoni* (Solien, 1979). 10–13, MPC25592, from KC02-14. 14–16, MPC25593, from KC02-14. 17–19, MPC25594, from KC02-15. 20–22, MPC25595, from KC02-15.

Subfamily Uncertain
Genus ***Icriospathodus*** Krahl, Kauffmann, Kozur, Richter, Foerster and Heinritzi, 1983

Type species: *Neospathodus collinsoni* Solien, 1979.

Icriospathodus collinsoni (Solien, 1979)
Figs. 186.10–186.22, 187–191, 192.1–192.6

Icriodus. Clark *et al*., 1964, pl. 60, figs. 1a, b.
Neospathodus sp. G. Sweet *et al*., 1971, pl. 1, fig. 13; Buryi, 1979, p. 49, pl. 9, figs. 3a–c, pl. 18, figs. 4a, b.
Neospathodus collinsoni Solien, 1979, p. 302, pl. 3, figs. 10, 12–20.; Clark *et al*., 1979, pl. 1, figs. 11, 12; Duan, 1987, pl. 2, figs. 1–6; Cao and Wang, 1993, pl. 55, figs.12, 13.
Neospathodus? *collinsoni* Solien, 1979. Koike, 1981, pl. 1, figs. 42–44.
Spathoicriodus collinsoni Budurov, Sudar and Gupta, 1987, p. 175.
Spathoicriodus collinsoni (Solien, 1979). Koike, 1992, p. 357–361, figs. 12.1–12.42, 12.44, 12.47–12.50, 13.8–13.37.
Icriospathodus collinsoni (Solien, 1979). Orchard, 1995, p. 113, figs. 2.22–2.24; Nakazawa *et al*., 1994, pl. 1, fig. 30; Lucas and Orchard, 2007, figs. 7.4–7.7, 7.13–7.15; Ji *et al*., 2011, figs. 4.5a-c.
multielement apparatuses, *Icriospathodus collinsoni* (Solien, 1979). Orchard, 2005, p. 96, text-fig. 22.

Material examined: Two specimens, MPC25592, 25593, from KC02-14, and fifty-four specimens, MPC25594–25647, from KC02-15.

Description: Blade-like robust elements 0.50–0.92 mm in length, average 0.64 mm; 0.20–0.36 mm in height, average 0.27 mm; length to height ratio 1.4–2.9, average 2.0 for fifty-six specimens, with rectangular general profile. Upper part of element consists of pointed node-like and ridge-like denticles. Prominent strong rib extended to posterior end in the middle part of element, flanged laterally above basal cavity. Lower margin straight or bowed at both anterior and posterior ends, downturned prominently. Denticles, varying in number from 10 to 18, average 12, change to spine or node-like form at both anterior and posterior ends, and exhibit biserial ribs or single ridge across platform. Line of denticulation straight, or slightly or strongly curved to sinistral or dextral sides of element at posterior end. Some specimens have small pointed denticles extended along the posterior margin. Denticles show some variation in size and form. Ridge-like denticles widest in middle or slightly posterior part of element, gradually decreasing to both anterior and posterior ends, highest point situated in posterior one-fourth, and lowest in anterior end. Strongly concave basal cavity exhibits various shapes: subround, triangular, square, parallelogram, pentagon. Some posterior margins branched or remarkably elongated to lateral side at posterior end. Deep furrow extends from basal pit to anterior end.

Remarks: Koike (1992) demonstrated a wide range of intraspecific variation in the platform morphology and denticulation of *Spathoicriodus collinsoni* (Solien, 1979) (=*Icriospathodus collinsoni* [Solien, 1979]) from the Taho limestone, Southwest Japan, and consequently divided into three forms (α, β, γ) on the basis of the degree of development of its ridge-like denticles. Form α is marked by having transverse ridge-like denticles on the entire platform. Form β has narrow uniserial or a few biserial denticles on the middle portion of the platform. Form γ has laterally compressed or laterally rounded and tipped denticles (lacking ridge-like denticles or paired platform nodes) on the entire platform. Form γ and other forms co-occur in Oman, Southwest Japan, and Idaho, Form γ occurs by itself in the Spathian of California (Orchard, 1995). Orchard (1995) separated Form γ from the other forms based on their differences in denticulation and FAD (Form γ occurs earlier than the other forms), and proposed a new species, *Neospathodus crassatus* Orchard, 1995 (=*I.*? *crassatus* [Orchard, 1995]).

Occurrence: Described specimens from KC02-14 and KC02-15 within the portion of the *Triassospathodus symmetricus* Zone represented by the *Tirolites* sp. nov. beds (Lower

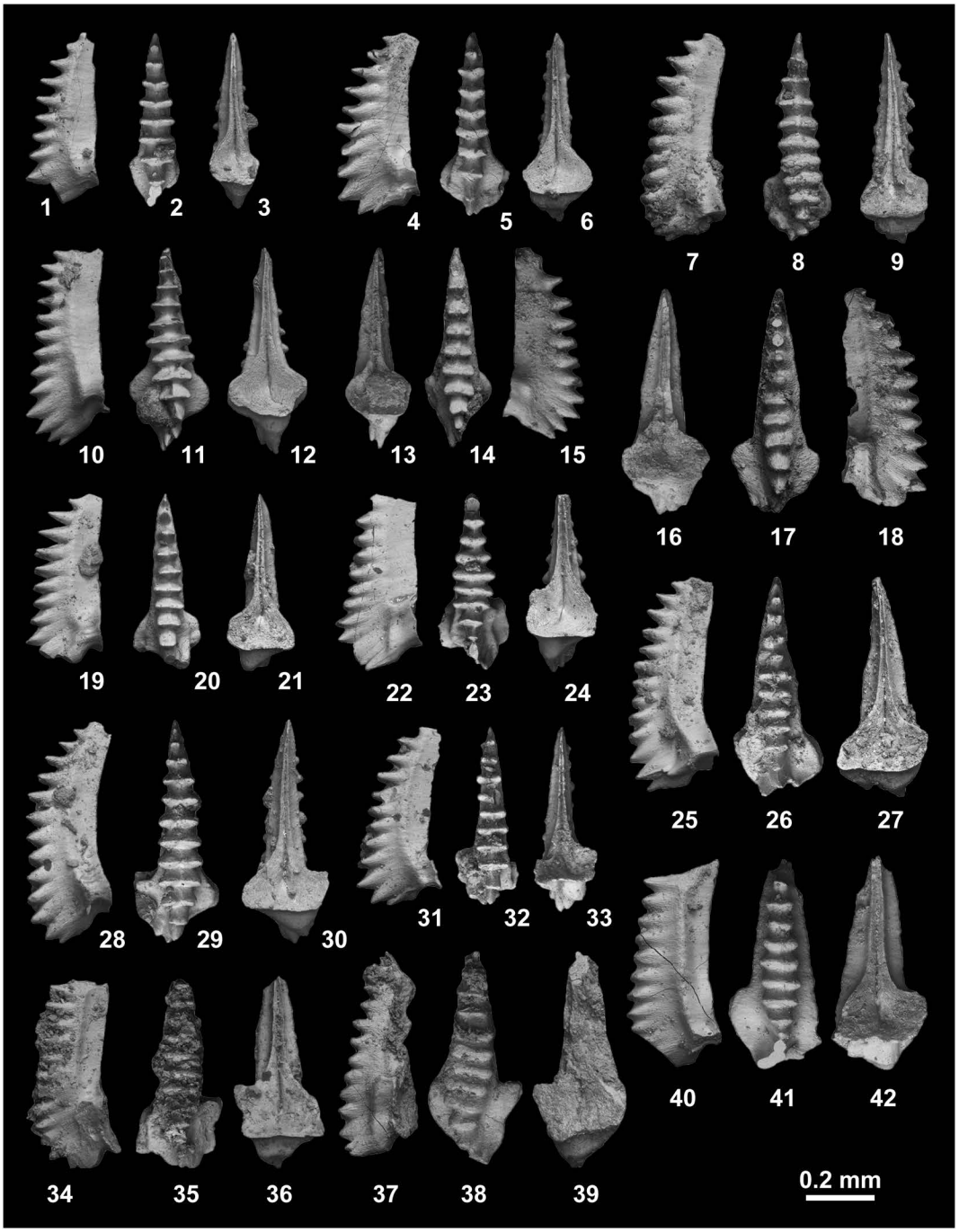

Fig. 187. *Icriospathodus collinsoni* (Solien, 1979) from KC02-15. 1–3, MPC25596. 4–6, MPC25597. 7–9, MPC25598. 10–12, MPC25599. 13–15, MPC25600. 16–18, MPC25601. 19–21, MPC25602. 22–24, MPC25603. 25–27, MPC25604. 28–30, MPC25605. 31–33, MPC25606. 34–36, MPC25607. 37–39, MPC25608. 40–42, MPC25609.

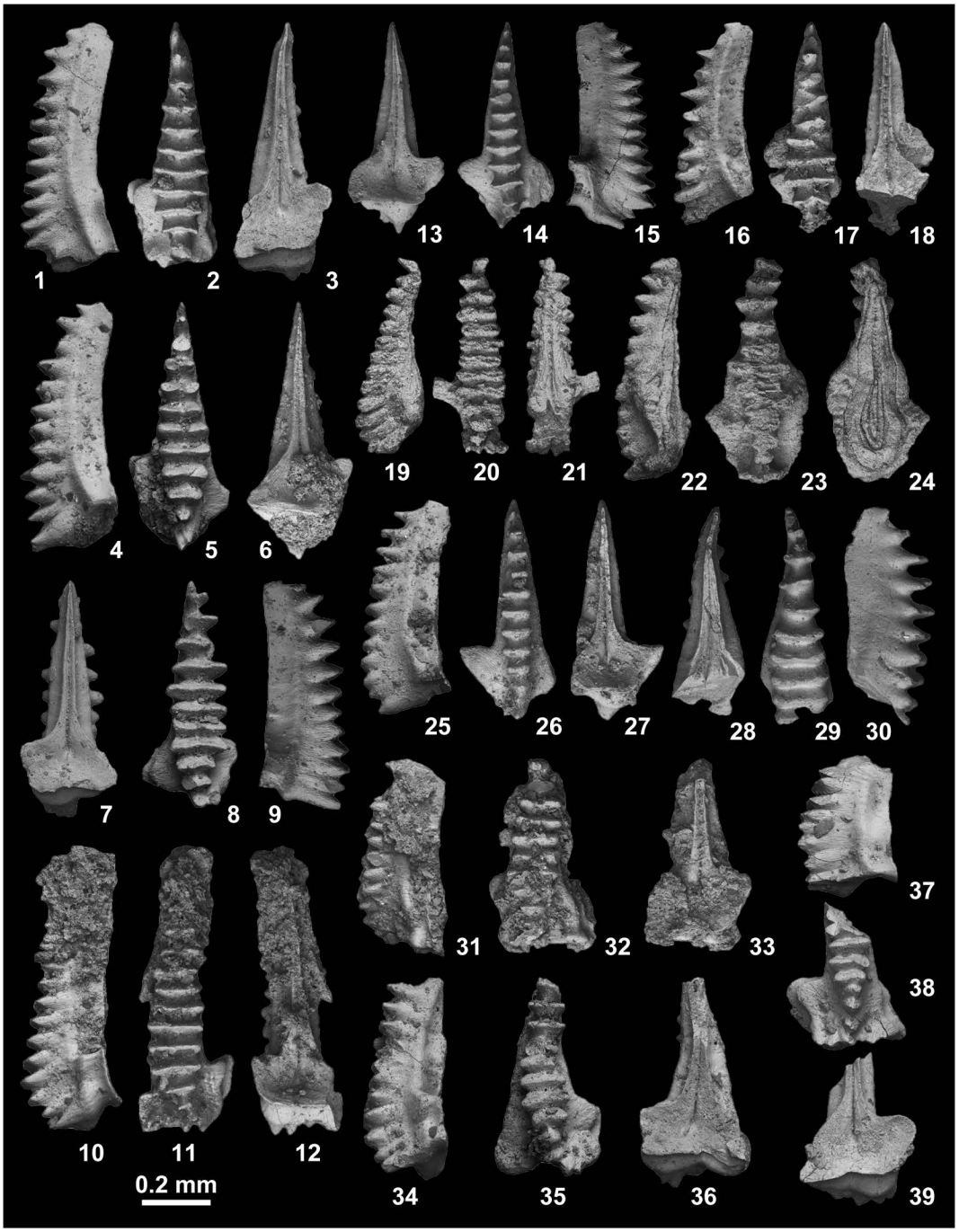

Fig. 188. *Icriospathodus collinsoni* (Solien, 1979) from KC02-15. 1–3, MPC25610. 4–6, MPC25611. 7–9, MPC25612. 10–12, MPC25613. 13–15, MPC25614. 16–18, MPC25615. 19–21, MPC25616. 22–24, MPC25617. 25–27, MPC25618. 28–30, MPC25619. 31–33, MPC25620. 34–36, MPC25621. 37–39, MPC25622.

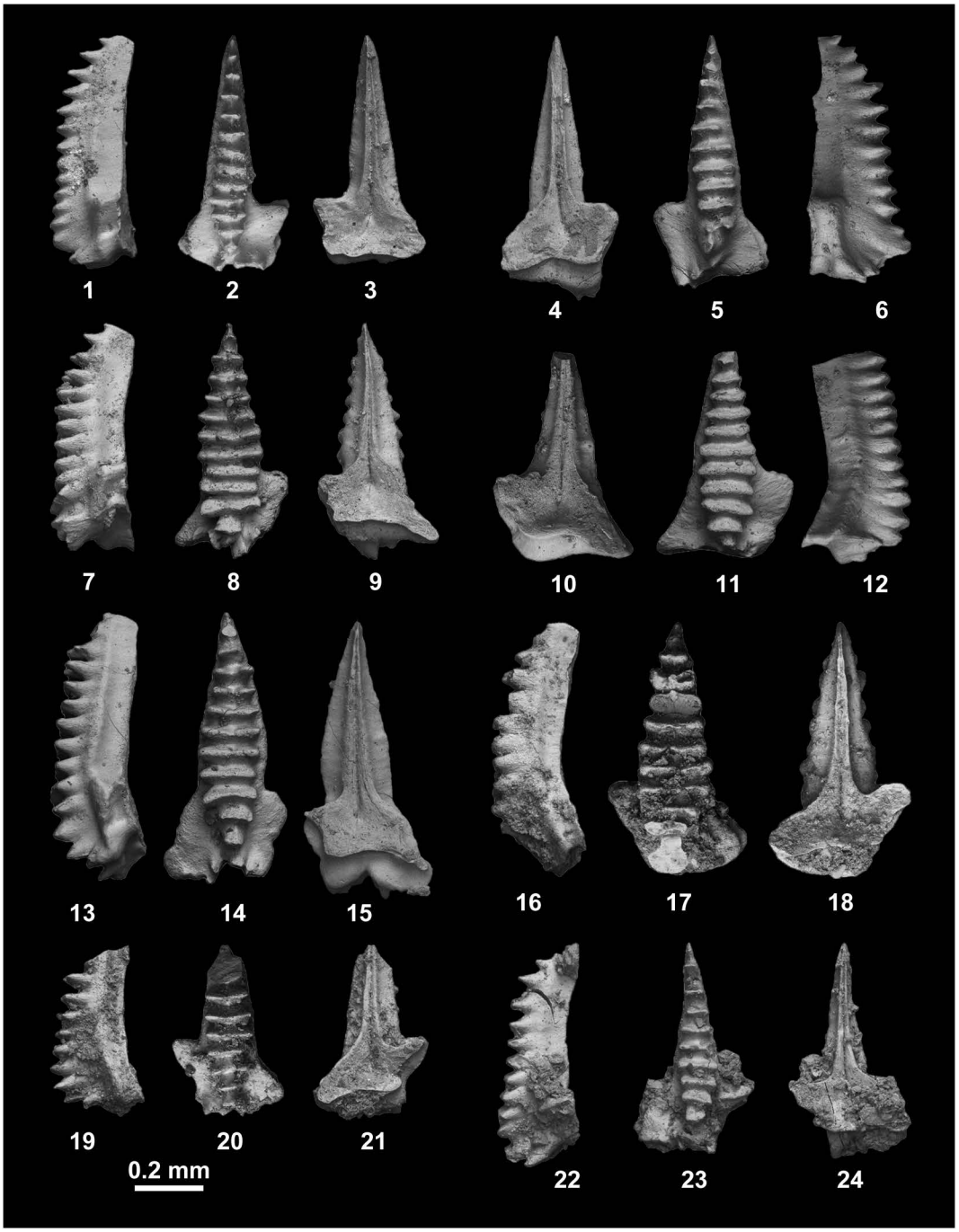

Fig. 189. *Icriospathodus collinsoni* (Solien, 1979) from KC02-15. 1–3, MPC25623. 4–6, MPC25624. 7–9, MPC25625. 10–12, MPC25626. 13–15, MPC25627. 16–18, MPC25628. 19–21, MPC25629. 22–24, MPC25630.

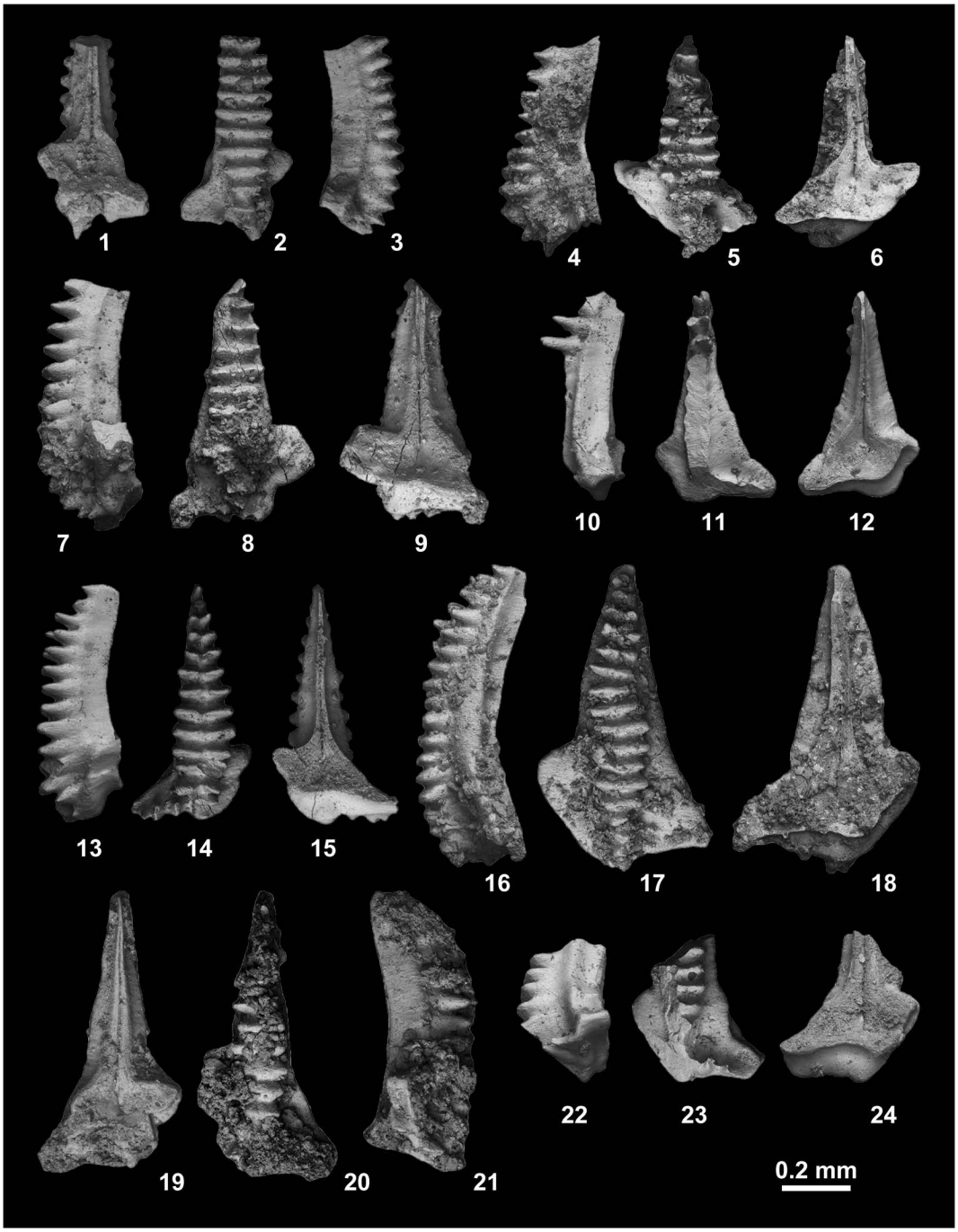

Fig. 190. *Icriospathodus collinsoni* (Solien, 1979) from KC02-15. 1–3, MPC25631. 4–6, MPC25632. 7–9, MPC25633. 10–12, MPC25634. 13–15, MPC25635. 16–18, MPC25636. 19–21, MPC25637. 22–24, MPC25638.

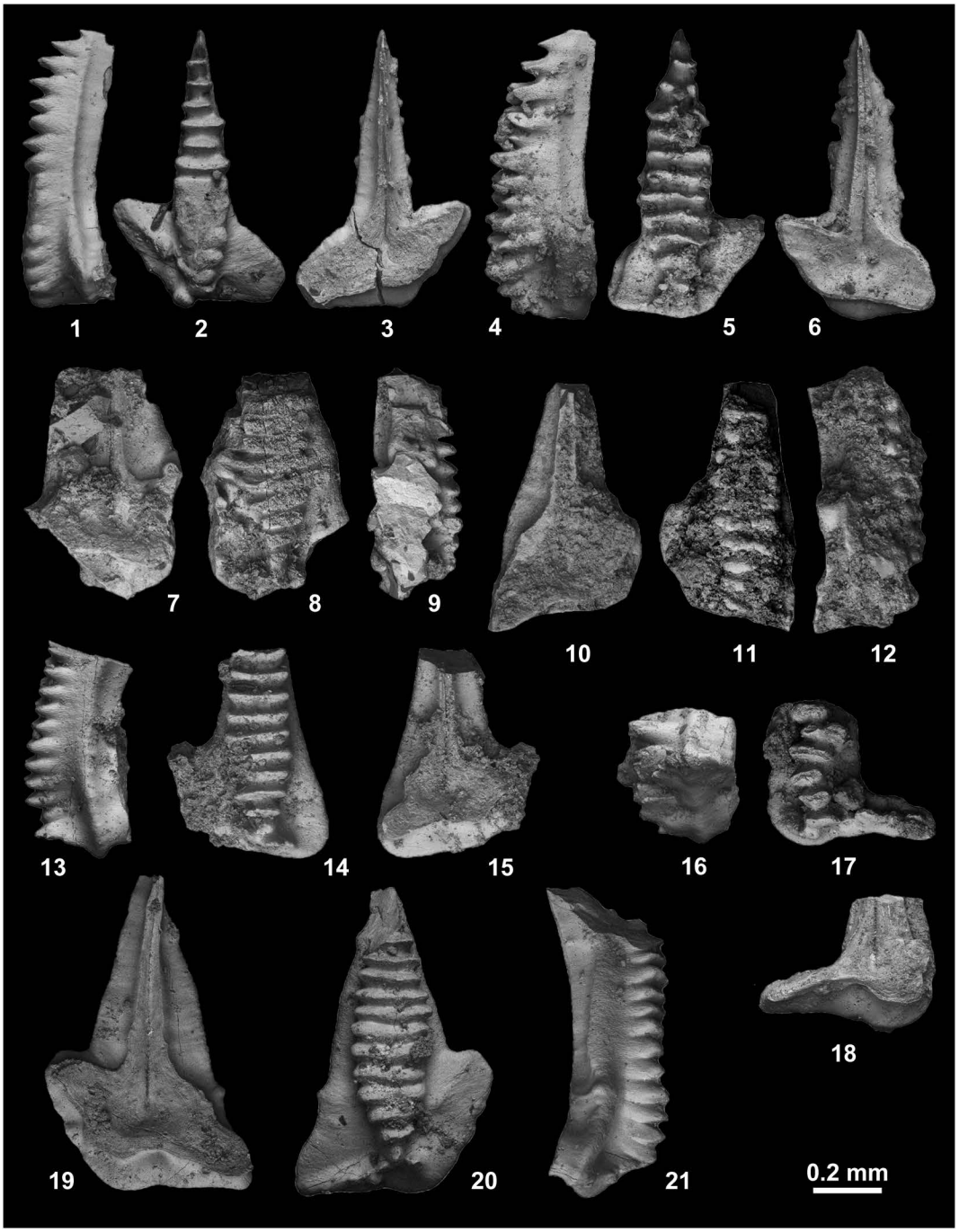

Fig. 191. *Icriospathodus collinsoni* (Solien, 1979) from KC02-15. 1–3, MPC25639. 4–6, MPC25640. 7–9, MPC25641. 10–12, MPC25642. 13–15, MPC25643. 16–18, MPC25644. 19–21, MPC25645.

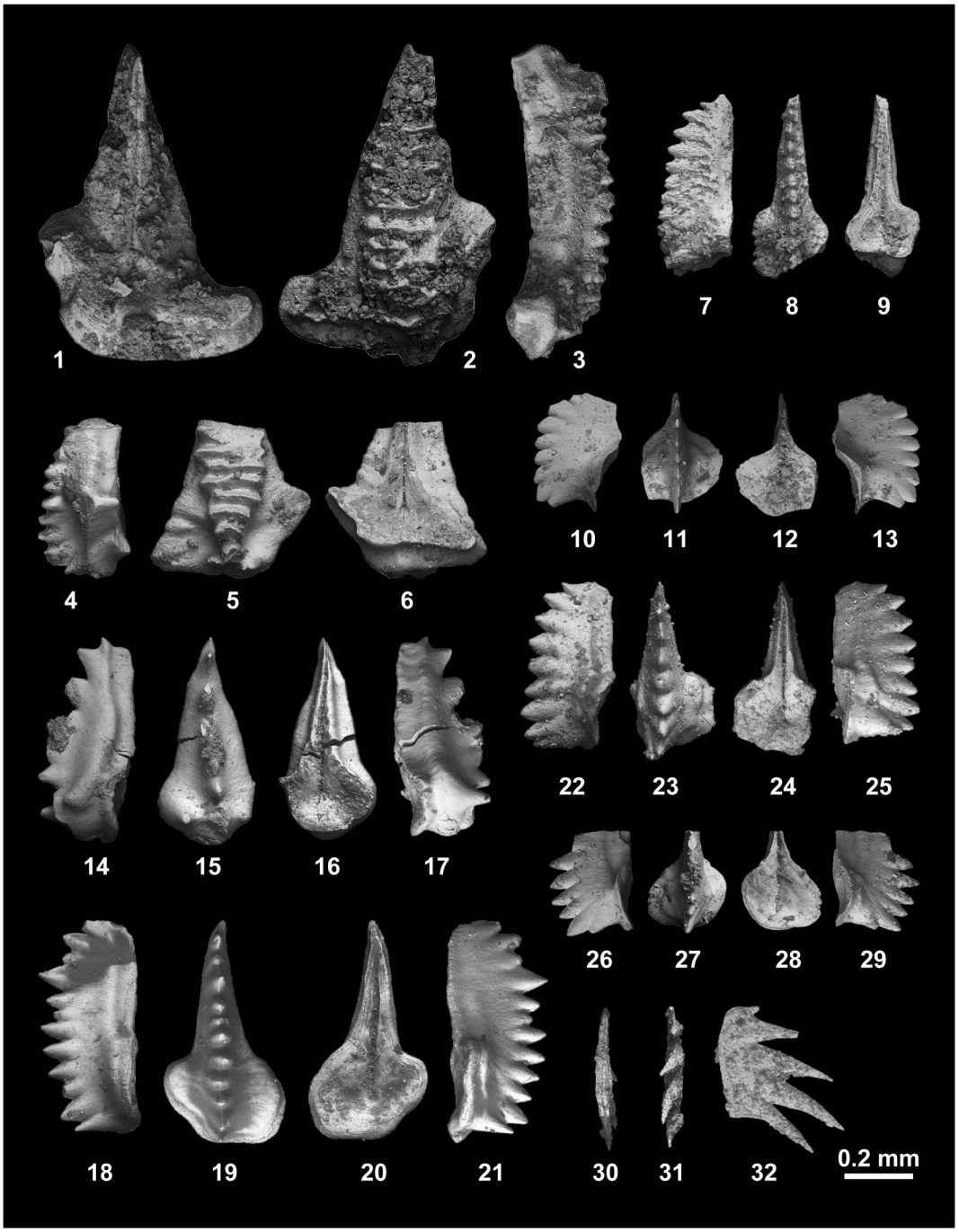

Fig. 192. 1–6, *Icriospathodus collinsoni* (Solien, 1979) from KC02-15. 1–3, MPC25646. 4–6, MPC25647. 7–9, *Icriospathodus*? *crassatus* (Orchard, 1995), MPC25648, from KC02-15. 10–29, *Icriospathodus*? *zaksi* (Buryi, 1979). 10–13, MPC25649, from KC02-08. 14–17, MPC25650, from KC02-10. 18–21, MPC25651, from KC02-10. 22–25, MPC25652, from NT01-07. 26–29, MPC25653, from NT01-09. 30–32, Genus gen. indet. A, MPC25654, from BT01-03.

Spathian = lower Upper Olenekian) in the Bac Thuy Formation, northeastern Vietnam. This species also occurs in the Lower Spathian in Idaho (upper part of Zone 10 and Zone 11, Sweet *et al*., 1971), the Thaynes Formation, Utah (middle and upper part of *Platyvillosus* Zone and *Neospathodus collinsoni* Zone, Solien, 1979), Nevada (Clark *et al.*, 1964; Lucas and Orchard, 2007), South Primorye (*Tirolites cassianus* Zone, Buryi, 1979), the Taho limestone, Southwest Japan (Koike, 1981, 1992), South China (Duan, 1987; Ji *et al*., 2011), and Svalvard (Hatleberg and Clark, 1984).

According to Sweet *et al*. (1971), Solien (1979), and Lucas and Orchard (2007), in North America, *I. collinsoni* occurs in the *Columbites* beds and its FAD is placed slightly above the Smithian/Spathian boundary (SSB), which is indicated by the FAD of *Platyvillosus asperatus* Clark, Sincavage and Stone. *P. asperatus* has been reported only from the western part of Panthalassa and it co-occurs with *Ns. homeri* (Bender, 1970) (= *Triassospathodus homeri* [Bender, 1970]) and *Ns. triangularis* (Bender, 1970) (= *Novispathodus triangularis* [Bender, 1970]). In the Bac Thuy Formation, *I. collinsoni* (KC02-14) co-occurs with *Columbites* sp. indet. and its FAD is placed slightly above the FAD of *Tirolites* cf. *cassianus* (KC02-11), the ammonoid that marks the SSB. This fact agrees with other reports.

Icriospathodus*? *crassatus (Orchard, 1995)

Fig. 192.7–192.9

Spathoicriodus collinsoni (Solien, 1979). Koike, 1992, p. 357, figs. 12.1–12.12, 12.43, 12.45–12.46, 12.51–12.53, 13.1–13.7.

Neospathodus crassatus Orcahrd, 1995, p. 120, figs. 2.19, 2.25–2.57, Ji *et al*., 2011, figs. 4.2a-c.

Icriospathodus? *crassatus* (Orchard, 1995). Orchard, 2007a, p. 60. fig. 2.

Material examined: One specimen, MPC25648, from KC02-15.

Description: Robust rectangular-shaped segminate element 0.52 mm in length; 0.22 mm in height; 0.23 mm in width; length to height ratio 2.4; length to width ratio 2.3, with rectangular lateral profile. Node-like denticles total 11 in number, and contain one small posterior process. Cusp situated near posterior end. Lower edge straight, slightly undulated below cusp. Square basal cavity expanded at posterior end with a deep pit. Furrow extends from pit to anterior end

Remarks: The described specimen closely resembles *Icriospathodus collinsoni* (Solien, 1979) in its lateral and lower views, but it lacks the ridge-like denticles on its platform. It also resembles *I.*? *zaksi* (Buryi, 1979), but the width of the element is smaller.

Occurrence: Described specimen from KC02-15 within the portion of the *Triassospathodus symmetricus* Zone represented by the *Tirolites* sp. nov. beds (Lower Spathian = lower Upper Olenekian) in the Bac Thuy Formation, northeastern Vietnam. This species also occurs in the Lower Spathian in Southwest Japan (Koike, 1992), Oman, Idaho and California (Orchard, 1995), and South China (Ji *et al*., 2011).

Icriospathodus*? *zaksi (Buryi, 1979)

Fig. 192.10–192.29

Neospathodus zaksi Buryi, 1979, p. 60, pl. 18, figs. 3a, b.

Neospathodus triangularis (Bender, 1970). Perri and Andraghetti, 1987, p. 311, pl. 33, figs. 1–4.

Icriosapthodus? *zaksi* (Buryi, 1979). Orchard, 2007a, p. 105, fig. 2.

Material examined: One specimen, MPC25469, from KC02-08, two specimens, MPC25450, 25451, from KC02-10, one specimen, MPC25452, from NT01-07, and one specimen, MPC25453, from NT01-09.

Description: Robust segminate elements 0.35–0.65 mm in length, average 0.48 mm; 0.25–0.30 mm in height, average 0.28 mm; 0.23–0.36 mm in width, average 0.27 mm; length to height ratio 1.3–2.1, average 1.7; length to width ratio 1.5–2.1, average 1.9 for five specimens, with rectangular lateral pro-

file. Short, robust, triangular-shaped denticles vary in number from 7 to 12, average 9, gradually becomes smaller towards both anterior and posterior ends, extremely small at posterior end. Terminal processes in some specimens turn to the sinistral side. Cusp situated in posterior one-third, except for MPC25651. Specimen (MPC25650) has terminal processes along the posterior margin of element. In lateral view, prominent lateral rib developed in middle part of element, becoming strong posteriorly. Lower margin straight or curved slightly upward in anterior-most part, downcurved or slightly deflected upward in posterior part. Sub-rounded or rectangular asymmetrical basal cavity strongly concave. Deep furrow extends from the basal pit to anterior end.

Remarks: The described specimens, which include a juvenile (MPC25649), show a broad morphological variation in the platform. Specifically, one specimen (MPC25650) has a laterally expanded element and terminal process at the posterior end. Koike (1992) reported similar morphological variations in *Icriospathodus collinsoni* (Solien, 1979) and *I.*? *crassatus* (Orchard, 1995).

Occurrence: Described specimens from KC02-08, KC02-10, NT01-07 and NT01-09 within the portion of the *Novispathodus pingdingshanensis* Zone that represents the *Xenoceltites variocostatus* beds (Upper Smithian=upper Lower Olenekian) in the Bac Thuy Formation, northeastern Vietnam. This species also ranges from the Upper Smithian (upper Lower Olenekian) to the Lower Spathian (lower Upper Olenekian) in South Primorye, Russia (upper part of *Anasibirites nevolini* Zone and lower part of *Tirolites cassianus* Zone, Buryi, 1979), and the Werfen Formation, southern Alps, Italy (Perri and Andraghetti, 1987).

Order Prioniodinida Sweet, 1988
Familly Ellisoniidae, Clark, 1972
Genus ***Hadrodontina*** Staesche, 1964

Type species: *Hadrodontina anceps* Staesche, 1964.

Hadrodontina? sp. indet. A

Fig. 186.4, 186.5

Material examined: one specimen, MPC25590, from BT01-07.

Remarks: The specimen is characterized by an arcuatiform element with robust denticles that are reclined posteriorly, and a cusp that is longer and larger than the other denticles. Assignment of this specimen to *Hadrodontina* is uncertain, but its arched form with strongly inclined pole-like processes and non-expanded basal cavity suggest that this element belongs to the family Ellisoniidae.

Occurrence: Described specimen from BT01-07 in the portion of the *Novispathodus* ex gr. *waageni* Zone between the *Flemingites rursiradiatus* beds (lowest Middle Smithian=middle Lower Olenekian) and *Urdyceras tulongensis* beds (lower Middle Smithian=middle Lower Olenekian) in the Bac Thuy Formation, northeastern Vietnam.

Hadrodontina? sp. indet. B

Fig. 186.6–186.9

Material examined: One specimen, MPC25591, from BT02-02.

Description: Angulate-like arcuatiform element 1.13 mm in length; 0.82 mm in height. Platform strongly bowed in lateral view, sigmoidal in upper view and V-shaped in lower view. Node-like denticles arranged in three rows: 13 on each side, with 6 in the center, inclination and size gradually increase posteriorly. Largest process situated in middle part of element, four times larger than other denticles.

Remarks: The assignment of this specimen to *Hadrodontina* is uncertain, but it is somewhat similar to the specimen of *Hadrodontina*

anceps Staesche, 1964 described by Perri and Andraghetti (1987, pl. 33, fig. 1a), in having three rows of denticles on the platform, but differs by its pole-like denticles arranged in a radial fashion on the symmetrical platform.

Occurrence: Described specimen from BT02-02 within the portion of the *Novispathodus* ex gr. *waageni* Zone represented by the *Urdyceras tulongensis* beds (lower Middle Smithian=middle Lower Olenekian) in the Bac Thuy Formation, northeastern Vietnam.

Incertae sedis

Genus gen. indet. A

Fig. 192.30–192.32

Material examined: One specimen, MPC25654, from BT01-03

Remarks: The completely discrete denticles, which total 5 in number, and the lack of an expanded basal cavity, indicate that this element belongs to the P_2 element of an uncertain species.

Occurrence: Described specimen from BT01-03 within the portion of the *Novispathodus* ex gr. *waageni* Zone that represents the *Flemingites rursiradiatus* beds (lowest Middle Smithian=middle Lower Olenekian) in the Bac Thuy Formation, northeastern Vietnam.

Genus gen. indet. B

Fig. 193.1–193.4

Material examined: One specimen, MPC25655, from BT01-06

Remarks: This specimen is similar to *Furnishius triserratus* Clark, 1959 in its branched anterior part, but the latter has double lines of denticles on both anterior branches. The lateral form of this specimen is close to species of the genus *Neospathodus*, but such an assignment would be uncertain based on only one specimen.

Occurrence: Described specimen from BT01-06 within the portion of the *Novispathodus* ex gr. *waageni* Zone between the *Flemingites rursiradiatus* beds (lowest Middle Smithian=middle Lower Olenekian) and *Urdyceras tulongensis* beds (lower Middle Smithian=middle Lower Olenekian) in the Bac Thuy Formation, northeastern Vietnam.

Genus gen. indet. C

Fig. 193.5–193.7

Material examined: One specimen, MPC25656, from BT01-06

Remarks: This specimen is similar to *Discretella* in having discrete denticles and a rounded basal cavity, but the more robust and strongly laterally curved posterior part of the element makes it difficult to determine an assignment.

Occurrence: Described specimen from BT01-06 within the portion of the *Novispathodus* ex gr. *waageni* Zone between the *Flemingites rursiradiatus* beds (lowest Middle Smithian=middle Lower Olenekian) and *Urdyceras tulongensis* beds (lower Middle Smithian=middle Lower Olenekian) in the Bac Thuy Formation, northeastern Vietnam.

Genus gen. indet. D

Fig. 193.8–193.12

Material examined: One specimen, MPC25657, from BT01-07, and one specimen, MPC25658, from PK01-02.

Remarks: The specimens have a large reclined cusp on a relatively short platform. Specimen MPC25658 has several processes on both the anterior and posterior sides of the cusp and a strongly expanded platform, when compared with specimen MPC25657. These elements probably exhibit different growth stages.

Occurrence: Described specimen from BT01-07 within the portion of the *Novispathodus* ex gr. *waageni* Zone between the *Flemingites rursiradiatus* beds (lowest Middle Smithian=middle Lower Olenekian) and *Urdyceras tulongensis* beds (lower Middle Smithian=middle Lower Olenekian), and from PK01-02 within the portion of the *Novispatho-*

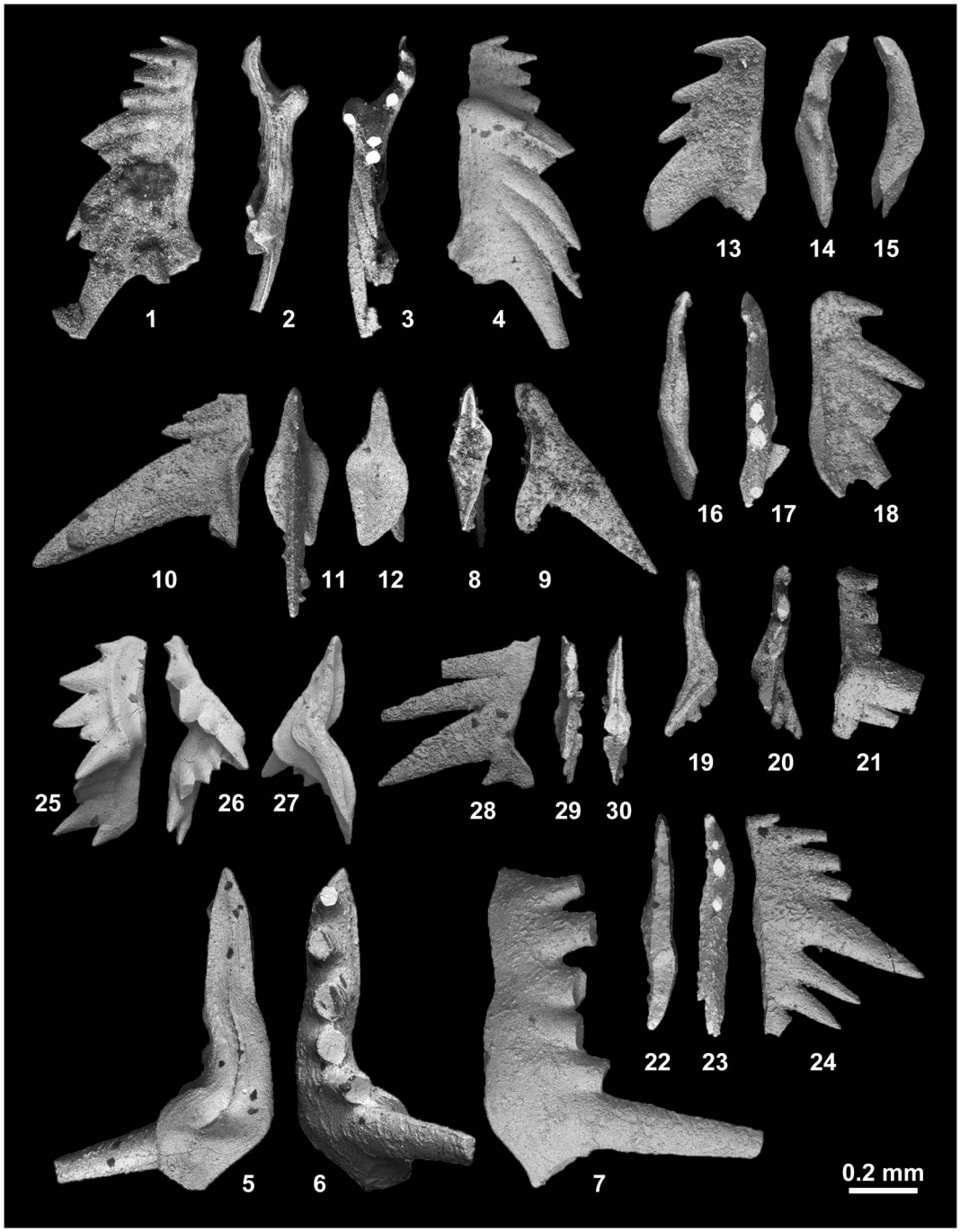

Fig. 193. 1–4, Genus gen. indet. B, MPC25655, from BT01-06. 5–7, Genus gen. indet. C, MPC25656, from BT01-06. 8–12, Genus gen. indet. D. 8–9, MPC25657, from BT01-07. 10–12, MPC25658, from PK01-02. 13–21, Genus gen. indet. E. 13–15, MPC25659, from BT02-01. 16–18, MPC25660, from BT02-01. 19–21, MPC25661, from BT03-01. 22–24, Genus gen. indet. F, MPC25662, from BT02-03. 25–27, Genus gen. indet. G, MPC25663, from KC01-05. 28–30, Genus gen. indet. H, MPC25664, from PK01-02.

dus ex gr. *waageni* Zone represented by the *Owenites koeneni* beds (middle Middle Smithian=middle Lower Olenekian) in the Bac Thuy Formation, northeastern Vietnam.

Genus gen. indet. E

Fig. 193.13–193.21

Material examined: Two specimens, MPC25659, 25660, from BT02-01, and one specimen, MPC25661, from BT03-01.

Remarks: The specimens are characterized by a laterally curved element with strongly reclined denticles and a large cusp situated in the posterior one-third. These features indicate that the specimens probably belong to the P_2 element of the family Gondolellidea.

Occurrence: Described specimens collected from BT02-01 within the portion of the *Novispathodus* ex gr. *waageni* Zone represented by the *Flemingites rursiradiatus* beds (lowest Middle Smithian=middle Lower Olenekian), and from BT03-01 within the portion of the *Novispathodus* ex gr. *waageni* Zone represented by the *Owenites koeneni* beds (middle Middle Smithian=middle Lower Olenekian) in the Bac Thuy Formation, northeastern Vietnam.

Genus gen. indet. F

Fig. 193.22–193.24

Material examined: One specimen, MPC25662, from BT02-03.

Remarks: The specimen lacks a part of its lower side, but discrete needle-like denticles on the upper side are similar to those of the P_2 element of species in the subfamily Mulleninae.

Occurrence: Described specimen from BT02-03 within the portion of the *Novispathodus* ex gr. *waageni* Zone represented by the *Leyeceras* horizon of the *Owenites koeneni* beds (middle Middle Smithian=middle Lower Olenekian) in the Bac Thuy Formation, northeastern Vietnam.

Genus gen. indet. G

Fig. 193.25–193.27

Material examined: One specimen, MPC25663, from KC01-05.

Remarks: This specimen exhibits a "V" shaped platform with laterally compressed short denticles in the upper view. An affiliation assignment of this element is not possible.

Occurrence: Described specimen from KC01-05 within the portion of the *Novispathodus* ex gr. *waageni* Zone below the *Owenites koeneni* beds (middle Middle Smithian=middle Lower Olenekian) in the Bac Thuy Formation, northeastern Vietnam.

Genus gen. indet. H

Fig. 193.28–193.30

Material examined: One specimen, MPC25664, from PK01-02.

Remarks: This bowed specimen lacks the anterior part of element. Discrete long processes and a slightly expanded basal cavity demonstrate that this element belongs to the P_2 element of species in the family Gondolellidea.

Occurrence: Described specimen from PK01-02 within the portion of the *Novispathodus* ex gr. *waageni* Zone represented by the *Owenites koeneni* beds (middle Middle Smithian=middle Lower Olenekian) in the Bac Thuy Formation, northeastern Vietnam.

Ostracods (by G. Tanaka,T. Komatsu and T. Maekawa)

Most of the ostracod specimens recovered by acid treatment of limestone samples have consisted of incomplete, fragmented, or crushed valves or carapaces, but six species belonging two genera have been recognized and several well-preserved specimens are described in this paper. The morphological terms used are based on the work of Moore (1961).

Abbreviations: L=length, H=height, W=width, LV=left valve, RV=right valve, C=carapace.

Institution abbreviation: MPC=Micropaleontology Collection, National Museum of Nature and Science, Tsukuba.

Phylum Arthropoda Latreille, 1829
Subphylum Crustacea Brünnich, 1772
Class Ostracoda Latreille, 1802
Order Podocopida Sars, 1866
Suborder Cypridocopina Jones, 1901
Superfamily Cypridoidea Baird, 1845
Family Candonidae Kaufmann, 1900
Genus ***Paracypris*** Sars, 1866

Type species: ***Paracypris polita*** Sars, 1866.

Paracypris vietnamensis
Tanaka and Komatsu sp. nov.
Figs. 194, 195

Type specimens: Holotype, MPC25845; paratypes, seven specimens, MPC25846–25852. Type specimens were collected from BR01-04.

Diagnosis: LV larger than RV, overlapping along anterior to posterior margin via dorsal margin. Posterior margin protruded with small curvature and protruding toward postero-ventral direction.

Etymology: After Vietnam, where the type specimens are from.

Description: Valve sub-trapezoidal in lateral view and anterior end higher than posterior end (Figs. 194.1, 195.1). LV larger than RV, overlapping along anterior to posterior margin via dorsal margin (Fig. 195.3). Anterior cardinal angle obtuse at about 150 degrees, posterior cardinal angle obtuse at about 140 degrees. In lateral view, lower half of anterior margin acutely rounded and protruded antero-ventrally; dorsal margin straight, inclined toward posterior; ventral margin sinuate and concave at middle; one-third of lower posterior margin protruded, with small curvature and protruding in a postero-ventral direction, and two-thirds of upper posterior margin broadly arched in RV (Fig. 195.3), broadly arched postero-dorsally in LV (Fig. 195.1). Surface of C finely reticulated (Figs. 194.3, 195.4), probably shrinking after diagenesis or acid-treatment. Reticulation probably due to shrinkage of the chitinous membrane, because same reticulation is observed on internal surface of the valve (Figs. 194.7, 194.8, 195.7). Extremely thin valve (1.5–5.0μm) (Figs. 194.5, 194.7, 194.8, 195.2, 195.5, 195.7). Normal pore canals (Fig. 194.3) are sporadically distributed, and diameter of each is about 1.5μm. In dorsal view, bullet-shaped carapace, LV larger than RV, anterior end protruding more than posterior end. In internal view, straight hinge line (Fig. 194.6) runs parallel to dorsal margin (Fig. 194.6) in LV. Sulcus of RV (Fig. 195.6) fit straight hinge bar of RV. Adont hinge. Duplicature developed in antero-dorsal to postero-dorsal areas along ventral area, broadly in antero-ventral and postero-ventral areas (Figs. 194.6, 194.7, 195.6, 195.7). Adductor muscle scars not observed. Sexual dimorphism unknown.

Discussion: *Paracypris vietnamensis* sp. nov. is similar to *Paracypris jinyaensis* Crasquin-Soleau, 2006 (in Crasquin-Soleau *et al*., 2006) from the Early Triassic (Olenekian) strata of the Fengshan area, Guangxi Province, South China, but differs from it in terms of its postero-ventrally bended caudal process, its more rounded lateral outline, and its slightly sinuated ventral margin. *Paracypris vietnamensis* sp. nov. resembles *Paracypris* sp. reported by Wei (1981) from the Middle Triassic Leikoupo Formation of Weiyuan of Sichuan, South China, but can be distinguished from *Paracypris* sp. by its small carapace and by its widely arched posterior margin and more rounded lateral outline in the RV. The new species is similar to *Paracypris*? *scalaris* Wei, 1981 from the Early Triassic Jialingjiang Formation of Sichuan, South China, but differs from the latter in terms of its more acute posterior margin, the tendency for its dorsal margin to be inclined toward the posterior, and its more blunt anterior and posterior cardinal angles.

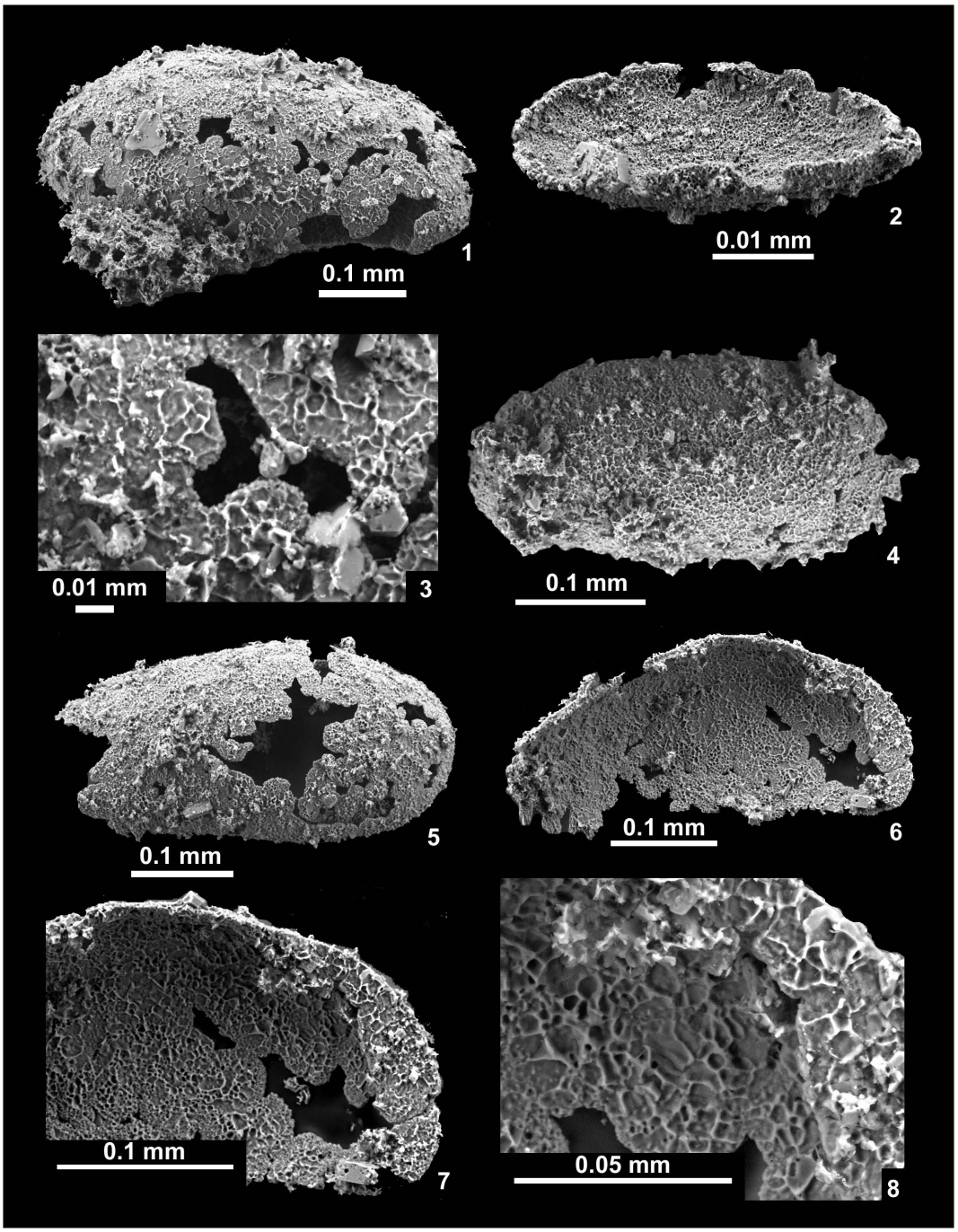

Fig. 194. *Paracypris vietnamensis* Tanaka and Komatsu sp. nov., from BR01-04. 1, 3, MPC25848, paratype. 1, Left lateral view of C. 3, Enlargement of mid-posterior area. 2, MPC25849, paratype, ventral view of internal valve of RV. 4, MPC25850, paratype, lateral view of RV. 5, MPC25851, paratype, lateral view of RV. 6–8, MPC25852, paratype. 6, Internal view of LV. 7, Enlargement of anterior area. 8, Magnified antero-dorsal margin.

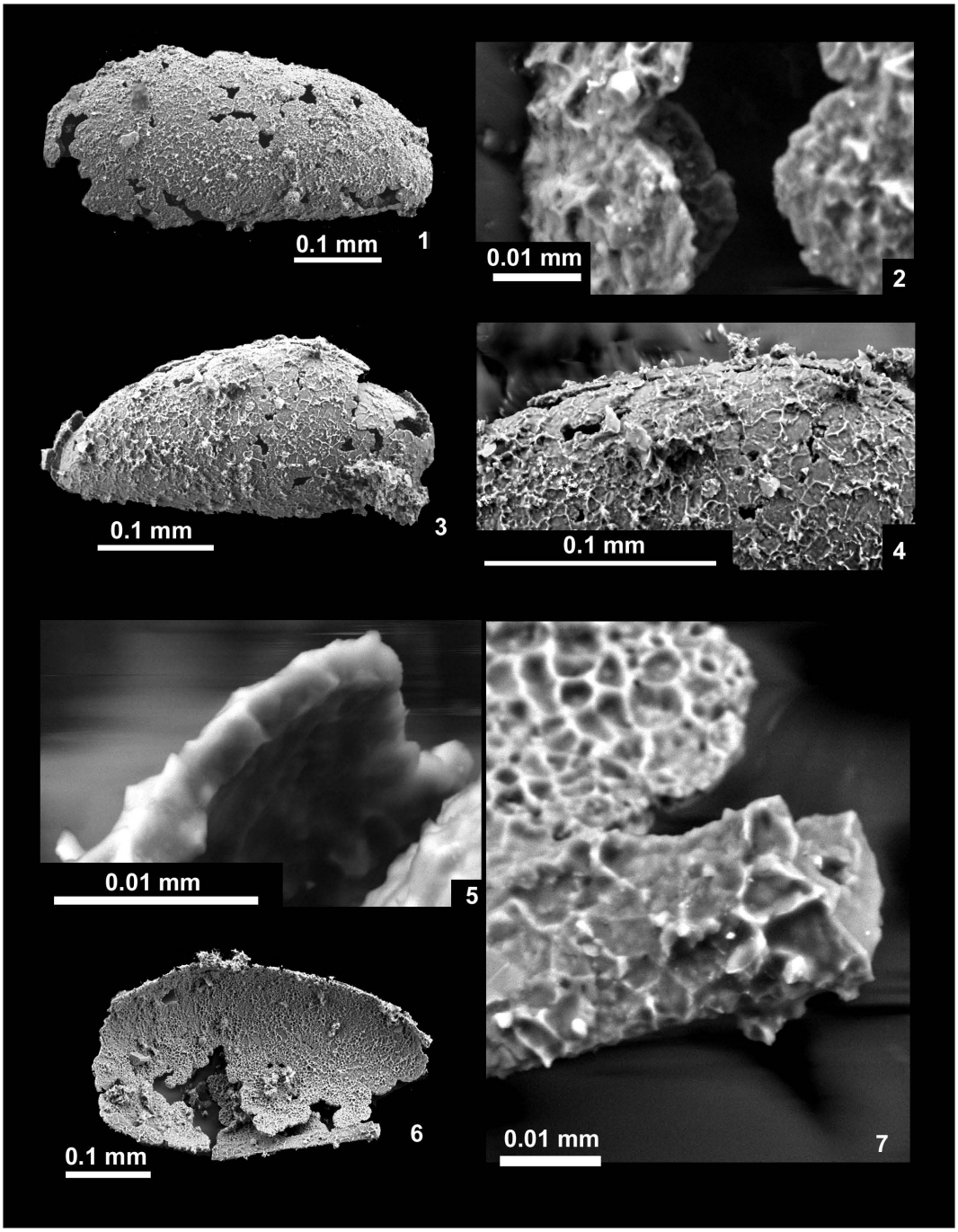

Fig. 195. *Paracypris vietnamensis* Tanaka and Komatsu sp. nov., from BR01-04. 1–2, MPC25846, paratype. 1, External view of LV. 2, Enlargement of antero-ventral area. 3–5, MPC25845, holotype. 3, Right lateral view of C. 4, Enlargement of mid-dorsal area. 5, Magnification of dorso-posterior area. 6–7, MPC25847, paratype. 6, Internal view of partly broken RV. 7, Enlagement of postro-ventral area.

Occurrence: Described specimens from BR01-04 within the *Novispathodus pingdingshanensis* Zone below the *Xenoceltites variocostatus* beds (Upper Smithian=upper Lower Olenekian) in the Bac Thuy Formation, northeastern Vietnam.

Paracypris sp. indet. A

Figs. 196.1–196.5, 197.3–197.5, 197.7, 197.8

Material examined: Five specimens, MPC25853–25857, from BR01-04.

Discussion: This species is similar to *P. jinyaensis* Crasquin-Soleau, 2006 (in Crasquin-Soleau *et al*., 2006) from the Early Triassic (Olenekian) strata of the Fengshan area, Guangxi Province, South China, but differs from it in the straight upper half of its anterior margin, its more acute caudal process, and its lack of an evenly rounded anterior margin. *Paracypris* sp. indet. A resembles *Paracypris* sp. reported by Wei (1981) from the Middle Triassic Leikoupo Formation of Weiyuan in Sichuan, South China, but it can be distinguished from *P.* sp. by its small carapace, ventrally arched anterior margin, and more rounded posterior margin. This species is similar to *Paracypris badongensis* Guan, 1985 from the Middle Triassic Baotahe Formation, Hubei Province, South China, but differs from it in that it has a more protruded caudal process, a straight dorsal margin, and a more inflated carapace from the dorsal view.

Occurrence: Described specimens from BR01-04 within the *Novispathodus pingdingshanensis* Zone below the *Xenoceltites variocostatus* beds (Upper Smithian=upper Lower Olenekian) in the Bac Thuy Formation, northeastern Vietnam.

Paracypris sp. indet. B

Figs. 196.6, 196.7, 197.6

Material examined: Two specimens, MPC25858–25859, from BR01-04.

Discussion: This species is similar to *Paracypris* sp. Wei, 1981 from the Middle Triassic Leikoupo Formation, Sichuan Province, South China, but differs from it in that it has a broadly arched anterior margin, higher lateral outline, and sinuated ventral margin.

Occurrence: Described specimens from BR01-04 within the *Novispathodus pingdingshanensis* Zone below the *Xenoceltites variocostatus* beds (Upper Smithian=upper Lower Olenekian) in the Bac Thuy Formation, northeastern Vietnam.

Paracypris sp. indet. C

Fig. 197.1, 197.2

Material examined: One specimen, MPC25860, from BR01-04.

Discussion: This species is similar to *Paracypris*? *scalaris* Wei, 1981 from the Early Triassic Jialingjiang Formation, Sichuan Province, South China, but it differs from the latter in terms of its broadly arched dorsal margin, evenly arched anterior margin, and higher lateral outline.

Occurrence: Described specimens from BR01-04 within the *Novispathodus pingdingshanensis* Zone below the *Xenoceltites variocostatus* beds (Upper Smithian=upper Lower Olenekian) in the Bac Thuy Formation, northeastern Vietnam.

Superfamily Bairdiacea Sars, 1887
Family Bairdiidae Sars, 1887
Genus ***Bairdia*** McCoy, 1844

Type species: ***Bairdia curia*** McCoy, 1844.

Bairdia sp. indet. A

Fig. 198.3–198.5

Material examined: One specimen, MPC25862, from NT01-08.

Discussion: This species is similar to *Bairdia wailiensis* Crasquin-Soleau, 2006 (in Crasquin-Soleau *et al*., 2006) from the Early Triassic (Olenekian) strata of the Jinya/Waili section, Guangxi Province, South China, but differs from it in the more steeply inclined

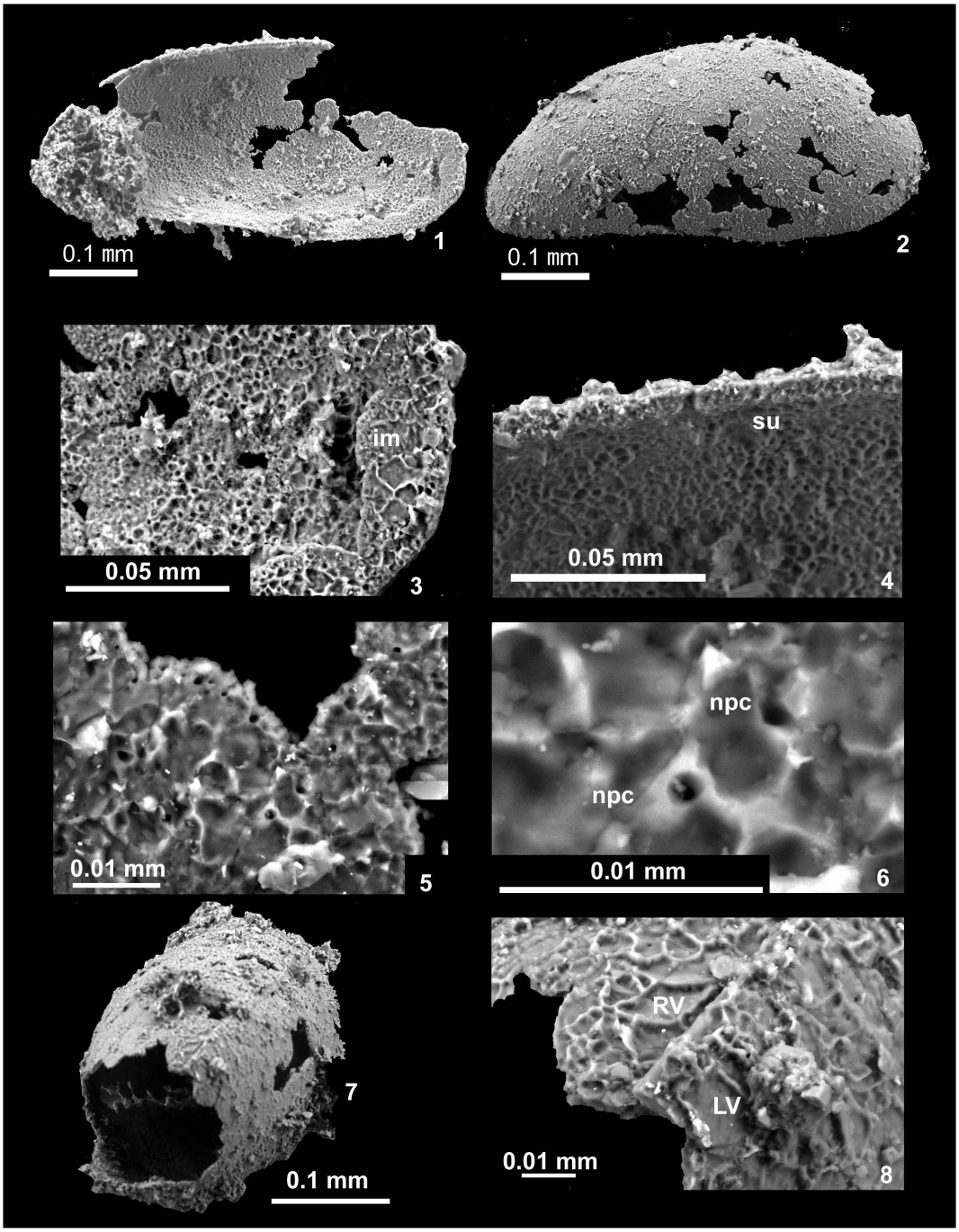

Fig. 196. 1–5, *Paracypris* sp. indet. A from BR01-04. 1, 2, MPC25853. 1, External view of LV. 2, Enlargement of broken part of anterior area, showing outer and inner shells. 3–5, MPC25854. 3, Right lateral view of C. 4, Enlargement of dorsal margin. 5, Magnified broken area of postero-dorsal margin. 6, 7, *Paracypris* sp. indet. B, MPC25858 from BR01-04. 6, Fragment of internal view of RV. 7, Enlargement of postero-ventral area, showing duplicature.

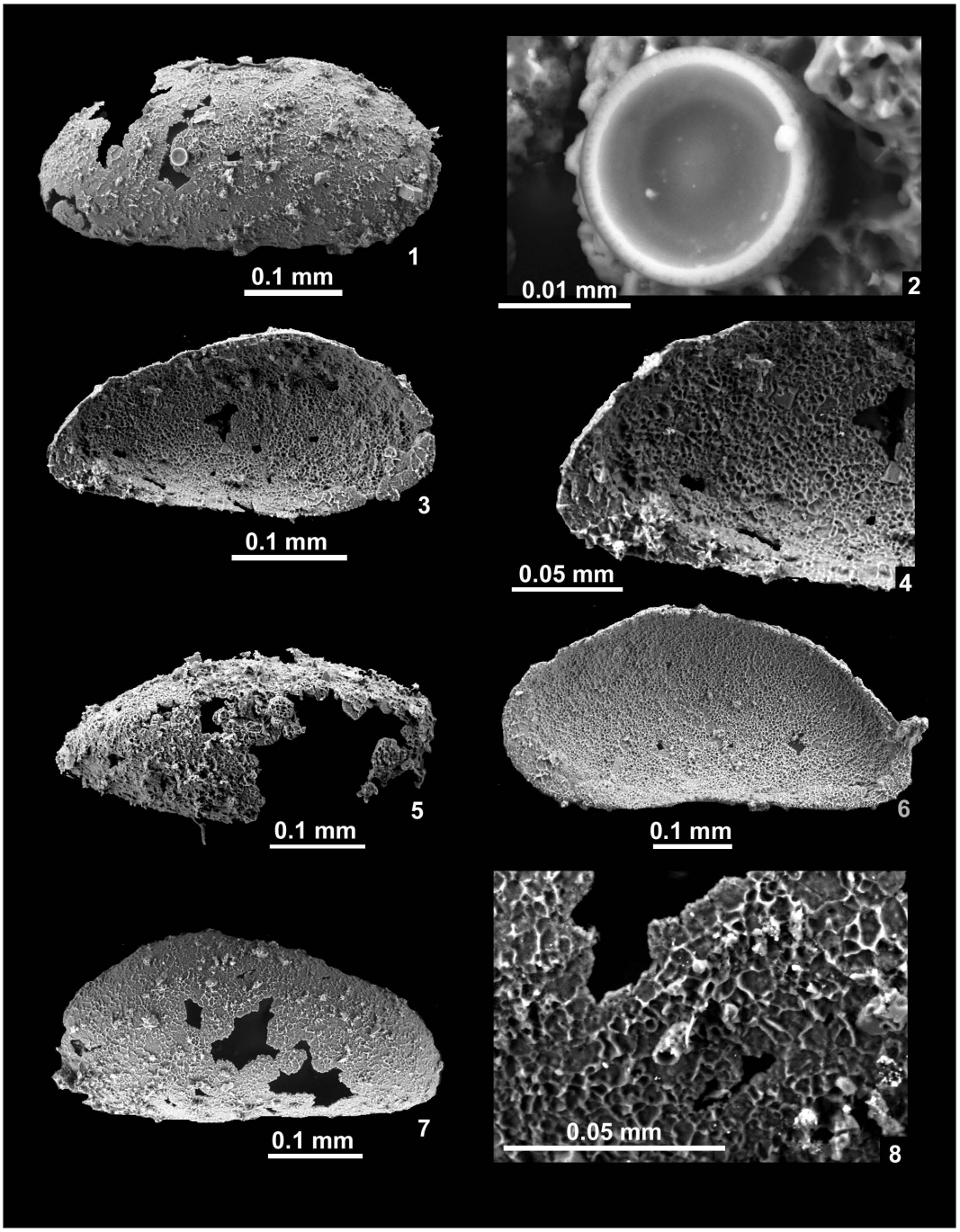

Fig. 197. 1, 2, *Paracypris* sp. indet. C, MPC25860 from BR01-04. 1, External view of RV. 2, Enlargement of central area showing attached diatom-like organism. 3–5, 7, 8, *Paracypris* sp. indet. A from BR01-04. 3, 4, MPC25855. 3, Internal view of LV. 4, Close-up of postero-ventral area. 5, MPC25856, dorsal view of C. 7–8, MPC25857. 7, External view of LV. 8, Enlargement of mid-ventral area, showing tube-like structure (center of image). 6, *Paracypris* sp. indet. B, MPC25859, from BR01-04, internal view of RV. im: inner margin, LV: left valve, npc: normal pore canal, RV: right valve, su: sulcus.

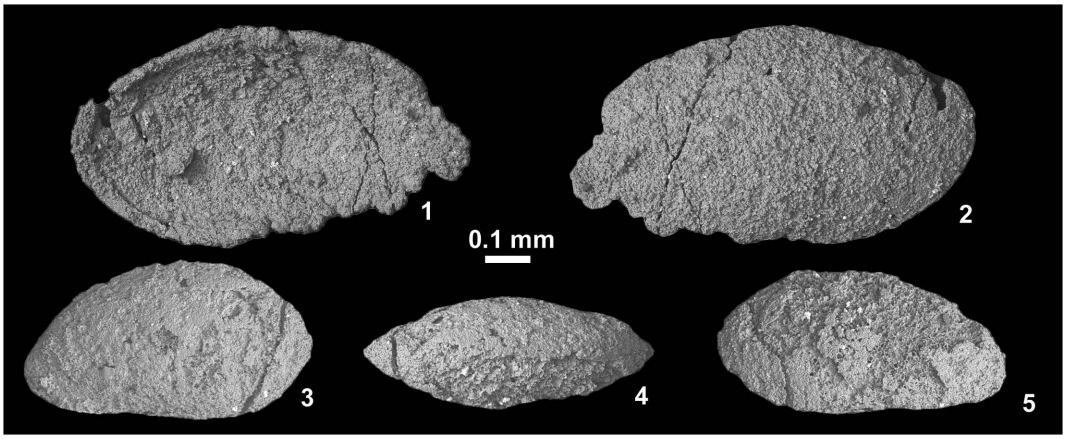

Fig. 198. 1, 2, *Bairdia* sp. indet. B, MPC25861, from NT01-09. 1, Internal view of RV. 2, External view. 3–5, *Bairdia* sp. indet. A, MPC25862, from NT01-08. 3, Right lateral view of C. 4, Dorsal view of C. 5, Left lateral view of C.

upper half of the posterior margin, more broadly arched dorsal margin, and sinuated ventral margin.

Occurrence: Described specimens from NT01-08 within the *Novispathodus pingdingshanensis* Zone represented by the *Xenoceltites variocostatus* beds (Upper Smithian=upper Lower Olenekian) in the Bac Thuy Formation, northeastern Vietnam.

Bairdia sp. indet. B

Fig. 198.1, 198.2

Material examined: One specimen, MPC25861, from NT01-09.

Discussion: This specimen is juvenile because of the presence of a weakly developed inner margin. This species is similar to *Bairdia* sp. Wei, 1981 from the Early Triassic Jialingjiang Formation, Sichuan Province, South China, but differs from the latter in that it has a longer upper half of anterior margin, broadly arched anterior margin, and longer dorsal margin.

Occurrence: Described specimen from NT01-09 within the *Novispathodus pingdingshanensis* Zone represented by the *Xenoceltites variocostatus* beds (Upper Smithian=upper Lower Olenekian) in the Bac Thuy Formation, northeastern Vietnam.

Radiolarians (by O. Takahashi and Y. Miyake)

Systematic descriptions are basically following the classification by De Wever *et al.* (2001).

Institution abbreviations: TGU=Tokyo Gakugei University.

Subclass Radiolaria Müller, 1858
Superorder Polycystina Ehrenberg, 1838, emend Riedel, 1967
Order Entactinaria Kozur and Mostler, 1982
Family Tetrentactiniidae Kozur and Mostler, 1979
Genus ***Multisphaera*** Nazarov and Afanasieva, 2000, emend Dumitrica, 2011

Type species: *Multisphaera impersepta* Nazarov and Afanasieva, 2000.

Remarks: The genus *Multisphaera* was first described by Nazarov and Afanasieva in Afanasieva (2000) from the Lower Permian Russian Platform. According to the emended description by Dumitrica (2011), *Multisphaera* possesses four or five concentric lattice spheres, which originated from an eccentric

four-rayed initial spicule, consisting of a double medullary shell, a single cortical shell, and one or two intermediary shells. The initial spicule has a very short median bar and four spines arranged tetrahedrally. Based on its morphological features, especially the tetrahedral arrangement of the initial spicule, Dumitrica (2011) transferred the genus to the family Tetrentactiniidae.

Multisphaera triassorobusta Takahashi, sp. nov.

Fig. 199

Material examined: Holotype, TGU 8717 (Fig. 199.1), from KC02-10. Seven specimens, TGU 8604, 8626, 8705, 8714, 8715, 8717, 8718, from KC02-10, seven specimens, TGU 9001, 9010, 9013, 9207, 9209, 9210, 9216, from NT01-05, and three specimens, TGU 8907, 8911, 8913, from NT01-07.

Diagnosis: Large robust concentric shell, comprising two medullary, one intermediary, and one cortical shells with up to about 15 three-bladed radial spines. Radial spines proximally cylindrical become three-bladed outside second medullary shell and increase their breadth distally up to the cortical shell.

Etymology: According to its occurrence in Triassic beds and the Latin noun robustus (robust) indicating its robust form.

Description: Fully grown specimens possess four concentric spheres comprising two medullary shells, one intermediary shell, and one cortical shell with up to about 15 three-bladed radial spines of uniform size and distribution. Inner medullary (1st) shell spherical and with small regularly arranged simple pores, approximately 20 on the half sphere. Outer medullary (2nd) shell also spherical and composed of an irregular network of very thin delicate anastomosing bars that sometimes has a sponge-like appearance. Between first and second medullary shell the radial spines are cylindrical. They become three-bladed outside second medullary shell and increase their breadth distally up to the cortical shell. Outside it they have not been observed because all of them are broken off. Numerous thorns or cylindrical thin short spines arise from the surface of the outer medullary shell. They may stop inside the space of the intermediary shell or may touch the wall of the latter when well preserved. Intermediary (3rd) shell composed of an irregular, delicate, anastomosing lace-like network of very thin bars; an almost identical texture is observed on the outer medullary shell. Cortical (4th) shell large, robust, rough-surfaced and composed of a very irregular loose spongy framework.

Measurements (3–5 specimens): Diameter of cortical shell 311–353 μm (mean = 329.7 μm); diameter of intermediary shell 207–225 μm (mean = 216.0 μm); diameter of outer medullary shell 92–116 μm (mean = 105.8 μm); and diameter of inner medullary shell 27–35 μm (mean = 31.2 μm).

Remarks: The observed specimens of this species were generally broken. Although the tetrahedral initial spicule allowed emendation of the diagnosis of the genus (Dumitrica, 2011) was not visible because of poor preservation, the set of several fragmentary images of this species shows all the other diagnostic features of the genus *Multisphaera* such as: double medullary shell, connected to the intermediary and cortical shells through about 15 three-bladed radial spines, which are thin and cylindrical between first and second medullary shells and three-bladed outside it. Also the structure of the intermediary shell resembles that of the type species of the genus *Multisphaera*. *Multisphaera triassorobusta* sp. nov. differs from *Multisphaera impersepta* Nazarov and Afanasieva, 2000 in having fewer radial spines and robust cortical shell.

Discussion: The genus *Multisphaera* has been represented until present only by its type species (*M. impersepta*) and considered to occur only in the Lower Permian. *M. triassorobusta* sp. nov., found in the Lower Triassic (upper Smithian), would prove that the genus *Multisphaera* crossed the P–T crisis. Although

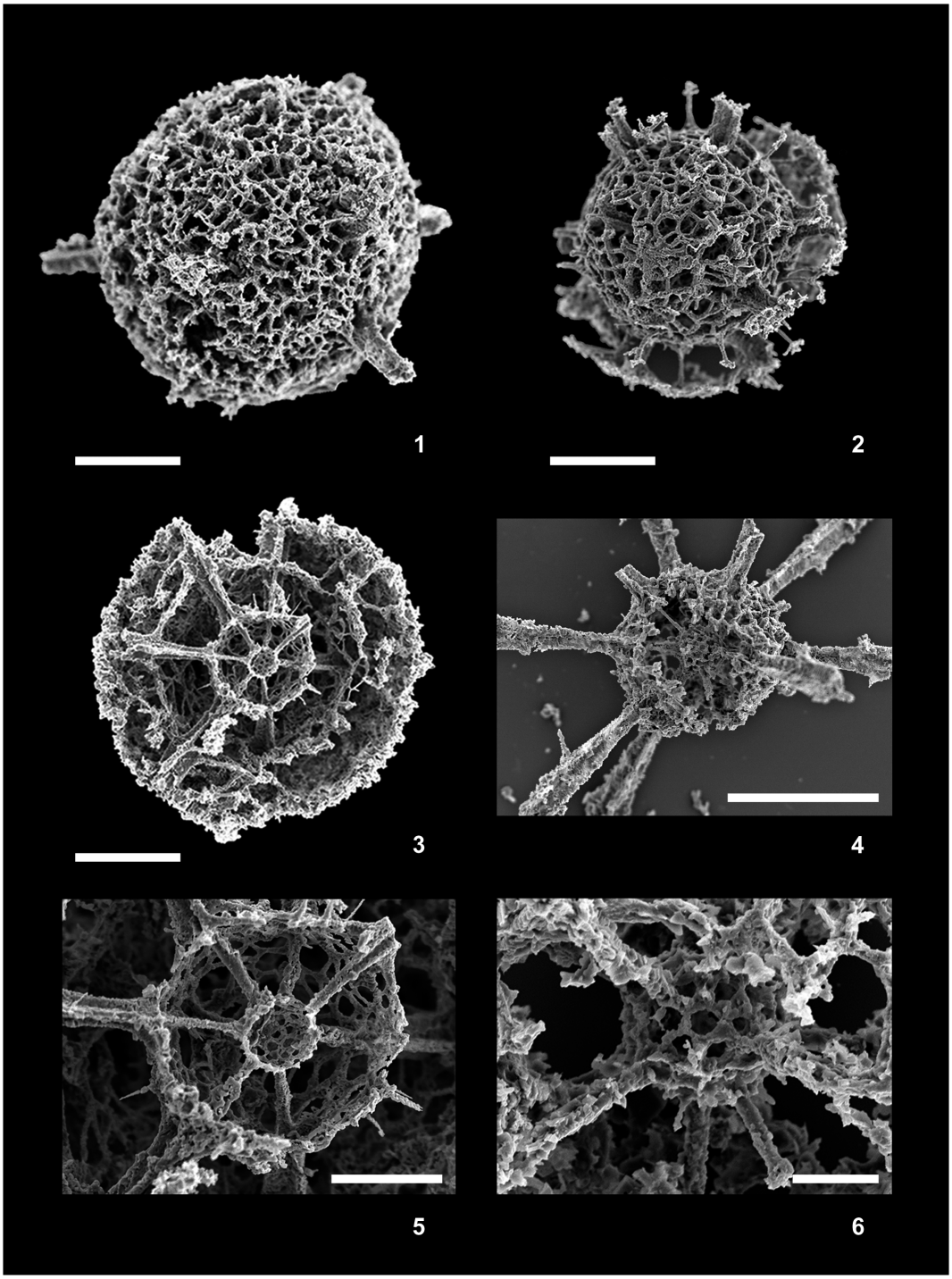

Fig 199. *Multisphaera triassorobusta* Takahashi, sp. nov. 1, TGU 8717, holotype, from KC02-10. 2, TGU 8714, from KC02-10. 3, 5, TGU 8705, from KC02-10. 4, TGU 9210, from NT01-05. 6, TGU 8626, from KC02-10. Scale bars = 100 μm (1–4), 50 μm (5), 20 μm (6).

the family Tetrentactiniidae lineage has been suggested to have a long gap between the Lower Permian (Afanasieva, 2000) and Upper Jurassic (Dumitrica and Zügel, 2000; Dumitrica, 2011), *M. triassorobusta* sp. nov. probably fills partly the gap between the Permian and Jurassic genera of this family. It might suggest that the radiolarians bearing tetrahedrally arranged initial spicule represent a single family during this period at least, although Dumitrica (2013) erected a new family for the Jurassic genera with tetrahedral spicule.

Occurrence: Described specimens from NT01-05, NT01-07 and KC02-10 within the *Novispathodus pingdingshanensis* Zone represented by the *Xenoceltites variocostatus* beds (Upper Smithian=upper Lower Olenekian) in the Bac Thuy Formation, northeastern Vietnam.

Family Spongentactiniidae Nazarov, 1975
(syn: Retentactiniinae Won, 1997)
Genus ***Retentactinia*** Won, 1997

Type species: *Retentactinia repleta* Won, 1997.

Remarks: According to Won (1997), the most characteristic feature of the genus *Retentactinia* is having a network frame (N-frame) structure. This structure appears as an inner shell and is clearly separated from the spongy tissue of the outer shell. The N-frame is connected directly to the inner surface of the outer shell by six rays of the initial spicule. This genus differs from the genus *Spongentactinia* Nazarov, 1975 in having the N-frame structure.

Retentactinia? ***kycungensis*** Takahashi, sp. nov.
Fig. 200

Material examined: Holotype, TGU 9118 (Fig. 200.1), from NT01-05. Eight specimens, TGU 8606, 8627, 8632, 8702, 8703, 8712, 8805, 8808, from KC02-10, and eight specimens, TGU 9015, 9020, 9021, 9108, 9113, 9118, 9208, 9212, from NT01-05.

Diagnosis: Moderately sized, loose spongy spinulate shell with six long, proximally three-bladed but distally cylindrical radial spines. Apophyses forming an N-frame structure.

Etymology: The species is named after the Ky Cung River, where the uppermost part of the Bac Thuy Formation is exposed and from where the radiolarian-bearing limestone samples come.

Description: Test spherical, consisting of thin uniform spongy tissue. Surface of the shell consisting of an irregular and loose spongy framework with numerous microthorns. Six long, straight, proximally three-bladed but distally cylindrical radial spines asymmetrically arranged. They are unequal in length, one or two being slightly longer. Spines directly connected to the six rays of the initial spicule that has a short median bar. Apophyses of the species forming an N-frame structure.

Measurements (8 specimens): Diameter of shell 116–156 μm (mean=138.0 μm); length of apical spine 100–156 μm (mean=131.1 μm); length of other spines 95–116 μm (mean=101.8 μm).

Remarks: The shell texture and the frame of the internal network of *Retentactinia*? *kycungensis* sp. nov. resemble those of *Retentactinia repleta* Won, 1997, the type species of the genus. However, our species differs from *R. repleta* in having six cylindrical long spines connected to the N-frame.

Occurrence: Described specimens from NT01-05 and KC02-10 within the *Novispathodus pingdingshanensis* Zone represented by the *Xenoceltites variocostatus* beds (Upper Smithian=upper Lower Olenekian) in the Bac Thuy Formation, northeastern Vietnam.

Retentactinia? ***parvisphaera*** Takahashi, sp. nov.
Fig. 201

Material examined: Holotype, TGU 9116 (Fig. 201.1), from NT01-05. Three specimens,

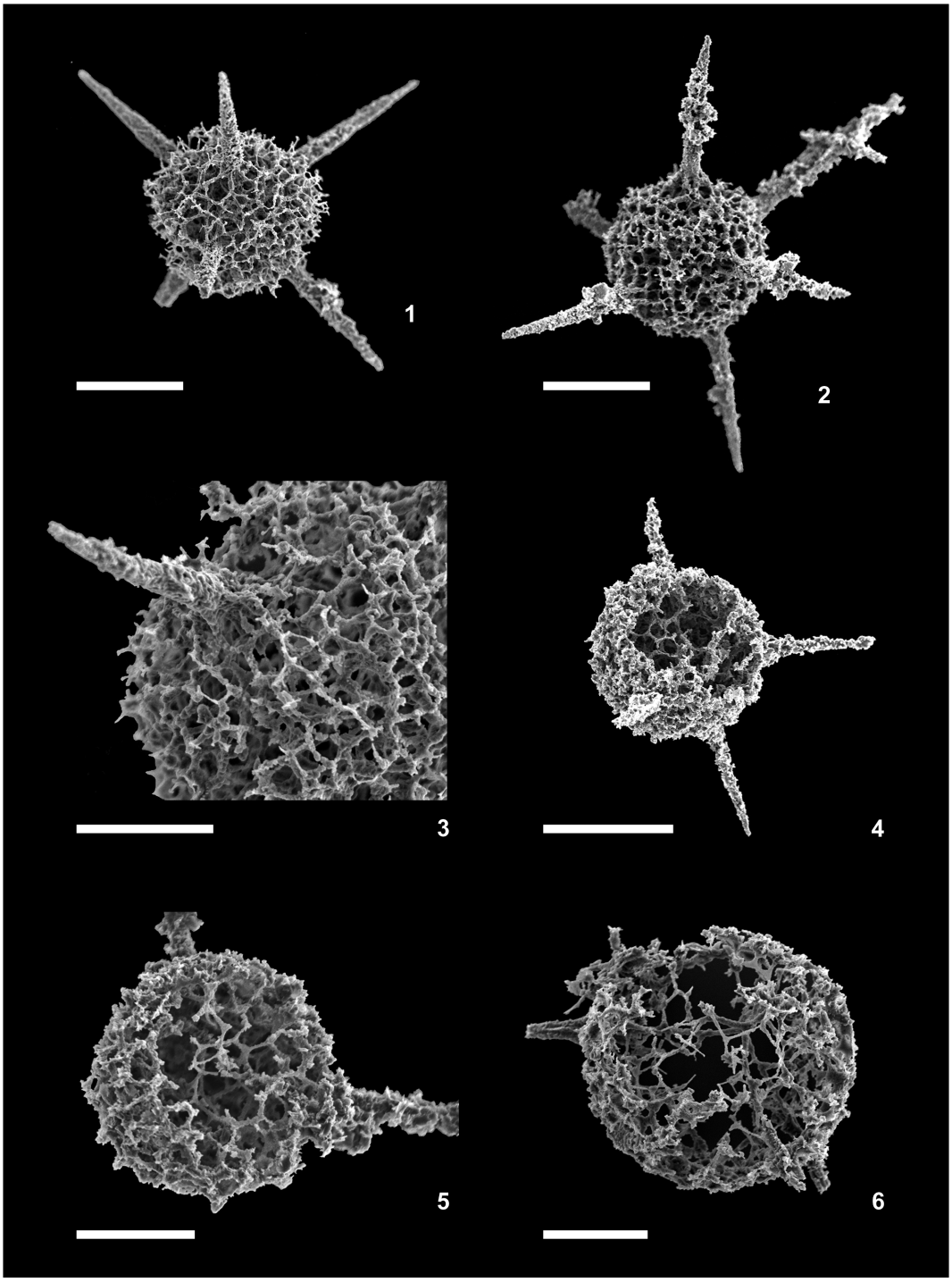

Fig. 200. *Retentactinia*? *kycungensis* Takahashi, sp. nov. 1, TGU 9118, holotype, from NT01-05. 2, TGU 8808, from KC02-10. 3, TGU 9021, from NT01-05. 4, TGU 8606, from KC02-10. 5, TGU 9020, from NT01-05. 6, TGU 8627, from KC02-10. Scale bars = 100 μm (1, 2, 4), 50 μm (3, 5, 6).

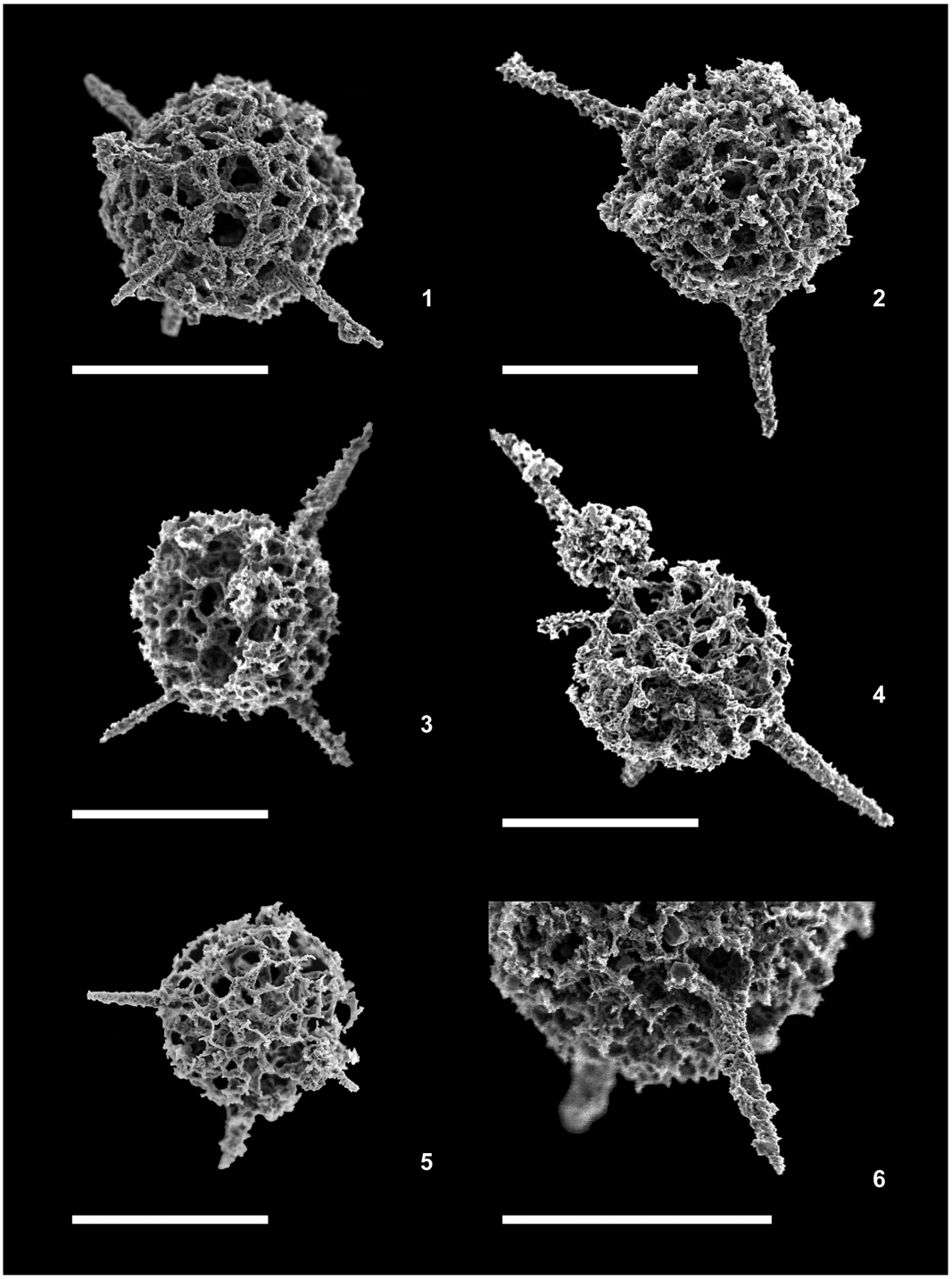

Fig. 201. *Retentactinia*? *parvisphaera* Takahashi, sp. nov. 1, TGU 9116, holotype, from NT01-05. 2, TGU 8607, from KC02-10. 3, TGU 8816, from KC02-10. 4, TGU 8819, from KC02-10. 5, TGU 9213, from NT01-05. 6, TGU 9101 from NT01-05. Scale bars = 100 μm.

TGU 8607, 8616, 8819, from KC02-10, ten specimens, TGU 9007, 9014, 9101, 9114, 9116, 9117, 9202–9204, 9213, from NT01-05, and five specimens, TGU 8903, 8908–8910, 8912, from NT01-07.

Diagnosis: Small spherical shell, consisting of a coarse fragile meshwork with six short conical spines. Spines robust, connected to initial spicule with very short median bar. Apophyses forming an N-frame structure.

Etymology: The Latin adjective parvus (small) and the noun sphaera (sphere), indicating its small size and spherical form.

Description: Test small and spherical, consisting of a coarse or middle coarse meshwork and six spines. In some specimens, a fine spongy tissue covers partly the coarse meshwork. Spines are robust and arranged asymmetrically. They are conical but slightly three-bladed proximally and connected to the six thick rays of the initial spicule that has a very short median bar. The four thick, straight, longer rays of the initial spicule arise from near the midpoint of the shell; two short rays also arise from the N-framed inner structure of the shell.

Measurements (8 specimens): Diameter of shell 87–126 μm (mean = 111.0 μm); length of spines 58–97 μm (mean = 74.2 μm).

Remarks: The genus *Retentactinia* has a spongy shell with weakly developed spines, except for *Retentactinia interreticulata* Won, 1997, which possesses robust three-bladed radial spines. *Retentactinia*? *parvisphaera* sp. nov. differs from other *Retentactinia* species in having a very coarse and fragile meshwork on the shell surface and small, straight, but robust spines.

Occurrence: Described specimens from NT01-05, NT01-07 and KC02-10 within the *Novispathodus pingdingshanensis* Zone represented by the *Xenoceltites variocostatus* beds (Upper Smithian = upper Lower Olenekian) in the Bac Thuy Formation, northeastern Vietnam.

Genus ***Plenoentactinia*** Won, 1997

Type species: *Plenoentactinia sexangula* Won, 1997.

Plenoentactinia? ***terespongia*** Takahashi, sp. nov.

Fig. 202

Material examined: Holotype, TGU 8719 (Fig. 202.2), from KC02-10. Four specimens, TGU 8620, 8621, 8701, 8706, from KC02-10, nine specimens, TGU 9003, 9004, 9006, 9017–9019, 9104, 9105, 9107, from NT01-05, and one specimen, TGU 8904, from NT01-07.

Diagnosis: Moderately sized, thick non-layered spongy shell with eight long, cylindrical slender spines. A six-rayed initial spicule with a short median bar.

Etymology: The Latin adjective teres (fine, smooth) and the noun spongia (sponge) indicate its compact spongy tissues of the shell.

Description: Test spherical, spongy, and non-layered with eight slender, cylindrical radial spines. Size of the test relatively variable; however, the inner and superficial structure of the shell and the arrangement of the main spines have a similar development within the species. Single unlayered shell consisting of very compact, thick spongy tissue and with eight long radial spines of uniform length and shape. Pores on the inner surface of the shell characteristically larger and more irregular in shape than those on the outer surface. A six-rayed initial spicule with a short median bar was observed in some specimens. This means that some spines are not prolongation of the spicule rays.

Measurements (5 specimens): Diameter of shell 139–170 μm (mean = 153.7 μm); length of spines 108–164 μm (mean = 140.8 μm).

Remarks: *Plenoentactinia*? *terespongia* sp. nov. differs from the species Won (1997) assigned unquestionably to this genus in having the spines circular in cross section and may be compared only with *Plenoentactinia*? *abstrusa* (Aitchison, 1993) (Won, 1997).

Occurrence: Described specimens from

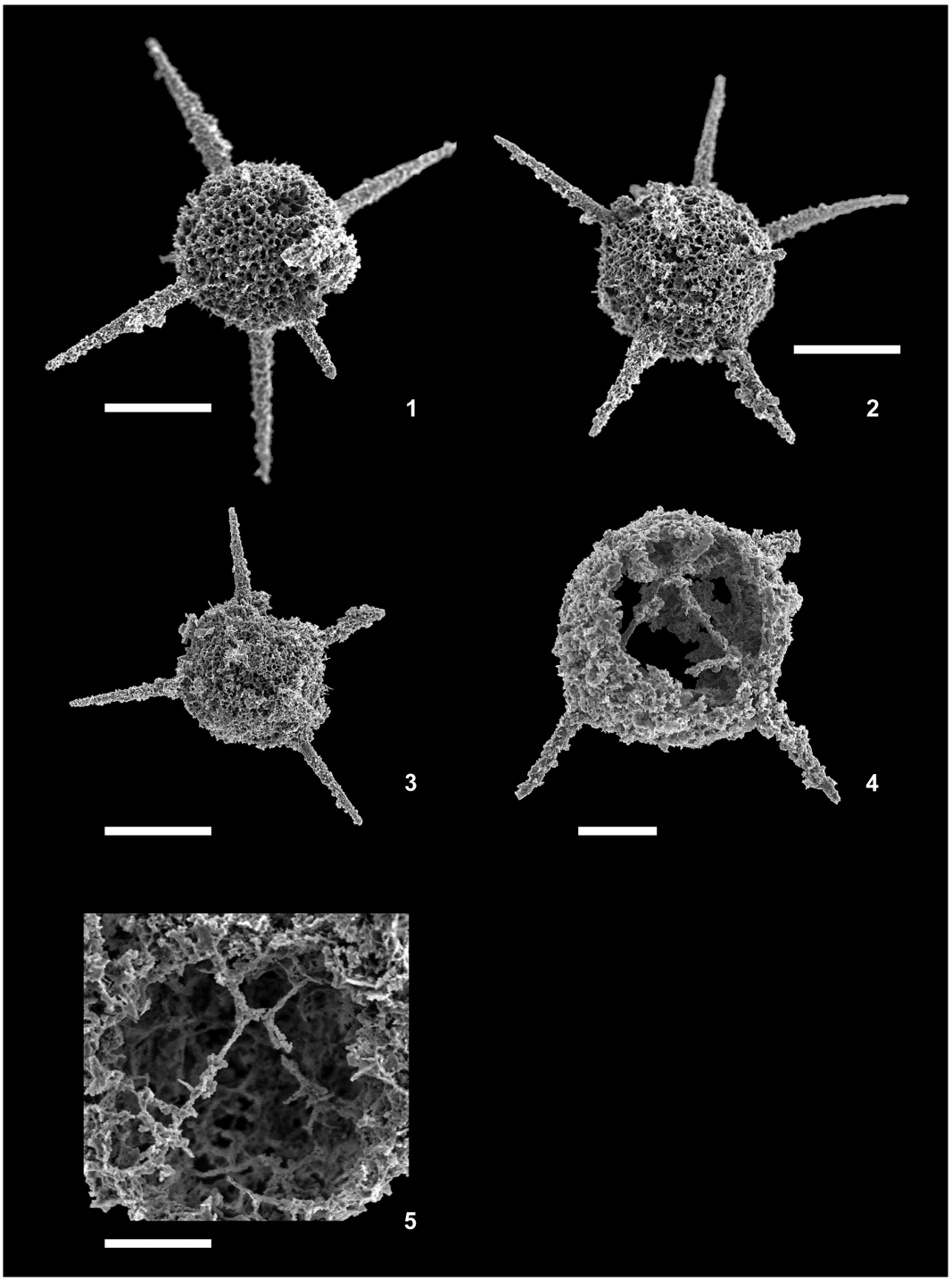

Fig. 202. *Plenoentactinia*? *terespongia* Takahashi, sp. nov. 1, TGU 8701, from KC02-10. 2, TGU 8719, holotype, from KC02-10. 3, TGU 8621, from KC02-10. 4, TGU 8620, from KC02-10. 5, TGU 8904, from NT01-07. Scale bars = 100 μm (1–3), 50 μm (4, 5).

NT01-05, NT01-07 and KC02-10 within the *Novispathodus pingdingshanensis* Zone represented by the *Xenoceltites variocostatus* beds (Upper Smithian=upper Lower Olenekian) in the Bac Thuy Formation, northeastern Vietnam.

Genus ***Spongentactinia*** Nazarov, 1975

Type species: *Spongentactinia fungosa* Nazarov, 1975.

Spongentactinia? sp. indet.

Fig. 203.1–203.4

Material examined: One specimen, TGU 9111, from NT01-05, and three specimens, TGU 8609, 8616, 8623, from KC02-10.

Remarks: We recovered only very poorly preserved and fragmental specimens of this species. The specimens have thin, fragile, spherical spongy shell with four or five, possibly six long, slender needle-like spines. Spongy shell has rather loose meshes, very thin and irregular bars and seems to be disposed in concentric layer and traversed by a series of thin radial bars. Spicule center is not visible due to the poor preservation.

Occurrence: Described specimens from NT01-05 and KC02-10 within the *Novispathodus pingdingshanensis* Zone represented by the *Xenoceltites variocostatus* beds (Upper Smithian=upper Lower Olenekian) in the Bac Thuy Formation, northeastern Vietnam.

Family Palaeoscenidiidae Riedel, 1967, emend Furutani, 1983
(syn: Parentactiniidae Kozur and Mostler, 1981; Protoentactiniidae Kozur, Mostler and Repetski, 1996)

Genus ***Parentactinia*** Dumitrica, 1978

Type species: *Parentactinia pugnax* Dumitrica, 1978.

Parentactinia nakatsugawaensis Sashida, 1983

Fig. 204.1–204.3

Parentactinia nakatsugawaensis Sashida, 1983, p. 172, pl. 37, figs. 1–9; Sashida, 1991, p. 687, figs. 5.15, 5.16, 6.1, 6.3–6.6; Sugiyama, 1992, p. 1212, 1213, figs. 14.7–14.10; Sugiyama, 1997, p. 184, figs. 27.2, 27.3; Sashida *et al*., 2000a, p. 801, fig. 8.24; Sashida *et al*., 2000b, p. 86, figs. 7.1–7.7.

Material examined: Two specimens, TGU 9115, 9211, from NT01-05, and two specimens, TGU 8902, 8905, from NT01-07.

Remarks: *Parentactinia nakatsugawaensis*, especially when poorly preserved, resembles the spiculate nassellarian species *Tandarnia recoarensis* Dumitrica, 1982, as suggested by Sashida (1983). However, both are distinguishable by the presence of a latticed shell and/or branching pattern of the spines. *P. nakatsugawaensis* has a loose hemispheric latticed shell, among the four basal spines; the basal spines are rather straight and are longer than those of *T. recoarensis*. Furthermore, *P. nakatsugawaensis* has no apical verticil.

Occurrence: Described specimens from NT01-05 and NT01-07 within the *Novispathodus pingdingshanensis* Zone represented by the *Xenoceltites variocostatus* beds (Upper Smithian=upper Lower Olenekian) in the Bac Thuy Formation, northeastern Vietnam. This species also occurs in the Lower Triassic (Spathian?) chert beds of central Japan (Sashida, 1983, 1991; Sugiyama, 1992, 1997) and the Spathian chert beds of the southern and northern Thailand (Sashida *et al*., 2000a, b).

Parentactinia cf. ***pugnax*** Dumitrica, 1978

Fig. 203.5

cf. *Parentactinia pugnax* Dumitrica, 1978, p. 50, pl. 4, figs. 4?, 5, pl. 5, figs. 1–3; Kozur and Mostler, 1994, p. 45, pl. 1, figs. 11, 12.

Material examined: One specimen, TGU 9215, from NT01-05.

Remarks: From this species we found only the fragment illustrated. It has a globular shell

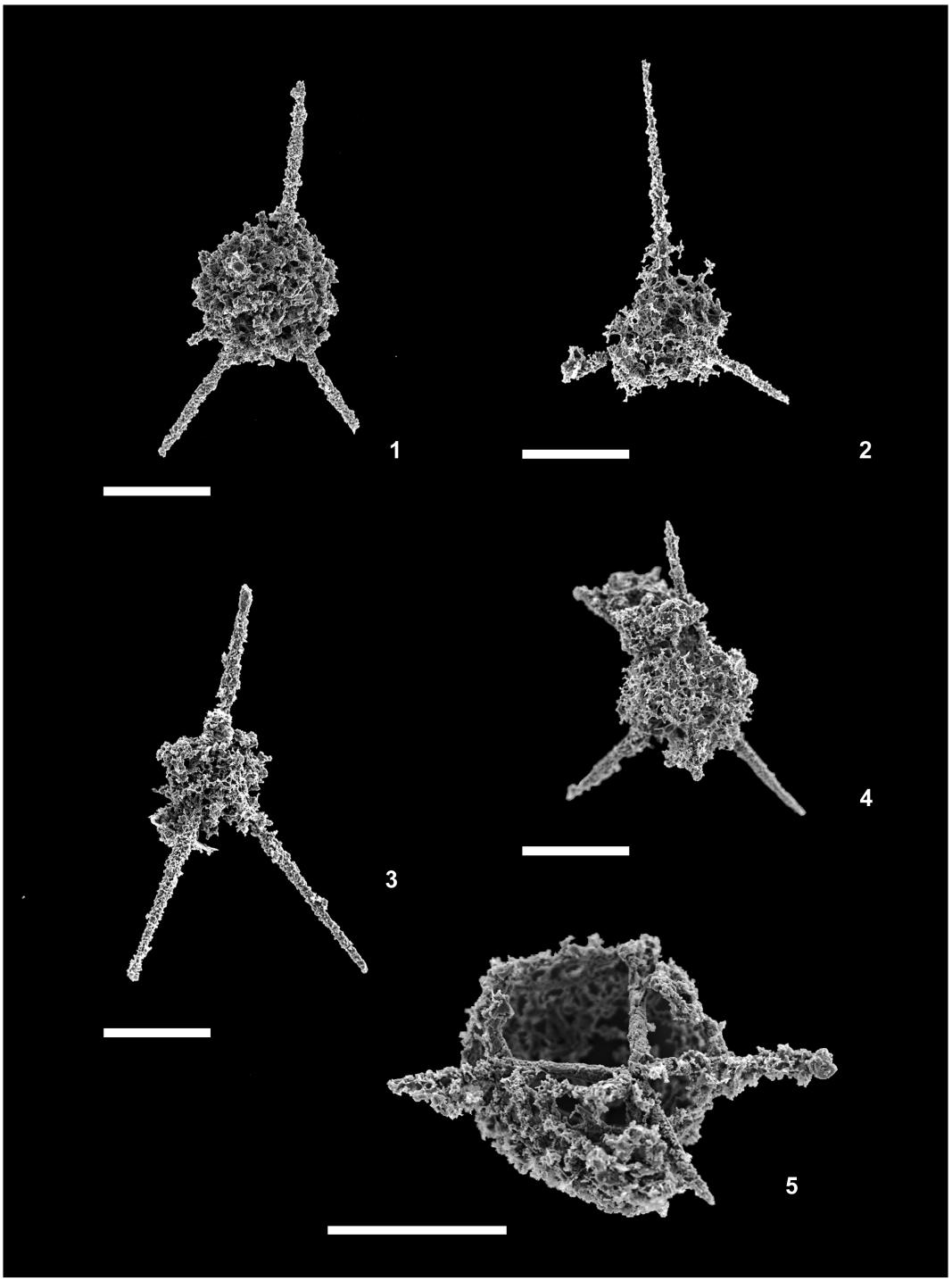

Fig. 203. 1–4, *Spongentactinia*? sp. indet. 1, TGU 8623, from KC02-10. 2, TGU 8616, from KC02-10. 3, TGU 8609, from KC02-10. 4, TGU 9111, from NT01-05. 5, *Parentactinia* cf. *pugnax* Dumitrica, 1978, TGU 9215, from NT01-05. Scale bars = 100 μm.

and an eccentric and robust initial spicule with an extremely short median bar, four basal spines and probably three apical spines of which only two are preserved. Basal spines are longer than the apical ones, relatively straight and arranged under different angles relative to the axis of shell. They are prolonged outside the shell as relatively long spines. Test is also robust with pores of irregular shape, size and arrangement. Our specimen resembles very much the late Illyrian or early Fassanian specimen questionably assigned to *Parentactinia pugnax* Dumitrica, 1978. This specimen has also three apical spines and a globular shell that includes in it also the medial bar.

Occurrence: Described specimens from NT01-05 within the *Novispathodus pingdingshanensis* Zone represented by the *Xenoceltites variocostatus* beds (Upper Smithian=upper Lower Olenekian) in the Bac Thuy Formation, northeastern Vietnam. *Parentactinia pugnax* occurs fairly rare in the upper Illyrian (=uppermost Anisian) or lower Fassanian (lowest Ladinian) at Recoaro, northern Italy (Dumitrica, 1978) and Balaton Highland, western Hungary (Kozur and Mostler, 1994).

Family Pentactinocarpidae Dumitrica, 1978
Genus ***Pentactinocarpus*** Dumitrica, 1978

Type species: *Pentactinocarpus fusiformis* Dumitrica, 1978.

Pentactinocarpus? aff. ***acanthicus*** Dumitrica, 1978
Fig. 204.4–204.7

aff. *Pentactinocarpus acanthicus* Dumitrica, 1978, p. 44, pl. 3, fig. 3; Kozur and Mostler, 1994, p. 46, pl. 2, figs. 3, 5.

Material examined: Four specimens, TGU 8614, 8618, 8625, 8806, from KC02-10, and four specimens, TGU 9008, 9112, 9120, 9214, from NT01-05.

Remarks: Our specimens have a large subspherical shell with long conical apical and antapical spines. Five or more basal spines extend laterally downward or slightly upward. Pores are elliptical or sub-circular and irregularly arranged. Although our specimens are poorly preserved, the characteristic features are similar to those of *Pentactinocarpus acanthicus* described from the uppermost Anisian to lowest Ladinian of Recoaro, Italy by Dumitrica (1978). However, our specimens differ from the type species in having more than four basal spines in some specimens, no primary ring around the spicule center and no intercalary spines between the four basal spines. Until present this genus was not yet recorded at stratigraphic levels older than late Anisian.

Occurrence: Described specimens from NT01-05 and KC02-10 within the *Novispathodus pingdingshanensis* Zone represented by the *Xenoceltites variocostatus* beds (Upper Smithian=upper Lower Olenekian) in the Bac Thuy Formation, northeastern Vietnam.

Family Thalassothamnidae Haecker, 1906
Genus ***Triassothamnus*** Kozur and Mostler, 1981
(syn: ***Archaeothamnulus*** Dumitrica, 1982)

Type species: *Palacantholithus*? *verticillatus* Dumitrica, 1978.

Triassothamnus verticillatus (Dumitrica, 1978)
Fig. 205

Palacantholithus? *verticillatus* Dumitrica, 1978, p. 42, pl. 1, fig. 1, pl. 2, fig. 5.
Archaeothamnulus verticillatus (Dumitrica, 1978). Dumitrica, 1982, p. 418, pl. 5, figs. 3, 4, pl. 7, fig. 4.

Material examined: Three specimens, TGU 8615, 8802, 8803, from KC02-10, one specimen, TGU 9011, from NT01-05, and one specimen, TGU 8906, from NT01-07.

Remarks: Our specimens have a long, straight, needle-like axial spine and four slightly curved basal spines arising from the spicule center. The apical spine has sometimes an apical verticil of three short and thin spinules, whereas the basal spines have generally a verticil of three or four spinules. The lengths of spinules vary from very short to moderately

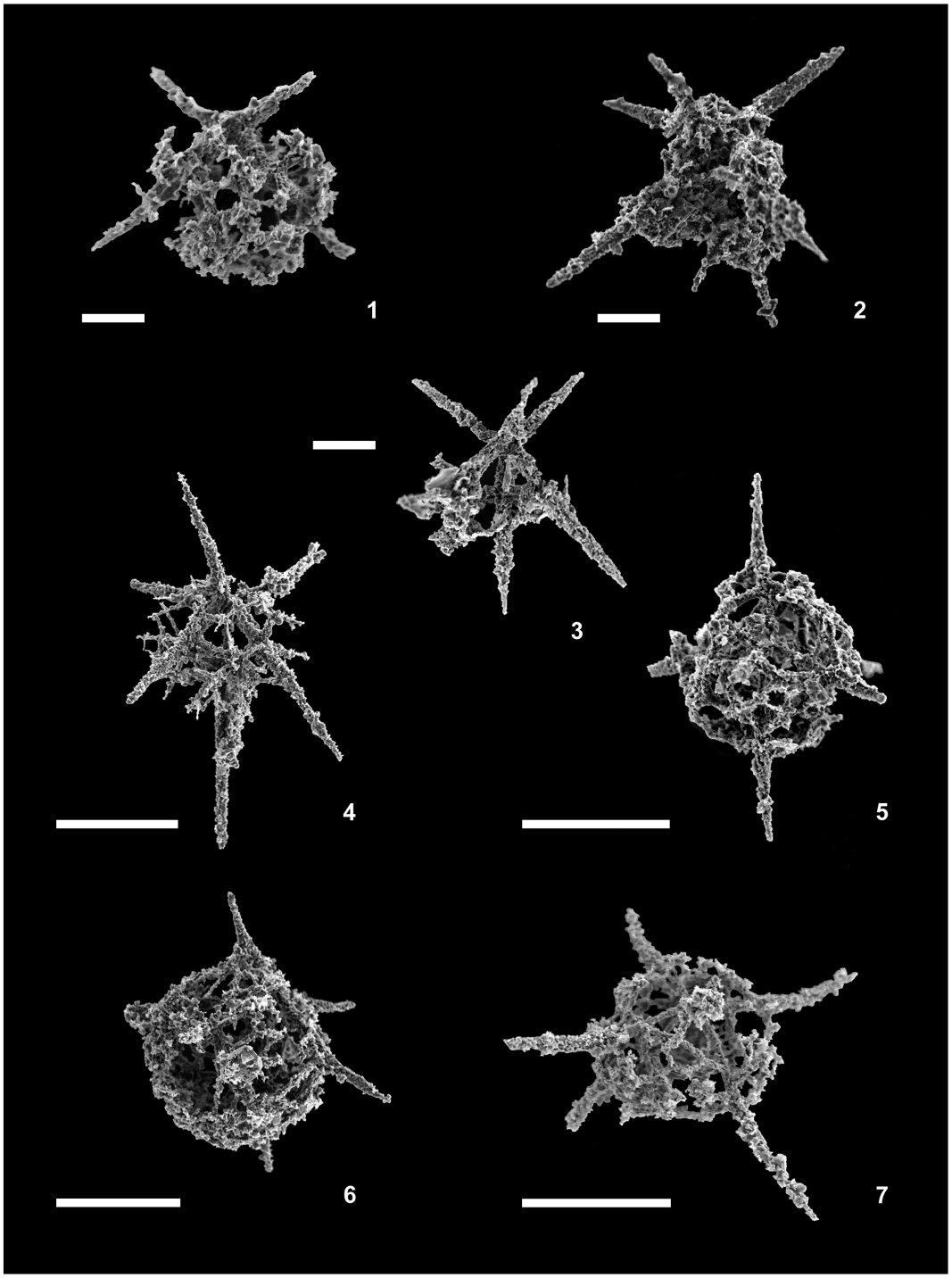

Fig. 204. 1–3, *Parentactinia nakatsugawaensis* Sashida, 1983. 1, TGU 8902, from NT01-07. 2, TGU 9115, from NT01-05. 3, TGU 9211, from NT01-05. 4–7, *Pentactinocarpus*? aff. *acanthicus* Dumitrica, 1978. 4, TGU 8618, from KC02-10. 5, TGU 9112, from NT01-05. 6, TGU 8614, from KC02-10. 7, TGU 8806, from KC02-10. Scale bars = 50 μm (1–3), 100 μm (4–7).

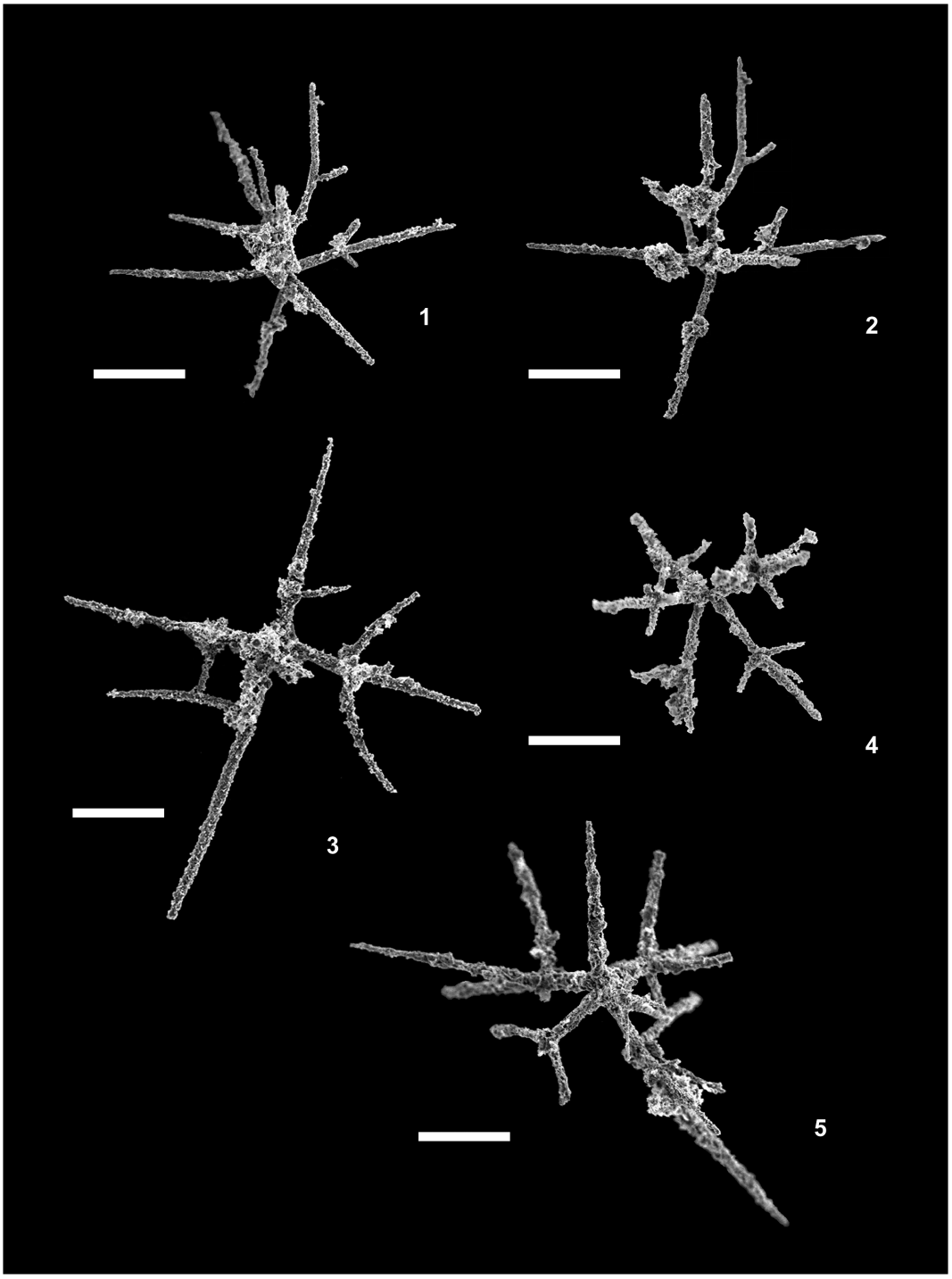

Fig. 205. *Triassothamnus verticillatus* (Dumitrica, 1978). 1, TGU 8802, from KC02-10. 2, TGU 8803, from KC02-10. 3, TGU 8615, from KC02-10. 4, TGU 8906, from NT01-07. 5, TGU 9011, from NT01-05. Scale bars = 100 μm.

long. As already suggested by Dumitrica (1982), we recognized also two morphotypes within the species, one without an apical verticil (Fig. 205.5) and the other with an apical verticil consisting of three spinules (Fig. 205.1–205.4).

Occurrence: Described specimens from NT01-05, NT01-07 and KC02-10 within the *Novispathodus pingdingshanensis* Zone represented by the *Xenoceltites variocostatus* beds (Upper Smithian=upper Lower Olenekian) in the Bac Thuy Formation, northeastern Vietnam. This species rarely occurs in the lower Fassanian (lowest Ladinian) at Recoaro, northern Italy (Dumitrica 1978, 1982).

Family Entactiniidae Riedel, 1967
Genus ***Entactinosphaera*** Foreman, 1963

Type species: *Entactinosphaera esostrongyla* Foreman, 1963.

Entactinosphaera sp. indet.
Fig. 206.1–206.2

Material examined: Two specimens, TGU 9103, 9110, from NT01-05.

Remarks: The test consists of two thin spherical shells interconnected through seemly six, three-bladed radial beams prolonged outside cortical shell into long and gently tapering three-bladed radial spines. Radial beams and spines not disposed in the three isometric axes. The wall of both shells perforated by small, polygonally-framed pores. Due to the poor preservation we could not see if inside the inner shell there is another shell or a spicule.

Occurrence: Described specimens from NT01-05 within the *Novispathodus pingdingshanensis* Zone represented by the *Xenoceltites variocostatus* beds (Upper Smithian=upper Lower Olenekian) in the Bac Thuy Formation, northeastern Vietnam.

Order Nassellaria Ehrenberg, 1875
Family Archaeosemantidae Kozur and Mostler, 1981, emend De Wever *et al.,* 2001
Genus ***Tandarnia*** Dumitrica, 1982, emend Dumitrica, 2004

Type species: *Tandarnia recoarense* Dumitrica, 1982.

Remarks: The genus *Tandarnia* is a Triassic spiculate genus with spicules very similar in arrangement to those of the entactinarian *Parentactinia* Dumitrica, 1978, but bearing no latticed shell as in *Parentactinia*. They are therefore easily distinguished by their general shape and, if possible, preserved ornamentation. Furthermore, the genus *Tandarnia* has typical disposition of spines as nassellarians; i.e., it has two homologous spines of apical and ventral, that are commonly longer than the other four lateral basal spines, and the arrangement is verticil, which is a system of branches disposed around the same point from the spicule center.

Tandarnia recoarensis Dumitrica, 1982
Fig. 206.3–206.5

Tandarnia recoarense Dumitrica, 1982, p. 415, pl. 3, figs. 6–10; Goričan and Buser, 1990, p. 159, pl. 7, fig. 4.
Tandarnia recoaroense Dumitrica, 1982. Kozur *et al*., 1996b, p. 219, pl. 11, figs. 1, 2, 4–7.
Tandarnia recoarensis Dumitrica, 1982. Sugiyama, 1997, p. 187, fig. 48.10; Dumitrica, 2004, p. 221, pl. 5, fig. 3, pl. 10, figs. 4–6.

Material examined: Three specimens, TGU 8613, 8709, 8713, from KC02-10.

Remarks: *Tandarnia recoarensis* resembles the entactinarian species of *Parentactinia nakatsugawaensis* Sashida, 1983. However, *T. recoarensis* differs from *P. nakatsugawaensis* in having two homologous apical and vertical spines, and four lateral upward-curved basal spines, and the arrangement of the all spines is verticil with three or four simple spinules. In addition, *T. recoarensis* has many short branching intricately crossed spinules.

Occurrence: Described specimens from

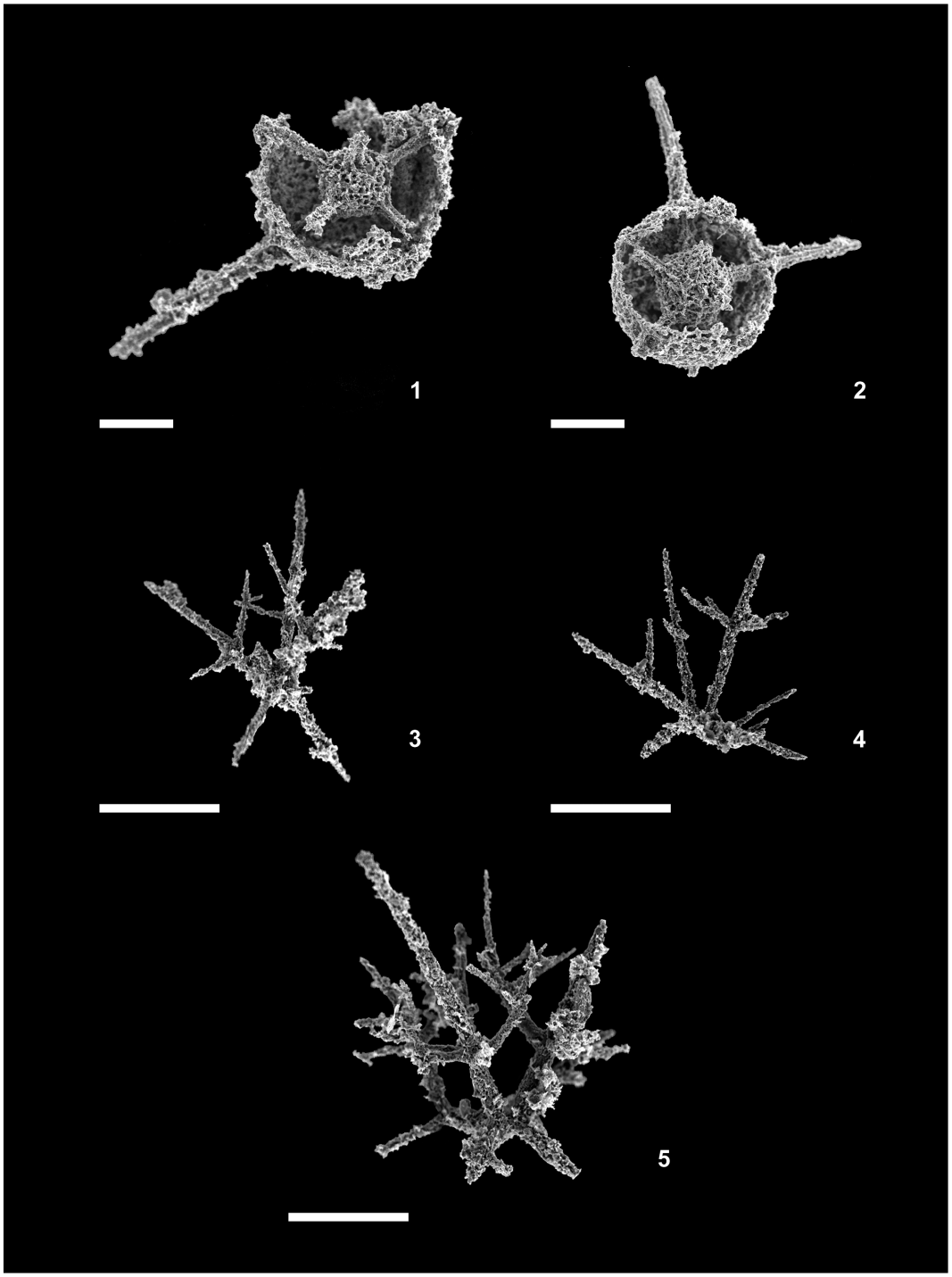

Fig. 206. 1–2, *Entactinosphaera* sp. indet. 1, TGU 9103, from NT01-05. 2, TGU 9110, from NT01-05. 3–5, *Tandarnia recoarensis* Dumitrica, 1982. 3, TGU 8709, from KC02-10. 4, TGU 8613, from KC02-10. 5, TGU 8713, from KC02-10. Scale bars = 100 μm.

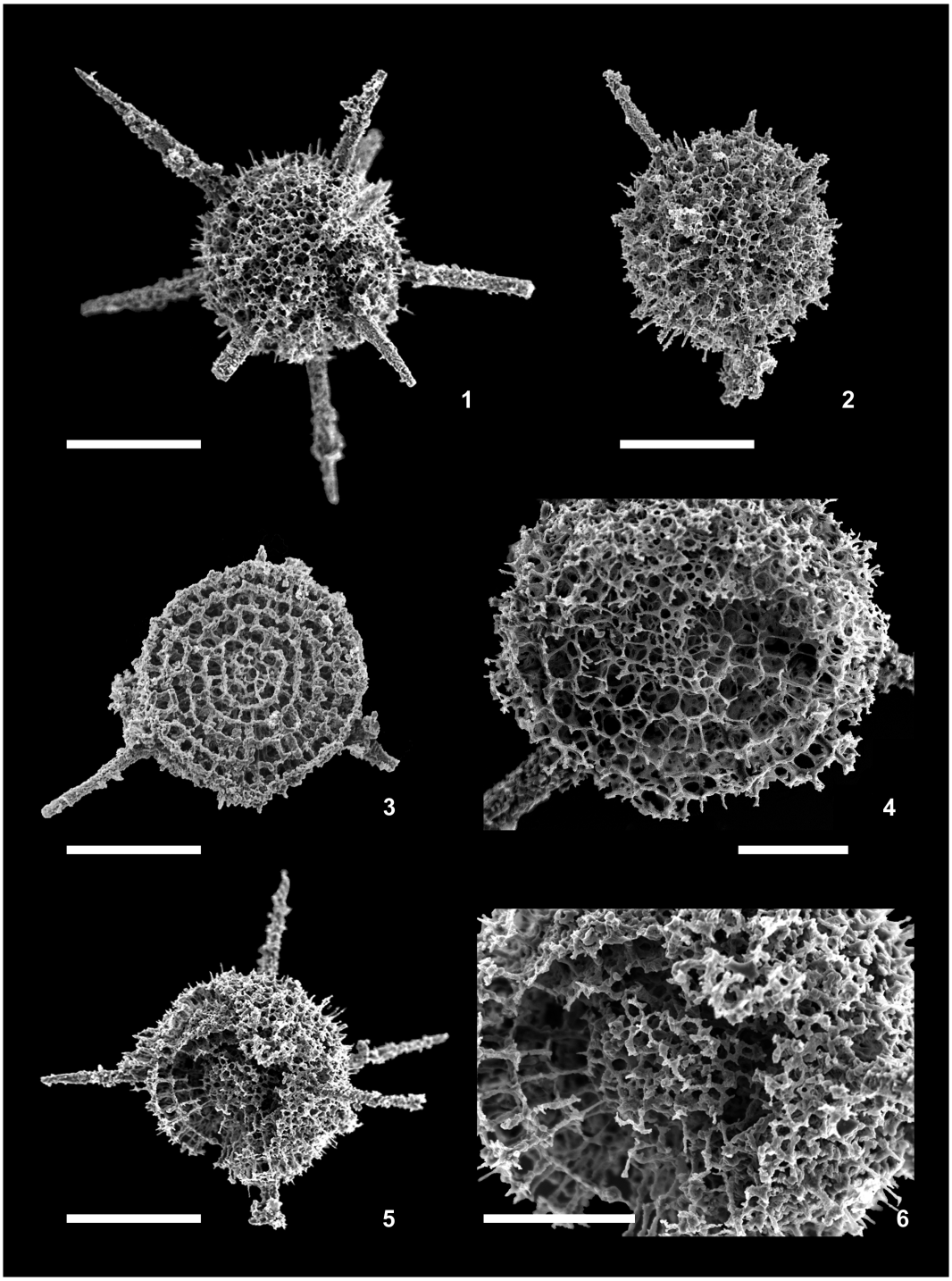

Fig. 207. *Paroertlispongus spinorientalis* Takahashi, sp. nov. 1, TGU 8809, holotype, from KC02-10. 2, TGU 8631, from KC02-10. 3, TGU 8914, from NT01-07. 4, TGU 8811, from KC02-10. 5–6, TGU 8708, from KC02-10. Scale bars = 100 μm (1–3, 5), 50 μm (4, 6).

KC02-10 within the *Novispathodus pingdingshanensis* Zone represented by the *Xenoceltites variocostatus* beds (Upper Smithian=upper Lower Olenekian) in the Bac Thuy Formation, northeastern Vietnam. This species occurs in the upper Illyrian (=uppermost Anisian) to lower Fassanian (lowest Ladinian) at Recoaro, northern Italy (Dumitrica, 1982, 2004), the Slovenian Carbonate Platform, Slovenia (Goričan and Buser, 1990), and the Loibl Formation, Austria (Kozur *et al*., 1996b). It also occurs in lower Anisian chert beds of central Japan (Sugiyama, 1997).

Order Spumellaria Ehrenberg, 1875, emend De Wever *et al.*, 2001

Family Oertlispongidae Kozur and Mostler, 1980 emend Kozur and Mostler, 1981

Genus ***Paroertlispongus*** Kozur and Mostler, 1981

Type species: *Paroertlispongus multispinosus* Kozur and Mostler, 1981.

Remarks: We use this genus in the wider sense used already by Feng *et al.* (2006) who included in it species with many spines.

Paroertlispongus spinorientalis
Takahashi, sp. nov.
Fig. 207

Material examined: Holotype, TGU 8809 (Fig. 207.1), from KC02-10. Five specimens, TGU 8502, 8631, 8708, 8811, 8815, from KC02-10, three specimens, TGU 9009, 9012, 9119, from NT01-05, and one specimen, TGU 8914, from NT01-07.

Diagnosis: Five to seven concentric spherical shells, consisting of an irregular, loose spongy framework with numerous thorns and nine long, slender, cylindrical spines. A three-dimensionally patterned framework of spongy tissues developed on each shell except in the innermost one.

Etymology: The Latin adjectives spinosus (thorny) and Orientalis (Oriental) indicate its morphology and the occurrence in the eastern Asia.

Description: Test composed of five to seven shells and nine long, slender radial spines. Spines straight and cylindrical with uniform length and shape. Innermost shell composed of a lattice with loose polygonal meshes. All other shells have a meshwork similar to that of the innermost shell; however, a three-dimensionally patterned framework of spongy tissues is developed on each shell except in the innermost shell. Surface of the outermost shell has an irregular, loose spongy framework and numerous thorns or cylindrical short by-spines.

Measurements (7 specimens): Diameter of shell 149–171 μm (mean=158.6 μm); length of spines 148–154 μm (mean=151.1 μm).

Remarks: The inner shell structure of the species was not possible to see because of the looseness and complexity of the shell meshwork. The general outline of the test of our specimens resembles those of the genus *Paroertlispongus*. This species resembles some multi-spiny species illustrated by Feng *et al.* (2006) from the latest Permian of South China.

Occurrence: Described specimens from NT0-05, NT01-07 and KC02-10 within the *Novispathodus pingdingshanensis* Zone represented by the *Xenoceltites variocostatus* beds (Upper Smithian=upper Lower Olenekian) in the Bac Thuy Formation, northeastern Vietnam.

Concluding Remarks

(by Y. Shigeta, T. Komatsu, T. Maekawa and H. T. Dang)

Our Japanese-Vietnamese Joint field investigation has described in detail the stratigraphy and faunal succession of the Lower Triassic in northeastern Vietnam. These studies have not only resulted in the reconstruction of depositional environments and the establishment of a biostratigraphic framework, but they also have contributed significantly to a better understanding of the global environmental change and dynamics of the biotic recovery

following the Permian-Triassic mass extinction. However, a considerable amount of work remains to be accomplished. Planned studies include stable isotope stratigraphy, magnetostratigraphy, biomarker analysis, spore analysis and the study of fish and shark teeth. Therefore, the future efforts of the joint research team will result in even greater contributions and will significantly broaden our knowledge of the Early Triassic.

Acknowledgements

We are very grateful to all personnel of the Vietnam Institute of Geosciences and Mineral Resources (Hanoi) for their kind help and cooperation throughout the field survey. Y. Shigeta is indebted to the following institutions for kindly providing him the opportunity to examine type and comparative specimens of Early Triassic ammonoids: Institute and Museum of Paleontology, University of Zurich (Zurich), Department of Palaeontology, University of Vienna (Vienna), Geological Survey of Austria (Vienna), Museum of Natural History of Vienna (Vienna), Goldfuss Museum (Steinmann Institute), Bonn University (Bonn), Geological Survey of India (Kolkata), Geologic Museum, Bao Tang Dia Chat (Hanoi), Nanjing Institute of Geology and Palaeontology (Nanjing), Central Research Geological Prospecting Museum (St. Petersburg), Paleontological Institute (Moscow), Far Eastern Geological Institute (Vladivostok), and Geological Survey of Canada (Ottawa). Thanks are extended to J. F. Jenks (Utah) for his helpful suggestions and improvement of the English text.

This study was financially supported by grants-in-aid from the Japanese Ministry of Education, Culture, Sports, Science, and Technology (no. 20740300), Japan Society for Promotion of Science (no. 25400500) and JSPS-VAST Joint Research Program to T. Komatsu, grants of the National Museum of Nature and Science in 2010–2012 to Y. Shigeta, a grant-in aid from the Japan Society for Promotion of Science (no. 24540501) to G. Tanaka, and the Fulbright Commission to A. Kaim.

References

Afanasieva, M. S., 2000. *Atlas of Paleozoic Radiolaria of the Russian Platform*. 480 pp, Scientific World. Moscow. (In Russian with English abstract)

Aitchison, J. C., 1993. Devonian (Frasnian) radiolarians from the Gogo Formation, Canning Basin, Western Australia. *Palaeontographica Abteilung A*, **228**: 105–128.

Arkadiev, V. V. and Vavilov, M. N., 1984. Middle Triassic Parapopanoceratidae and Nathorstitidae (Ammonoidea) of Boreal region: internal structure, ontogeny and phylogenetic patterns. *Geobios*, **17**: 397–415, pls. 1–5.

Arnold, W. H., 1965. A glossary of a thousand-and-one terms used in conchology. *Veliger, Supplement*, **7**: 1–50.

Arthaber, G., 1908. Über die Entdeckung von Untertrias in Albanien und ihre faunistische Bewertung. *Mitteilungen der Geologischen Gesellschaft in Wien*, **1**: 245–289, pls. 11–13.

Arthaber, G., 1911. Die Trias von Albanien. *Beiträge zur Paläontologie und Geologie Öesterreich-Ungarns und des Orients,* **24**: 169–277.

Baird, W., 1845. Arrangement of the British Entomostraca, with a list of species, particularly noticing those which have as yet been discovered within the bounds of the Club. *History of the Berwickshire Naturalists' Club, Edinburgh,* **2**: 145–158.

Bandel, K., 1982. Morphologie und Bildung der frühontogenetischen Gehäuse bei conchiferen Mollusken. *Facies*, **7**: 1–198, pls. 1–22.

Bandel, K., 1991. Über triassische "Loxonematoidea" und ihre Beziehungen zu rezenten und paläozoischen Schnecken. *Paläontologische Zeitschrift*, **65**: 239–268.

Bandel, K., 1993. Trochomorpha (Archaeogastropoda) aus den St.-Cassian-Schichten (Dolomiten, Mittlere Trias). *Annalen des Naturhistorischen Museums in Wien A*, **95**: 1–99.

Bandel, K., 2009. The slit bearing nacreous Archaeogastropoda of the Triassic tropical reefs in the St. Cassian Formation with evaluation of the taxonomic value of the selenizone. *Berliner Paläobiologische Abhandlungen*, **10**: 5–47.

Bando, Y., 1981. Lower Triassic ammonoids from Guryul Ravine and the Spur three kilometers north of Burus. *Palaeontologia Indica, New Series*, 46: 137–170, pls. 14–20.

Batten, R. L. and Stokes, W. L., 1986. Early Triassic gastropods from the Sinbad Member of the Moenkopi Formation, San Rafael Swell, Utah. *American Museum Novitates*, **2864**: 1–33.

Bender, H., 1970. Zur Gliederung der Mediterranen Trias II. Die Conodonten–chronologie der Mediterranen Trias. *Annales Geologiques des Pays Helleniques*, **19**: 465–540.

Beranek, L. P., Mortensen, J. K., Orchard, M. J. and Ullrich, T., 2010. Provenance of North American Trissic strata from west-central and southeastern Yukon: correlations with coeval strata in the Western Canada Sedimentary Basin and Canadian Arctic Islands. *Canadian Journal of Earth Sciences*, **47**: 53–73.

Beyers, J. M. and Orchard, M. J., 1991. Upper Permian and Triassic conodont faunas from the type area of the Cacke Creek complex, south-central British Columbia, Canada. *Geological Survey of Canada Bulletin*, **417**: 269–297.

Birkenmajor, K. and Trammer, J., 1975. Lower Triassic conodonts from Hornsund, South Spitsbergen. *Acta Geologica Polonica*, **25**: 229–308, pls. 1–2.

Bittner, A., 1891. Triaspetrefacten von Balia in Kleinasien. *Jahrbuch der Kaiserlich-Königlichen Geologischen Reichsanstalt*, **41**: 97–116.

Bittner, A., 1899. Trias Brachiopoda and Lamellibranchiata. *Palaeontologia Indica, Series 15*, **3**: 1–76, pls. 1–12.

Blome, C. D. and Reed, K. M., 1992. Permian and early (?) Triassic radiolarian faunas from the Grindstone Terrane, central Oregon. *Journal of Paleontology*, **66**: 351–383.

Bockelie, T. G. and Yochelson, E. L., 1979. Variation in a species of "worm" from the Ordovician of Spitzbergen. *Skrifter Norsk Polarinstitutt,* **167,** 225–237.

Bondarenko, L. G., Buryi, G. I., Zakharov, Y. D., Bushkareva, X. Y. and Popov, A. M., 2013. Late Smithian (Early Triassic) conodonts from Artyom, South Primorye, Russian Far East. *New Mexico Museum of Natural History and Science Bulletin*, **61**: 55–66.

Bouchet, P., Rocroi, J. P., Frýda, J., Hausdorf, B., Ponder, W. F., Valdés, Á. and Warén, A., 2005. Classification and nomenclator of gastropod families. *Malacologia*, **47**: 1–368.

Bragin, N. J., 1991. Radiolaria and Lower Mesozoic units of the USSR east regions. *Academy of Sciences of the USSR, Transactions*, **469**: 1–122. (In Russian with English abstract)

Brayard, A., Brühwiler, T., Bucher, H. and Jenks, J., 2009. *Guodunites*, a low-palaeolatitude and trans-panthalassic Smithian (Early Triassic) ammonoid genus. *Palaeontology*, **52**: 471–481.

Brayard, A. and Bucher, H., 2008. Smithian (Early Triassic) ammonoid faunas from northwestern Guangxi (South China): taxonomy and biochronology. *Fossil and Strata*, **55**: 1–179.

Brayard, A., Bucher, H., Escarguel, G., Fluteau, F., Bourquin, S. and Galfetti, T., 2006. The Early Triassic ammonoid recovery: paleoclimatic significance of diversity gradients. *Palaeogeography, Palaeoclimatology, Palaeoecology*, **239**: 374–395.

Brayard, A., Bylund, K. G., Jenks, J. F., Stephen, D. A., Oliver, N., Escarguel, G., Fara, E. and Vennin, E., 2013. Smithian ammonoid faunas from Utah: implications for Early Triassic biostratigraphy, correlation and basinal paleogeography. *Swiss Journal of Palaeontology*, **132**: 141–219.

Brayard, A., Escarguel, G., Bucher, H. and Brühwiler, T., 2009. Smithian and Spathian (Early Triassic) ammonoid assemblages from terranes: paleoceanographic and paleogeographic implications. *Journal of Asian Earth Sciences*, **36**: 420–433.

Bromley, R. G., 1996. *Trace Fossils. Biology, Taphonomy and Applications.* 361 pp. Chapman and Hall, London.

Bronn, H. G., 1828. *Posidonia becheri*, eine neue fossile Muschel der Üebergangs-Periode. *Zeitschrift oder Taschenbuch fur Mineralogie von Leonhard*, **1**: 262–269.

Brühwiler, T., Brayard, A., Bucher, H. and Guodun, K., 2008. Griesbachian and Dienerian (Early Triassic) ammonoid faunas from northeastern Guangxi and southern Guizhou (South China). *Palaeontology*, **51**: 1151–1180.

Brühwiler, T., Bucher, H. and Goudemand, N., 2010. Smithian (Early Triassic) ammonoid from Tulong, South Tibet. *Geobios*, **43**: 403–431.

Brühwiler, T., Bucher, H., Goudemand, H. and Galfetti, T., 2012a. Smithian (Early Triassic) ammonoid faunas from Exotic Blocks from Oman: taxonomy and biochronology. *Palaeontographica, Abteilung A*, **296**: 3–107, pls. 1–26.

Brühwiler, T., Bucher, H. and Krystyn, L., 2012c. Middle and late Smithian (Early Triassic) ammonoids from Spiti, India. *Special Papers in Palaeontology*, **88**: 115–174.

Brühwiler, T., Bucher, H., Ware, D., Schneebeli-Hermann, E., Hochuli, P. A., Roohi, G., Rehman, K. and Yaseen, A., 2012b. Smithian (Early Triassic) ammonoids from the Salt Range, Pakistan. *Special Papers in Palaeontology*, **88**: 1–114.

Brünnich, M. T., 1772. *Zoologiae fundamenta praelectionibus academicis accommodate*. 253 pp. Leipzig.

Budurov, K. J., Buryi, G. I. and Sudar, M. N., 1988.

Smithodus n. gen. (Conodonta) from the Smithian stage of the Lower Triassic. *Mittelilungen der Österreichischen Geologischen Bergbaustud*, **34**: 295–299.

Budurov, K. and Pantic, S., 1973. Conodonten aus den Capiller Schichten von Brassina (Westerbien). *Burgarian Academy of Sciences*. *Ministry of Heavy Industry Bulletin of the Geological Institute-Series of Paleontology*, **22**: 49–64, pls. 1–4.

Budurov, K., Sudar, M. N. and Gupta, V. J., 1987. *Spathoicriodus*, a new Early Triassic conodont genus. *Bulletin of the Indian Geologists Association*, **20:** 175–176.

Bui, D. T., 1989. Lower Triassic conodonts from North Vietnam. *Acta Palaeontologica Polonica*, **34**: 391–416, pls. 29–34.

Buryi, G. I., 1979. *Nizhnetriasovye Konodonty Yuzhnogo Primorya*. 144 pp. Nauk, Moscow. [*Lower Triassic conodonts of the South Primorye*] (In Russian)

Buryi, G. I., 1989. *Konodonty i stratigrafiya triasa Sikhote-alinya*. 136 pp. Akademiya Nauk SSSR, Dal'nevostochnoe otdelenie, Dal'nevostochnyj Geologicheskij Institut, Vladivostok. [*Triassic conodonts and stratigraphy of Sikhote-alin*] (In Russian)

Buryi, G., 1997. Early Triassic conodont biofacies of Primorye. *Mémoires de Géologie* (*Lausanne*), **30**: 35–44.

Cao, Y. and Wang, Z., 1993. Triassic conodont biostratigraphy and lithofacies paleogeography. Triassic biostratigraphy section bearing conodonts. Triassic conodont biostratigraphy. *In*, Wang, C. *ed*., *Conodonts of Lower Yangtze Valley–an Indexes to Biostratigraphy and Organic Metamorphic Maturity*, 103–117, pls. 54–64. Science Press, Beijing. (In Chinese)

Chao, K., 1950. Some new ammonite genera of Lower Triassic from western Kwangsi. *Palaeontological Novitates*, **5**: 1–11.

Chao, K., 1959. Lower Triassic ammonoids from Western Kwangsi, China. *Palaeontologia Sinica, New Series B*, **9**: 1–355, pls. 1–45.

Chen, Y., Twitchett, R. J., Jiang, H., Richoz, S., Lai, X., Yan, C. and Sun, Y., 2013. Size variation of conodonts during the Smithian–Spathian (Early Triassic) global warming event. *Geology*, **41**: 823–826.

Clark, D. L., 1972. Early Permian crisis and its bearing on Permo-Triassic conodont taxonomy. *Geologica et Palaeontologica*, **1**: 147–158.

Clark, D. L., Paull, R. K., Solien, M. N. amd Morgan, W. A., 1979. Triassic Conodont biostratigraphy in the Great Basin. *In*, Sandberg, C. A. and Clark, D. L. *eds*., *Conodont Biostratigraphy of the Great Basin and Rocky Mountains*. Brigham Young University Geology Studies, **6**, 179–183.

Clark, D. L., Sincavage, J. P. and Stone, D. D., 1964. New conodont from the Lower Triassic of Nevada. *Journal of Paleontology*, **38**: 375–377, pl. 60.

Collignon, M., 1933. Paléontologie de Madagascar 20 - Les céphalopodes du Trias infériur. *Annales de Paléontologie*, **22**: 151–180, pls. 14–20.

Collignon, M., 1973. Ammonites du Trias inférieur et moyen d'Afghanistan. *Annales de Paléontologie*, **59**: 127–163, pls. 1–10.

Conrad, T. A., 1835. Description of five new species of fossil shells in the collection presented by Mr. Edward Miller to the Geological Society. *Transactions of the Geological Society of Pennsylvania*, **1**: 267–270.

Cossmann, M. 1895. *Essais de paléoconchologie comparée. Première Livraison*. 159 pp. M. Cossmann, Comptoir Géologique, Paris.

Cox, L. R., 1960. Gastropoda. General characteristics of Gastropoda. *In*, Knight, J. B., Cox, L. R., Keen, A. M., Smith, A. G., Batten, R. L., Yochelson, E. L., Ludbrook, N. H., Robertson, R., Yonge, C. M. and Moore, R. C. *eds*., *Treatise on Invertebrate Paleontology Part I Mollusca 1*, 84–169. Geological Society of America, New York and University of Kansas Press, Lawrence.

Crasquin-Soleau, S., Galfetti, T., Bucher, H. and Brayard, A., 2006. Palaeoecological changes after the end-Permian mass extinction: early Triassic ostracods from northwestern Guangxi Province, South China. *Rivista Italiana di Paleontologia e Stratigrafia*, **112**: 55–75.

Cuvier, G., 1797. Second Mémoire sur l'organisation et les rapports des animaux à sang blanc, dans lequel on traite de la structure des Mollusques et de leur division en ordre, lu à la société d'Histoire Naturelle de Paris, le 11 prairial an troisième [30 May 1795]. *Magazin Encyclopédique, ou Journal des Sciences, des Letters et des Arts, 1795*, **2**: 433–449.

Dalrymple, R. W., 1992. Tidal depositional systems. *In,* Walker, R. G. and James, N. P. *eds*., *Facies Models: Response to Sea Level Change*, 195–218. Geological Association of Canada, Ontario.

Dalrymple, R. W., 2010. Tidal depositional systems. *In,* James, N. P. and Dalrymple, R. W. *eds.*, *Facies Models 4*, 201–232. Geological Association of Canada, Ontario.

Dang, T. H., 2006. Mesozoic. *In*, Thanh, T. D. *ed*., *Stratigraphic Units of Vietnam*, 245–366. Vietnam National University Publishing House, Hanoi.

Dang, T. H. and Nguyen, K. Q., 2000. Stratigraphical and paleontological data of Lower Triassic sediments in the An Chau structure facies zone. *Geology and*

Mineral Resources, **7**: 9–249. (In Vietnamese with English abstract)

Dang, T. H. and Ngyen D. H., 2005. Fossil zones and stratigraphic correlation of the Lower Triassic sediments of East Bac Bo. *Journal of Geology*, *Series A*, **11–12**: 1–9.

De Gregorio, A. 1886. Monographie des fossiles de Valpore (Mont Grappa) du sous-horizon Grappin de Greg. *Annales de Géologie et de Paléontologie*, **2**: 1–20.

De Wever, P., Dumitrica, P., Caulet, J. P., Nigrini C. and Caridroit, M., 2001. *Radiolarians in the Sedimentary Record*. 533 pp. Gordon and Breach Science Publishers, Amsterdam.

Diener, C., 1895. Triasdische Cephalopodenfaunen der otsibirischen küstenprovinz. *Mémoires du Comité Géologique St. Pétersbourg*, **14** (3): 1–59, pls. 1–5.

Diener, C., 1909. See Krafft, A. and Diener, C., 1909.

Diener, C., 1913. Triassic faunae of Kashmir. *Palaeontologia Indica, New Series*, **5** (1): 1–133, pls. 1–13.

Druschits, V. V. and Doguzhaeva, L. A., 1974. O nekotorykh osobennostyakh morfogeneza fillotseratid i litotseratid (Ammonoidea). *Paleontologicheskij Zhurnal*, 1974 (1): 42–53, pls. 3, 4. [Some morphogenetic characteristics of phylloceratids and lytoceratis (Ammonoidea)] (In Russian)

Druschits, V. V. and Doguzhaeva, L. A., 1981. *Ammonity pod elektronnym mikroskopom*, 238 pp., Moscow University Press, Moscow. [*Ammonites under the electron microscope*] (In Russian)

Druschits, V. V. and Khiami, N., 1970. Stroyeniye sept, stenki protokonkha i nachal'nykh oborotov rakoviny nekotorykh rannemelovykh ammonitov. *Paleontologicheskij Zhurnal*, 1970 (1): 35–47, pls. 1, 2. [Structure of the septa, protoconch walls and initial whorls in early Cretaceous ammonites] (In Russian)

Duan, J., 1987. Permian-Triassic conodonts from southern Jiangsu and adjacent areas, with indexes of their colour alteration. *Acta Micropalaeontologica Sinica*, **4**: 351–368, pls. 1–4. (In Chinese with English abstract)

Dumitrica, P., 1978. Triassic Palaeoscenidiidae and Entactiniidae from the Vicentinian Alps (Italy) and eastern Carpathians (Romania). *Deri de Seama ale sedinfelor*, **64**: 39–54.

Dumitrica, P., 1982. Middle Triassic spicular Radiolaria. *Revista Española de Micropaleontologia*, **14**: 401–428.

Dumitrica, P., 2004. New Mesozoic and early Cenozoic specular Nassellaria and Nassellaria-like Radiolaria. *Revue de Micropaléontologie*, **47**: 193–224.

Dumitrica, P., 2011. On the status of the Permian radiolarian genus *Multisphaera* Nazarov and Afanasieva, 2000. *Revue de Micropaléontologie*, **54**: 207–213.

Dumitrica, P., 2013. Early Tithonian entactinarian Radiolaria from the Solnhofen area (southern Germany). Part I. *Revue de Micropaléontologie*, **56**: 75–95.

Dumitrica, P., Kozur, H. and Mostler, H., 1980. Contribution to the radiolarian fauna of the Middle Triassic of the Southern Alps. *Geologisch-Paläontologische Mitteilungen Innsbruck*, **10**: 1–46.

Dumitrica, P. and Zügel, P., 2000. Lower Tithonian entactinarian Radiolaria from the Solnhofen area (southern Franconian Alb, southern Germany). *INTERRAD 2000, IX meeting, Reno, Program with Abstracts*: 28–29.

Dzik, J., 1976. Remarks on the evolution of Ordovician conodonts. *Acta Palaeontologica Polonica*, **21**: 395–453, pls. 41–44.

Eggins, S. M., Kinsley, L. P. J. and Shelley, J. M. G., 1998. Deposition and element fractionation processes during atmospheric pressure laser sampling for analysis by ICP-MS. *Applied Surface Science*, **129**: 278–286.

Ehrenberg, C. G., 1838. Über die Bildung der Kreidefelsen und des Kreidemergels durch unsichtbare Organismen. *Königlichen Akademie der Wissenschaften zu Berlin, Abhandlungen, Jahre 1838*: 59–147.

Ehrenberg, C. G., 1875. Fortsetzung der mikrogeologischen Studien als Gesammt-Uebersicht der mikroskopischen Paläontologie gleichartig analysirter Gebirgsarten der Erde, mit specieller Rücksicht auf den Polycystinen-Mergel von Barbados. *Königlichen Akademie der Wissenschaften zu Berlin, Abhandlungen, Jahre 1875*: 1–225.

Eichwald, E., 1851. Naturhistorische Bemerkungen, als Beitrag zu einer vergleichenden Geognosie, auf einer Reise durch die Eifel, Tryol, Italien, Sizilien und Algier. *Memoirs de la Societe Imperiale de Naturalistes d'Histoire de Moscou*, **9**: 1–464.

Ekdale, A. A. and Mason, T. R., 1988. Characteristic trace fossil associations in oxygen-poor sedimentary environments. *Geology*, **16**: 720–723.

Feng, Q., He, W., Gu, S., Jin, Y. and Meng, Y., 2006. Latest Permian Spumellaria and Entactinaria (Radiolaria) from South China. *Revue de Micropaléontologie*, **49**: 21–43.

Enos, P., Lehrmann, D. J., Jiayong, W., Youyi, Y., Jiafei, X., Chaikin, D. H., Minzoni, M., Berry, A. K. and Montgomery, P., 2006. Triassic evolution of the Yangtze Platform in Guizhou Province, People's Republic of China. *Geological Society of America, Special Paper*, **417**: 1–105.

Foreman, H. P., 1963. Upper Devonian Radiolaria from the Huron member of the Ohio shale. *Micropaleontology*, **9**: 267–304.

Frebold, H., 1930. Die Altersstellung des Fischhorizontes, des Grippianniveaus und des unteren Saurierhorizontes in Spitzbergen. *Skrifter om Svalbard og Ishavet*, **28**: 1–36.

Frech, F., 1902. Die Dyas: Lethaea Geognostica, Theil 1. *Lethaea Palaeozoica*, **2**: 579–788.

Frech, F., 1909. Die Leitfossilien der Werfener Schichten und Nachträge zur Fauna des Muschelkalkes der Cassianer und Raibler Schichten sowie der Rhät und des Dachsteindolomites (Hauptdolomit). *Resultate der Wissenschaftlichen Erforschung des Balatonsees*, **1** (1), Anhang: *Palaeontologie der Umgebung des Balatonsees*, **2** (6): 1–95.

Furutani, H., 1983. Middle Palaeozoic Palaeoscenidiidae (Radiolaria) from Mt. Yokokura, Shikoku, Japan. Part I. *Transactions and Proceedings of the Palaeontological Society of Japan, New Series*, **130**: 96–116.

Galfetti, T., Bucher, H., Martini, R., Hochuli, P. A., Weissert, H., Crasquin-Soleau, S., Brayard, A., Goudemand, N., Brühwiler, T. and Guodun, K., 2008. Evolution of Early Triassic outer platform paleoenvironments in the Nanpanjiang Basin (South China) and their significance for the biotic recovery. *Sedimentary Geology*, **204**: 36–60.

Goel, R. K., 1977. Triassic conodonts from Spiti (Himachal Pradesh), India. *Journal of Paleontology*, **51**: 1085–1101, pls. 1–3.

Goričan, Š. and Buser, S., 1990. Middle Triassic radiolarians from Slovenia (Yugoslavia). *Geologija Ljubljana*, **31**: 133–197.

Goudemand, N., Orchard, M. J., Tafforeau, P., Urdy, S., Brühwiler, T., Brayard, A., Galfetti, T. and Bucher, H., 2012. Early Triassic conodont clusters from South China: Revision of the Architecture of the 15 element apparatuses of the superfamily Gondolellidea. *Palaeontology*, **55**: 1021–1034.

Goudemand, N. and Orchard, M. J., 2012. See Goudemand, N., Orchard, M. J., Tafforeau, P., Urdy, S., Brühwiler, T., Brayard, A., Galfetti, T. and Bucher, H., 2012.

Gavrilova, V. A., 1996. On the systematics of Triassic Pterinopectinidae (Bivalvia). *Paleontological Journal*, **30**: 497–505.

Gu, H., 1976. *Fossil Lamellibranchiata of China*. 522 pp., 150 pls. Science Press, Beijing. (In Chinese)

Guex, J., 1978. Le Trias inférieur des Salt Ranges (Pakistan): problèmes biochronologiques. *Eclogae geologicae Helvetiae*, **71**: 105–141.

Guex, J., Hungerbühler, A., Jenks, J. F., O'Dogherty, L., Atudorei, V., Taylor, D. G., Bucher H. and Bartolini, A., 2010. Spathian (Lower Triassic) ammonoids from western USA (Idaho, California, Utah and Nevada). *Mémoires de Géologie (Lausanne), Université de Lausanne*, **49**: 1–82, pls. 1–60.

Guex, J., Hungerbühler, A., Jenks, J., Taylor D. and Bucher, H., 2005. Dix-huit nouveaux genres d'ammonites du Spathien (Trias inférieur) de l'Ouest américain (Idaho, Nevada, Utah et California): Note préliminaire. *Bulletin de Géologie Lausanne*, **362**: 1–31.

Guizhou Bureau of Geology and Mineral Resources, 1987. Regional geology of Guizhou Province: People's Republic of China, Ministry of Geology and Mineral Resources, Geological Memoirs, Series. 1, no. 7, 700 pp., Geologic map 1:500,000. Geological Publishing House, Beijing. (In Chinese with English summary)

Guo, F., 1985. *Fossil Bivalves of Yunnan*. 319 pp., 46 pls. Yunnan Science and Technology Publishing House, Kunming.

Haas, O., 1953. Mesozoic invertebrate fauna of Peru. Part 1, General introduction, Part 2, Late Triassic gastropods from Central Peru. *Bulletin of the American Museum of Natural History*, **101**: 1–328.

Hada, S., 1966. Discovery of Early Triassic ammonoids from Gua Musang, Kelantan, Malaya. *Journal of Geosciences, Osaka University*, **9**: 111–121.

Haecker, V., 1906. Über einige grosse Tiefsee-Radiolarien. *Zoologischer Anzeiger*, **30**: 878–895.

Haggart, J. W., 1989. New and revised ammonites from the Upper Cretaceous Nanaimo Group of British Columbia and Washington State. *Geological Survey of Canada Bulletin*, **396**: 181–221.

Hatleberg, E. W. and Clark, D. L., 1984. Lower Triassic conodonts and biofacies interpretations: Nepal and Svalbard. *Geologica et Palaeontologica*, **18**: 101–125.

Hauer, F., 1865. Die Cephalopoden der unter Trias der Alpen. *Sitzungsberichte der Akademie der Wissenschaften mathematisch-naturwissenschaftliche Klasse*, **52**: 605–640, pls. 1–3.

Herholz, M., 1992: Mikromorphe Gastropoden aus dem rheinisch-westfälischen Steinkohlenrevier (Oberkarbon). *Neues Jahrbuch für Geologie und Paläontologie, Monatshefte*, **1992**: 242–256.

Hirsch, F., 1994. Triassic conodonts as ecological and eustatic senosors. *In*, Empry, A. F., Beauchamp, B. and Glass, D. J. *eds*., *Pangea: Global Environments and Resources*, 949–959, Memoir of the Canadian Society of Petroleum Geologists 17.

Hoffet, J. H., 1940. Sur une faune de céphalopodes Werféniens de Na-Canh (Tonkin). Comptes Rendus du Conseil de Recherches Scientifiques de l'Indochine, 1940: 17–24.

Hoffmann, R., 2010. New insights on the phylogeny of the Lytoceratoidea (Ammonitina) from the septal lobe and its functional interpretation. *Revue de*

Paléobiologie, **29**: 1–156.

Hori, R. S., Yamakita, S., Ikehara, M., Kodama, K., Aita, Y., Sakai, T., Takemura, A., Kamata, Y., Suzuki, N., Takahashi, S., Spörli, K. B. and Grant-Mackie, J. A., 2011. Early Triassic (Induan) Radiolaria and carbon-isotope ratios of a deep-sea sequence from Waiheke Island, North Island, New Zealand. *Palaeoworld*, **20**: 166–178.

Huckriede, R., 1958. Die Conodonten der mediterranen Trias und ihr stratigraphischer Wert. *Paläontologische Zeitschrift*, **32**: 141–175, pls. 10–14.

Hyatt, A., 1883–1884. Genera of fossil cephalopods. *Proceedings of the Boston Society of Natural History*, **22**: 253–338.

Hyatt, A., 1900. Cephalopoda. *In*, Zittel, K. A. *ed*., *Textbook of Palaeontology*, 502–592. C. R. Eastman, London.

Hyatt, A. and Smith, J. P., 1905. The Triassic cephalopod genera of America. *United States Geological Survey Professional Paper*, **40**: 1–394.

Igo, H., 2009. Conodonts. *In*, Shigeta, Y., Zakharov, Y. D., Maeda, H. and Popov, A. M. *eds*., *The Lower Triassic System in the Abrek Bay area, South Primorye, Russia*, 181–196. National Museum of Nature and Science Monographs No. 38, Tokyo.

Jenks, J. F., Brayard, A., Brühwiler, T. and Bucher, H., 2010. New Smithian (Early Triassic) ammonoids from Crittenden Springs, Elko County, Nevada: implications for taxonomy, biostratigraphy and biogeography. *New Mexico Museum of Natural History and Science Bulletin*, **48**: 1–41.

Ji, W., Tong, J., Zhao, L., Zhuo, S. and Chen, J., 2011. Lower-Middle Triassic conodont biostratigraphy of the Qingyan section, Guizhou Province, Southwest China. *Palaeogeography, Palaeoclimatology, Palaeoecology*, **308**: 213–223.

Jia, J. T., Zheng, H. B., Huang, X. T., Wu, F. Y., Yang, S. Y., Wang, K. and He, M. Y., 2010. Detrital zircon U-Pb ages of Late Cenozoic sediments from the Yangtze delta: implication for the evolution of the Yangtze River. *Chinese Science Bulletin*, **55**: 1520–1528.

Jones, T. R., 1901. On some fossils of Wenlock age from Mulde, near Klinteberg, Gotland. *Annals and Magazine of Natural History*, **7**: 141–160.

Kaim, A., 2009. Gastropods. *In*, Shigeta, Y., Zakharov, Y. D., Maeda, H. and Popov, A. M. *eds*., *The Lower Triassic System in the Abrek Bay area, South Primorye, Russia*, 141–156. National Museum of Nature and Science Monographs No. 38, Tokyo.

Kaim, A., Nützel, A., Bucher, H., Brühwiler, T. and Goudemand, N., 2010. Early Triassic (Late Griesbachian) gastropods from South China (Shanggan, Guangxi). *Swiss Journal of Geosciences*, **103**: 121–128.

Kaim, A., Nützel, A., Hautmann, M. and Bucher, H., 2013. Early Triassic gastropods from Salt Range, Pakistan. *Bulletin of Geosciences*, **88**: 505–516.

Kamata, Y., Matsuo, A., Takemura, A., Yamakita, S., Aita, Y., Sakai, T., Suzuki, N. and Hori, R. S., 2007. Late Induan (Dienerian) primitive nassellarians from Arrow Rocks, Northland, New Zealand. *In*, Spörli, K. B., Takemura, A. and Hori, R. S. *eds*., *The Oceanic Permian/Triassic Boundary Sequence at Arrow Rocks (Oruatemanu), Northland, New Zealand*, 109–116. Institute of Geological and Nuclear Sciences Monograph 24.

Kaufmann, A., 1900. Cypriden und Darwinuliden der Schweig. Revue Suisse de Zoologie. *Annales de la Société Zoologique de Suisse*, **8**: 209–423.

Kidwell, S. M., Fürsich, F. T. and Aigner, T., 1986. Conceptual framework for the analysis and classification of fossil concentration. *Palaios*, **1**: 228–238.

Kiparisova, L. D., 1938. Nizhnetriasovye plastinchatozhabernye Ussurijskogo kraya. *Trudy Geologicheskogo Instituta*, **7**: 197–311, pls. 1–6. [Lower Triassic bivalves of the Ussuri region] (In Russian with English descriptions for new species)

Kiparisova, L. D. (ed.), 1947. *Atras rukovodyashshikh form iskopaemykh faun SSSR, 7: triasovaya sistema*. 253 pp., 51 pls. Gosudarstvennoe Izdatel'stvo Geologicheskoj Literatury Ministerstva Geologii SSSR, Moscow. [*Atlas of the guide forms of the fossil faunas of the USSR, 7: Triassic*] (In Russian)

Kiparisova, L. D., 1954. See Kiparisova, L. D. and Krishtofovich, A. N., 1954.

Kiparisova, L. D., 1961. Paleontologicheskoe obosnovanie stratigrafii triasovykh otlozhyenij primorskogo kraya. 1. Golovonogie mollyuski. *Trudy Vsyesoyuzhogo Nauchno-isslyedovatyel'skogo Geologichyeskogo Instityta (VSEGEI), Novaya seriya*, **48**: 1–278. [Paleontological fundamentals for the stratigraphy of Triaasic deposits of Primorye region. 1. Cephalopod Mollusca] (In Russian)

Kiparisova, L. D. and Krishtofovich, A. N., 1954. *Polevoj atlas kharakternykh kompleksov fauny i flory triasovykh otlozhenij primorskogo kraya*. 127 pp. Gosgeoltekhizdat, Moscow. [*Field atlas of typical complexes of fauna and flora of Triassic deposits in Primorye region*] (In Russian)

Kittl, E., 1894. Die Gastropoden der Schichten von St. Cassian der südalpinen Trias. 3. Theil. *Annalen des Kaiserlich-Königlichen Naturhistorischen Hofmuseums*, **9**: 143–275.

Kittl, E., 1903. Die Cephalopoden der oberen Werfener Schichten von Muć in Dalmatien sowie von anderen dalmatinischen, bosnisch-herzegowinischen und alpinen Lokalitäten. *Abhandlungen der Geolo-*

gischen Reichsanstalt Wien, **20**: 1–77, pls. 1–11.

Koike, T. 1981. Biostratigraphy of Triassic Conodonts in Japan. *Science Reports of the Yokohama National University, Section 2, Biological and Geological Sciences*, **28**: 25–42, pls. 1–2.

Koike, T., 1982. Triassic conodont biostratigraphy in Kedah, West Malaysia. *In*, Kobayashi, T., Toriyama, R. and Hashimoto, W. *eds*., *Geology and Palaeontology of Southeast Asia 23*, 9–51, pls. 4–10. University of Tokyo Press, Tokyo.

Koike, T., 1988. Lower Triassic conodonts *Platyvillosus* from the Taho Limestone in Japan. *Science Reports of the Yokohama National University, Section 2, Biological and Geological Sciences*, **35**: 61–79.

Koike, T., 1992. Morphological variation in Spathian conodonts *Spathoicriodus collinsoni* (Solien) from the Taho Limestone, Japan. *In*, Ishizaki K. and Saito T., *eds*., *Centenary of Japanese Micropaleontology,* 355–364. Terra Scientific Publishing Company, Tokyo.

Koike, T., 2004. Early Triassic *Neospathodus* (Conodonta) apparatuses from the Taho Formation, southwest Japan. *Paleontological Research*, **8**: 129–140.

Koken, E. 1896. Die Gastropoden der Trias um Hallstatt. *Jahrbuch der Kaiserlich-Königlichen Geologischen Reichsanstalt*, **46**: 37–126.

Komatsu, T. and Dang, T. H., 2007. Lower Triassic bivalve fossils from the Song Da and An Chau Basins, North Vietnam. *Paleontological Research*, **11**: 135–144.

Komatsu, T and Dang, T. H., 2013. See Komatsu, T., Shigeta, Y. Dang, T. H., Nguyen, D. H., Dinh, C. T., Maekawa, T. and Tanaka, G., 2013.

Komatsu, T., Dang, T. H. and Nguyen, D. H., 2010. Radiation of Middle Triassic bivalve: Bivalve assemblages characterized by infaunal and semi-infaunal burrowers in a storm- and wave-dominated shelf, An Chau Basin, North Vietnam. *Palaeogeography, Palaeoclimatology, Palaeoecology*, **291**: 190–204.

Komatsu, T., Maekawa, T., Shigeta, Y., Dang, T. H. and Nguyen, D. H., 2011. Lower Triassic stratigraphy and fossils in North Vietnam (a preliminary work). *Abstracts with Programs, the 2011 Annual Meeting, the Palaeontological Society of Japan (July, 1–3, 2011, Kanazawa, Ishikawa Prefecture)*: 26. (In Japanese)

Komatsu, T., Naruse, H., Shigeta, Y., Takashima, R., Maekawa, T., Dang, T. H., Dinh, C. T., Nguyen, D. P., Nguyen, H. H., Tanaka G. and Sone, M., 2014. Lower Triassic mixed carbonate and siliciclastic setting with Smithian–Spathian anoxic to dysoxic facies, An Chau basin, northeastern Vietnam. *Sedimentary Geology*, **300**: 28–48.

Komatsu, T., Shigeta, Y., Dang, T. H., Nguyen, D. H., Dinh, T. C., Maekawa, T. and Tanaka, G., 2013. *Crittendenia* (Bivalvia) from the Lower Triassic Olenekian Bac Thuy Formation, An Chau Basin, North Vietnam. *Paleontological Research*, **17**: 1–11.

Koninck, L. G. de, 1863. Descriptions of some fossils from India, discovered by Dr. A. Fleming, of Edinburgh. *The Quarterly Journal of the Geological Society of London*, **19**: 1–19, pls. 1–8.

Koninck, L. G. de, 1881. Faune du calcaire carbonifère de la Belgique. Troisième partie, Gastéropodes. *Annales du Musée royal d'Histoire naturelle de Belgique, série paléontologique*, **6**: 1–170.

Koninck, L. G. de, 1883. Faune du calcaire carbonifère de la Belgique. Quatrième partie, Gastéropodes suite et fin. *Annales du Musée royal d'Histoire naturelle de Belgique, série paléontologique*, **8**: 1–240.

Kozur, H. W., Kaya, O. and Mostler, H., 1996a. First evidence of Lower to Middle Scythian (Dienerian–Lower Olenekian) radiolarians from the Karakaya Zone of northwestern Turkey. *Geologisch-Paläontologische Mitteilungen Innsbruck*, *Sonderband*, **4**: 271–285.

Kozur, H.W., Krainer, K, and Mostler, H., 1996b. Radiolarians and facies of the Middle Triassic Loibl Formation, South Alpine Karawanken Mountains (Carinthia, Austria). *Geologisch-Paläontologische Mitteilungen Innsbruck*, *Sonderband*, **4**: 195–269.

Kozur, H. W. and Mostler, H., 1979. Beiträge zur Erforschung der mesozoischen Radiolarien. Teil III: Die Oberfamilien Actinommacea Haeckel 1862 emend., Artiscacea Haeckel 1882, Multiarcusellacea nov. der Spumellaria und triassische Nassellaria. *Geologisch-Paläontologische Mitteilungen Innsbruck*, **9**: 1–132.

Kozur H. W. and Mostler, H., 1980. See Dumitrica, P., Kozur, H. W. and Mostler, H., 1980.

Kozur, H. W. and Mostler, H., 1981, Beiträge zur Erforschung der mesozoischen Radiolarien. Teil IV: Thalassosphaeracea Haeckel, 1862, Hexastylacea Haeckel, 1882 emend. Petruschevskaya, 1979, Sponguracea Haeckel, 1862 emend. und weitere triassische Lithocycliacea, Trematodiscacea, Actinommacea und Nassellaria. *Geologisch-Paläontologische Mitteilungen Innsbruck, Sonderband*, **1**: 1–208.

Kozur, H. W. and Mostler, H., 1982. Entactinaria subordo nov., a new radiolarian suborder. *Geologisch-Paläontologische Mitteilungen Innsbruck*, **11/12**: 399–414.

Kozur, H. W. and Mostler, H., 1994. Anisian to Middle Carnian radiolarian zonation and description of some stratigraphically important radiolarians. *Geologisch-Paläontologische Mitteilungen Inns-*

bruck, *Sonderband*, **3**: 39–255.

Kozur, H. W., Mostler, H. and Krainer, K., 1998. *Sweetospathodus* n. gen. and *Triassospathodus* n. gen., two important Lower Triassic conodont genera. *Geologia Croatica*, **51**: 1–5.

Kozur, H. W., Mostler, H. and Repetski, J. E., 1996. Well-preserved Tremadocian primitive Radiolaria from the Windfall Formation of the Antelope Range, Eureka County, Nevada, U.S.A. *Geologisch-Paläontologische Mitteilungen Innsbruck*, **21**: 245–271.

Krafft, A. V. and Diener, C., 1909. Lower Triassic cephalopoda from Spiti, Malla Johar, and Byans. *Palaeontologia Indica, Series 15*, **6** (1): 1–186, pls. 1–31.

Krahl, J., Kauffmann, G., Kozur, H., Richter, D., Föerster, O. and Heinritzi, F., 1983. Neue Daten zur Biostratigraphie und zur tektonischen Lagerung der Phyllit-Gruppe und der Trypali-Gruppe anf der Insel Kreta (Griechenland). *Geologische Rundschau*, **72**: 1147–1166.

Krumbeck, L., 1924. Die Brachiopoden, Lamellibranchiaten und Gastropoden der Trias von Timor II. Paläontologischer Teil. *Paläontologie von Timor*, **22**, 1–275, pls. 179–198.

Krystyn, L., 1974. Die *Tirolites*-Fauna (Ammonoidea) der untertriassischen Werfener Schichten Europas und ihre stratigraphische Bedeutung. *Sitzungsberichte der Akademie der Wissenschaften mathematisch-naturwissenschaftliche Klasse, Abteilung 1*, **183**: 29–50.

Krystyn, L., Bhargava, O. N. and Richoz, S., 2007. A candidate GSSP for the base of the Olenekian Stage: Mud at Pin Valley; district Lahul and Spiti, Himachal Pradesh (Western Himalaya), India. *Albertiana*, **35**: 5–29.

Kuenzi, W. D., 1965. Early Triassic (Scythian) ammonoids from northeastern Washington. *Journal of Paleontology*, **39**: 365–378, pl. 53.

Kuhn, O., 1940. *Paläozoologie in Tabellen*. 50 pp. Fischer Verlag, Jena.

Kumagae, T. and Nakazawa, K., 2009. Bivalves. *In,* Shigeta, Y., Zakharov, Y. D., Maeda, H. and Popov, A. N. *eds.*, *Lower Triassic System in the Abrek Bay area, South Primorye*, 156–173. National Museum of Nature and Science Monographs No. 38, Tokyo.

Kummel, B., 1959. Lower Triassic ammonoids from Western Southland, New Zealand. *New Zealand Journal of Geology and Geophysics*, **2**: 429–447.

Kummel, B., 1966. The Lower Triassic formations of the Salt Range and Trans-Indus Ranges, West Pakistan. *Bulletin of the Museum of Comparative Zoology*, *Harvard University*, **134**: 361–429.

Kummel, B., 1969. Ammonoids of the late Scythian (Lower Triassic). *Bulletin of the Museum of Comparative Zoology*, *Harvard University*, **137**: 311–702.

Kummel, B. and Erben, H. K., 1968. Lower and Middle Triassic cephalopods from Afghanistan. *Palaeontographica Abteilung A*, **129**: 95–148, pls. 19–24.

Kummel, B. and Sakagami, S., 1960. Mid-Scythian ammonites from Iwai Formation, Japan. *Breviora*, **126**: 1–11, pls 1–3.

Kummel, B. and Steele, G., 1962. Ammonites from the *Meekoceras gracilitatus* Zone at Crittenden Spring, Elko County, Nevada. *Journal of Paleontology*, **36**: 638–703, pls. 99–104.

Kutassy, A., 1937. Triadisch Faunen aus dem Bihar-Gebirge. I. Teil: Gastropoden. *Geologica Hungarica Series Palaeontologica*, **13**: 1–80.

Landman, N. H. and Bandel, K., 1985. Internal structures in the early whorls of Mesozoic ammonites. *American Museum Novitates*, **2823**: 1–21.

Landman, N. H., Tanabe K. and Shigeta, Y., 1996. Ammonoid embryonic development. *In*, Landman, N. H., Tanabe, K. and Davis, R. *eds*., *Ammonoid Paleobiology*, 343–405. Plenum Press, New York.

Latreille, P. A., 1802. *Histoire Naturelle des Fourmis, et recueil de memoires et d'observations sur les abeilles, les faucheurs, et autres insects*. 445 pp. Craoelet, Paris.

Latreille, P. A., 1829. *Les crustacés, les arachnides et les insectes, distribués en familles naturelles. Ouvrage formant les tomes 4 et 5 de celui de M. le Baron Cuvier sur le Règne Animal (deuxième édition), vol. 2*. 556 pp. Deterville and Crochard, Paris.

Lehrmann, D. J., Donghong, P., Enos, P., Minzoni, M., Ellwood, B. B., Orchard, M. J., Jiyan, Z., Jiayong, W., Dillett, P., Koenig, J., Steffen, K., Druke, D., Druke, J., Kessel, B. and Newkirk, T., 2007a. Impact of differential tectonic subsidence on isolated carbonate-platform evolution: Triassic of the Nanpanjiang Basin, south China. *The American Association of Petroleum Geologists Bulletin*, **91**: 287–320.

Lehrmann, D. J., Payne, J. L., Felix, S. V., Dillett, P. M., Wang, H., Yu, Y. and Wei, J., 2003. Permian-Triassic boundary sections from shallow-marine carbonate platforms of the Nanpanjiang Basin, South China: implications for oceanic conditions associated with the end-Permian extinction and its aftermath. *Palaios*, **18**: 138–152.

Lehrmann, D. J., Payne, J. L., Pei, D., Enos, P., Druke, D., Steffen, K., Zhang, J., Wei, J., Orchard, M. J. and Ellwood, B., 2007b. Record of the end-Permian extinction and Triassic biotic recovery in the Chongzuo-Pingguo platform, southern Nanpanjiang basin, Guangxi, south China. *Palaeogeogra-*

phy, Palaeoclimatology, Palaeoecology, **252**: 200–217.

Lehrmann, D. J., Wang, W., Wei, J., Yu, Y. and Xiao, J., 2001. Lower Triassic peritidal cyclic limestone: an example of anachronistic carbonate facies from the Great Bank of Guizhou, Nanpanjiang Basin, Guizhou Province, South China. *Palaeogeography, Palaeoclimatology, Palaeoecology*, **173**: 103–123.

Lepvrier, C., Maluski, H., Vu, T. V., Leyreloup, A., Phan, T. T. and Nguyen, V. V., 2004. The Early Triassic Indosinian orogeny in Vietnam (Truong Son Belt and Kontum Massif); implications for the geodynamic evolution of Indochina. *Tectonophysics*, **393**: 87–118.

Liang, D., Tong, J., and Zhao, L., 2011. Lower Triassic Smithian-Spathian boundary at West Pingdingshan section in Chaohu, Anhui Province. *Science: China Earth Science*, **54**: 372–379.

Lindström, M., 1970. A suprageneric taxonomy of the conodonts. *Lethaia*, **3**: 427–445.

Linné, C., 1758. *Systema naturae per regna tria naturae, secundum classes, ordines, genera, species, cum characteribus, differentiis, synonymis, locis. Vol. 1: Regnum animale. Editio decimal, reformata*. 824 pp. Laurentii Salvii, Stockholm.

Lucas, S. G. and Orchard, M. J., 2007. Triassic lithostratigraphy and biostratigraphy North of Currie, Elko Country, Nevada. *New Mexico Museum of Natural History and Science Bulletin*, **40**: 119–126.

Ludwig, K. R., 2003. *User's manual for Isoplot 3.00. A geochronological toolkit for Microsoft Excel. Berkeley Geochronology Center Special Publication No. 4*. 70 pp. Berkeley Geochronology Center, Berkeley.

Luppov, N. P. and Drushchits, V. V., 1958. *Osnovy paleontologii. Mollyusk-golovonogiye. 2, Ammonoidyei (ceratity i ammonity)*. 359 pp. Gosudarstvennoye, Naucho-Tekhnicheskoye Izdatel'stvo Liiteratury po Geologii i Okhrane Nedr, Moscow. [*Fundamentals of Palaeontology, Mollusca-Cephalopoda 2, Ammonoidea (Ceratites and Ammonites)*] (In Russian)

Maeda, H. and Seilacher, A., 1996. Ammonoid taphonomy. *In*, Landman, N. H., Tanabe K. and Davis R. *eds*., *Ammonoid Paleobiology*, 543–578. Plenum Press, New York.

Maekawa, T., Komatsu, T., Shigeta, Y., Dang, T. H. and Nguyen, D. H., 2012. Biostratigraphy of the Lower Triassic Bac Thuy Formation in Lang Son area, Northern Vietnam. *Abstracts with Programs, the 2012 Annual Meeting, the Palaeontological Society of Japan (June, 29–July, 1, 2012, Nagoya, Aichi Prefecture)*: 35. (In Japanese)

Mansuy, H., 1908. *Contribution à la carte géologique de l'Indo-Chine. Paléontologie*. 73 pp., 28 pls. Imprimerie d'Extrême-Orient, Hanoi.

Mapes, R. H. and Nützel, A., 2009. Late Palaeozoic mollusk reproduction: cephalopod egg-laying behavior and gastropod larval palaeobiology. *Lethaia*, **42**: 341–356.

Marsella, E., Kozur, H. W. and D'Argenio, B., 1993. Monte Facito Formation (Scythian–Middle Carnian). A deposit of the ancestral Lagonegro Basin in the Southern Apennines. *Bollettino del Servizio Geologico d'Italia*, **119**: 225–248.

Matsuda, T., 1982. Early Triassic conodonts from Kashmir, India, part 2: *Neospathodus* 1. *Journal of Geoscience, Osaka City University*, **25**: 87–102, pls. 1–4.

Matsuda, T., 1983. Early Triassic conodonts from Kashmir, India, part 3: *Neospathodus* 2. *Journal of Geosciece, Osaka City University*, **26**: 87–110, pls. 1–5.

Matsuda, T., 1984. Early Triassic conodonts from Kashmir, India, part 4: *Gondolella* and *Platyvillosus*. *Journal of Geosciece, Osaka City University*, **27**: 119–141, pls. 1–6.

Matsumoto, T., 1954. *The Cretaceous System in the Japanese Islands*, 324 pp. Japan Society for the Promotion of Science, Tokyo.

McCoy, F., 1844. *A Synopsis of the Characters of Carboniferous Limestone Fossils of Ireland*. 274 pp. McGloshan and Gill, Dublin.

McTavish, B. R., 1973. Triassic conodont faunas from Western Australia. *Neues Jahrbuch fur Geologie und Paläontologie, Abhandlungen*, **143**: 275–303, pls. 1–2.

Meek, F. B. and Worthen, A. H., 1867. Contributions to the paleontology of Illinois and other western states. *Proceedings of the Academy of Natural Sciences Philadelphia*, 1866: 251–275.

Metcalfe, I., 1998. Palaeozoic and Mesozoic geological evolution of the SE Asian region: multidisciplinary constraints and implications for biogeography. *In,* Hall, R. and Holloway, J. D. *eds*., *Biogeography and Geological Evolution of SE Asia*, 25–41, Backhuys Publishers, Leiden.

Metcalfe, I., 2009. Late Palaeozoic and Mesozoic tectonic and palaeogeographical evolution SE Asia. *In,* Buffetaut, E., Cuny, G., Loeuff, J. Le and Suteethorn, V. *eds.*, *Late Palaeozoic and Mesozoic Ecosystems in SE Asia*, 7–23. Geological Society of London Special Publication 315.

Mojsisovics, E., 1879. Vorläufige kurze Übersicht der Ammoniten Gattungen der mediterranen und juvavischen Trias. *Verhandlungen der Geologischen*

Reichsanstalt Wien, 1895: 133–143.

Mojsisovics, E., 1882. Die Cephalopoden der mediterranen Triasprovinz. *Abhandlungen der Geologischen Reichsanstalt Wien*, **10**: 1–322, pls. 1–94.

Mojsisovics, E., 1896. Beiträge zur Kenntniss der obertriadischen Cephalopoden-Faunen des Himalaya. *Denkschriften der Kaiserlichen Akademie der Wissenschaften*, **63**: 575–701, pls. 1–22.

Moore, R. C. (ed.), 1957. *Treatise on Invertebrate Paleontology Part L Mollusca 4, Cephalopoda, Ammonoidea*. 490 pp. Geological Society of America, New York and University of Kansas Press, Lawrence.

Moore, R. C. (ed.), 1961. *Treatise on Invertebrate Paleontology, Part Q, Arthropoda 3*. 442 pp. Geological Society of America, New York and University of Kansas Press, Lawrence.

Moore, R. C. (ed.), 1964. *Treatise on Invertebrate Paleontology Part K Mollusca 3, Cephalopoda, General features, Endoceratoidea, Actinoceratoidea, Nautiloidea, Bactritoidea*. 519 pp. Geological Society of America, New York and University of Kansas Press, Lawrence.

Moore, R. C. (ed.), 1969. *Treatise on Invertebrate Paleontology part N (1, 2), Mollusca 6*. 952 pp. Geological Society of America, New York and University of Kansas Press, Lawrence.

Mosher, L. C., 1968. Triassic conodonts from western North America and Europe and their correlation. *Journal of Paleontology*, **42**: 895–946, pls. 113–118.

Mosher, L. C., 1973. Triassic conodonts from British Columbia and the northern Arctic Island. *Geological Survey of Canada Bulletin*, **222**: 141–193, pls. 17–20.

Mulder, T., 2011. Gravity processes and deposits on continental slope, rise and abyssal plains. *In*, Hüneke, H. and Mulder, T. *eds*., *Deep-Sea Sediments. Developments in Sedimentology, 63*, 25–148. Elsevier, Amsterdam.

Mulder, T. and Alexander, J., 2001. The physical character of sedimentary density currents and their deposits. *Sedimentology*, **48**: 269–299.

Müller, J., 1858. Über die Thalassicollen, Polycystinen und Acanthometren des Mittelmeeres. *Königlichen Akademie der Wissenschaften zu Berlin, Abhandlungen, Jahre 1858*: 1–62.

Müller, K. J., 1956. Triassic conodonts from Nevada. *Journal of Paleontology*, **30**: 818–830, pls. 95–96.

Münster, G. G. zu, 1841. *Beiträge zur Geognosie und Petrefacten-Kunde des Südöstlichen Tirol's vorzüglich der Schichten von St. Cassian*. 152 pp. Buchner'schen Buchhandlung, Bayreuth.

Nakano, N., Osanai, Y. and Owada, M., 2008. Textural varieties in the Indochinese metamorphic rocks: A key for understanding Asian Tectonics. *Island Arc*, **17**: 2–5.

Nakano, N., Osanai, Y., Sajeev, K., Hayasaka, Y., Miyamoto, T., Minh, N. T., Owada, M. and Windley, B., 2010. Triassic eclogite from northern Vietnam: inferences and geological significance. *Journal of Metamorphic Geology*, **28**: 59–76.

Nakazawa, K., 1996. Lower Triassic bivalves from the Salt Range region, Pakistan. *In,* Geological Survey of India *ed*., *Gondwana Nine,* Volume 1*, Ninth International Gondwana Symposium*, 207–229, Balkema Publishers, Brookfield.

Nakazawa, K., Ishibashi, T., Kimura, T., Koike, T., Shimizu, D. and Yao, A., 1994. Triassic biostratigraphy of Japan based on various taxa. *Mémoires de Géologie* (*Lausanne*), **22**: 83–103.

Nakrem, H. A., Orchard, M. J., Weitschat, W., Hounslow, M. W., Beatty, T. W. and Mørk, A., 2008. Triassic conodonts from Svalbard and their Boreal correlations. *Polar Research*, **27**: 523–539.

Nazarov, B. B., 1975. Radiolyarii nizhnego-srednego paleozoya Kazakhstana (metody issledovanii, sistematika, stratigraficheskoe znachenie). *Trudy Akademiya Nauk SSSR, Geologicheskii Institut, Moscow, USSR, Izdatelstvo Nauka,* **275**: 1–203. [Lower and middle Paleozoic radiolarians of Kazakhstan (methods of investigation, systematics, and stratigraphic significance)] (In Russian)

Nazarov, B. B. and Afanasieva, M. S., 2000. See Afanasieva, M. S., 2000.

Newell, N. D., 1937–1938. Late Paleozoic pelecypods: Pectinacea. *Kansas State Geological Survey Publication*, **10**: 1–123.

Newell, N. D., 1965. Classification of the Bivalvia. *American Museum Novitates*, **2206**: 1–25.

Newell, N. D. and Boyd, D. W., 1995. Pectinoid bivalves of the Permian-Triassic crisis. *Bulletin of the American Museum of Natural History*, **227**: 1–95.

Nguyen, D. H., 1977. Some Olenekian Cephalopod fossils from Lower Triassic sediments in Lang Son. *Journal of Biology and Earth Sciences*, **15**: 15–23. (In Vietnamese with English abstract)

Nichols, K. M. and Silberling, N. J., 1979. Early Triassic (Smithian) ammonites of paleoequatorial affinity from the Chulitna terrane, south-central Alaska. *United States Geological Survey Professional Paper*, **1121**(B): 1–5, pls. 1–3.

Noetling, F., 1905a. Untersuchungen über den Bau der Lobenlinie von *Pseudosageceras multilobatum* Noetling. *Palaeontographica*, **51**: 155–260, pls. 19–27.

Noetling, F., 1905b. Die asiatische Trias. *In*, Frech, F., *ed*., *Lethaea geognostica. Theil 2, Das Mesozoicum 1,*

Trias (2), 107–221, pls. 9–33. Handbuch der Erdgeschichte mit Abbildungen der für die Formationen bezeichnendsten Versteinerungen. Schweizerbart, Stuttgart.

Nützel, A., 1998. Über die Stammesgeschichte der Ptenoglossa (Gastropoda). *Berliner Geowissenschaftliche Abhandlungen, Reihe E* (*Paläobiologie*), **26**:1–229.

Nützel, A., 2005. Recovery of gastropods in the Early Triassic. *Comptes Rendus Palevol*, **4**: 501–515.

Nützel, A., Lehnert, O. and Frýda, J., 2007. Origin of planktotrophy – evidence from early molluscs: a response to Freeman and Lundelius. *Evolution & Development*, **9**: 313–318.

Nützel, A. and Mapes, R. H., 2001. Larval and juvenile gastropods from a Mississippian black shale: paleoecology, and implications for the evolution of the Gastropoda. *Lethaia*, **34**:143–162.

Nützel, A. and Nakazawa, K., 2012. Permian (Capitanian) gastropods from the Akasaka Limestone (Gifu Prefecture, Japan). *Journal of Systematic Palaeontology*, **10**: 103–169.

Nützel, A. and Schulbert, C., 2005. Facies of two important Early Triassic gastropod lagerstätten: implications for diversity patterns in the aftermath of the end-Permian mass extinction. *Facies*, **51**: 480–500.

Ohtsuka, Y., 1986. Early internal shell microstructure of some Mesozoic Ammonoidea: implications for higher taxonomy. *Transactions and Proceedings of the Palaeontological Society of Japan, New Series*, **141**: 275–288, pls. 45–50.

Orchard, M. J., 1994. Conodont biochronology around the Early-Middle Triassic boundary: new data from North America, Oman and Timor. *Mémoire de Géologie* (*Lausanne*), **22**: 105–114, pl. 1.

Orchard, M. J., 1995. Taxonomy and correlation of Lower Triassic (Spathian) segminate conodonts from Oman and revision of some species of *Neospathodus*. *Journal of Paleontology*, **69**: 110–122.

Orchard, M. J., 2005. Multielement conodont apparatuses of Triassic Gondolelloidea. *Special Papers in Palaeontology*, **73**: 73–101.

Orchard, M. J., 2007a. Conodont diversity and evolution through the latest Permian and Early Triassic upheavals. *Palaeogeography, Palaeoclimatology, Palaeoecology*, **252**: 93–117.

Orchard, M. J., 2007b. Report on 2007 conodont collections from Mud, Spiti. *Albertiana*, **36**: 46–49.

Orchard, M. J., 2008. Lower Triassic conodonts from the Canadian Arctic, their intercalibration with ammonoid-based stages and a comparison with other North American Olenekian faunas. *Polar Research*, **27**: 393–412.

Orchard, M. J., 2010. Triassic conodonts and their role in stage boundary definition. *In*, Lucas, S. G. *ed.*, *The Triassic Timescale*, 139–161. Geological Society of London Special Publication 334.

Orchard, M. J., Grădinaru, E. and Nicora, A., 2007a. A summary of the conodont succession around the Olenekian-Anisian boundary at Desli Caire, North Dobrogea, Romania. *New Mexico Museum of Natural History and Science, Bulletin*, **41**: 341–346.

Orchard, M. J., and Krystyn, L., 2007. Conodonts from the Induan-Olenekian boundary interval at Mud, Spiti. *Albertiana*, **35**: 30–34.

Orchard, M. J., Lehrmann, D. I., Wei, J., Wang, H. and Taylor, H. J., 2007b. Conodons from the Olenekian-Anisian boundary beds, Guandao, Guizhou Province, China. *New Mexico Museum of Natural History and Science Bulletin*, **41**: 347–354.

Pakistani-Japanese Research Group, 1985. Permian and Triassic Systems in the Salt Range and Surghar Range, Pakistan. *In*, Nakazawa, K. and Dickins, J. M. *eds*., *The Tethys: Her Paleogeography and Paleobiogeography from Paleozoic to Mesozoic*, 221–312. Tokai University Press, Tokyo.

Pan, H. Z., 1982. Triassic marine fossil gastropods from SW China. *Bulletin of Nanjing Institute of Geology and Palaeontology, Academia Sinica*, **4**: 153–188. (In Chinese)

Péron, S., Bourquin, S., Fluteau, F. and Guillocheau, F., 2005. Paleoenvironment reconstructions and climate simulations of the Early Triassic: impact of the water and sediment supply on the preservation of fluvial system. *Geodinamica Acta*, **18**: 431–446.

Perri, M. C. and Andraghetti, M., 1987. Permian-Triassic boundary and Early Triassic conodonts from the southern Alps, Italy. *Rivista Italiana di Paleontologia e Stratigrafia*, **93**: 291–328.

Popov, Y. N., 1962. Nektorye rannetriasovye ammonoidei severnogo Kavkaza. *Paleontologicheskij Zhurnal*, 1962 (3): 40–46. [Some early Triassic ammonites from the northern Caucasus] (In Russian)

Posenato, R., 1992. *Tirolites* (Ammonoidea) from the Dolomites, Bakony and Dalmatia: taxonomy and biostratigraphy. *Eclogae Geologicae Helvetiae*, **85**: 893–929.

Pratt, B. R., 2010. Peritidal carbonates. *In*, James, N. P. and Dalrymple, R. W. *eds*., *Facies Model 4*, 401–420. Geological Association of Canada, Ontario.

Purnell, M. A, Donghue, P. C. J. and Aldridge, R. J., 2000. Orientation and anatomical notation in conodonts. *Journal of Paleonotology*, **74**: 113–122.

Quenstedt, F. A., 1845–1849. *Petrefactenkunde Deutschlands. Bd. 1. Cephalopoden*. 580 pp., 36 pls. Tübingen.

Quenstedt, F. A. von, 1856–1858. *Der Jura*. (1) 1856,

1–576, pls. 1–72; (2) 1857, 577–823, pls. 73–100; (3) 1858, title-page and index. 824–842. H. Laupp'schen, Tübingen.

Rafinesque, C. S. 1815. *Analyse de nature, ou tableau de l'univers et des corps organisés*. 224 pp. L' Imprimérie de Jean Barravecchia, Palermo.

Reading, H. G. and Collinson, J. D., 1996. Clastic coasts. *In*, Reading, H. G. *ed*., *Sedimentary Environments, Processes, Facies and Stratigraphy*, 154–231, Blackwell Science, Oxford.

Riedel, W. R., 1967. Subclass Radiolaria. *In*, Harland, W. B., Holland, C. H. and House M. R. *eds*., *The Fossil Record. A Symposium with Documentation.* 291–298. Geological Society of London, London.

Sakagami, S., 1955. Lower Triassic ammonites from Iwai, Oguno-mura, Nishitama-gun, Kwanto massif, Japan. *Science Reports Tokyo Kyoiku Daigaku, Series C*, **30**: 131–140, pls. 1–2.

Salvini-Plawen, L. von, 1980. A reconsideration of systematics in the Mollusca (phylogeny and higher classification). *Malacologia*, **19**: 249–278.

Sars, G. O., 1866. Oversigt af Norges marine Ostracoder. *Forhandlinger* i *Videnskabs-Selskabet Christiania*, **8**: 1–130. (In Norwegian)

Sars, G. O. 1887. Nye bidrag til kundskaben om Middelhavets invertebratfauna: 4. Ostracoda mediterranea (Sydeuropaeiske Ostracoder). *Archiv for Mathematik og Naturvidenskab*, **12**: 173–324. (In Norwegian)

Sashida, K., 1983. Lower Triassic Radiolaria from the Kanto Mountains, central Japan. Part 1: Palaeoscenidiidae. *Transactions and Proceedings of the Palaeontological Society of Japan, New Series*, **131**: 168–176.

Sashida, K., 1991. Early Triassic radiolarians from the Ogamata Formation, Kanto Mountains, central Japan. Part 2. *Transactions and Proceedings of the Palaeontological Society of Japan, New Series*, **161**: 681–696.

Sashida, K. and Igo, H., 1992. Triassic radiolarians from a limestone exposed at Khao Chiak near Phatthalung, southern Thailand. *Transactions and Proceedings of the Palaeontological Society of Japan, New Series*, **168**: 1296–1310.

Sashida, K., Igo, H., Adachi, S., Ueno, K., Kajiwara, Y., Nakornsri, N. and Sardsud, A., 2000a. Late Permian to Middle Triassic radiolarian faunas from northern Thailand. *Journal of Paleontology*, **74**: 789–811.

Sashida, K., Nakornsri, N., Ueno, K. and Sardsud, A., 2000b. Carboniferous and Triassic radiolaria faunas from the Saba Yoi area, southernmost part of Peninsular Thailand and their paleogeographic significance. *Science Reports of the Institute of Geoscience, University of Tsukuba, Section B, Geological Sciences*, **21**: 71–99.

Sashida, K., Sardsud, A., Igo, H., Nakornsri, N., Adachi, S. and Ueno, K., 1998. Occurrence of Dienerian (Lower Triassic) radiolarians from the Phatthalung area of Peninsular Thailand and radiolarian biostratigraphy around the Permian/Triassic (P/T) boundary. *News of Osaka Micropaleontologists, Special Volume*, **11**: 59–70. (In Japanese with English abstract)

Schastlivtceva, N. P., 1981. O sistematicheskom polozhenii triasovykh ortotseratoidej yuga SSSR. *Byulleten Moskovskogo Obschestva Ispytatelej Prirody, Otdeleniye Geologicheskoye*, **56**: 76–82. [On systematic position of Triassic Orthoceratoidea of the South USSR] (In Russian)

Schastlivtceva, N. P., 1986. Nekotorye triasovye ortotseratidy i nautilidy Severo-Vostoka SSSR. *Byulleten Moskovskogo Obschestva Ispytatelej Prirody, Otdeleniye Geologicheskoye*, **61**: 122–129. [Some Triassic orthoceratids and nautilids of the Northeast Russia.] (In Russian)

Schastlivtceva, N. P., 1988. Triasovye ortotseratidy i nautilidy SSSR. *Trudy Paleontologicheskogo Instituta*, **299**: 1–104, pls. 1–8. [Triassic Orthoceratids and Nautilods of the USSR] (In Russian)

Scotese, C. R., 2002. http://www.scotese.com, (PALEOMAP website).

Shevyrev, A. A., 1968. Triasovye ammonoidei yuga SSSR. *Trudy Paleontologicheskogo Instituta, Akademiya Nauk SSSR*, **119**: 1–272. [Triassic ammonoids of the southern USSR] (In Russian)

Shevyrev, A. A., 1990. Ammonoidyei i khronostratifrafiya triasa. *Trudy Paleontologicheskogo Instituta, Rossijskaya Akademiya Nauk*, **241**: 1–179. [Ammonoids and chronostratigraphy of the Triassic] (In Russian)

Shevyrev, A. A., 1995. Triasovye ammonity Severo-Zapadnogo Kavkaza. *Trudy Paleontologicheskogo Instituta, Rossijskaya Akademiya Nauk*, **264**: 1–174. [Triassic ammonites of northwestern Caucasus] (In Russian)

Shigeta, Y. and Zakarov, Y. D., 2009. Cephalopods. *In,* Shigeta, Y., Zakharov, Y. D., Maeda, H. and Popov, A. M. *eds*., *The Lower Triassic System in the Abrek Bay area, South Primorye, Russia*, 44–140. National Museum of Nature and Science Monographs No. 38, Tokyo.

Shigeta, Y. and Weitschat, W., 2004. Origin of the Ammonitina (Ammonoidea) inferred from the internal shell features. *Mitteilungen aus dem Geologisch-Paläontologischen Institut der Universität Hamburg*, **88**: 179–194.

Shigeta, Y., Zakharov, Y. D., Maeda, H. and Popov, A. M.

(eds.), 2009. *Lower Triassic System in the Abrek Bay area, South Primorye*. 218 pp. National Museum of Nature and Science Monographs 38, Tokyo.

Shigeta, Y., Zakharov, Y. D. and Mapes, R. H., 2001. Origin of the Ceratitida (Ammonoidea) inferred from the early internal shell features. *Paleontological Research*, **5**: 201–213.

Smith, J. P., 1927. Upper Triassic marine invertebrate faunas of North America. *United States Geological Survey Professional Paper*, **141**: 1–262.

Smith, J. P., 1932. Lower Triassic ammonoids of North America. *United States Geological Survey Professional Paper*, **167**: 1–199.

Solien, M. A., 1979. Conodont biostratigraphy of the Lower Triassic Thaynes Formation, Utah. *Journal of Paleontology*, **53**: 276–306, pls. 1–3.

Spath, L. F., 1930. The Eo-Triassic invertebrate fauna of East Greenland. *Meddelelser om Grønland*, **83**: 1–90, pls. 1–12.

Spath, L. F., 1934. *Catalogue of the fossil Cephalopoda in the British Museum (Natural History). Part 4, The Ammonoidea of the Trias*. 521 pp., 18 pls. The Trustees of the British Museum, London.

Spath, L. F., 1935. Additions to the Eo-Triassic invertebrate fauna of east Greenland. *Meddelelser om Grønland*, **98**: 1–115. pls. 1–23.

Spath, L. F., 1951. *Catalogue of the fossil Cephalopoda in the British Museum (Natural History). Part 5, The Ammonoidea of the Trias 2*. 228 pp. The Trustees of the British Museum, London.

Stacey, J. S. and Kramers, J. D., 1975. Approximation of terrestrial lead isotope evolution by a two-stage model. *Earth and Planetary Science Letters*, **26**: 207–221.

Staesche, U., 1964. Conodont aus dem Skyth von Südtirol. *Neues Jahrbuch für Geologie und Paläontologie*, *Abhandlungen*, **119**: 247–306.

Sugiyama, K., 1992. Lower and Middle Triassic radiolarians from Mt. Kinkazan, Gifu Prefecture, Central Japan. *Transactions and Proceedings of the Palaeontological Society of Japan, New Series*, **167**: 1180–1223.

Sugiyama, K., 1997. Triassic and Lower Jurassic radiolarian biostratigraphy in the siliceous claystone and bedded chert units of the southeastern Mino Terrane, Central Japan. *Bulletin of the Mizunami Fossil Museum*, **24**: 79–193.

Sweet, W. C., 1964. Nautiloidea–Orthocerida. *In*, Moore, R. C. *ed*., *Treatise on Invertebrate Paleontology Part K Mollusca 3*, 216–261. Geological Society of America, New York and University of Kansas Press, Lawrence.

Sweet, W. C., 1970a. Permian and Triassic conodonts from Guryul Ravine, Vihi district, Kashmir. *University of Kansas Paleontological Contributions, Paper*, **49**: 1–10, pl. 1.

Sweet, W. C., 1970b. Uppermost Permian and Lower Triassic conodonts of the Salt Range and Trans-Indus Ranges, West Pakistan. *In*, Kummel, B. and Teichert, C. *eds*., *Stratigraphic Boundary Problems: Permian and Triassic of West Pakistan*, 207–275. University of Kansas Special Publications 4.

Sweet, W. C., 1988. *The conodont Morphology, Taxonomy, Paleoecology, and Evolutionary History of a Long-Extinct Animal Phylum*. 212 pp. Oxford Monography on Geology and Geophysics 10, Clarendon Press, Oxford.

Sweet, W. C., Mosher, L. C., Clark, D. L., Collinson, J. W. and Hasenmueller, W. H., 1971. Conodont biostratigraphy of the Triassic. *In*, Sweet, W. C. and Bergstrom, S. M. *eds*., *Symposium on Conodont Biostratigraphy*, 441–465. Geological Society of America Memoir 127.

Takemura, A., Sakai, M., Sakamoto, S., Aono, R., Takemura, S. and Yamakita, S., 2007. Earliest Triassic radiolarians from the ARH and ARF sections on Arrow Rocks, Waipapa Terrane, Northland, New Zealand. *In*, Spörli, K. B., Takemura, A. and Hori, R. S. *eds*., *The Oceanic Permian/Triassic Boundary Sequence at Arrow Rocks (Oruatemanu), Northland, New Zealand*, 97–107. GNS Science Monograph 24.

Tanabe, K., Landman, N. H. and Mapes, R. H., 1994. Early shell features of some Late Paleozoic ammonoids and their systematic implications. *Transactions and Proceedings of the Palaeontological Society of Japan, New Series*, **173**: 384–400.

Tanabe, K., Landman, N. H. and Yoshioka, Y., 2003. Intra- and interspecific variation in the early internal shell features of some Cretaceous ammonoids. *Journal of Paleontology*, **77**: 876–887.

Tanabe, K., Obata, I., Fukuda, Y. and Futakami, M., 1979. Early shell growth in some Upper Cretaceous ammonites and its implications to major taxonomy. *Bulletin of the National Science Museum, Tokyo, Series C (Geology)*, **5** (4): 155–176, pls. 1–6.

Tanabe, K. and Ohtsuka, Y., 1985. Ammonoid early internal shell structure: its bearing on early life history. *Paleobiology*, **11**: 310–322.

Tian, C., Dai, J. and Tian, S., 1983. Triassic conodonts. *In*, Chenghu Institute of Geology and Mineral Resources *ed*., *Paleontological Atlas of Southwest China, Volume of Microfossils*, 345–398, pls. 79–100. (In Chinese)

Tong, J. N., Zakharov, Y. D. and Wu, S. B., 2004. Early Triassic ammonoid succession in Chaohu, Anhui Province. *Acta Palaeontologica Sinica*, **43**: 192–204, pls. 1–2.

Tozer, E. T., 1961. Triassic stratigraphy and faunas, Queen Elizabeth Islands, Arctic archipelago. *Geological Survey of Canada Memoir*, **316**: 1–116, pls. 1–30.

Tozer, E. T., 1971. Triassic time and ammonoids. *Canadian Journal of Earth Sciences*, **8**: 989–1031.

Tozer, E. T., 1981. Triassic ammonoidea: classification, evolution and relationship with Permian and Jurassic forms. *In*, House M. R. and Senior, J. R. *eds*., *The Ammonoidea*, 65–100. Systematic Association, Special volume 18, London.

Tozer, E. T., 1994. Canadian Triassic ammonoid faunas. *Geological Survey of Canada Bulletin*, **467**: 1–663.

Tsutsumi, Y., Horie, K., Sano, T., Miyawaki, R., Momma, K., Matsubara, S., Shigeoka, M. and Yokoyama, K., 2012. LA-ICP-MS and SHRIMP ages of zircons in chevkinite and monazite tuffs from the Boso Peninsula, Central Japan. *Bulletin of the National Museum of Nature and Science, Series C*, **38**: 15–32.

Tucker, M. E., 1991. *Sedimentary Petrology, An Introduction to the Origin of Sedimentary Rocks*. 260 pp. Blackwell Scientific Publications, Oxford.

Tucker, M. E. and Wright, V. P., 1990. *Carbonate Sedimentology*. 482 pp. Blackwell, Oxford.

Vavilov, M. N., 1992. *Stratigrafiya i ammonoidei srednetriasovykh otlozhenij Severo-Vostochnoj Azii*, 234 pp. Nedra, Moscow. [Stratigraphy and ammonoids of the Middle Triassic in Northeast Asia] (In Rusian)

Vu Khuc, 1980. Stratigrafija Triasa Vietnama. *V Geologija i poleznye iskopaemye stran Azii, Afriki i Lat. Ameriki*, 33–34. Universitet Druzhby Narodov imeni Patrisa Lumumby, Moscow. [Stratigraphy of the Triassic in Vietnam. *Geology and Minerals of Asia, Africa and Latin American countries*] (In Russian)

Vu Khuc, 1984. *Triassic Ammonoids in Vietnam*. 134 pp. Geoinform and Geodate Institute, Hanoi. (In Vietnamese with English summary)

Vu Khuc, 1991. *Paleontological Atlas of Vietnam, Vol. 3, Mollusca*. 207 pp. Science and Technics Publishing House, Hanoi.

Waagen, W., 1880. Salt-Range fossils. 1, Productus-limestone fossils. 2, Pisces-Cephalopoda: supplement. Gasteropoda. *Palaeontologia Indica*, **13**: 73–183, pls. 7–16.

Waagen, W., 1895. Salt Range fossils. 2, Fossils from the ceratite formation. 1, Pisces-Ammonoidea. *Palaeontologia Indica*, **13**: 1–323, pls. 1–40.

Waller, T. R. and Stanley, G. D. Jr., 2005. Middle Triassic pteriomorphian bivalvia (mollusca) from the New Pass Range, west-central Nevada: systematic, biostratigraphy, paleoecology, and paleobiogeography. *Journal of Paleontology*, **61** (supplement 79): 1–64.

Wang, Y., 1978. Latest Early Triassic ammonoids of Ziyun, Guizhou–with notes on the relationship between Early and Middle Triassic ammonoids. *Acta Palaeontologica Sinica*, **17**: 151–177, pls. 1–3. (In Chainese with English abstract)

Wang, Z. and Cao, Y., 1981, Early Triassic conodonts from Lichuan, Western Hubei. *Acta Palaeontologica, Sinica,* **20**: 363–375, pls. 1–3. (In Chinese with English abstract)

Wang, C. and Wang, Z., 1976. Triassic conodonts from the Mount Jolmo Lungma region. *In, A Report of Scientific Expedition in the Mount Jolmo Lungma region (1966–1968), Paleontology, 2*, 387–416. Science Press, Beijing. (In Chinese)

Wang, Z. and Zhong, D., 1994. Triassic conodonts from different facies in eastern Yunnan, western Guizhou and northern Guangxi. *Acta Micropalaeontologica Sinica*, **11**: 379–412, pls. 1–5.

Waterhouse, J. B., 2000. Early Triassic Pectinidina (Mollusca: Bivalvia) from Dolpo and Manang, Nepal Himalaya. *Records of the Canterbury Museum*, **14**: 155–186.

Wei, M., 1981. Early and Middle Triassic ostracods from Sichuan. *Acta Palaeontologica Sinica*, **20**: 501–507. (In Chinese with English abstract and description of new species)

Weitschat, W., 1986. Phosphatisierte Ammonoideen aus der Mittleren Trias von Central-Spitzbergen. *Mitteilungen aus dem Geologisch-Paläontologischen Institut der Universität Hamburg*, **61**: 249–279. (In Germany with English summary)

Weitschat, W. and Lehmann, U., 1978. Biostratigraphy of the uppermost part of the Smithian stage (Lower Triassic) at the Botneheia, W.-Spitsbergen. *Mitteilungen aus dem Geologisch-Paläontologischen Institut, Universität Hamburg*, **48**: 85–100.

Welter, O. A., 1922. Die Ammoniten der Unteren Trias von Timor. *Paläontologie von Timor*, **11**: 83–154, pls. 155–171.

Wenz, W., 1938. Gastropoda. Teil 2: Prosobranchia. *In*, Schindewolf, O. H. *ed*., *Handbuch der Paläozoologie, Band 6*, 241–480, Gebrüder. Borntraeger, Berlin.

Wheeley, J. R. and Twitchett, R. J., 2005. Palaeoecological significance of a new Griesbachian (Early Triassic) gastropod assemblage from Oman. *Lethaia*, **38**: 37–45.

White, C. A., 1879. Paleontological paper no. 9: fossil from the Jura-Trias of south-eastern Idaho. *Bulletin of the United States Geological and Geographical Survey of the Territories*, **5**: 105–117.

Williams, I. S., 1998. U-Th-Pb geochronology by ion mi-

croprobe. *In*, McKibben, M. A., Shanks, W. C. P. and Ridley, W. I. *eds*., *Applications of Microanalytical Techniques to Understanding Mineralizing Processes*, 1–35. Reviews in Economic Geology 7, Society of Economic Geologists, Littleton, Co.

Won, M.-Z., 1990. Lower Carboniferous radiolarian fauna from Riescheid (Germany). *Journal of the Palaeontological Society of Korea*, **6**: 111–143.

Won, M.-Z., 1997. Review of family Entactiniidae (Radiolaria), and taxonomy and morphology of Entactiniidae in the late Devonian (Frasnian) Gogo Formation, Australia. *Micropaleontology*, **43**: 333–369.

Wright, V. P., 1990. Peritidal carbonates. *In,* Tucker, M. E. and Wright, V. P. *eds*., *Carbonate Sedimentology*, 137–164. Blackwell Science, Oxford.

Wright, V. P. and Burchette, T. P., 1996. Shallow-water carbonate environments. *In,* Reading, H. G. *ed*., *Sedimentary Environments: Processes, Facies and Stratigraphy*, 325–392. Blackwell Science, Oxford.

Xu, X., O'Reilly, S. Y., Griffin, W. L. Wang, X., Pearson, N. J. and He, Z., 2007. The crust of Cathaysia: Age, assembly and reworking of two terranes. *Precambrian Research*, **158**: 51–78.

Zakharov, Y. D., 1968. *Biostratigraphiya i ammonoidei nizhnego triasa Yuzhnogo Primorya*. 175 pp. Nauk, Moscow. [Lower Triassic biostratigraphy and ammonoids of South Primorye] (In Russian)

Zakharov, Y. D., 1978. *Rannetriasovye ammonoidei Vostoka SSSR*. 224 pp. Nauka, Moscow. [*Lower Triassic ammonids of East USSR*] (In Russian)

Zhang, S. and Yang, Z., 1991. On multielement taxonomy of the Early Triassic conodonts. *Stratigraphy and Paleontology of China*, **1**: 17–47, pls. 1–4.

Zhao, L., Orchard, M. J. and Tong, J., 2004. Lower Triassic conodont biostratigraphy and speciation of *Neospathodus waageni* around the Induan-Olenekian boundary of Chaohu, Anhui Province, China. *Albertiana*, **29**: 41–43.

Zhao, L., Orchard, M. J., Tong, J., Sun, Z., Zuo, J., Zhang, S. and Yun, A., 2007. Lower Triassic conodont sequence in Chaohu, Anhui Province, China and its global correlation. *Palaeogeography, Palaeoclimatology, Palaeoecology*, **252**: 24–38, pl. 1.

Zhao, L. and Orchard, M. J., 2007. See Zhao, L., Orchard, M. J., Tong, J., Sun, Z., Zuo, J., Zhang, S. and Yun, A., 2007.

Zittel, K. A., 1884. Cephalopoda. *In*, Zittel, K. A.. *ed*., *Handbuch der Palaeontologie, Band 1, Abt. 2*, 329–522. München and Leipzig.

Zittel, K. A., 1895. *Grundzüge der Paläontologie (Paläozoologie), Abt. I, Invertebrata*. 971 pp. Oldenburg, München and Leipzig.

Zhu, X. G., 1995. Palaeontology-Gastropods. *In*, Sha, J.G. *ed*., *Palaeontology of the Hoh Xil Region, Qinghai*, 69–81. Kexue Chubanshe, Beijin.

National Museum of Nature and Science Monographs

(Nos. 1–35 were published as "National Science Museum Monographs)

No. 1*. Early Cretaceous marine and brackish-water Gastropoda from Japan. By Tomoki Kase, 199 pp., 31 pls., 1984.

No. 2*. A taxonomic study on the subfamily Herminiinae of Japan (Lepidoptera, Noctuidae). By Mamoru Owada, 208 pp., 1987.

No. 3*. Small mammal fossils and correlation of continental deposits, Safford and Duncan Basins, Arizona, USA. By Yukimitsu Tomida, 141 pp., 1987.

No. 4. Late Miocene floras in northeast Honshu, Japan. By Kazuhiko Uemura, 174 pp., 11 pls., 1988.

No. 5. A revisional study of the spider family Thomisidae (Arachnida, Araneae) of Japan. By Hirotsugu Ono, 252 pp., 1988.

No. 6. The taxonomic study of Japanese dictyostelid cellular slime molds. By Hiromitsu Hagiwara, 131 pp., 1989.

No. 7. A systematic study of the Japanese Chiroptera. By Mizuko Yoshiyuki, 242 pp., 1989.

No. 8. Rodent and lagomorph families of Asian origins and diversification: Proceedings of Workshop WC-2 29th International Geological Congress, Kyoto, Japan. Edited by Yukimitsu Tomida, Chuankuei Li, and Takeshi Setoguchi, 195 pp., 1994.

No. 9. A microevolutional history of the Japanese people as viewed from dental morphology. By Hirofumi Matsumura, 130 pp., 1995.

No. 10. Studies on the human skeletal remains from Jiangnan, China. Edited by Bin Yamaguchi and Huan Xianghon, 108 pp., 3 pls., 1995.

No. 11. Annoted checklist of the inshore fishes of the Ogasawara Islands. By John E. Randall, Hitoshi Ida, Kenji Kato, Richard L. Pyle, and John L. Earle, 74 pp., 19 pls., 1997.

No. 12. Deep-sea fauna and pollutants in Suruga Bay. By Tsunemi Kubodera and Masaaki Machida, *et al*., 336 pp., 12 pls., 1997.

No. 13. Polychaetous annelids from Sagami Bay and Sagami Sea collected by the Emperor Showa of Japan and deposited at the Showa Memorial Institute, National Science Museum, Tokyo. Families Polynoidae and Acoetidae. By Minoru Imajima, 131 pp., 1997.

No. 14. Advance in vertebrate paleontology and geochronology. Edited by Yukimitsu Tomida, Lawrence J. Flynn, and Louis L. Jacobs, 292 pp., 1998.

No. 15. Proceedings of the Second Gondwanan Dinosaur Symposium. Edited by Yukimitsu Tomida, Thomas H. Rich, and Patricia Vickers-Rich, 296 pp., 1999.

No. 16. Onuphidae (Annelida, Polychaeta) from Japan, excluding the genus *Onuphis*. By Minoru Imajima, 115 pp., 1999.

No. 17. Description of a new species of Anhangueridae (Pterodactyloidea) with comments on the pterosaur fauna from the Santana Formation (Aptian-Albian), northeastern Brazil. By Alexander W. A. Kellner and Yukimitsu Tomida, 135 pp., 2000.

No. 18. Proceedings of the First and Second Symposia on Collection Building and Natural History Studies in Asia. Edited by Keiichi Matsuura, 188 pp., 2000

No. 19. A taxonomic revision of the marine species of *Cladophora* (Chlorophyta) along the coasts of Japan and the Russian Far-east. By Christiaan van den Hoek and Mitsuo Chihara, 242 pp., 2000.

No. 20. Deep-sea fauna and pollutants in Tosa Bay. Edited by Toshihiko Fujita, Hiroshi Saito and Masatsune Takeda, 380 pp., 2001.

No. 21. Marine Fauna of the Shallow Waters around Hainan Island, South China Sea. Edited by Keiichi Matsu-ura, 126 pp., 2001.

No. 22. Proceedings of the Third and Fourth Symposia on Collection Buildings and Natural History Studies in Asia and the Pacific Rim. Edited by Tsunemi Kubodera, Masanobu Higuchi, and Ritsuro Miyawaki, 193 pp., 2002.

No. 23. Polychaetous Annelids from Sagami Bay and Sagami Sea Collected by the Emperor Showa of Japan and Deposited at the Showa Memorial Institute, National Science Museum, Tokyo (II). Orders included within the Phyllodocida, Amphinomida, Spintherida and Eunicida. By Minoru Imajima, 221 pp., 2003.

No. 24. Proceedings of the Fifth and Sixth Symposia on Collection Building and Natural History Studies in Asia and the Pacific Rim. Edited by Shinobu Akiyama, Ritsuro Miyawaki, Tsunemi Kubodera, and Masanobu Higuchi 292 pp., 2004.

No. 25. Revision of scydmaenid beetles of the genus *Syndicus* Motschulsky (Coleoptera, Scydmaenidae). By Pawel Jaloszynski, 108 pp., 2004.

No. 26. A new specimen of *Apatosaurus ajax* (Sauropoda: Diplodocidae) from the Morrison Formation (Upper Jurassic) of Wyoming, USA. By Paul Upchurch, Yukimitsu Tomida, and Paul M. Barrett, 108 pp., 10 pls., 2004.

No. 27. Leaf-rolling Sawflies of the *Pamphilius vafer* complex (Hymenoptera, Pamphiliidae). By Akihiko Shinohara, 116 pp., 2005.

No. 28. Types of Japanese Bird. By Hiroyuki Morioka, Edward C. Dickinson, Takashi Hiraoka, Desmond Allen and Takeshi Yamasaki, 154 pp., 2005.

No. 29. Deep-sea fauna and pollutants in Nansei Islands. Edited by Kazunori Hasegawa, Gento Shinohara and Masatsune Takeda, 476 pp., 2005.

No. 30. Phenology and Growth Habits of Tropical Trees: Long-term Observations in the Bogor and Cibodas Botanic Garden, Indonesia. Edited by Hiroaki Hatta and Dedy Darnaedi, 436 pp., 2005.

No. 31. The Cretaceous System in the Makarov area, southern Sakhalin, Russian Far East. Edited by Yasunari Shigeta and Haruyoshi Maeda, 136 pp., 2005.

No. 32. Revision of the Palearctic species of the myrmecophilous genus *Pella* (Coleoptera, Staphylinidae, Aleocharinae). By Munetoshi Maruyama, 207 pp., 2006.

No. 33. Checklist of Japanese lichens and allied fungi. By Syo Kurokawa and Hiroyuki Kashiwadani, 157 pp., 2006.

No. 34. Proceedings of the Seventh and Eighth Symposia on Collection Building and Natural History Studies in Asia and the Pacific Rim. Edited by Yukimitsu Tomida, Tsunemi Kubodera, Shinobu Akiyama and Taiju Kitayama, 294 pp., 2006.

No. 35. Anatomy of a Japanese Tomistomine Crocodylian, *Toyotamaphimeia Machikanensis* (Kamei et Matsumoto, 1965), from the Middle Pleistocene of Osaka Prefecture: The Reassessment of its Phylogenetic Status within Crocodylia. By Yoshitsugu Kobayashi, Yukimitsu Tomida, Tadao Kamei and Taro Eguchi, 121 pp., 2006.

No. 36. A systematic study of the genus *Siriella* (Crustacea: Mysida) from the Pacific and Indian oceans, with descriptions of fifteen new species. Edited by Masaaki Murano and Kouki Fukuoka, 173 pp., 2008.

No. 37. Chromosome atlas of flowering plants in Japan. Edited by Tsunehiko Nishikawa, 706 pp., 2008.

No. 38. The Lower Triassic System in the Abrek Bay area, South Primorye, Russia. Edited by Yasunari Shigeta, Yuri D. Zakharov, Haruyoshi Maeda and Alexander M. Popov, 218 pp., 2009.

No. 39. Deep-sea Fauna and Pollutants off Pacific Coast of Northern Japan. Edited by Toshihiko Fujita, 755 pp., 2009.

No. 40. Joint Haeckel and Ehrenberg Project: Reexamination of the Haeckel and Ehrenberg Mircofossil Collections as a Historical and Scientific Legacy. Edited by Yoshihiro Tanimura and Yoshiaki Aita, 106 pp., 2009.

No. 41. Middle and Late Miocene Marie Bivalvua from the Northeern Kanto Region, Central Japan. Edited by Yukito Kurihara, 87 pp., 2010.

No. 42. Chemical Compositions of Electrum Grains in Ore and Placer Deposits in the Japanese Islands. By Kazumi Yokoyama, Shogo Takeuchi, Izumi Nakai, Yukiyasu Tsutsumi, Takashi Sano, Masako Shigeoka, Ritsuro Miyawaki and Satoshi Matsubara, 80 pp., 2011.

No. 43 Digeneans (Trematoda) Parasitic in Freshwater Fishes (Osteichthyes) of the Lake Biwa Basin in Shiga Prefecture, Centeral Honshu, Japan. By Takeshi Shimazu, Misako Urabe and Mark J. Grygier, 105 pp., 2011.

No. 44 Deep-sea Fauna of the sea of Japan. Edited by Toshihiko Fujita, 291 pp., 2014.

(* out of print)

All inquiries concerning the Monographs should be addressed to:
Library
National Museum of Nature and Science
4-1-1 Amakubo, Tsukuba, Ibaraki 305-0005 Japan